UNIVERSITY OF ADELAIDE LIBRARY
22-3-96

SEDIMENTARY ARCHITECTURE OF RIFT RELATED DEPOSITIONAL SYSTEMS WITHIN THE DAMPIER PROVINCE, NORTH WEST SHELF, AUSTRALIA

LYNDON ROBERT MILLER

Thesis submitted for the degree of
Doctor of Philosophy
at
The University of Adelaide
and the
National Centre for Petroleum Geology and Geophysics
July, 1995

This work contains no material which has been accepted for the award of any other degree or diploma in any university or other tertiary institution and, to the best of my knowledge and belief, contains no material previously published or written by another person, except where due reference has been made in the text.

I give consent to this copy of my thesis, when deposited in the University Library, being available for loan and photocopying.

Lyndon R. Miller
April, 1995

ABSTRACT

Detailed stratigraphy and high resolution seismic mapping is essential in areas such as the Dampier Sub-Basin where exploration for conventional structural plays has reached a mature stage, and only more subtle stratigraphic plays provide new strategies. It is in the analysis of the vertical and lateral architecture of reservoir units and their relationships with sealing rocks that these stratigraphic plays may be defined.

A review of the sequence stratigraphy literature suggests to me a shortcoming in which many interpretations are driven by previously conceived sequence stratigraphic and sedimentological models. This work demonstrates that any particular area must be considered individually on the basis of available data with respect to the age of the rocks, structural regime, style of sedimentary basin and depositional setting. Depositional systems should be defined on an independent basis, and then 'characterised' by the style of deposition that is observed by sedimentological evidence. The style of deposition observed may be qualified only by considering numerous sedimentological models as end-members which are 'type' examples of these variables, and then allocated accordingly within a spectrum of possibilities. When this is achieved, the effect that sediment influx, eustacy and tectonics had on the defined depositional systems may be objectively evaluated.

The depositional systems of the Mesozoic succession of the Dampier Sub-basin can be described elegantly in terms of *tectonic systems tracts* (Prosser, 1993) which characterise the styles of sedimentation that occur during progressive rift-related stages of structural evolution of the basin. This framework is used on a 'super-cycle' scale and is relevant to all the basins of the North West Shelf. The structural inheritance of older basin morphologies and fault patterns, vulnerable to reactivation (Hill, 1994), is interpreted as an additional controlling factor in the Dampier Sub-basin. This factor is considered in addition to the effect that rifting and sea floor spreading events and the tectonic effects that the adjacent cratons had on the stratigraphy of the Western Margin of Australia during the Mesozoic.

Detailed chronostratigraphic correlations of the Aptian to Callovian section within and adjacent to the Lewis Trough of the Dampier Sub-Basin has led to the definition of five major chronostratigraphic cycles. The sedimentary architecture (geometries, thicknesses and lateral extents) of depositional systems within each cycle reflects the tectonic stage of basin development in terms of a tectonic systems tract. Detailed seismic facies mapping, integrated with chronostratigraphic well log correlations, has allowed the architecture of many of these units to be described.

The early rift climax systems tract of Calypso Formation equivalents (Mid-Callovian - Oxfordian) is dominantly a marine shelf succession where seismic reflection terminations reveal half graben sediment filling under static to slightly transgressive changes in relative sea level. During lower Oxfordian time, an increased rate of half graben fault movement gave way to pronounced deeper marine conditions in the Lewis Trough and adjacent Elliassen Terrace, as subsidence dramatically outpaced sediment supply. At this time the Elliassen Formation was deposited as part of the mid-late rift climax systems tract. Gravity induced slope apron depositional systems

formed along a contemporaneously developing fault scarp. These slope apron systems contain depositional elements such as braided channels, levee complexes and discrete sand lobes. As sedimentation progressed, increasingly mud rich conditions accompanied the deposition of muddy turbidites, contourites and levee complexes, and hemipelagic ponding.

The formation of an unconformity near the end of Oxfordian time is directly attributed to break up and subsequent sea floor spreading on the Argo Abyssal Plain. Marginward, isostatic uplift operating contemporaneously with sediment cannibalization via headward erosion of a previously developed fault scarp provided high rates of sediment influx. Deposition of the Angel Formation and equivalents as an immediate post-rift systems tract resulted. Ever increasing sand rich conditions ensued as sedimentary gradients subsided and progressive sediment 'filling' of the basin depocentre occurred. Concommittently, there was an evolutionary progression of depositional systems from sandy slope aprons, to channel lobe complexes, to a shelf fed depositional ramp as sedimentation became more widespread up section. This vertical succession of depositional systems resulted as topographic relief progressively decreased due to basin filling and then gave way to thermal subsidence related to basin tilting (flexure). Six genetically related units were defined using well logs and high resolution palynology. These units were interpreted to be the result of variations in sediment influx and tectonically influenced changes in relative sea level. This led to the mapping of three seismic units, which, together with the well correlations, demonstrate the progression that is described above.

Diminishing sediment supply signalled the end of widespread Angel Sandstone deposition during the Berriasian. The Dampier rift basin was dominantly filled at this time and deposition of a marine claystone, the Forestier Claystone, became widespread. Onlap onto the adjacent Enderby Terrace commenced as a late post rift systems tract as sands of the Talisman Sandstone Member and muds of the Forestier Claystone slumped into the eastern margin of the Lewis Trough. This filled any remnant relief of the Rosemary Fault scarp that may have existed. Mild, synsedimentary, left-lateral wrenching movements that occurred sporadically over the Rosemary Fault system during Angel Formation time and continued in the Early Cretaceous may have also had some palaeotopographic control of sedimentation. Sediment starvation persisted in the basin depocentre. A disconformity within the Valanginian marks the onset of a regional transgression where the Birdrong Sandstone and the Mardie Greensand transgressed over the Enderby Terrace, primarily due to thermal isostatic subsidence of the basin margin. A disconformity near the top of the Aptian marks the establishment of fully open marine conditions with deposition of the Windalia Sandstone, Gearle Siltstone, and Haycock Marl in a passive margin setting.

ACKNOWLEDGEMENTS

There are several people and institutions whom I gratefully acknowledge, as they made this research possible.

This project was primarily sponsored by Ampolex Ltd. They provided a scholarship and much of the data for this project. The initial work was performed at the Ampolex office in Perth, where the staff offered helpful support. Other funding has been also provided by the Australian Petroleum Cooperative Research Centre (APCRC). In addition, I was a receiver of a grant of the 1994 Grants-in Aid Program, which is provided by the Grants-in-Aid Fund of the American Association of Petroleum Geologists Foundation.

Basic data was supplied by numerous Australian contracting companies within the oil industry who were willing to provide this data for the purpose of academic research. Seismic on paper, sepia and in digital form was provided by Australian Seismic Brokers in Perth. Philips Petroleum Ltd. were also generous in supplying much of the needed seismic over Permit WA-208-P. Shot point location data was provided by Digimap Consultants (Sydney). Palynological data was supplied by Morgan Palaeo Associates of Maitland, South Australia. Digital electric log data was supplied by Wiltshire Geological Services in Adelaide. Core data was viewed at the West Australian Department of Mines, and also at Woodside Offshore Petroleum Pty. Ltd., both of Perth.

The majority of this project work was performed at the National Centre for Petroleum Geology and Geophysics (NCPGG) in Adelaide. I would like to thank the staff and students at the NCPGG who provided helpful advice and moral support during the course of this work. Specifically, I thank my head supervisor, Dr. W.J. Stuart, and also Dr Nick Lemon and Mr. Andy Mitchell, who all provided invaluable advice and support when it was needed. Professor Cedric Griffiths and Dr. Ian Dysan kindly provided helpful advice and comments with respect to the transcript. Simon Polomka, Alex Kaiko, and Anthony Hayball were a few of my fellow students who were always willing to assist, or contribute helpful feedback on this work, or to simply be the source of stimulating and friendly conversation.

TABLE OF CONTENTS

Abstract iii
Acknowledgements v
List of figures xii
List of tables xvi
List of appendices xvii
List of enclosures xviii

CHAPTER 1: INTRODUCTION

THE DAMPIER SUB-BASIN

1.1 Objectives 1
1.2 Database 1
1.3 Methods 6
Core logging
Seismic interpretation
Stratigraphic well log correlations
1.4 Regional geology 10
1.4.1 Regional framework 10
1.4.2 Structural framework 13
1.4.3 Lithostratigraphy 16
Athol Formation
Legendre Formation
Calypso Formation
Eliassen Formation
Dingo Claystone
Angel Formation
Forestier Claystone
Talisman Sandstone Member
Lower Winning Group
Muderong Shale
Mardie Greensand
Birdrong Sandstone
Upper Winning Group
Windalia Radiolarite
Gearle Siltstone / Haycock Marl
Toolonga Calcilutite

1.5 Petroleum exploration and production in the Dampier Sub-basin 23
Legendre Field
Angel Field
Eaglehawk Field
Egret Field
Lambert Field
Talisman Field
Wanaea Field
Cossack Field
Wandoo Field

CHAPTER 2: THEORY
SEDIMENTARY AND STRATIGRAPHIC MODELS TO REPRESENT ARCHITECTURAL RELATIONSHIPS OF DEPOSITIONAL SYSTEMS

2.1 Genetic stratigraphy 30
2.2 Sedimentology in genetic stratigraphy 34
2.3 Marine resedimentation models applicable to the Dampier Sub-basin 37

CHAPTER 3: INTERPRETATION
CORE, SEISMIC AND WELL DATA

3.1 Lithofacies 51
3.1.1 Introduction 51
3.1.2 Results 56
Facies A2.1 - stratified gravel
Facies B1.1 - thick/medium-bedded disorganized sands
Facies B2.1 - parallel-stratified sands
Facies B2.2 - cross-stratified sands
Facies C1.1 - poorly sorted muddy sands
Facies C1.2 - mottled muddy sands
Facies C2.1 - thick-bedded sand-mud couplets
Facies C2.3 - thin-bedded sand-mud couplets
Facies D1.1 - structureless silts
Facies D1.3 - mottled silt and mud
Facies E1.1 - structureless muds
Facies E1.3 - mottled muds
Facies F2.2 - brecciated and balled strata

3.1.3 Conclusions 73
3.2 Depositional elements 75
3.2.1 Introduction 75
3.2.2 Results 78
Hemipelagic Basin Fill
Condensed Sections
Contourites or Levees
Distal Low Density Turbidites
Distal or Levee Channels and Crevasse Splays
Depositional Lobe Sheet Sands
Depositional Lobe Massive Sand
Braided Channels and Chutes
Channel Fill
Slope Apron Massive Sand
Slope Apron Braided Channels
Slope Apron Sandy Slides
Slope Apron Slides and Slumps
Slope Apron Drape
Retrograding Upper Slope Apron
Upper Slope Apron
Slope Channels
Aggrading Shelf
Transgressive Shelf Sand
3.2.3 Depositional models 94
3.2.4 Conclusions 98
3.3 Chronostratigraphy 100
3.3.1 Introduction 100
3.3.2 Biostratigraphy 101

3.3.3 Results 105
Top Toolonga Calcilutite horizon
Aptian Disconformity
Valanginian Disconformity
Horizon 'A'
Horizon 'B'
Horizon 'C'
Horizon 'D'
Horizon 'E'
Horizon 'F'
Horizon 'G'
Horizon 'H'
Horizon 'I'
Horizon 'J'
3.3.4 Conclusions 110
3.4 Seismic facies 112
3.4.1 Introduction 112
3.4.2 Results 118
Convergence
Asymptotic downlap
Eliassen Formation
Calypso Formation
Hemipelagic Basin Fill
Depositional Lobe Sheet Sands
Depositional Lobe Massive Sand
Braided Channels and Chutes
Channel Fill
Slope Apron Braided Channels
Slope Apron Sandy Slides
Slope Apron Slides and Slumps
Slope Apron Depositional Sand
Levees and Contourites
Erosional channel features

3.4.3 Conclusions 140

CHAPTER 4: RESULTS AND DISCUSSION

DEPOSITIONAL SYSTEMS, TECTONIC DEVELOPMENT AND GENETIC STRATIGRAPHY

4.1 Depositional systems 148

4.1.1 Introduction 148

4.1.2 Discussion 154

Calypso Formation Unit C1

Eliassen Formation Unit E2

Eliassen Formation Unit E1

Angel Formation Unit A6

Angel Formation Unit A5

Angel Formation Units A3 and A4

Angel Formation Units A1 and A2

Forestier Claystone

Winning Group Units M1 and M2

Late Cretaceous development

4.1.3 Conclusions 177

4.2 Tectonic development and structure with respect to sedimentation 182

4.2.1 Introduction 182

Tectonic history

Sea floor spreading

4.2.2 Discussion 189

Tectonic systems tracts

Pre-rift

Rift initiation

Rift climax

Immediate post-rift

Late post-rift

Passive Margin

Subsidence history

Seismic evidence for structural events

4.2.3 Conclusions 218
4.3 Sequence stratigraphy, depositional surfaces and eustacy 220
4.3.1 Introduction 220
The use of geological time scales and age dating
Comparison of sequence definitions to similar studies
4.3.2 Discussion 228
Early rift climax
Mid to late rift climax
Immediate post-rift
Late post-rift
Passive margin
4.3.3 Conclusions 237

CHAPTER 5: CONCLUSIONS

SUMMARY AND IMPLICATIONS FOR PETROLEUM EXPLORATION IN THE DAMPIER SUB-BASIN

5.1 Summary 239
5.2 Implications of methodology 242
5.3 Implications for petroleum exploration..... 244
5.4 Further work 246
5.5 Comment 247
REFERENCES 248

LIST OF FIGURES

1.1 Location map
1.2 Seismic and well data base map
1.3 Structural framework map of the Westralian Super Basin
1.4 Phanerozoic tectonic setting diagram of the North West Shelf
1.5 Structural units and Sub-basins map of the northern Carnarvon Basin
1.6 Tectonic elements map of the Dampier Sub-basin
1.7 Stratigraphic column of the Dampier Sub-basin
2.1 Sequence stratigraphy 'slug' diagram
2.2 Genetic stratigraphic sequence diagram
2.3 Geometric systems tract diagram
2.4 Modifiers for depositional systems diagram
2.5 Hierarchy of genetic stratigraphic units diagram
2.6 Hierarchy of stratigraphic nomenclatures chart
2.7 Flow types of resedimented deposits classification scheme
2.8 High density turbidity current vertical profile
2.9 Slope failure trigger mechanisms representation
2.10 a) types I, II and III turbidity deposits diagram and b) stages of growth of turbidite systems with respect to sea level diagram
2.11 Lowstand deep-water siliciclastic systems model with limitations
2.12 'Genetic' submarine fan deposition model
2.13 a) active-margin fan model and b) passive-margin fan model
2.14 Point-source gravel-rich submarine fan model
2.15 Linear-source mud/sand-rich slope apron model
2.16 Linear-source sand-rich slope apron model
2.17 Multiple-source mud/sand-rich ramp model
2.18 Multiple-source sand-rich slope apron model
3.1 Core data well location map
3.2 Deep water sediment classification scheme
3.3 Type verticle succession diagram of Facies B2.1
3.4 a) *Cruziana* and b) *Zoophycos* ichnofacies diagrams
3.5 Core photographs:
a) Angel 2 core 1, 2703.2m
b) Wanaea 1 core 1, 2848.4m
c) Montague 1 core 1, 3228.3m
d) Legendre 1 core 16, 2974.5m
e) Talisman 3 core 2, 1971.2m
f) Angel 3 core 2, 2755.3m
g) Wanaea 2 core 4, 2907m
h) Wanaea 2 core 4, 2918.5m
i) Angel 4 core 2, 2722.2m
j) Madeleine 1 core 3, 3186.2m
k) Angel 1 core 3, 3408.9m
3.6 Prograding turbidite systems schematic verticle successions diagram
3.7 Wire line log facies classification scheme
3.8 Type gamma ray wire line log facies of depositional elements diagram (examples 'a' to 'i')

3.9 Type gamma ray wire line log facies of depositional elements diagram (examples 'j' to 's')
3.10 Channel/lobe complex depositional elements diagram
3.11 Gravity driven processes conceptual model
3.12 Slope apron deposits vertical succession diagram
3.13 Detailed chronostratigraphy of the Dampier Sub-basin
3.14 Idealised asymptotic downlap and convergence diagram
3.15 a) legend, and b) seismic facies analysis code system for seismic facies maps
3.16 Seismic example location map and accompanying table
3.17 Seismic example legend
3.18 Line CD88-16 seismic example of convergence
3.19 Line CD88-16 seismic example of asymptotic downlap
3.20 Line CD88-13 seismic example of Eliassen Formation
3.21 Line CD88-66 seismic example of Calypso Formation
3.22 Hemipelagic Basin Fill seismic and gamma ray log example
3.23 Upper Slope Apron seismic and gamma ray log example
3.24 Distal Channels and Sheet Sands seismic and gamma ray log example
3.25 Sheet Sands seismic and gamma ray log example
3.26 Depositional Lobe Massive Sand seismic and gamma ray log example
3.27 Braided Channels and Chutes seismic and gamma ray log example
3.28 Channel Fill seismic and gamma ray log example
3.29 Channel Fill seismic and gamma ray log example
3.30 Channel Fill/Braided Channels seismic and gamma ray log example
3.31 Channel Fill seismic and gamma ray log example
3.32 Slope Apron Braided Channels and Channel Fill seismic and gamma ray log example
3.33 Slope Apron Sandy Slides seismic and gamma ray log example
3.34 Slope Apron Sandy Slides seismic and gamma ray log example
3.35 Slope Apron Sandy Slides seismic and gamma ray log example
3.36 Slope Apron Slumps and Slides seismic and gamma ray log example
3.37 Slope Apron Slumps and Slides seismic and gamma ray log example
3.38 Slope Apron Depositional Sand seismic and gamma ray log example
3.39 Slope Apron Depositional Sand seismic and gamma ray log example
3.40 Slope Apron Depositional Sand seismic and gamma ray log example
3.41 Slope Apron Depositional Sand seismic and gamma ray log example
3.42 Slope Apron Depositional Sand seismic and gamma ray log example
3.43 Slope Apron Depositional Sand seismic and gamma ray log example
3.44 Levee and Crevasse Splays and Channel Fill seismic and gamma ray log example
3.45 Levees or Contourites seismic and gamma ray log example
3.46 Levee Complex seismic and gamma ray log example
3.47 Levees or Contourites seismic and gamma ray log example
3.48 Line CD88-23 stratal configuration diagram and seismic example of Levee Complex
3.49 Line CD88-17 stratal configuration diagram and seismic example of incised channel feature (strike section)
3.50 Line CD88-56 stratal configuration diagram and seismic example of incised channel feature (dip section)
3.51 Line CD88-17 stratal configuration diagram and seismic example of channel cut and fill sequence

3.52 Line CD88-20 stratal configuration diagram and seismic example of seismic lens
3.53 Line CD88-46 stratal configuration diagram and seismic example at Lauchie 1
3.54 Line CD88-52 stratal configuration diagram and seismic example at Lewis 1
3.55 Line CD88-66 stratal configuration diagram and seismic example at Samson 1
3.56 Line 85-2953 stratal configuration diagram and seismic example at Legendre 1
3.57 Line 85-2953 stratal configuration diagram and seismic example at Angel 3
4.1 Textural spectrum of turbidite channels diagram
4.2 Textural spectrum of turbidite lobes diagram
4.3 Legend of schematic palaeogeography
4.4 Location map of stratigraphic log correlation - sections H - H' and I - I'
4.5 Section H - H' stratigraphic log correlation
4.6 Section I - I' stratigraphic log correlation
4.7 Calypso Formation Unit C1 isochron map
4.8 Calypso Formation Horizon 'J' structure/isochron map (depositional structure)
4.9 Eliassen Formation Unit E2 schematic palaeogeography diagram
4.10 Eliassen Formation Unit E2 seismic facies map
4.11 Eliassen Formation Unit E2 isochron map
4.12 Eliassen Formation Horizon 'I' structure/isochron map (depositional structure)
4.13 Eliassen Formation Horizon 'H' top structure map
4.14 Angel Formation Unit A6 schematic palaeogeography diagram
4.15 Location map of stratigraphic log correlation - sections C - C', D - D', E - E', F - F' and G - G'
4.16 Section C - C' stratigraphic log correlation
4.17 Section D - D' stratigraphic log correlation
4.18 Section E - E' stratigraphic log correlation
4.19 Section F - F' stratigraphic log correlation
4.20 Section G - G' stratigraphic log correlation
4.21 Angel Formation Unit A6 seismic facies map
4.22 Angel Formation Unit A6 isochron map
4.23 Angel Formation Horizon 'G' structure/isochron map (depositional structure)
4.24 Angel Formation Horizon 'G' base structure map
4.25 Angel Formation Unit A5 schematic palaeogeography diagram
4.26 Angel Formation Unit A5 seismic facies map
4.27 Angel Formation Unit A5 isochron map
4.28 Angel Formation Unit A3 and 4 schematic palaeogeography diagram
4.29 Angel Formation Unit A3 and 4 seismic facies map
4.30 Angel Formation Unit A3 and 4 isochron map
4.31 Angel Formation Horizon 'C' structure/isochron map (depositional structure)
4.32 Angel Formation Horizon 'C' structure map
4.33 Angel Formation Unit A1 and 2 schematic palaeogeography diagram
4.34 Angel Formation Unit A1 and 2 seismic facies map
4.35 Angel Formation Unit A1 and 2 isochron map
4.36 Angel Formation (top) Horizon 'A' structure map
4.37 Forestier Claystone isochron map

4.38 Valanginian disconformity structure map
4.39 Location map of stratigraphic log correlation - sections A - A'and B - B'
4.40 Section A - A' stratigraphic log correlation
4.41 Section B - B' stratigraphic log correlation
4.42 Winning Group isochron map
4.43 Aptian disconformity structure map
4.44 Campanian to Aptian isochron map
4.45 Top Toolonga structure map
4.46 Lewis Trough structural cross section
4.47 Schematic prograding wedge comparison diagrams of a) fault scarp and b) broad shelf
4.48 Tectonic elements map with seismic line locations
4.49 Structural development of the Dampier Sub-basin evolutionary diagrams
4.50 Gravity profile across the Dampier Sub-basin
4.51 Lister detachment model for extension
4.52 Abyssal plains magnetic anomalies and lineaments map of the North West Shelf
4.53 Mesozoic tectonic systems tracts stratigraphic table of the Dampier Sub-basin
4.54 Idealised vertical succession diagram of rift related tectonic systems tracts
4.55 Seismic stratal patterns of tectonic systems tracts diagram
4.56 Lauchie 1 subsidence curves a) and b)
4.57 Regional structural/stratigraphic seismic interpretation - section A - A'
4.58 Regional structural/stratigraphic seismic interpretation - section B - B'
4.59 Regional structural/stratigraphic seismic interpretation - section C - C'
4.60 Generalised faults and structure of the Lewis Trough schematic diagram
4.61 Line CD88-66 seismic example of collapse graben structure
4.62 Line CD88-40 seismic example low displacement normal faults
4.63 Line CD88-16 small scale seismic example of inversion events
4.64 Line CD88-16 detailed seismic example of inversion events
4.65 Line 84-104 seismic example of Talisman area anticline and 'kinked' reflectors
4.66 Line 85-2953 seismic example at Legendre 1 of fault scarp
4.67 Line 85-2953 flattened seismic example at Legendre 1 of fault scarp
4.68 Stratigraphic table with comparison of sequence stratigraphy studies and eustatic sea level curve
4.69 Stratigraphic table with relative sea level and eustatic sea level
4.70 Idealised genetic stratigraphy and sedimentary architecture 'slug' for the Dampier Sub-basin

LIST OF TABLES

1.1 Project wells list
1.2 Project core data list
1.3 Project seismic data vintages and line kilometres list
1.4 Mapped seismic horizons list
1.5 Project seismic maps list
1.6 Project stratigraphic log correlation cross sections list
2.1 Sedimentological characteristics of deep-water basin margin systems versus grain size and sediment source
2.2 Subsurface and reservoir attributes of deep-water basin margin systems versus grain size and sediment source
3.1 Genetic units versus core data chart
3.2 Core data versus Pickering facies classes chart
3.3 Identified depositional facies list
3.4 Genetic units versus depositional elements chart
3.5 Pickering facies classes versus depositional elements chart
3.6 Defined depositional elements list
3.7 Seismic characteristics and stratal configurations of depositional elements summary chart
4.1 Reworked palynomorphs list of the Angel Formation
4.2 Lauchie 1 horizon information for subsidence analysis
4.3 Various time scales used for sequence stratigraphy on the North West Shelf
4.4 Sequence stratigraphy varying factors summary chart for the Dampier Sub-basin

LIST OF APPENDICES

I Core logs 265

II Core log to electric log annotation diagrams 325

III Thin section descriptions 365

IV Interpreted unit well tops 385

V Subsidence curves 387

a) Lauchie 1 subsidence

b) Legendre 1 subsidence

c) Rosemary 1 subsidence

LIST OF ENCLOSURES

(contained in separate volumes)

I Regional structural/stratigraphic seismic interpretations

a) Montage of tectonic elements and seismic sections A - A', B - B', and C - C' (interpreted - Figures 4.48, 4.57, 4.58, and 4.59)

b) Seismic section A -A' (uninterpreted; location of Figure 4.65)

c) Seismic section B - B' (uninterpreted)

d) Seismic section C - C' (uninterpreted)

II Dampier Sub-basin genetic stratigraphy, lithostratigraphy and palaeogeography legend - Montage (Figures 3.13, 4.3, 4.54, 4.70)

III Structure and depositional systems montages

a) Rift climax - stratigraphy, depositional structure, seismic facies and depositional systems (Figures 4.4, 4.5, 4.6, 4.7, 4.8, 4.9, 4.10, 4.12, 4.13)

b) Immediate post-rift - stratigraphy and depositional structure (Figures 4.15, 4.16, 4.17, 4.18, 4.19, 4.20, 4.23, 4.31, 4.36)

c) Immediate post-rift - seismic facies and depositional systems (Figures 4.14, 4.21, 4.25, 4.26, 4.28, 4.29, 4.33, 4.34)

d) Late post-rift - structure and stratigraphy (Figures 4.37, 4.38, 4.39, 4.40, 4.41, 4.42, 4.43)

IV Uninterpreted seismic sections showing seismic example locations

a) Line CD88-16 (locations of Figures 3.18, 3.19, 4.63, 4.64)

b) Line CD88-13 (location of Figure 3.20)

c) Line CD88-66 (locations of Figures 3.21, 3.55, 4.61)

d) Line CD88-23 (location of Figure 3.48)

e) Line CD88-17 (locations of Figures 3.49, 3.51)

f) Line CD88-56 (location of Figure 3.50)

g) Line CD88-20 (location of Figure 3.52)

h) Line CD88-46 (location of Figure 3.53)

i) Line CD88-52 (location of Figure 3.54)

j) Line 85-2953 (locations of Figures 3.56, 3.57, 4.66, 4.67)

k) Line CD88-40 (location of Figure 4.62)

UNIVERSITY OF ADELAIDE LIBRARY

CHAPTER 1: INTRODUCTION

THE DAMPIER SUB-BASIN

1.1 OBJECTIVES

The objective of this research project was to define the depositional systems and assess the sedimentary architecture in the Aptian to Callovian Age succession of the Dampier Sub-basin, North West Shelf, Australia. In this study, I applied sequence stratigraphic methods and concepts by integrating sedimentology, log sequence analysis and seismic interpretation in an attempt to understand the effect of tectonics, eustacy and sediment source on reservoir development and sedimentation. The ultimate aim was to identify new petroleum stratigraphic trapping mechanisms, whilst assessing present play concepts that have been applied to the area.

The study area (Figure 1.1), covers approximately 6000 km^2 over the northern portion of the Dampier Sub-basin, and centres on the Lewis Trough depocentre.

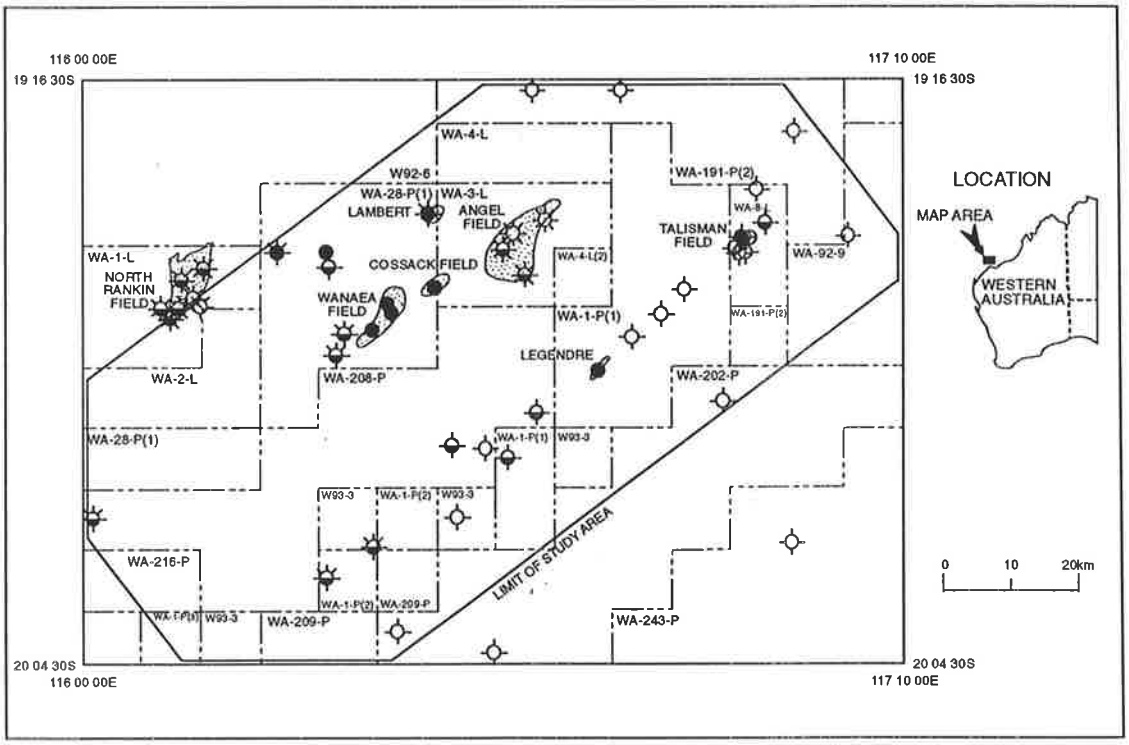


Figure 1.1. Location map of the study area showing wells, oil and gas fields, and petroleum exploration and production permits.

1.2 DATABASE

The well database comprises relevant data from 34 non-proprietary petroleum exploration wells (Table 1.1, Figure 1.2). This well data includes geological and palynological reports and velocity surveys from well completion reports. Wireline log data in digital form of all open file wells in the Barrow and Dampier Sub-basins, obtained from Wiltshire Geological Services, exists on the Sun station hard disk at the NCPGG. This database functions as part of the continuing Barrow Project at the

NCPGG. Software from Mincom, specifically Geolog, were used to plot and manipulate these data.

Well Name	Year	Operator	Permit
Alpha North 1	1989	Marathon	WA-8-L
Angel 1	1972	Woodside	WA-3-L
Angel 2	1972	Woodside	WA-3-L
Angel 3	1973	Woodside	WA-3-L
Angel 4	1990	Woodside	WA-3-L
Aurora 1	1990	Marathon	WA-191-P
Bounty 1	1983	Marathon	WA-191-P
Calypso 1	1985	Marathon	WA-8-L
Cossack 1	1990	Woodside	WA-28-P
Cygnus 1	1989	Arco	WA-202-P
Dampier 1	1969	Woodside	WA-208-P
De Grey 1	1971	Woodside	WA-92-9
Eaglehawk 1	1972	Woodside	WA-28-P
Egret 1	1973	Woodside	WA-28-P
Finucane 1	1978	Woodside	WA-191-P
Forestier 1	1978	Woodside	WA-1-P
Lambert 1	1974	Woodside	WA-28-P
Lauchie 1	1990	Phillips	WA-208-P
Legendre 1	1968	Woodside	WA-1-P
Legendre 2	1970	Woodside	WA-1-P
Lewis 1/1a	1976	Woodside	WA-1-P
Madeleine 1	1969	Woodside	WA-28-P
Montague 1	1985	Esso	WA-28-P
Nelson Rocks 1	1973	Woodside	WA-1-P
Orion 1	1990	Woodside	W93-3
Rosemary 1	1973	Woodside	WA-1-P
Rosemary North 1	1982	Woodside	W93-3
Samson 1	1984	Woodside	WA-208-P
Talisman 1	1984	Marathon	WA-8-L
Talisman 2	1985	Marathon	WA-8-L
Talisman 3	1987	Marathon	WA-8-L
Walcott 1	1979	Woodside	WA-28-P
Wanaea 1	1990	Woodside	WA-28-P
Wanaea 2	1990	Woodside	WA-28-P

Table 1.1. List of the 34 wells used in the study showing the year the well was drilled, the permit number and the permit operator. Refer to the bibliography for full company names.

Palynological data sheets for each of the wells in this study were obtained from Morgan Palaeo Associates. They provided high quality age dating information that was crucial to the sequence analysis. The data sheets are "quick look" interpretations of dinoflagellates, spores and pollen using the palynological zonation scheme of Helby, Morgan, and Partridge (1987). A limited number of detailed interpretations were also used in which placement of data into subzones or 'events' provided a means of high resolution dating. These detailed reports are listed as 'Palynological Reviews' for specific wells in the bibliography.

Most of the wells that occur on the Madeleine Trend (Figures 1.1, 1.6) have a relatively complete Upper Jurassic to Lower Cretaceous succession. Many wells on the Legendre Trend did not intersect Oxfordian age sediments, but revealed important information about unconformities of Callovian, Oxfordian, Berriasian, Valanginian and Aptian ages. Wells drilled down flank from the Legendre Trend, for example Lauchie 1, have a more complete section due to continuous deposition of sediment with little erosion. However, wells located along the margins of the study area, for example on the Rankin Platform and the Enderby Platform, have significant amount of Upper Jurassic section missing and were of little use for detailed sequence analysis.

Cores from 16 of the database wells (Table 1.2) were studied to define lithological facies and facies associations, and to interpret depositional environment. These associations were correlated with well logs and seismic for the interpretation of depositional systems. The interval length of these cores generally vary from a few metres to 18m. The total length of core that was used for this study is 495.5m. Three cores from Angel 4 and two cores from Cossack 1 are continuous 80m and 38m sections, respectively, from near the top of the Angel Sandstone. These two sections of core provided an excellent opportunity to examine the vertical facies variations that occur in this unit, and their correlation with wireline logs and seismic profiles. The Dampier 1, Madeleine 1 and Legendre 1 wells were drilled previous to 1970, and as such, were bound by the guidelines under the 'Petroleum Search Subsidy Act' that was operative between 1958 and 1974 by the Commonwealth Government. As a result of these wells being 'subsidised', they contain a section of core from each of the Mesozoic formations that they penetrated, thereby providing a good lithological summary of Dampier Basin stratigraphy in a relatively continuous sedimentary section. There is, however, limited core available for the defined Oxfordian, Kimmeridgian and Lower Tithonian Age units. Interpretation of these units therefore relied on well logs, palynology and drill cuttings.

Well	#	Depth (M)	Metres
Angel 1	1	2662.1 - 2667.0	4.9
	3	3408.3 - 3411.7	3.4
Angel 2	1	2702.0 - 2707.0	4.1
	3	2746.9 - 2754.0	7.1
Angel 3	1	2604.5 - 2613.4	8.9
	2	2746.6 - 2755.7	9.1
Angel 4	1	2698.0 - 2711.0	13.0
	2	2716.5 - 2744.0	27.5
	3	2744.0 - 2771.0	27.0
	4	2771.0 - 2798.3	27.3
Cossack 1	1	2891.0 - 2909.6	18.6
	2	2909.6 - 2928.7	19.1
Dampier 1	9	2834.6 - 2838.3	3.7
	10	2898.3 - 2905.0	6.7
	11	3063.5 - 3070.9	7.4
	12	3282.4 - 3287.0	4.6
	13	3487.5 - 3492.7	5.2
	14	3710.6 - 3715.2	4.6
	15	3931.0 - 3935.6	4.6
	16	4134.9 - 4140.4	5.5
Lambert 1	1	3104.0 - 3109.6	5.6
Legendre 1	10	1933.7 - 1938.2	4.5
	11	2127.2 - 2128.7	1.5
	12	2354.6 - 2359.6	5.0
	13	2485.6 - 2488.7	3.1
	14	2534.7 - 2538.9	4.2
	16	2974.2 - 2977.8	3.6
	17	3180.0 - 3184.2	4.2
	18	3383.9 - 3386.6	2.7
Legendre 2	1	2080.3 - 2083.2	2.9

Well	#	Depth (M)	Metres
Madeleine 1	1	2900.1 - 2907.8	7.7
	2	2979.1 - 2984.9	5.8
	3	3185.5 - 3191.9	6.4
	4	3404.0 - 3408.6	4.6
	5	3632.6 - 3636.3	3.7
	6	3856.9 - 3867.3	10.4
	7	3942.3 - 3947.8	5.5
	8	4160.0 - 4164.5	4.5
Montague 1	1	3219.5 - 3237.5	18.0
Rosemary 1	1	2794.4 - 2803.6	9.2
	2	2918.2 - 2927.3	9.1
	3	3185.5 - 3193.7	8.2
Talisman 2	3	1994.0 - 2011.3	17.3
	4	2012.0 - 2030.1	18.1
	5	2030.0 - 2048.2	18.2
	6	2055.0 - 2058.7	3.7
Talisman 3	1	1962.0 - 1965.0	3.0
	2	1965.0 - 1973.0	8.0
Wanaea 1	1	2832.0 - 2845.5	13.5
	2	2889.0 - 2904.8	15.8
Wanaea 2	1	2075.0 - 2077.0	2.0
	2	2869.0 - 2886.0	17.0
	3	2886.0 - 2907.0	21.0
	4	2907.0 - 2930.0	23.0

Table 1.2. List of core that was logged for the project. A total of 495.5m is listed.

Table 1.3 lists the seismic database used in this study. Seismic in paper and digital form comprises a total of 2168.9 line kilometres. The majority of the seismic consists of the 'Beluga survey', shot in 1988 by Command Petroleum N.L. over WA-208-P. This seismic provides good data coverage on an approximate 1 x 2 km grid over the Lewis Trough (Figure 1.2) between Dampier 1 and Legendre 1. Further seismic selected from various 1976 - 1988 vintages provide essential infills, well ties, and extensions out of the area. The seismic grid to the north of the Legendre and Angel area is more widely spaced, and is dominantly composed of paper sections only.

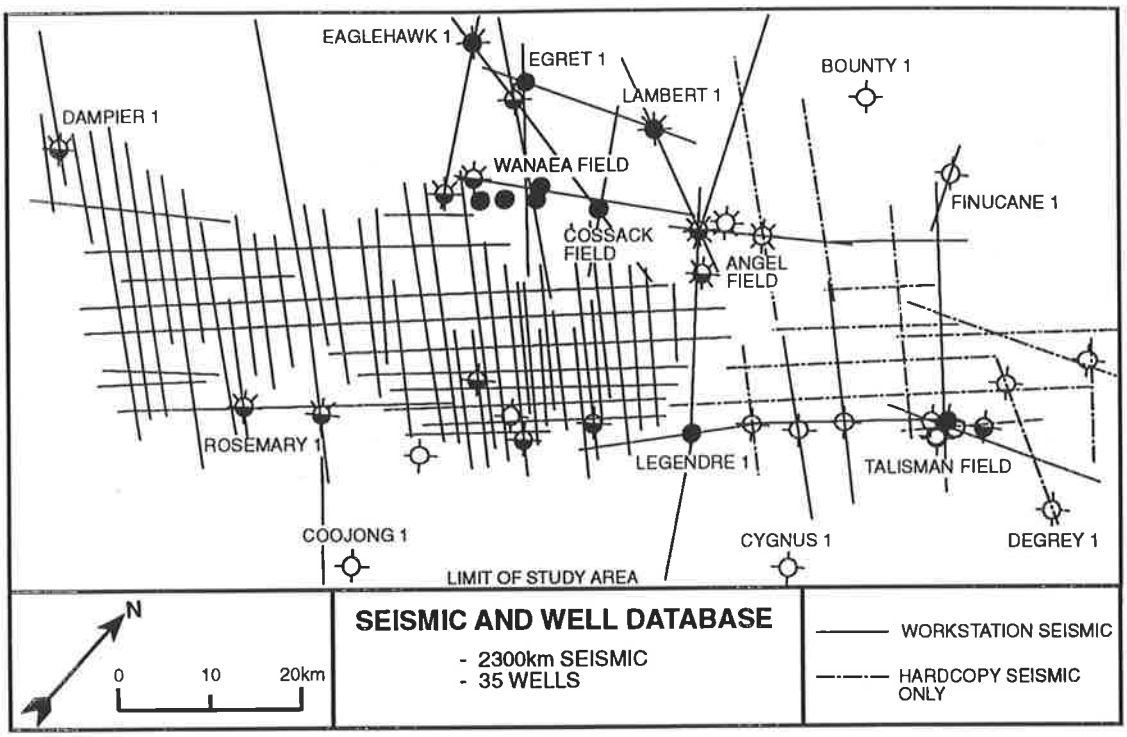


Figure 1.2. Seismic and well database for this study.

Survey	Company	Permit	Year	Prefix	Fold	Traces	Km On Work-Station	Km On Paper Only
	Woodside	WA-28-P	1976	76	48	96	18.4	
	Woodside	WA-28-P	1977	77	48	96	32	
	Hudson's Bay	WA-58-P	1980	HL80	36	96	16	
North-East Kendrew	Woodside	WA-28-P	1981	81B2	48	96	27.4	
Marathon - Angel	Marathon	WA-191-P	1982	82MPA	48	96	103.5	30
Boronia	Marathon	WA-191-P	1983	83MPB	60	240		78
Mawby - East Angel	Woodside	WA-1-P	1984	84	60	240	93.2	94.5
Dampier Basin Scientific Survey	Non-Exclusive		1985	85DBX	60	240	35	
Kendrew - Dixon	Woodside	WA-28-P	1985	85	60	240	142.5	
	Marathon	WA-191-P	1986	86MPE	60	240		19
Eaglehawk	Woodside	WA-28-P	1986	86A	60	240	162.8	61.6
Firetail	Marathon	WA-191-P	1988	88MPF	75	300		15
Beluga	Command	WA-208-P	1988	CD88	100	300	1240	
Total Seismic	**2168.9 km**					**Totals**	**1870.8 km**	**298.1 km**

Table 1.3. Listing of seismic vintages and the line kilometres of paper and workstation seismic data.

The quality of the seismic ranges from fair to excellent, and varies with the area covered and seismic vintage. The 'Beluga survey' is generally of excellent quality, which made high resolution definition of seismic units possible on the Legendre Trend and Lewis Trough areas southwest of Legendre 1. Generally, seismic quality diminishes gradually north of the Legendre area towards the Talisman area in the Lewis Trough. In general, data quality over the length of the Madeleine Trend is fair, a downfall to the good core and well control over this area. Data quality over the Kendrew Trough area varies from fair in the southwest, to good in the northeast, near Lambert 1 and Montague 1. The seismic coverage over this area is, however, the main factor that constricts the interpretation.

Seismic quality has historically been a problem over the North West Shelf, owing primarily to the velocity inversion and intrabed and water bottom multiples caused by the thick overlying Tertiary Carbonate wedge (Ramsden et al., 1988). For instance, over this area, the Eaglehawk survey suffered severely from water bottom multiples due to the large energy source of 4075 cu in used in an effort to penetrate the carbonates. In addition, the velocities of the multiples are near the stacking velocities of the Upper Jurassic section, which makes attempts to attenuate multiples without attenuating data difficult. This problem is compounded by large lateral velocity variations due to faulting and facies changes within the carbonates. These factors have also made the application of statics problematic.

The digital seismic data used in this study were loaded on the Sun work station at the NCPGG and interpreted using the 'SIERRA 2DI' software package. It proved to be advantageous over paper seismic interpretation, thereby allowing for better and easier high resolution mapping of seismic units.

1.3 METHODS

Core Logging

Approximately 500m of core from 16 wells were examined during the course of study. Core logs at 1:50 and 1:100 representing this core are found in Appendix I. The core was logged with an emphasis on lithology, grainsize and sorting (determined by hand lens), sedimentary structures, trace fossils, and large scale diagenetic features. These features helped to identify sedimentary processes such as energy regime, rate of deposition, and degree of reworking to characterise the environment of deposition and water depth on individual depositional elements. Each core was annotated to the complete suite of electric logs at 1:100 or 1:200 scale (Appendix II) to calibrate and determine the lithological cause of log response. Together with the core logs, these were an aid in placing the established wire line log facies into respective depositional elements.

Core sampling was conducted and a limited number of thin sections were cut. These were examined for general petrology and to establish general diagenetic trends. Thin section descriptions are contained in Appendix III.

Seismic Interpretation

A synthetic seismogram was generated for each of the wells in the study area using either the Crocker Petrophysical Software or the SIERRA Sierraseis software packages. Stratigraphic information from the wells, such as sequence boundary horizons, defined by stratigraphic well log correlations could then be tied to the seismic.

Seismic horizons (Table 1.4) were correlated throughout the grid using the SIERRA 2DI interactive seismic interpretation workstation. During this exercise, the well log correlations were continuously updated according to the seismic interpretation. Also, seismic horizon correlations were verified against well log correlations. In effect, the seismic horizon correlation was an interactive interpretive exercise with the stratigraphic well log correlation, each complementing the other in their accuracy.

	Seismic Horizon	**Palynological Zone**
1.	Top Toolonga Calcilutite	None
2.	Aptian Disconformity	Middle *O. operculata*
3.	Valanginian Disconformity	Top *B. reticulatum*
4.	Top Angel Formation	Middle *K. wisemaniae*
5.	Angel Fm Horizon C	Middle *D. jurassicum* 'bii'
6.	Angel Fm Horizon E	Middle *O. montgomeryi* 'd'
7.	Angel Fm Horizon F	Top *D. swanense*
8.	Angel Fm Horizon G	Base *W. clathrata*
9.	Top Eliassen Member	Middle *W. spectabilis* 'c'
10.	Base Eliassen Member	Middle *W. spectabilis* 'a'
11.	Callovian Flooding Event	Middle *W. digitata* 'b'

Table 1.4. List of seismic horizons correlated over the seismic grid with their palynological zones and subzones indicated.

Various two way time thickness (isochron) and two way time structure maps were produced (Table 1.5). These maps, including seismic facies analysis maps are all included within section 4.1 as detachable figures. Many of them are also included on various montages that are contained in Enclosures IIIa to IIId. For each map, time values were posted over the seismic grid and plotted on hardcopy. Contour maps were then hand drawn and drafted.

Unit or Horizon	TWT Structure Map	TWT Isochron Map	TWT Isochron/ Structure Map	Seismic Facies Analysis Map
Top Toolonga Calcilutite	4.45			
Aptian Disconformity	4.43			
Aptian to Valanginian Disconformity		4.42		
Valanginian Disconformity	4.38			
Forestier Claystone		4.37		
Top Angel Formation (Horizon 'A')	4.36			
Angel Fm Units A_1 and A_2		4.35		4.34
Angel Fm Horizon 'C'	4.32		4.31	
Angel Fm Units A_3 and A_4		4.30		4.29
Angel Fm Unit A_5		4.27		4.26
Angel Fm Unit A_6		4.22		4.21
Base Angel Fm (Horizon 'G')	4.24		4.23	
Eliassen Fm Horizon 'H'	4.13			
Eliassen Fm Unit E2		4.11		4.10
Base Eliassen Formation (Horizon 'I')			4.12	
Calypso Formation Unit C1		4.7		
Calypso Formation Horizon 'I'			4.8	

Table 1.5. List of two way time structure, two way time isochron and seismic facies analysis maps created for the seismic units and horizons. The two way time isochron/structure maps are isochron maps from the Valanginian Disconformity to the horizon listed, and include fault cuts to the lower horizon. Each map is indicated by the figure number.

Seismic units with significant sand development were the focus of detailed seismic facies analysis. There are five constructed seismic facies analysis maps, each containing mapped seismic facies, selected gamma ray motifs, dipmeter rosettes (where available), and 100 millisecond interval isochron contours.

The lateral extent and three dimensional geometry of sandstone intervals were inferred using seismic facies analysis maps along with isochron maps and two way time structure maps. These maps were also useful in determining palaeogeography and depositional structure, factors which play an important role in controlling the shape and extent of sand bodies.

Stratigraphic Well Log Correlations

The study includes eight stratigraphic well log correlations constructed over three chronostratigraphic levels (Table 1.6). These cross sections were designed to cross the study area in strike and dip directions, while choosing wells that best represent the interval in a specific area. They are also included in section 4.1 as detachable figures and on the montages contained in Enclosures IIIa to IIId.

	Aptian - Valanginian Interval (Valanginian datum)
Section A - A' (Figure 4.40)	Rosemary 1 - Rosemary North - Orion 1 - Legendre 1 - Angel 3 - Finucane 1
Section B - B' (Figure 4.41)	Cygnus 1 - Talisman 2 - Alpha North 1 - Angel 2 - Walcott 1 - Montague 1
	Valanginian - Oxfordian Interval (Valanginian datum)
Section C - C' (Figure 4.16)	Rosemary 1 - Lewis 1 - Legendre 1 - Forestier 1
Section D - D' (Figure 4.17)	Dampier 1 - Madeleine 1 - Wanaea 1 - Angel 3 - Calypso 1
Section E - E' (Figure 4.18)	Egret 1 - Montague 1 - Walcott 1 - Lauchie 1 - Samson 1
Section F - F' (Figure 4.19)	Lambert 1 - Angel 1 - Angel 3 - Legendre 1
Section G - G' (Figure 4.20)	Finucane 1 - Calypso 1 - Talisman 2
	Oxfordian - Callovian Interval (Oxfordian datum)
Section H - H' (Figure 4.5)	Rosemary 1 - Lewis 1 - Angel 3 - Calypso 1
Section I - I' (Figure 4.6)	Montague 1 - Madeleine 1 - Lauchie 1 - Legendre 1

Table 1.6. List of stratigraphic cross sections used in the study.

The Aptian to Valanginian interval is represented by two regional sections with the Valanginian Disconformity as a datum. This disconformity is also used as the datum for five regional cross sections produced for the Valanginian to Oxfordian interval. The Oxfordian to Callovian interval is represented by two cross sections, and the base of the Eliassen Member horizon is the datum.

Regional well log correlations show the gamma ray (GR), sonic (DT), and density (RHOB) electric log profiles at a vertical scale of 1:2500. These wire line logs were chosen to infer lithological and seismic acoustical information from well to well. Palynological zones are annotated with each well to provide important age dating information. In addition, locations of available core intervals were also annotated on these sections. These cross sections show major facies changes between wells and also time equivalent horizons that divide the section into genetically related sequences. These time equivalent horizons, defined by the wireline logs, correspond with mapped seismic reflections.

As an initial part of the study, individual well sequence summary sheets were constructed at 1:2000 scale. They contain gamma ray and sonic logs, and have annotated lithologies, palynology, core and side wall core points as well as proposed sequence boundaries and systems tracts. These are not included in this thesis, but were used for the interpretation process. In addition to providing stratigraphic summaries to individual wells, the summary sheets were used to help establish wireline log facies in order to infer depositional elements of the various sections.

1.4 REGIONAL GEOLOGY

1.4.1 Regional Framework

The continental shelf of northwestern Australia, better known as the North West Shelf region, is underlain by four sedimentary basins comprising the Northern Carnarvon, the Offshore Canning, the Browse and the Bonaparte basins from south to north respectively. These basins, some consisting of several sub-basins, make up the northern part of the Westralian Super Basin, a thick, contiguous Permian and Mesozoic fill along the western Margin of Australia (Bradshaw et al., 1988). The Westralian Super Basin is a 4000 km long Permian to Cretaceous basin that continues south of the Carnarvon Basin to include the Perth Basin along the western margin of Australia (Veevers, 1988). The Perth Basin is contemporaneous with the North West Shelf, but had its origin not as a rim basin, but as a "failed arm" basin. This failed arm extended from a triple junction located northwest of Cape Range, at a change in trend of the continental margin (Veevers, 1988). The structural Framework of the Westralian Super Basin is shown in Figure 1.3.

The basins of the North West Shelf are the northeast part of overlapping rim basins that extended along the Indian continent's northern margin during the break up of Gondwanaland. These basins initially formed in response to break up of the continent sliver by sliver due to the southeastward advance of sea floor spreading ridges (stages I - III) in the northwest, and finally, to the drifting away of India (stage IV) off the western margin of Australia (Veevers, 1988; see Figure 1.4).

The Dampier Sub-basin is located in the northern most part of the Carnarvon Basin (Figure 1.5). It borders the Barrow Sub-basin in the southeast and the Beagle Sub-basin (of the Canning Basin) in the northeast. The Rankin Platform forms the northeast margin of the basin, and the Lambert shelf (a tectonic shelf) lies to the southeast of the basin. The basin is arbitrarily separated from the Barrow Sub-basin to the south by the Mermaid Nose. Broad structural and stratigraphic similarities exist between the Barrow and Dampier Sub-basins and they are often referred to as

one geological entity in the literature (ie. the Barrow-Dampier Sub-basin). The most obvious difference is the change in structural orientation, where the Barrow area trends north-northeast and the Dampier area trends to the North-East. The Cossigny Fault defines the northerly limit of the Dampier Sub-basin and separates it from the Beagle Sub-basin, the northerly limit of the Carnarvon Basin (Forrest & Horstman, 1986).

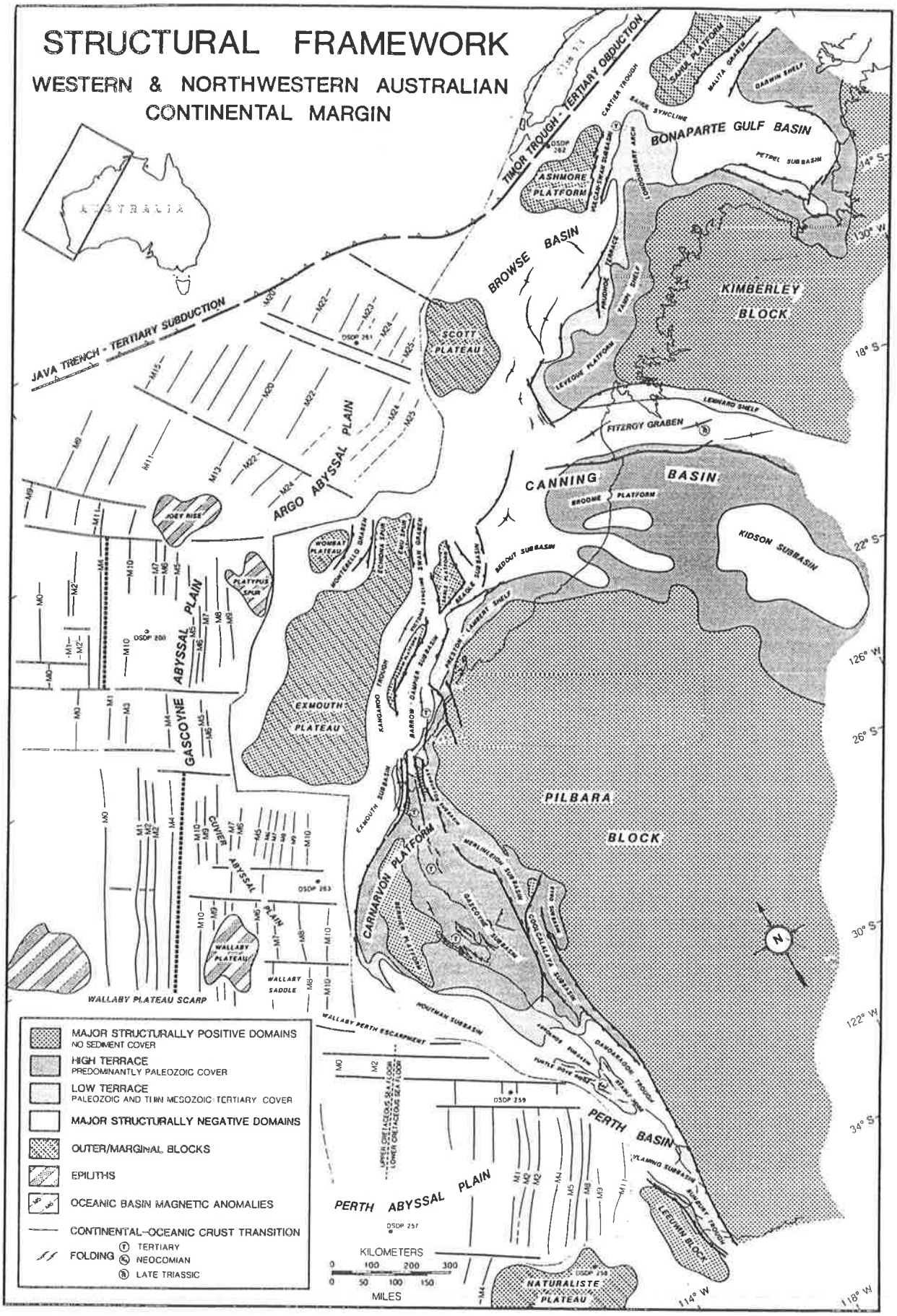


Figure 1.3. Structural framework of the Westralian Super Basin and the Western Australian Continental Margin (after Boote & Kirk, 1989).

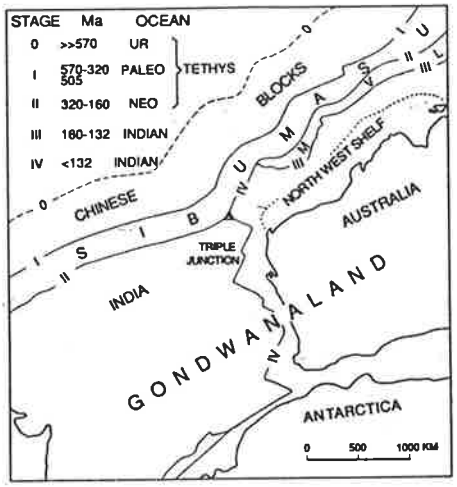


Figure 1.4. Phanerozoic tectonic setting of the North West Shelf (after Veevers, 1988).

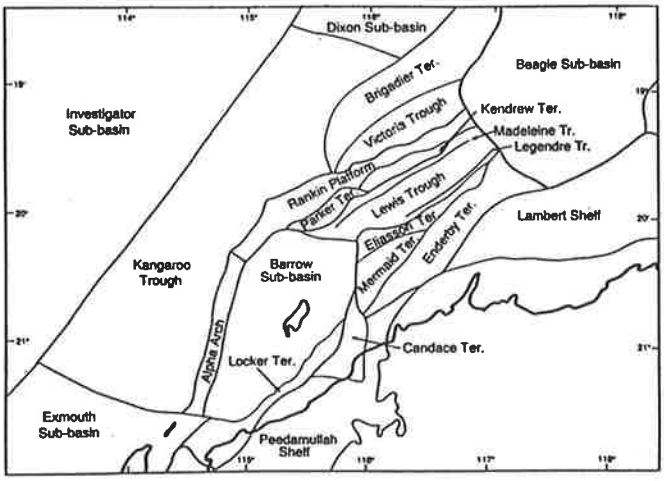


Figure 1.5. Structural units and Sub-basins of the northern Carnarvon Basin. The Dampier Sub-basin includes the structural units that are highlighted. Ter: terrace; Tr: trend; SB: sub-basin; Pl: platform (after Hocking, 1992).

1.4.2 Structural Framework

The tectonic elements of the Dampier Sub-basin are shown in Figure 1.6. The present day morphological structure consists of two linear synclines, namely the Lewis Trough and Kendrew Trough. These are separated by the Madeleine Trend, an intra-basinal anticline. The Legendre trend is another anticlinal trend that occurs on the south eastern flank of the Lewis Trough. The history of tectonic development is discussed in detail in Section 4.2.

Hocking (1993) provided a concise description of the structural elements of the Dampier Sub-basin. The following is a brief morphological description of the individual tectonic elements that comprise the Dampier Sub-basin.

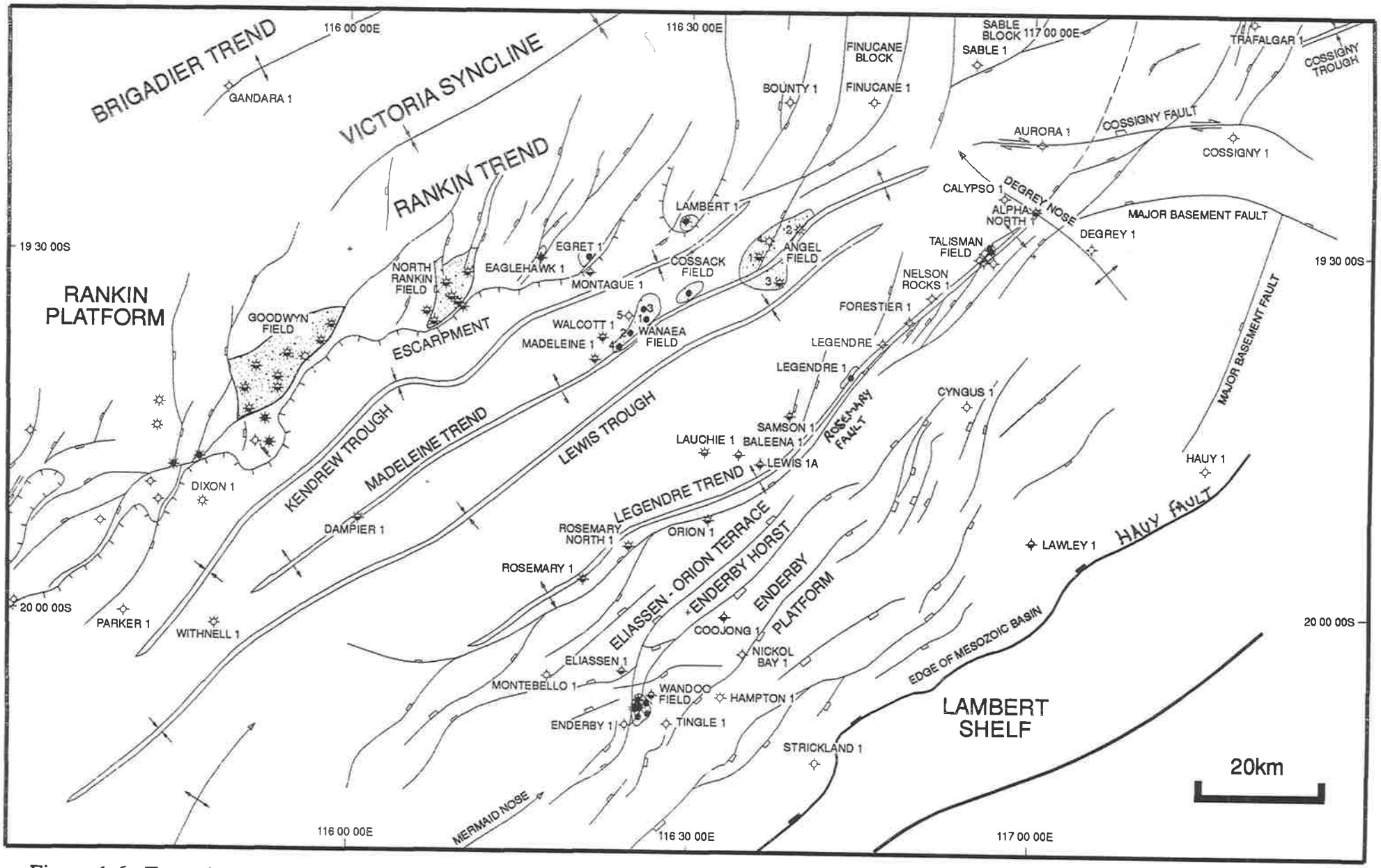


Figure 1.6. Tectonic elements map of the Dampier Sub-basin (modified after Woodside, 1988; Delfos and Boardman, 1994).

The Lewis Trough is a southwest plunging asymmetric syncline that comprises the main basin depocentre. It is relatively unfaulted. However, on the southwest flank near the Legendre Trend, north to south normal faults with minor throw occur. The Lewis Trough represents continuous deposition throughout the Mesozoic (Barber, 1994; Kopsen & McGann, 1985) and contains in excess of 13 km of sedimentary fill (Hill, 1994).

The Legendre Trend is a northeast trending anticline that formed due to various compressional events from as early as Late Jurassic to the Tertiary. This compressional component coincides with rollover associated to listric growth of the Rosemary Fault during the Callovian.

The Rosemary Fault System consists of one main fault (the Rosemary Fault) next to the Legendre Trend and includes northeast trending faults that splay off the main fault. These are normal faults that throw to the northwest. The Rosemary Fault system separates the Lewis Trough from the Eliassen-Orion Terrace.

The Eliassen-Orion Terrace borders the Rosemary Fault and to the southeast, the Eliassen Fault. This terrace formed as a result of half-graben development associated with syntectonic movement of the Eliassen Fault (Barber, 1994). It narrows to the northeast and disappears northwest of Orion 1 as the Eliassen and Rosemary Faults merge.

The Enderby Platform occurs southeast of the Eliassen Fault and is a submerged offshore portion of the stable Pilbara Craton. It features a series of northeast trending, southeast dipping listric growth faults. These faults were active from the Permian to the Middle Jurassic, with the main growth taking place in the Early Triassic (Veenstra, 1985).

The northeastern edge of the Lambert Shelf, defined by the Hauy Fault, marks the southeastern limit of the Dampier Sub-basin. This is an offshore area of shallow basement (Pilbara Craton) onto which Upper Cretaceous sediments and Tertiary carbonates onlap.

Parallel to the Lewis Trough to the northwest is the Madeleine Trend, a narrow southwest plunging anticlinal trend. This anticline is partially a result of sediments onlapping and draping the edge of a half graben. It is suggested that it is also related to inversion or reactivation of major basin forming fault terraces during the Cretaceous (Stagg and Colwell, 1994).

The Kendrew Trough is the subsequent synclinal trend adjacent to the Madeleine Trend. This syncline is partially the result of sediments onlapping this half graben that developed beside the Rankin Platform. Unlike the Lewis Trough, it is more shallow, and wells and seismic indicate that the Middle to Lower Jurassic synrift section is missing, owing to either non-deposition or erosion.

The Rankin Trend occurs along the northwestern edge of the Dampier Sub-basin and forms the southeastern margin of the Exmouth Plateau. This trend is a series of north to northeast trending *en echelon* tilted fault blocks of Triassic to Middle Jurassic strata. This platform consists of Triassic Mungaroo Formation sediments that is

overlain by a condensed shale section. The first appearance of this shale section varies laterally from Neocomian to Aptian in age.

The southeastern edge of the Rankin Trend is a fault trend which forms a palaeoescarpment onto which Upper Jurassic and younger sediments of the Dampier Sub-basin onlap (Veenstra, 1985). This escarpment surface is part of the main unconformity which separates the rift sequence from the drift sequence in the Northern Carnarvon Basin.

The Cossigny Fault defines the boundary between the Lewis Trough and the Cossigny Trough of the Beagle Sub-basin. This fault is a deep seated normal east-west oriented fault, probably originating in the Palaeozoic as a result of north - south extension. Lemon and Mahmood (1994) demonstrated that this fault probably acted as a side ramp of oblique extension that resulted in the development of the near parallel Cossigny Trough during the Lower to Middle Jurassic.

The De Grey Nose was a structural high during the Mesozoic. Middle to Lower Jurassic deltas associated with this high indicate that it was a major controlling factor in deposition of fluvial systems (Hocking et al., 1987). De Grey 1 was drilled on this high. It penetrated Berriasian to Barremian age nearshore marine sandstones that unconformably overlie a Lower to Middle Jurassic nearshore marine deltaic section.

1.4.3 Lithostratigraphy

Hocking (1992) summarised the lithostratigraphic terminology of the Barrow and Dampier Sub-basins. He provided a good regional framework for more detailed studies. The nomenclature used on the North West Shelf is generally functional and informal. The following is a brief introduction to the lithostratigraphic nomenclature as it applies to this study. Local and regional stratigraphic sections are shown in Figures 1.7, 3.13, and 4.54.

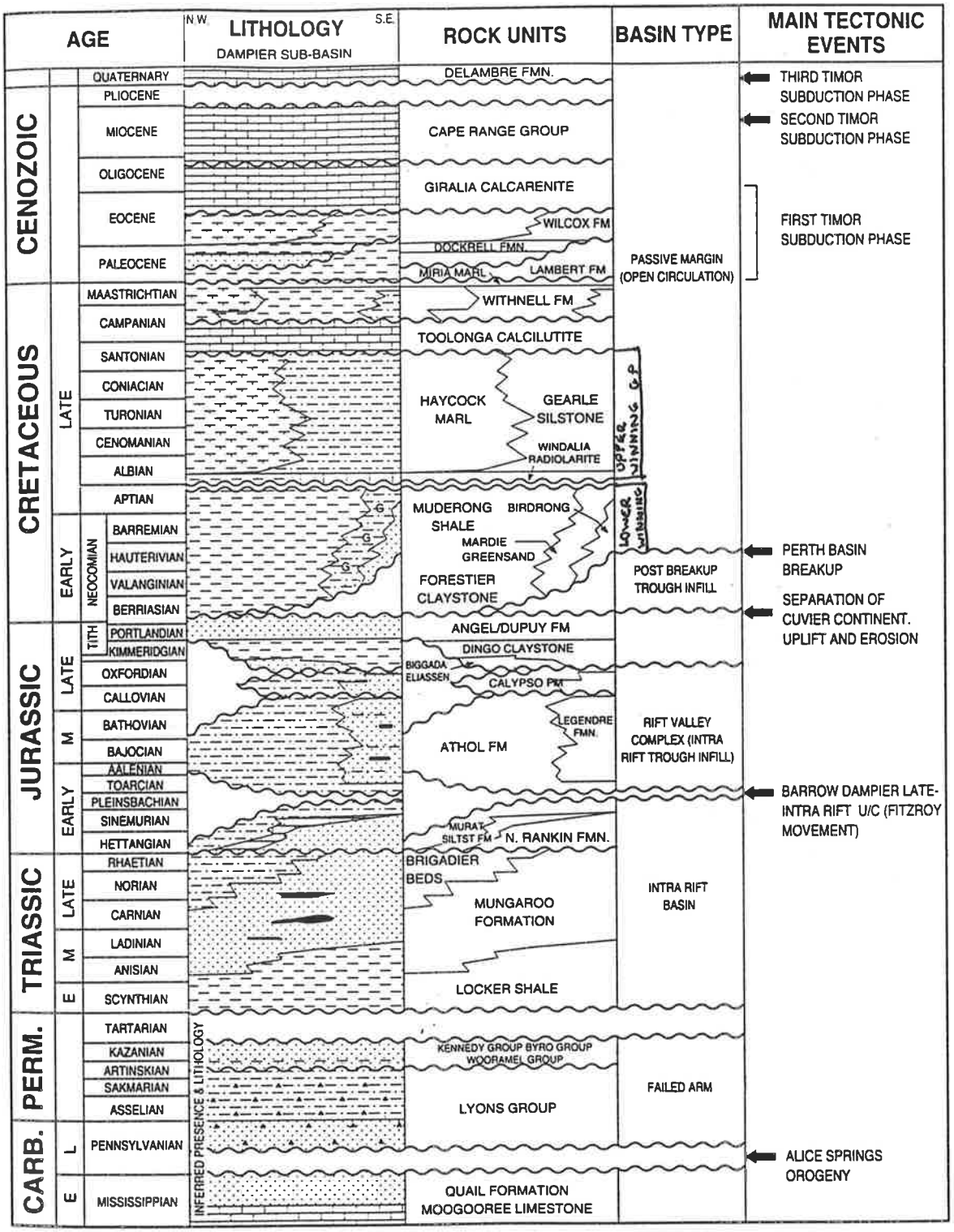


Figure 1.7. Stratigraphy of the Dampier Sub-basin (modified after Barber, 1988, 1994; Woodside, 1988; Hocking, 1992).

Athol Formation

The Athol Formation was named by Hocking in 1988 and replaces the informally used "middle Dingo Claystone" (Kopsen and McGann, 1985). This formation is represented by the fine-grained sequence between the "breakup unconformity" and the "rift onset unconformity", as suggested by Hocking, 1992. It is time equivalent to the coarser, near shore to deltaic sediments of the Legendre Formation. The Athol Formation ranges in age from the top of *W. indotata* to the top of *C. turbatus* (Hocking, 1992).

Legendre Formation

Hocking (1985) defined the Legendre Formation and it was subsequently described by Hocking (1992) and Hocking et al. (1987). It was deposited as a line source or a multiple point source depositional system, and contains sections of coarsening-upwards deltaic cycles, mouth bar and beach ridge sands, crevasse splays and includes thin coal splits (Hocking, 1992).

The Legendre Formation ranges in age from the top of *W. indotata* to the middle of *C. turbatus* palynozones (Hocking, 1992). It extends over the entire study area and is intersected at depth by Rosemary 1, Samson 1, Legendre 1 and 2 , Talisman 1 and Angel 2 wells near or at total depth.

Calypso Formation

The Calypso Formation comprises fine-grained rocks deposited between the onset and the completion of the Callovian - Oxfordian rifting episode (Hocking, 1992). It contains dominant siltstone and fine sandstone and limited claystone. The entire section averages approximately 700m in thickness and occurs in Legendre 1 and 2, Rosemary 1, Lewis 1, Samson 1 and Calypso 1. Hocking (1992) interpreted these sediments to have been deposited in a low energy and restricted offshore marine setting that was partly a deep marine trough but included areas below wavebase on marine shelves along the basin margins.

The age range of the Calypso Formation extends from near the base of *W. spectabilis* to the base of *W. digitata* palynozones.

Eliassen Formation

The Eliassen Formation is the formal name of the former "Biggada equivalent", referring to the same section in the Barrow Sub-basin (Hocking, 1992). It is a blocky mass flow deposit and is intersected by most wells along the Legendre Trend. The Biggada Formation of the Barrow Sub-basin has a more ragged gamma-ray character, consists of finer grained sand and is separated by considerable intercalations of siltstone (Hocking, 1992).

The sand distribution of this formation, defined by seismic profiles, is discussed in detail in this study. Hocking (1992) considered it to be a section of coalesced submarine fan sands which were deposited in response to movement of the Rosemary

and Eliassen Faults. In this study, it is also considered to be dominated by slope-apron wedges (see section 4.1).

The Eliassen Formation covers a relatively short time interval, spanning from the base of *W. spectabilis* 'b' palynological sub-zone to near the base of *W. Clathrata* zone.

Dingo Claystone

The Dingo Claystone was redefined by Cockbain and Hocking (1989) to exclude Middle and Upper Jurassic claystones such as the Calypso and Athol Formations. This formation represents the distal claystone time equivalent of the Angel and Eliassen Formations. It is an open-marine, low-energy claystone that developed in the trough area of the Dampier Sub-basin (Hocking, 1992). This formation is considered in detail in this study.

The time span of the Dingo Claystone ranges from *K. wisemaniae* to near the base of the *W. spectabilis* palynozone.

Angel Formation

The Angel Formation was first proposed by Hocking (1985). It referred to the Upper Jurassic sand-dominated sequence that consists of massive sandstones with thin shale splits in the eastern Dampier Sub-basin. The formation was formally grouped by Kaye et al. (1972) with the Dupuy Sand Member. Hocking (1985) proposed that the Dupuy Sand Member should be restricted to the Barrow Sub-Basin.

The Angel Formation extends over most of the Dampier Sub-basin and this study describes the sand distribution in detail. Hocking (1992) noted that the section south of Madeleine 1 at Dampier 1 and Withnell 1 shows more resemblance to the Dupuy Sand Member. He also interpreted the Angel Formation as a sand-dominated, multiple feeder, coalesced submarine fan sequence with two separate provenance directions corresponding to the Angel Field area and the Legendre Trend.

Hocking (1992) state that the age range of the Angel Formation is from above the top of *P. iehiense* to the base of *D. swanense* palynozones. This thesis places the age range from the middle of *K. wisemaniae* to near the base of *W. clathrata* palynozones.

Forestier Claystone

Thompson et al. (1990) defined the Forestier Claystone as a claystone-dominated sequence of Lower Neocomian age in the northern Barrow and Dampier Sub-basins. This section was previously unnamed or considered as part of the Dingo Claystone. It consists of basinal shales which were deposited prior to and during deposition of the Barrow Group (Thompson et al., 1990). In this study area the formation contains the Talisman Sandstone Member.

The Forestier Claystone disconformably overlies the Angel Formation in the study area and varies from 50 to 100m thick along the Legendre Trend to nearly 300m over the depocentre at Madeleine 1.

The age range of the Forestier Claystone ranges from lower *E. torynum* to *P. iehiense* palynozones (Thompson et al., 1990).

Talisman Sandstone Member

The Talisman Member of the Forestier Claystone is a Berriasian succession of medium to coarse and fine-grained sandstone, siltstone and shale (Thompson et al., 1990) which occurs in the northeastern portion of the study area. It is of probable shelf origin, and varies from a thin transgressive sand 5 to 20 m thick in some wells (Calypso 1, Forestier 1, Nelson Rocks 1, Lewis 1, Samson 1), to a more massive blocky unit in other wells where it is up to 80m thick (Alpha North 1, Legendre 1, Legendre 2, Talisman 1, Talisman 2).

The age of the Talisman Member ranges from *B. reticulatum* to *K. wisemaniae* palynozones (this study).

Lower Winning Group

The informally known lower Winning Group is a super-cycle that was deposited from Aptian to middle Valanginian time (121 - 138Ma, this study). It is composed of various facies that are appropriately arranged to represent a classical transgression. These facies include, from distal to proximal, the Muderong Shale, Mardie Greensand, Birdrong Sandstone, Nanutarra Formation and the Yarraloola Conglomerate, respectively. Although it is tenuous as to whether they should be considered formations or members, these respective facies have distinct characteristics. A comprehensive description of these lithofacies is provided by Hocking et al. (1988). In addition, Parry and Smith (1988), provided generalised definitions of the Winning Group stratigraphy with respect to the Barrow and Exmouth Sub-basins.

Muderong Shale

The Muderong Shale is the distal facies of the Winning Group. It is composed of an argillaceous siltstone with lesser shale, fine-grained sandstone and greensand (Hocking 1987, 1990; Wiseman, 1979). This shale forms the regional seal for the majority of producing reservoirs of Cretaceous age.

Over the project area, the thickness of the Muderong Shale ranges from nearly 600m in the vicinity of Rosemary 1, to less than 70m in the northwest near Finucane 1, where it represents an aggradational wedge to a sediment starved section, respectively.

The age range of the Muderong Shale spans the complete Winning Group interval, which is from middle *O. operculata* to near top *B. reticulatum* (121 - 138Ma, this study).

Mardie Greensand

The Mardie Greensand Member is contained within the Muderong Shale and its facies are transitional with the Birdrong Sandstone. The Mardie Greensand commonly overlies and/or occurs laterally to the Birdrong Sandstone (Hocking, 1988). It is grossly correlative to other glauconitic units on the North West Shelf, and globally to sands such as the Kuparak Formation on the North Slope of Alaska.

The Mardie Greensand is a sandstone that commonly contains more than 30% glauconite. Other components include quartz sand (5 - 85%), mud, silt and secondary cements such as carbonate and pyrite. It was deposited and evolved on a shallow, moderate to low-energy marine shelf, with most of the glauconite forming *in situ* (Hocking, 1990).

The Mardie Greensand can be observed within the project area in wells over and to the northeast of the Talisman Field. It varies in thickness from 5 to 20m. The age of the Mardie Greensand is restricted to the *S. tabulata* palynozone over the project area.

Birdrong Sandstone

The Birdrong Sandstone is a diachronous, basal transgressive lag of the Muderong Shale that was deposited in a littoral to sub-littoral environment. It is a relatively clean, locally glauconitic sandstone which contains minor siltstone or conglomerate (Thompson et al., 1990). A minor fluvial component in channels has been noted in some areas at the base of the unit by Hocking (1987, 1988). This base is commonly an angular unconformity that typically overlies Callovian to early Triassic sediments towards the basin margin. Over the project area, the Birdrong Sandstone is noted in wells over the Enderby Platform (e.g. Nickol Bay 1, Cygnus 1). It also occurs over the Talisman region and in some wells north of this area. It is as 90m at Cygnus 1, and is expected to have varying degrees of development over the Enderby Platform.

The relationship of the transgressive nature of formations in the Winning Group has been discussed in a sequence stratigraphic framework over the Barrow Sub-basin by Arditto (1993). Although limited data with respect to the Birdrong Sandstone was observed in this project, the maximum age range for the Birdrong Sandstone is considered to extend from middle *M. australis* subzone 'a' to *E. torynum* palynozone.

Upper Winning Group

The upper Winning Group is informally grouped into the Windalia Radiolarite, Gearle Siltstone, Alinga Formation and the Haycock Marl. The most comprehensive description of these formations with respect to the North West Shelf is provided by Apthorpe (1979).

Windalia Radiolarite

The Windalia Radiolarite was described by Hocking (1990) as a "varicoloured radiolarian siltstone and calcilutite; minor argillaceous sandstone, chert and calcareous claystone to marl". It is attributed to a major global rise in sea level with subsequent onset of open marine circulation across the North West Shelf. The Windalia Radiolarite and time equivalent Gearle Siltstone are unique for their high dissolved silica content. This silica content has been attributed by some authors to possible contemporaneous submarine volcanism or deep tropical weathering of nearby continental areas. It also was deposited under conditions of very low terrigenous input (Hocking, 1988).

Sandstone lithofacies occur adjacent to and southeast of Rosemary 1 and Rosemary North 1 areas. The thickness of the Windalia Radiolarite is typically 5 to 20m. Its facies are transitional with the Gearle Siltstone and the Haycock Marl. The base of the Windalia Radiolarite is a regionally correlatable event on both seismic and electric well logs and occurs within the middle of the *O. operculata* palynozone. The youngest extent of the Windalia Radiolarite is uncertain, but possibly occurs near the *D. davidii* palynozone.

Gearle Siltstone / Haycock Marl

The Gearle Siltstone is a dark grey to black argillaceous siltstone, silty claystone and radiolarian siltstone (Hocking, 1990). The depositional setting is low energy and shallow marine with restricted circulation (Hocking, 1990). It is the proximal time equivalent to the Haycock Marl.

The Haycock Marl was first described by Heath and Apthorpe (1984). It is a grey to greenish-grey argillaceous marl and calcilutite. The depositional setting ranges from open marine, outer shelf to slope (Hocking, 1990).

Over the project area, the facies transition from the proximal Gearle Siltstone to the distally associated Haycock Marl occurs approximately in the middle of the Lewis Trough.

The age range for the Haycock Marl and Gearle Siltstone is from middle Santonian (approx. 85Ma) to middle Aptian (121Ma).

Toolonga Calcilutite

The Toolonga Calcilutite is disconformable with the underlying Gearle Siltstone and conformable with the Haycock Marl, possibly as a result of marine transgression. It is a fossiliferous pale calcilutite and calcisiltite (Hocking, 1990). This calcilutite is a regionally correlable formation on well logs and seismic.

The age range for the Toolonga Calcilutite (79 - 85Ma) is from lower Campanian to middle Santonian (Barber, 1988).

1.5 PETROLEUM EXPLORATION AND PRODUCTION IN THE DAMPIER SUB-BASIN

The Northern Carnarvon Basin is presently Australia's richest oil and gas province with total basin reserves of some 9.1 BBOE (billion barrels of oil equivalent) (Kopsen, 1994). Kopsen (1994) provided a humble estimate of an additional 1 to 2 BBOE by the year 2010. These reserves resulted from at least 80 wildcat discoveries, including four giant fields and seven major fields (Kopsen, 1994).

Petroleum exploration in the Northern Carnarvon Basin began in 1951 with the formation of the West Australian Petroleum Pty Ltd (WAPET). Sir Harold Raggatt, the director of the BMR at the time, encouraged William Walkley, an executive at Ampol, to explore for oil around the Carnarvon Basin. Ampol had previously acquired leases (1947) covering most of the Phanerozoic basins of Western Australia. Walkley sought a partner with the necessary expertise and capital for petroleum exploration. After several years of difficult negotiations in the late 1940's, Walkley formed a partnership with Caltex, and WAPET was set up for oil exploration in the Carnarvon Basin region (Parry and Smith, 1988).

The first well to be drilled using conventional style exploration techniques in Australia yielded overwhelming optimism for the future petroleum potential in Australia. This optimism was unfortunately short-lived. On September 5, 1953, Rough Range 1 was spudded on the Rough Range anticline within the Exmouth Sub-basin. In November, the well flowed 850 BOPD at a depth of 1100m (Wilkinson, 1988). However this well soon proved to be uneconomic, and it was eleven years before WAPET discovered the Barrow Island Oil Field in 1964 (McClure et al., 1988). The remainder of the 1950's proved to be virtually unfruitful for petroleum companies in Australia. Interestingly, the Barrow Island Oil Field has produced the largest quantity of oil of any field in the Carnarvon Basin, with the extraction of over 200 million barrels.

Offshore exploration in the Carnarvon basin began in 1961 when WAPET acquired marine seismic and gravity data (Wilkinson, 1988). The first reconnaissance seismic was shot over the Dampier Sub-basin in 1965 after BOCAL (British Oil Company of Australia Ltd, now Woodside Offshore Petroleum Pty Ltd) was awarded most of the permits in this region. Again, as for onshore drilling, it was the first offshore well that yielded artificial success and fuelled optimism for the Dampier Sub-basin. Legendre 1 was drilled in 1968 by Woodside (Legendre 1 WCR). It encountered a 6.7m section of net pay sandstone that flowed oil at a rate of 1014 BOPD (Vincent and Tilbury, 1988). Although the Legendre area is presently being re-evaluated for potential economic feasibility, this well inspired the drilling of further wells on the Legendre Trend as well as on the Madeleine Trend.

The conventional style of play on the Madeleine Trend is Lower Cretaceous / Upper Jurassic Angel Formation Sandstones that have anticlinal drape closure over an underlying eroded faulted crest. This sandstone is sealed by the Forestier Claystone and the primary source is considered to be the Dingo Claystone. Madeleine 1 and Dampier 1 were drilled in 1969, and a subsequent gas discovery was achieved by Angel 1 in 1972 (refer to Figure 1.1 and Table 1.1). The Angel Field has an

estimated 1.69 TCF gas in place (Oil and Gas Australia, 1992). The prior discovery of gas at North Rankin and Goodwyn in 1971 on Triassic horst blocks delayed development of the Angel Field (the lack of demand for more gas). Dampier 1 had no suitable reservoir as an objective. In 1979, Walcott 1 was positioned to re-test the Madeleine 1 objective structure. The acquisition of a grid of modern seismic in 1985 and 1986 by Woodside showed that these wells were off structure (Bint, 1991). Subsequently, the discoveries of the Wanaea Oil Field and the Cossack Oil Field were made in 1989 and 1990, respectively (Bint, 1991). Combined recoverable reserves from these fields is presently estimated at 264.1 MMBOE (Kopsen, 1994).

The Cossack Field had original reserve estimates of 123.2 MMBO. Early in 1992, the identification of problems in statics corrections revealed that this figure was optimistic, and recoverable reserves now stand at 30 MMBO, only 25% of the original reserve estimates. With drilling of the preceding Madeleine 1 and Walcott 1 wells off structure, it appears that statics corrections and velocities of overlying Tertiary Carbonates has plagued the history of exploration on the Madeleine Trend. Bearing this in mind, the Madeleine Trend has proved to be relatively more prosperous than the Legendre Trend on the opposite flank of the Lewis Trough.

The objective reservoirs on the Legendre Trend included sandstones from the Angel Formation, Talisman Sandstone Member, Eliassen Formation and the Calypso Formation. The seal includes the Muderong Shale, Forestier Claystone and Dingo Claystone. The primary source is considered to be the Dingo Claystone. The trap style is typically a compressionally closed anticlinal structure on the down-thrown block of a normal fault.

After the discovery of Legendre 1, it was 16 years and the drilling of 8 wildcat wells over the length of the Legendre Trend before another discovery on this structure was made at Talisman 1 in 1984. Sporadic drilling during the 1970's and early 1980's included Legendre 2 (1970), Nelson Rocks (1973), Rosemary 1 (1973), Lewis 1/1A (1976), Forestier 1 (1978), Rosemary North 1 (1982), Bounty 1 (1983) and Samson 1 (1984). Most of these wells were drilled on closed structures, but many depended on fault seals. It is suspected that in most cases, breach of a fault seal caused the failure of these wells. Indeed, the success of the Talisman field may be partially attributed to the fact that it lies over the footwall block of the Rosemary Fault and does not rely as much on a fault seal.

Subsequent to the Talisman discovery, wells tested closures on the Degrey Nose (i.e. Calypso 1, 1985; and Alpha North 1, 1989) and the Cossigny Fault (Aurora 1, 1990). Orion 1 (1990) was another well drilled to test sandstones of the Angel Formation on the footwall block of the Rosemary Fault (see Figure 1.6 for well locations).

The most recent exploration efforts in and around the Lewis Trough have focused on structural/stratigraphic style plays, lower on the flank of the Lewis trough. This style of play requires sandstones of the Angel Formation and/or Eliassen Formation to pinch-out up-dip on the flank of the Lewis Trough due to submarine resedimentation processes. Lauchie 1 (1989) failed due to lack of an overlying shale seal. The Baleena 1 (1993) Angel objective failed for the same reason (Barber, 1994). However, the deeper Eliassen Formation objective at Baleena 1 failed due to the lack

of sandstone. Spinner 1 is another dry well that has recently been drilled near the Lauchie - Baleena area with the same objective.

Interestingly, the discovery of oil and gas at Wandoo 1 in June 1991 heralded a new hydrocarbon trend on the adjacently lying Enderby Platform. A flow of 4560 barrels of 19^0 API oil per day flowed from a depth of 600m (Delfos and Boardman, 1994). This field consists of Barremian age transgressive sands with drape style closure overlying a horst block which contain oil and gas. In addition, underlying lower Jurassic Aalenian sands were found to contain gas. The seal is the Muderong Shale. The interesting factor of this hydrocarbon trend is that it raises the issue of long range migration of oil from Dingo Claystones and/or Locker Shale within the Lewis Trough. There is no known mature source rock in the vicinity of the Wandoo Field. This migration would require leakage of hydrocarbons through the Rosemary Fault, as suggested by Christiansen (1992). It would also help to explain the lack of success of the large number of dry wells along the Legendre Trend.

In order to assess the future hydrocarbon prospectivity of the Dampier Sub-basin, it is helpful to review the history of success within the region. The following is a review of some of the vital statistics for hydrocarbon fields over the Dampier Sub-basin. Refer to Figure 1.6 for field and well locations.

Legendre Field

Year discovered: 1968. *Water depth:* 52m.
Initial production rate: 1014 BOPD.
Oil gravity: 145.7^0 API.
Estimated recoverable reserves: 5 MMBO.
Reservoir net pay thickness: 6.7m.
Hydrocarbon-water contact depth: 1896m.
Reservoir: Talisman Member - *B. reticulatum* palynozone.
Reservoir porosity: 14%.
Seal: Muderong Shale.
Source: Dingo Claystone.
Trap style: Faulted anticline on Legendre Trend.
Present status: Suspended.
Reference: Vincent and Tilbury (1988).

Angel Field

Year discovered: 1972. *Water depth:* 80m.
Initial production rate: Angel 2 - 7.4 MMscf/day gas, 377 bbls/day condensate;
Angel 3 - 13.6 MMscf/day gas, 704bbls/day condensate.
Estimated recoverable reserves: 83 MMBO; 1700 BCFG.
Reservoir net pay thickness: 82m.
Hydrocarbon-water contact depth: 2745m.
Reservoir: Angel Formation - *P. iehiense* palynozone.
Reservoir porosity: 14-20%. *Reservoir permeability:* 150-727 mD.
Seal: Forestier Claystone.
Source: Dingo Claystone; Locker Shale possible.
Trap style: Structural drape over an eroded fault crest.
Present status: Suspended.
Reference: Vincent and Tilbury (1988).

Eaglehawk Field

Year discovered: 1972. *Water depth:* 120m.
Initial production rate: 1645 bbls/day oil; 0.141 MMscf gas.
Estimated recoverable reserves: 3 MMBO.
Oil gravity: 30^0 API.
Reservoir net pay thickness: 13.9m.
Hydrocarbon-water contact depth: 2795.6m.
Reservoir: Upper Triassic Mungaroo Formation.
Reservoir porosity: 15-22%.
Seal: Muderong Shale.
Source: Locker Shale.
Trap style: Structural drape over a horst block.
Present status: Suspended.
Reference: Vincent and Tilbury (1988).

Egret Field

Year discovered: 1973. *Water depth:* 118m.
Initial production rate: 2729 bbls/day oil; 2.8 MMscf/day gas.
Estimated recoverable reserves: 6 MMBO.
Oil gravity: 39° API.
Reservoir net pay thickness: 9.4m.
Hydrocarbon-water contact depth: 3129m.
Reservoir: Angel Formation - *P. iehiense* palynozone.
Reservoir porosity: 19%. *Reservoir permeability:* 100-200 mD.
Seal: Dingo Claystone.
Source: Dingo Claystone; Locker Shale possible.
Trap style: Structural drape over an eroded fault crest.
Present status: Suspended.
Reference: Vincent and Tilbury (1988).

Lambert Field

Year discovered: 1974. *Water depth:* 125m.
Initial production rate: 375 bbls/day oil; 7.4 MMscf/day gas.
Estimated recoverable reserves: 20 MMBO.
Oil gravity: 45° API. *Water saturation:* 61%.
Reservoir net pay thickness: 10m.
Hydrocarbon-water contact depth: 3111m.
Reservoir: Angel Formation - *P. iehiense* palynozone.
Reservoir porosity: 18%. *Reservoir permeability:* 300-700 mD.
Seal: Forestier Claystone.
Source: Dingo Claystone; Locker Shale possible.
Trap style: Structural drape over an eroded listric fault crest.
Present status: Suspended.
Reference: Vincent and Tilbury (1988).

Talisman Field

Year discovered: 1984. *Water depth:* 78m.
Initial production rate: 11239 bbls/day oil.
Total recoverable reserves: 7.8 MMBO.
Oil gravity: 'A' Sand - 62^0 API; 'B' Sand - 42.7^0 API;
'C' Sand - 41.60 API.
Reservoir net pay thickness: 60m gross column over 3 zones.
Hydrocarbon-water contact depth: 1971.2m.
Reservoir: Mardie Greensand, Birdrong Sandstone, Talisman Sandstone Member - *S. tabulata, D. lobospinum, C. delicata* palynozones.
Reservoir porosity: 'A' Sand - 15-24%; 'B' Sand - 17-25%; 'C' Sand - 16-23%.
Reservoir permeability: 'A' Sand - 127 mD; 'B' Sand - 1534 mD;
'C' Sand - 3027 mD.
Seal: Muderong Shale.
Source: Dingo Claystone.
Trap style: Anticline structure over footwall block.
Present status: Depleted 1993.
Reference: Ellis (1988).

Wanaea Field

Year discovered: 1989. *Water depth:* 85m.
Initial production rate: 5856 bbls/day oil.
Total recoverable reserves: 199 MMBO; 210 BCFG.
Oil gravity: 49^0 API.
Reservoir net pay thickness: 103m gross oil column.
Hydrocarbon-water contact depth: 2900m.
Reservoir: Angel Formation - *P. iehiense, D. jurassicum* palynozones.
Reservoir porosity: 17%. *Reservoir permeability:* 300 mD (average).
Seal: Dingo Claystone.
Source: Dingo Claystone.
Trap style: Structural drape over a fault crest.
Present status: In development.
Reference: Bint (1991).

Cossack Field

Year discovered: 1989. *Water depth:* 85m.
Initial production rate: 7200 bbls/day oil.
Total recoverable reserves: 30 MMBO.
Oil gravity: 49° API.
Reservoir net pay thickness: 54m gross oil column.
Hydrocarbon-water contact depth: 2918m.
Reservoir: Angel Formation - *P. iehiense* palynozone.
Reservoir porosity: 17%. *Reservoir permeability:* 500 mD (average).
Seal: Forestier Claystone, Dingo Claystone.
Source: Dingo Claystone.
Trap style: Structural drape over a fault crest.
Present status: In development.
Reference: Bint (1991).

Wandoo Field

Year discovered: 1991. *Water depth:* 55m.
Initial production rate: 4560 bbls/day oil.
Total recoverable reserves: 50 MMBO.
Oil gravity: 19° API.
Reservoir net pay thickness: 30m.
Hydrocarbon-water contact depth: 600m.
Reservoir: M. australis Sandstone Member of the Muderong Shale - *M. australis* palynozone.
Reservoir porosity: 33% (average).
Reservoir permeability: 2000-15000 mD.
Seal: Muderong Shale.
Source: Uncertain, Dingo Claystone probable, Locker Shale possible.
Trap style: Structural drape over a horst block.
Present status: In development.
Reference: Delfos and Boardman (1994).

CHAPTER 2: THEORY

SEDIMENTARY AND STRATIGRAPHIC MODELS TO REPRESENT ARCHITECTURAL RELATIONSHIPS OF DEPOSITIONAL SYSTEMS

2.1 GENETIC STRATIGRAPHY

A sequence was originally defined by Sloss, Krumbein and Dapples in 1949 as unconformity-bounded masses of strata. In 1963 Sloss modified this definition to state that these masses of strata were greater than group or supergroup rank in the American Code of Stratigraphic Nomenclature. These bounding unconformities referred originally to "significant inter-regional unconformities which can be traced in outcrop and in the subsurface over vast distances", and which covered much of the North American continental interior (Krumbein and Sloss, 1963). In addition, these six reference sequences represented "the rock record of a major tectonic cycle". They were named from oldest to youngest as the Sauk, Tippecanoe, Kaskaskia, Absaroka, Zuni and Tejas sequences. In this context, 'sequence stratigraphy' was referred to by Sloss as the study of genetically-related strata that are bounded by unconformities (Sloss, 1988; Weimer, 1992a). Although the original definition of a sequence was initially intended to occur within the lithostratigraphic hierarchy, it was suggested by Chang in 1975 that it should be regarded as a 'synthem', a position that was sanctioned by the International Commission on Stratigraphic Classification but it was not ruled to be accepted. The idea was that the 'unconformity bounded unit' should be separated from the lithostratigraphic hierarchy because it had chronostratigraphic applications that made it unique (Sloss, 1988).

In 1977, Memoir 26 (Payton, editor) defined the 'depositional sequence' as a "stratigraphic unit ... bounded at its top and base by unconformities *or their correlative conformities*" (Mitchum et al., 1977). While the definition appears to complement Sloss's original definition, the term 'sequence' referred to stratal packages at a much smaller scale. In the terminology of Memoir 26, the previous 'sequences' were referred to as 'supersequences' (Sloss, 1988). A new generation of nomenclature was then introduced to support what was considered to be a new way to study stratigraphy. Many stratigraphers feel that the only new aspect that was introduced by sequence stratigraphy was the terminology. Indeed, this terminology is not completely accepted throughout the stratigraphic community (e.g. Sloss, 1988: Weimer, 1992b).

The International Commission on Stratigraphy (ICS) have recently recognised the continuing resistance to some sequence stratigraphic concepts. They are presently establishing a forum to reconcile the divergent opinions. It will be called the 'Committee on Genetic Stratigraphy'. There is also contention on the difference between sequence stratigraphy, event stratigraphy, and cyclic stratigraphy because of their similarities of study. However, each "involve the establishment of explanations for sequences of rocks in the context of their origin and the causes of their deposition"("International Commission on Stratigraphy", *Episodes* Newsmagazine, September 1994). The ICS ~~have~~ has recently intended that the name 'Genetic Stratigraphy' is to embrace all three of these categories.

There are primarily two frameworks or 'schools of thought' regarding sequence stratigraphy. The 'Vail' framework of 'sequence stratigraphy' (Figure 2.1) regards a sequence to be bounded by unconformities that have formed due to falls in relative sea level. Geometric systems tracts occur within each sequence which are implied (by name) to occur during a particular stage of relative sea-level (i.e. highstand systems tract, lowstand systems tract). The dominating theme is that relative sea-level is driving the stratigraphy of the sediments.

The Galloway framework of 'genetic sequence stratigraphy' (Figure 2.2) is the framework that is adopted for use in this study, albeit slightly modified. The formal definition of the 'genetic stratigraphic unit' (Galloway, 1994) can be found in Section 3.3.1. A 'genetic stratigraphic sequence' using the Galloway approach (1989a) is regarded to be bounded at the top and bottom by maximum flooding surfaces. It was defined as a regressive depositional unit bounded by transgressive surfaces. This definition was formulated after consideration of Frazier's (1974) concept that depositional episodes were bounded by regional flooding events or hiatuses formed during sea level rise or by shifting delta lobes. Previous to this, the concept of a genetic chronostratigraphic unit had been used since the late 1950's (e.g. Busch, 1959; Hollenshead and Pritchard, 1961).

Using the genetic sequence stratigraphic approach, systems tracts are referred to by their geometric shape rather than by any mechanism that may be driving the stratigraphy. While genetic sequence stratigraphy accommodates factors such as relative sea-level and tectonics, the framework (particularly Galloway's 1994 definition of the genetic stratigraphic unit) puts greater emphasis on sediment source and the sediment processes. Although this framework was initially designed to apply to shelf systems, it has proved to be equally appropriate for 'slope and basin systems' also.

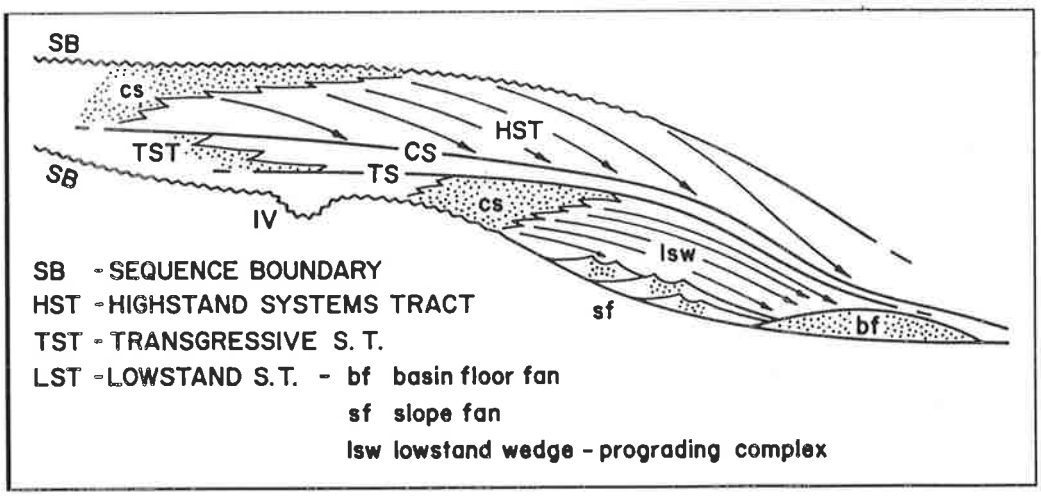


Figure 2.1. The Vail 'slug' diagram of the depositional sequence that is driven primarily by changes in sea level. This sequence is bounded by unconformity surfaces thought to be caused by falls in relative sea level (from Walker, 1992 p. 258; modified after Vail et al., 1987 and Posamentier and Vail 1988). Note that submarine fan development is shown to only occur within the low stand systems tract. TS - transgressive surface; CS - condensed section (or maximum flooding surface); IV - incised valley; cs - coastal sandstones.

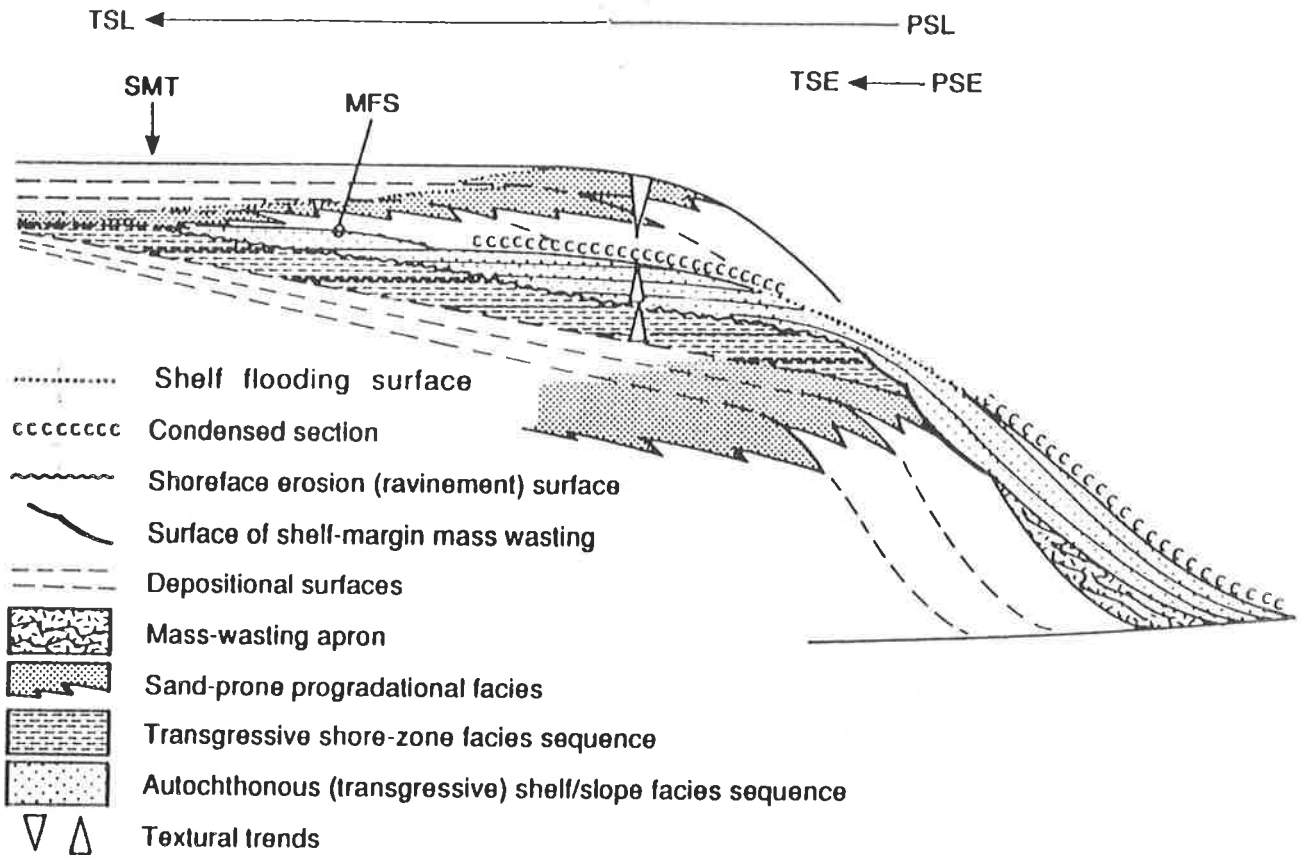


Figure 2.2. Facies architecture of a genetic stratigraphic sequence for the Galloway framework of genetic sequence stratigraphy (from Galloway, 1994). This particular diagram represents the depositional and stratigraphic framework of the transgressive backstep wedge with component diastems that form the maximum flooding surface, and the condensed section. TSL - transgressive shoreline location; PSL - progradational shoreline location; TSE - transgressive shelf edge location; PSE - progradational shelf edge location; SMT - shoreline of maximum transgression; MFS - maximum flooding surface.

Transgressive surfaces, or, as referred to herein, 'primary flooding surfaces' form the boundaries of many of the depositional episodes described in this study. The primary flooding surface was observed to be less diachronous than the maximum flooding surface. This surface also forms the boundary of the 'transgressive - regressive sequence' (T - R cycle), used in regional basin analysis studies (e.g. Embry, 1993; Johnson et al., 1985).

One of the advantages that have been realised in using the genetic sequence stratigraphic framework is that the effect of various driving mechanisms may be evaluated objectively at the end of the sequence stratigraphic exercise, when crucial data and evidence ~~has~~ have been collated. This is conducted by using 'generic' geometric terms for wedges or 'systems tracts' that are observed in the geological record (e.g. Figure 2.3). These systems tracts can be modified according to the sand body architecture that is observed (Figure 2.4).

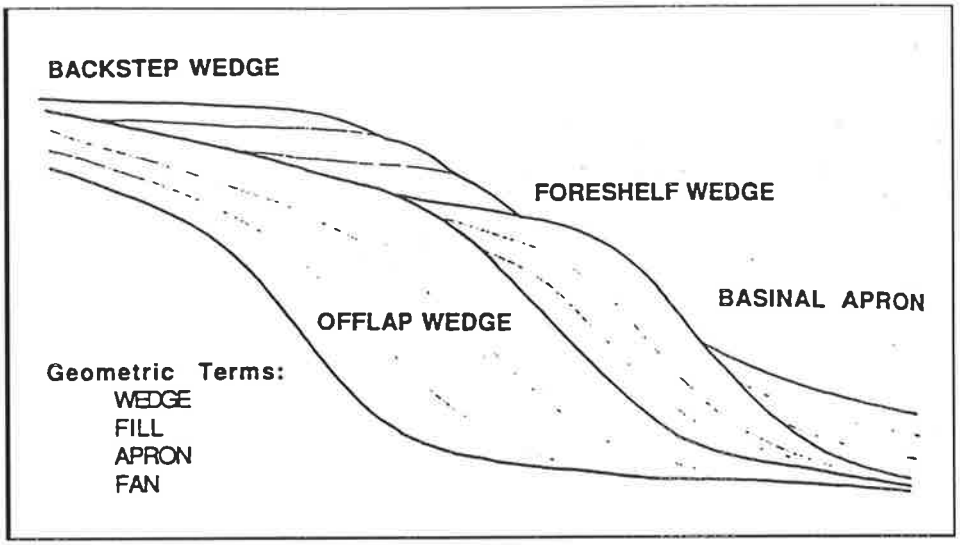


Figure 2.3. Geometric systems tracts found within progradational marine basin fill. Alternative geometric terms include fill (distinctly enclosed sub-basin or erosional depression) and fan (point-source with radial plan form). Note that these terms are divorced from interpretation of depositional processes or boundary conditions (from Galloway, 1994).

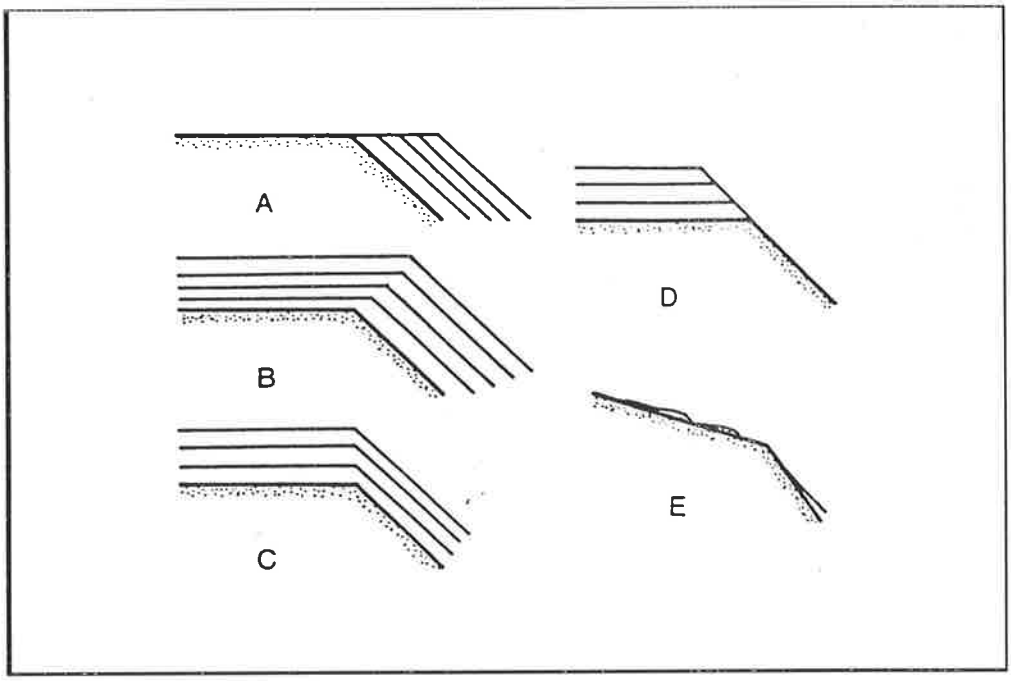


Figure 2.4. Sand body architecture of progradational (A, B), aggradational (C), retrogradational (D) and transgressive (E) depositional systems (from Galloway, 1994; after Leithold and Bourgeois, 1989).

2.2 SEDIMENTOLOGY IN GENETIC STRATIGRAPHY

Sedimentology is crucial in genetic stratigraphy to evaluate the three-dimensional shape and size of a lithostratigraphic body of rock. By determining the variations of depositional processes that occur within a particular depositional system and attributing these variations to parameters such as sediment source and provenance, palaeogeography, changes in relative sea-level (if any), and tectonic regime and tectonic stage in basin development, the architecture of the lithostratigraphy will be better understood. In addition, an evolutionary progression of the style of the depositional systems may be observed over the depositional history of the basin. This observed progression of depositional systems will help to confirm and to better understand these rock body geometries.

Rather than establishing a unifying model or concept, it is more important to conceive and establish relationships and identify the responsible parameter(s) for the character of the depositional system. The 'extremes' of these relationships may be represented in depositional models that account for one or more relevant parameters. These models should be used as end-members of a spectrum of possibilities, with each plane of the spectrum accommodating one of the parameters. The more parameters involved, the more planes within the spectrum. In this study, models of marine resedimented depositional systems that represent end-members of various parameters have been chosen. The depositional systems observed in the Dampier Sub-basin can be explained with respect to end-member submarine fan models arranged over a spectrum of parameters. These models are outlined in Section 2.3.

The hierarchy of genetic stratigraphic units (after Galloway, 1994) is shown in Figure 2.5. The hierarchy of terminology for this study with respect to various stratigraphic nomenclatures and with respect to data types are represented in Figure 2.6. In this study, depositional systems are composed of depositional elements. One or more depositional processes have been identified as being responsible for the formation of a depositional element. Type examples have been made up using the available data to represent various depositional elements (i.e. wire line log profiles, seismic facies and stratal patterns). By using these examples to show some of the variations of depositional elements represented by this database, numerous depositional systems within the Aptian to Callovian succession of the Dampier Sub-basin have been defined and characterised.

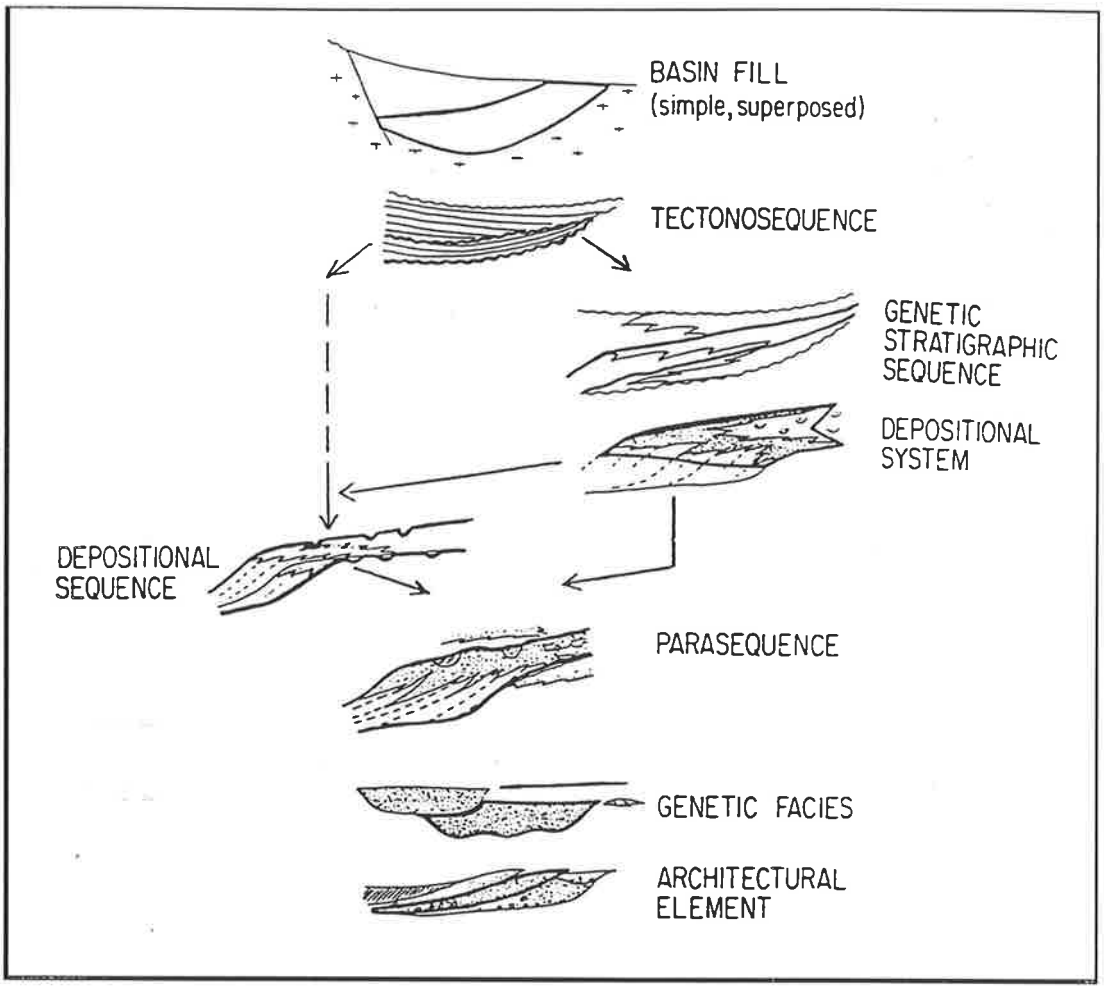


Figure 2.5. Hierarchy of genetic stratigraphic units (after Galloway, 1994).

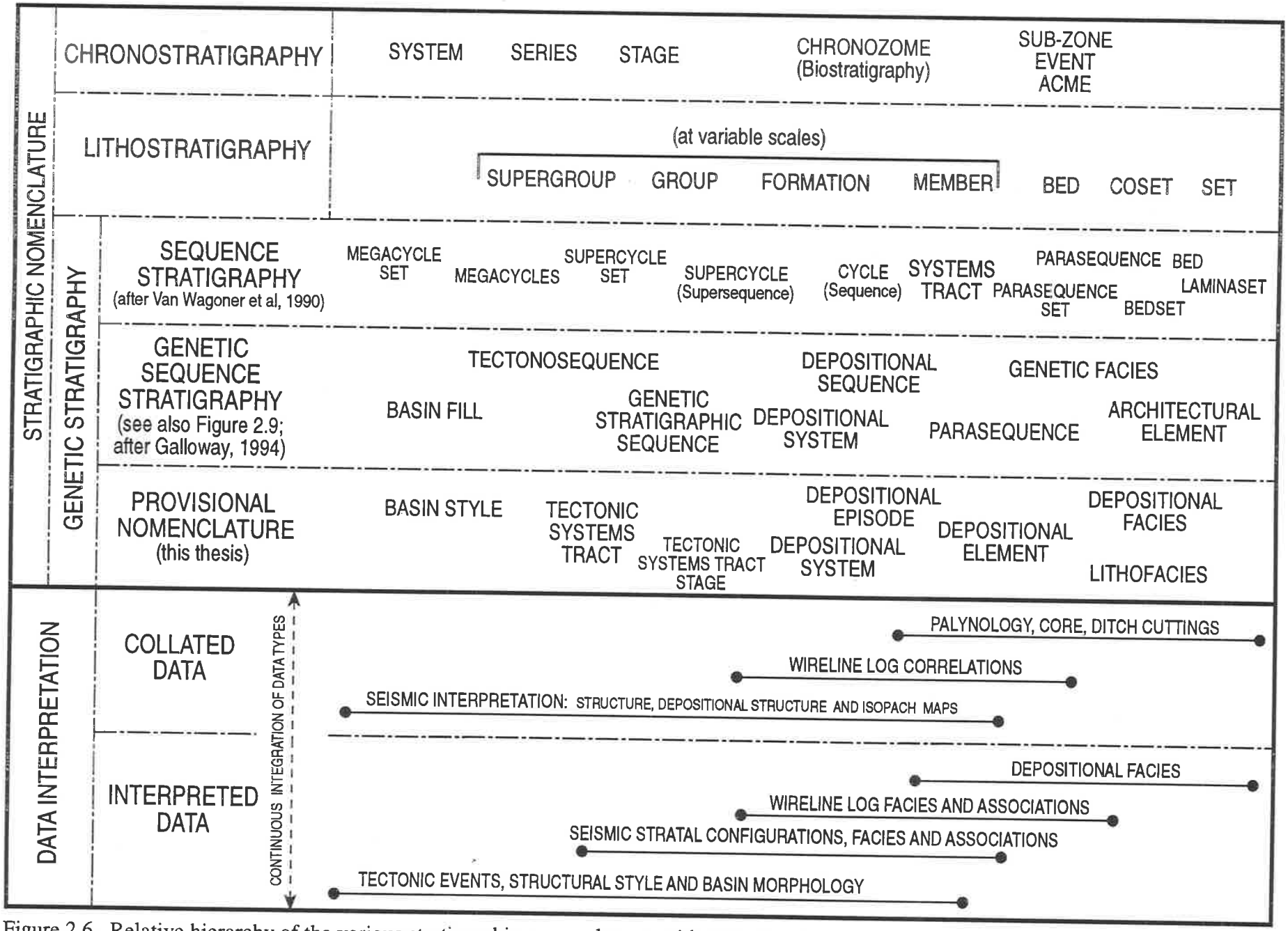


Figure 2.6. Relative hierarchy of the various stratigraphic nomenclatures with respect to the scale ranges of pertinent data types used in this study. A relative increase in time and size is implied from right to left of the diagram.

2.3 MARINE RESEDIMENTATION MODELS APPLICABLE TO THE DAMPIER SUB-BASIN

The morphology, internal structure and facies associations of submarine fans are primarily controlled by the long-term stability of the basin and the volume of sediment supplied to the depositional area (Mutti and Normark, 1987). Turbidite basins formed in active tectonic settings tend to be short lived, especially in cases where both the source area and depositional basin were affected by crustal movements (Mutti and Normark, 1987). In these short-lived systems, local tectonic control greatly influenced the development of the turbidite deposit (Mutti and Normark, 1987).

The Valanginian to Callovian resedimented succession of the Dampier Sub-basin is classified within type 'D' of Mutti and Normark (1987). "Type 'D' basins are those formed on continental crust where continuing tectonic activity resulted in relatively rapid changes in basin shape and in short lived sediment sources. The resulting turbidite deposits formed in relatively short time spans (10^4 to 10^5 years), are dominantly coarse-grained channel and lobe units, and are volumetrically much smaller than turbidite fill of the other three basin types (types A to C). These small, actively deforming and short-lived basins formed on active margins: during early rifting phases of an opening ocean, along active transform margins and during final stages of continental collision" (Mutti and Normark, 1987).

There are two misleading factors in discussing the Dampier Sub-basin succession in terms of a 'turbidite fan'. The use of the term 'turbidite' implies that fluid turbulence was the dominant sediment transport process (Figures 2.7 and 2.8).

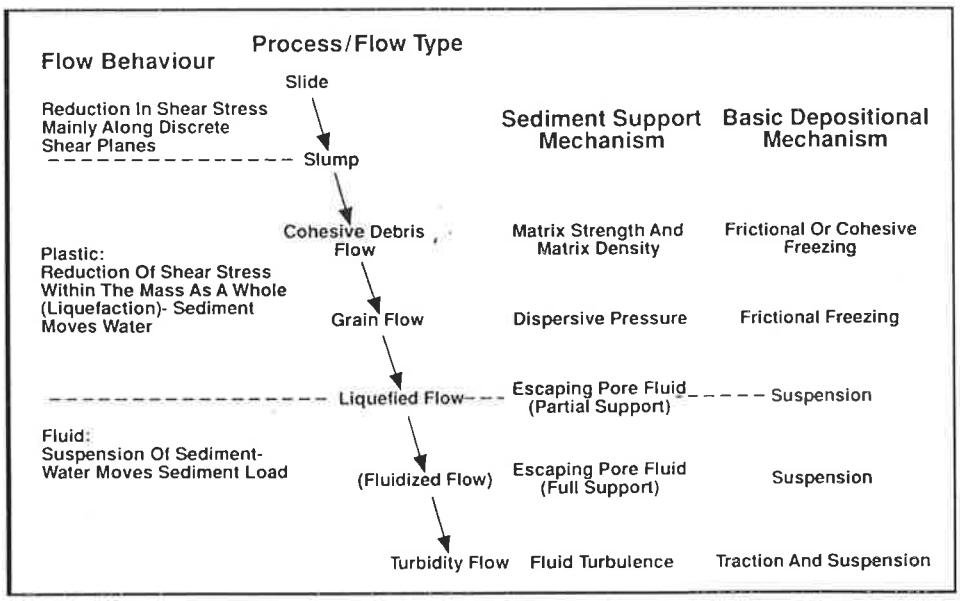


Figure 2.7. Classification scheme of flow types for resedimented deposits (from Guy, 1992).

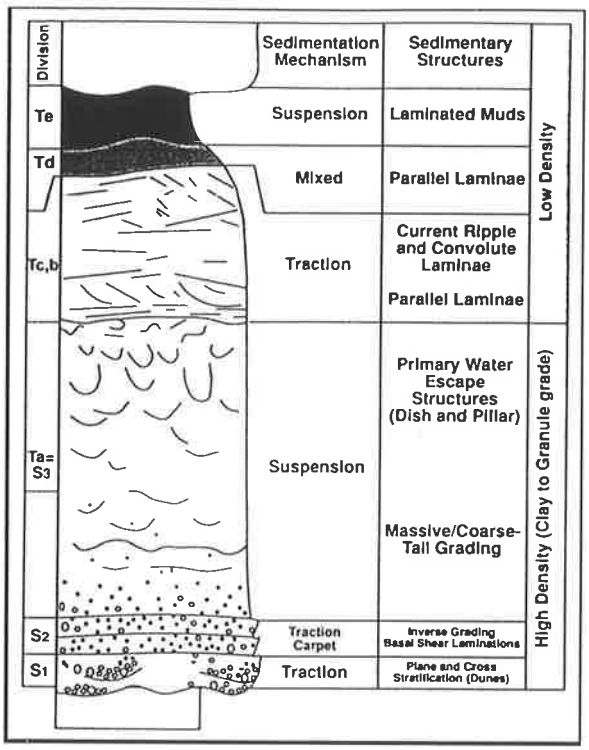


Figure 2.8. Idealised depositional sequence from a sandy high density turbidity current (after Lowe, 1982).

Although sections attributed to turbidity currents (as in Figure 2.8) were identified in this study, many were also attributed to gravity flow mechanisms (e.g. see Sections 3.2.3 and 4.1.3). These observations were also supported by recent publications (e.g. Shanmugam et al. 1994). The morphologic distinction is that turbidite deposits are usually detached from more proximal sediments, while gravity flow deposits will have proximal sediments attached.

The second misleading factor is the use of the term 'fan'. This term resulted from studies of recent submarine fans deposited on the ocean floor which have a fan-shaped morphology. In this study, none of the depositional systems were fan-shaped, but rather manifest the previous morphology of the basin. "The complexities of the slope/basin system have led to limited and over generalised models. These systems are variously referred to as turbidite or gravity-flow systems, fan systems and deep marine systems. Each name emphasizes an important element of their deposition but is an incomplete expression of the diversity of systems and processes inherent in the geomorphic setting" (Galloway, 1993). The successions described in this study are referred to as 'resedimented depositional systems' so that no particular aspect of sedimentation is excluded.

This study differs from previous investigations of the Dampier Sub-basin in giving gravity-flow mechanisms greater emphasis. A flow chart showing the sources of gravity-flow mechanisms induced on the slope of a basin is depicted in Figure 2.9.

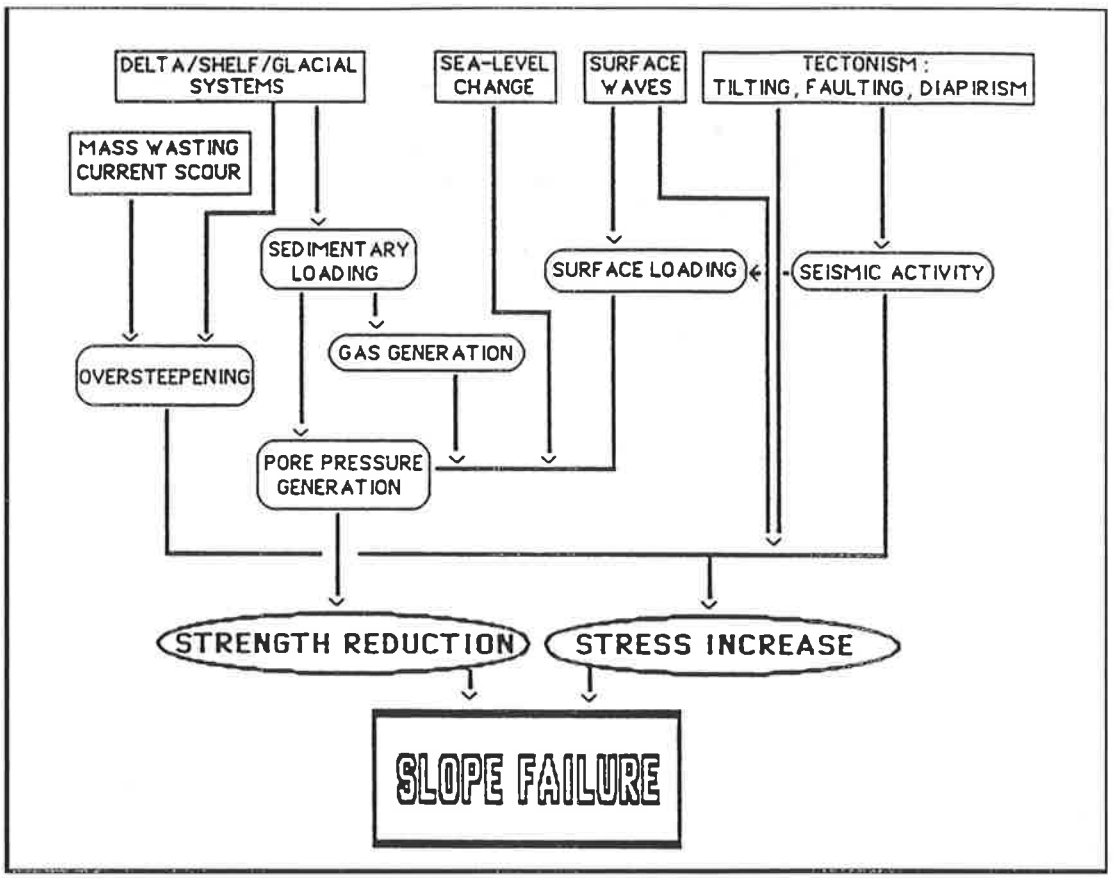
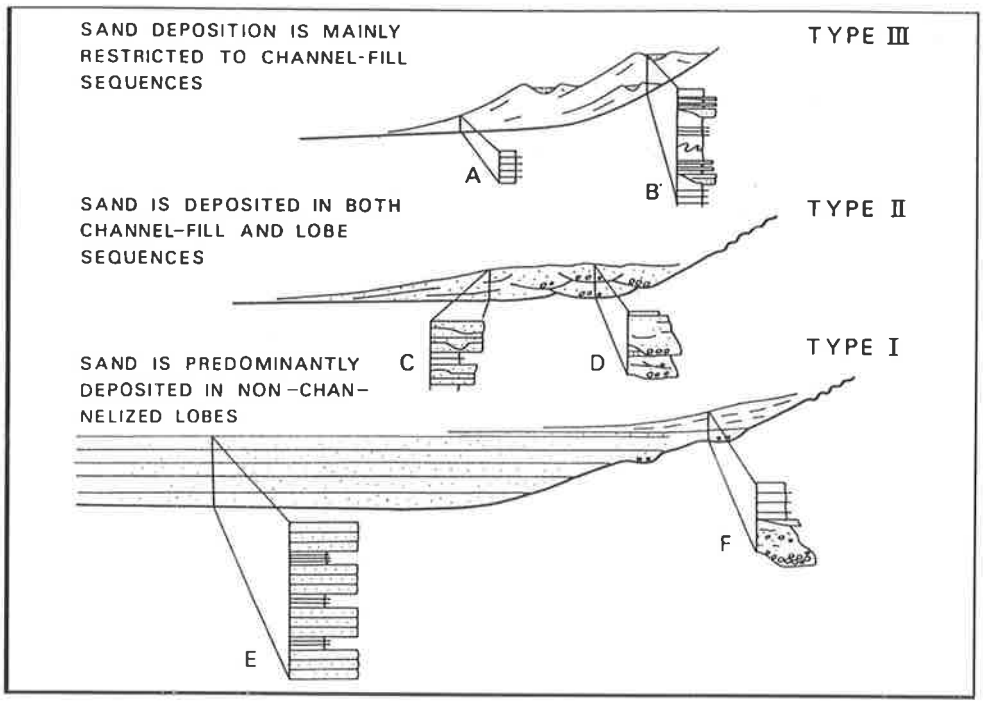


Figure 2.9. Trigger mechanisms for slope failure (from Galloway, 1994; after Coleman and Prior, 1988).

In reviews of the petroleum potential of the Barrow and Dampier Sub-basins, the Calypso, Eliassen and Angel Formations were not discussed as separate entities with respect to the Barrow Sub-basin (e.g. Kopsen and McGann, 1985; Woodside, 1988; Boote and Kirk, 1989). In these papers, these formations were discussed in the context of their respective equivalents in the Barrow Sub-basin, namely the Biggada Sand and the Dupuy Sandstone Member of the Upper Dingo Claystone. These sandstone units were discussed with reference to 'prograding submarine fans', 'turbidity-flow' and debris-flow' deposits in limited detail.

The Angel Formation was interpreted by Buswell (1989) to consist of submarine fan sands with respect to the Mutti (1985) Type I, II and III turbidite deposits (Figure 2.10). This study was mainly a petrological study of the Angel 3 well, and the depositional environment was not a major issue in the study. In 1994, Barber discussed the Aptian to Callovian succession of the Dampier Sub-basin in terms of 'Vail' sequence stratigraphy and Mutti Type I, II and III turbidite systems.

a)



b)

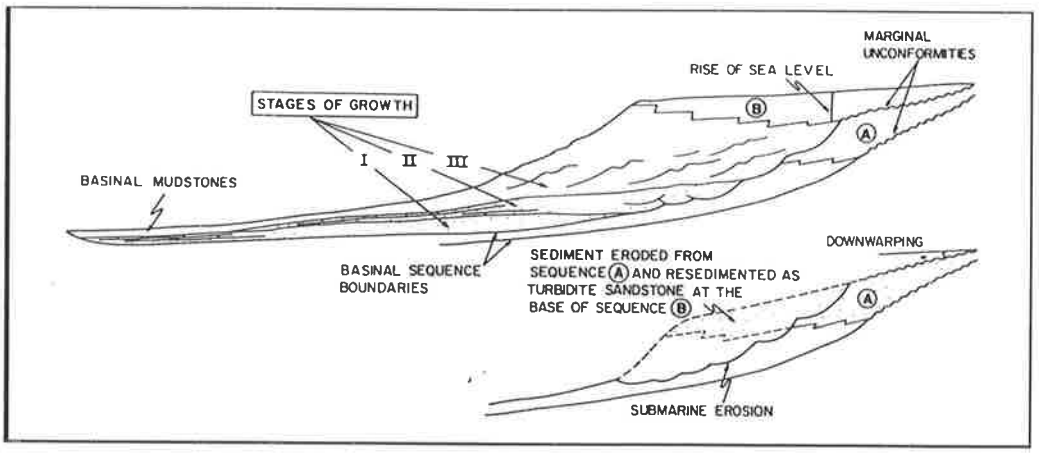


Figure 2.10. a) The three main types of turbidite deposits (From Mutti and Normark, 1987, after Mutti, 1985). b) The relation of relative changes of sea level to the different stages of growth of turbidite systems for depositional systems developed in elongate flysch basins (From Mutti and Normark, 1987, after Mutti, 1985).

The use of the sequence stratigraphic framework for rifted margins is discussed in detail in Sections 4.1 and 4.3 of this thesis. In addition, the problems involved with use of this framework for 'deep-water siliciclastic systems' are outlined after Mutti (1992) in Figure 2.11. It is interesting to note that Mutti (1985) intended that the three types of turbidite systems to represent end members in the stages of growth of turbidite systems. The only suggestion that Mutti provides with respect to how relative sea level effects the type of turbidite system is shown in Figure 2.10b. It was later that these turbidite system types were related to sequence stratigraphic systems tracts (i.e. the basin floor sand and slope fan systems tracts) by independent authors (e.g. Barber, 1994).

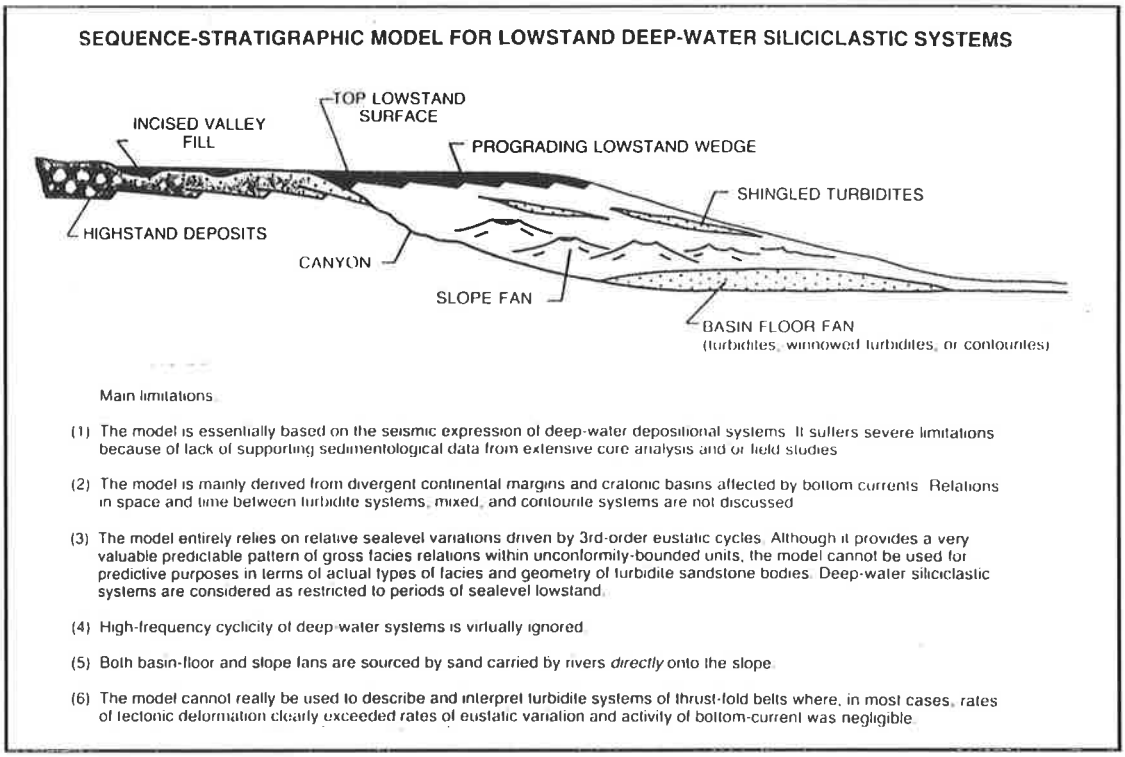


Figure 2.11. The limitations associated with the sequence stratigraphic model for lowstand deep-water siliciclastic systems (From Mutti, 1992).

A generalised facies distribution for a rather 'generic' type of submarine fan setting (Walker, 1978) is shown in Figure 2.12. This model is practical because it shows typical relative locations and facies distributions and associations with no relative scale implied. It contains the submarine fan morphologic sub-divisions suggested by Normark (1970). By applying additional knowledge of fan morphology, depositional processes and relative sizes of depositional facies that occur as a result of the type of basin, tectonic setting, basin morphology and sediment texture, these basic facies distributions and associations are valid, albeit with the exemplification of one or more facies and the disappearance of others. In addition, by knowing the transport and depositional processes that produce these facies, the prediction of some depositional facies in various locations of the system may be achieved. Note, for example, the similarity of the 'thin-bedded turbidites on levee' and the 'thin-bedded classical turbidites' of the lower fan. By making these distinctions and comparisons, more accurate palaeogeographies of resedimented marine systems can be established.

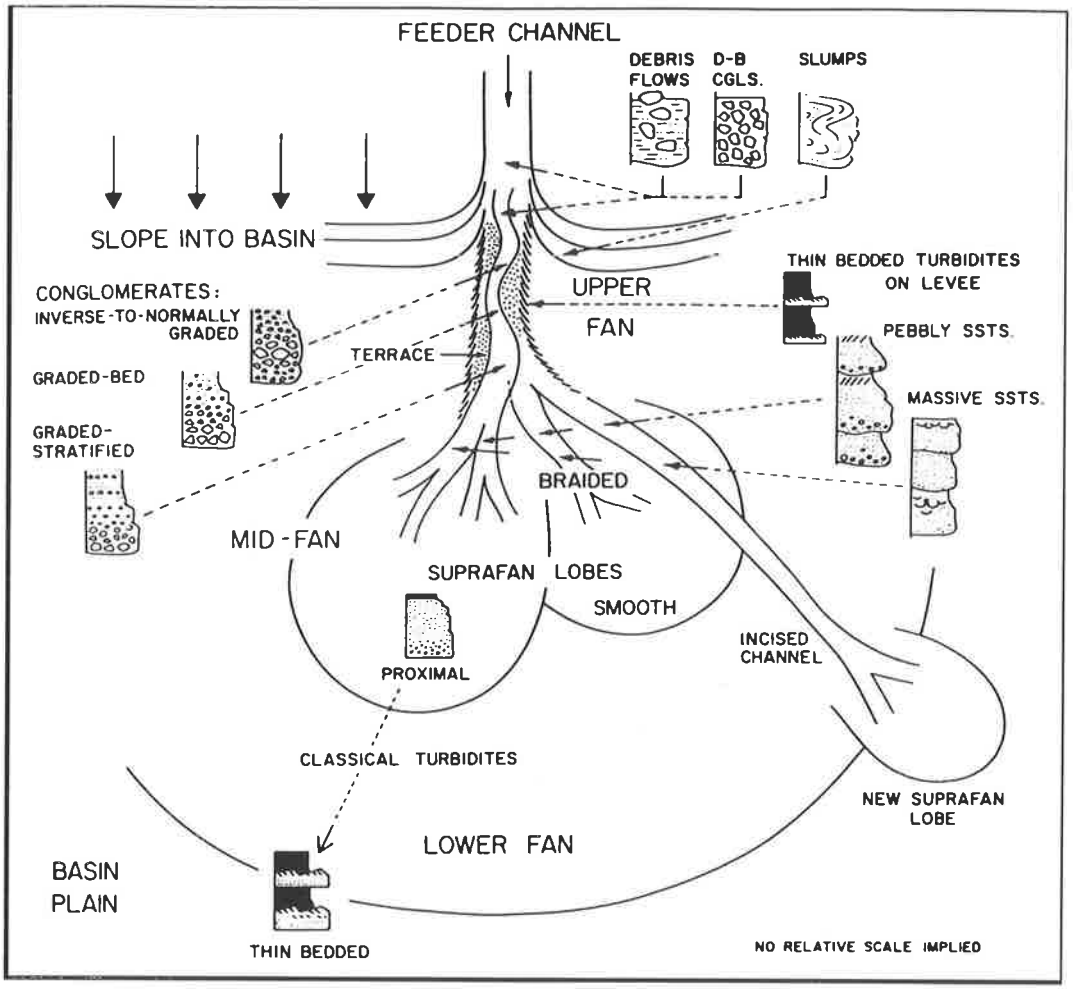
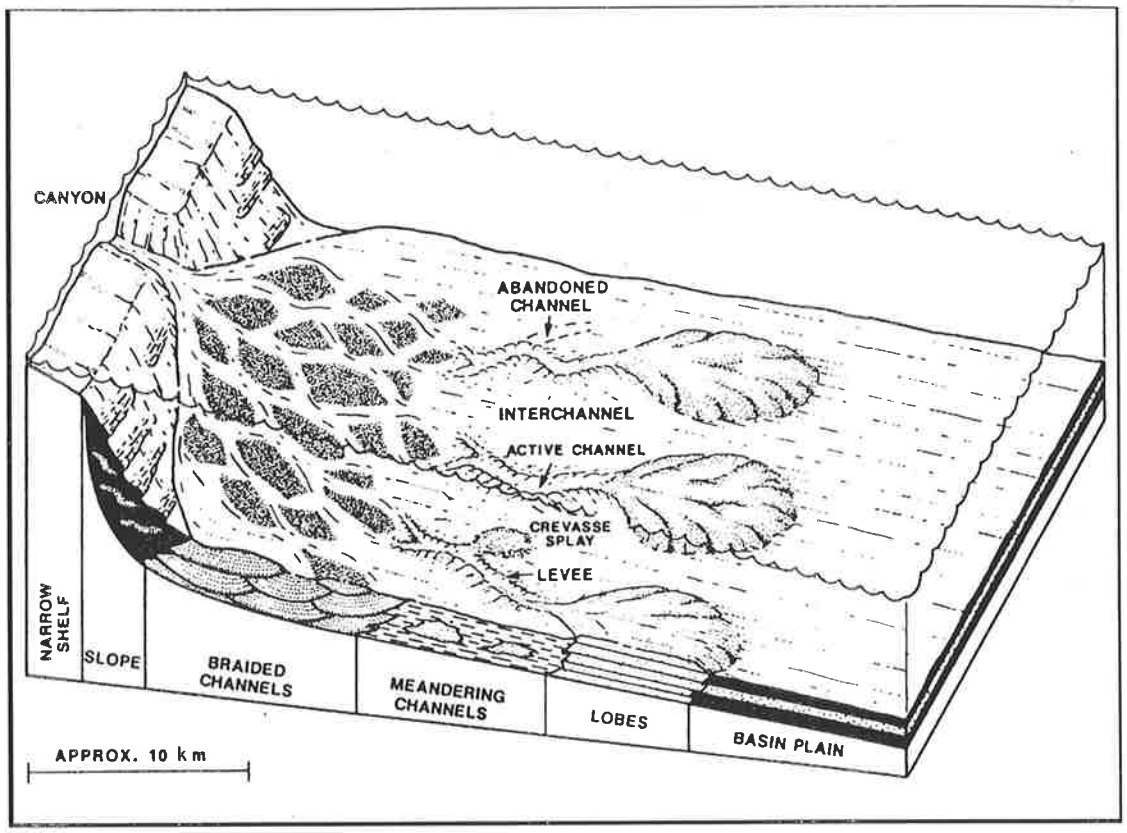


Figure 2.12. Model of submarine fan deposition, relating facies, fan morphology and depositional environment. D-B indicates disorganised bed conglomerates (from Walker, 1978).

An example of the variations in marine resedimentation due to basin type is shown in Figure 2.13. Note the differences of scale, sand content and fan elements between the model of an active-margin setting and a passive margin in which certain presumptions have been placed on the basin setting. The passive margin example is large scale, highly channelled and relatively low in relief, a common result in mud-rich systems. One of the presumptions made in this case is that most passive margins are relatively mud-rich and so this is a 'typical' passive-margin fan. It is interesting to note that the active-margin example is a favorable 'type' example of the pertinent section in this study without considering the varying factors of each individual depositional episode. This model is on a scale of ten's of kilometres and contains sandy slumps on the slope. It also contains a relatively sandy 'slope apron' area of braided channels and channel-lobe complexes, and interchannel areas with possible levees and crevasse splays. All of these factors are applicable to this study.

a)



b)

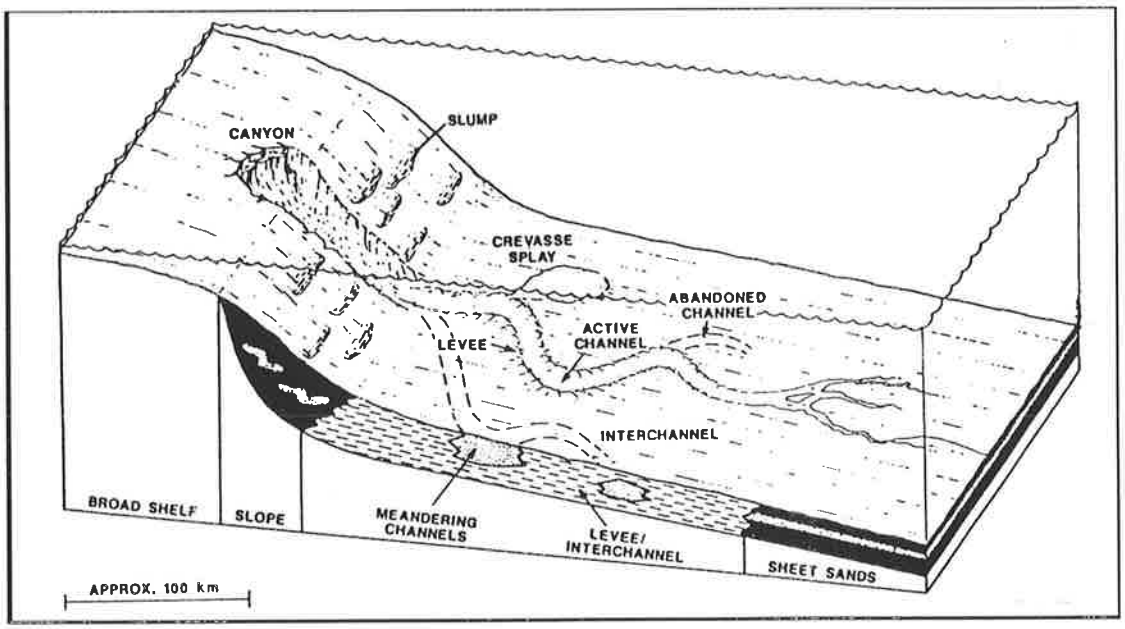


Figure 2.13. Schematic views of: a) an active-margin fan with channel-mouth lobes; and b) a mature passive-margin fan without channel-mouth lobes (from Shanmugam et al., 1988). See text for discussion.

Turbidite systems were distingushed from apron systems in modern settings by Nelson et al. (1990). Reading and Richards (1994) classified depositional systems in deep-water basin margins into twelve classes. These classes were based on mud-rich, mud/sand-rich, sand-rich and gravel-rich textural factors variably combined with point-sourced submarine fan, multiple-sourced submarine ramp and linear-source slope apron system morphologies. The major sedimentological characteristics of the various possible types of deep-water basin margin systems were based on grain size and sediment source (Table 2.1). In addition, the major subsurface and reservoir attributes of these depositional systems were also outlined (Table 2.2). Depositional models were presented for each possible system in an 'end-member' fashion. They stated: "The exact positioning of any one depositional system within the scheme cannot always be precise, and the position may be altered by changes in tectonics, climate, sediment supply and sea level" (Reading and Richards, 1994).

The associations that Readings and Richards made on the various styles of depositional systems are also applicable to this study. The depositional systems thus defined can be characterised according to the models of Reading and Richards (1994), and subsequently provides a vehicle to evaluate the attributes of various depositional systems described in this study. All of these models can be considered as end-members of a spectrum.

Feeder System Type / Dominant Grain Size	Single Point-Source Submarine Fans				Multiple-Source Submarine Ramps				Linear-Source Slope Aprons			
	Mud	Mud/Sand	Sand	Gravel	Mud	Mud/Sand	Sand	Gravel	Mud	Mud/Sand	Sand	Gravel
Size	Large	Large-moderate	Moderate	Small	Moderate	Moderate	Moderate	Small	Large	Moderate	Small	Very small
Slope Gradient	Low 0.20–18 m/km	Low-moderate 2.5–18.0 m/km	Moderate 2.5–36 m/km	High 20–250 m/km	Moderate 2.5–25 m/km m/km	Moderate 7–35 m/km	Moderate >35 m/km	High 2 0 - 2 5 0	Moderate-high 40–150 m/km	Moderate-high 40–150 m/km	Moderate-high 40–150 m/km	Very high 20–500 m/km
Shape Radius/Length	Elongate 100–3000 km	Lobate 10–450 km	Radial/lobate 10–100 km	Radial 1–50 km	Lobate 50–200 km	Lobate 5–75 km	Linear-belt 1–50 km	Linear-belt 1–10 km	Linear belt 10–100 km	Linear belt 10–100 km	Linear belt 1–10 km	Linear belt 1–5 km
Source Area Size Gradient Distance	 Large Low Distant	 Moderate Moderate Moderate	 Moderate-small Moderate Close	 Small High Close	 Moderate Low Distant	 Moderate-small Moderate Moderate	 Small Moderate Close	 Very small High Close	 Large Low Moderate	 Moderate Moderate Moderate	 Small Moderate Close	 Very small High Close
Feeding Systems	Large, mud-rich river delta	Large, mixed load, river delta and/or downdip canyon	Shelf failure or shelf canyon	Fan delta or alluvial cone	Large, mud-rich river delta	Mixed-load delta, linear shoreline	Sand-rich, clastic shoreline/ shelf	Alluvial fan/braid plain/ fan delta	Wide, starved shelf	Relict/ Narrow shelf	Narrow shelf	Braid plain
Supply Mechanism	Infrequent slumps and slump-initiated low-density turbidity currents; contour currents	Mainly high- and low-density turbidity currents	Reworking or direct access to shelf clastics; low-efficiency turbidity currents	Frequent mass flows, slumps; river-generated turbidity currents	Infrequent slumps and slump-initiated low-density turbidity currents; contour currents	Mainly high- and low-density turbidity currents	Reworking or direct access to shelf clastics; low-efficiency turbidity currents	Frequent mass flows, slumps; river-generated turbidity currents	Major slumps and related low-density turbidity currents; contour currents	Combination low- and high-density turbidity currents	Collapse of shelfal clastics generating low-efficiency turbidity currents	Frequent mass-flow slumps; river-generated turbidity currents
Size of Flows	Very large	Moderate	Moderate-small	Very small	Large	Moderate	Moderate-small	Small	Large	Moderate	Small	Small
Channel System	Large, persistent; meandering to straight with well-developed stable levee system	Moderate scale; meandering to braided systems laterally migrating with levees	Braided to low-sinuosity impersistent channels and chutes; rapid lateral migration	Braided, small impersistent chutes	Moderate sizes; channel-levee systems	Multiple, leveed channels with meandering to straight platform	Multiple, laterally migrating braided to low-sinuosity channels	Small, impersistent chutes	None; dominance of failure chutes	Multiple, straight to meandering leveed channels	Multiple chutes & poorly developed impersistent channels	Small, impersistent chutes
Distal Slope/ Lower Fan Sediments	Thin, sheet-like flows forming interbedded sands, silts, and muds; coarse intervals forming thin clastic sheets	Mixed-load turbidity current flows forming lobes of interbedded sands and muds	Sand-rich turbidity current flows forming low-relief lobes and sand sheets	Thin, dilute turbidity current flows forming thin distal turbidites	Thin, sheet-like flows forming interbedded sands, silts and muds	Mixed-load turbidity current flows forming lobes of interbedded sands and muds	Sand-rich turbidity current flows forming low-relief lobes and sand sheets	Thin, dilute turbidity current flows forming thin distal turbidites	Slumps and debris flows, largely mud dominated	Rare sandy turbidity current flows, slumps	Impersistent sand-rich turbidity current flows	Dilute turbidity current flows depositing largely mud and occasional sands
Principal Basin Plain Deposits	Turbidites> Hemipelagics	Hemipelagics> Turbidites	Hemipelagics	Hemipelagics	Turbidites> Hemipelagics	Hemipelagics>	Hemipelagics		High-density mud flows	Hemipelagics	Hemipelagics	Hemipelagics

Table 2.1. Major sedimentological characteristics of deep-water basin margin systems based on grain size and sediment source (after Reading and Richards, 1994).

Feeder System Type / Dominant Grain Size	Point-Source Submarine Fans				Multiple-Source Submarine Ramps				Linear-Source Slope Aprons			
	Mud	Mud/Sand	Sand	Gravel	Mud	Mud/Sand	Sand	Gravel	Mud	Mud/Sand	Sand	Gravel
Principal Architectural Elements Proximal Area Distal Area	Channel levees Distal sheets	Channel levees Lobes	Channels Channelized lobes	Wedges Distal sheets	Channel levees Distal sheets	Channel levees Lobes	Channels Channelized lobes	Wedges Distal sheets	Slumps Slides	Slides Offset lobes	Channels Slumps	Wedges Debris flows
Seismic Architecture	Channel levees; distal parallel reflectors	Channel levees and mounds	Constructional, low-relief mounds	Wedges	Channel levees and distal parallel reflectors	Channel levees and mounds	Constructional, low-relief mounds	Wedges	Chaotic mounds	Chaotic mounds	Mounds	Wedges
Sand Percentage	≤30% sand	≥30–≤70% sand	≥70% sand	Variable 5–50% (>50% gravel)	≤30% sand	≥30–≤70% sand	≥70% sand	Variable 5–50% (>50% gravel)	Highly variable 0–20%	Highly variable	Highly variable	Highly variable
Sand-Body Geometry	Large, lenticular channels with multiple, variable-scale sand, silt, and mud fills; high degree of heterogeneity; distal fan dominated by thin sand, silt, and mud sheets	Lenticular channels dominated by sand or mud fill; downdip lobes formed of interbedded and alternating sands, silts, and muds	Broad, sheet-like to low-relief lobate sand-body geometries dominated internally by channelized sandstone units	Irregular interconnected gravels; proximal areas dominated by conglomerates and breccias; sands dominant within medial to distal parts of system	Moderate size sand bodies within overall large channel form; sands commonly isolated in both downdip and updip directions	Offset stacked, lenticular channel sand bodies bounded by fines; levee passing downdip into offset stacked lobate sand bodies formed of sandstones and mudstones	Broad, sheet-like to low-relief lobate sand-body geometries dominated internally by channelized sandstone units	Irregular interconnected gravels; proximal areas dominated by conglomerates and breccias; sands dominant within medial to distal parts of system	Limited sand development; commonly confined to slide scars and slump-generated lows	Laterally extensive; separated by silts and muds	Lobate sand bodies dominated by interconnected channelized units	Laterally extensive; distally limited
Turbidite Facies	A, B, E, F	C, D	B, C	A, B, F	A, B, E, F	C, D	B, C	A, B, E, F	F	D, F	D, E	A, B, F
Reservoir Heterogeneity	High	High-moderate	Low	High	High	High-moderate	Low	High	High	High-moderate	Low	High
Sand-Body Communication Vertical Lateral	 Poor Poor	 Moderate Poor	 Good Good	 Good Poor	 Poor-moderate Moderate	 Moderate Moderate	 Good Good	 Good Moderate	 Poor Poor	 Moderate Moderate	 Very good Very good	 Good Very good
Common Reservoir Trap Type	Stratigraphic	Stratigraphic	Structural	Structural	Stratigraphic	Stratigraphic	Structural	Structural	Stratigraphic	Stratigraphic	Structural	Structural
Play Concepts	(1) Stratigraphic trapping within terminal lobes (2) Stratigraphic trapping of channel levee and splay deposits	(1) Stratigraphic trapping of channel and lobe deposits (2) Trapping of sands in canyons from slope failure and flow stripping	(1) Updip pinch-out of inner fan channel sandstones (2) Stratigraphic trapping of mid-fan channelized lobes	(1) Structural trapping of fan conglomerates adjacent to footwall scarps (2) Structural trapping of medial/distal sandstones	(1) Stratigraphic trapping within terminal lobes (2) Stratigraphic trapping of channel levee/splay sands	(1) Combined structural-stratigraphic trap in proximal ramp channels (2) Updip pinch-out of channel and/or ramp-lobe sands	Combined structural and stratigraphic traps of ramp sandstones	(1) Structural trapping of fan conglomerates and sandstones against footwall scarps (2) Structural closure of medial/distal sandstones	Stratigraphic trapping of detached slumped clastics derived from active or relict updip deltaic systems	Stratigraphic trapping of detached slumped clastics derived from active or relict updip deltaic systems	Combined structural and stratigraphic traps involving slope apron turbidite sandstones	Structural closure of fan conglomerates and sandstones against footwall scarps
Key Exploration Risks	Reservoir and trap presence; extent and identification	Reservoir presence; extent and identification; seal integrity	Trap requires structural component; seal integrity	Reservoir quality and seal integrity	Reservoir quality; trap presence; extent and identification	Reservoir definition, delineation, and quality; seal integrity	Trap requires structural component; seal integrity	Reservoir quality and seal integrity	Reservoir and trap presence; extent and identification; seal integrity	Reservoir and trap presence; extent and identification; seal integrity	Trap requires structural component; seal integrity	Reservoir quality and seal integrity
Importance and Position on Relative Sea Level Cycle	Important Lowstands	Potentially important Highstand and lowstands	Not important	Not important	Important Lowstand	Potentially important; highstand and lowstand	Not important; highstand and lowstand; major flooding events	Important; lowstand and highstand	High importance, highstand and rising base level	Low importance; rising and falling base level	Low importance; falling base level	Low importance; falling base level

Table 2.2. Major subsurface and reservoir attributes of deep-water basin margin systems based on grain size and sediment source (after Reading and Richards, 1994).

The deep-water basin margin depositional systems that bear particular relevance to the depositional systems described in this study include the point-source gravel-rich submarine fan (Figure 2.14), the linear-source mud/sand-rich slope apron (Figure 2.15), the linear-source sand-rich slope apron (Figure 2.16), the multiple-source mud/sand-rich ramp (Figure 2.17) and the multiple-source sand-rich apron (Figure 2.18).

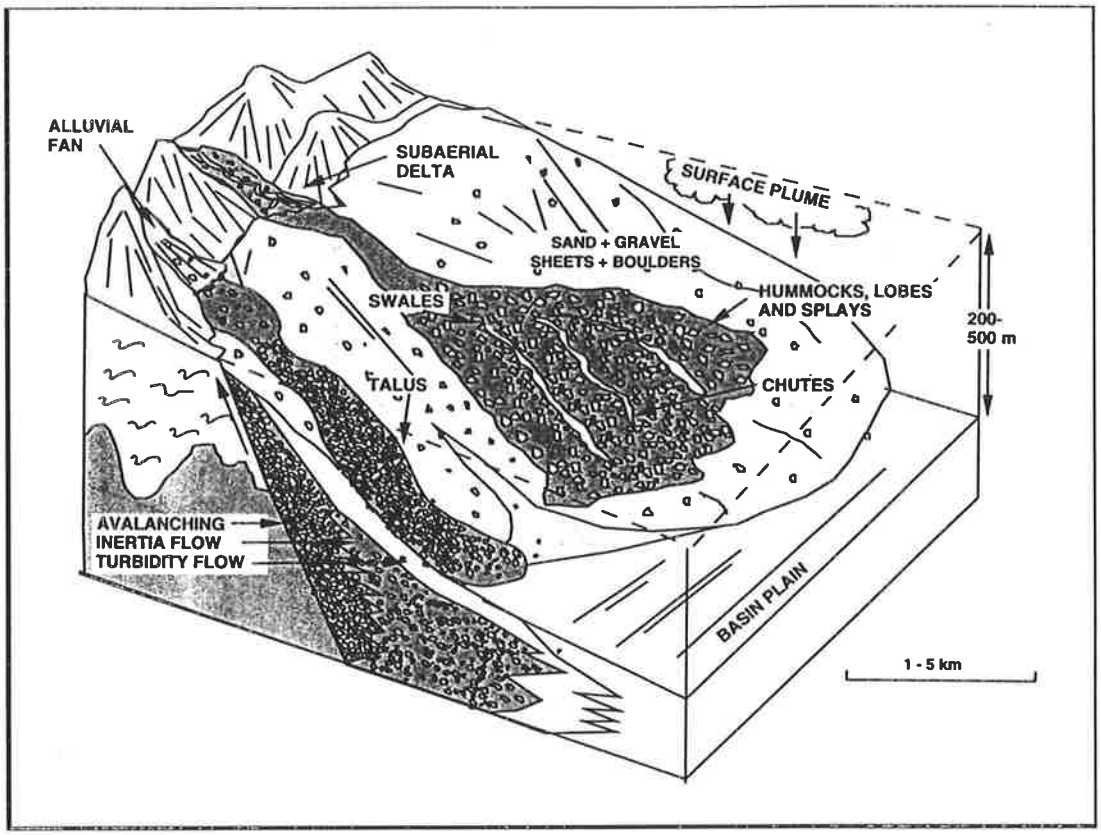


Figure 2.14. Depositional model for a point-source gravel-rich submarine fan (after Reading and Richards, 1994).

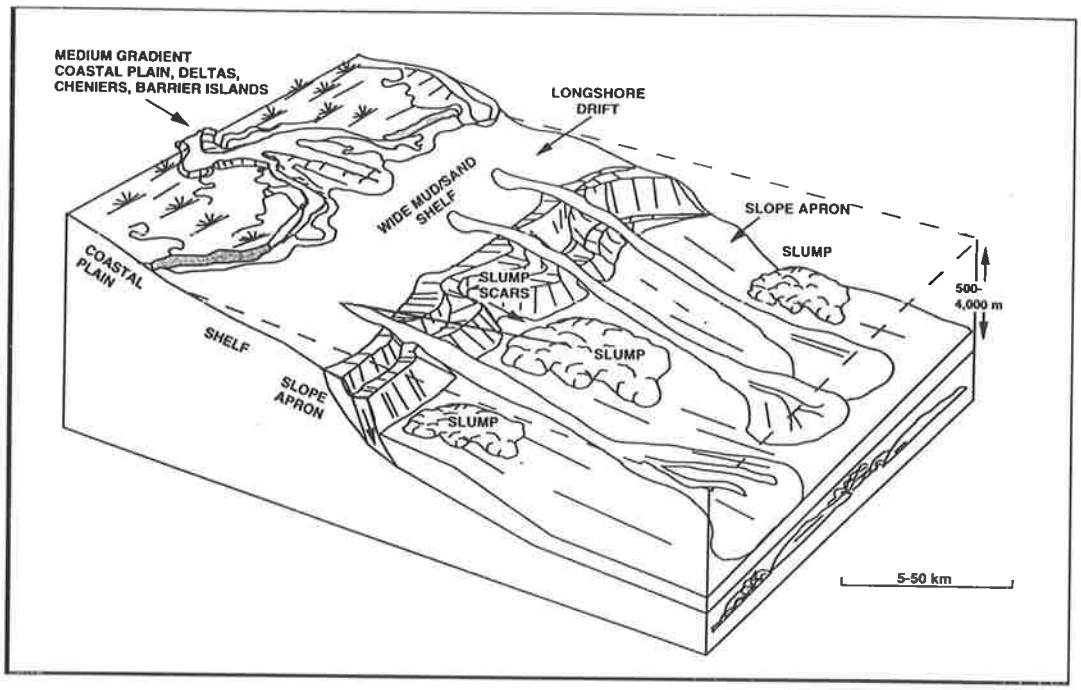


Figure 2.15. Depositional model for a linear-source mud/sand-rich slope apron (after Reading and Richards, 1994).

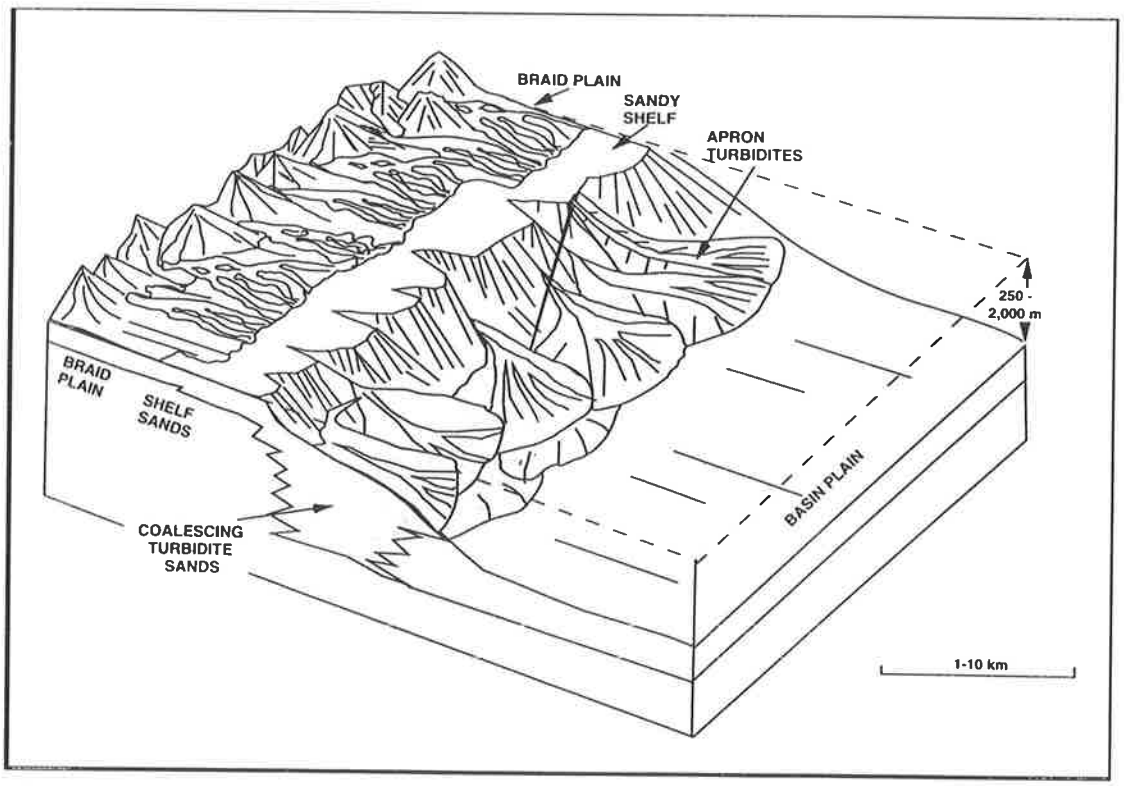


Figure 2.16. Depositional model for a linear-source sand-rich slope apron (after Reading and Richards, 1994).

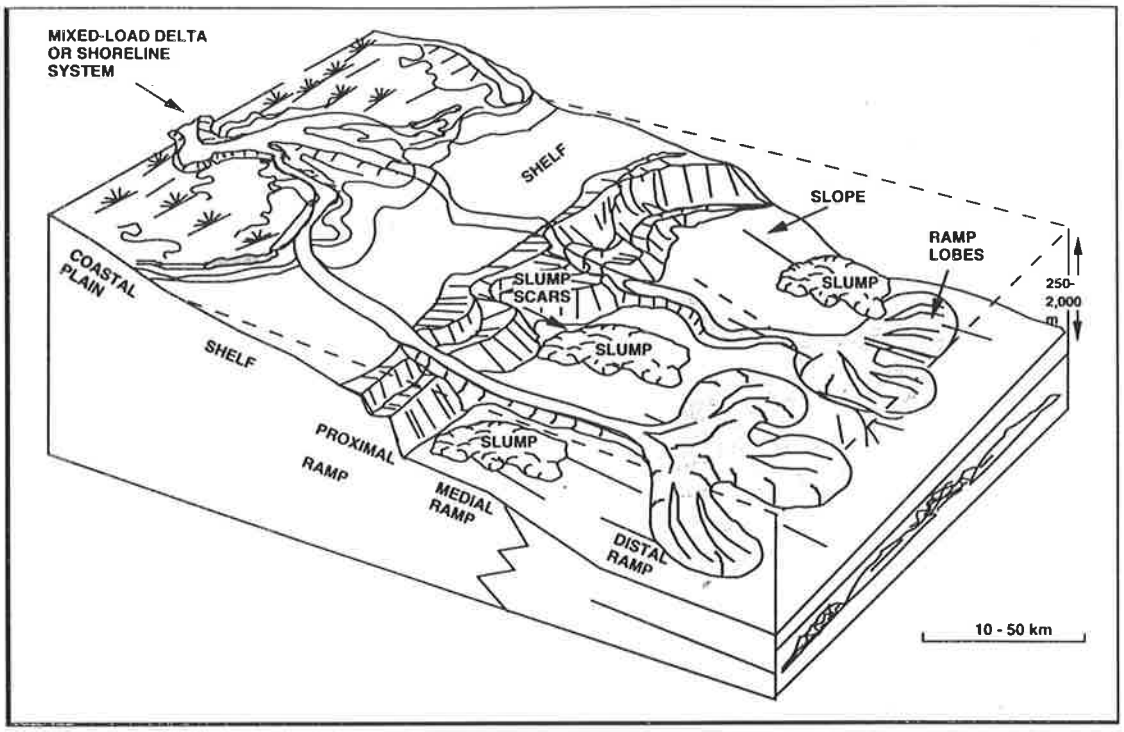


Figure 2.17. Depositional model for a multiple-source mud/sand-rich ramp (after Reading and Richards, 1994).

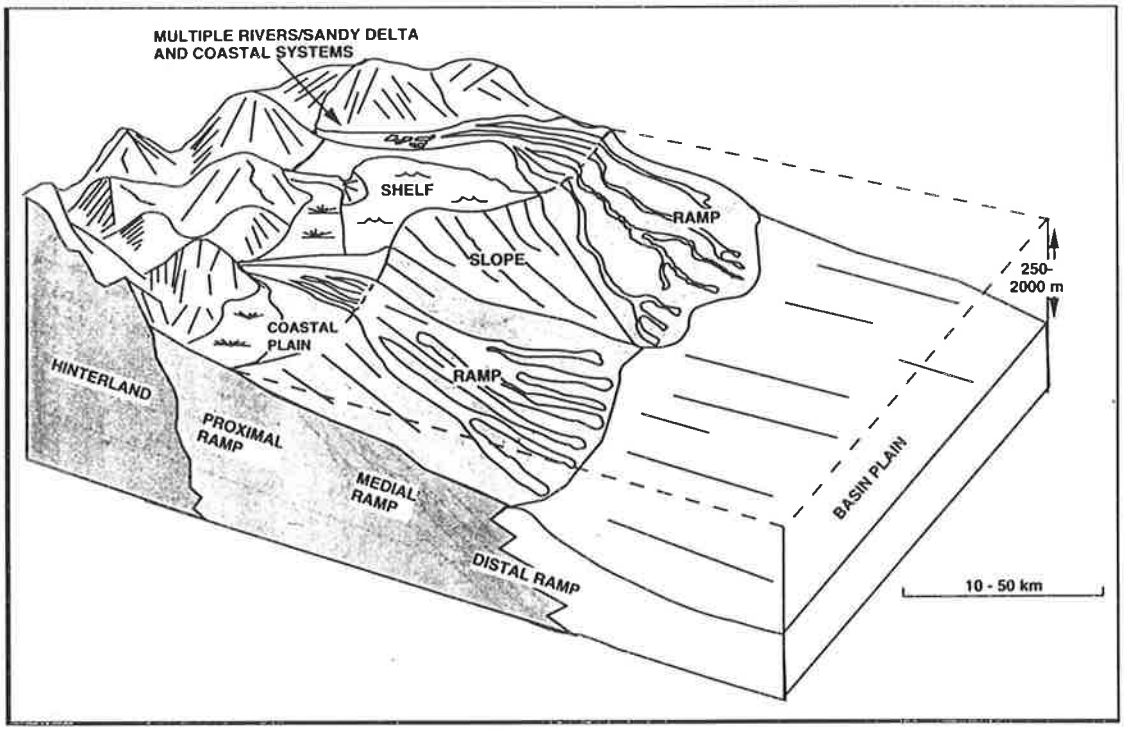


Figure 2.18. Depositional model for a multiple-source sand-rich slope apron (after Reading and Richards, 1994).

Aspects of these depositional systems that bear relevance to systems described in this study are not discussed here. However, these aspects will become apparent during the course of this thesis. In particular, it is suggested that Figures 2.14 and 2.15 be considered with respect to unit E2 of the Eliassen Formation, Figures 2.15 and 2.16 with respect to unit A6 of the Angel Formation, Figures 2.16 and 2.17 with respect to unit A5, Figures 2.17 and 2.18 with respect to units A3 and A4, and Figure 2.18 with respect to units A1 and A2.

CHAPTER 3: INTERPRETATION

CORE, SEISMIC AND WELL DATA

3.1 LITHOFACIES

3.1.1 Introduction

The lithofacies in this study ~~is~~ are primarily defined from core logs. This section is a summary of 501.3m (Table 1.2) of logged core that occurs within the Aptian to Callovian section over the study area. The locations of the wells containing cored sections over this interval is shown in Figure 3.1.

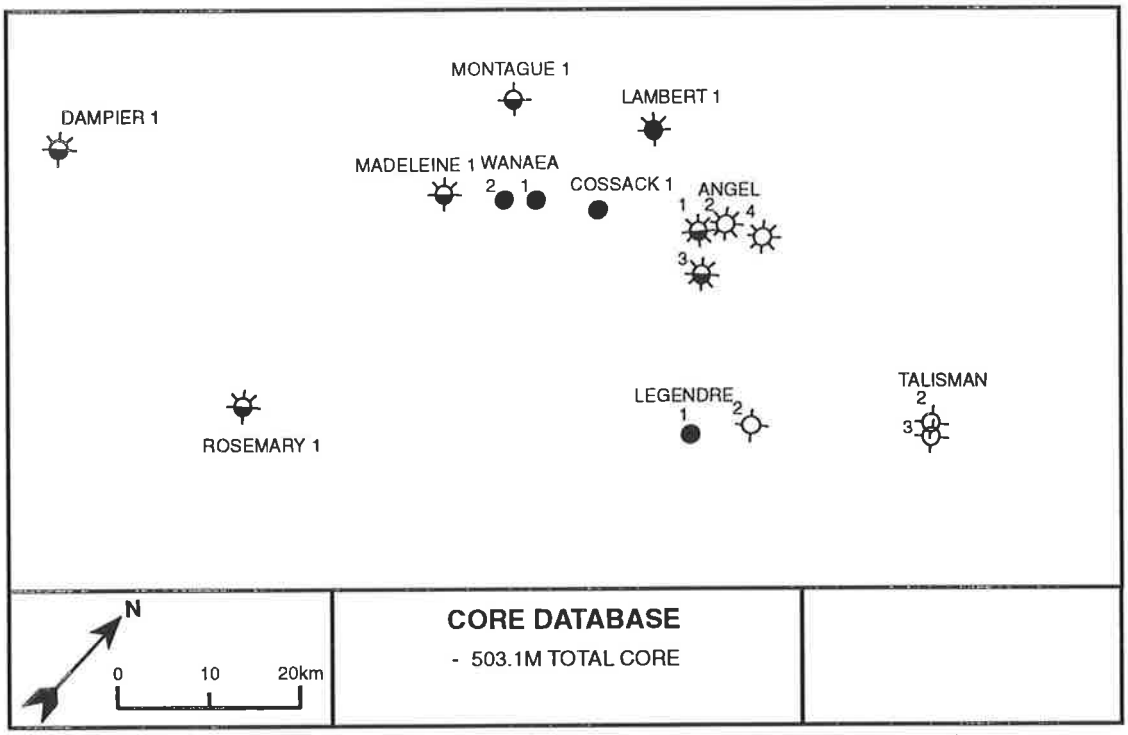


Figure 3.1. Distribution of wells for core that was logged during the project.

The core logs are found in Appendix I. They were drawn at either 1:50 scale or 1:100 scale. Photographs over pertinent sections of core are included with some of the core logs. The core was logged and described using Miall's lithofacies codes (1978).

Lithology, sedimentary structures, and ichnofacies, and large scale diagenetic trends were the focus of the logging. The primary objective was to identify depositional processes and environments of deposition. To achieve this objective, it was appropriate to class the variations of these given factors into the 'facies groups' and 'facies constituents' that were defined by Pickering et al. (1986, 1989) for deep water siliciclastic facies (Figure 3.2). By grouping these variations in the core set and placing them appropriately into this classification scheme, I imply the broad transport and depositional processes that Pickering et al. (1989) have described for each facies constituent.

Palynological interpretations by Morgan Palaeo Associates (1987 - 1993) that designate strata into nearshore marine or offshore marine environments are also considered. Morgan Palaeo Associates interpreted these environments by establishing the relative dinoflagellate diversities, where high diversities are considered to be offshore and low diversities are considered to be nearshore. Their Palynological Data Sheets were referred to for this information.

Additional interpretations were inferred from distinct features that are seen in the core. Trace fossils were noted to ascertain an approximate marine depositional setting. All of the various factors were then used to place the designated 'facies constituents' into appropriate depositional elements and environments.

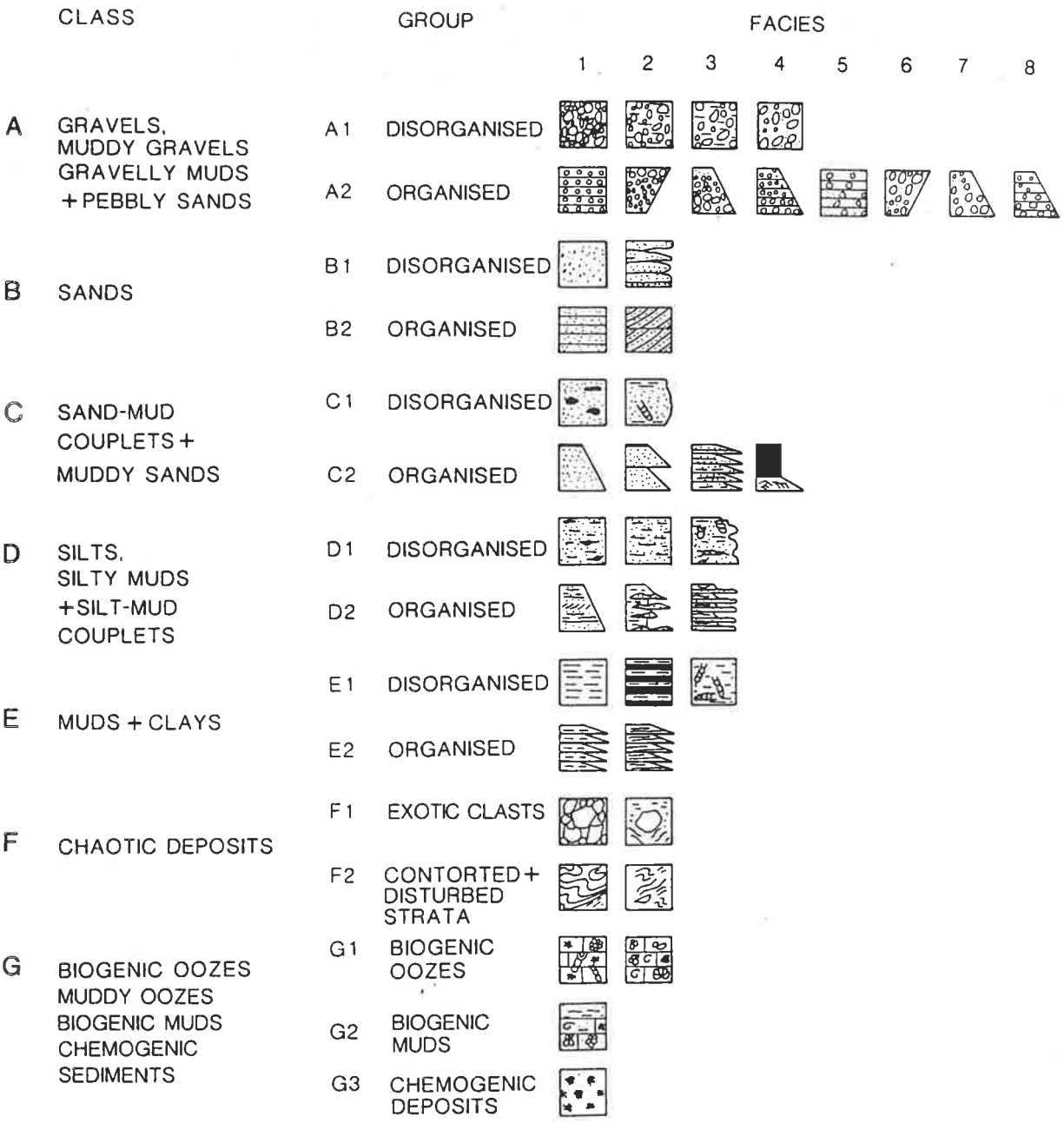


Figure 3.2. Classification scheme for deep water sediments used in this study. Classes A - E are defined on the basis of grain size, while class F is based on internal organisation, and class G is based on composition. Each 'group' is distinguished on the basis of the internal organisation of structures and textures. Each 'facies' is based on internal structures, bed thicknesses and composition (after Pickering et al., 1989).

Depositional elements were delineated by defining wireline log characters which are discussed in section 3.2. In order to associate depositional environments and processes to the log signatures, core logs were annotated to wireline logs at scales of either 1:100 or 1:200. These are found in Appendix II.

The distribution of core that exists over the mapped time units (Table 3.1) was considered to broadly represent the style of deposition that is associated with the defined depositional elements and systems in this thesis and to show the units exert the most control on lithofacies.

The following section is a description of the core with respect to their designated facies constituent. The allocation of core sections into these constituents is represented in Table 3.2. For the sake of brevity, the terms sand, silt and mud/clay are used here to describe the equivalent lithified rock types as seen in the core. In addition, the facies constituents are referred to in the text by letter and number only, thereby assuming that the reader knows that it is a facies constituent (e.g. 'B1.1' rather than 'facies B1.1').

Unit	Angel 1	Angel 2	Angel 3	Angel 4	Cossack 1	Dampier 1	Lambert 1	Legendre 1	Legendre 2	Madeleine 1
M_1										
M_2										
F			1			9		10	1	
A_1	1	1	2	1, 2	1, 2	10, 11	1			
A_2		3		2, 3, 4						1, 2
A_3										
A_4						12		11		3
A_5						13				4
A_6	3					14, 15,16				5
E_1								12, 13, 14		6, 7
E_2										8
C_1								16, 17, 18		

Unit	Montague 1	Rosemary 1	Talisman 2	Talisman 3	Wanaea 1	Wanaea 2
M_1						
M_2			3	1		
F			3, 4, 5, 6	2		1
A_1	1					2, 3, 4
A_2					1, 2	4
A_3						
A_4						
A_5						
A_6						
E_1						
E_2						
C_1		1, 2, 3				

Table 3.1. Distribution of cores representing the defined units in the study. Refer to Figure 3.13 for formation names and ages of given units.

	A2.1	B1.1	B2.1	B2.2	C1.1	C1.2	C2.1	C2.3	D1.1	D1.3	E1.1	E1.3	F2.2
Angel 1		1								1			3
Angel 2		1, 3											
Angel 3		2				2					1		
Angel 4		1, 2, 4	2, 3, 4			1				2, 3, 4			
Cossack 1		1,2					1, 2			2			
Dampier 1						10, 11				10, 11	9, 12, 13, 14, 15, 16		
Lambert 1		1											
Legendre 1	12		10, 11	16			13			14, 17	18		
Legendre 2		1											
Madeleine 1		2						5, 7			1, 4, 5, 6, 8	2, 3	
Montague 1			1										
Rosemary 1						2, 3			1, 2	3	1		
Talisman 2					3, 4, 5	3, 6							3, 4, 5
Talisman 3					2	1							2
Wanaea 1		2					1			1, 2			
Wanaea 2		4					2, 3, 4	2		2, 3, 4	1, 2, 3		

Table 3.2. Allocation of whole cores into the various facies classes of Pickering et al., (1989).

3.1.2 Results

Facies A2.1 - STRATIFIED GRAVEL Legendre 1, core 12.
Core 12 in Legendre 1 is a poorly sorted, pebbly to medium grained sandstone. It is massive with imbricated pebbles and granules. The imbrication is inclined at approximately a 30 degree angle of repose and decreases to horizontal at the base of the core. Pebbles and granules consist of quartz, jasper and lithic fragments suggesting a fluvial source from the Pilbara Craton. Up to 5% detrital glauconite occurs as medium grained sand, suggesting a marine shelf was an additional sediment source (Odin, 1984).

No trace fossils were identified, possibly due to the high energy of deposition. Palynology suggests a nearshore environment of deposition. The massive texture indicates a relative episodic deposition. This facies constituent indicates high concentration turbidity current transport with grain by grain deposition from suspension followed by traction transport as bedload (Pickering et al., 1989). This constituent is related to B2.2, and a higher energy, is suggested by the grain size.

The core interval occurs within a 7m bed as part of a 190m sequence comprising dominantly mud with 5 - 20m sand beds. The gamma ray signature is a smooth cylinder shape (refer to core to wire line log annotations, Appendix III.

Deposition of this facies probably occurred within the confines of a channel or chute on a relatively steep muddy gradient.

Facies B1.1 - THICK/MEDIUM BEDDED, DISORGANISED SANDS Angel 1 core 1; Angel 2 core 1, 3; Angel 3 core 2; Angel 4 core 4 (2772 - 2798.3m); Cossack 1 core 1, 2; Lambert 1 core 1; Legendre 2 core 1; Madeleine 1 core 2 (2981.8 - 2984.9m); Wanaea 1 core 2 (2894 - 2904m); Wanaea 2 core 4 (2919.5 - 2930m).

This is a massive sand that contains common dish structures caused by fluid escape, occasional 'floating' granules and clay rip up clasts, and rare coarse tail grading with small pebbles and granules concentrated in thin basal layers (Figure 3.5a). Grading is subtle fining up or absent. The sand is well sorted, fine to medium grained and quartzose which contains up to 5% detrital glauconite (Figure 3.5b), and often grades up to a slightly silty or muddy matrix.

B1.1 occurs as very thick sections of sand, commonly 20 to 100m thick in the Angel and Cossack area which are separated by thin clay splits. Over the Wanaea and Madeleine area, the sand breaks up into beds 1 - 20m thick. The gamma ray signature is a smooth cylinder shape and commonly displays variation of <5 API units. Bed contacts with silts and clays are well defined and the bases occasionally display soft sediment deformation such as flame structures, and ball and pillows.

Offshore indicators are noted in the palynology interpretation of this facies with the exception of the Wanaea 2 core which are all nearshore. Although no trace fossils were identified in this facies, silty and muddy sections have a mottled appearance due to burrowing. This facies is considered to have been deposited episodically, and so the ichnofacies identified in the interbedded silts and clays of C2.1, D1.3, and E1.1

(see facies descriptions) can be considered to indicate the relative marine position represented by these massive sands.

The B1.1 facies implies a transport process of high concentration turbidity currents. The depositional process is rapid mass deposition due to intergranular friction (or freezing) in a concentrated dispersion near the bed. This results in an open grain packing that may later collapse, forming fluid escape structures due to the escape of surplus pore fluids (Pickering et al., 1989). This group of rocks has characteristics that are transitional to B2.1, as in the cores of Cossack 1.

B1.1 in this area is probably associated with non-channelised areas of decelerating sediment flow, such as the mouths of distributary chutes or channels, where depositional lobes tend to form (Shanmugam et al., 1988; Mutti and Ricci Lucchi, 1972).

Facies B2.1 - PARALLEL-STRATIFIED SANDS Angel 4 core 2, 3, 4 (2721 - 2772m); Legendre 1 core 10, 11; Montague 1 core 1.

B2.1 is transitional and interbedded with B1.1. The lithology is identical to B1.1 sands. It is distinguished from B1.1 by the presence of scoured bases with common rip up clasts and granules of clay, and by common faint horizontal and inclined planar bedding. The Angel 4 core has approximately 51m of continuous section of B2.1. It predominantly consists of 7 to 10m sections of sand that are separated by .1 to 1m thick silt beds of D1.3.

Bedding commonly occurs within 1 to 2m of the bed base or top. The middle of the sand beds are typically massive like B1.1. For example, 2758.4 to 2769.6m in Angel 4 consists of a soft sediment deformed contact at the base, and contains scoured bed contacts 1 to 5m apart within the section. Granules tend to occur just above the scoured base that is commonly overlain by < .5m of inclined bedded sand that, in turn passes gradationally upwards into massive sand. The bedding is often accompanied by long and narrow clay rip ups (.5 x 3cm) that are imbricated parallel to the bedding planes. Near the top, faint horizontal bedding is commonly noted. The bedding is commonly faint, possibly owing to the lack of a significant grain size range. A typical sequence of B2.1 is represented in Figure 3.3.

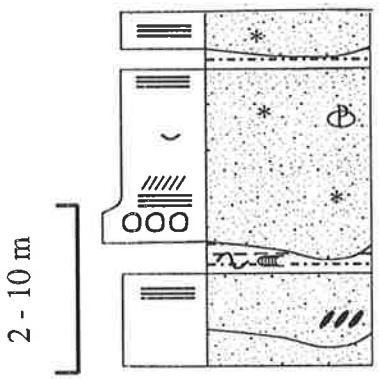


Figure 3.3. Typical vertical successions noted in B2.1. See Appendix I for symbol codes.

Grading of B2.1 appears to be dominantly absent, with the exception of a subtle upward-fining up unit in Core 11 of Legendre 1.

B2.1 occurs over the Angel area, comprising very thick sections of sand 20 to 100m thick, and coexists with B1.1. The gamma ray signature for B2.1 is noted as a bumpy cylinder shape, having common 5 to 10 API unit variation, distinguishing it from the smooth cylinder shape of B1.1.

Ripple cross-stratification is rarely associated with horizontal bedding (Legendre 1 core 11 2127.5m and Angel 4 core 3 2771.2m). The Montague 1 core, unique to other representations of B2.1, is a fine to very fine grained, well sorted sand. It displays possible polymodal trough cross bedding, suggesting multi-directional currents (Figure 3.5c).

The matrix of B2.1 is typically clean and porosity is commonly near 20%. However, core 10 and 11 of Legendre 1 contains a slightly muddy matrix of kaolin, and porosity is occasionally reduced to 10%. Core 10 at Legendre 1, being from the younger Talisman Sand Member rather than the Angel Formation, contains up to 20% glauconite.

No trace fossils were identified in B2.1 due to the episodic nature of deposition and lack of mud. Offshore marine indicators are noted in the palynology reports with the exception of the Wanaea 2 cores.

The implied transport process of the B2.1 Facies is high concentration turbidity currents. The depositional process is 'freezing' of successive traction carpets at the base of the flow. Intense grain interaction produces strong imbrication and, although not seen in this core, inverse grading. The structureless sections are due to rapid fall out from suspension, like B1.1 (Pickering et al., 1989).

It is likely that B2.1 in this area makes up amalgamated and braided channel and chute sands over a gradient. These commonly form sheet sand geometries according to Shanmugam et al. (1988).

Facies B2.2 - CROSS-STRATIFIED SANDS Legendre 1 core 16.

The core interval occurs within a 40m thick sand unit within a sequence of silt, fine sand, and mud beds 10 to 40m thick. The gamma ray is generally moderate to high value with a serrated to irregular signature.

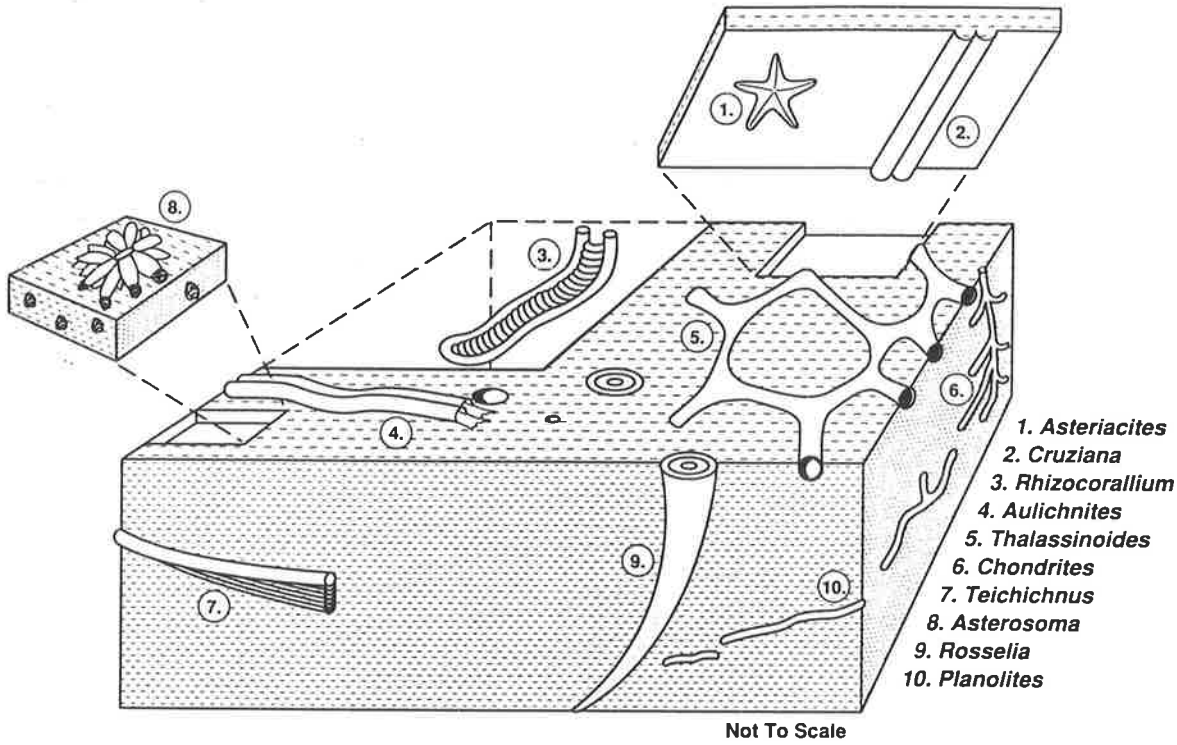
This core consists of a very well sorted, very fine grained quartzose sand. Bedsets 30 to 70cm thick over the full core interval consist of a scoured base with a thin massive sand bed overlain by a low angle, planar bedded unit. The top 10 to 30cm of the bed set is highly bioturbated. Microfaulting and intraformational breccias occur within a few of these units, suggesting mild, incipient slumping. Palynology indicates a near shore environment of deposition.

The transport process implicated by the B2.2 Facies is bed-load transport beneath dilute turbidity currents. Deposition occurs as intermittent suspension transport of grain dispersions over bedforms and into scours (Pickering et al., 1989).

Horizontal and subhorizontal burrows such as possible *Teichichnuss, Rhizocorallium,* and *Rosselia* trace fossils are noted (Figure 3.5d). These fall into the *Cruziana* ichnofacies (Figure 3.4). This ichnofacies can occur in shallow waters below fair weather base but above storm wave base according to Pemberton et al., 1992.

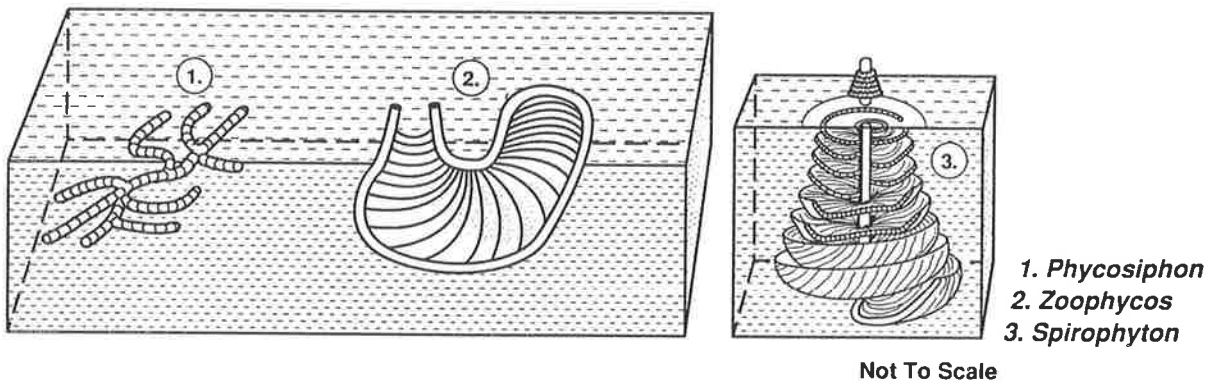
Low angle cross-bedding with any divergent, curving laminae would suggest hummocky cross stratification. However, the cross bedding noted in this core interval suggest waning flow such as episodic turbidity currents or storm derived currents that are interluded by quiescent periods and intense bioturbation. The palynology and suggested ichnofacies favour a relatively shallow water environment of deposition. This interval is therefore interpreted to have accumulated on a storm influenced shelf, below normal wave base.

a)



***Cruziana* Ichnofacies**

b)



***Zoophycos* Ichnofacies**

Figure 3.4. Trace fossil association characteristics of the a) *Cruziana* and b) *Zoophycos* ichnofacies (after Pemberton et al., 1992).

Facies C1.1 - POORLY SORTED MUDDY SANDS Talisman 2 core 3, 4, 5; Talisman 3 core 2.

C1.1 is noted as a poorly sorted, sandy and glauconitic mud (Figure 3.5e). It occurs interbedded with debrites defined as F2.2 in beds .5 to several metres thick. Convolute laminations are noted in silty sections, and wavy horizontal lamination is common in relatively massive sections. These features give the rock a 'swirled' appearance of that described by Pickering et al. (1989).

Chondrites burrows occur occasionally, some of which are pyritized, in massive mud sections. The pyritization and low diversity of these burrows suggests an anaerobic environment of deposition.

The gamma ray signature is a high value serrated character. The above core intervals occur within the Forestier Claystone. They are 20 to 45m thick muddy sections that separate the Birdrong/Mardie Sand Members from the Talisman Sand Member. Palynology indicates a marine environment of deposition.

The transport process for the C1.1 Facies is mud rich, very high density turbidity currents or fluid sand-mud debris flows. The depositional process is rapid mass deposition due to increased intergranular friction or cohesion where the deposit remains sufficiently plastic for gravitationally induced loading to occur (Pickering et al., 1989).

C1.1 as observed here was possibly deposited in relatively deep water where there was a steep gradient and where sediment was sourced from hemipelagic deposition mixed with a near-shore influence.

Facies C1.2 - MOTTLED MUDDY SANDS Angel 3 core 2 (2754.5 - 2755.7m); Angel 4 core 1 (2704.3 - 2706.7m); Dampier 1 core 10 (2901.4 - 2905m), 11 (3063.5 - 3070.9m); Rosemary 1 core 2, 3; Talisman 2 core 3 (1994 - 2007.5m), core 6; Talisman 3 core 1.

C1.2 is associated with B1.1 in the Angel area and D1.2 in the Dampier and Rosemary cores. It is typically a fine to very fine grained quartzose sand with a muddy matrix with intense bioturbation (Figure 3.5f). This gives the facies a characteristic 'mottled' appearance. Wavy horizontal laminations are also noted. The sections in the Talisman cores are 'greensands' that contain 30 - 40% detrital and diagenetic glauconite. They are fine to coarse grained, poorly and well sorted, and argillaceous.

Palynology indicates variable offshore and nearshore marine environments of deposition. Distinct trace fossil identification is limited, however *Terebellina* and *Planolites* are noted in the Angel cores. The general appearance of the bioturbation and these trace fossils is characteristic of the distal *Cruziana* ichnofacies.

The gamma ray signature is commonly flat and irregular. When C1.2 is noted to be associated with B1.1, 2 to 8m thick B1.1 beds are interbedded with .5 to 5m C2.1 beds. These bed contacts are gradational.

The transport process for the C1.2 Facies is winnowing of fines and short, repeated bed-load transport of sands by strong bottom currents. The depositional process is grain by grain deposition of coarse load and thorough post-depositional mixing of sand and mud by burrowers (Pickering et al., 1989).

C1.2 is interpreted from the palynology, ichnofacies and depositional processes to have occurred at varying positions on a marine shelf during periods of waning mass flow sand deposition. This waning occurred when sediment supply ceased or was redirected during transgression or tectonically quiescent periods.

Facies C2.1 - VERY THICK AND THICK-BEDDED SAND-MUD COUPLETS

Cossack 1 core 1, 2 (transitional with B1.1); Legendre 1 core 13; Wanaea 1 core 1; Wanaea 2 core 2, 3, 4.

C2.1 consists of sand beds .2 to 2m thick, typically interbedded with relatively thicker silt and clay beds of D1.3 and E1.1. It is also transitional to the B1.1 sand in the Wanaea and Cossack areas. By definition, C2.1 normally contains Bouma turbidite divisions 'a' and 'b' (Bouma, 1962). It is transitional with the more distal C2.2 which contains Bouma 'T_{bcd}' divisions. Sections in Wanaea 2 core 2 and 3 are a variation that may be more appropriately C2.2, but are discussed here for simplicity. In the Wanaea and Cossack areas, the C2.1 sand is lithologically identical to B1.1 and B1.2 there.

Grading is virtually absent in C2.1 which is unusual for rocks containing Bouma turbidite divisions. Sand beds consist of a massive and/or faint horizontal bedded base that are occasionally overlain by a thin cross bedded section. Soft sediment deformation is common, with occasional sand balls and flame structures.

Legendre 1 core 13 consists of graded beds with poorly sorted, dominantly coarse sand at the base, grading upwards to well sorted dominantly fine sand. The bases are scoured, contain rip up clasts and severe soft sediment deformation structures. Porosity is generally poor due to an argillaceous matrix.

Palynology indicates both nearshore and offshore environments of deposition, depending on the well. This may be the result of one of two factors. Conditions may be transitional, resulting in a subjective interpretation, since many interpretations were based on qualitative dinoflagellate diversity charts. Alternatively, the palynological sample points may consist of resedimented nearshore indicators in an offshore environment. These two factors are particularly controversial in the Wanaea area, where Wanaea 2 and 3 indicate nearshore conditions and while the more proximal Wanaea 1, and Cossack and Angel areas are all offshore.

The latter interpretation is the most favoured, particularly due to the resedimented nature of these facies. This problem exists also in other areas containing turbidite sequences. In an area of the North Sea, for instance, 18 of 20 interpreted samples were considered nearshore in a suspected offshore setting (Roger Morgan, pers. comm.).

The gamma ray signature of C2.1 is a highly serrated spike character. At large scale, it however appears cylindrical.

The transport process implied by the C2.1 Facies is high concentration turbidity flows (Pickering et al., 1989). This facies possibly occurred in areas fringing sand rich depositional lobes. An exception to this interpretation is shown by Legendre 1 core 13, thought to represent more proximal deposition such as within an interchannel area and may be part of a crevasse splay or a meandering channel within a muddy wedge during relatively mud-rich sedimentation.

Facies C2.3 - THIN-BEDDED SAND-MUD COUPLETS Madeleine 1 core 5, 7; Wanaea 2 core 2.

Facies C2.3 is defined as consisting of sand beds less than 10cm thick with Bouma T_{bc} and less frequently, T_a divisions. In the core, the sand is well sorted, fine to very fine grained, and is interbedded with E1.1. Ripple cross lamination and convoluted laminations are typical. Palynology indicates an offshore setting.

The high gamma ray signature displays an irregular to slightly serrated character.

Facies C2.3 is transported by relatively dilute turbidity currents with a depositional process of grain by grain deposition from suspension, followed by tractional transport as bedload (Pickering et al., 1989).

C2.3 probably represents the deposition of distal turbidites in a basinal setting, periodically interrupted by hemipelagic sedimentation of E1.1.

Facies D1.1 - STRUCTURELESS SILTS Rosemary 1 core 1, 2.

These cores are from the Calypso Formation. D1.1 contains massive silt sections. Bioturbation varies from intense to minor. Gamma ray character is typically bumpy.

Rosemary 1 core 1 is a massive silt that is part of an approximate 60m section as defined by the wireline logs. Core 2 consists of silt beds .3 to 3m thick that are intensely bioturbated and with wavy horizontal lamination.

The transport process for Facies D1.1 is high concentration silt dominated turbidity currents or highly fluid silty debris flows (Pickering et al., 1989). Rapid mass deposition occurs from a concentrated dispersion.

D1.1 probably accumulated on a marine shelf below storm wave base. Palynology indicates a nearshore setting. Sedimentation rate was probably high and kept pace with subsidence.

Facies D1.3 - MOTTLED SILT AND MUD Angel 1 core 1; Angel 4 core 2, 3, 4; Cossack 1 core 2; Dampier 1 core 10, 11; Legendre 1 core 14, 17; Rosemary 1 core 3; Wanaea 1 core 1, 2; Wanaea 2 core 2, 3, 4.

The majority of this core consists of the Dingo Claystone, except Rosemary 1 core 1 and Legendre 1 core 17 which are from the Calypso Formation. D1.3 consists of mottled silts and silty muds. Some of the core sections may appropriately be classed as D1.2, but are grouped here for simplicity. D1.3 is transitional with C1.2 based on increasing grain size; and transitional with E1.3 with increasing mud.

Bedding of D1.3 is typically .2 to 8m thick and interbedded with B1.1, B2.1, C1.2, C2.1, and C2.3. Bed contacts are typically sharp. Wavy horizontal lamination and common intense bioturbation gives the rock a mottled appearance (Figure 3.5g).

Siderite nodules are common in the Wanaea core. Figure 3.5g displays *Chondrites* burrows through a siderite nodule. It suggests siderite formation shortly after deposition and within a few centimetres of burial. Syndepositional siderite formation indicates disaerobic water conditions. The relative size of the trace fossils above the nodule (relatively small), and the horizontal and shallow nature of the burrows would agree with this interpretation.

Intense bioturbation is ubiquitous in D1.3. Commonly identified burrows are *Chondrites, Planolites, Terebellina,* and *Rhizocorallium* . Abundant *Gastrochaenolites* are noted in Wanaea 2, core 4 (Figure 3.5h) which suggests the interval here is a 'firmground'. Likely *Zoophycos* is also noted occasionally. The above assemblage of trace fossils is common in the *Cruziana* Ichnofacies of the Pemberton et al. (1992) scheme (Figure 3.4a). In addition, the predominance of horizontal forms rather than inclined forms, and the presence of *Zoophycos* attests to a possible distal *Cruziana* assemblage. *Cruziana* is inferred to generally occur within the sublittoral zone of a marine environment (Pemberton et al., 1992).

D1.3 typically has a moderate to high, bumpy signature. It is primarily D1.3 that is the cause of the 'shale splits' between thick massive sands of B1.1 and B2.1.

Facies D1.3 implies long lived bottom currents as the transport process. Grain by grain deposition from suspension occurs with subsequent pervasive bioturbation destroying most of the original sedimentary structures (Pickering et al., 1989).

Palynology indicates both offshore and nearshore marine conditions. As with C2.1, the same interpretational problem may exist. Nearshore conditions are interpreted in the Wanaea 2, Legendre 1 and Rosemary 1 core, while the rest are all offshore marine. The offshore/nearshore discussion under the section for C2.1 is valid here.

The lithology, sedimentary structures, and trace fossil assemblage indicate a sublittoral environment of deposition. Sedimentation was slow and continuous which allowed intense bioturbation of the sediment. While wavy lamination may suggest an oscillatory influence, it may also indicate a continuous current that is typical for a longshore drift. This style of deposition was episodically interrupted by deposition of B1.1, B2.1, C1.2, C2.1 and/or C2.3 turbidite sands.

Facies E1.1 - STRUCTURELESS MUDS Angel 3 core 1; Angel 4 core 2 2722-22.7m; Dampier 1 core 9, 12, 13, 14, 15, 16; Legendre 1 core 18; Madeleine 1 core 1, 4, 5, 6, 8; Rosemary 1 core 1; Wanaea 2 core 1, 2, 3.

E1.1 occurs in core taken from the Forestier Claystone, Dingo Claystone and the Calypso Formation. It is generally a massive claystone that is transitional with D1.3 (for example, Dampier 1 core 9). Distal turbidites C2.1 and C2.3, and the D1.3 transition are commonly interbedded with E1.1. It is typically slightly silty, with silt occurring both within the matrix and as laminae. Bioturbation ranges from non-existent to slightly bioturbated. Micaceous and fissile sections are common. They are described as 'shale' in the core logs.

Shell fragments and Belemnite guards occur rarely to occasionally in E1.1. Disseminated pyrite and pyrite nodules are common. The Madeleine 1, Dampier 1 and Rosemary core are slightly calcareous and contain dolomite nodules. Septarian nodules are noted in Rosemary 1 core 1. Slickensides occur in Legendre 1 core 18, Madeleine 1 core 8, and Dampier 1 core 15, suggesting evidence of post-diagenetic faulting.

E1.1 typically has a high value, flat to wavy gamma ray signature. At small scale (1:2500), it shows a high value serrated character. This signature commonly occurs for several hundreds of metres, suggesting very thick sections of E1.1 with occasional beds of C2.3 and D1.3.

E1.1 is offshore marine as indicated from palynology. However, Dampier 1 core 9, Rosemary 1 core 1 and Legendre 1 core 18 are exceptions that contain nearshore marine palynological indicators.

Bioturbation in E1.1 is typically slight. Figure 3.5i shows *Planolites, Phycosiphon,* and *Spirophyton,* all of which are common in E1.1. *Chondrites* is also common throughout E1.1. This assemblage is common to the *Zoophycos* ichnofacies (Figure 3.4b). Zoophycos is commonly associated with areas of lowered oxygen levels in quiet water settings, such as across the shelf-slope break (Pemberton et al., 1992).

The transport process implied by Facies E1.1 is not clear, but may include thick, mud-rich turbidity currents and lateral transfer of hemipelagic material by deep water currents or sliding. Rapid deposition may result from ponding of mud rich turbidity currents in confined basins (Pickering and Hiscott, 1986).

E1.1 represents basinal hemipelagic sedimentation that occurred in the Dampier Sub-basin. Turbidites associated with E1.1 are commonly distal C2.1 and C2.3. This deposition probably occurred over the distal sublittoral zone to the maximum extent of the depocentre including any associated slope. The nearshore Facies interpreted in the Rosemary and Legendre core may have been physically near to the shoreline, but positioned near the base of a steep scarp under low energy conditions.

Facies E1.3 - MOTTLED MUDS Madeleine 1 core 2, 3.

E1.3 is closely related to E1.1, and is discussed in comparison to E1.1. E1.3 has a mottled appearance due to moderate to high bioturbation and sandy laminae (Figure 3.5j). The wavy, discontinuous laminae consist of very fine grained well sorted sand.

Bioturbation consists of dominantly *Planolites* and *Chondrites* burrows. The gamma ray signature is slightly more irregular than that of E1.1. At a small scale, it is indistinguishable from E1.1. The palynology indicates an offshore marine setting.

Contour currents are suggested as a transport process for Facies E1.3. Deposition occurred as settling of particles or particle aggregates from suspension with extensive post-depositional bioturbation (Pickering et al., 1989).

E1.3 is a variation of the basinal E1.1 and represents a slower rate of deposition noted by the increased bioturbation. The sand laminae suggest long lived low intensity currents such as contour currents.

Facies F2.2 - BRECCIATED AND BALLED STRATA Angel 1 core 3; Talisman 2 core 3, 4, 5 (2007.5 - 2048.2m); Talisman 3 core 2; Angel 3 (2770 - 2770.5m).

In the Talisman wells, F2.2 occurs as intraformational conglomerates and breccias that are interbedded with C1.1.

Angel 1 core 3 is a sand with brecciated clasts of the underlying clay. The sand matrix is muddy and has no visual porosity (Figure 3.5k).

The Talisman core contain abundant microfaulting and convoluted laminae in silty mud. Beds of .2 to .7m thick intraformational conglomerates or breccias are interbedded with relatively thicker beds of C1.1.

An interpreted slide block occurs in Talisman 2 at 2015.5 to 2019.5m. It is a section of sandy mud that is bound by soft sediment faulting and sheared surfaces and which directly overlies a contorted mud unit.

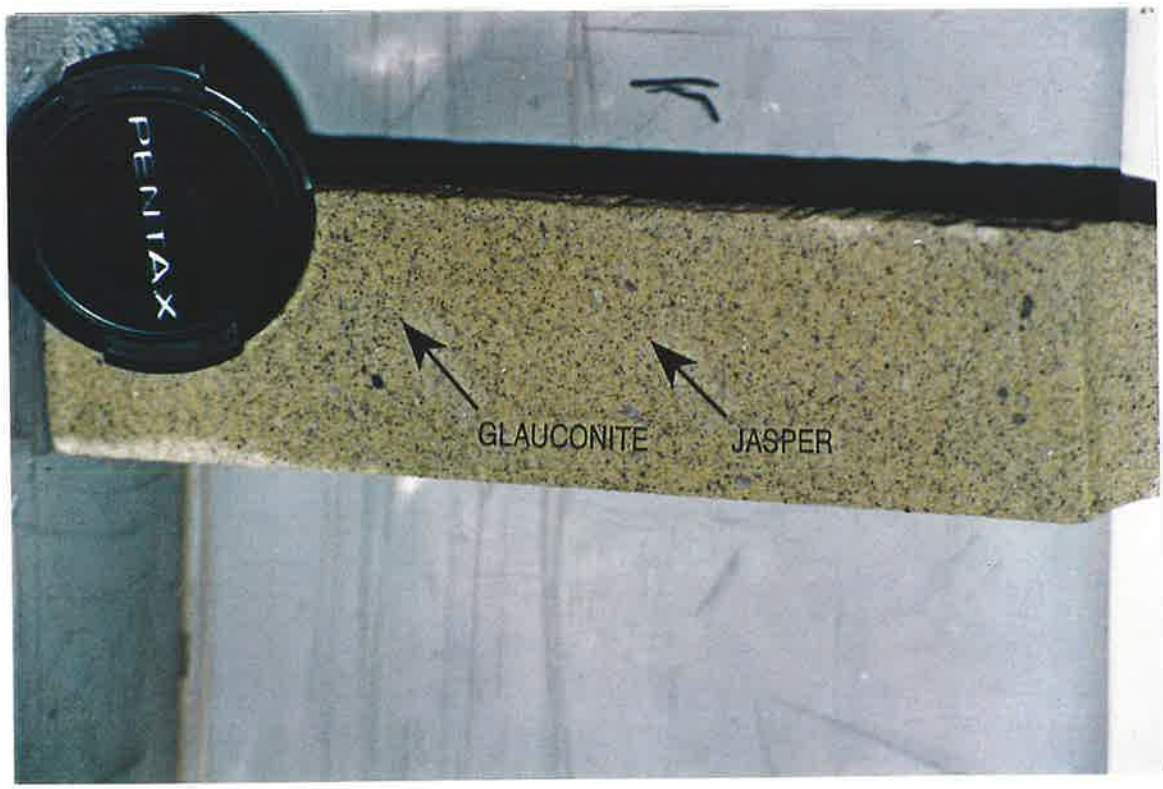
The gamma ray character is a high value, irregular and serrated one which appears 'ragged'. This ragged appearance is considered to be closely associated with debris flows and slide blocks. Angel 1 core 3 was cut below the total depth of the logging runs. Therefore, the log character was not observed.

In the Talisman core, F2.2 is attributed to sliding and slumping within a C1.1 setting. Angel 1 core 3 is more suggestive of a debris flow, where an overlying sand was eroding and picking up material from the underlying mud. This erosional surface is probably associated with the A_5 - A_6 unit boundary defined in this study (e.g. See Figure 4.19).

In both of the Talisman and Angel core, these gravity driven sediments are at or near a relatively steep gradient and are attributed to emplacement by tectonic activity or seismicity.



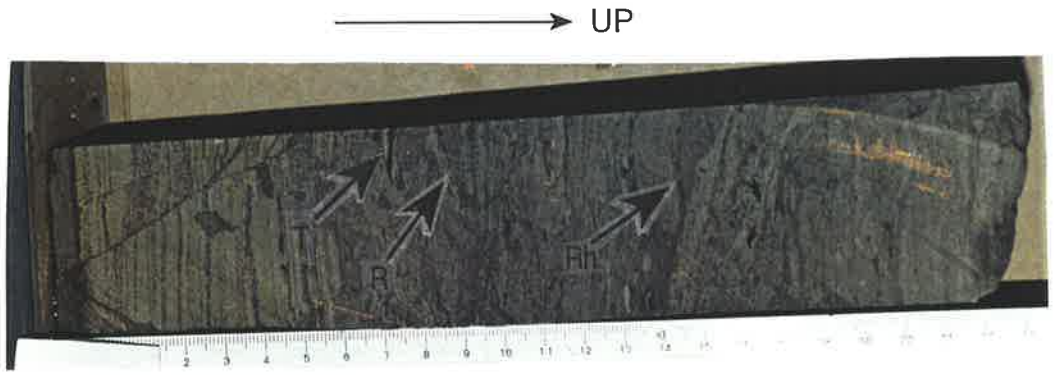
Figure 3.5. a) Angel 2 core 1, 2703.2m. Example of coarse tail grading that is occasionally noted in B1.1. Upper portion of core reveals a dish structure, a common occurrence in B1.1.



b) Typical B1.1 appearance with common floating quartz granules, detrital glauconite (dark green), and rare jasper fragments (red).



Figure 3.5. c) Possible trough cross bedding with multiple current directions, a unique example of B2.1.



d) Legendre 1 core 16, 2974.5m. Bioturbated unit with planar bedded sand of B2.2. Noted trace fossils include *Rosselia* (R), *Rhizocorallium* (Rh), and *Teichichnus* (T).

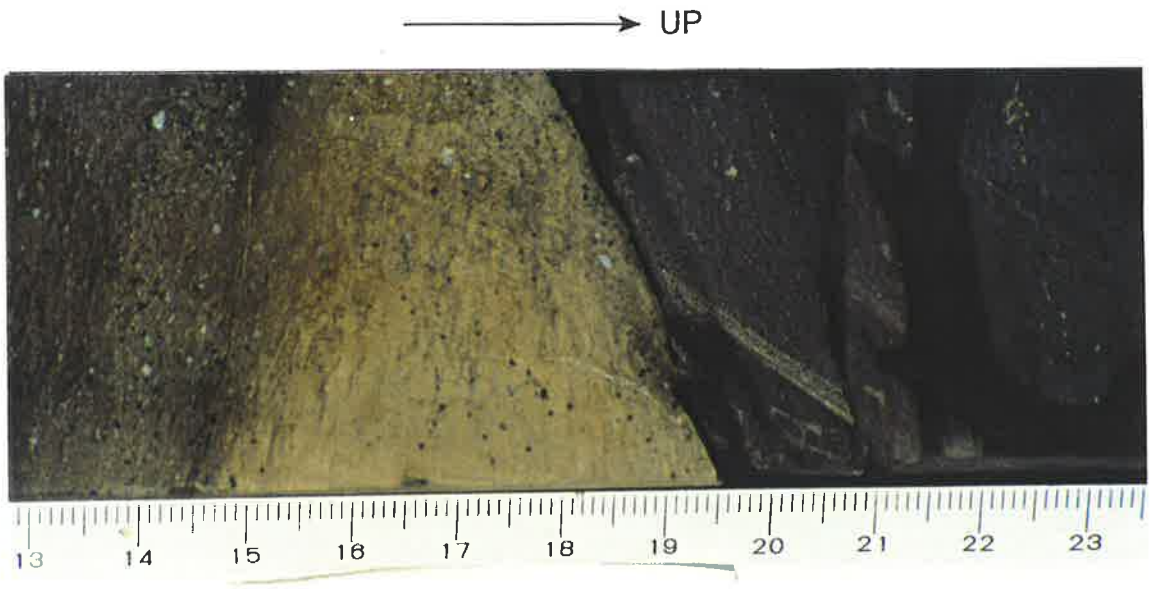
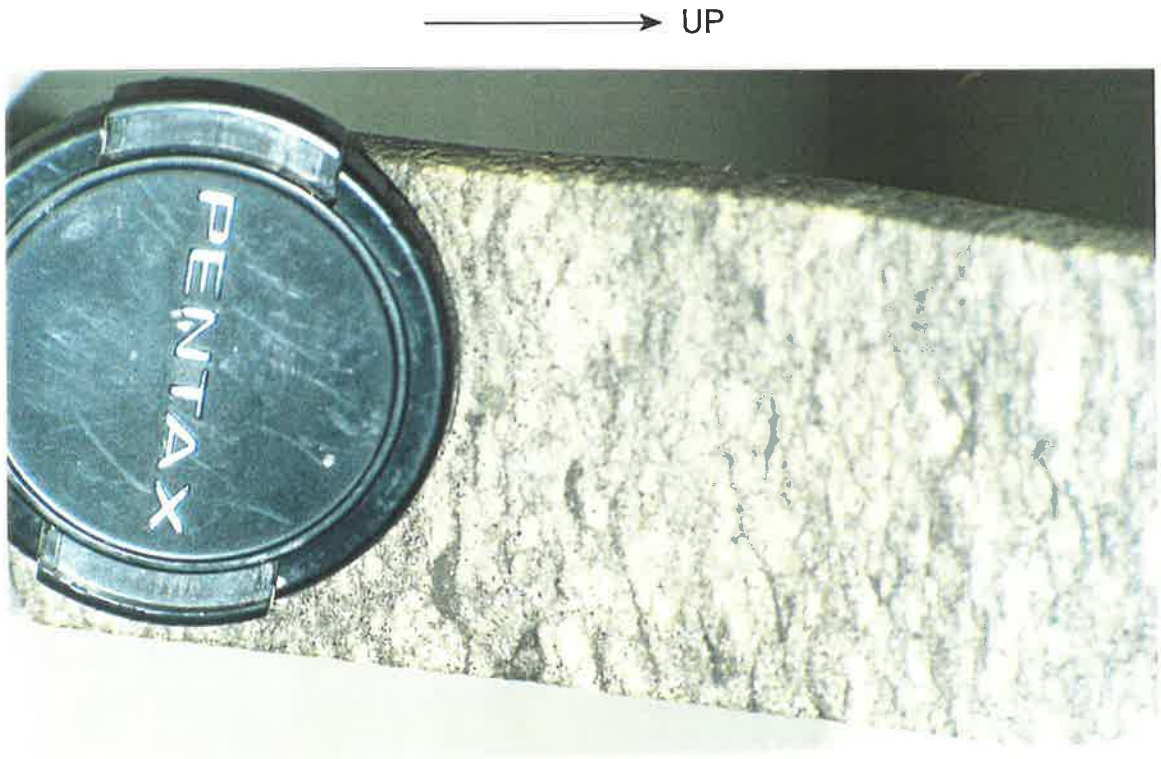


Figure 3.5. e) Talisman 3 core 2, 1971.2m. Typical C1.1 facies.



f) Angel 3 core 2 2755.3m. The highly bioturbated, mottled appearance of C1.2 is shown here.



Figure 3.5. g) Typical mottled appearance of D1.3. *Chondrites* burrowed into a siderite nodule near the core base. Thin Bouma 'T_c' unit occurs at the core base. Other noted trace fossils are *Terrebellina* (Te) and *Rhizocorallium* (Rh).



Figure 3.5. h) D1.3 with abundant *Gastrochaenolites* burrows, indicative of a possible firm ground.



Figure 3.5. i) Relatively high bioturbated example for E1.1. Noted trace fossils are *Planolites* (white specks), *Phycosiphon* (Ph), and likely *Spirophyton* (Sp).



j) Madeleine 1 core 3, 3186.2m. Mottled appearance of moderate to highly bioturbated example of E1.3. Note small sandstone core with a Bouma 'T_c' unit with small escape burrow.

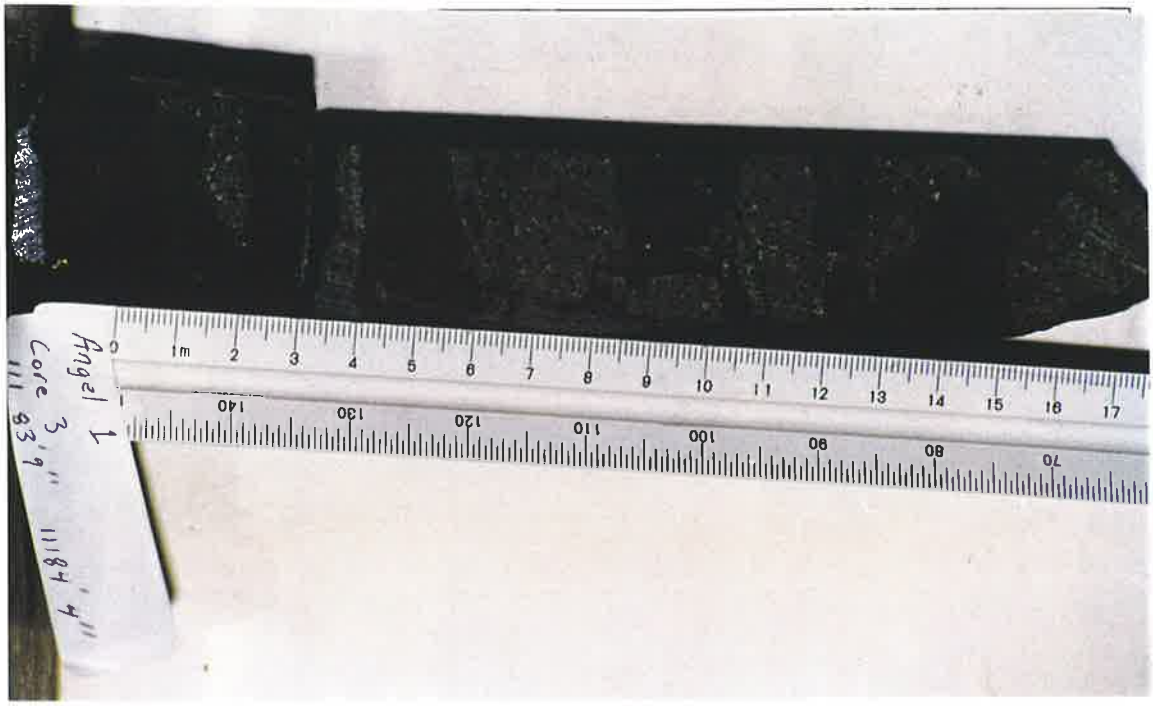


Figure 3.5. k) Angel 1 core 3, 3408.9m. Interpreted debris flow example of F2.2.

3.1.3 Conclusions

The various depositional facies and suggested associated settings observed in this study are outlined in Table 3.3. This chapter provides a basis for interpretation of wireline log signatures (discussed in Section 3.2) that may be used to infer depositional elements from these types of settings.

Facies Code	Depositional Setting
A2.1	Gravelly channels
B1.1	Depositional Sand Lobes
B2.1	Channelled Lobes
B2.2	Shelf Storm Sediments
C1.1	Slope
C1.2	Shelf Sands
C2.1	Fan Fringe Turbidites
C2.3	Distal Turbidites
D1.1	Shelf Silts
D1.3	Sublittoral
E1.1	Basinal Hemipelagic
E1.3	Basinal Contourites
F2.2	Slumps, Slides & Debris Flows

Table 3.3. The depositional facies that were identified in this study are indicated by the facies code. An interpreted and suggested depositional setting is indicated for each facies code. Note that these facies codes are not necessarily exclusive to the indicated depositional setting.

A striking aspect of this core set is the lack of grading observed in the sand. This is possibly the result of a texturally mature sediment source. In addition, it may be attributed to a ramp style of basinal resedimentation system that I refer to in this study. According to Hellar and Dickinson (1985), "ramp deposits generally lack the facies segregation of more familiar fan sequences, and rarely contain the asymmetric cycles observed in conventional fan sequences. They are instead composed of relatively monotonous sheets of sand, the average thickness of which gradually diminishes down ramp as the sand to shale ratio gradually decreases." This variation in style of submarine fan deposition is demonstrated in Figure 3.6.

The ubiquitous well sorted sand of the mass flow facies B1.1, which makes up a large portion of this core set, is attributed to a sand rich sediment source with a high degree of sediment recycling. B1.1, typically representative of the Angel Formation, was likely sourced from a shelf where a good degree of reworking occurred. This shelf area may have been closely associated with the area of deposition, located in a more proximal position on a relatively consistent gradient as implied by a 'ramp' setting. These sands may have undergone repeated mass flow events before becoming a part of the geological record.

The lack of grain size variation of B1.1 and B1.2 is considered to be the major cause of faint bedding. Bedding features are more easily seen if there is some variation of grain size in the sediment. If it were plausible, a study using x-ray tomography may reveal more information with respect to the style of bedding.

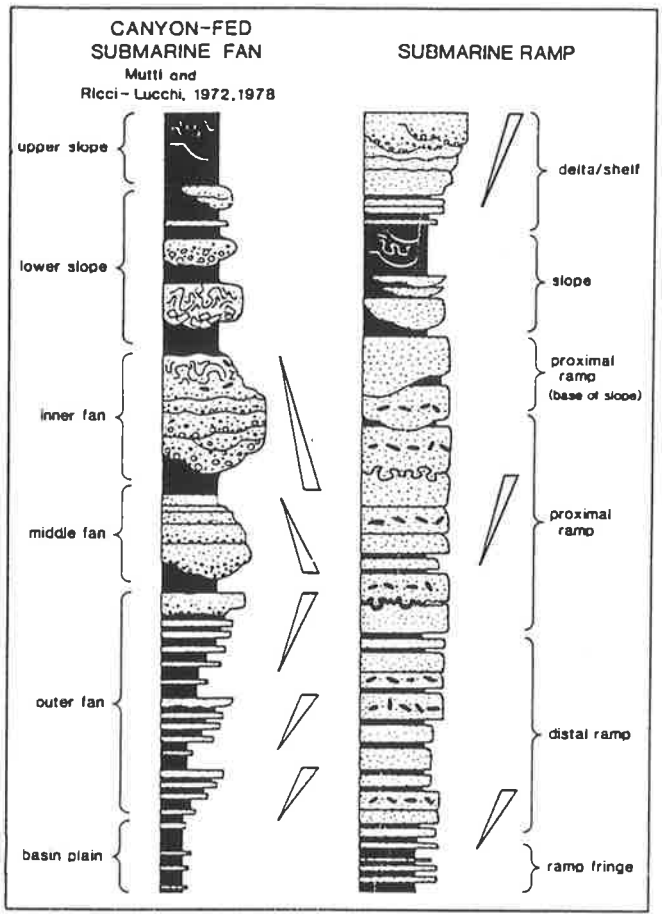


Figure 3.6. Schematic stratigraphic successions produced by prograding turbidite systems. The ramp style of fan has a ubiquitous lack of grading when compared to the more conventional 'canyon fed' submarine fan.

3.2 DEPOSITIONAL ELEMENTS

3.2.1 Introduction

In the previous section, the basinal setting was established with depositional sites ranging from the shelf, slope and basinal areas of a marine environment. Processes included traction currents, turbidites, hemipelagic sedimentation and gravity induced sediments. The depositional elements discussed in this section are described with respect to wire line log facies and includes: a) these identified processes and environments of deposition; b) general seismic knowledge of the area which indicates the relative basinal position of the well; and c) other studies of log profiles in marine resedimented successions. This information is integrated to characterise and establish wire line log facies in order to delineate various depositional elements. The interpreted depositional elements are subsequently referred to, with respect to the seismic facies that they occur in (section 3.4), and the various depositional systems that they comprise (section 4.1).

The depositional elements are primarily delineated and defined on the basis of gamma ray log character or 'wire line log facies'. In addition to the gamma ray log, other wire line logs such as the sonic, density, and dipmeter (where available) logs, were considered to a lesser degree during the interpretation. The term 'electrofacies' is defined by Serra (1970) as: "the set of log responses which characterises a bed and permits it to be distinguished from the others" (Serra, in Schlumberger Well Evaluation Conference, Algeria, 1979; Serra, 1984). All log responses that indicate the quantitative as well as qualitative aspects represent, therefore, the component elements of the electrofacies (Serra, 1984). In order to accommodate radioactivity based logs, I use the expression 'wire line log facies' here to replace Serra's term 'electrofacies'. It is important to note that, as other log motif based studies have stressed (e.g. Rider, 1990; Selley, 1979), direct diagnosis of the depositional setting from log profiles alone is not conclusive by any means. They are however useful to delineate vertical successions of rock based on log signature when annotated to core and ditch cuttings.

In addition to depositional elements, depositional surfaces such as unconformities, downlap intervals or condensed sections may also be qualified by noting wireline log 'breaks' that occur within, and more often, between wire line log facies. These are discussed in section 3.3.2 (Definition of Chronostratigraphic Horizons).

The gamma ray log response is often used by geologists to infer sandstone grain size trends and hence depositional facies (Rider, 1990). As Rider (1990) clarifies, the actual gamma ray signature is in response to the clay content, normally associated with finer grained sand. In addition, he notes that the gamma ray will also respond to the natural radioactivity of minerals such as glauconite, feldspars, and micas; minerals which commonly occur as sand grains. This further diminishes the assumption that gamma ray response can be associated to grain size trends. These factors are considered in this study. Although there is a not always a good relationship between grain size and gamma ray response, I consider that there is a good association of gamma ray signature to interpreted depositional elements. This association is however, indirect, and each depositional element is further supported

by lithological information. For the purposes of this study, relative gamma ray responses are referred to as 'fining upwards' and 'coarsening upwards' sequences (Figure 3.7), when successions may, in fact, be 'muddying upwards' or 'cleaning upwards'. This is particularly applicable here because of the lack of grading observed in core. Gamma ray responses that are suspected of being affected by detrital minerals are noted within the depositional element discussion.

The following discussion describes each depositional element with respect to the defined wire line log facies and lithologies and refers to the previous section on lithofacies. The depositional elements are listed with respect to the units or formations in which they occur, as well as with respect to the expected or known lithofacies that are to consist of (Tables 3.4 and 3.5). The primary source of the log profiles for this section is the stratigraphic log correlation cross sections (see Table 1.6, Enclosures IIIa to IIId, and/or detachable figures in section 4.1) which are at a vertical scale of 1:2500. These were also useful to observe lateral transitions that occur within and between the identified depositional elements. In order to observe the wire line response of the detailed sedimentological variations, core logs were annotated to wire line logs (Appendix II) at scales of 1:100 and 1:200 (see lithofacies section).

Figure 3.7 schematically defines the log response descriptors and should be referred to while reading the section. In addition, type examples of the gamma ray profiles for each of the depositional elements are displayed in Figures 3.8 and 3.9.

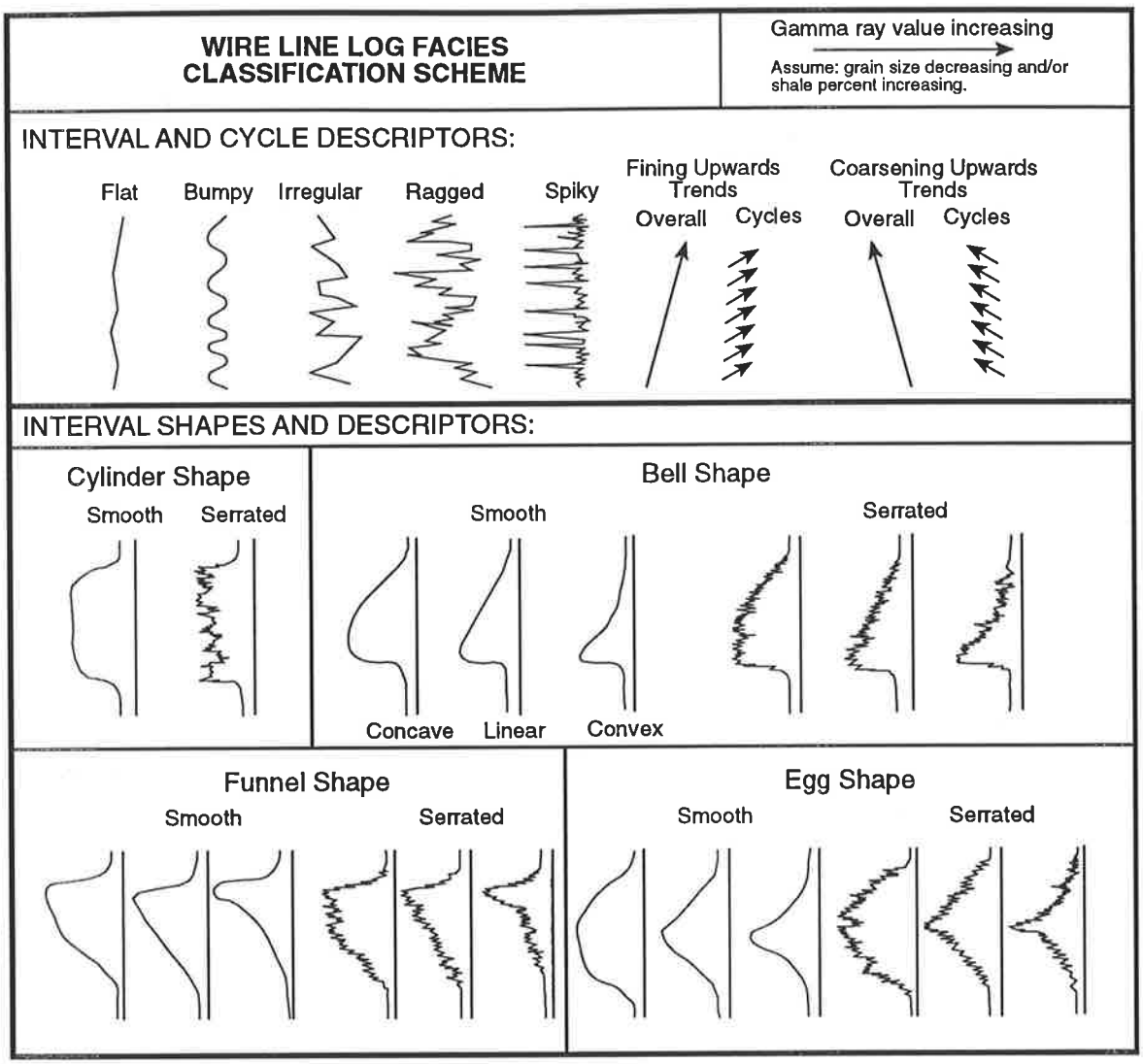


Figure 3.7. Schematic definition of wireline log profile shapes, descriptors, and symbols that are used in classifying wire line log facies (modified after Serra, 1984).

3.2.2 Results

	Depositional Element	M_1	M_2	F	A_1	A_2	A_3	A_4	A_5	A_6	E_1	E_2	C_1	C_2
1.	Hemipelagic Basin Fill	X	X	X	X	X	X	X	X	X	X	X	X	X
2.	Condensed Sections	X	X								X	X		
3.	Contourites or Levees		X									X		
4.	Distal Low Density Turbidites						X	X	X	X				
5.	Distal or Levee Channels and Crevasse Splays						X	X	X		X			
6.	Depositional Lobe Sheet Sands				X	X	X	X		X				
7.	Depositional Lobe Massive Sand				X	X								
8.	Braided Channels/Chutes					X	X	X						
9.	Channel Fill					X	X	X	X	X	X	X		
10.	Slope Apron Massive Sand						X		X	X				
11.	Slope Apron Braided Channels							X	X			X		
12.	Slope Apron Sandy Slides					X		X	X	X				
13.	Slope Apron Slides and Slumps					X	X	X		X				
14.	Slope Apron Drape			X				X						
15.	Retrograding Upper Slope Apron		X	X		X								
16.	Upper Slope Apron			X					X					
17.	Slope Channels	X	X											
18.	Aggrading Shelf												X	X
19.	Transgressive Shelf Sand		X											

Table 3.4. The depositional elements defined in this section and the various units that exhibit their known occurrence. Refer to Figure 3.13 for formation names and ages of unit abbreviations.

Depositional Element	A2.1	B1.1	B2.1	B2.2	C1.1	C1.2	C2.1	C2.3	D1.1	D1.3	E1.1	E1.3	F2.2
Hemipelagic Basin Fill								S		S	D		
Condensed Sections											D?	S?	
Contourites or Levees								S			S	D	
Distal Low Density Turbidites							D?	D?					
Distal or Levee Channels and Crevasse Splays	S		D?				S						
Depositional Lobe Sheet Sands		D					S	S		S			
Depositional Lobe Massive Sand		D	S			S				S			
Braided Channels/Chutes			D			S				S			
Channel Fill	S?		D							S			
Slope Apron Massive Sand		D?											
Slope Apron Braided Channels	S?		D										S?
Slope Apron Sandy Slides		S?											D?
Slope Apron Slides and Slumps		S?	S?										D?
Slope Apron Drape					S?	S?					D?		
Retrograding Upper Slope Apron					S?	D?							
Upper Slope Apron					S	D							S
Slope Channels			D?				S?						
Aggrading Shelf						S			S	D	S		
Transgressive Shelf Sand					D?	S?							

Table 3.5. The dominating lithofacies (D) and secondary lithofacies (S), observed in core that occurs within each depositional element. Entries denoted by '?' were not observed in core, but are expected to occur within the depositional element.

Hemipelagic Basin Fill

Typical examples: Dampier 1 3090 - 4144.5m (TD); Walcott 1 3425 - 3740m; (see Figure 3.8a).

Wire line log facies description: thick (commonly several hundreds of metres), monotonous sections of relative high gamma ray value which are slightly to moderately serrated.

Lithofacies: dominantly E1.1; may contain thin sections of C2.3 and/or D1.3.

Formations: Muderong Shale, Forestier Claystone, Dingo Claystone and Calypso Formation.

Gradational elements: Distal Low Density Turbidites, Contourites, Upper Slope Apron.

Hemipelagic Basin Fill consists of sedimentary successions that are dominated by hemipelagic sedimentation. Sediment influx is slow and continuous with periodic low density turbidites.

Condensed Sections

Typical examples: Finucane 1 2740 - 2813.5m; Walcott 1 2650 - 2710m; (see Figure 3.8b).

Wire line log facies description: relatively high gamma ray value, serrated and often egg shaped profiles. Compared to Hemipelagic Basin Fill, sonic values are relatively low, and density values are relatively high. Complete palynological zones are covered over one to several sample points (e.g. often < 5m).

Lithofacies: no core data available, but thought to be typical of E1.1 and E1.3. Ditch cutting descriptions indicate that these sections contain dolomitic, calcitic, and siliceous ~~rich~~ sediment zones. These zones often produce spikes on the sonic and density profiles. In relatively proximal wells, condensed sections are rich in glauconite sand (Mardie Greensand).

Formations: Muderong Shale units M_1 and M_2; Mardie Greensand.

Gradational elements: Hemipelagic Basin Fill.

Condensed Sections represent long periods of geological time with relatively little sediment influx. The condensed section described here is initiated above the Valanginian Disconformity. This disconformity represents a relative sea level flooding surface. In wells distal to sedimentation, the condensed section is a downlap interval.

Contourites or Levees

Typical examples: Legendre 1 1798 - 2000.5m; Lewis 1 2506.5 - 2742m; Madeleine 1 3937.5 - 4228m; (see Figure 3.8c).

Wire line log facies description: overall egg shape interval 100 to 250m thick which contains serrated, coarsening upwards trends 5 to 25m thick.

Lithofacies: C2.3, E1.1, and E1.3 (Madeleine 1 core 3, 7, and 8).

Formations: Muderong Formation unit M_2; Dingo Claystone unit E_2.

Gradational elements: Hemipelagic Basin Fill. It is differentiated from Distal Low Density Turbidites by the absence of sharp spikes on the gamma ray log.

Contourites are considered to form as a result of contour currents. Levees form as a result of channel induced currents. Both considered to occur in mud dominated systems. Contourites are differentiated from Levees by the basinal position of the well.

Distal Low Density Turbidites

Typical examples: Angel 1 3192 - 3409m; Lambert 1 3313.5 - 3400.5m; Walcott 1 3282.5 - 3439.5m; Wanaea 1 3129.5 - 3298.5m; (see Figure 3.8d).

Wire line log facies description: spiky character within a relatively high background of gamma ray values. Individual spikes appear sharp (average 1m thick), approach 'clean sand' gamma ray values, and typically fine upwards. Overall coarsening upwards cycles 10 to 20m thick are common. Unit thicknesses are of the order of one metre to several hundreds of metres.

Lithofacies: No core data are available within this depositional element. The Bouma turbidite successions characteristic of C2.1 and C2.2 are anticipated.

Formations: Dingo Claystone/Angel Formation transition (units A_3 A_6).

Gradational elements: Hemipelagic Basin Fill, Depositional Lobe Sheet Sands. It is differentiated from Levees by overall thickness and relative basinal position. Contourites are similar in appearance but do not display spikes.

Distal Low Density Turbidites are though to fringe depositional lobes. The sandy 'spikes' are expected to thin distally to zero thickness. This element is visibly limited to units A_3 to A_6 and lower A_2. This is considered to be, in part, a result of the style of deposition where channel/lobe complexes dominate.

Distal or Levee Channels and Crevasse Splays

Typical examples: Angel 3 2998 - 3041m; Lauchie 1 2368.5 - 2383m, 2749 - 2757m; Legendre 1 2174 - 2193m; (see Figure 3.8e).

Wire line log facies description: 7 to 10m thick spiky beds which have convex fining upwards trends or convex coarsening upwards trends. Fining upwards trends are associated with channels. Coarsening upwards trends are associated with crevasse splays.

Lithofacies: A2.1 and C2.1 are identified from Legendre 1 core 12 and 13. It is anticipated that B2.1 will also occur.

Formations: Angel Formation units A_3 to A_5; Eliassen Member unit E_1.

Gradational elements: may occur within levees of Contourites or Levees. It is differentiated from Distal Low Density Turbidites by the relative frequency and overall thickness of spikes in vertical sections.

Distal or Levee Channels and Crevasse Splays occur in relatively mud dominated systems, such as unit E_1. Crevasse splays represent more sand rich systems overlying abandoned channel complexes. Whether a spike is considered a distal channel, a channel within a levee complex, or a crevasse splay within a levee complex depends on several interrelated factors. These are: a) relative basinal position of the well; b) whether the system is sand or mud dominated; and c) whether the gamma ray spike is fining upwards or coarsening upwards.

Depositional Lobe Sheet Sands

Typical examples: Lambert 1 3083 - 3313.5m; Walcott 1 3006.5 - 3110m; Wanaea 1 2822 - 3069.5m; (see Figure 3.8f).

Wire line log facies description: slightly serrated cylindrical beds 5 to 20m thick separated by serrated beds 5 to 20m thick of relatively high gamma ray values. No vertical thickness trends are observed, suggesting aggradation. Grading is typically slightly coarsening upwards, slightly fining upwards, or absent. Unit thicknesses range from one metre to several hundred metres thick.

Lithofacies: sandy beds are represented by B1.1. Muddy successions contain C2.1, C2.3, and D1.3.

Formations: Angel Formation units A_1 to A_4.

Gradational elements: Distal Low Density Turbidites, Depositional Lobe Massive Sand.

Individual sand units are laterally continuous and decrease in thickness distally. Vertical successions are aggradational. These 'sheet sands' compose the distal portion of depositional lobes.

Depositional Lobe Massive Sand

Typical examples: Angel 1 2649 - 2935.5m; Angel 3 2735 - 2825m; Finucane 1 2982.5 - 3104m; (see Figure 3.8g).

Wire line log facies description: slightly serrated, cylindrical successions over the full interval of one metre to several hundred metres. Thin clay splits <1m thick occur sporadically every 40 to >100m. No vertical thickness or grading trends are observed which suggests aggradation.

Lithofacies: dominantly B1.1, and B2.1 to a lesser degree. Thin clay splits consist of C1.2 or D1.3.

Formations: Angel Formation units A_1 and A_2.

Gradational elements: Depositional Lobe Sheet Sands, Braided Channels and Chutes.

The Depositional Lobe Massive Sand ideally represents amalgamated massive sand that is deposited at the mouths of channels. They are thought to be the proximal equivalent of Depositional Sheet Sands. Both make up a depositional lobe. Vertical successions are aggradational.

Braided Channels and Chutes

Typical examples: Angel 1 2935.5 - 3192m; Angel 2 2932 - 3111.5m; Angel 3 2825 - 2984m; (see Figure 3.8h).

Wire line log facies description: slightly serrated, cylindrical intervals ranging from one metre to two hundred metres thick that contain thin clay splits and spiky sands 1 to 3m thick every 20 to 40m. Individual 20 to 40m thick cycles are usually fining upward. The character is similar to that of Depositional Lobe Massive Sand and clay splits are more frequent. Sandy cycles are more serrated and irregular in shape.

Lithofacies: Sandy beds are ideally represented by B2.1. Clay splits contain C1.2 and D1.3.

Formations: Angel Formation units A2, A3, and A4.

Gradational elements: Channel Fill; often occurs closely related to Depositional Lobe Massive Sand. In relatively more muddy systems (e.g. Angel 1 units A3 and A4, Angel 3 unit A4) it occurs with Depositional Lobe Sheet Sands. It is less serrated than Slope Apron Slides.

Braided Channels and Chutes are considered to form suprafan lobes or channelled lobes. These are also expected to form sheet-like sand body geometries (Shanmugam et al., 1988). They are very massive in sand rich systems, and contain increasingly more clay breaks with increased mud.

Channel Fill

Typical examples: Lauchie 1 2905 - 3003m; Legendre 1 1893 - 1969.5m, 2540 - 2680m; Lewis 1 2160.5 - 2314.5m; (see Figure 3.8i).

Wire line log facies description: slightly serrated to irregular cylindrical intervals 60 to 100m thick which contain thin clay splits commonly every 20 to 30 metres. Fining upwards shapes occur near the interval tops which are commonly succeeded by spiky sand beds approximately 5m thick. The character is similar to Braided Channels and Chutes, and is usually more serrated in shape.

Lithofacies: limited core information is available, however Legendre 1 core 10 and 11 consist of B2.1. A2.1 may also occur near some channel bases. Clay splits contain D1.3.

Formations: Eliassen Formation units E_1 and E_2; Angel Formation units A_2 to A_6; Talisman Sandstone Member.

Gradational elements: Braided Channels and Chutes; Slope Apron Sandy Slides. It is differentiated from Levee Channels And Distal Channels by overall cycle thickness.

Channel Fill is associated with areas of relatively steep gradients where channel incision was succeeded by sand deposition during the waning phase. They are commonly associated with slope apron successions (Figure 3.12). They often overlie and are interbedded with Slope Apron Sandy Slides.

Slope Apron Massive Sand

Typical examples: Lauchie 1 2208 - 2368.5m; (see Figure 3.9j).

Wire line log facies description: cylindrical intervals approximately 200m thick that contain slightly serrated and slightly egg shaped beds 40 to 50m thick (see Lauchie 1).

Lithofacies: no core data available. The occurrence of dominantly B1.1 lithofacies is anticipated. The sand sections in Lauchie 1 have low porosities and permeabilities due to an argillaceous matrix.

Formations: Angel Formation units A_2, A_5, A_6.

Gradational elements: Slope Apron Sandy Slides. It is differentiated from Depositional Lobe Massive Sand by the slight egg shape of the gamma ray log, basinal position, and the argillaceous matrix.

Slope Apron Massive Sand occurs down slope from Slope Apron Sandy Slides. It resulted from the transformation of relatively coherent sand rich slumps and slides to relatively liquefied muddy mass flow sands.

Slope Apron Braided Channels

Typical examples: Legendre 1 2699 - 2848.5m; Montague 1 3219 - 3766.5m; (see Figure 3.9k).

Wire line log facies description: 5 to 40m thick cylindrical intervals that are internally serrated and often fining upwards. These intervals are separated by relatively high value gamma ray clay splits 1 to 2m thick. Montague 1 has an overall fining upwards trend from 3428.5 to 3761.5m. Legendre 1 has a vertical aggradational trend.

Lithofacies: Montague 1 core 1, the only core within this signature, contains B2.1 with possible multi-directional trough cross bedding. This element may also contain A2.1 and F2.2.

Formations: Eliassen Member unit E2; Angel Formation units A3 and A4.

Gradational elements: Channel Fill. It is differentiated from Slope Apron Sandy Slides by containing shale splits and fining upwards sequences.

Slope Apron Braided Channels are defined on the basis of gamma ray signature and the relative basinal positions of the well locations that contain this element. Legendre 1 and Montague 1 are considered to be adjacent palaeo-scarps or slopes. The depositional element is considered to be a braided channel complex on a slope environment.

Slope Apron Sandy Slides

Typical examples: Forestier 1 2186.5 - 2394.5m; Samson 1 2129 - 2205m; Talisman 2 2075 - 2256m; (see Figure 3.9l).

Wire line log facies description: cylindrical intervals one to several hundred metres thick with slightly to moderately serrated and irregular internal character. The frequency of the serrations is characteristically intense.

Lithofacies: no core data available. Sandy lithologies of F2.2 are anticipated to occur here.

Formations: Angel Formation units A2, A4 to A6.

Gradational elements: Slope Apron Braided Channels; Slope Apron Slides and Slumps. It frequently displays a vertical association with Channel Fill. It can be differentiated from Braided Channels and Chutes by the intensity of serration of the gamma ray log.

Slope Apron Sandy Slides is defined on the basis of a unique wire line log facies which is associated with wells along the Legendre Trend. It is interpreted that the Legendre Trend was in the vicinity of a scarp or gradient during deposition of this element. An analogy is that of Shanmugam et al. (1994), where there is a description of slope related slump and debris flow lithofacies are described from the Upper Cretaceous of offshore regions of Norway. The gamma ray signatures of their Facies 2 (their Figure 5A, p. 916) have a strikingly similar character to this wire line log facies. Facies 2 is described as "contorted sandstone, fine to medium grained, steep layers, variable dips, shear zones, brecciated jumble of fragments, floating mudstone clasts, planar clast fabric, water-escape structures, sandstone dikes". The depositional process for Facies 2 is "sandy slump and debris flows (freezing, in a non-channelized slope environment;" Shanmugam et al., 1994). This same process is suspected here, based on the basinal position of these wells and the similar gamma signatures of the facies between the two areas.

Slope Apron Slides and Slumps

Typical examples: Forestier 1 2080 - 2137.5m; Lewis 1 2001 - 2149m; (see Figure 3.9m).

Wire line log facies description: highly irregular, ragged appearance with both sandy and muddy lithologies.

Lithofacies: no core data available. F2.2, and some B1.1 and B2.1 are anticipated to occur.

Formations: Angel Formation A2 to A4, A6.

Gradational elements: Slope Apron Sandy Slides, Upper Slope Apron.

This element contains both sandy and muddy lithologies associated with slumping on a slope environment. It is defined on the basis of log signature and slope association.

Slope Apron Drape

Typical examples: Legendre 1 1967 - 1974.5m; Lewis 1 2150.5 - 2160.5m; Samson 1 2308.5 - 2328.5m; (see Figure 3.9n).

Wire line log facies description: 5 to 20m thick serrated beds with overall high gamma ray values. Relatively high sonic and density values are also noted. It tends to occur between lower slope depositional elements (Slope Apron Braided Channels, Slope Apron Sandy Slides, and/or Slope Apron Slides and Slumps).

Lithofacies: no core data available. The log character is similar to that of the Upper Slope, and similar lithologies are inferred. These include C1.1, C1.2 and E1.1.

Formations: Forestier Claystone, Dingo Claystone unit A4.

Gradational elements: Distal or Levee Channels.

Slope Apron Drape is associated with depositional elements of the lower slope. In all noted cases, the top and/or bottom of the interval is a unit boundary. It is interpreted to be a relatively condensed sediment, deposited as drape when gravity induced sedimentation had ceased.

Retrograding Upper Slope Apron

Typical examples: Calypso 1 2212 - 2226m; Samson 1 2100 - 2119m; Talisman 2 1982.5 - 2005.5m; (see Figure 3.9o).

Wire line log facies description: serrated egg shape intervals 12 to 50m thick. Glauconite influences the gamma ray response.

Lithofacies: C1.1 and C1.2. It generally consists of >15% glauconite sand.

Formations: Angel Formation unit A_2; Talisman Sandstone; Mardie Greensand; Birdrong Sandstone.

Gradational elements: Upper Slope Apron.

Retrograding Upper Slope Apron is interpreted to occur at the base of upper slope apron deposits. It is deposited during periods of waning soft sediment deformation, sand supply and overall low sediment input. Contour currents may have been involved in reworking the glauconite rich sands.

Upper Slope Apron

Typical examples: Calypso 1 2089 - 2212m; Forestier 1 2020 - 2080m; Talisman 2 2005.5 - 2048.5m; (see Figure 3.9p).

Wire line log facies description: high gamma ray value, highly and intensely serrated. It can also be slightly irregular. Relatively high density values are noted.

Lithofacies: contains C1.1, C1.2, and F2.2 (Talisman 2 and 3 core).

Formations: Forestier Claystone, Angel Formation unit A_5.

Gradational elements: Hemipelagic Basin Fill, Slope Apron Slumps and Slides.

Upper Slope Apron occurs in wells that penetrate the Forestier Claystone along the Legendre Trend. It also occurs adjacent to the Rankin Trend (e.g. Montague 1). It is interpreted as outer shelf or upper slope apron sediments that were deposited as a result of a terminated sand supply to the basin.

Slope Channels

Typical examples: Orion 1 1688 - 1766m; Rosemary North 2012 - 2032m; (see Figure 3.9q).

Wire line log facies description: slightly serrated, cylindrical beds 5 to 20m thick. Fining upwards trends are common within the beds.

Lithofacies: no core data available; B2.1 and C2.1 are anticipated.

Formations: Birdrong Sandstone.

Gradational elements: this element is associated with a retrograding delta system. There are no defined gradational elements present.

Slope Channels occurs within a thick prograding (approximately 600m thick at Rosemary 1) wedge of dominantly hemipelagic mud or outer shelf and slope sediments. Foresets that correspond to this wedge are observed on seismic. These relatively cylindrical sands are interpreted to have been deposited within a relatively muddy system.

Aggrading Shelf

Typical examples: Legendre 1 2848.5 - 3245m; Samson 1 2700 - 3415.5m; Rosemary 1 2781.5 - 3252m (TD); (see Figure 3.9r).

Wire line log facies description: relatively high gamma ray value, spiky and highly serrated sections. Coarsening upwards cycles, and to a lesser degree, fining upwards cycles 5 to 10m thick are common. Slight egg shapes occasionally occur over 50 to 70m intervals. The dominant feature of this wire line log facies is overall vertical aggradation. Complete sections are very thick (e.g. 715m thick at Samson 1).

Lithofacies: C1.2, D1.1, D1.3, and E1.1 (Rosemary 1 core 1, 2 and 3; Legendre 1 core 16 and 17). Palynology indicates nearshore and marginal marine conditions.

Formations: Calypso Formation.

Gradational elements: Hemipelagic Basin Fill

Aggrading Shelf consists of very thick sections of overall aggrading shelf sediment. It is interpreted that tectonic influence was strong, and sediment influx kept pace with basin subsidence.

Transgressive Shelf Sand

Typical examples: Cygnus 1 1055 - 1147m; (see Figure 3.9s).

Wire line log facies description: intensely serrated, cylindrical to bell shape beds 10 to 30m thick.

Lithofacies: no core data available. Similar lithofacies to Retrograding Upper Slope Apron, incorporating C1.1, and C1.2 are anticipated. This section contains abundant glauconite and pyrite, vari-colored lithics including feldspar, and quartz grains are noted to be clear to frosted (Cygnus 1 Well Completion Report).

Formations: Birdrong Sandstone

Gradational elements: none.

Transgressive Shelf Sand is interpreted to be a transgressive marine sand on a marine shelf or shoreface.

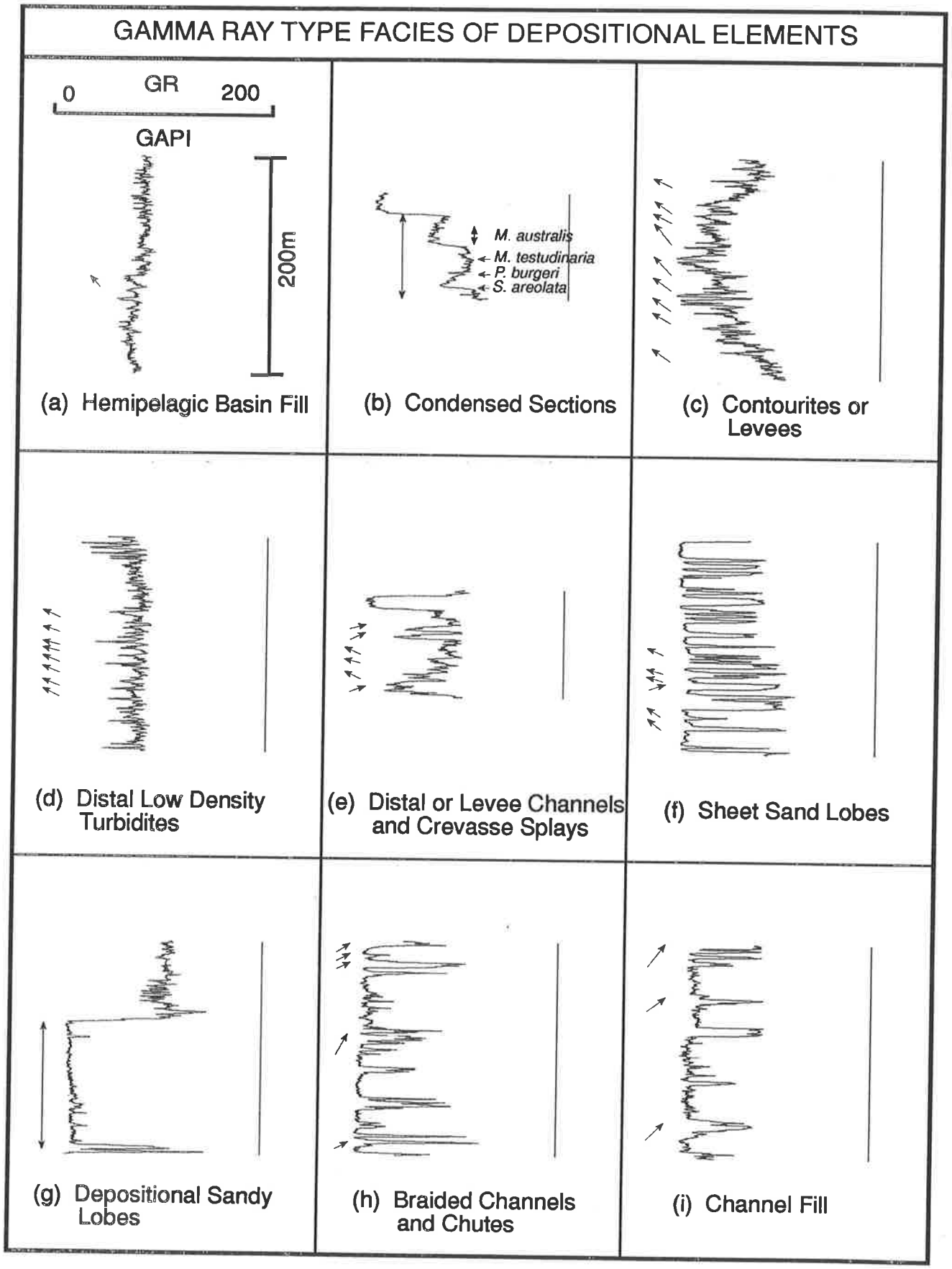


Figure 3.8. Gamma ray type wire line log facies of depositional elements, examples (a) to (i).

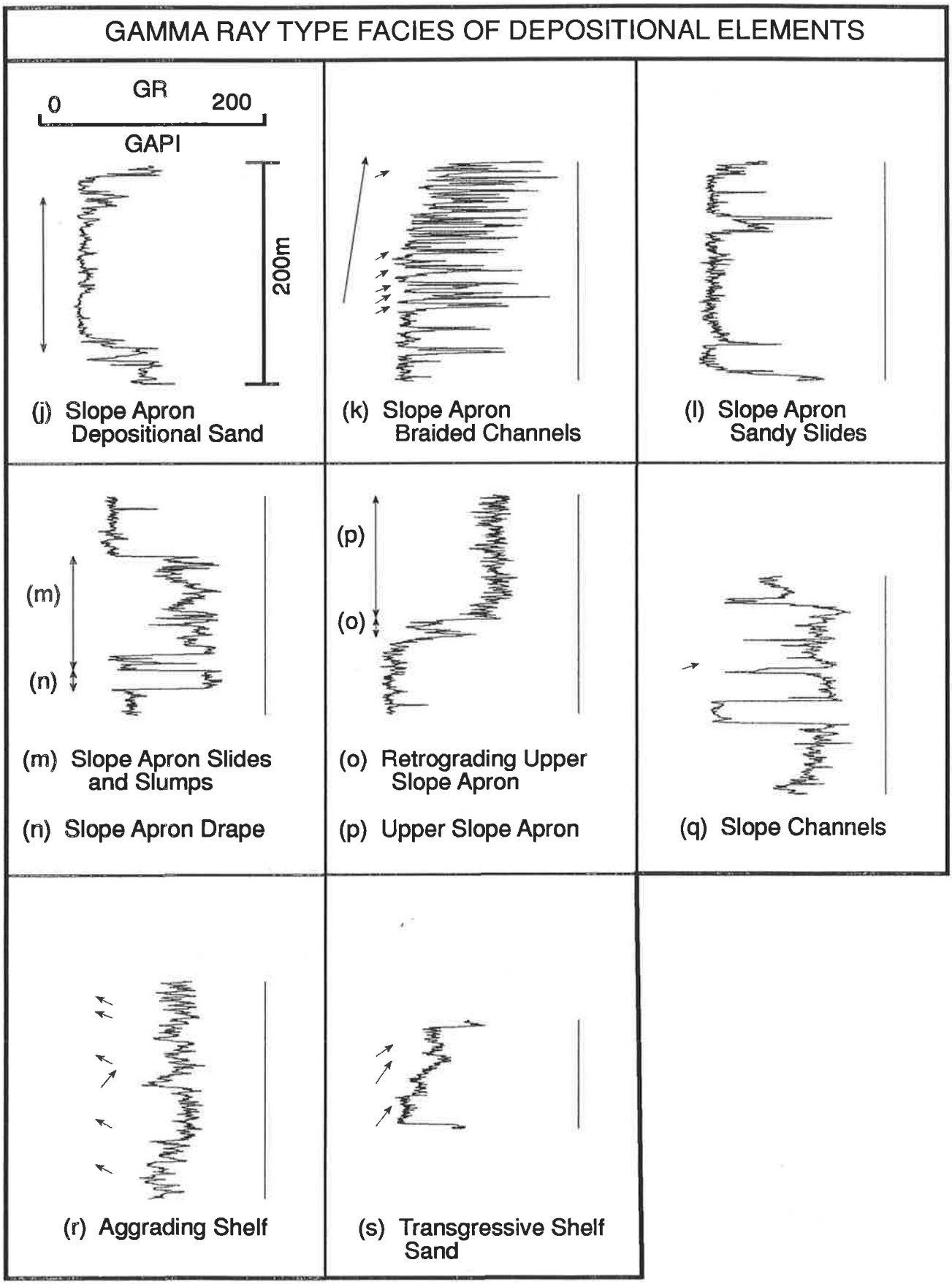


Figure 3.9. Gamma ray type wire line log facies of depositional elements, examples (j) to (s).

3.2.3 Depositional Models

Most of the defined depositional elements can be attributed to either one or both of the following processes: a) turbidity current associated channel/lobe complexes; and b) gravity induced slope apron deposits. In general, most of the vertical sections on the Legendre Trend are slope apron type elements, while those on the Madeleine Trend are considered with respect to a channel/lobe complex. The lateral distribution of the depositional elements is discussed further in section 4.1 (Depositional Systems).

Figure 3.10 shows the lateral distribution of depositional elements over an idealised channel/lobe complex. As with any schematic depositional model, it is important to note that geomorphologies and/or existence of the depositional elements listed are dependant on several variables concerning the particular depositional system. These are the sand to shale ratio, dominant grain size, and total volume of the sediment influx; sedimentary gradients, palaeobathymetry and basin type (e.g. see Galloway 1993; Pickering et al., 1989). In particular, the extent to which braided channels and chutes occur with Levees, and their relative sizes is contentious, but are ultimately vary with the content of the sediment influx and the local depositional slope. Braided channelling is characteristic of sand rich environments and areas of relatively steep gradients. Levees are associated with mud rich environments and relatively low depositional gradients.

Shanmugam and Moiola (1991) define the usages and meanings of the term 'lobe' for describing resedimented sand bodies. Their definition of 'depositional lobe' is implied in the Depositional Lobe Sheet Sands and Depositional Lobe Massive Sand elements. They state that depositional lobes are considered to exhibit overall sheet-like geometry. Also by their definition, depositional lobes occur at the mouths of channels and show an absence of channelling. They consider that Facies C dominates in depositional lobes. However, the depositional lobe elements defined in this study have an affinity to Facies B1.1. This variation probably reflects the lack of grain size variation that occurs in this ramp style of setting.

Eight of the defined depositional elements are considered to consist of slope apron deposits. The processes of these dominantly 'gravity induced' deposits are idealistically shown in Figure 3.11. Shanmugam et al. (1994), with the use of this diagram, distinguish the terms slide, slump, debris flow and turbidity current. These distinctions are implied in the context of this study. While slides and slumps are both gravity driven, downslope movements of sediment as a coherent mass, one implies translational movement and the other implies rotational movement, respectively (Shanmugam et al., 1994). A slide mass moves on a planar glide plane and shows no internal deformation; a slump moves on a concave up glide plane and undergoes rotational movements causing internal deformation (Dingle, 1977, Shanmugam et al., 1994). A debris flow represents a variety of sediment gravity flows, such as cohesive debris flows, density modified grain flows and liquefied flows in which the flow behavior is plastic. 'Debris flow' and 'mass flow' are used interchangeably because each exhibits plastic flow behavior (Dott, 1963) with shear stress distributed throughout the mass (Shanmugam et al., 1994). They also point out ten distinctions

between debris flows and turbidity currents; the common theme being that the flow rheology of turbidity currents is fluid, while the rheology of debris flows is plastic.

Due to the chaotic nature of slope apron successions, there is no predictable vertical stacking sequence of facies (e.g. see Figure 3.12; Pickering et al., 1989). In this study, the Upper Slope Apron is often bounded by the Retrogradational Slope Apron at the base. In addition, the distinction between the upper slope apron and the lower slope apron appears to be the abundance of sand-bearing beds in Lower Slope Apron successions. Galloway (pers. comm. 1994) suggested that a natural progression to more organised channel/turbidite sands above slumps and slides of a slope apron commonly occurs. The slide and slump glide planes act as a palaeo-low, steeply graded area to which turbidite sands may be directed. These sites can also be a source of inertia for channel/turbidite sand bypass and transport to the basin proper.

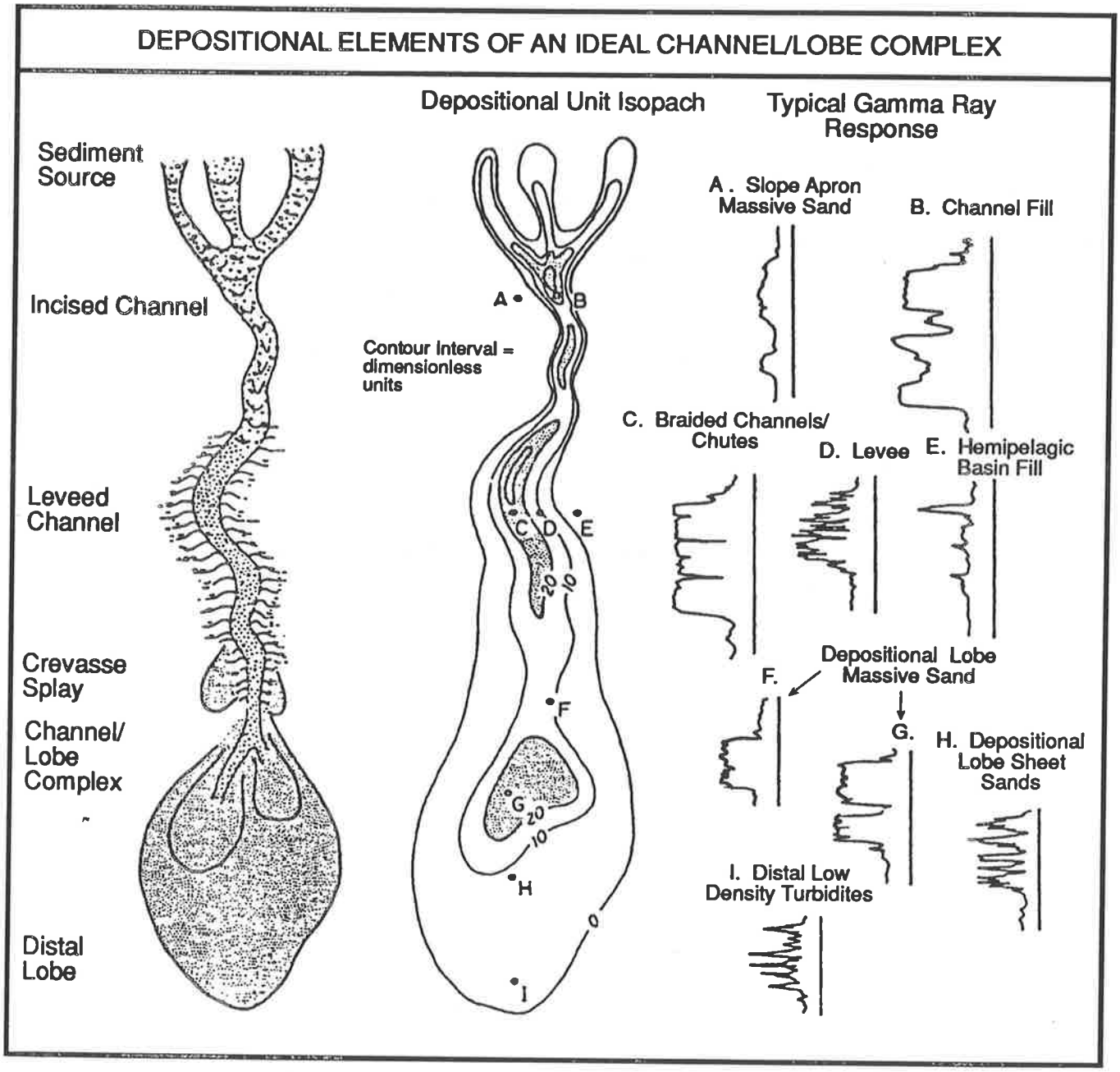


Figure 3.10. The various depositional elements of this study that ideally compose a channel/lobe complex. The respective geomorphic elements, depositional isopach, and typical log responses are shown (modified after Galloway, 1993).

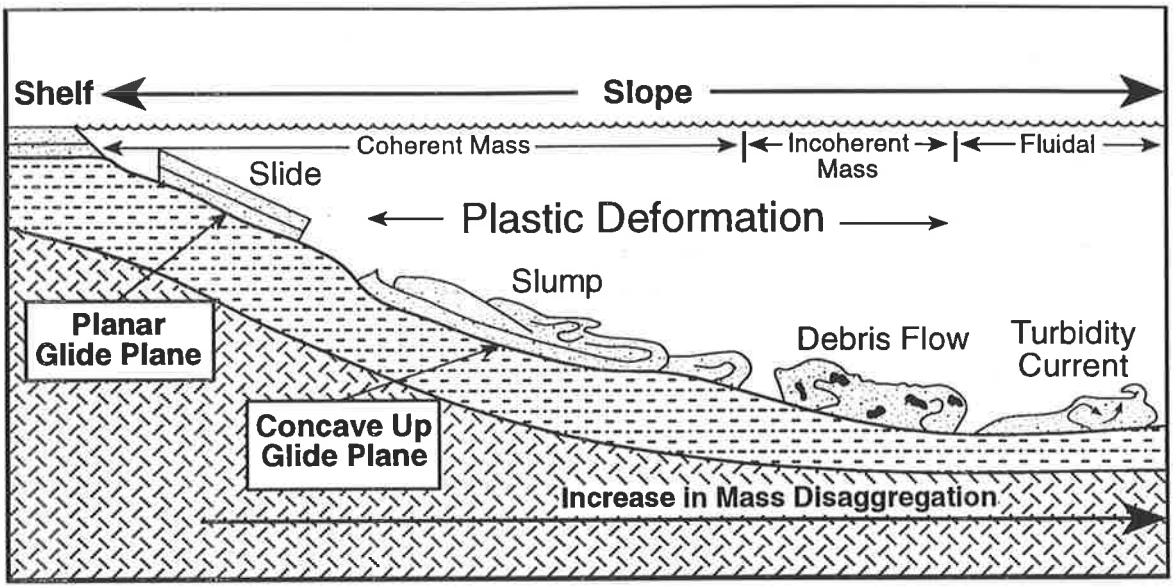


Figure 3.11. A conceptual model showing sediment failure and initiation of slides near the shelf break, and progressive downslope transformation of slides into slumps, debris flows and turbidity currents (after Shanmugam et al., 1994).

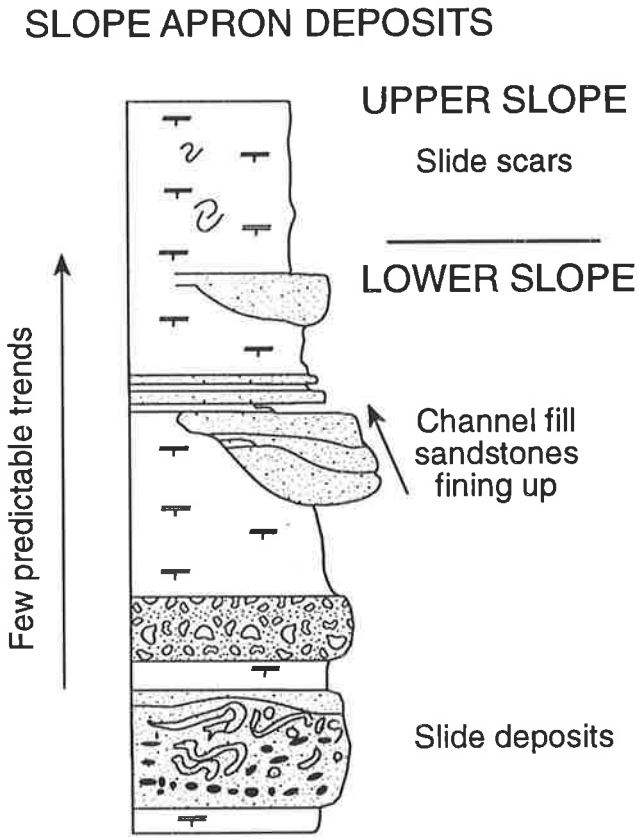


Figure 3.12. Facies and sequences characteristic of slope apron environments (from Pickering et al., 1989).

3.2.4 Conclusions

Nineteen depositional elements were defined and described in this section (Table 3.6). Eight of those are considered to occur as a result of gravity induced processes. Six occur as a result of turbidite currents in the context of a channel/lobe complex. Other depositional elements are caused by sediment starvation (Condensed Sections) and others by continuous traction currents (Contourites or Levees). The Aggrading Shelf and Transgressive Shelf Sands exist in the context of basin type (syn-rift and subsiding passive margin, respectively).

It is important to understand that the depositional elements cited in this study are end-members of a spectrum of depositional sites. Many are gradational to others. Some are similar but are distinguished on the basis of external factors such as basinal location, sand/mud supply and stage of basin development. In addition, the spatial distribution and occurrence of various suites of depositional elements is a reflection of these factors. This is discussed in section 3.5 (Depositional Systems). In some cases, the style of deposition that is implied by the hard 'labelling' of a depositional element may occasionally seem pretentious and may not always be correct. However, this manner is simply a method of associating the available data to the style of deposition that the element has affinities towards, or to relate them to similar types of processes.

1.	Hemipelagic Basin Fill
2.	Condensed Sections
3.	Contourites or Levees
4.	Distal Low Density Turbidites
5.	Distal or Levee Channels and Crevasse Splays
6.	Depositional Lobe Sheet Sands
7.	Depositional Lobe Massive Sand
8.	Braided Channels/Chutes
9.	Channel Fill
10.	Slope Apron Massive Sand
11.	Slope Apron Braided Channels
12.	Slope Apron Sandy Slides
13.	Slope Apron Slumps and Slides
14.	Slope Apron Drape
15.	Retrograding Upper Slope Apron
16.	Upper Slope Apron
17.	Slope Channels
18.	Aggrading Shelf
19.	Transgressive Shelf Sand

Table 3.6. List of the various depositional elements defined and described in this section. They are listed in approximate relative order from the most distal to the most proximal depositional environments.

The influence of gravity induced processes on the geological record in ancient slope and basin systems may be underestimated in the literature. Recently however, many known turbidite deposits in sand rich active margin settings have been reconsidered in this context (e.g. pers. comm., Galloway 1994; Shanmugam et al., 1994; Reading, 1994). This has subsequently led to the re-interpretation of apparent 'turbidite sands' as slide, slump and debris deposits (e.g. Frigg Field, Balder Field, pers. comm., Galloway, 1994).

3.3 CHRONOSTRATIGRAPHIC HORIZONS

3.3.1 Introduction

Time lines, or 'chronostratigraphic horizons' were defined iteratively with seismic and well log correlations. Eight stratigraphic log correlations were constructed in the process (Table 1.6; also refer to 'Methods'). Gross correlations were initially conducted on wireline logs using palynological zonations. Significant log breaks on the gamma ray, sonic and density logs were noted and then correlated between wells. The character of the log break defined the nature of the chronostratigraphic surfaces. The palynology was used for broader, overall time control. In sections of sparse palynological control, the log break character was relied upon to a greater degree. In these areas, confidence in the pick was usually gained by associating the nature of the log break in wells of good palynological control with the sections of poor time control.

Density and sonic logs were an essential tool in the correlation exercise, particularly for the Angel Formation sandstone. Morgan (Morgan Palaeo Associates, 1989) commented on the use of the palynology and the sonic log: "correlation of individual sands and shales is not conclusive based on the palynology alone, but significant constraints can be placed on log correlations. Clearly, the sonic log provides more hope of effective correlation than the gamma ray log, although a general association of higher gamma response with the *D. jurassicum* 'a' and 'b' subzones is evident". The density and sonic logs contain the values which are factors used for impedance calculations. For this reason, they were highly useful together in locating and correlating seismic surfaces at well locations.

Log correlations were tested when the wells were tied to the seismic data with synthetic seismograms (calibrated with check-shot surveys). In many instances, well correlations were readjusted based on confident seismic horizon correlations. One horizon (Horizon 'H') was initially picked and mapped on seismic before picking it from well logs. It appeared as a significant seismic event and could not be ignored. When the event was tied to well control, it was discovered that the seismic event was a satisfactory time line. The process of seismic horizon definition and mapping occurred by using one of three approaches: a) first defined on well logs and satisfactorily mapped on seismic; b) first defined on well logs and later readjusted due to seismic horizon interpretation; or c) defined by a seismic event and subsequently defined on well logs. In any case, no gross time discrepancies occurred by seismic horizon correlation. In certain instances, seismic horizon correlation ultimately increased the accuracy of the well log correlations. For these reasons, the mapped seismic horizons are satisfactorily considered time lines for the intense purposes of this study. The definition of each of the horizons is described in Section 3.3.3 (Results).

The hypothesis that seismic reflections could be considered to be reasonable 'time markers' was first proposed by Vail et al., (1977). The validity of this concept at the regional scale is a tenuous issue as discussed by Cartwright et al. (1993). By regarding both seismic events and seismic reflection character on an integrated basis, time constrained surfaces were successfully mapped on seismic. This achievement is

UNIVERSITY OF ADELAIDE LIBRARY

based on the premise that lithological variations are the primary cause of varying seismic signatures (varying seismic frequencies and amplitudes) and do not necessarily result in individual seismic horizons.

The method used in this study encompasses the 'genetic stratigraphic unit' approach as defined by Galloway (1994) which:

- "groups all sediments that record a common palaeogeographic array of depositional systems;
- is bounded by stratal surfaces that reflect major reorganisations in the array of depositional surfaces;
- is a meaningful, mappable unit that fosters interpretation of the depositional systems, their component facies, and historical evolution. The practical application is prediction of the distribution of reservoir sand bodies and stratigraphic geometries that form traps;
- must comfortably recognise and incorporate the full range of stratigraphic surfaces as potential sequence boundaries which depend on the local genetic and temporal significance of the surface."

The significance of each defined time line mapped in this study is discussed in the context stated above. In addition, each is discussed with respect to the seismic response, well log response and the formations that they encompass.

The seismic polarity is discussed with reference to 'normal polarity'. For the purpose of this study, normal polarity is defined by a compression pulse in the field representing a negative number in digital form, which in turn, is represented by a trough in display format. Seismic peaks and troughs with respect to normal polarity are discussed herein.

Although a 'formation' (*senso-stricto*) does not encompass time, the lithostratigraphy in this study is discussed in terms of maximum time constraints based on palynological zonations. The chronostratigraphic significance of these horizons with respect to formations, is shown in Figure 3.13. The montages contained in Enclosure IIIa, IIIb, and IIIc should be referred to while reading the following discussion of horizon definition (Section 3.3.3).

3.3.2 Biostratigraphy

Biostratigraphy, and more specifically, palynostratigraphy, forms the basis from which age dating of time lines on seismic and wireline log correlations were made in this study. The palynostratigraphy is adopted from Helby, Morgan and Partridge Dinoflagellate Zonation Scheme (1987). This scheme is based on the assemblages of dominantly dynoflagellate cysts. A good summary as to how this zonation scheme applies to the North West Shelf is provided by Ingram and Morgan (1988). The palynostratigraphic chart is their Figure 2 (p. 586-7). The interpretations for wells in this study are contained within Morgan's "Palynological Data Sheets" (1987 - 1993) and are 'quick look' interpretations.

The palynological zonations as applied to the Geological Age Scale, have subsequently been updated but are unpublished. The updated form was acquired from

Roger Morgan and was compiled by Partridge and Helby (1988), based on the Cretaceous and Jurassic Global Cycle Chart (Haq et al.,1987). The time scale used in this thesis is from Harland (1989) and was used in the construction of Figures 3.13 and 4.54. Unfortunately, both sets of time scales and Dynoflagellate Zonation allocations have been used in recent publications (e.g. see Figure 4.68). This inconsistency is discussed in detail in section 4.3.

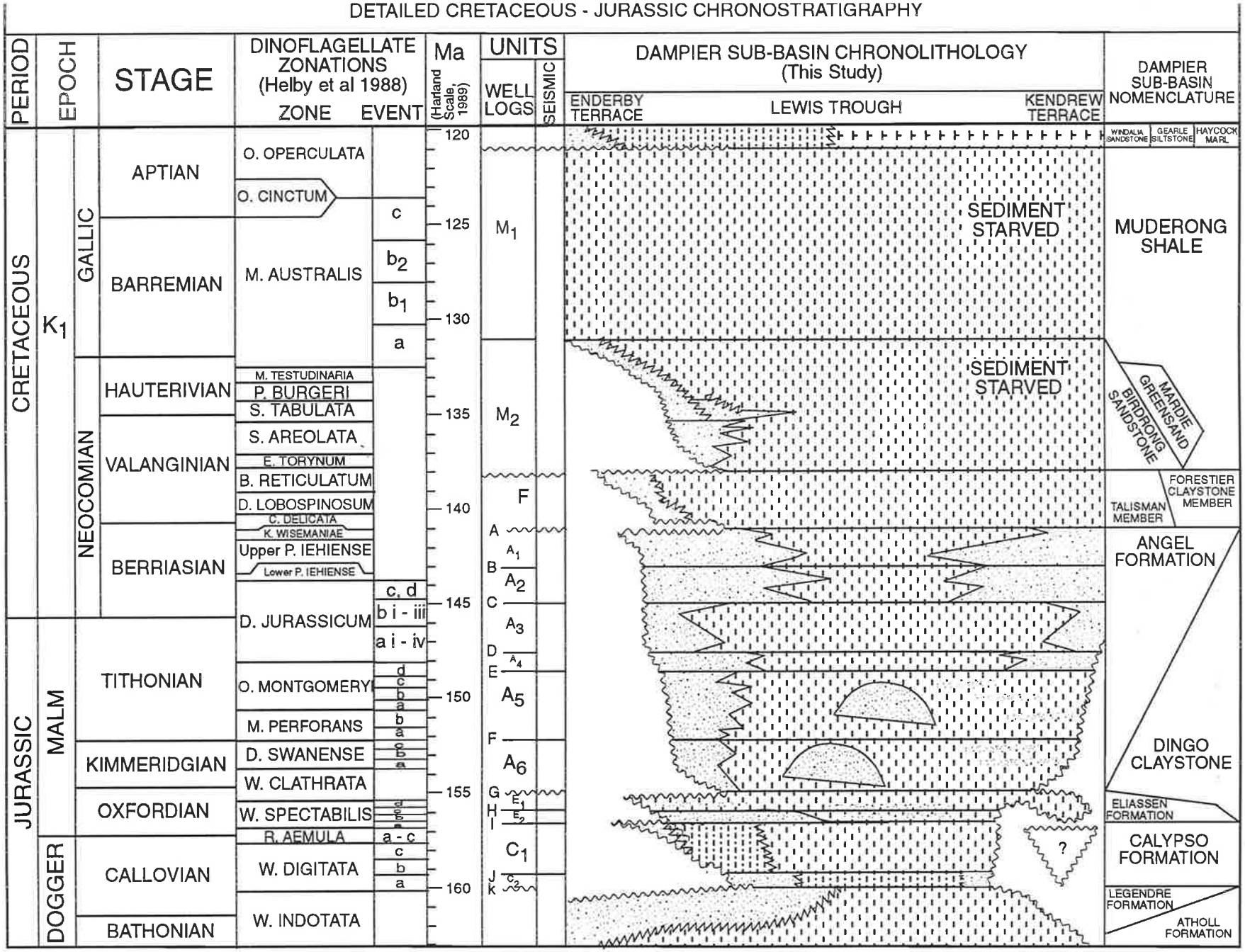


Figure 3.13. Detailed chronostratigraphy of the Dampier Sub-basin.

The palynological zonations have also been subsequently subdivided into subzones which are based on 'Acme Events' (see Figure 3.13). These detailed interpretations of subzones were available for a limited number of wells in the study area in the form of "Palynological Review" and "Rapid Restudy" reports by Morgan (1989). These interpretations proved invaluable to precise dating and verify the consistency of the previously defined horizons of this project. In addition, high resolution palynostratigraphy has recently been applied to the Angel Formation over the Wanaea and Cossack Oil Fields (Bint and Marshall, 1994).

In addition to time and age control, the palynological interpretations give an overall impression of depositional environment. These are divided into nonmarine, lacustrine, brackish, nearshore marine, offshore marine and oceanic. Comments are also included with the data sheets which provide information about caved samples, reworking of palynomorphs, condensed sections, unconformities, and basin oxicity levels at the time of deposition. Further statistical studies using palynomorph diversities and abundances are suggested to provide possible details of relative depositional environments, erosional surfaces, flooding surfaces, and condensed sections (Roger Morgan, pers. comm. 1991).

3.3.3 Results

Top Toolonga Calcilutite Horizon

Palynological Zone/Age: palynology was not used at this level. The horizon is a disconformity of approximately middle Campanian Age (Figure 1.7 or 4.54). This is dated at approximately 79Ma using the Harland Time Scale.

Formations delineated: top of Toolonga Calcilutite; base of Withnell Formation.

Seismic response: top (zero intersection) of a high amplitude trough.

Wireline log response: abrupt decrease in gamma ray value and abrupt increase in sonic value. Correlation is based on individual well picks. No well log correlations were conducted at this level.

This horizon is very ubiquitous over the seismic grid and so was easily mapped. Detailed well correlation and age dating of this horizon was not part of this study. The dating accuracy of this horizon is unknown. The Toolonga Calcilutite is considered to be the result of a rise in sea level and a period of low clastic influx. This study suggests that it represents approximately the first point at which there was no topographic expression of the Dampier Sub-basin (discussed in section 4.2).

Aptian Disconformity

Palynological Zone/Age: middle *O. operculata*, above *O. cinctum;* middle Aptian Age; 121Ma.

Formations delineated: top of Muderong Shale; base of Windalia Sandstone, Windalia Radiolarite, and Haycock Marl/Gearle Siltstone.

Seismic response: top of a moderate amplitude peak.

Wireline log response: consistent abrupt increase in gamma ray and sonic values. The density value commonly abruptly decreases, but can be increasing depending on the relative basinal position of the well (e.g. Enclosure IIId or Figures 4.40 and 4.41).

The Aptian Disconformity is a regionally significant surface across the North West Shelf. It is a flooding surface that marks the change from restricted marine claystone deposits to open marine deposits (Butcher, 1989). It is the base of a condensed section over the middle of the Lewis Trough and to the northwest. Wells on the Legendre Trend are usually interpreted to have missing section from the base of *M. tetracantha* to the top of *O. cinctum* , possibly as a result of erosion.

Valanginian Disconformity

Palynological Zone/Age: near top *B. reticulatum* ; middle Valanginian; 138Ma.

Formations delineated: top Forestier Claystone, and Talisman Sand Member; base Winning Group Muderong Shale, Mardie Greensand and Birdrong Sandstone.

Seismic response: top of a low to moderate amplitude trough. This horizon can sometimes be difficult to pick and is occasionally picked by delineating seismic characters.

Wireline log response: The surface is the base of a condensed section. Gamma ray shape is often a serrated convex funnel shape and varies to a convex bell shape. Where the condensed section above is significant, the gamma ray value is high and drops significantly below the surface, and visa versa for the sonic log (e.g. Enclosure IIId or Figures 4.40 and 4.41; note Walcott 1 horizon at 2705m).

The Valanginian Disconformity is a regional surface across the North West Shelf. In most cases, it is considered to be an erosional surface associated with a fall in relative sea level (Wiseman, 1979; Butcher, 1989). In the Dampier area, it appears however, to be associated with sediment starvation and transgressive ravinement due to a rise in relative sea level.

Along the Madeleine Trend and to the northwest, condensed intervals occur above the surface. The exact time period of these intervals varies depending on the well location. They occur with variable tops and bases between the base *P. burgeri* and near the top *B. reticulatum* Zones. Based on Palynological data sheets (e.g. Wanaea 1 and 2, Walcott 1, Madeleine 1; Morgan Palaeo Associates) these intervals are condensed and complete with no missing section.

Along the Legendre Trend, an interpreted erosional surface exists, with missing section occurring from near the base *S. tabulata* to near the top *B. reticulatum* (e.g. see Calypso 1, 2084m; Talisman 2, 2005.5m; Forestier 1, 2020m).

This disconformity is commonly known as the 'Intra-Valanginian Unconformity' across the North West Shelf (e.g. see Barber, 1994; Labutis, 1994). In this area, this surface is interpreted as a disconformity because there is no evidence of angular discontinuity of strata across this surface. In addition, other studies such as those stated above, pick the disconformity at the base of, or near the base of *S. areolata* . In the Dampier Sub-basin, I picked the surface at near the top of *B. reticulatum* because of fewer difficulties in seismic correlation. Also, this surface is interpreted here to represent the onset of transgression (ie. primary flooding surface), above which condensed intervals occur distally (ie. Madeleine Trend and to the northwest). In the proximal direction (ie. Legendre Trend and to the southeast) the disconformity represents an interpreted transgressive ravinement surface. The choice of the surfaces mapped and their reflection of relative sea level is discussed further in section 4.3.

Horizon 'A'

Palynological Zone/Age: middle *K. wisemaniae* Zone; near top Berriasian; 141Ma.

Formations delineated: base Forestier Claystone and Talisman Sand Member; top Angel Formation and Dingo Claystone.

Seismic response: typically this surface is the top of a low amplitude, moderate frequency trough. It is often difficult to pick, and the nature of the seismic character is frequently relied upon. A possible explanation for the poor seismic response is given below. In addition, Woodside attributes other factors such as propagating multiples from the Tertiary carbonates, geometry of reflectors, crestal faulting, and overburden geology (di Toro, 1994).

Wireline log response: The gamma ray pick is usually a subtle break in character often accompanied by a high gamma ray value spike. It sometimes, but not always coincides with the top Angel Formation Sandstone (e.g. Finucane 1 2982.5m, Figure 4.20). The density log break is an abrupt break from relatively high to relatively low. The sonic break is usually a more gradual convex bell shape containing a small, abrupt shift to relatively higher value (e.g. Dampier 1 2899m, Figure 4.17; Angel 3 2735m Figure 4.17; Lauchie 1 2208m, Figure 4.18; refer to figures in Enclosure IIIb).

The difficulty in picking this surface on seismic is due to the low impedance contrast that occurs across it. It is a result of the decreasing density values and increasing sonic values that occur crossing the surface, effectively cancelling the other out to some degree. The problem is currently being addressed by Sarah Ryan at the NCPGG (Ph.D student).

Horizon 'A' corresponds approximately to Woodside's 'K' geological marker over the Wanaea and Cossack Fields (di Toro, 1994). This marker is defined by a sequence of altered volcanic ash beds which they interpret to occur at the base *K. wisemaniae* Zone (Bint and Marshall, 1994). A wireline log correlation of their 'K' marker picks (di Toro, 1994, their Figures 11 and 12, p.564-5), correspond to Morgan's' (Morgan Palaeo Associates Palynological Data Sheets) near top *P. iehiense* Zone in Wanaea 1 (2805m, Figure 4.17), near base *C. delicata* Zone in Madeleine 1 (2987m, Figure 4.17), and one metre above (2886m) Morgan's' only *K. wisemaniae* interpreted sample (at 2887m, Figure 4.18) in Walcott 1. The marker is either diachronous or interpretation discrepancies based on subjectivity exist. I believe the latter to be the most likely cause. The ash beds are not observed over the whole study area, owing to nondeposition or erosion. It is however, a logical marker with which to define Horizon 'A'. Based on my regional correlations, and Morgan's palynological interpretations, the middle *K. wisemaniae* Zone is the best position to pick this surface.

The correlation of Horizon 'A' reveals that the lithological top of the Angel Formation Sandstone is diachronous. It occurs near the top of *D. jurassicum* in wells on the Kendrew Terrace (e.g. Montague 1 3029m, and Egret 1 3110m, Figure 4.18); near middle *P. iehiense* at Wanaea 1 (2822m); and near middle *K. wisemaniae* at Angel 3 (2736m). Sandstones that occur above near middle *K. wisemaniae* (Horizon 'A') in wells along the Legendre Trend (e.g. Legendre 1,

Figure 4.16; Calypso 1, Figure 4.17) therefore belong to the Talisman Member Sandstone, according to the definition in this thesis.

Horizon 'B'

Palynological Zone/Age: Upper - Lower *P. iehiense* boundary; middle Berriasian; 143Ma.

Formations delineated: Angel Formation, base of unit A_1, this study.

Seismic response: no seismic event was mapped at this horizon.

Wireline log response: sharp shale spike, or either the top or bottom of a sand bed on gamma ray log; small abrupt increase in sonic and density values (e.g. Enclosure IIIb).

Horizon 'B' defines the base of unit A_1. This unit is characterised as a phase of retrogradation of sand supply. Sand deposition is thought to have occurred no further to the southwest than the Angel Wells.

Horizon 'C'

Palynological Zone/Age: approximately middle *D. jurassicum* "bii' Subzone; near base Berriasian; 145Ma.

Formations delineated: A_2 to A_3 unit boundary, this study; base of Woodside's Angel Formation for the Wanaea and Cossack Fields (Bint & Marshall, 1994).

Seismic response: top of a low to high amplitude trough. The mappability of this event varies from excellent where it defines the base of a sand section, to fair within shaly sections.

Wireline log response: noted on gamma ray logs as the base of significant sandy intervals over most of the area; occasional low abrupt increase in sonic value; abrupt increases in density values are common (e.g. Enclosure IIIb).

Horizon 'D'

Palynological Zone/Age: approximately within *D. jurassicum* 'aii' Subzone; upper Tithonian; approximately 147.5Ma.

Formations delineated: A_3 to A_4 unit boundary, this study.

Seismic response: no seismic event was mapped at this horizon.

Wireline log response: base of a relatively shaly section on the gamma ray log; undescriptive character breaks occur in sonic and density logs (e.g. Enclosure IIIb).

Horizon 'E'

Palynological Zone/Age: near top *O. montgomeryi* Zone; upper Tithonian; approximately 148.5Ma.

Formations delineated: A4 to A5 unit boundary, this study.

Seismic response: top of a high amplitude peak; occasionally varies to the top of a moderate amplitude trough.

Wireline log response: horizon is picked on the gamma ray log as the base of sandy sections at Angel 1 and northeast thereof (Lambert 1 and Montague 1, Figures 4.18 and 4.19). The gamma ray log break is significant but is not easily definable along the Legendre Trend. Funnel shaped decrease on sonic log is common. The break in the density log is commonly ill-defined and may abruptly increase or decrease in value (refer to figures in Enclosure IIIb).

Horizon 'F'

Palynological Zone/Age: near top *D. swanense* 'c' Subzone; base Tithonian; 152Ma.

Formations delineated: A5 to A6 unit boundary; this study.

Seismic response: top of a high amplitude trough and varies less commonly to a high amplitude peak. This event is highly continuous and easy to map.

Wireline log response: gamma ray, density and sonic log breaks are variable in character. The sonic and density values either both decrease or, more commonly, both increase (e.g. Enclosure IIIb).

Horizon 'G'

Palynological Zone/Age: near base *W. clathrata* ; near top Oxfordian; 155Ma.

Formations delineated: Base Angel Formation; unit A6, this study; top Eliassen Member.

Seismic response: base of a high amplitude trough; may occur at the top of a low to moderate amplitude peak. This event is easy to pick on the basin flanks where underlying reflectors are erosionally truncated at the surface.

Wireline log response: base of significant sand intervals on gamma ray logs in wells on the Legendre Trend. On the Madeleine Trend, it is commonly picked at the base of one to several discrete distal channels (e.g. see Walcott 1 3767m, Figure 4.18; Madeleine 1 3659.5m, Figure 4.17). Sonic and density log breaks are distinct but variable. They are, however, noted overall by a decrease in log values. Ideal log breaks typical of this surface occur at Wanaea 1 (3641.5m, Figure 4.17) and Lauchie 1 (2620m, Figure 4.18) (refer to figures in Enclosure IIIb).

Horizon 'G' is the surface of a major unconformity where significant section can be missing above this surface, particularly in wells along the Legendre Trend (typically base *O. montgomeryi* to base *W. clathrata* is commonly missing). Where this surface is picked at the immediate top of *W. spectabilis* (ie. base of *W. clathrata* missing), erosion is certain. This is evident by reworked *W. spectabilis* palynomorphs occurring in sand intervals above this surface in Rosemary 1, Lewis 1,

Lauchie 1 and Legendre 1 (Morgan Palaeo Associates, 1989). In addition, Morgan comments about the "turbidites reworking particularly the *W. spectabilis* zone have made a very significant contribution to the section".

Horizon 'H'

Palynological Zone/Age: approximately above top *W. spectabilis* 'c' subzone; middle Oxfordian; 156Ma.

Formations delineated: Eliassen Member E_1 to E_2 unit boundary, this study.

Seismic response: top of a high amplitude, moderate frequency peak. This event is easy to map. It was defined and correlated on seismic before it was picked on wireline logs.

Wireline log response: subtle character break in gamma ray log; sonic and density values both commonly decrease (e.g. Enclosure IIIa).

Horizon 'H' was mapped due to the ubiquity of the seismic event. It represents the end of sedimentation which causes significant mounding on seismic.

Horizon 'I'

Palynological Zone/Age: near middle *W. spectabilis* 'a' subzone; lower Oxfordian; 156.5Ma.

Formations delineated: base Eliassen Member; top Calypso Formation.

Seismic response: top of a moderate amplitude, low frequency trough and varies to a low amplitude peak in some areas. This horizon separates mounded reflection character above from highly monotonous, parallel and continuous reflectors below.

Wireline log response: base of significant sand intervals on gamma ray logs in many wells along the Legendre Trend. In other wells the pick is at the base of an egg shaped gamma ray log motif. Sonic and density log breaks are highly variable. The most flamboyant of those occurs in Lewis 1 (2742m, Figure 4.5), where there is a high, abrupt increase in both the sonic and density logs (refer to figures in Enclosure IIIa).

Horizon 'I' marks the time of a very significant increase in water depth or marine flooding. It divides an anoxic, offshore marine section above, from a dominantly nearshore section below, as noted from palynological interpretations.

Horizon 'J'

Palynological Zone/Age: middle *W. digitata* 'b' subzone; middle Callovian; 159Ma.

Formations delineated: Calypso Formation C_1 to C_2 unit boundary, this study.

Seismic response: top of a moderate amplitude, low frequency trough.

Wireline log response: this surface is only intersected by Rosemary 1, Samson 1, Calypso 1 and Aurora 1 in the study area. It is picked on the gamma ray log as a very high value spike. There is a consistent abrupt increase in sonic and density values (e.g. Enclosure IIIa).

Horizon 'J' is an interpreted flooding surface that occurs within a very thick section of interpreted shelfal siltstone and claystone (approximately 700m thick in Samson 1).

3.3.4 Conclusions

The definition of the Toolonga Calcilutite, Aptian Disconformity, Valanginian Disconformity, and Horizons 'A' through to 'J' have been substantiated on well logs, seismic and palynological data. These horizons are all considered to be chronostratigraphic surfaces that are reasonably constrained by time. In addition, they often coincide with depositional element boundaries, major erosional surfaces, flooding surfaces, and/or simply mappable surfaces that are attributed to an intricate interplay of sea level, sediment supply and tectonics. This interplay is discussed in chapter 4.

3.4 SEISMIC FACIES

3.4.1 Introduction

The principles of seismic facies mapping in petroleum exploration to infer lithofacies and subsequently identify potential stratigraphic traps has been documented by Mitchum et al. (1977), Mitchum (1977, 1985), Mutti and Normark, (1990) and Posamentier and Erskine, (1990). Ramsayer (1979) outlined a seismic mapping technique with a coding system. Thorne (1992) examined the assumptions used for the seismic sequence stratigraphy methodology. These principles and methodology are the basis for seismic facies definition and mapping in this study.

A seismic facies unit is defined as "a mappable three dimensional seismic reflection pattern whose characteristics differ from those of adjacent patterns" (Mitchum et al., 1977; Ramsayer, 1979). The term 'facies', as with lithofacies, is used here in an informal fashion for the purpose of distinguishing characteristics of a unit from those around it. The underlying purpose of seismic stratigraphy and seismic facies mapping is that by studying the geometries exhibited on seismic, palaeogeographies and their environments of deposition may be reconstructed. The ultimate goal of this study is to infer and identify sand-shale relationships that have hydrocarbon trapping potential.

In the previous section it was demonstrated that most of the mapped seismic horizons in this project were satisfactory time lines. Vail et al., (1977) stated that "no seismic reflector will follow the top of a time transgressive lithostratigraphic boundary". The lateral extent of sequence boundaries or stratal surfaces is scrutinised by Cartwright et al. (1993). They demonstrate several situations where, particularly in this age of increasing seismic resolution and use of 3-D seismic, "surfaces of stratal discontinuity can only be discrete and correlatable over an extremely limited area", and that they "should not be expected to be correlatable as discrete and valid stratigraphic surfaces over large distances". Bearing this statement, I have qualified the mapped seismic horizons in the previous section. The assumption as to whether the mapped stratal surfaces are time lines should be qualified before seismic facies analysis is conducted in any seismic stratigraphic study. When this is achieved, however, seismic facies analysis of the amplitude, frequency, continuity, geometry, and termination pattern may be conducted on the seismic units that are bounded by the mapped stratal surfaces or horizons.

Five seismic facies maps (see table 1.5) were constructed in the course of the project work and are contained in Enclosures IIIa, and IIIc. They pertain to the seismic units that are considered to have significant reservoir potential and varying seismic character that can be used to define seismic facies. These maps incorporate parameters of the seismic facies unit including reflection continuity, frequency, amplitude, geometry and termination pattern. Isochron contours are drawn on these maps at an interval of 100ms. Informative gamma ray log motifs and dipmeter rosettes (where dipmeter data was available) of the pertinent sections were annotated near some well locations. Basic lithology and unit thickness are indicated for each of the wells that intersected the unit.

Seismic stratigraphy studies that involve seismic facies on the North West Shelf include that of Kirk (1985), Boote and Kirk (1989), Kirk (1991) and Miller and Stuart (1992). These studies address the seismic expression of marine systems, and in particular, 'submarine fan sands'. While papers that address seismic facies are limited in number, there are many recent papers that address sequence stratigraphy on the North West Shelf. This contrast may be attributed in part to the lack of resolution in the seismic data over the region. The data set used in this study (see section 1.2) varies from fair to exceptional over the study area.

The legend and seismic facies analysis code system which were used for the seismic facies analysis are shown in Figure 3.15. Note that the term 'convergence' refers to when two parallel reflections converge to form one reflection (e.g. Figure 3.14).

The use of the term 'downlap' can be used to describe two types of progradational wedges. This is a distinction made by Cartwright et al. (1993, see their Figure 7 p.28). The first instance is where clinoforms downlap a discrete downlap surface. The second instance occurs when there is sediment aggrading ahead of prograding clinoforms which results in 'asymptotic downlap'. In this case, an apparent downlap surface may be observed on poor resolution seismic which will cross time lines within this 'downlap interval'. Subsequently, the apparent downlap surface gets younger in the distal direction. Both occurrences of downlap are mapped in this study. Generally, discrete downlap occurs as foresets within channels, as pinch-outs of seismic 'mounds', or within the wedges of slope apron deposits. Asymptotic downlap (Figure 3.14) pertains to the distal portions of the study area and is considered to consist primarily of hemipelagic accumulations that have bypassed the slope of the prograding clinoforms. The aggrading downlap interval reflectors may thin or thicken distally, while those near the base of the unit may onlap rising palaeobathymetry.

'Uplap' is a ~~relatively new~~ reflection configuration term that is defined by Galloway (1993). after Brown and Fisher (1977) This term is used in basins where the slope coincides with a relatively steep tectonic scarp which may be undergoing differential subsidence. Slope and basin strata may 'uplap' the structural features (Galloway, 1993). Uplap occurs in some sections along the Legendre Trend and the Rankin Platform.

The following portfolio of seismic stratal patterns outlines the characteristic features of the many depositional elements and formations that can be observed within the Valanginian to Callovian succession. Gamma ray log motifs were annotated to seismic profiles of individual units in order to associate the depositional elements, defined by wire line log facies in the previous section, to the seismic stratal patterns. Other examples include profiles showing the typical seismic character of units or formations.

The numerous illustrations of seismic examples and seismic stratal configurations are an essential visual aid to interpret lithofacies. Refer to Figure 3.16 for the locations of the seismic examples. Cut-out seismic examples of distinct depositional elements are referred to larger window seismic examples. The locations of the 'window' seismic examples are, in turn, outlined on the respective uninterpreted seismic sections and are included as enclosures. The legend pertaining to these examples is shown in Figure 3.17. The seismic examples were displayed on the SIERRA 2di Workstation and printed. They are at a relatively compressed scale to provide an approximate vertical exaggeration of 3:1. In addition, amplitude was reduced by using the gain control.

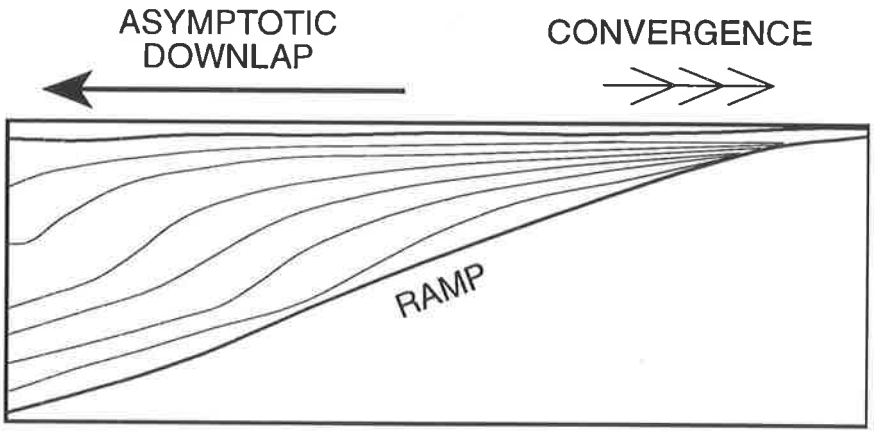
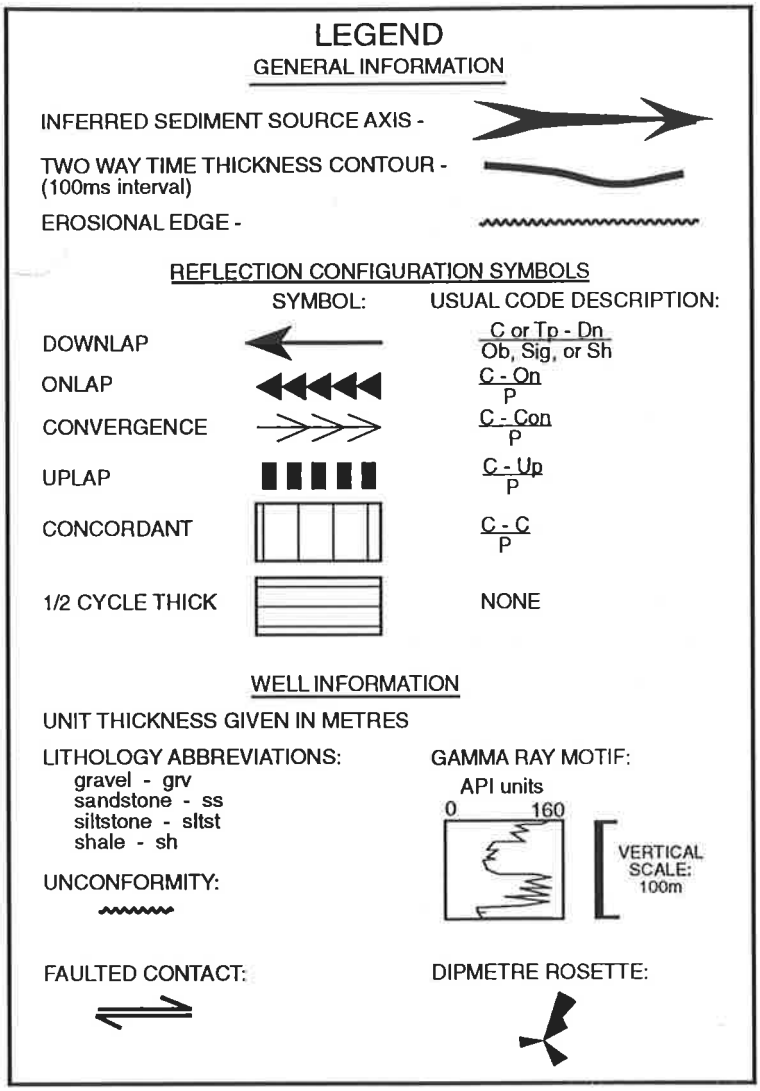


Figure 3.14. Idealised stratal configuration for asymptotic downlap and convergence (see also seismic examples Figures 3.18 and 3.19).

a)



b)

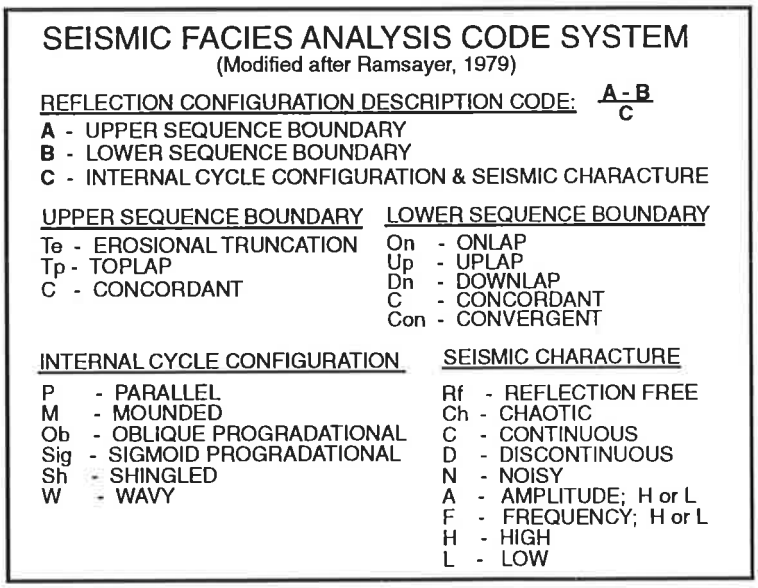
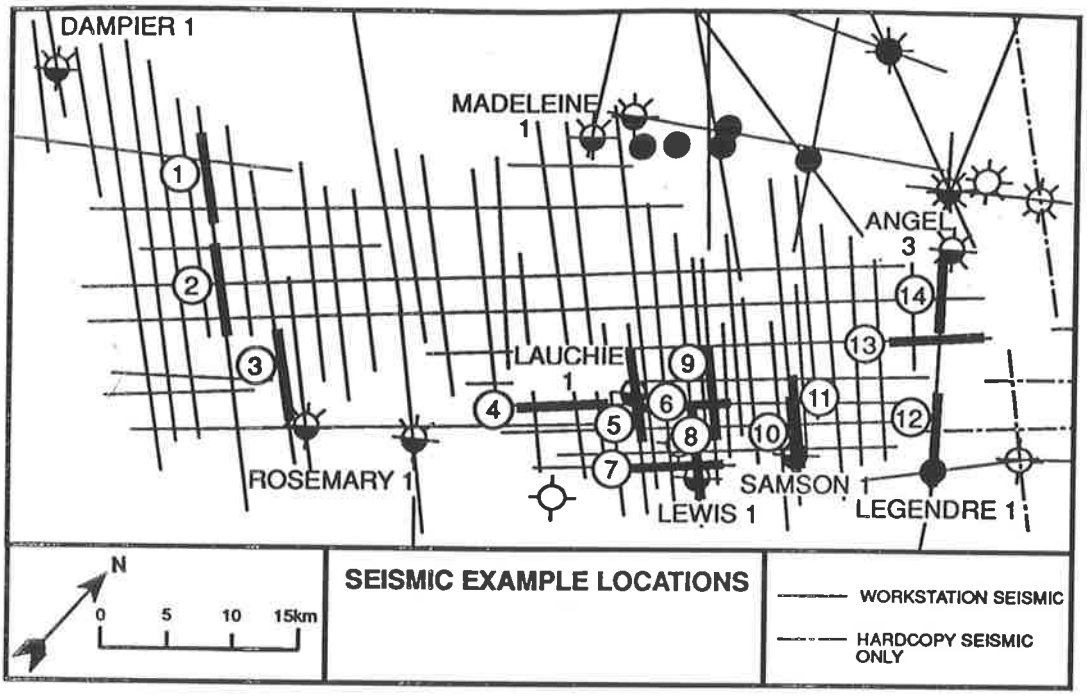


Figure 3.15. Legend a), and seismic facies analysis code system b), for seismic facies maps (part of Enclosures IIIa and IIIc).



Location No.	Figures
1	3.79
2	3.18
3	3.39, 3.40, 3.52
4	3.51
5	3.22, 3.41, 3.42, 3.43, 3.53
6	3.49
7	3.48
8	3.23, 3.31, 3.37, 3.38, 3.45, 3.54
9	3.50
10	3.21, 3.47
11	3.33, 3.34, 3.35, 3.36, 3.46, 3.55
12	3.27, 3.28, 3.29, 3.30, 3.32, 3.44, 3.56
13	3.20
14	3.24, 3.25, 3.26, 3.57

Figure 3.16. Location map of the seismic examples in Figures 3.18 to 3.57. The table lists the figures that pertain to each of the numbered seismic locations.

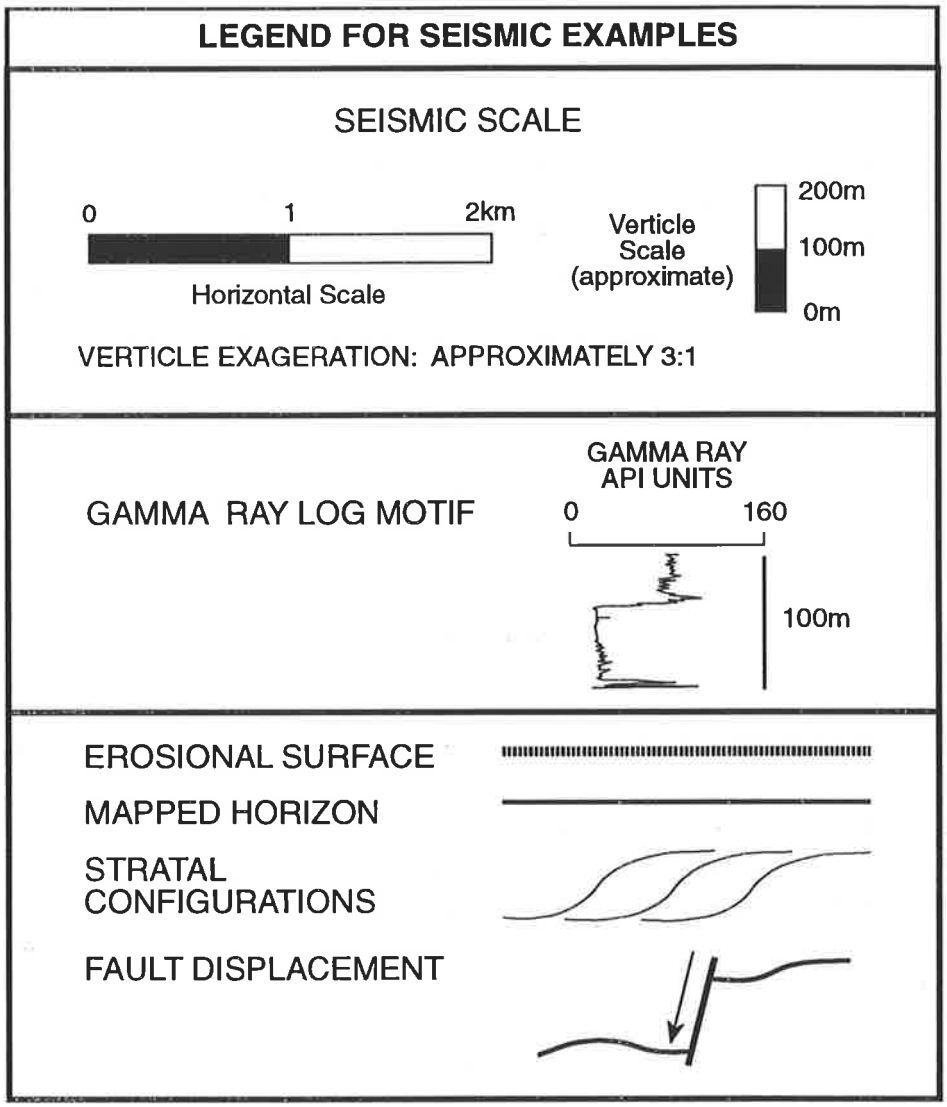


Figure 3.17. Legend pertaining to the seismic examples in Figures 3.18 to 3.57.

3.4.2 Results

Convergence

Convergence, as illustrated in Figure 3.18, displays the convergence of continuous, moderate amplitude and frequency events. This character is typical along the southeast flank of the Lewis Trough over the time equivalent succession of the Angel Formation. It is interpreted to dominantly represent the fine grained basinal sediment of the Dingo Claystone. Isolated sand bodies may pinch out in the down-dip direction near the position of horizon convergence.

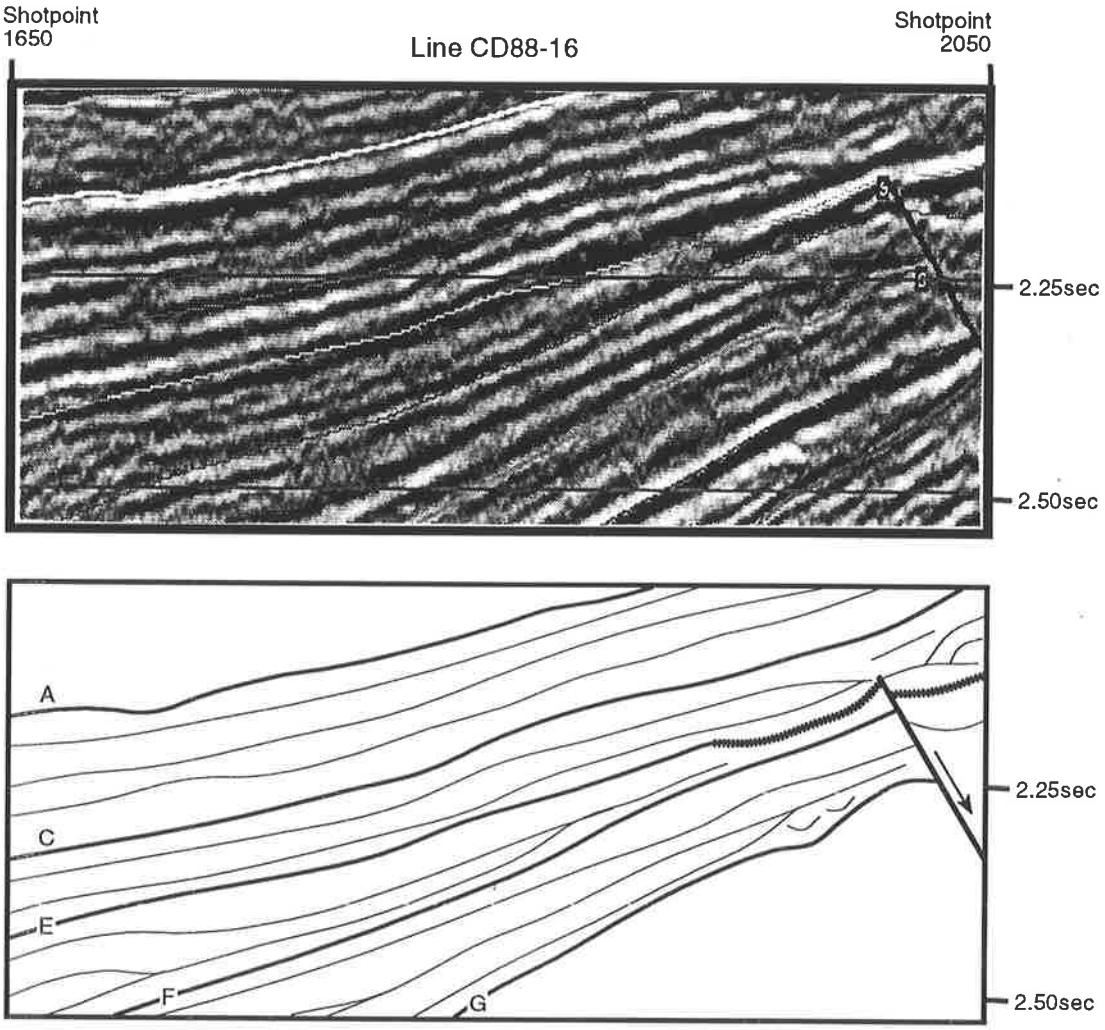


Figure 3.18. Seismic example and stratal configuration showing convergence. Note the overall reduction of amplitude and frequency of many events in the down-dip direction. Refer to Figure 3.14 for idealised stratal configuration of convergence. See Enclosure IVa for position on uninterpreted seismic section.

Asymptotic Downlap

Figure 3.19 is a seismic example illustrating asymptotic downlap. This type of downlap is characteristic of the stratal configurations that occurs in distal Dingo Claystone. Unfortunately, most of the data is relatively noisy where asymptotic downlap occurs, making it a difficult pattern to delineate. This configuration is associated entirely with Hemipelagic Basin Fill of the Dingo Claystone that was intersected, for example, in Dampier 1 and Madeleine 1.

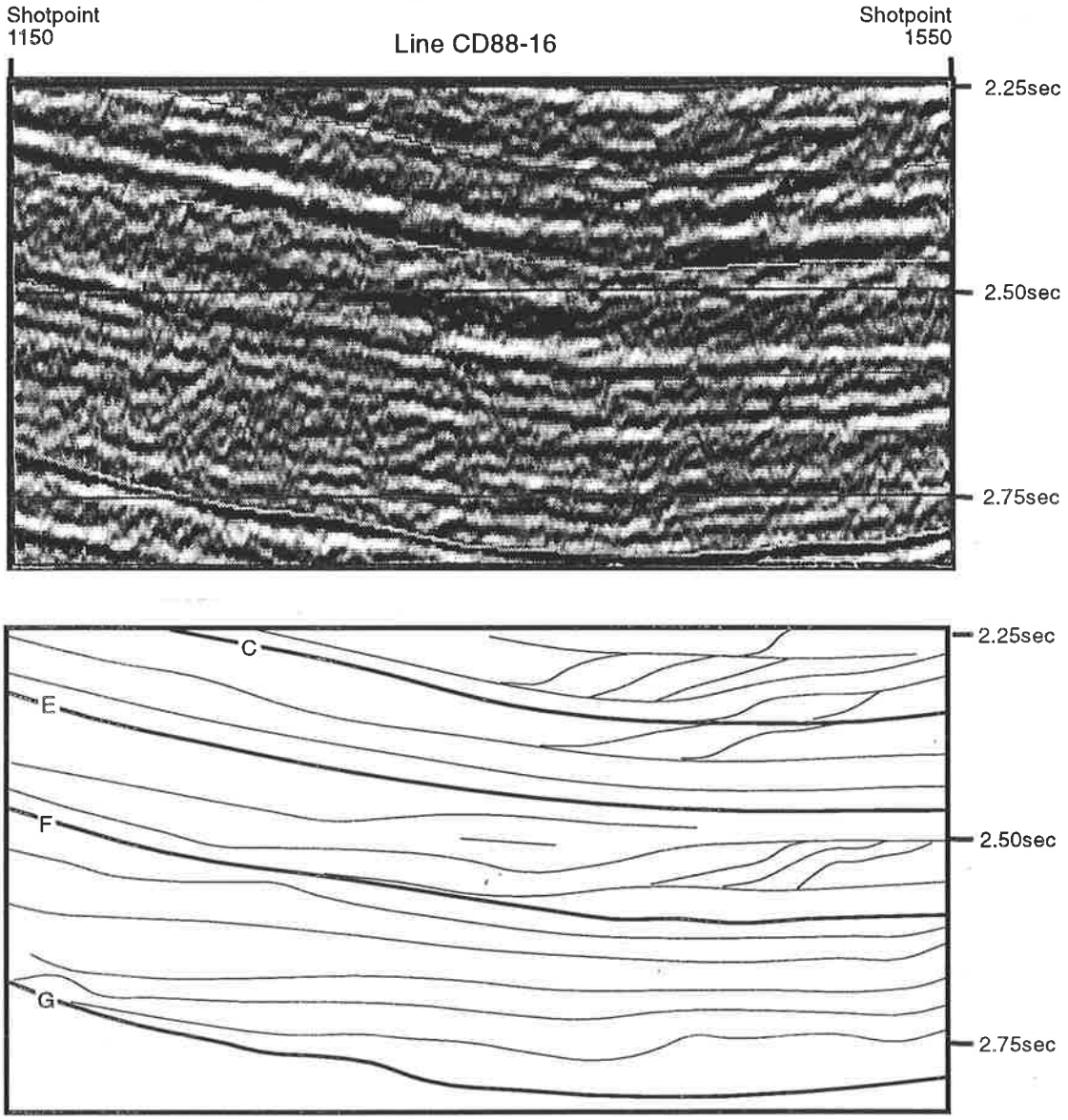


Figure 3.19. Seismic example and stratal configuration of asymptotic downlap. Note the aggradation of stratal reflectors distal to the prograding clinoforms. See Figure 3.14 for idealised stratal configuration of asymptotic downlap. See Enclosure IVa for position on uninterpreted seismic section.

Eliassen Formation

The basal unit E_2 of the Eliassen Member has mounded geometries in strike section which are bound by continuous high amplitude events at the top and base (Figure 3.20). The mounded geometry is rare in dip sections. Dip sections typically have wedge shaped geometries. The internal character of unit E_2 is low amplitude, discontinuous and often chaotic patterns. High amplitude troughs (normal polarity), interpreted as possible sand bodies, are noted cutting the low amplitude background character. Unit E_1 often contains one or two continuous cycles near the base which occur parallel to the mounded geometries of E_2. The upper portion of E_1 usually contains low amplitude and discontinuous non-descript character. The Eliassen Member is considered to be a mud rich system that is interpreted to contain contourites and muddy channels and levee complexes (e.g. Figures 3.47, 3.48, 3.49).

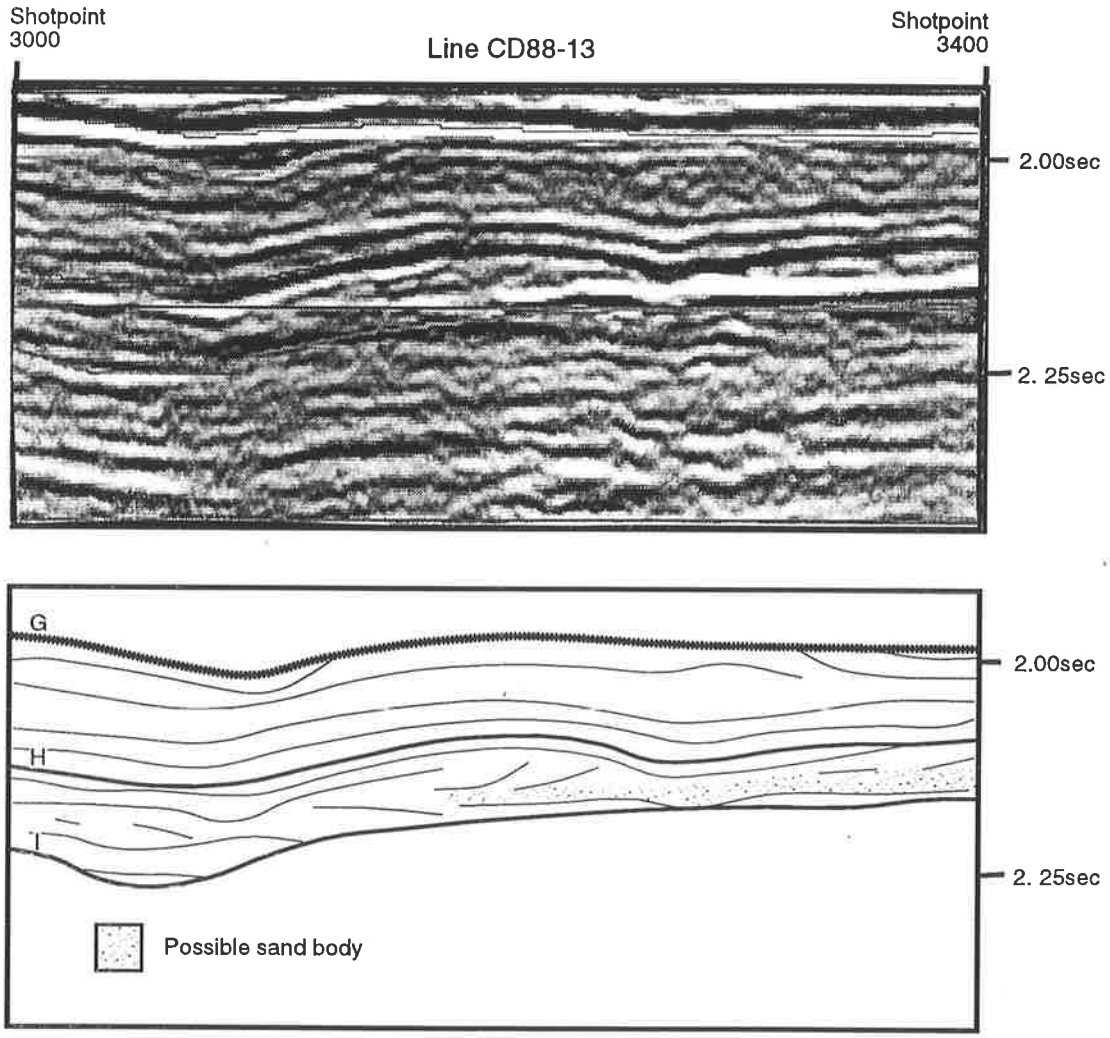


Figure 3.20. Seismic example and stratal configuration of a strike section of the Eliassen Member. The dimensions of the mounded configuration near the centre of the figure is 2.6km long and ranges from approximately 75 to 150m in thickness. Note the high amplitude trough that is interpreted as a possible sand body. See Enclosure IVb for position on uninterpreted seismic section.

Calypso Formation

The Calypso Formation displays a relatively monotonous seismic character of continuous, moderate to high frequency and moderate to low amplitude (Figure 3.21), and lacks any specific stratal patterns. The stratal configuration is primarily parallel and minor onlap occurs rarely at the base reflector. The seismic facies of the Calypso Formation was not mapped owing to the lack of variation in stratal configuration.

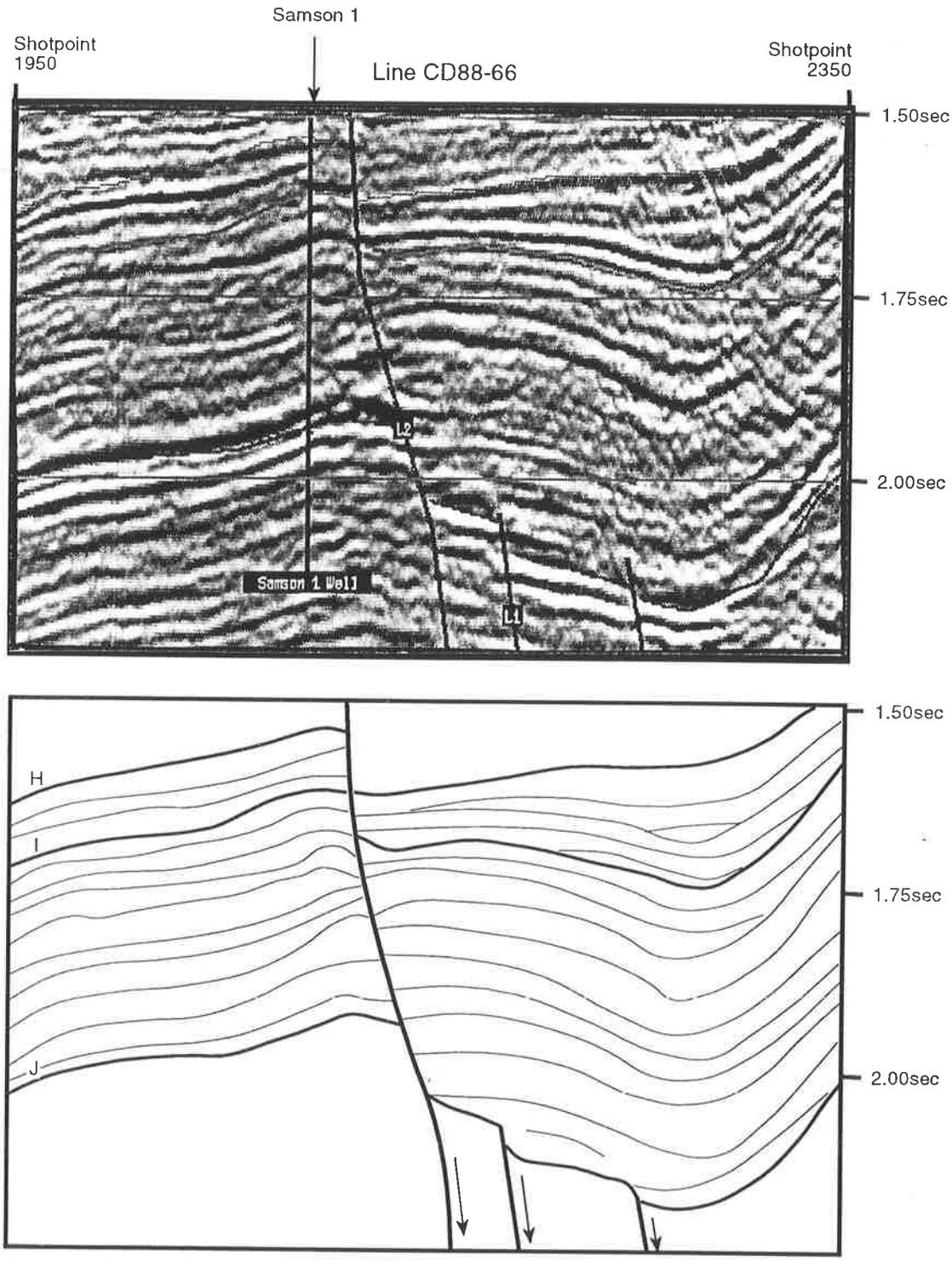


Figure 3.21. Seismic example and stratal configuration of the Calypso Formation. The steep fault to the right of Samson 1 is part of a collapse graben that is adjacent to the Rosemary Fault. See Enclosure IVc for position on uninterpreted seismic section.

Hemipelagic Basin Fill

Hemipelagic Basin Fill has a poorly defined seismic character. Low to moderate amplitudes and relatively discontinuous events prevail. Very low frequency events may be continuous. Stratal configurations include aggradation, convergence (Figure 3.18), asymptotic downlap (Figure 3.19) and onlap (Figures 3.22 and 3.23). The seismic facies of the Hemipelagic Basin Fill is defined by the lack of high amplitudes, low frequencies and sharply defined stratal configurations.

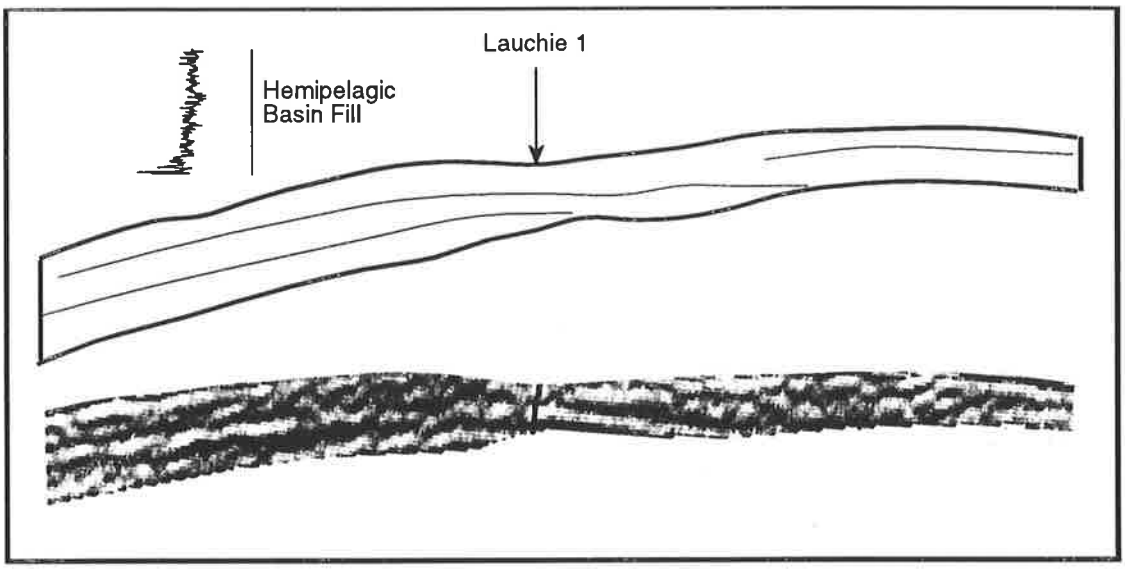


Figure 3.22. Seismic example and stratal configuration of the Hemipelagic Basin Fill of the Forestier Claystone at Lauchie 1. Note the onlapping horizons. See also Figure 3.53.

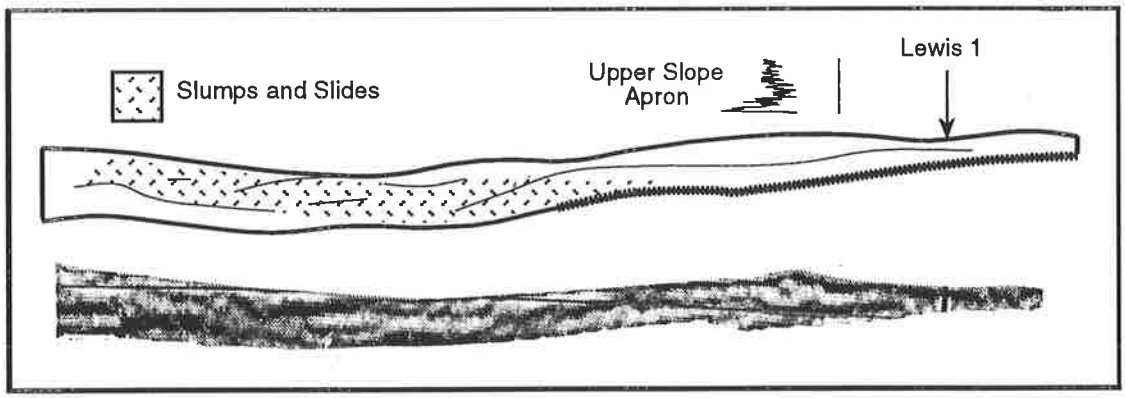


Figure 3.23. Example of the Upper Slope Apron, Forestier Claystone intersected at Lewis 1. It is interpreted to be slightly condensed and deposited on a slide scar, up-slope to possible Slumps and Slides. See also Figure 3.54.

Depositional Lobe Sheet Sands

Sheet sands have a continuous and parallel seismic character, characterised by low amplitude and moderate to high frequency. Examples are displayed in Figures 3.24 and 3.25.

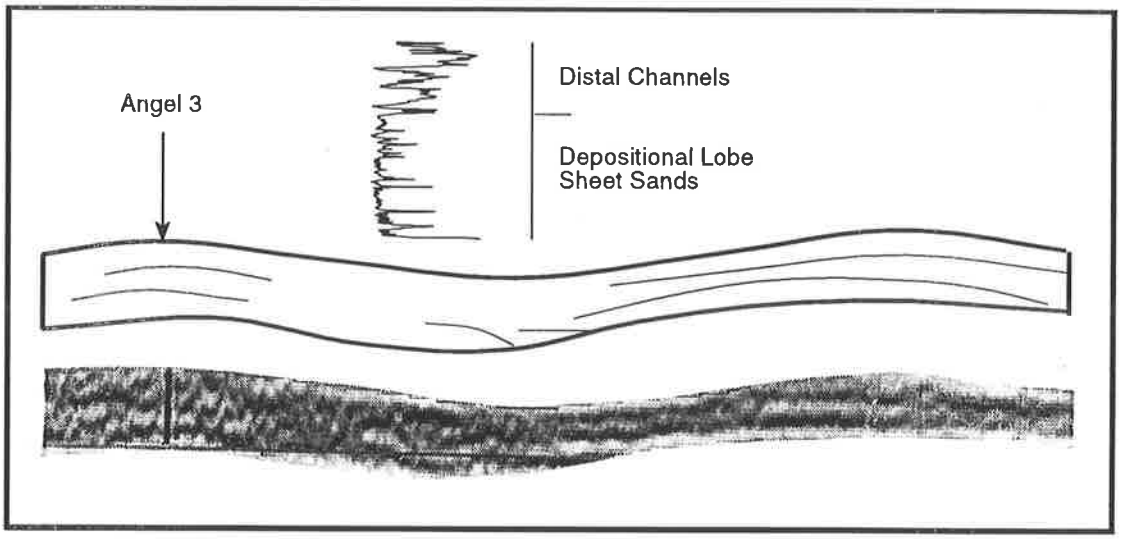


Figure 3.24. Unit A3&4 example of interpreted sheet sands at Angel 3. See also Figure 3.57.

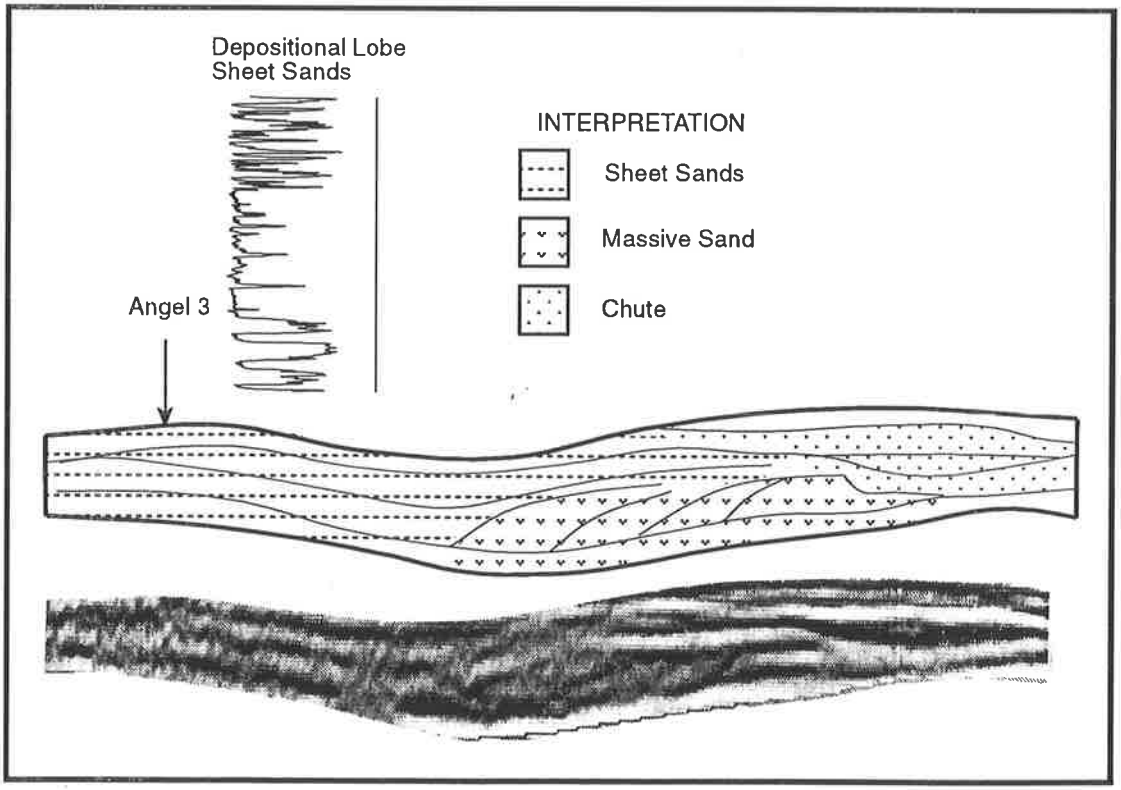


Figure 3.25. Example of unit A5 sheet sands at Angel 3. The section also includes configurations to suggest the presence of a massive sand and sand chute. See also Figure 3.57.

Depositional Lobe Massive Sand

Massive sands are considered to have mounded configurations, similar to the example in Figure 3.26. There, the outer mounded geometry may be delineated by a high amplitude event, but the internal character is often relatively transparent.

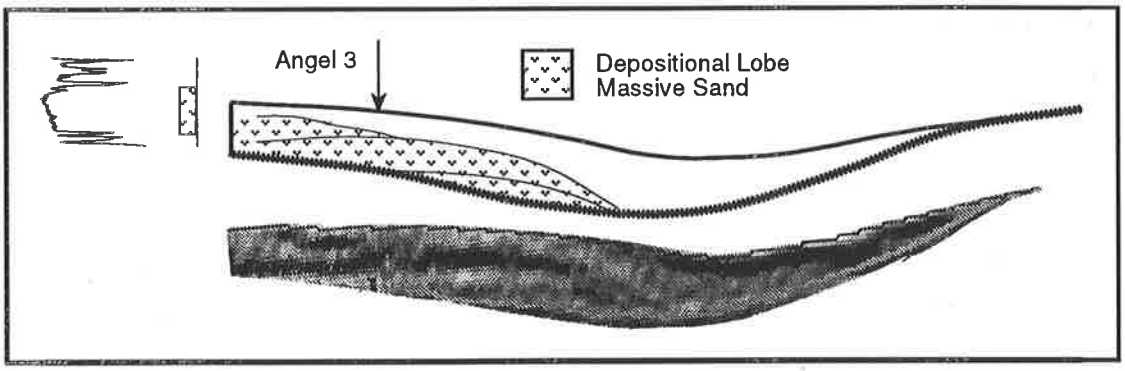


Figure 3.26. Seismic mound interpreted as a massive sand of a depositional lobe. The section is Unit A6 intersected at Angel 3. See also Figure 3.57.

Braided Channels and Chutes

Figure 3.27 displays continuous high amplitude events that converge at the margins of the complex. These are considered typical of Braided Channels and Chutes. Similar geometries are also noted in Figures 3.25 and 3.39. This character is also associated with broad, erosional cut and fill features (e.g. Figure 3.51).

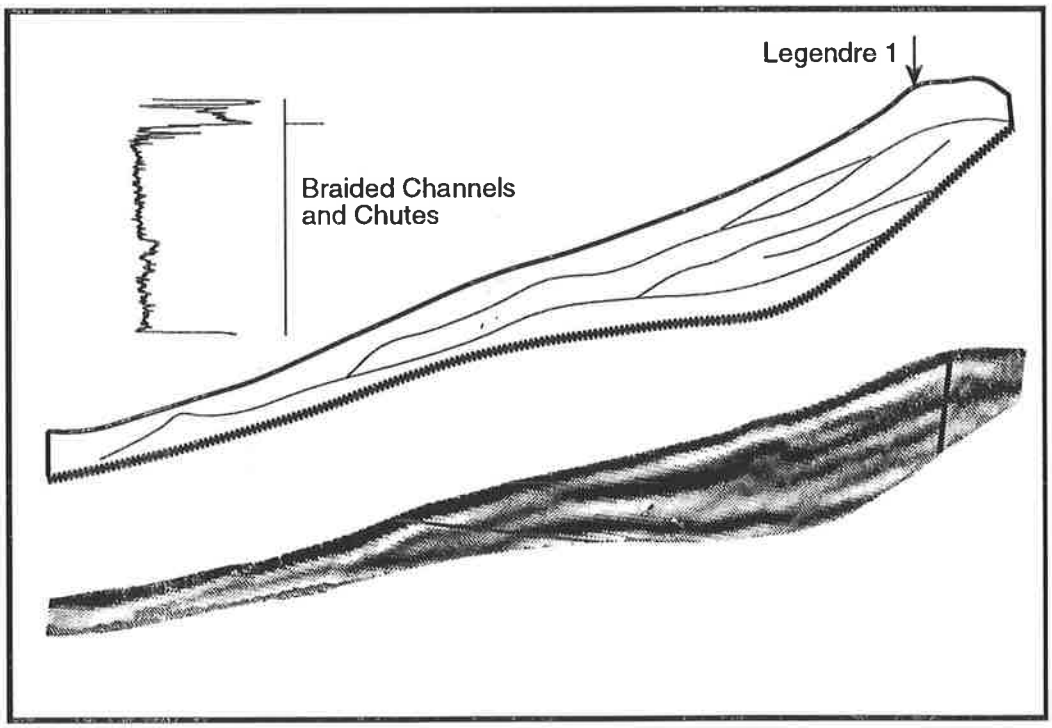


Figure 3.27 Braided Channels and Chutes at Legendre 1 Unit A5. See also Figure 3.56.

Channel Fill

Interpretations of Channel Fill are illustrated in Figures 3.28, 3.29, 3.30, 3.31 and 3.32. Channel Fill is usually associated with an erosional surface identified by erosionally truncated reflectors (e.g. Figures 3.28 and 3.29). Internal seismic character is characterised by continuous, low amplitude and high frequency (e.g. Figure 3.28), or may display discontinuous concave up events as in Figure 3.31.

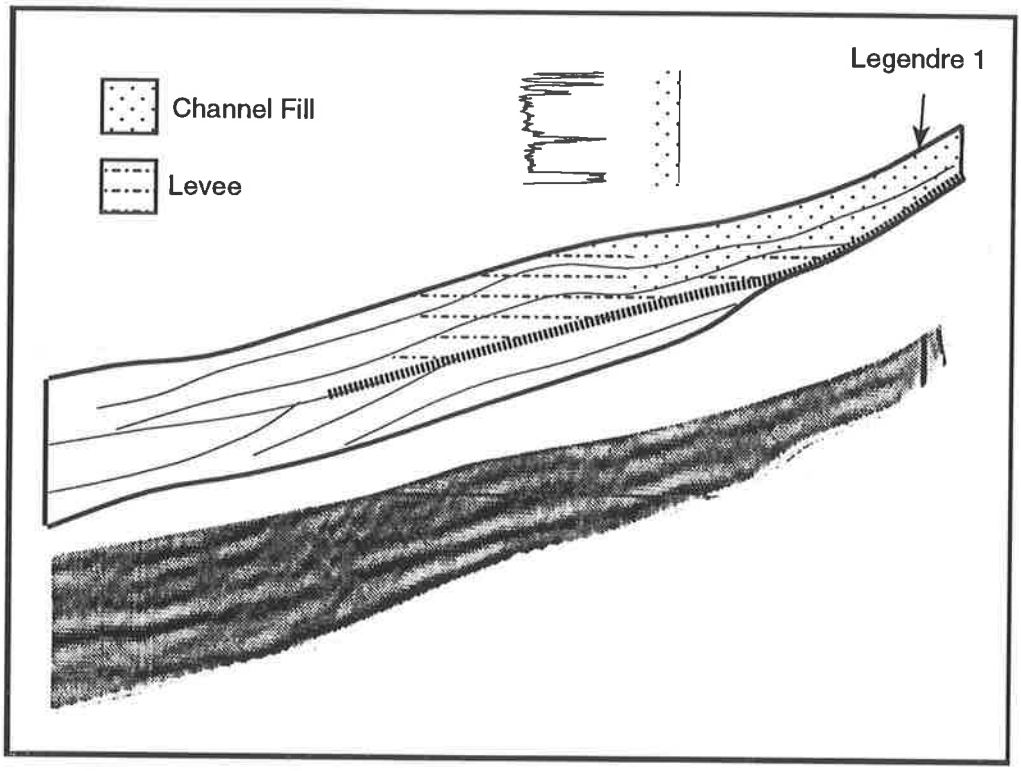


Figure 3.28. Talisman Sand Member at Legendre 1. Interpreted channel fill is associated with erosional surface and possible levee. See also Figure 3.56.

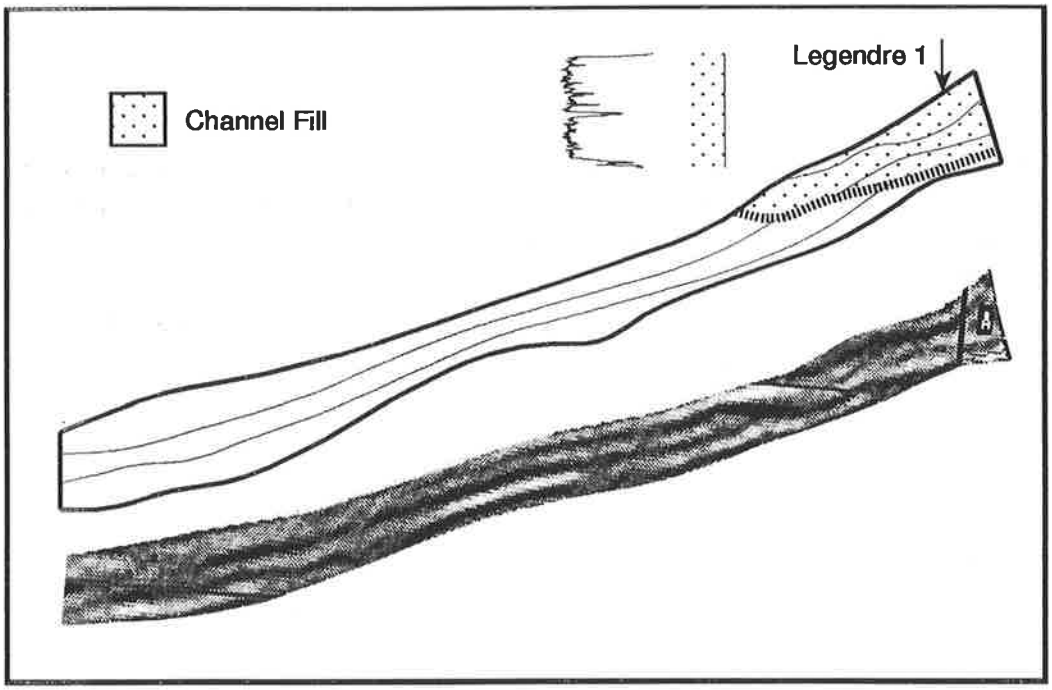


Figure 3.29. Unit A1&2 at Legendre 1, interpreted as Channel Fill. See also Figure 3.56.

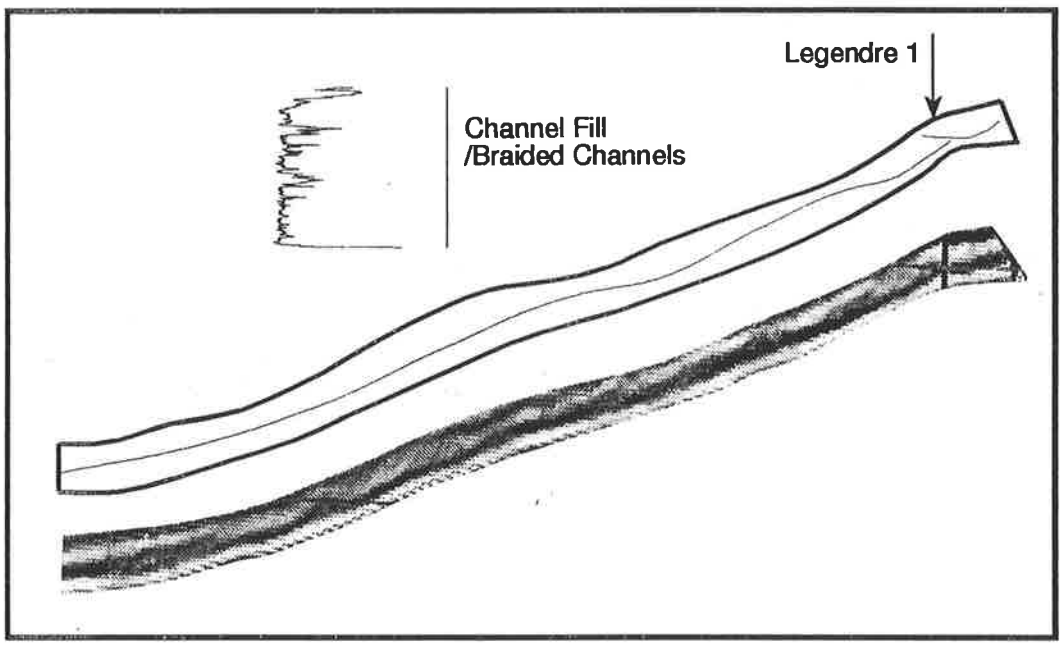


Figure 3.30. Unit A3&4 at Legendre 1 is considered to be transitional with Channel Fill and Braided Channels and Chutes. See also Figure 3.56.

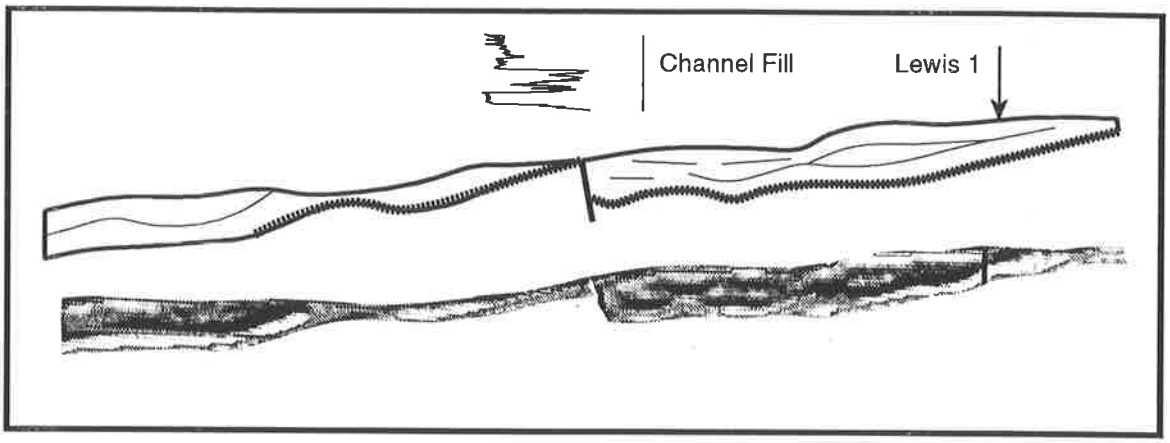


Figure 3.31. Interpreted Channel Fill example at Lewis 1, Unit A_6. Note the discontinuous, slightly concave up events in the down-faulted area. See also Figure 3.54.

Slope Apron Braided Channels

A section of Braided Channels within an interpreted Slope Apron is displayed in Figure 3.32. It has a low amplitude, high frequency and slightly chaotic seismic character. The overall wedge shape supports the slope apron interpretation. The seismic character of this example would not suggest a sand prone affinity without direct well evidence.

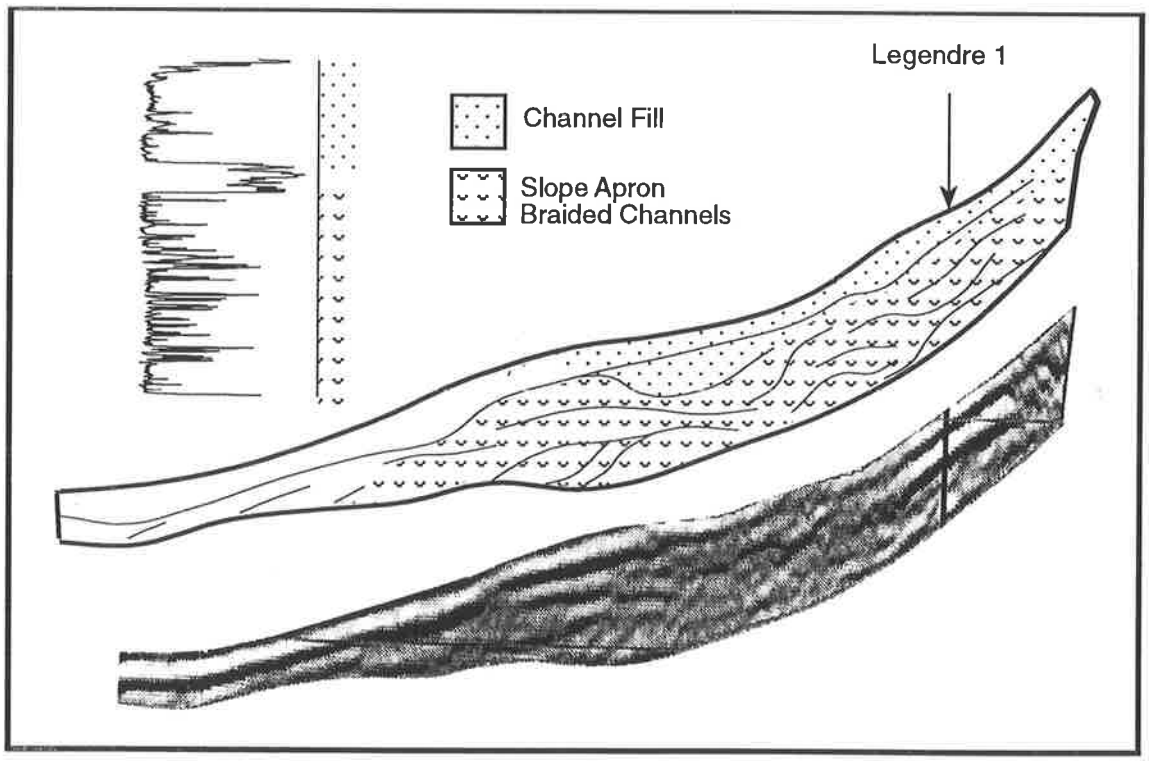


Figure 3.32. Unit E_2 at Legendre 1 interpreted as a slope apron deposit. Note the overall wedge shape of the unit. See also Figure 3.56.

Slope Apron Sandy Slides

Examples of Slope Apron Sandy Slides are displayed in Figures 3.33, 3.34 and 3.35. It is difficult to typify the seismic character because no section was thick enough in the data set to obtain a representative seismic character. One possible characteristic is a broad concave up configuration or dish shape of relatively high amplitude peaks or troughs.

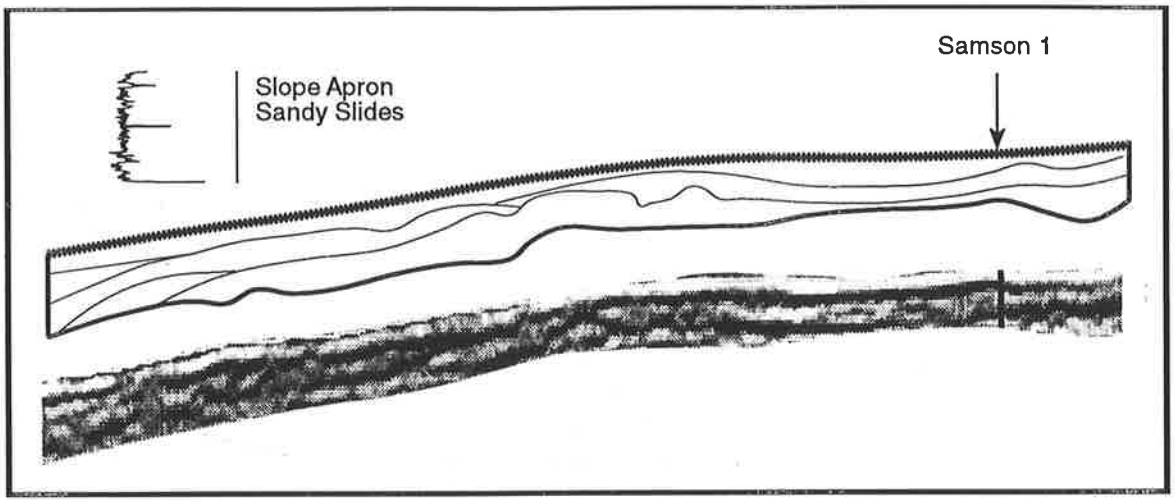


Figure 3.33. Unit A1&2 at Samson 1 of interpreted Slope Apron Sandy Slides. See also Figure 3.55.

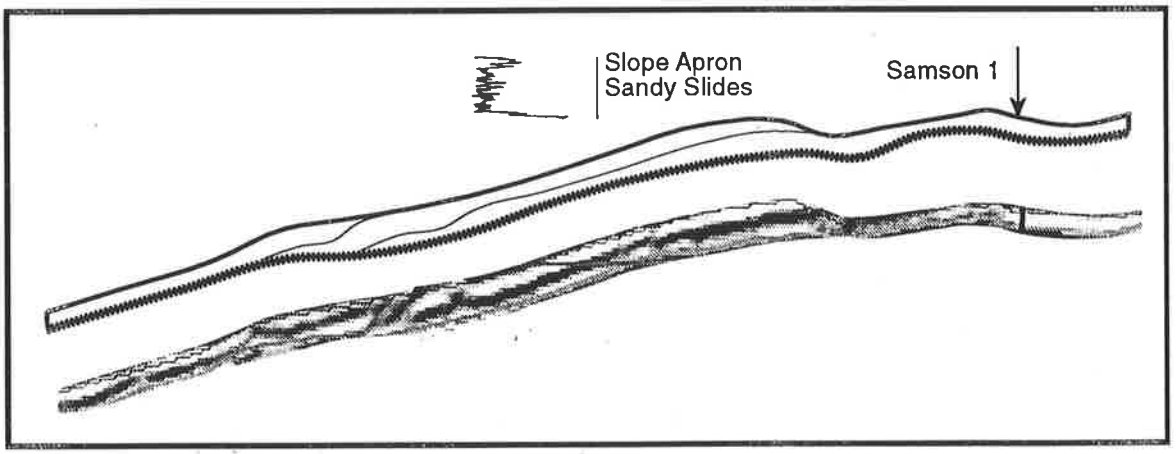


Figure 3.34. Unit A6 at Samson 1 of interpreted Slope Apron Sandy Slides. See also Figure 3.55.

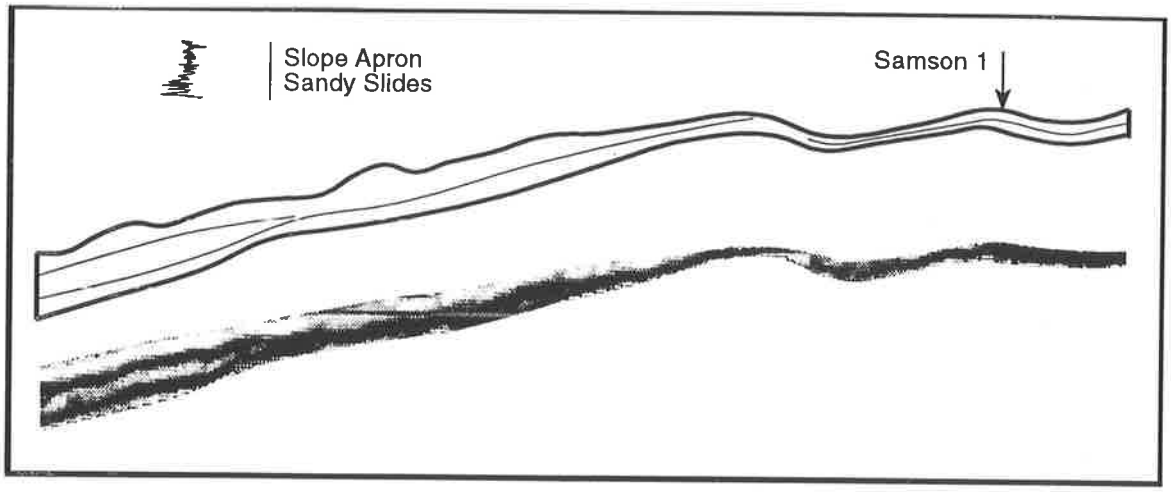


Figure 3.35. Unit A5 at Samson 1 of interpreted Slope Apron Sandy Slides. See also Figure 3.55.

Slope Apron Slides and Slumps

Slope Apron Slide and Slumps contain discontinuous, concave up and chaotic events. The examples (Figures 3.36 and 3.37) have subtle wedge shapes, typical of slope apron deposits.

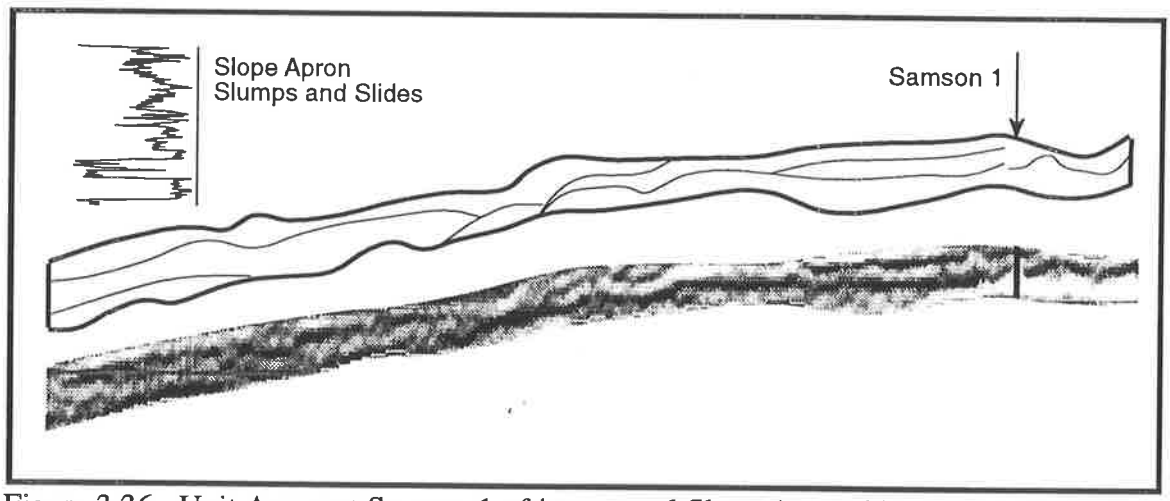


Figure 3.36. Unit A3&4 at Samson 1 of interpreted Slope Apron Slumps and Slides. See also Figure 3.55.

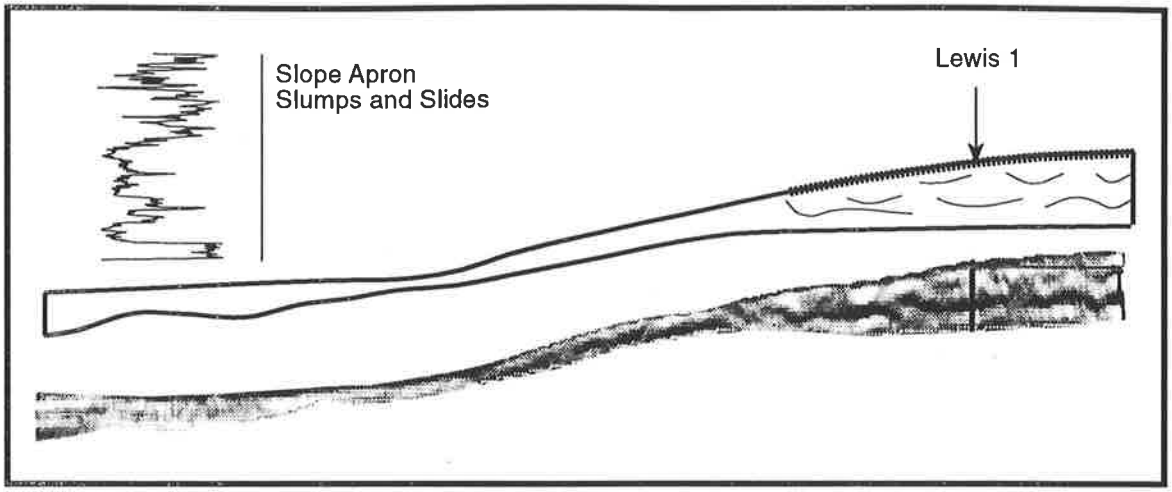


Figure 3.37. Unit A3&4 at Lewis 1 of interpreted Slope Apron Slumps and Slides. See also Figure 3.54.

Slope Apron Depositional Sand

Slope Apron Depositional Sand examples are shown in Figures 3.38, 3.39, 3.40, 3.41, 3.42, and 3.43. Overall lens shaped packages are noted in many of the examples. These discontinuous and low amplitude seismic 'lenses' tend to be outlined by continuous, low frequency, high amplitude events.

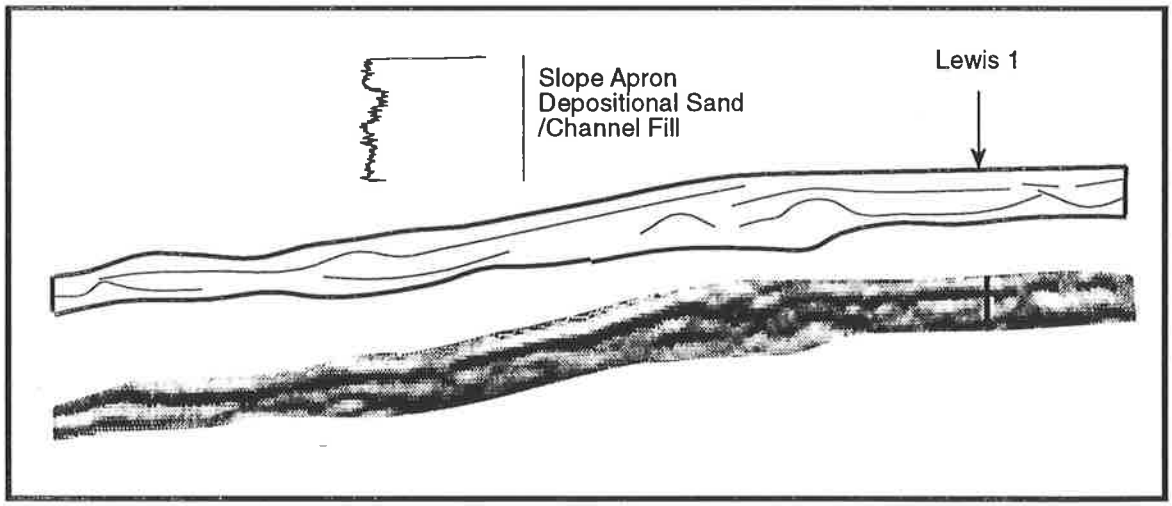


Figure 3.38. Unit A5 at Lewis 1, interpreted as Slope Apron Depositional Sand gradational with Channel Fill. See also Figure 3.54.

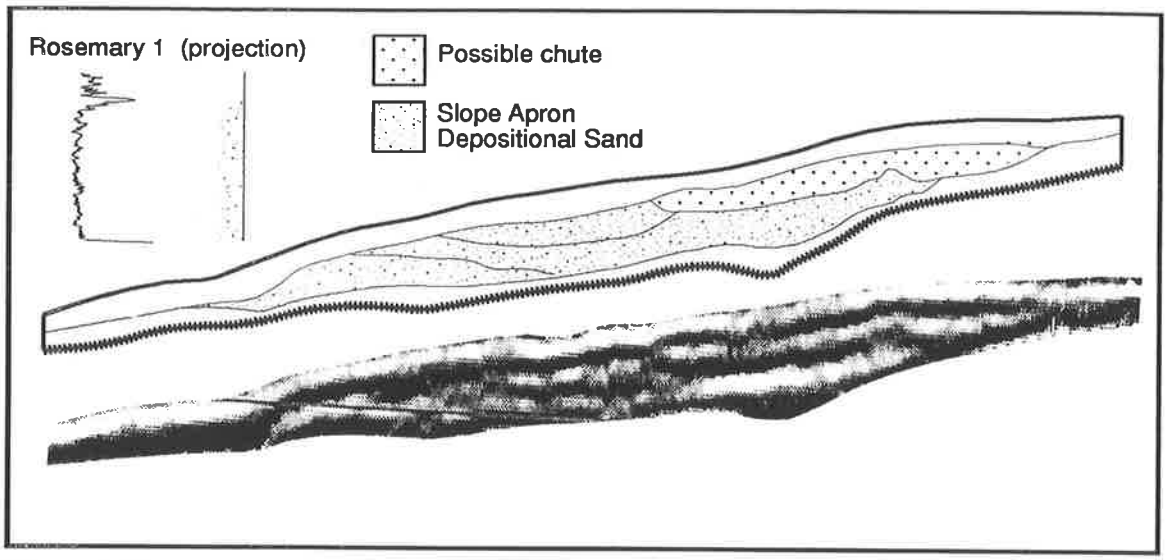


Figure 3.39. Slope Apron Depositional Sand projected from unit A5 at Rosemary 1 (1 - 2km). See also Figure 3.52.

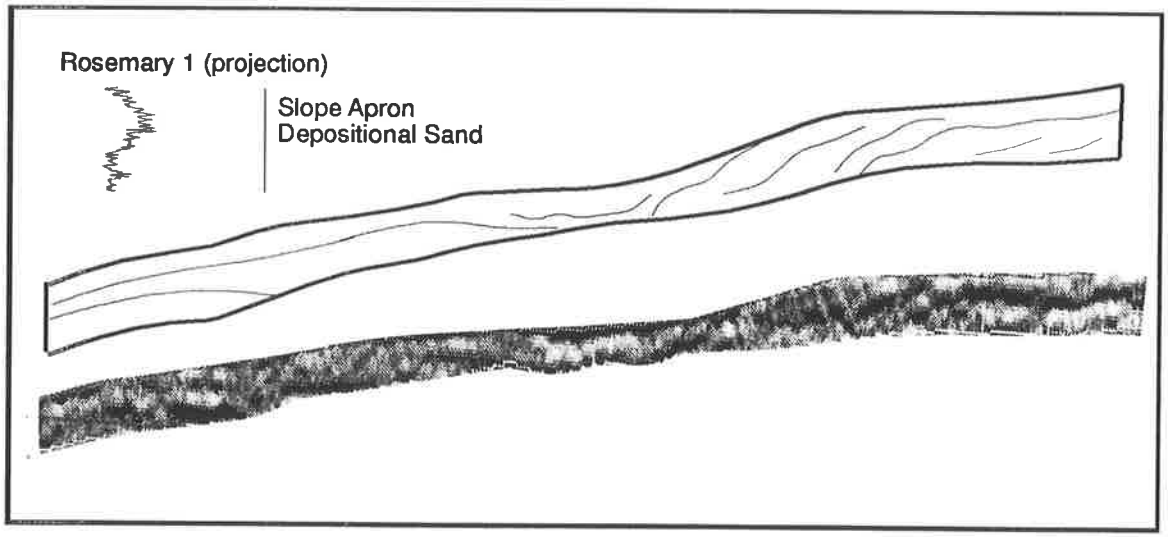


Figure 3.40. Slope Apron Depositional Sand projected from unit A3&4 at Rosemary 1 (1 - 2km). See Also Figure 3.52.

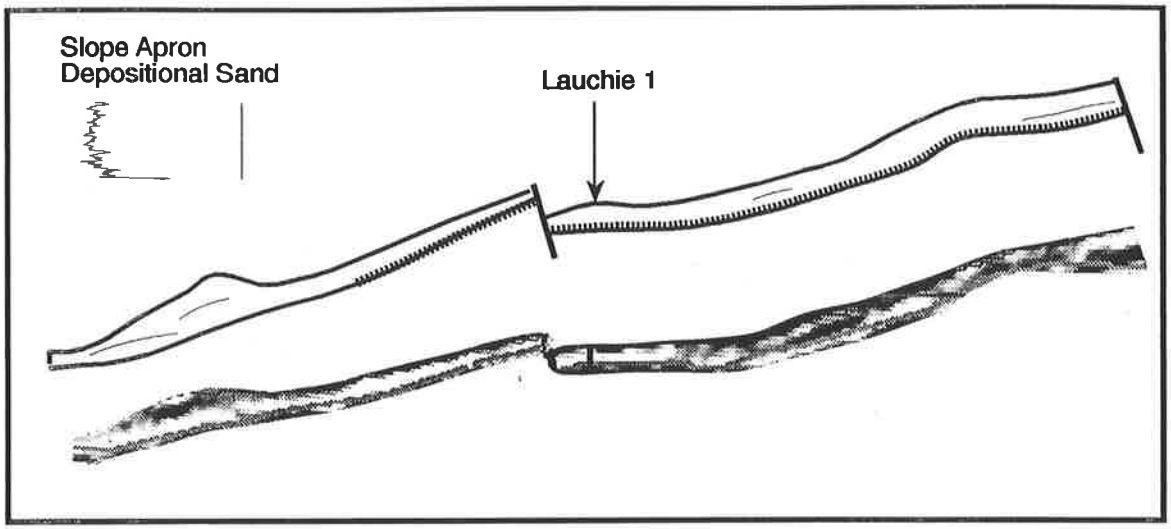


Figure 3.41. Unit A6 at Lauchie 1 of interpreted Slope Apron Depositional Sand. See also Figure 3.53.

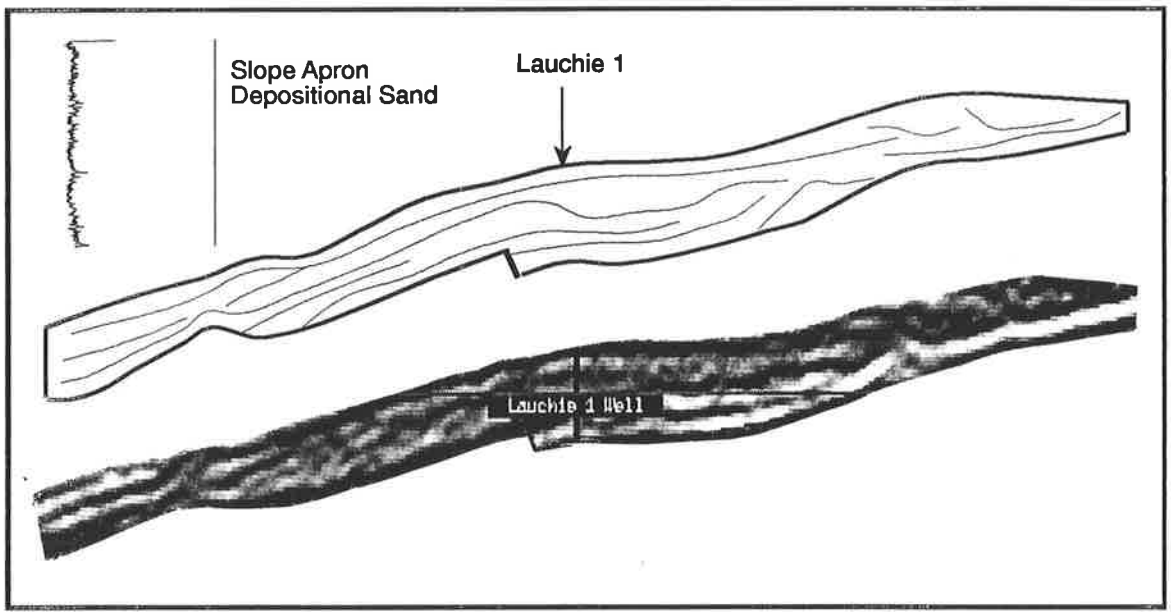


Figure 3.42. Unit A5 at Lauchie 1 of interpreted Slope Apron Depositional Sand. Note the relatively lower amplitudes within the seismic lens. See also Figure 3.53.

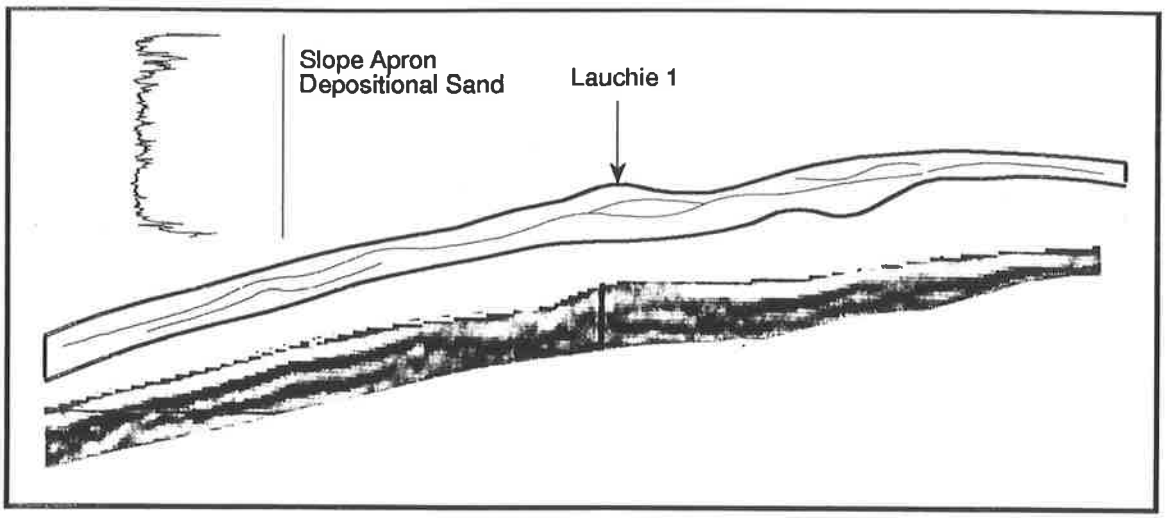


Figure 3.43. Slope Apron Depositional Sand example of unit $A_{1\&2}$ at Lauchie 1. See also Figure 3.53.

Levees and Contourites

Levees and Contourites display similar log profiles and seismic characters, and therefore discussed here together. Examples are displayed in Figures 3.44, 3.45, 3.46, 3.47 and 3.48. It is possible that these examples are more like levees than contourites since they are all associated with nearby incised channel features, interpreted to be mud filled (e.g. Figures 3.47 and 3.48). The seismic is characterised by continuous, low amplitude and moderate to high frequency, and parallel events with mounded geometries.

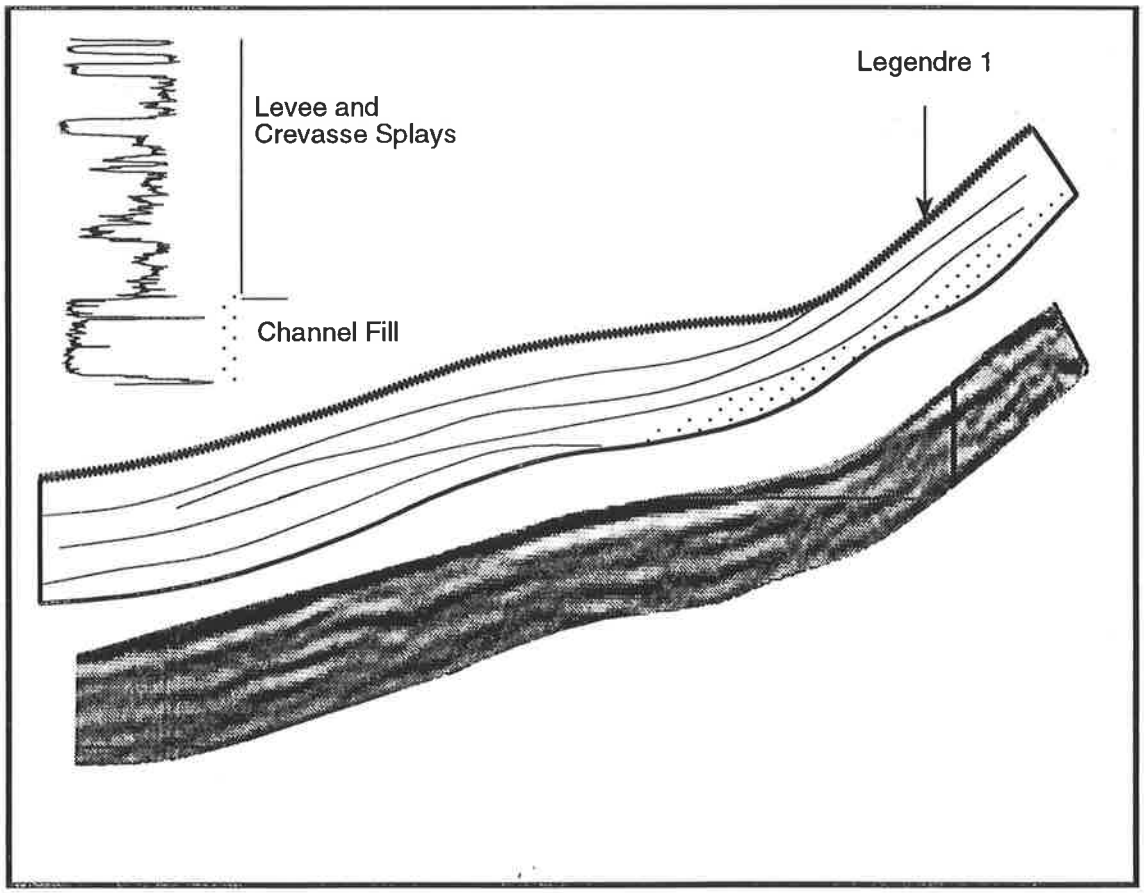


Figure 3.44. Interpreted Crevasse Splays within a levee complex at Legendre 1 unit E1. See also Figure 3.56.

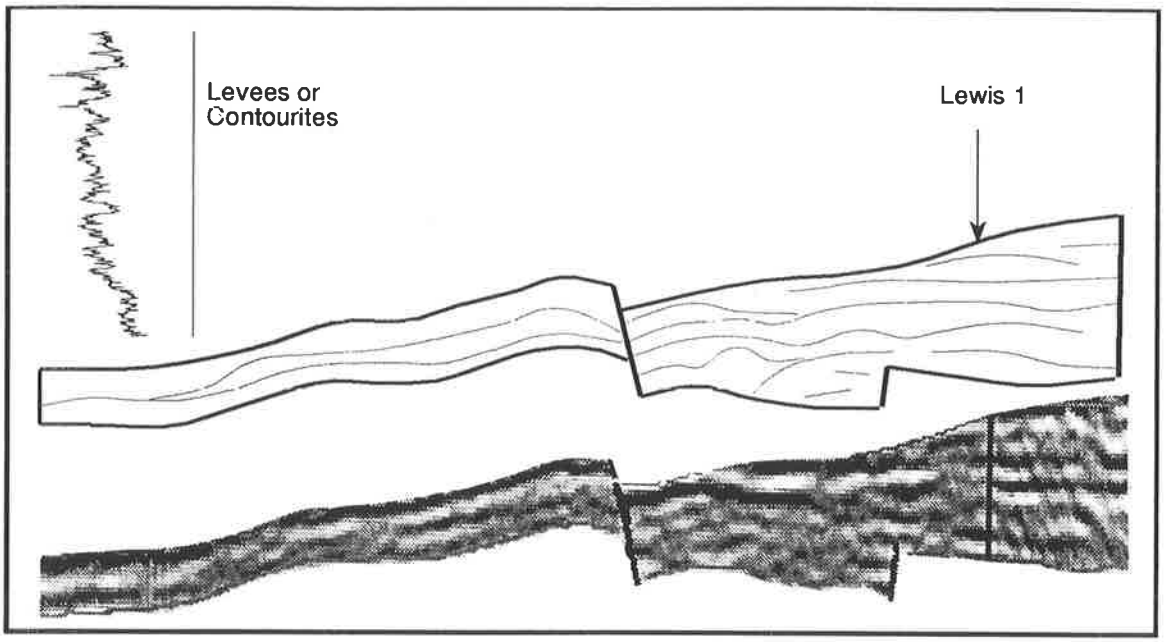


Figure 3.45. Dip section of interpreted Levee complex at Lewis 1 unit E_2. See Figure 3.47 for a nearby strike section. See also Figure 3.54.

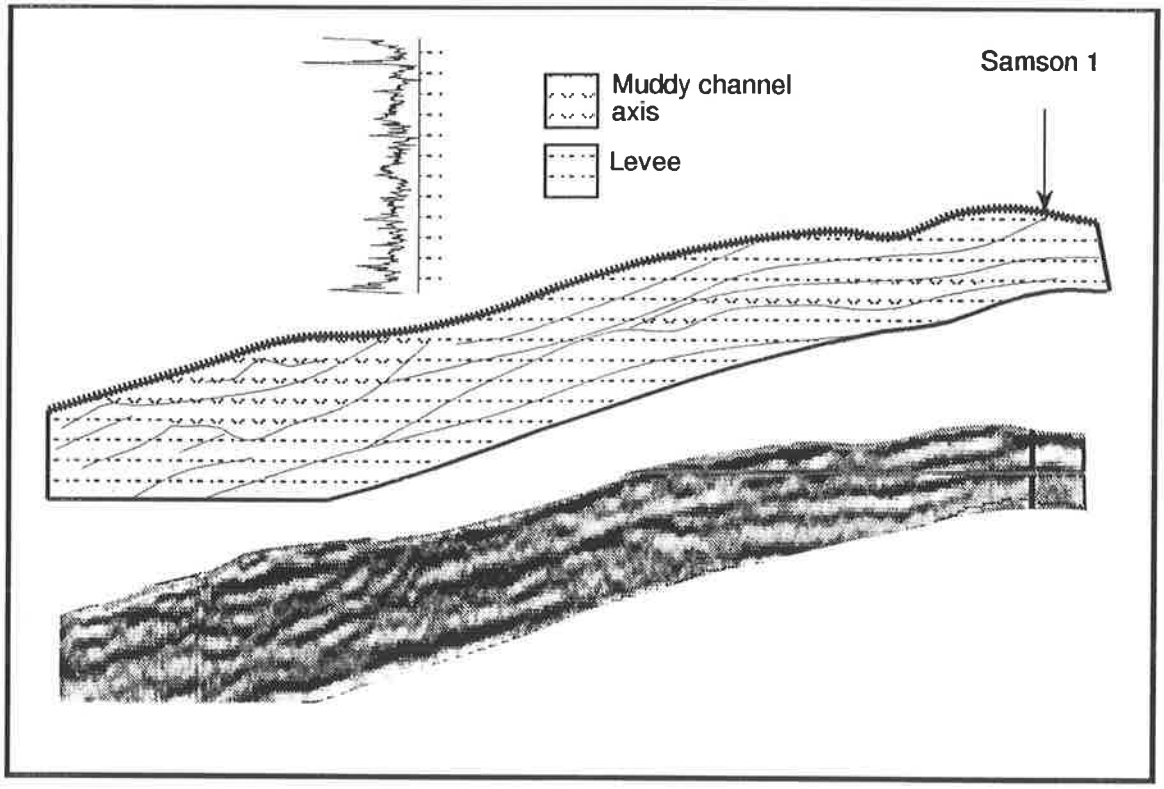


Figure 3.46. Interpreted levee complex within unit E_1 at Samson 1. Note possible muddy channel axes. See also Figure 3.55.

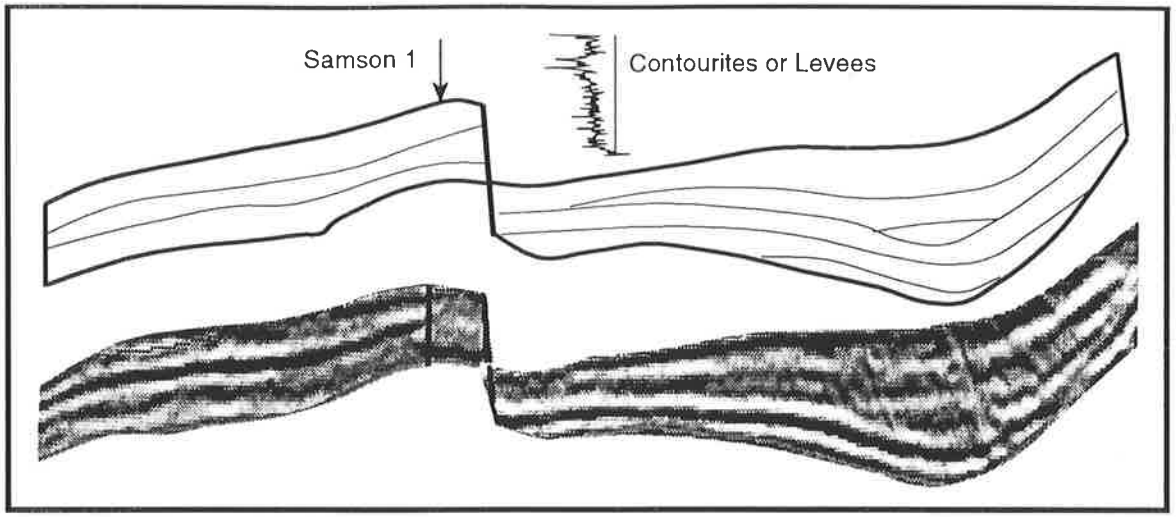


Figure 3.47. Interpreted Levees or Contourites within unit E_2 at Samson 1. See also Figure 3.21.

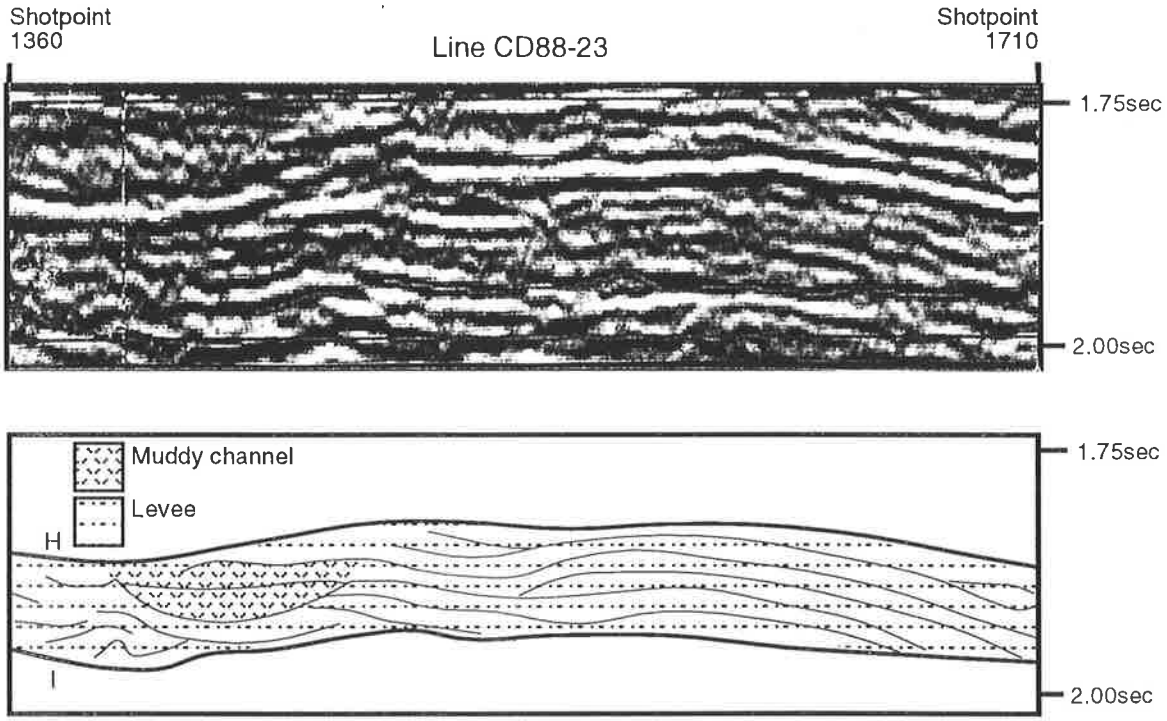


Figure 3.48. Strike section example of interpreted levee complex and possible muddy channel. See Figure 3.45 for nearby dip section and well profile. See Enclosure IVd for position on uninterpreted seismic section.

Erosional Channel Features

A fault controlled channel scour feature is highlighted in Figure 3.49 (strike example) and Figure 3.50 (dip example). Prograding clinoforms are seen in both sections. This channel has a maximum depth of 100m and is between 1 - 2km across. This equates to a width to depth ratio of about 10 to 1. The channel is thought to be sand filled with a gamma ray log profile similar to that of the Channel Fill depositional element.

A broad erosional feature is shown in Figure 3.51. Three episodes of cut and fill can be observed. It is expected that the lithofacies over this section would be similar to the Braided Channels and Chutes depositional element.

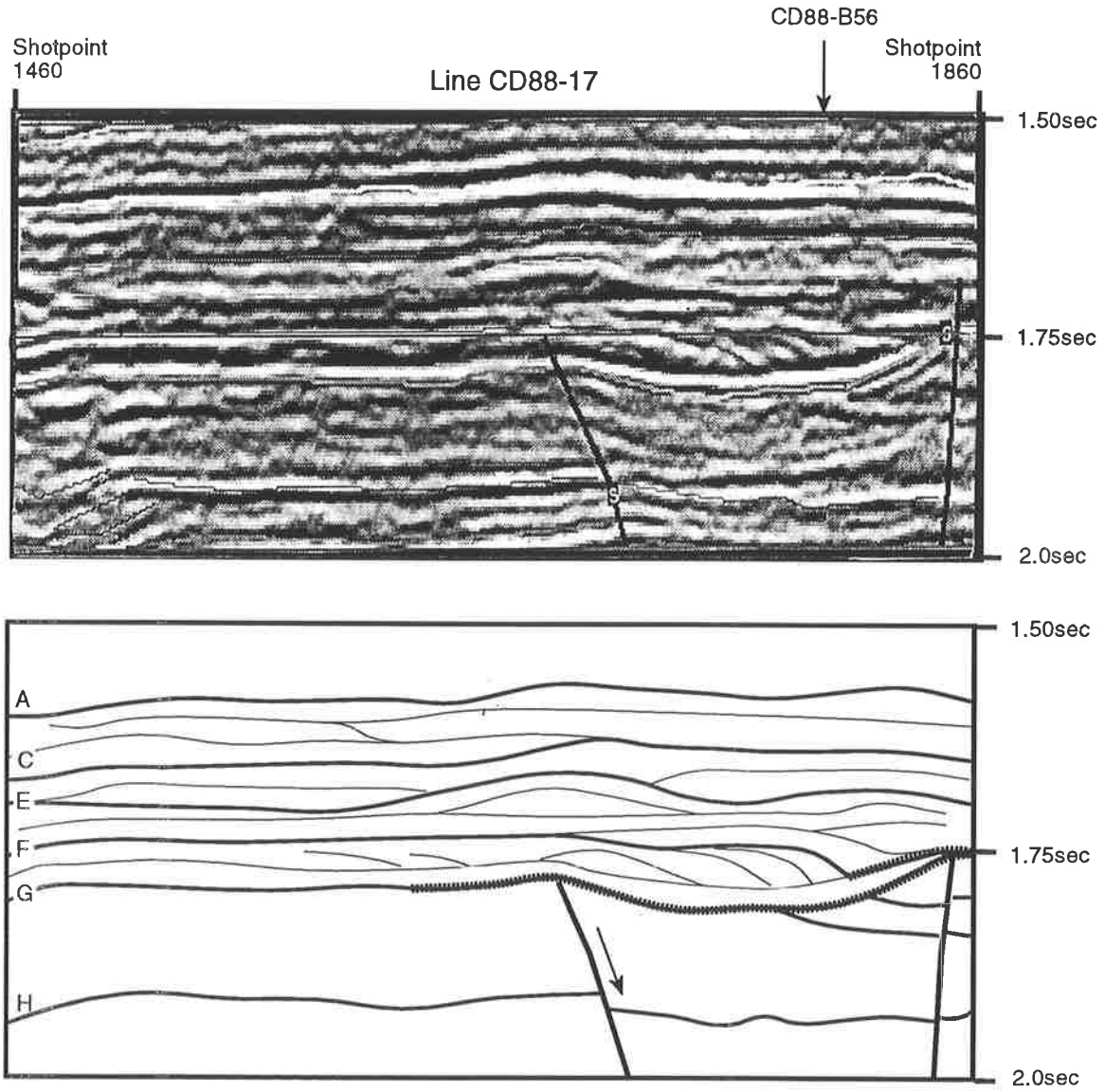


Figure 3.49. Strike section showing clinoforms within an incised channel feature. See Figure 3.50 for the dip profile of channel. See Enclosure IVe for position on uninterpreted seismic section.

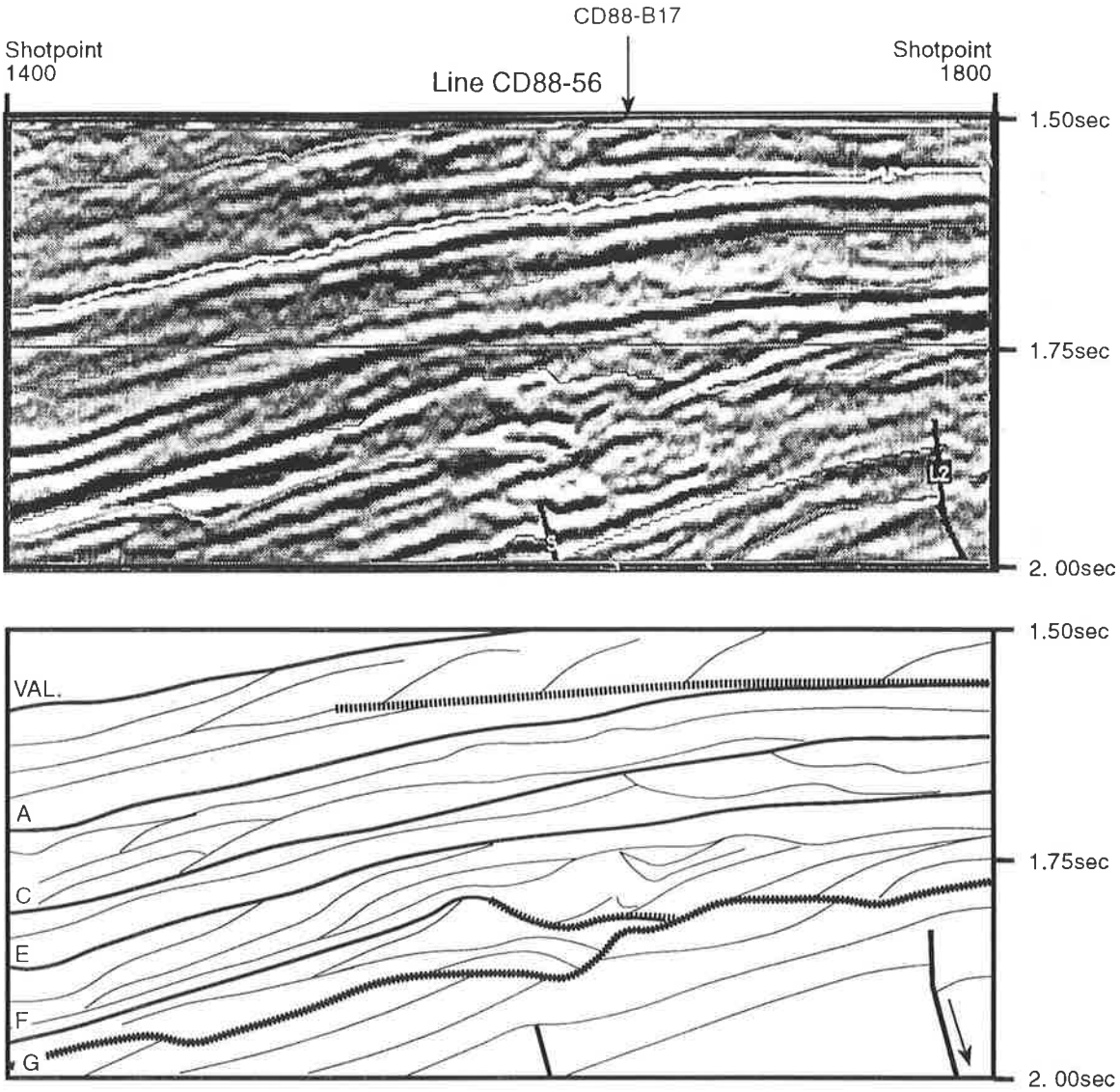


Figure 3.50. Dip section of incised channel feature. See Figure 3.49 for the strike profile of this feature. See Enclosure IVf for position on uninterpreted seismic section.

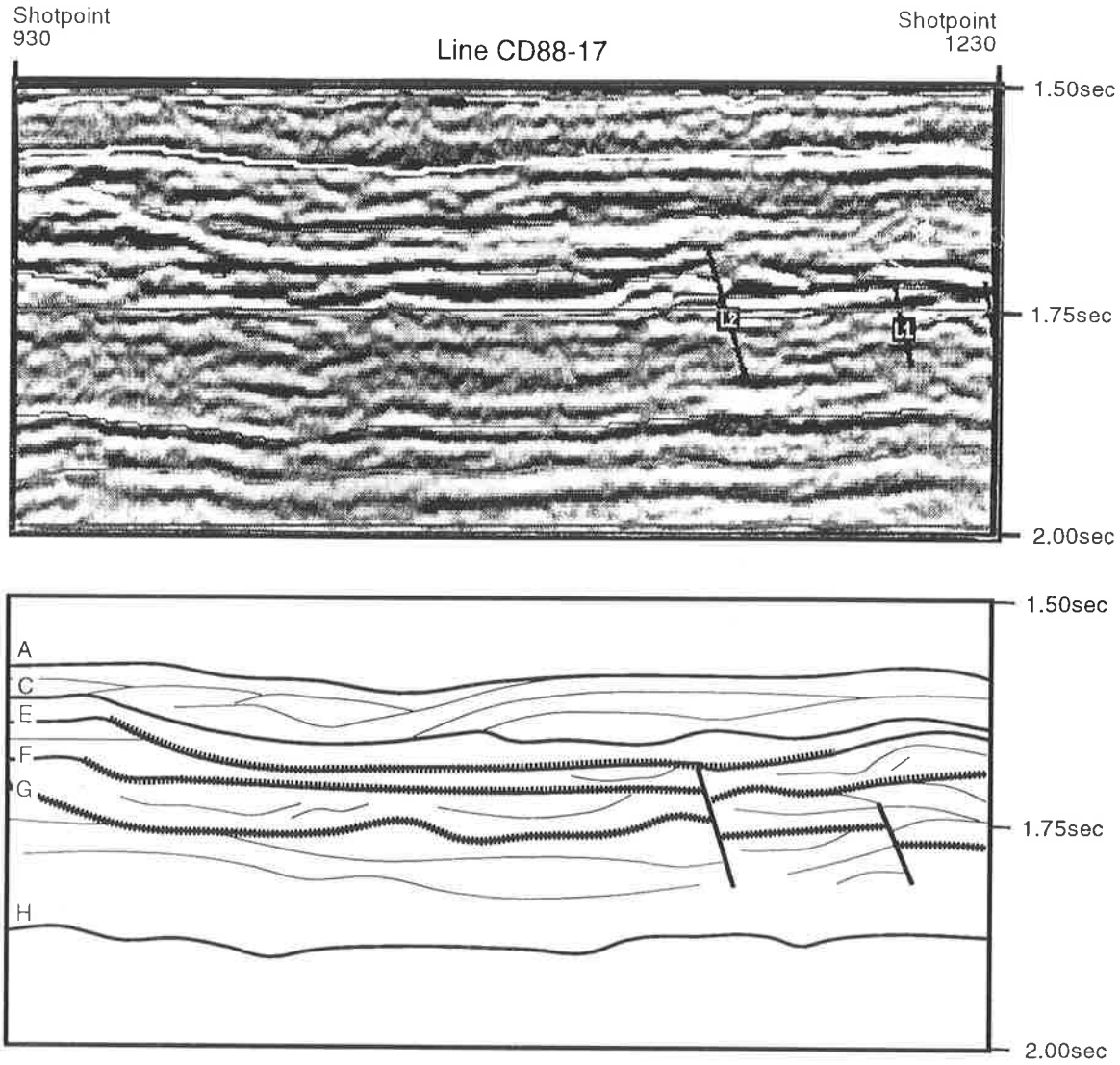


Figure 3.51. Seismic profile of a broad channel cut and fill sequence. See Enclosure IVe for position on uninterpreted seismic section.

3.4.3 Conclusions

Seismic characters and typical seismic stratal configurations for various depositional elements are summarised in Table 3.7. It is difficult, and perhaps dangerous to directly infer lithologies from seismic frequency and amplitude alone. It is observed, however, that many high amplitude events are often associated with sandy lithologies. By studying the seismic stratal configurations and relating them to various depositional elements, more accurate predictions of the lithofacies can be inferred. The examples shown in this section, although numerous, highlight typical seismic stratal configurations and seismic character of specific depositional features, depositional elements, and formations. In addition to the use of direct reference in this project area, they may be used as a guide to infer lithofacies in areas of similar depositional settings and limited well data.

Depositional Element	Seismic Character	Stratal Configuration	Outer Shape
Aggrading shelf (Calypso Formation)	continuous, moderate to high frequency, moderate to low amplitude	parallel, minor rare onlap	
Hemipelagic Basin Fill	discontinuous, low to moderate frequency, low to moderate amplitude; also occurs continuous with very low frequencies	onlap, convergence, asymptotic downlap, aggradation	
Depositional Lobe Sheet Sands	continuous, moderate to high frequency, low amplitude	parallel, possible onlap	
Depositional Lobe Massive Sand	discontinuous, convex up, moderate frequency, high amplitude; mounds may be internally transparent	bi-directional downlap	mound
Braided Channels and Chutes	continuous, high amplitude	bi-directional convergence, erosional truncations	lens
Channel Fill	continuous and discontinuous, concave up, high frequency, low amplitude	erosional truncation	channel or 'U' shape
Slope Apron Braided Channels	chaotic, high frequency, low amplitude		wedge
Slope Apron Sandy Slides	broad concave up or dish shaped events, high amplitude		
Slope Apron Slumps and Slides	discontinuous, concave up, chaotic	downlap	wedge
Slope Apron Depositional Sand	continuous, high amplitude; internally discontinuous, low amplitude	bi-directional convergence	lens
Levees and contourites	continuous, moderate to high frequency, low amplitude	bi-directional downlap	mound

Table 3.7. Summary of seismic characters and stratal configurations of depositional elements.

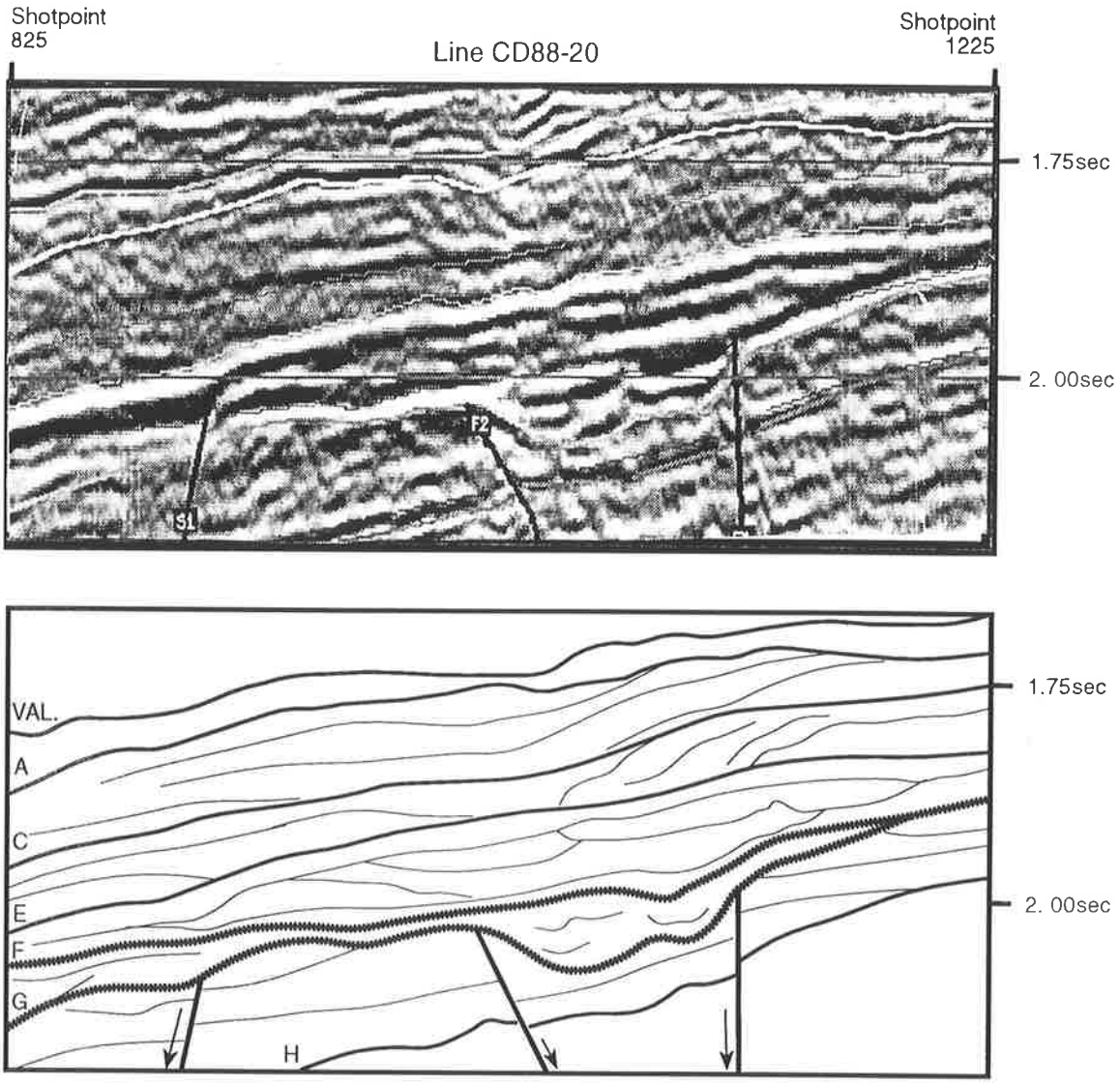


Figure 3.52. Seismic profile near Rosemary displaying a seismic 'lens'. See Enclosure IVg for position on uninterpreted seismic section.

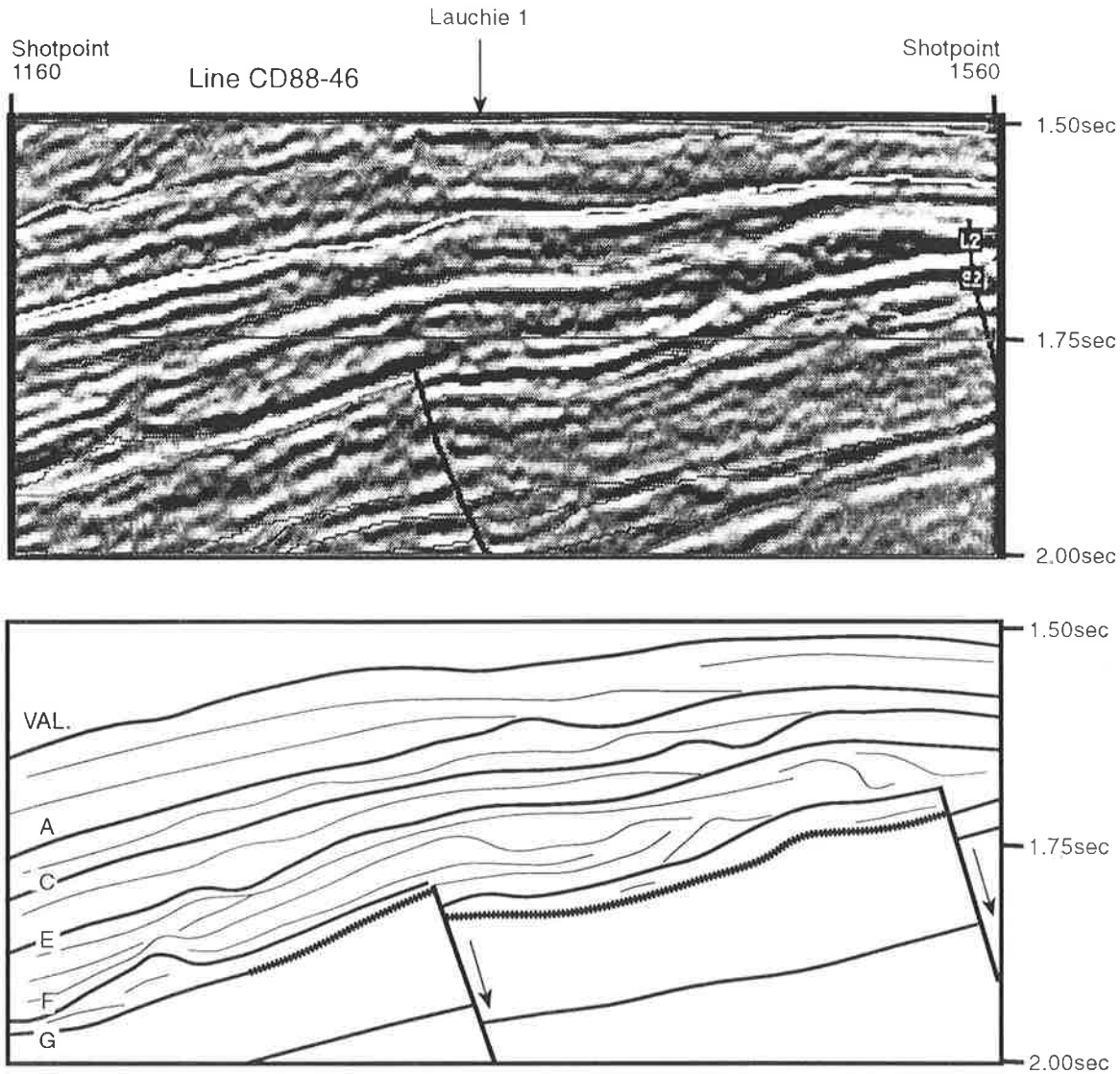


Figure 3.53. Seismic profile and stratal configuration diagram at Lauchie 1. See Enclosure IVh for position on uninterpreted seismic section.

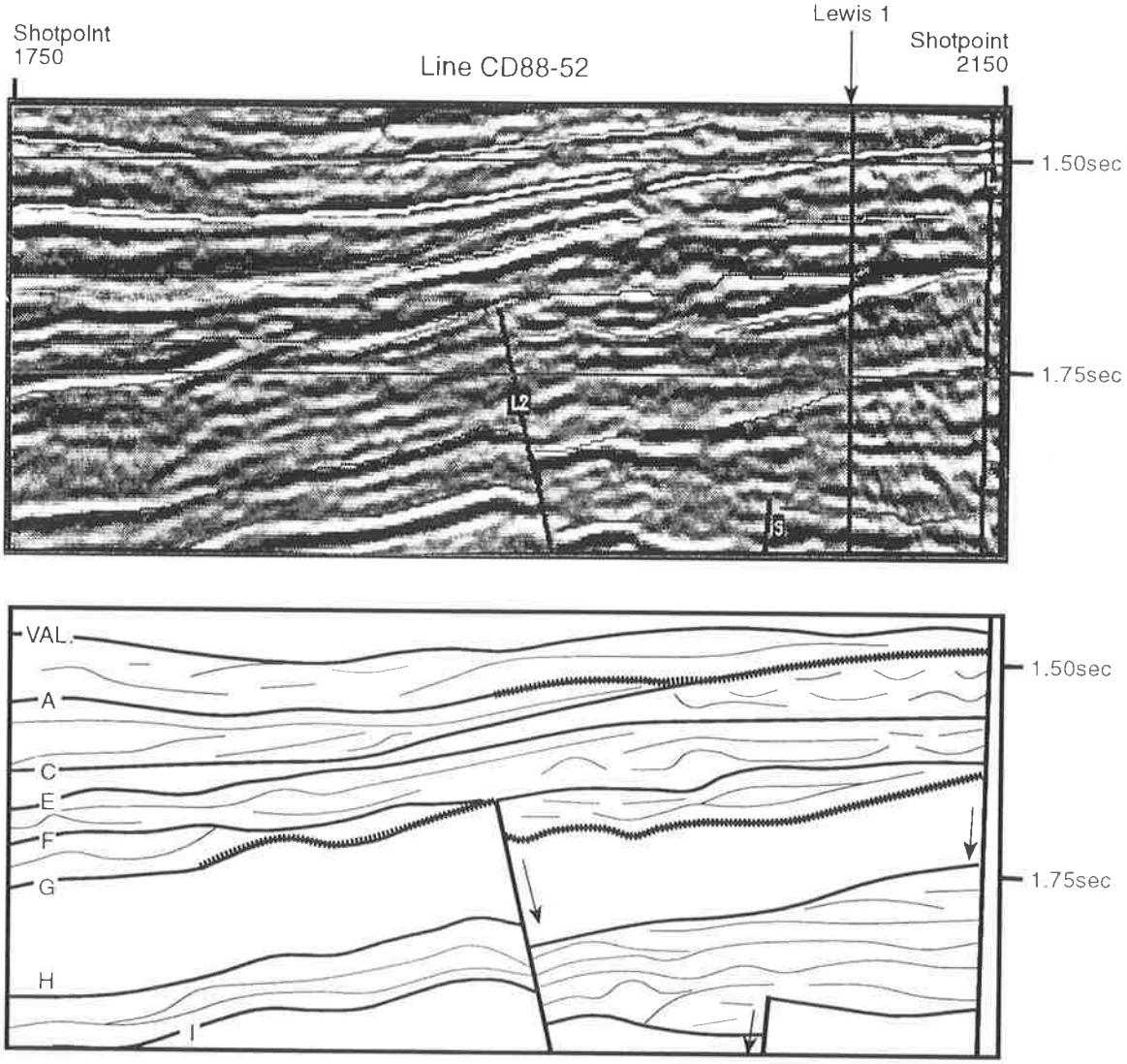


Figure 3.54. Seismic profile and stratal configuration diagram at Lewis 1. See Enclosure IVi for position on uninterpreted seismic section.

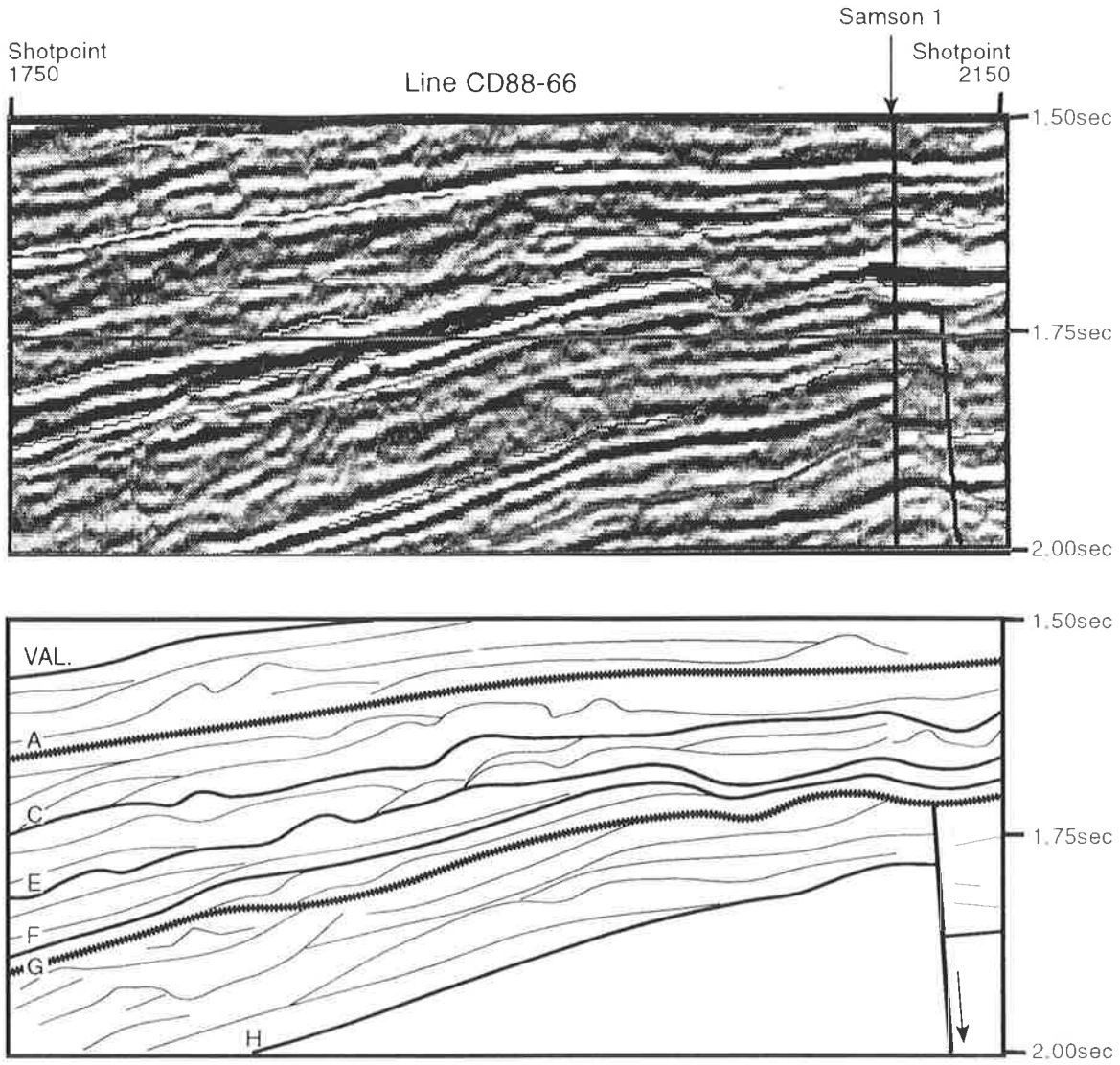


Figure 3.55. Seismic profile and stratal configuration diagram at Samson 1. See Enclosure IVc for position on uninterpreted seismic section.

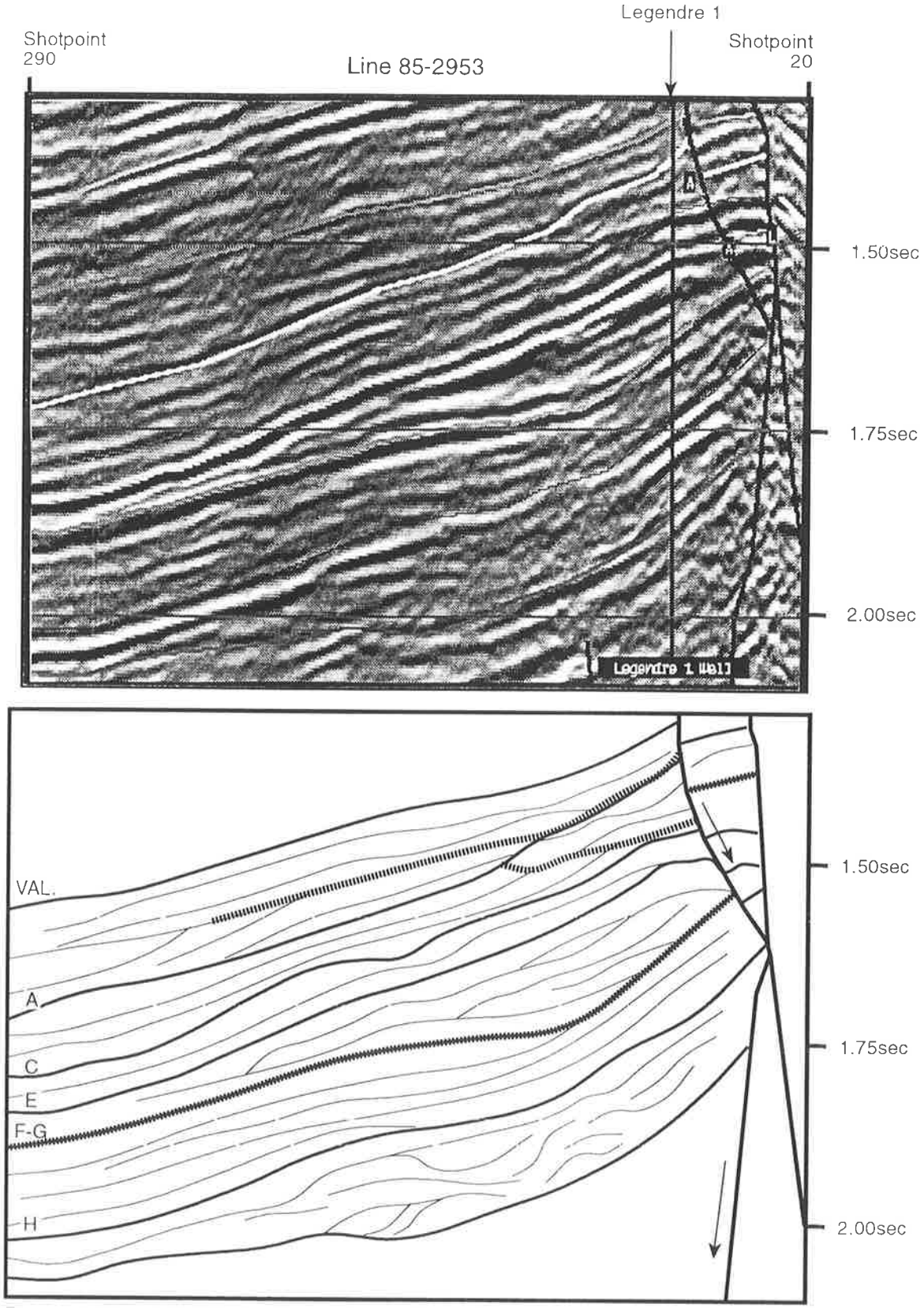


Figure 3.56. Seismic profile and stratal configuration diagram at Legendre 1. See Enclosure IVj for position on uninterpreted seismic section.

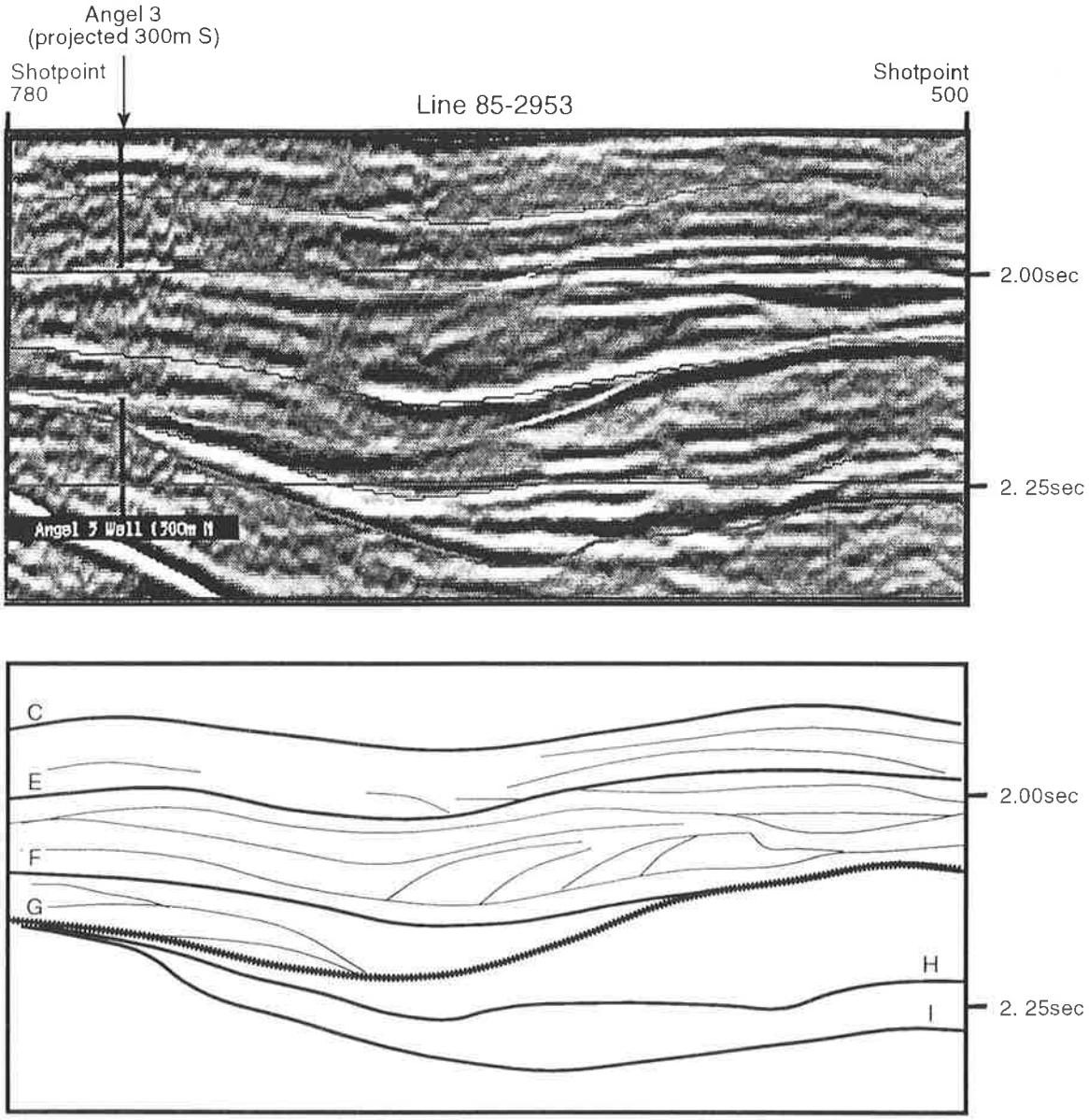


Figure 3.57. Seismic profile and stratal configuration diagram near Angel 3. See Enclosure IVj for position on uninterpreted seismic section.

CHAPTER 4: RESULTS AND DISCUSSION

DEPOSITIONAL SYSTEMS, TECTONIC DEVELOPMENT AND GENETIC STRATIGRAPHY

4.1 DEPOSITIONAL SYSTEMS

4.1.1 Introduction

Depositional systems in the Dampier Sub-basin are outlined by Barber (1994) in the context of the 'Vail' sequence stratigraphic approach. He defined sequences (see Figure 4.68) which are attributed to eustatic sea level using the Haq et al. (1988) sea level curve. The prediction of sand prone depositional periods are outlined in a temporal sense and associated with eustatic falls of sea level. Much of the same data is used in this project. Discrete episodes of deposition have been defined based on palynology, well log and seismic correlations (Section 3.3). Lithofacies have been defined using core log interpretations. These lithofacies have been associated to depositional elements that were fundamentally defined using wire line log facies (Section 3.2). Gamma ray log motifs were annotated to seismic profiles (Section 3.4) in order to assess the seismic configurations and character of the various depositional elements. The lithofacies, depositional elements and seismic facies form an integral part of this chapter. These aspects are used to characterise each depositional system. The influence of sediment source, palaeo-topography, syn-sedimentary tectonics, and sea level for each of the defined episodes of deposition were then evaluated.

There are many papers on sequence stratigraphy over the North West Shelf (e.g. Barber, 1994; Ross and Vail, 1994; Arditto, 1993; Spring and Newell, 1993; Wulff, 1992) that discuss sand-shale development in a temporal sense. This study, however, focuses on the spatial and three dimensional development of sand-shale interplays. This method utilises depositional models to help characterise the style of sedimentation within each depositional episode by using seismic facies maps, lithofacies and depositional elements. Each proposed style of deposition helps to explain lateral lithologies and sand body distributions which are, in turn, inferred from seismic facies maps, isopach maps, and structure maps.

Palaeo-bathymetry and overall basin shape is the primary controlling factor of the morphology of marine resedimented facies. Sandy lithologies can often be inferred to occur in palaeo-bathymetric low areas, while thinner, hemipelagic sediments may occur on local topographical highs. In the case of submarine canyons and incised channels, these generalisations should be met with caution. This is because many canyons and channels that have been drilled as exploration targets have been mud filled (pers. comm., W. Galloway, 1994).

Isopach maps are typically used to infer palaeo-topography, where relatively thick areas are local lows, and thin areas are local highs. There are two assumptions that need to be considered and accounted for, in order to interpret the palaeo-topography. Firstly, it must be assumed that the top of the unit was relatively flat near the end of the depositional episode. It is reasonable to suggest that relief probably existed at the end of depositional episodes in active margin settings such as the Dampier Sub-basin.

For example, slope aprons can be relatively thick with respect to the rest of the unit, but they are not necessarily deposited in the lowest areas of the basin. The relative thicknesses of slope apron deposits were the result of sediment source and palaeo-relief rather than selectively filling palaeo-topographic lows within the basin. A good counter-example to this would be a channel-lobe complex, where depositional morphology is strongly controlled by palaeo-topography. The style of depositional system and basin setting needs to be considered in this manner to objectively use isopachs to infer palaeo-topography.

The second assumption deals with the differential compaction of different lithologies. Mud is typically highly compacted, sand is variably compacted and mixed lithologies are relatively the least compacted. Therefore, relatively thicker areas on isopach maps may represent sandier areas that have undergone less compaction, rather than just palaeo-topographic low areas. However, if the palaeo-topography is controlling the distribution of sand deposition, this factor may amplify the real palaeo-topography. Again, the style of depositional system and basin setting needs to be considered to evaluate the influence of compaction in a given area. Although there is little knowledge of the relative timing of compaction of underlying sediment, it may also effect the palaeo-topography.

Another assumption must be considered when isochron maps are used as effective isopach maps. It deals with velocity contrasts of varying lithologies. The assumption is that velocities of the lithologies within the unit are the same, and therefore two-way-time is directly proportional to unit thickness. A unit that contains varying lithologies with large velocity contrasts, if unaccounted for, may result in unrealistic observations of relative unit thickness. Here, the factor of varying lithologies usually has a negative effect. For example, if the sand has a higher velocity than the mud within the unit, sandier areas will appear to by relatively thin. In this case, palaeo-topographic low areas may not be obvious.

In many cases, an isochron map of a single unit may not reflect the palaeo-topography as well as one would expect. The assumptions outlined above need to be checked throughout the interpretation of any isochron map. Some of these factors have been alleviated to some extent in this study by using combination structural/isochron maps.

Combination structural/isochron maps were constructed from the Valanginian Disconformity to: Horizon 'C' (middle Angel Formation); Horizon 'E' lower-middle Angel Formation); Horizon 'G' (base Angel Formation); Horizon 'I' (base Eliassen Formation); and Horizon 'J' (Callovian flooding event). Fault cuts at the base of the isochron intervals were drawn on these maps. Using these maps, overall palaeo-topography of the intervening depositional episodes was inferred. By using the Valanginian Disconformity as the top of the isochron units, I assumed that there was little, if no relief of the Lewis Trough depocentre during the Valanginian. This interpretation is supported by the Stratigraphic Log Correlations 'C' to 'G' (Figures 4.16 to 4.20) which have the Valanginian Disconformity as the datum. The horizon correlations appear relatively uniform across the sections with no significant thickness variations. In addition, the Valanginian Disconformity Structure Map (Figure 4.38) displays a relatively uniform structure. Although there is definition of the Lewis Trough on this structure map, it is interpreted that this syncline formed

later by differential subsidence in the Middle Cretaceous. This is discussed in detail in Section 4.2 (Structural and Tectonic Development With Relation to Sedimentation).

The isochron/structural maps from the Valanginian Disconformity were used to interpret overall basin shape and relief at the time of deposition of the overlying tectonic sequence. Individual variations of each depositional system were considered using the unit isochron maps. Mapped stratal patterns provided clues to the lateral extent of these lithologies. Local lithologies are included in the interpretation from nearby wells. Mapped seismic stratal configurations provided clues to the lateral extent of these lithologies. Two way time structure maps, isochron maps, isochron/structure maps and seismic facies maps are listed in Table 1.5.

The lithological content and morphologies of submarine channels and lobes is highly dependent on the relative grain size and the sand to mud and/or sand to gravel ratio that exists in the sediment supply (Galloway, 1993). For example, 'transport efficiency' is a concept developed by Mutti (1979) which is dependent on the sediment supply and qualifies the transportability of sand into the basin. Relatively muddy systems are highly efficient systems that transport isolated sand lobes onto the basin floor. Poorly efficient systems have a high sand to mud ratio, and lobes are less extensive and are dominantly composed of depositional and mixed channel fill types. Factors affected by the sediment supply in channels include the width to depth ratio, channel sinuosity, levee height and overall stability (see Figure 4.1).

The degree to which lobes are 'sheet lobes' or 'mounded lobes' is also dependent on the sediment supply and varies with the amount of channelisation and areal extent of the lobe (Figure 4.2). These concepts are used here to help explain the development of the depositional episodes.

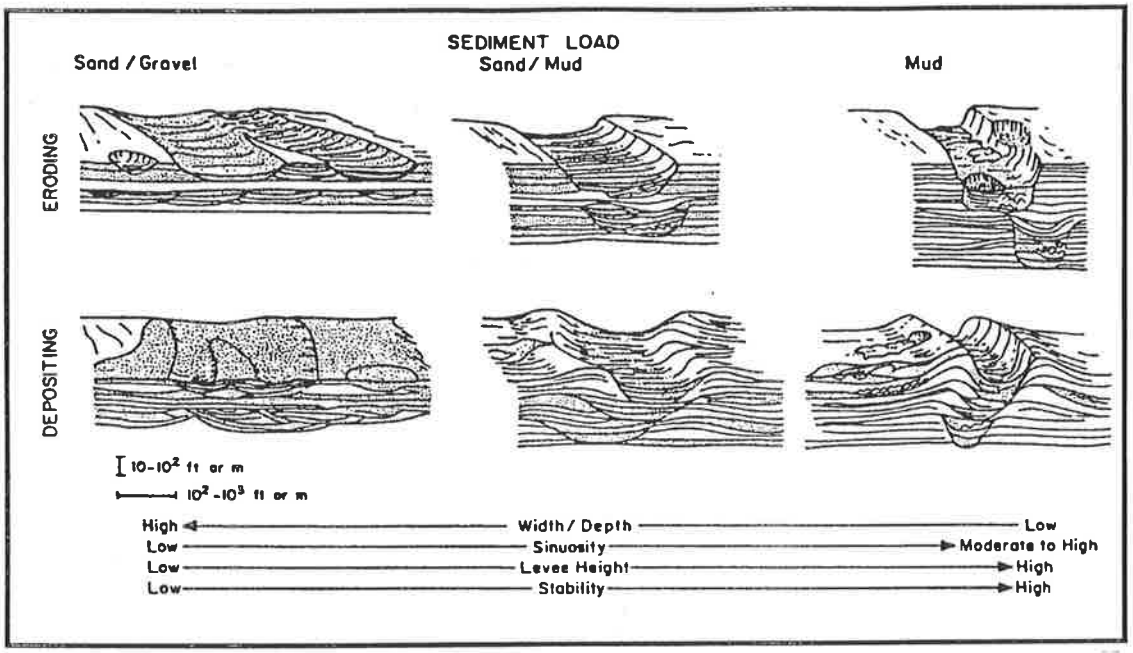


Figure 4.1. The textural spectrum of turbidite channels contrasting the geometric and depositional attributes of erosional and depositional types. Changes in width/depth ratio, sinuosity, levee height and channel stability parallel the patterns that are documented for fluvial settings (after Galloway, 1993).

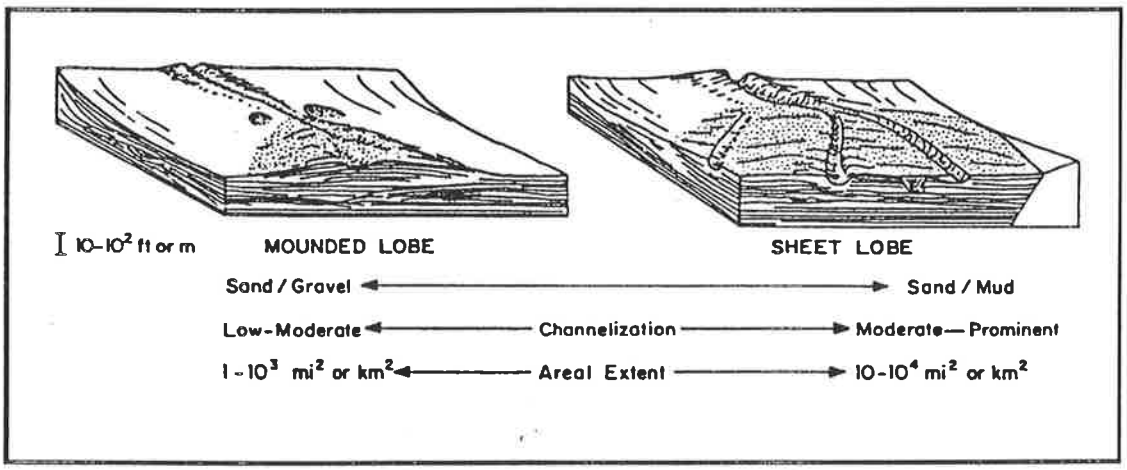


Figure 4.2. Block diagrams illustrating the geometry and characteristics of coarse sandy and mixed sandy to muddy turbidite lobes.

The following discussion is a description of each depositional episode which together represent the evolution of a rifted margin. Each episode was interpreted with respect to the various depositional models and processes that are discussed previously throughout this thesis. The interpretations are based on the available data and constructed maps. Schematic palaeo-geography diagrams, seismic facies maps, seismic examples, stratigraphic log correlations, isochron maps, structure/isochron maps, and structure maps relevant to each depositional episode are listed at the beginning of the particular discussion. The figures and maps listed for each depositional episode are often numerous, and it is suggested that they be referred to throughout the discussion. In addition, the detailed chronostratigraphy (Figure 3.13) should also be referred to throughout the discussion. In order for the key figures and maps to be crossed referenced with convenience, they have been compiled as various montages that are contained within the thesis as enclosures. The relevant montages should be hung on a nearby wall when the relevant section is being read.

Schematic palaeogeography diagrams were drawn for each of the units that seismic facies maps were constructed for. Where available, these figures are used to show the interpreted depositional element associations and their lateral distributions. The legend for the schematic palaeogeography diagrams is shown in Figure 4.3.

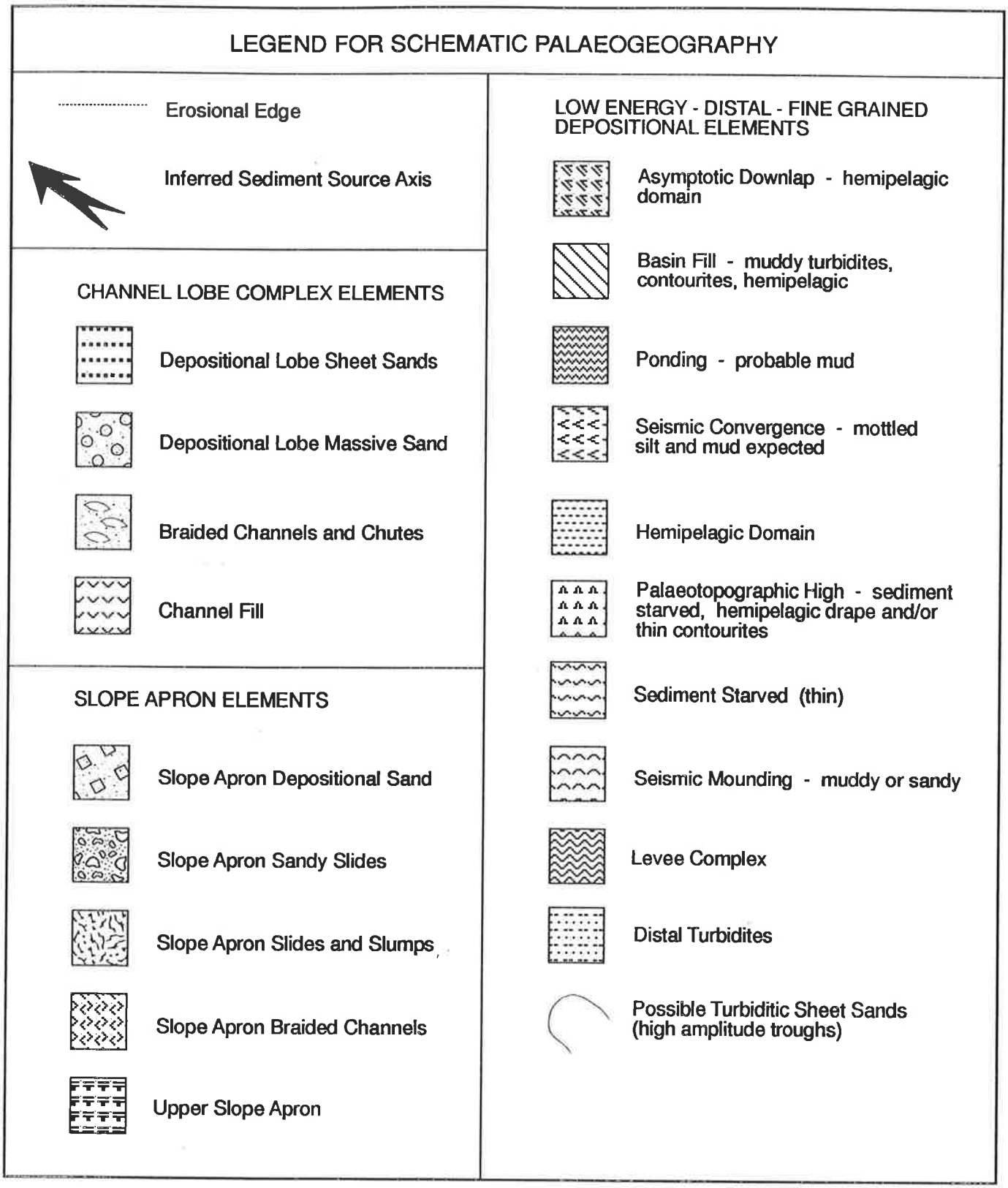


Figure 4.3. Schematic palaeogeography symbols that pertain to diagrams in this section.

4.1.2 Discussion

Calypso Formation Unit C_1

Seismic example : Figure 3.21

Stratigraphic log correlations : location map, Figure 4.4; section H - H', Figure 4.5; section I - I', Figure 4.6.

Isochron map : Calypso Formation unit C_1, Figure 4.7.

Structure/isochron map : Valanginian Disconformity to base Calypso Formation unit C_1, Figure 4.8.

Montage: Enclosure IIIa.

Core data : Legendre 1 core 16, 17, 18, Facies B2.2, D1.3, and E1.1; Rosemary 1 core 1, 2 and 3, Facies D1.1, D1.3 and E1.1.

Limited data was collated for Calypso Formation unit C_1. Many of the wells reached total depth within this unit (e.g. sections I - I', H - H', Figures 4.5 and 4.6). In addition, there is little variation in seismic stratal configuration, and so little stratigraphic information could be obtained by seismic facies analysis. Seismic character is typically represented by continuous, parallel events which onlap and uplap the basin margins or uplap fault scarps (e.g. Figure 3.21). This unit was studied in order to contrast sedimentation style and evaluate basin evolution with respect to the overlying Eliassen and Angel Formations. While these formations are considered to be post-rift, the Calypso Formation is interpreted to have been deposited during intra-rift half graben development. The Rosemary Fault was active during this period (e.g. Barber, 1994; see his figure 20). This fault movement appears to have been initiated near the onset of Calypso Formation deposition (e.g. see Figure 3.21; note fault cuts).

Half graben development provided subsidence of the Lewis Trough area which kept pace with sedimentation. The seismic facies, wire line log facies and depositional facies observed in core attest to this interpretation. The depositional elements are interpreted as Aggrading Shelf in proximal areas, grading to Hemipelagic Basin Fill in distal areas. Legendre 1 core 16 contains Facies B2.2 (cross-stratified sands), core 17 has Facies D1.3 (mottled silt and mud), and core 18 has Facies E1.1. Core 1, 2 and 3 at Rosemary 1 contain Facies C1.2 (mottled silt and mud), D1.1 (structureless silts), D1.3 and E1.1. These facies are interbedded with each other.

Nearshore palynological indicators occur in all wells that penetrate this section along the Legendre Trend. Distal wells such as Walcott 1 and Madeleine 1 have offshore palynological indicators.

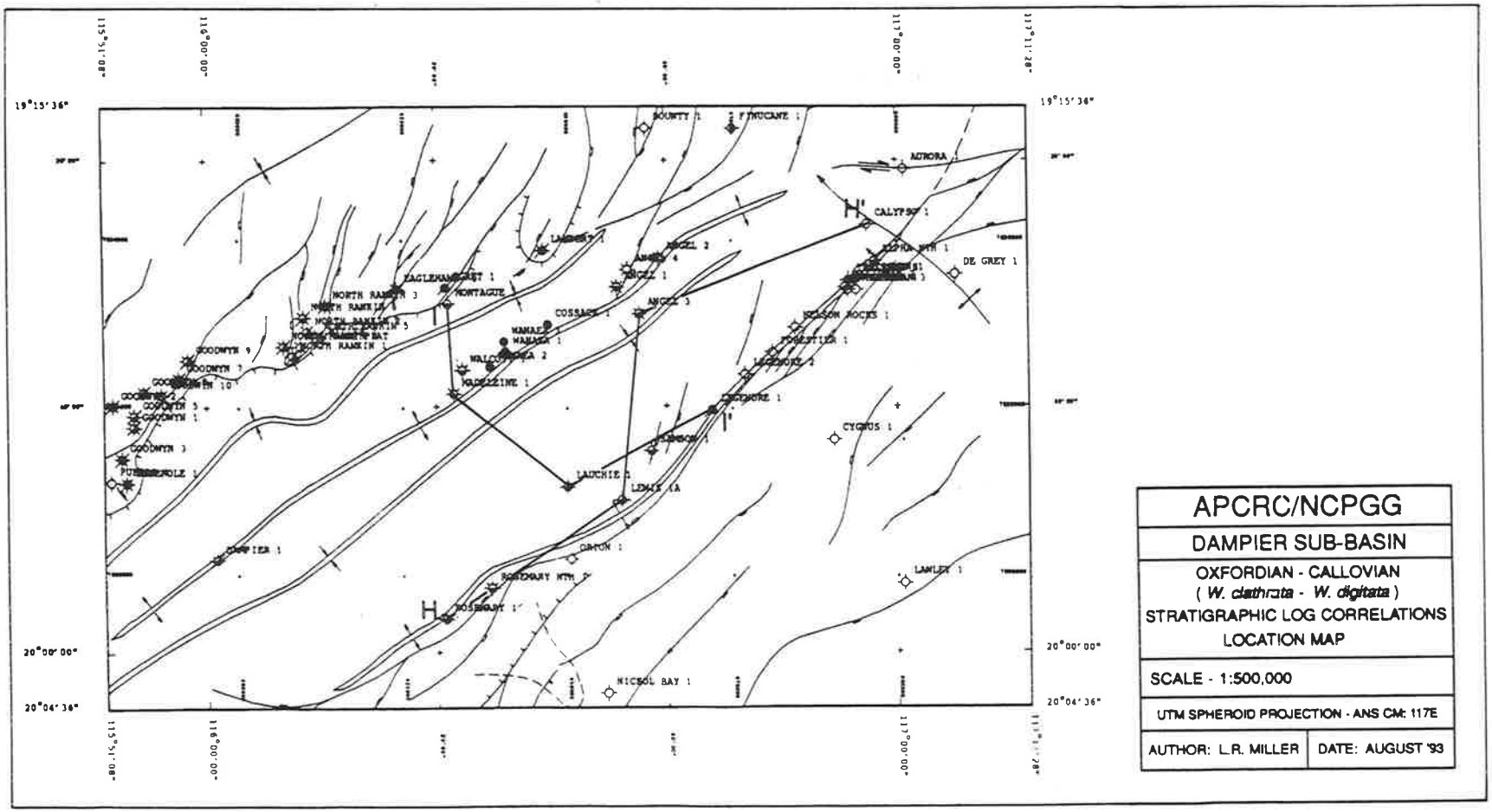

APCRC/NCPGG
DAMPIER SUB-BASIN
OXFORDIAN - CALLOVIAN
(W. clathrata - W. digitata)
STRATIGRAPHIC LOG CORRELATIONS
LOCATION MAP
SCALE - 1:500,000
UTM SPHEROID PROJECTION - ANS CM: 117E
AUTHOR: L.R. MILLER
DATE: AUGUST '93
19°15'36"
20°00'00"
20°04'36"
117°00'00"
AURORA 1
CALYPSO 1
DE GREY 1
CYGNUS 1
LAMLEY 1
NICSOL BAY 1
DAMPIER 1
LAUCHIE 1
ANGEL 1
ANGEL 2
ANGEL 3
COSSACK 1
MONTAGUE
GOODWYN 1
GOODWYN 3
GOODWYN 9
GOODWYN 10
PUBERULE 1
ROSEMARY 1

Figure 4.4.

It is interesting to note that Legendre 1 core 18 is a black shale of Facies E1.1 with nearshore palynological indicators. This shale probably represents a low energy environment with low sediment influx and anoxic water which is near to a shoreline. It is impossible to comment on water depth in this situation. Thin coals can be interpreted from ditch cuttings above and below the shale unit, attesting to a terrigenous influence. This core also contains slickensides, providing evidence that fault movement of the Rosemary Fault succeeded deposition and lithification.

An asymmetrical morphology of unit C_1 is revealed by the isochron map (Figure 4.7). This also attests to the proposed half graben development. A large sediment source can be inferred to occur to the east of Samson 1. This area contains a collapse graben (see structure/isochron map, Figure 4.8), part of which is shown in Figure 3.21. A smaller concentration of sediment is noted to the northwest of Rosemary 1 and is defined by the 320ms isochron (Figure 4.7).

The Rosemary Fault was mapped with reasonable confidence on the structure/isochron map. This accuracy is, however, limited because the fault occurs near the ends of seismic lines and does not intersect other lines. North - south faults are observed to splay from the Rosemary Fault over the Lauchie 1 to Legendre 1 area. Many of these faults continue up section into the overlying Eliassen and Angel Formations.

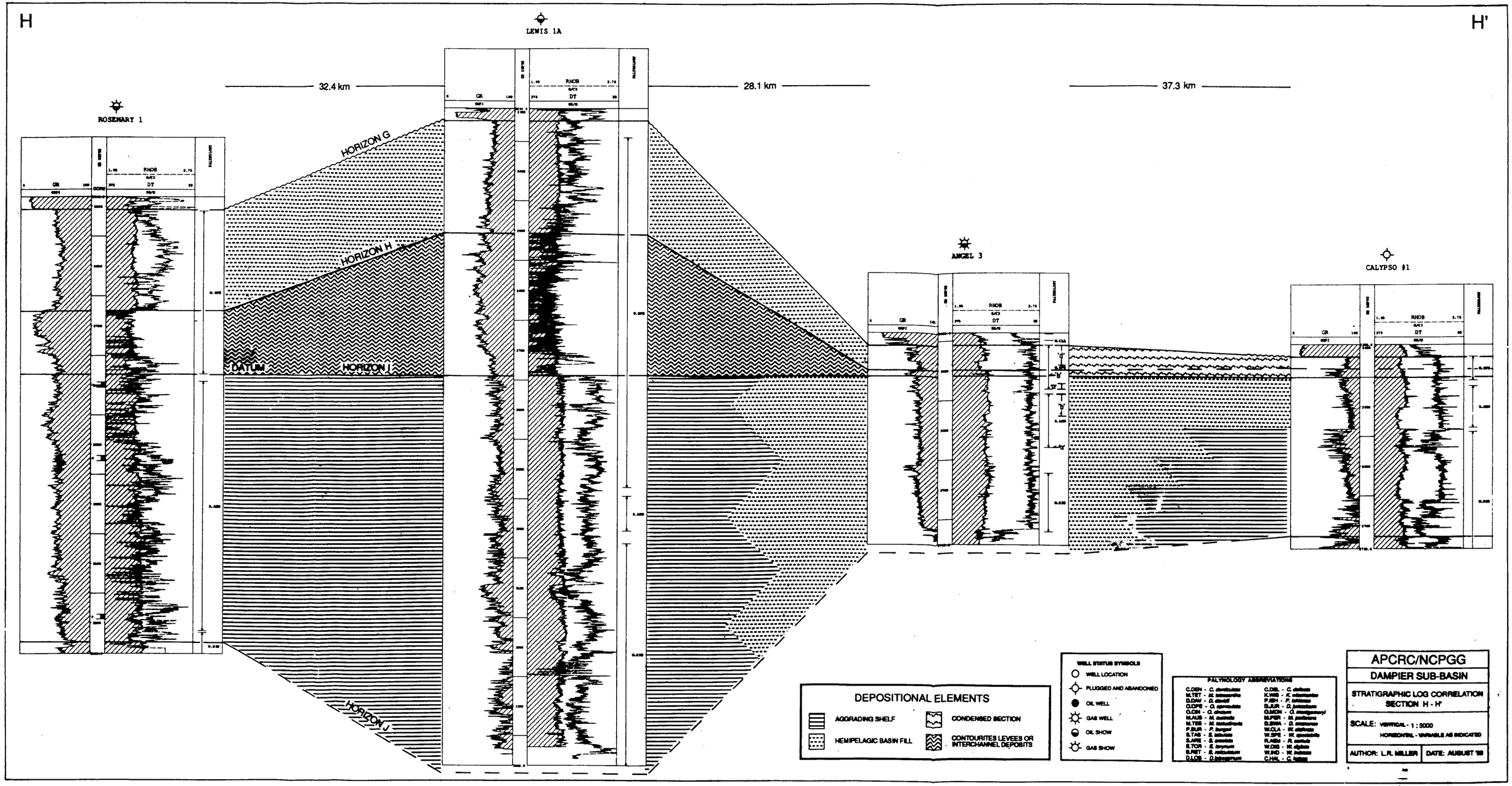

H
H'
LEWIS 1A
ROSEMARY 1
ANGEL 3
CALYPSO #1
32.4 km
28.1 km
37.3 km
HORIZON G
HORIZON H
HORIZON I
HORIZON J
DATUM
DEPOSITIONAL ELEMENTS
AGGRADING SHELF
HEMIPELAGIC BASIN FILL
CONDENSED SECTION
CONTOURITES LEVEES OR INTERCHANNEL DEPOSITS
WELL STATUS SYMBOLS
WELL LOCATION
PLUGGED AND ABANDONED
OIL WELL
GAS WELL
OIL SHOW
GAS SHOW
PALYNOLOGY ABBREVIATIONS
APCRC/NCPGG
DAMPIER SUB-BASIN
STRATIGRAPHIC LOG CORRELATION
SECTION H - H'
SCALE: VERTICAL - 1 : 5000
HORIZONTAL - VARIABLE AS INDICATED
AUTHOR: L.R. MILLER
DATE: AUGUST '89

Figure 4.5.

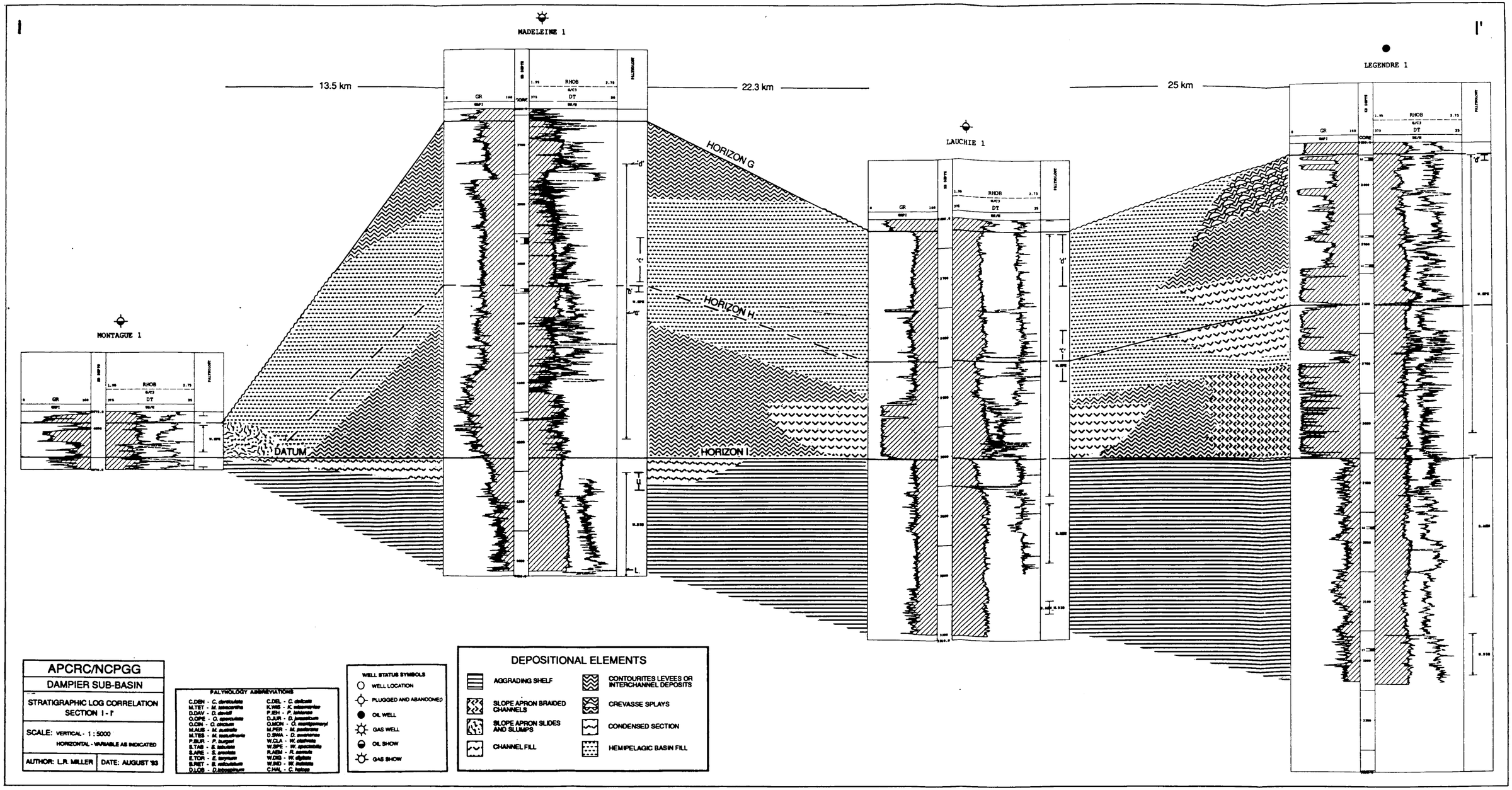

I
I'
MADELEINE 1
LEGENDRE 1
LAUCHIE 1
MONTAGUE 1
13.5 km
22.3 km
25 km
HORIZON G
HORIZON H
HORIZON I
DATUM
APCRC/NCPGG
DAMPIER SUB-BASIN
STRATIGRAPHIC LOG CORRELATION SECTION I - I'
SCALE: VERTICAL - 1 : 5000
HORIZONTAL - VARIABLE AS INDICATED
AUTHOR: L.R. MILLER
DATE: AUGUST '93
PALYNOLOGY ABBREVIATIONS
WELL STATUS SYMBOLS
WELL LOCATION
PLUGGED AND ABANDONED
OIL WELL
GAS WELL
OIL SHOW
GAS SHOW
DEPOSITIONAL ELEMENTS
AGGRADING SHELF
SLOPE APRON BRAIDED CHANNELS
SLOPE APRON SLIDES AND SLUMPS
CHANNEL FILL
CONTOURITES LEVEES OR INTERCHANNEL DEPOSITS
CREVASSE SPLAYS
CONDENSED SECTION
HEMIPELAGIC BASIN FILL

Figure 4.6.

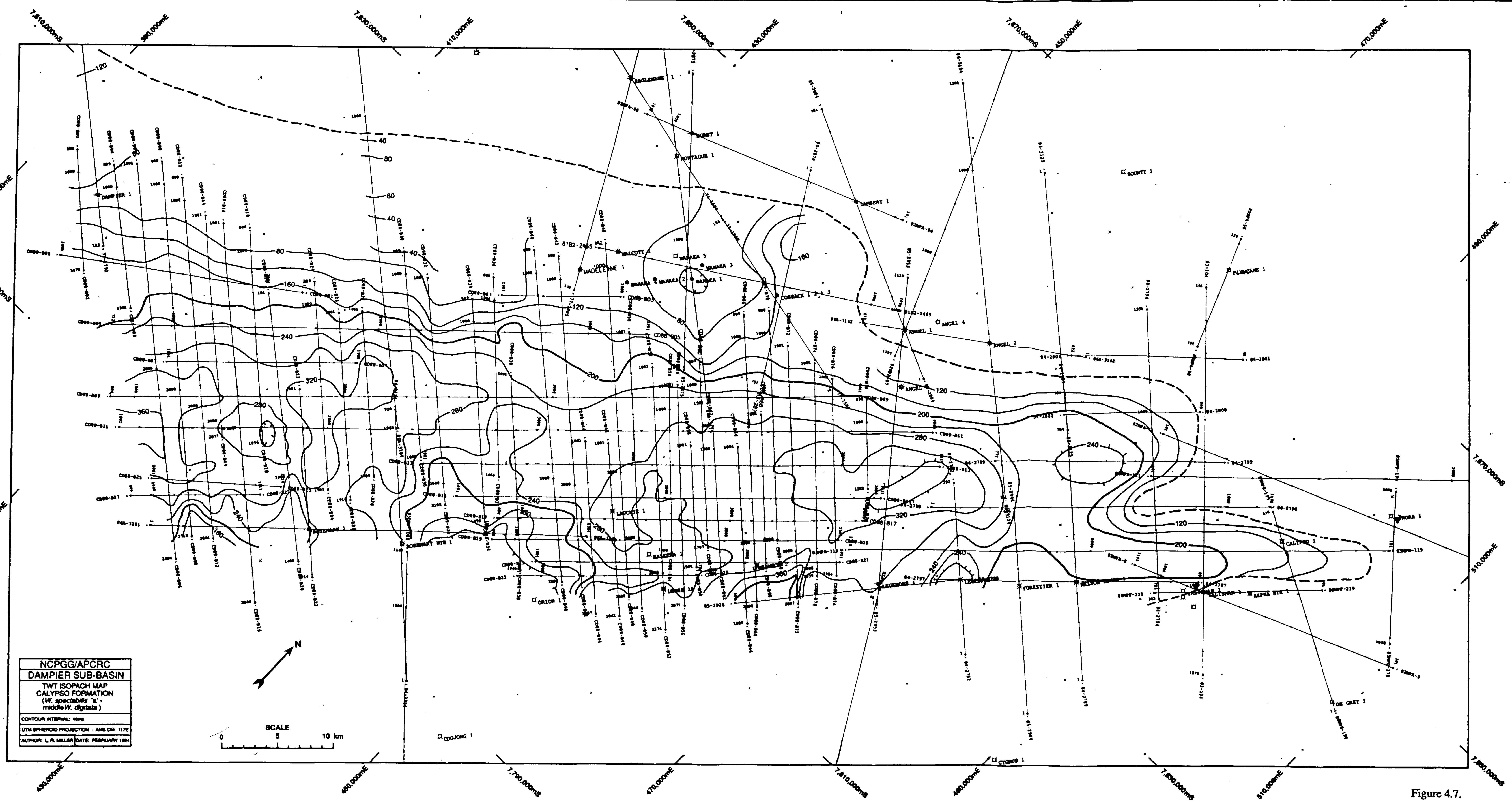

NCPGG/APCRC
DAMPIER SUB-BASIN
TWT ISOPACH MAP
CALYPSO FORMATION
(W. spectabilis 'a' -
middle W. digitata)
CONTOUR INTERVAL: 40ms
UTM SPHEROID PROJECTION - AMG CM: 117E
AUTHOR: L. R. MILLER
DATE: FEBRUARY 1994
SCALE
0
5
10 km
N
7,810,000mS
390,000mE
7,830,000mS
410,000mE
7,850,000mS
430,000mE
7,870,000mS
450,000mE
470,000mE
490,000mE
7,870,000mS
510,000mE
7,890,000mS
430,000mE
450,000mE
7,790,000mS
470,000mE
7,810,000mS
490,000mE
7,830,000mS
510,000mE
390,000mE
7,790,000mS
410,000mE
DAMPIER 1
MADELEINE 1
MONTAGUE 1
LAMBERT 1
BOUNTY 1
ANGEL 1
ANGEL 2
ANGEL 4
COSSACK 1
CALYPSO 1
DE GREY 1
COOJONG 1
CYGNUS 1
ORION 1
FORESTIER 1
40
80
120
160
200
240
280
320
360

Figure 4.7.

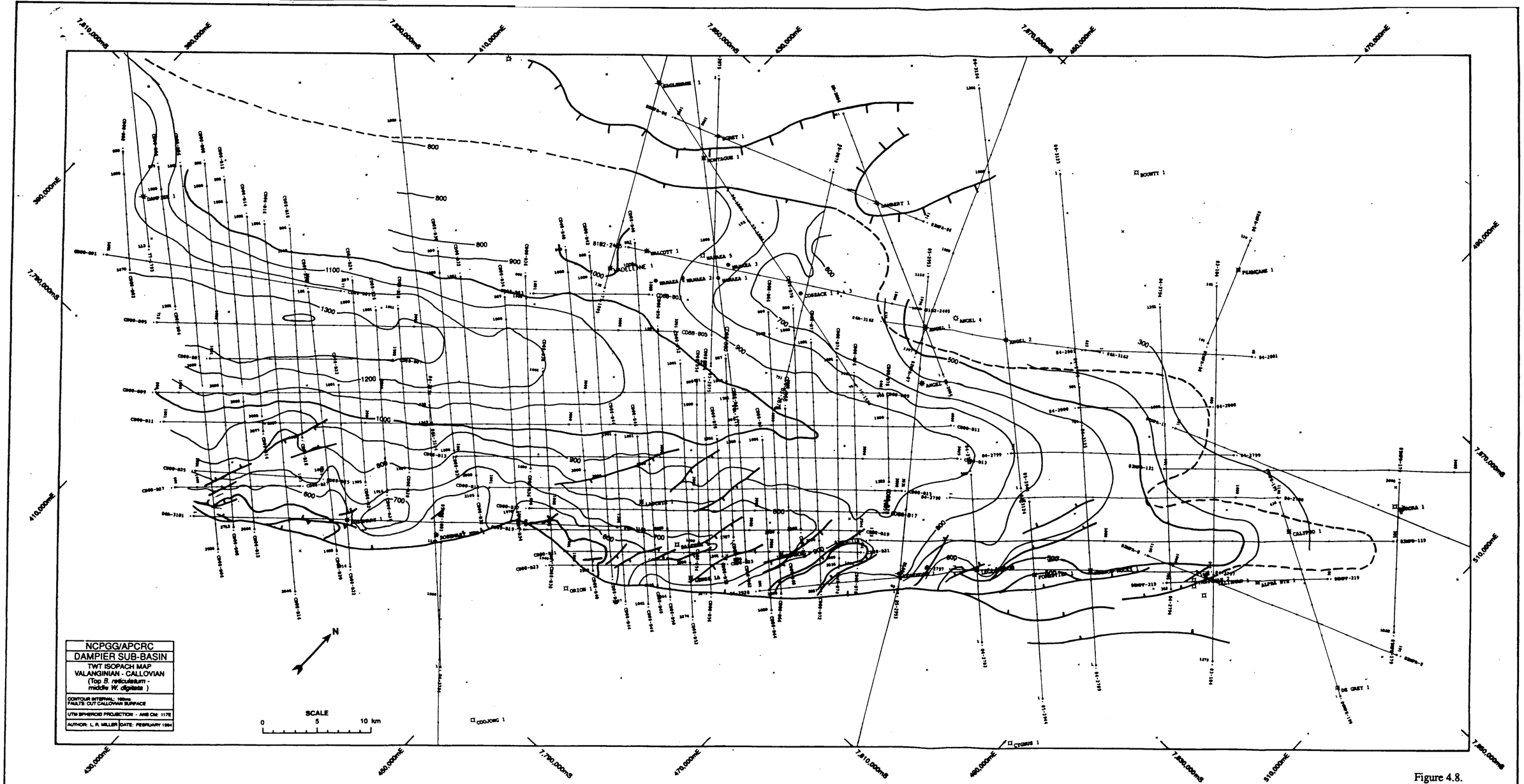

NCPGG/APCRC
DAMPIER SUB-BASIN
TWT ISOPACH MAP
VALANGINIAN - CALLOVIAN
(Top B. reticulatum - middle W. digitata)
CONTOUR INTERVAL: 100ms
FAULTS: CUT CALLOVIAN SURFACE
UTM SPHEROID PROJECTION - ANS Clrc 1178
AUTHOR: L. R. MILLER DATE: FEBRUARY 1994
SCALE
0 5 10 km
N
7,810,000mS
390,000mE
7,830,000mS
410,000mE
7,850,000mS
430,000mE
7,870,000mS
450,000mE
470,000mE
490,000mE
510,000mE
7,790,000mS
7,770,000mS
7,750,000mS
430,000mE
450,000mE
470,000mE
490,000mE
510,000mE
MONTAGUE 1
BOUNTY 1
DAMPIER 1
ADELEINE 1
MALCOTT 1
MAIDAEA 1
MAIDAEA 2
MAIDAEA 3
MAIDAEA 5
COSSACK 1
ANGEL 1
ANGEL 2
ANGEL 4
FUSILIER 1
CALYPSO 1
ORION 1
COOJONG 1
CTONUS 1
DE GREY 1
1100
1300
1200
1000
900
800
700
600
500
300

Figure 4.8.

Eliassen Formation Unit E_2

Schematic palaeogeography : Figure 4.9.

Seismic facies map : Figure 4.10.

Seismic examples : Figures 3.20, 3.32, 3.45, 3.47, 3.48, 3.54, 3.56, and 3.57.

Stratigraphic log correlations : location map, Figure 4.4; section H - H', Figure 4.5; section I - I', Figure 4.6.

Isochron map : Figure 4.11.

Structure/isochron map : Figure 4.12.

Structure map : top Eliassen Formation unit E_2, Figure 4.13.

Montage: Enclosure IIIa.

Core data : Madeleine 1 core 7 - Facies E2.3, E1.3; core 8 - Facies E1.1.

Unit E_2 of the Eliassen Formation is considered to be a mud rich system where sand efficient transport processes occurred. It contains evidence of significant levee and contourite development. Sandy sections observed at Lauchie 1 and Legendre 1 contain Channel Fill and Slope Apron Braided Channels (Figure 3.32), respectively. These sections coincide with interpreted sediment source axes that trend to the northwest and the north, respectively. These sediment source axes correspond with relatively thicker areas noted on the isochron map. In addition, they correspond to inferred palaeo-topographic low areas noted on the structural/isochron map. Conversely, the adjacent palaeo-topographic high areas contain interpreted condensed sections (e.g. Orion 1), and contourites (e.g. Rosemary 1; Samson 1, Figure 3.47). Levees also occur adjacent to the sediment source axes and can be observed at Lewis 1 (Figures 3.45 and 3.48).

A possible Depositional Lobe Massive Sand is interpreted to the south of Angel 3, distal to one of the sediment source axes. This area is highlighted by mounded stratal patterns that contain high amplitude events (Figures 3.20, 3.57). Adjacent to this, Angel 3 (23m thick) is on a palaeo-high and is relatively condensed.

Sediment starvation is noted at Calypso 1. It contains a 14.5m section of mud that is not necessarily on a palaeo-high. The controlling factor in this area is thought to be the lack of sediment source and possible relatively continuous current activity that prevented any significant hemipelagic sedimentation.

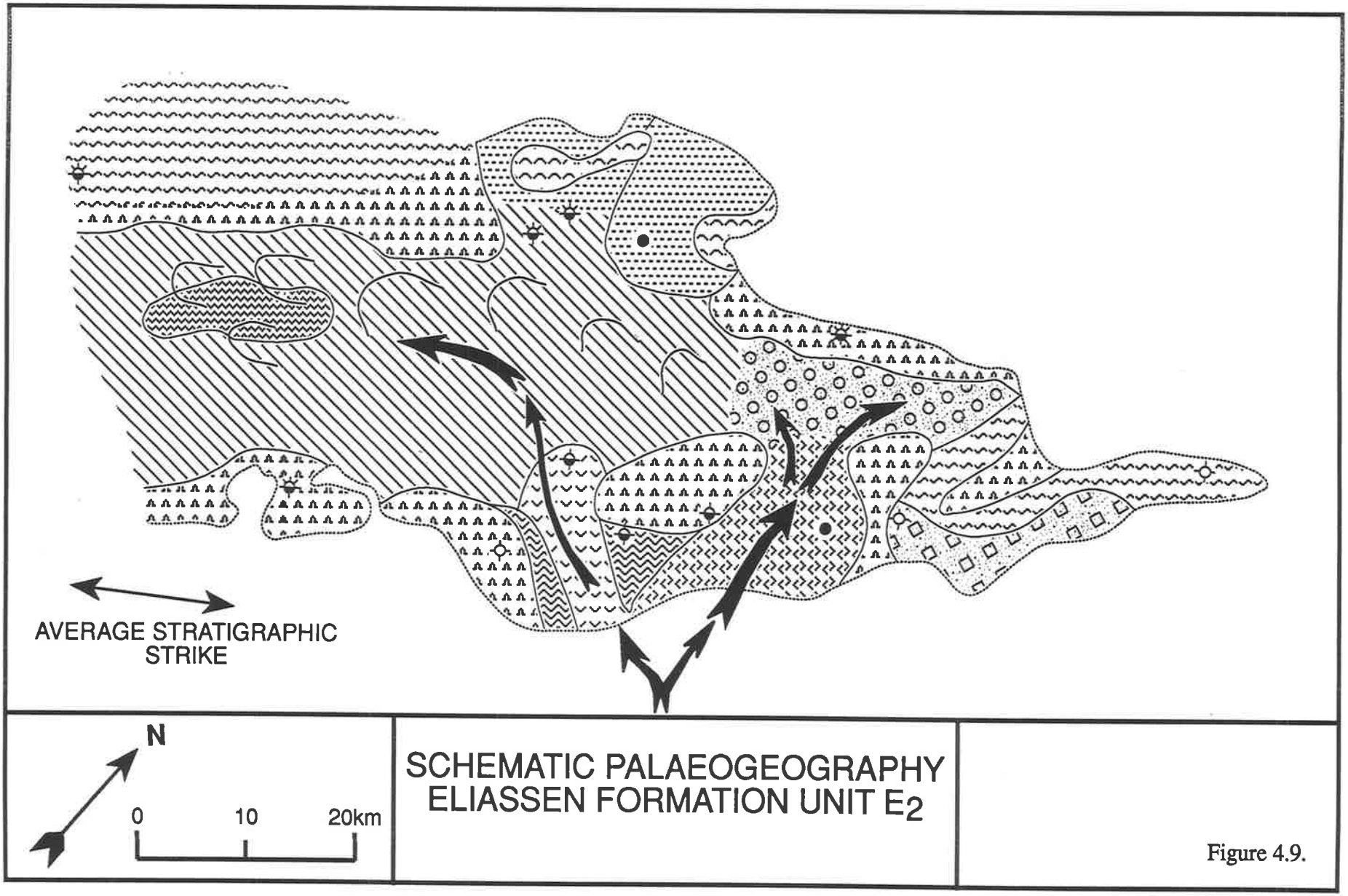

AVERAGE STRATIGRAPHIC STRIKE
N
0
10
20km
SCHEMATIC PALAEOGEOGRAPHY
ELIASSEN FORMATION UNIT E2

Figure 4.9.

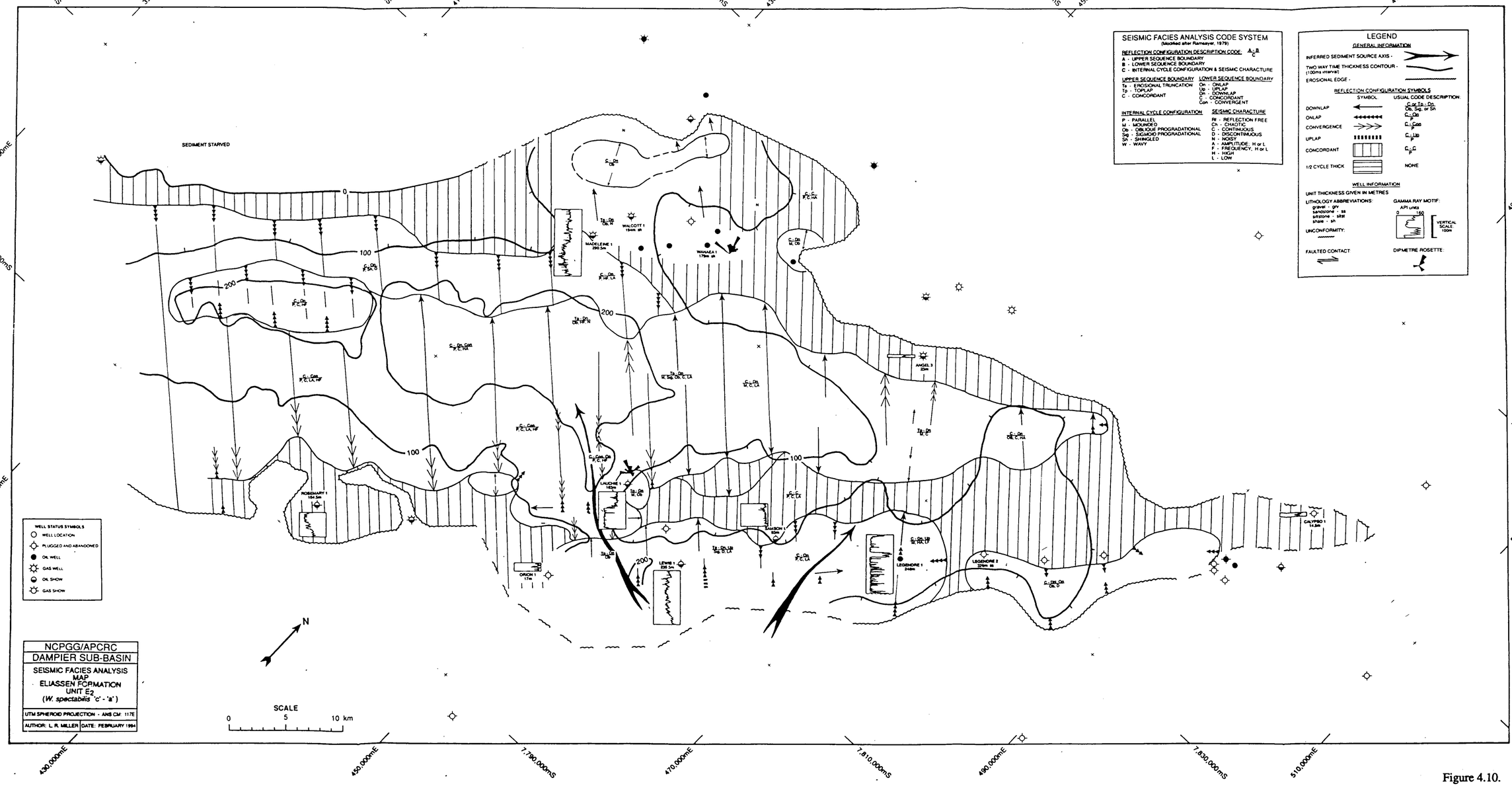

SEISMIC FACIES ANALYSIS CODE SYSTEM
(Modified after Ramsayer, 1979)
REFLECTION CONFIGURATION DESCRIPTION CODE: A-B/C
A - UPPER SEQUENCE BOUNDARY
B - LOWER SEQUENCE BOUNDARY
C - INTERNAL CYCLE CONFIGURATION & SEISMIC CHARACTURE
UPPER SEQUENCE BOUNDARY
Te - EROSIONAL TRUNCATION
Tp - TOPLAP
C - CONCORDANT
LOWER SEQUENCE BOUNDARY
On - ONLAP
Do - DOWNLAP
Cp - CONCORDANT
Con - CONVERGENT
INTERNAL CYCLE CONFIGURATION
P - PARALLEL
M - MOUNDED
Ob - OBLIQUE PROGRADATIONAL
Sig - SIGMOID PROGRADATIONAL
Sh - SHINGLED
W - WAVY
SEISMIC CHARACTURE
RF - REFLECTION FREE
Ch - CHAOTIC
C - CONTINUOUS
D - DISCONTINUOUS
N - NOISY
A - AMPLITUDE, H or L
F - FREQUENCY, H or L
H - HIGH
L - LOW
LEGEND
GENERAL INFORMATION
INFERRED SEDIMENT SOURCE AXIS -
TWO WAY TIME THICKNESS CONTOUR - (100ms interval)
EROSIONAL EDGE -
REFLECTION CONFIGURATION SYMBOLS
SYMBOL
USUAL CODE DESCRIPTION
DOWNLAP
ONLAP
CONVERGENCE
UPLAP
CONCORDANT
1/2 CYCLE THICK
NONE
WELL INFORMATION
UNIT THICKNESS GIVEN IN METRES
LITHOLOGY ABBREVIATIONS:
gravel - grv
sandstone - ss
siltstone - sltst
shale - sh
UNCONFORMITY:
FAULTED CONTACT
GAMMA RAY MOTIF:
API units
0
150
VERTICAL SCALE 100m
DIPMETRE ROSETTE
SEDIMENT STARVED
0
100
200
WELL STATUS SYMBOLS
WELL LOCATION
PLUGGED AND ABANDONED
OIL WELL
GAS WELL
OIL SHOW
GAS SHOW
WALCOTT 1
MADELEINE 1
WANAEA 1
ANGEL 3
ROSEMARY 1
LAURIE 1
LAVERSHAM 1
LEWIS 1
ORION 1
LEGENDRE 1
LEGENDRE 2
CALYPSO 1
N
SCALE
0
5
10 km
NCPGG/APCRC
DAMPIER SUB-BASIN
SEISMIC FACIES ANALYSIS MAP
ELIASSEN FORMATION
UNIT E2
(W. spectabilis 'c' - 'a')
UTM SPHEROID PROJECTION - ANS CM: 117E
AUTHOR: L. R. MILLER
DATE: FEBRUARY 1994
390,000mE
410,000mE
430,000mE
450,000mE
470,000mE
490,000mE
510,000mE
7,810,000mS
7,830,000mS
7,850,000mS
7,870,000mS
7,790,000mS

Figure 4.10.


NCPGG/APCRC
DAMPIER SUB-BASIN
TWT ISOPACH MAP
ELIASSEN FORMATION
UNIT E_2
(*W. spectabilis* 'c' - 'a')
CONTOUR INTERVAL: 40ms
UTM SPHEROID PROJECTION - AMG CM: 117E
AUTHOR: L. R. MILLER
DATE: FEBRUARY 1994
SCALE
0
5
10 km
N
DAMPIER 1
MADELEINE 1
WALCOTT 1
LAMBERT 1
ANGEL 1
ANGEL 2
ANGEL 4
BOUNTY 1
MONTAGUE 1
FORESTIER 1
NELSON ROCKS 1
ALPHA NTH 1
DE GREY 1
CALIFSO 1
ORION 1
CYGNUS 1
GOODWYN 1
REGAL 1
7,810,000mS
7,830,000mS
7,850,000mS
7,870,000mS
7,790,000mS
390,000mE
410,000mE
430,000mE
450,000mE
470,000mE
490,000mE
510,000mE
7,880,000mS

Figure 4.11.

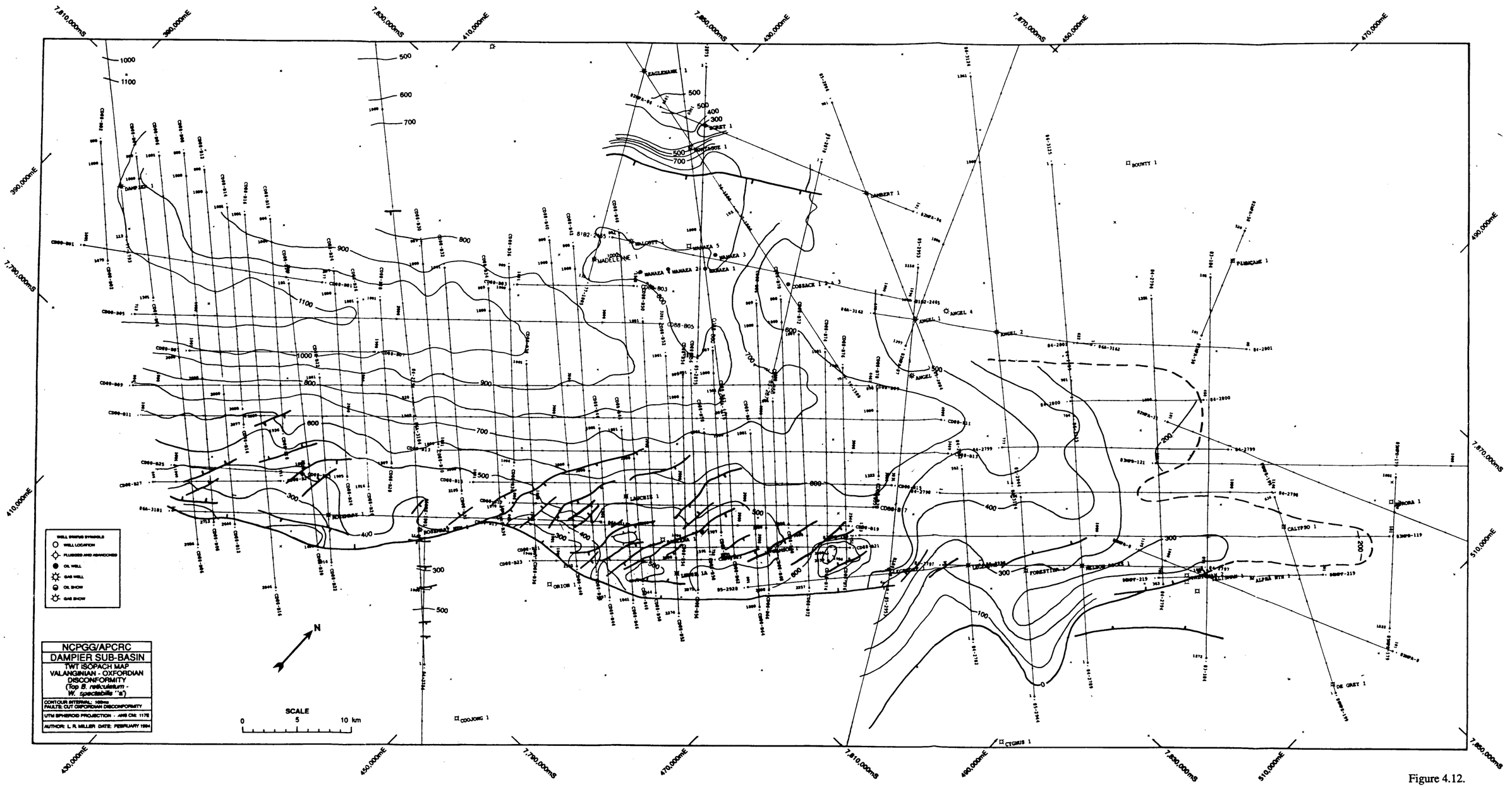

NCPGG/APCRC
DAMPIER SUB-BASIN
TWT ISOPACH MAP
VALANGINIAN - OXFORDIAN
DISCONFORMITY
(Top B. reticulatum - W. spectabilis "a")
CONTOUR INTERVAL: 100ms
FAULTS: CUT OXFORDIAN DISCONFORMITY
UTM SPHEROID PROJECTION - AMG CM: 117E
AUTHOR: L. R. MILLER DATE: FEBRUARY 1994
WELL LOCATION
PLUGGED AND ABANDONED
OIL WELL
GAS WELL
OIL SHOW
GAS SHOW
SCALE
0 5 10 km
N
7,810,000mS
390,000mE
7,830,000mS
410,000mE
7,850,000mS
430,000mE
7,870,000mS
450,000mE
470,000mE
490,000mE
510,000mE
7,790,000mS
7,770,000mS
7,750,000mS
430,000mE
450,000mE
470,000mE
490,000mE
510,000mE
EAGLEHAWK 1
DAMPIER 1
MADELEINE 1
WAHAZA 1
WAHAZA 2
WAHAZA 3
WAHAZA 5
COSSACK 1
ANGEL 1
ANGEL 2
ANGEL 3
ANGEL 4
LAMBERT 1
BOUNTY 1
PLUMBLINE 1
LARCHIE 1
ROSEBRIE 1
ORION 1
COOJONG 1
CTGHUS 1
CALTPSO 1
FORESTIER 1
DE GREY 1
ALPHA WH 1
ORORA 1

Figure 4.12.

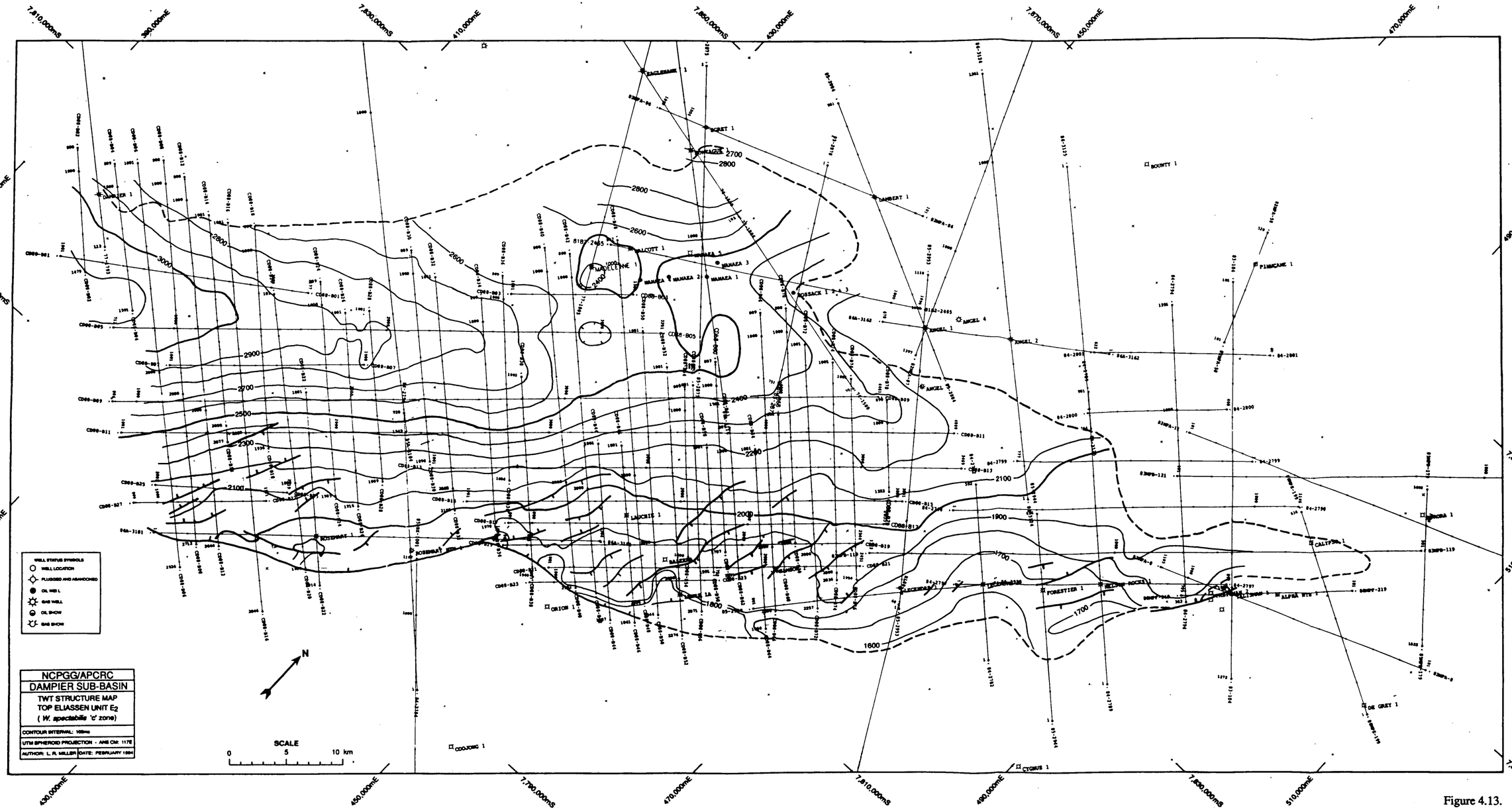

NCPGG/APCRC
DAMPIER SUB-BASIN
TWT STRUCTURE MAP
TOP ELIASSEN UNIT E2
(W. spectabilis 'c' zone)
CONTOUR INTERVAL: 100ms
UTM SPHEROID PROJECTION - ANS Clrk 1178
AUTHOR: L. R. MILLER
DATE: FEBRUARY 1994
WELL STATUS SYMBOLS
WELL LOCATION
PLUGGED AND ABANDONED
OIL WELL
GAS WELL
OIL SHOW
GAS SHOW
SCALE
0 5 10 km
N
7,810,000mS
390,000mE
7,830,000mS
410,000mE
7,850,000mS
430,000mE
7,870,000mS
450,000mE
470,000mE
490,000mE
510,000mE
7,790,000mS
7,850,000mS
430,000mE
450,000mE
470,000mE
7,790,000mS
7,810,000mS
490,000mE
7,830,000mS
510,000mE
2700
2800
2800
2600
2600
3000
2900
2700
2500
2300
2100
2400
2200
2000
1900
1700
1800
1600
2100
ROSEMARY 1
ROSEMARY 1A
LAICHIC 1
BALCHER 1
ORION 1
COOJONG 1
MADELEINE 1
BALCOTT 1
WAHAZA 1
WAHAZA 2
WAHAZA 3
WAHAZA 5
ROSSACK 1, 2, 3
ANGEL 1
ANGEL 2
ANGEL 3
ANGEL 4
BOUNTY 1
PISMIRE 1
FORESTER 1
ARCHER ROCKS 1
ALPHA NTH 1
CALYPSO 1
DE GREY 1
CYGNUS 1

Figure 4.13.

An area of ponding is interpreted to the east of Dampier 1 within the Lewis Trough. High frequency events that onlap the lowermost palaeo-low portion of the trough are noted on seismic. The seismic character does not reveal any particularly sandy attributes. It is likely that the ponding is mud dominated.

Most of the Lewis Trough is interpreted to be undifferentiated basin fill. Muddy turbidites, contourites and hemiplegic sediments are noted at Madeleine 1 and Walcott 1. This is consistent with core data from Madeleine 1. Hemipelagic sediments occur at Wanaea 1. These wells are considered to represent the representative style of deposition that dominated the Basin Fill portion of the Lewis Trough. This basin fill contains seismic convergence onto the flank of the Legendre Trend, and onlap onto the flank of the Madeleine Trend. Bi-directional downlap occurs in areas of seismic mounding. The relative thinning onto the flanks and the overall kidney shape of the isochron thickness contours suggests that much of the available accommodation provided by the Lewis Trough was filled by this unit.

The unit thickness is 0ms immediately north of Dampier 1. It is interpreted that this area represents deep water which was sediment starved. No sediment is evident to have been sourced from the Rankin Platform area to the northwest. There is, however, some mounding that occurs in the northern portion of the unit, and it is unknown as to whether it represents sandy or muddy sediment.

The seismic character of this unit is discussed in section 3.3.2. Sand bodies of possible reservoir potential may also occur within the basin fill area of the Lewis Trough. Considering the expected transport efficiency of this system, it is possible that turbidite sheet sands may occur in areas flagged by the allocated symbol on the schematic palaeogeography diagram. They refer to high amplitude trough anomalies which can be observed on seismic (e.g. Figures 3.20, and 3.57) at or near the base of the unit. The flagged locations are mostly speculative and further mapping is required to evaluated the exact extent of these anomalies.

Eliassen Formation Unit E_1

Seismic examples : Figures 3.20, 3.44 and 3.46.

Stratigraphic log correlations : location map, Figure 4.4; section H - H', Figure 4.5; section I - I', Figure 4.6.

Structure maps : top Eliassen Formation unit E_2, Figure 4.13; base Angel Formation, Figure 4.24.

Montage: Enclosure IIIa.

Core data : Legendre 1 core 12, 13 and 14, Facies A2.1, C2.1 and D1.3; Madeleine 1 core 6 and 7, Facies C2.3, E1.1.

Seismic facies analysis was not conducted on unit E_1 because it lacks variation in seismic stratal configurations. The typical seismic character is discontinuous and continuous, parallel, low amplitude and moderate frequency (e.g. see Figure 3.20). The top of the unit is erosionally truncated by the overlying Angel Formation. The base of the unit has continuous parallel events that often parallel the mounded configuration of unit E_1.

The system is mud dominated. Sandstone sections occur only at Legendre 1 where Channel Fill Levees and Crevasse Splay depositional elements are interpreted (Figure 3.44). Core 12 at Legendre 1 contains Facies A2.1 (stratified gravel), core 13 has Facies C2.1 (very thick and thick bedded sand-mud couplets), and core 14 contains Facies D1.3 (mottled silt and mud). The other wells contain muddy sections of Hemipelagic Basin Fill, Condensed Sections and Contourites or Levees. A muddy channel axis is shown in Figure 3.46.

It appears that there is little sand development within unit E_1. This unit is probably associated with transgression and flooding of low relief topography. Although this is a muddy system where sand efficient transport processes can occur, there is little sand available in the system for transport. The only sand that is evident occurs as Channel Fill, Levees and Crevasse Splays at Legendre 1.

Angel Formation Unit A_6

Schematic palaeogeography : Figure 4.14.

Seismic facies map : Figure 4.21.

Seismic examples : Figures 3.26, 3.31, 3.34, 3.41, 3.49, 3.50, 3.51, 3.52, 3.53 and 3.54.

Stratigraphic log correlations : location map, Figure 4.15; section C - C', Figure 4.16; section D - D', Figure 4.17; section E - E', Figure 4.18; section F - F', Figure 4.19; section G - G', Figure 4.20.

Isochron map : Figure 4.22.

Structure/isochron map : Valanginian Disconformity to base Angel Formation, Figure 4.23.

Structure map : base Angel Formation, Figure 4.24.

Montages: Enclosures IIIb and IIIc.

Core data : Madeleine 1 core 5 - Facies E1.1; Dampier 1 core 14, 15, 16 - Facies E1.1.

The basal member of the Angel Formation, Unit A_6, overlies a major unconformity. In addition to missing palynological zones noted on well log correlations, erosional truncation can be observed along the southeastern flank of the Lewis Trough (see Figures 3.49, 3.50, 3.51, 3.52, 3.53, 3.54 and 3.56). Synsedimentary normal faults, some of which terminate within this unit, are displayed in Figures 3.49, 3.51, 3.52, 3.53 and 3.54. The footwall components of most of these examples are interpreted to be filled with Channel Fill sand, which demonstrates that these faults, being active at the time of sedimentation, strongly controlled palaeo-topography and hence sand distribution.

The stratigraphic log correlation D - D' in Figure 4.17 shows a thickening hemipelagic wedge (defined by asymptotic downlap seismic facies) in the vicinity of Dampier 1. This wedge is interpreted from the isochron map to thicken to the north-northwest (perpendicular to average stratigraphic strike shown on the schematic palaeogeography). Very little definition of the Lewis Trough can be observed on the isochron map, suggesting that it was virtually filled with sediment prior to deposition of this unit. In addition, considerable unit thickness exists over the Kendrew Trough region, suggesting that active sedimentation had taken place.

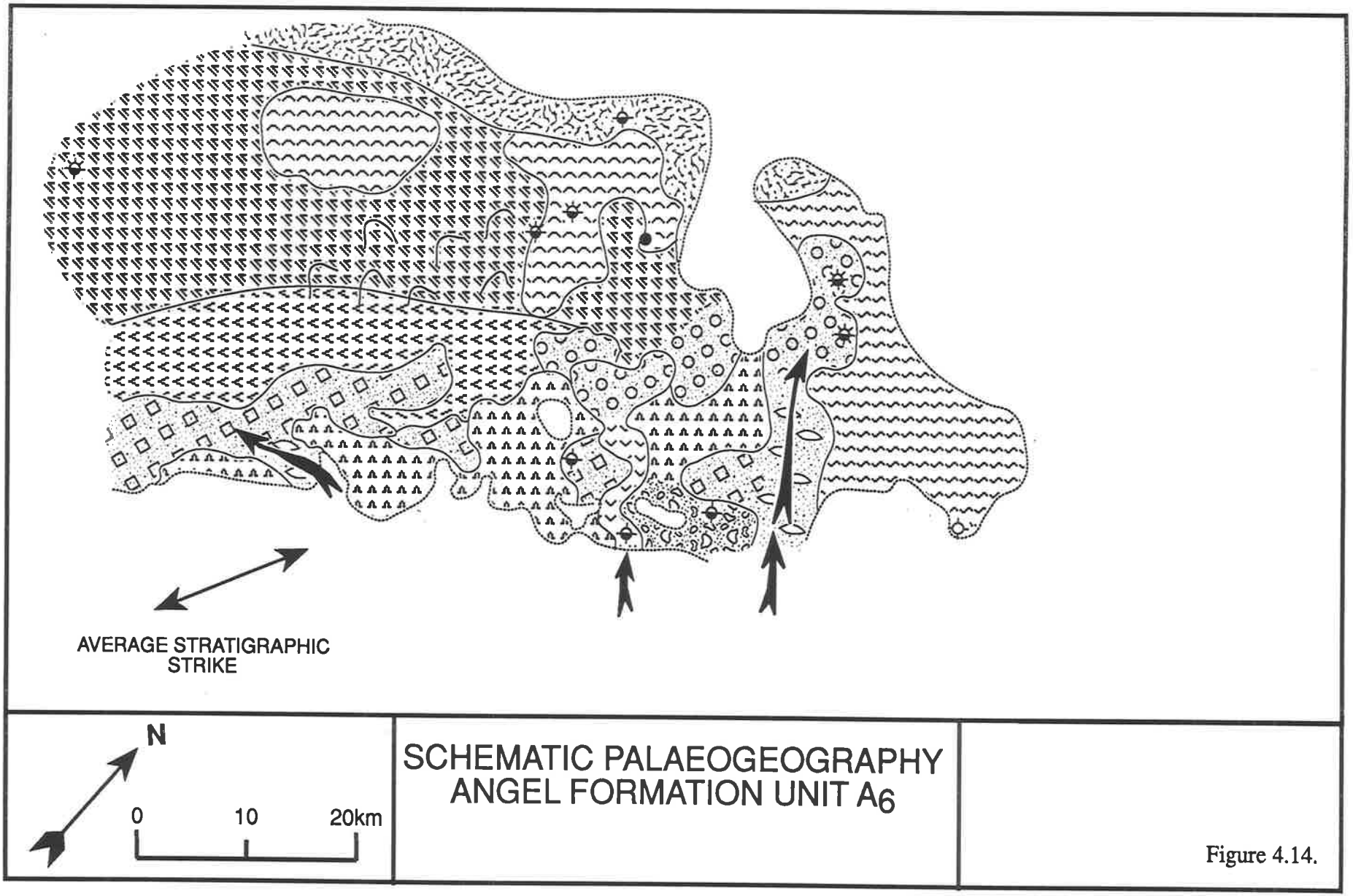

AVERAGE STRATIGRAPHIC STRIKE
N
0
10
20km
SCHEMATIC PALAEOGEOGRAPHY
ANGEL FORMATION UNIT A6

Figure 4.14.

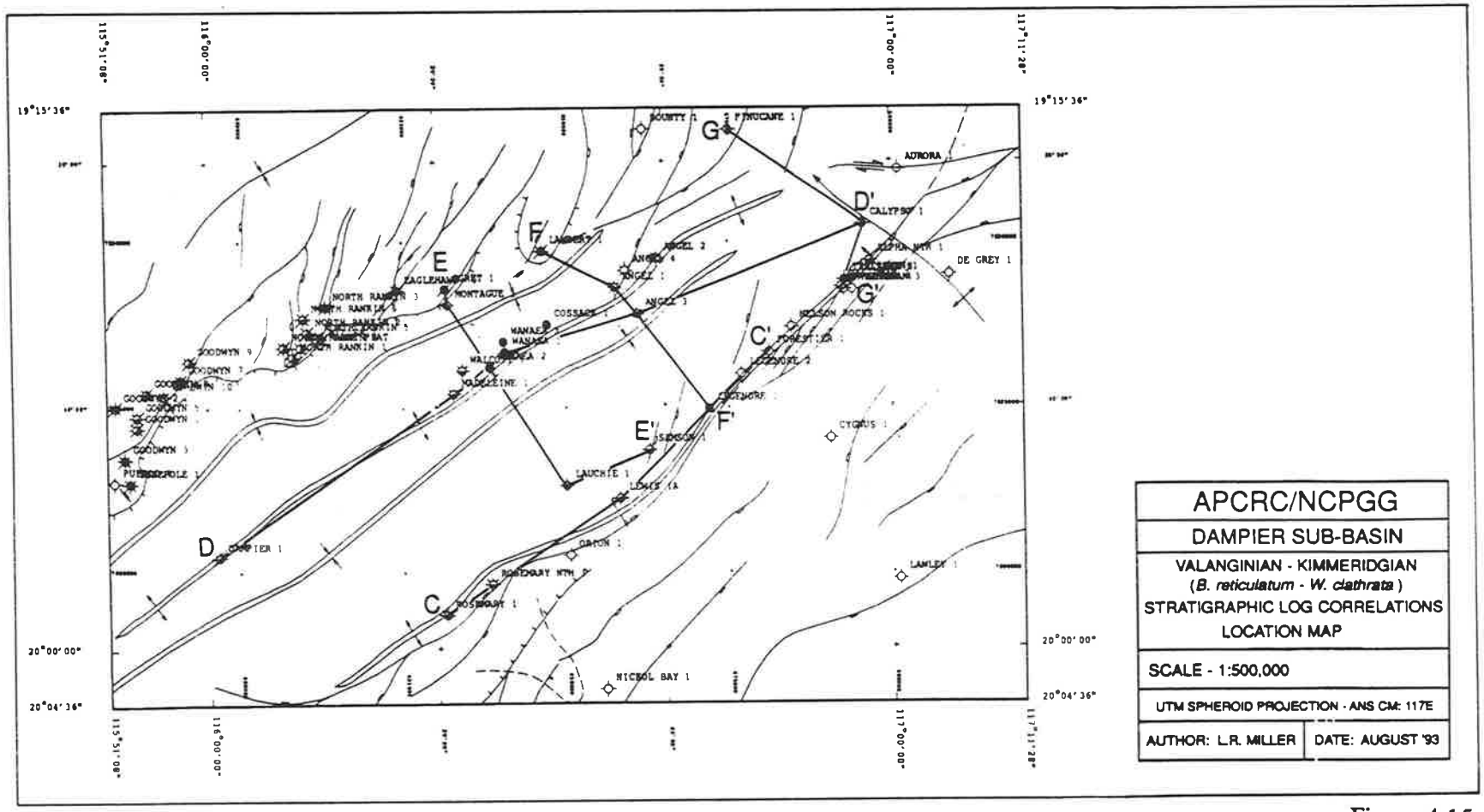

APCRC/NCPGG
DAMPIER SUB-BASIN
VALANGINIAN - KIMMERIDGIAN
(B. reticulatum - W. clathrata)
STRATIGRAPHIC LOG CORRELATIONS
LOCATION MAP
SCALE - 1:500,000
UTM SPHEROID PROJECTION - ANS CM: 117E
AUTHOR: L.R. MILLER
DATE: AUGUST '93
A
A'
B
B'
C
C'
D
D'
E
E'
F
F'
G
G'
AURORA
CALYPSO 1
DE GREY 1
NICOL BAY 1
LANLEY 1
CYGNUS 1
19°15'36"
20°00'00"
20°04'36"

Figure 4.15.

It is suggested that the morphology of this unit was controlled by basin tilting in the direction approximately perpendicular to the average stratigraphic strike. This tilting would have included relative isostatic uplift occurring near the margin of the Lewis Trough adjacent to the Rosemary - Legendre Fault. The region of relative uplift is designated on the schematic palaeo-geographic diagram by areas of palaeo-topographic highs, Slope Apron Depositional Sand, and incised channel areas that contain Channel Fill sand. Channel fill stratal patterns can be seen in Figures 3.31, 3.49 and 3.50. This region was probably an intermediate platform that succumbed to north-northeast faulting (see structure/isochron map, Figure 4.23). This platform area was adjacent to an area of increasing gradient, as defined by the areas of seismic convergence. These areas of seismic convergence possibly contain mottled silt and mud lithologies such as Facies D1.3.

The incised channel at Lewis 1 extends to an area of interpreted Depositional Lobe Massive Sand in the distal direction. A channel-lobe complex is interpreted to occur between Samson 1 and Legendre 1 where Braided Channels and Chutes are interpreted. This complex extends to the Angel area where Depositional Lobe Massive Sands occur (Figure 3.26). Slope Apron Sandy Slides (Figure 3.34) occur adjacent to this channel-lobe complex at Samson 1. The area to the west of Angel area channel-lobe complex is thin as indicated by seismic isochrons. Although Sandy Slides are interpreted from well data at Forestier 1, this area was subjected to continual sediment remobilisation and considerable erosion prior to the onset of deposition of unit A_5.

Slope Apron Slides and Slumps are noted at Montague 1. This is the only direct evidence of sediment being sourced from the North Rankin Platform area. Seismic reflections uplap onto this palaeo-escarpment as shown on the seismic facies map. Seismic mounding can be noted over two areas in the Kendrew Trough region. Hemipelagic sections at Walcott 1 and Wanaea 1 suggest that this mounding is probably mud dominated. If sandy seismic characters, such as high amplitude troughs can be observed within the palaeo-low portions of these mounded areas, potential for good sealing exists. In addition, areas of high amplitude trough anomalies occur within the region of asymptotic downlap (see schematic palaeography diagram). Further mapping is required to assess the extent of these anomalies.

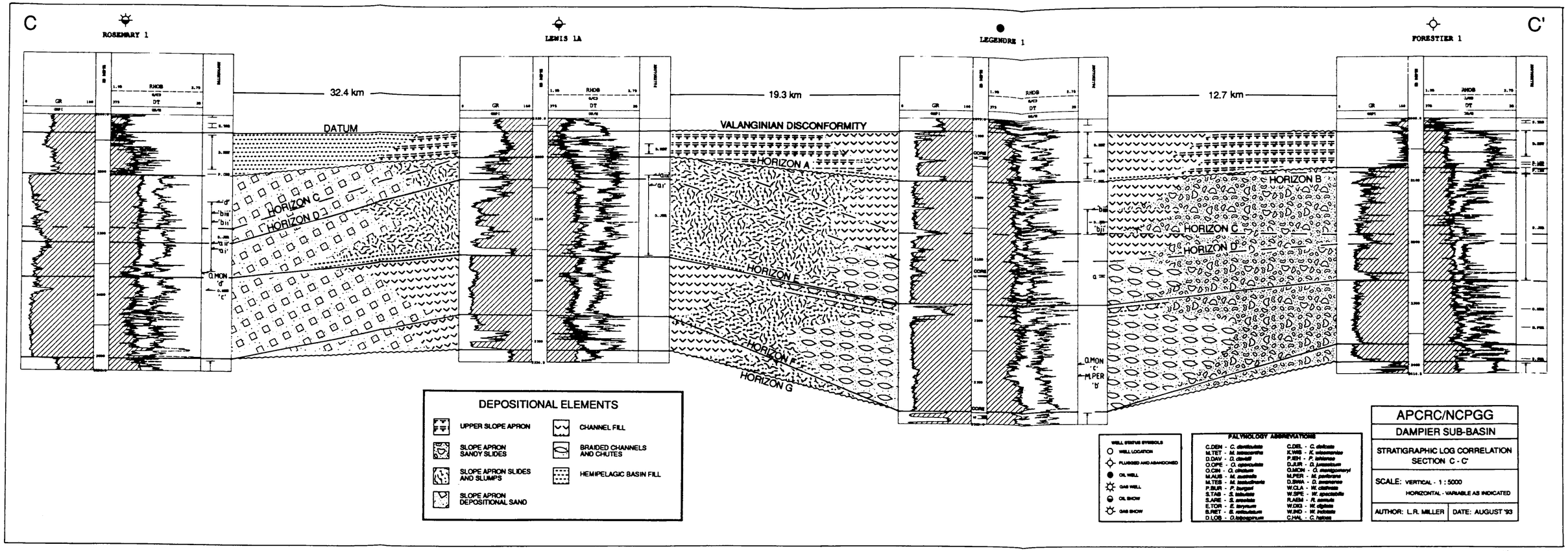

C
C'
ROSEMARY 1
LEWIS 1A
LEGENDRE 1
FORESTIER 1
32.4 km
19.3 km
12.7 km
DATUM
VALANGINIAN DISCONFORMITY
HORIZON A
HORIZON B
HORIZON C
HORIZON D
HORIZON E
HORIZON F
HORIZON G
Q.MON
M.PER
DEPOSITIONAL ELEMENTS
UPPER SLOPE APRON
SLOPE APRON SANDY SLIDES
SLOPE APRON SLIDES AND SLUMPS
SLOPE APRON DEPOSITIONAL SAND
CHANNEL FILL
BRAIDED CHANNELS AND CHUTES
HEMIPELAGIC BASIN FILL
APCRC/NCPGG
DAMPIER SUB-BASIN
STRATIGRAPHIC LOG CORRELATION SECTION C - C'
SCALE: VERTICAL - 1 : 5000
HORIZONTAL - VARIABLE AS INDICATED
AUTHOR: L.R. MILLER
DATE: AUGUST '93

Figure 4.16.

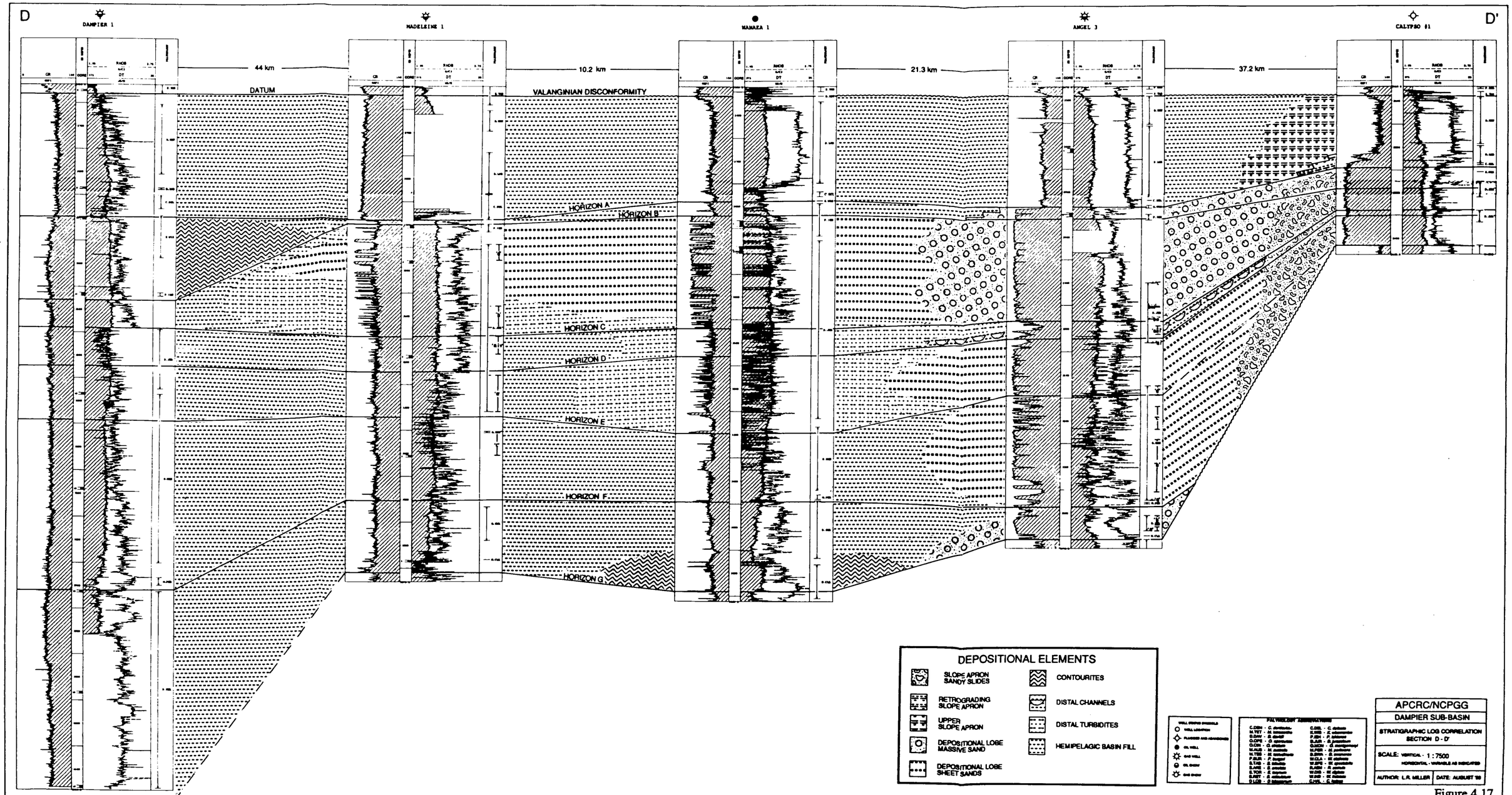
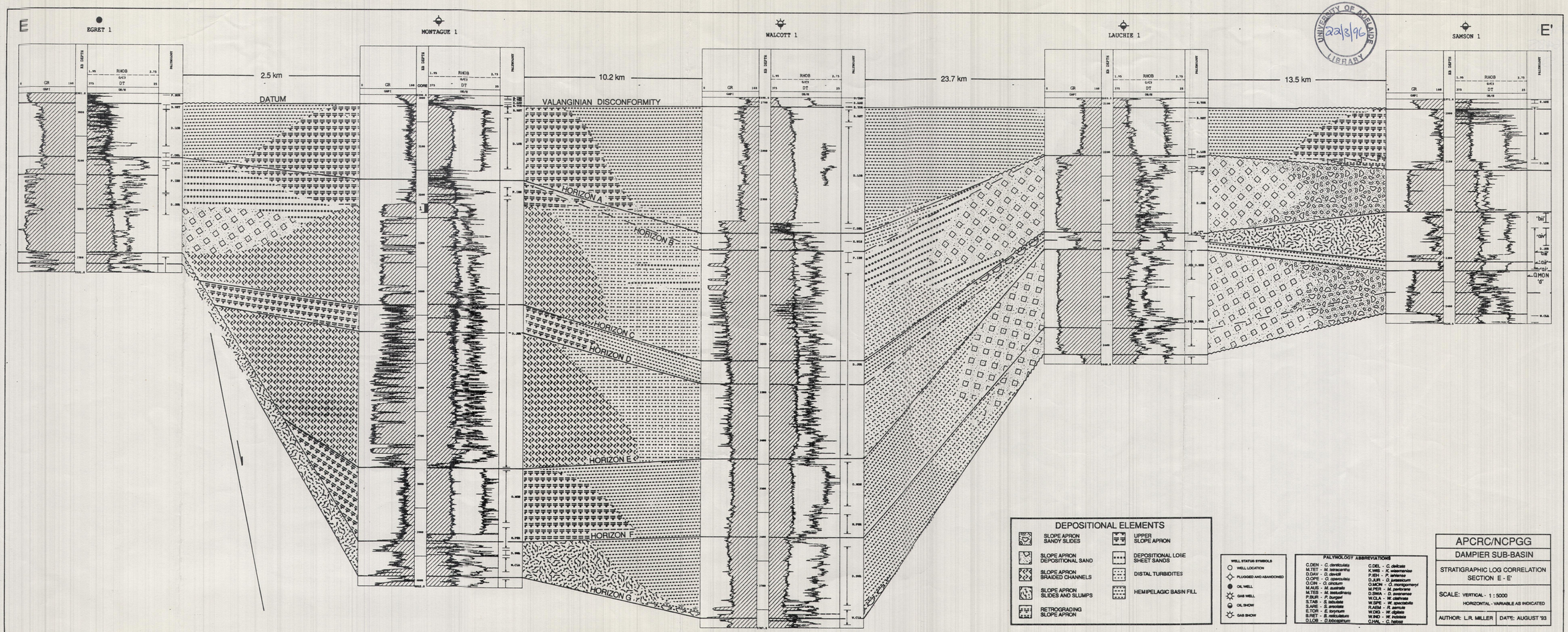

D
D'
DAMPIER 1
MADELEINE 1
MAHAZA 1
ANGEL 3
CALYPSO 01
44 km
10.2 km
21.3 km
37.2 km
DATUM
VALANGINIAN DISCONFORMITY
HORIZON A
HORIZON B
HORIZON C
HORIZON D
HORIZON E
HORIZON F
HORIZON G
DEPOSITIONAL ELEMENTS
SLOPE APRON SANDY SLIDES
RETROGRADING SLOPE APRON
UPPER SLOPE APRON
DEPOSITIONAL LOBE MASSIVE SAND
DEPOSITIONAL LOBE SHEET SANDS
CONTOURITES
DISTAL CHANNELS
DISTAL TURBIDITES
HEMIPELAGIC BASIN FILL
APCRC/NCPGG
DAMPIER SUB-BASIN
STRATIGRAPHIC LOG CORRELATION SECTION D - D'
SCALE: VERTICAL - 1 : 7500
HORIZONTAL - VARIABLE AS INDICATED
AUTHOR: L.R. MILLER
DATE: AUGUST '89

Figure 4.17.



UNIVERSITY OF ADELAIDE LIBRARY 22/3/96

Figure 4.18.

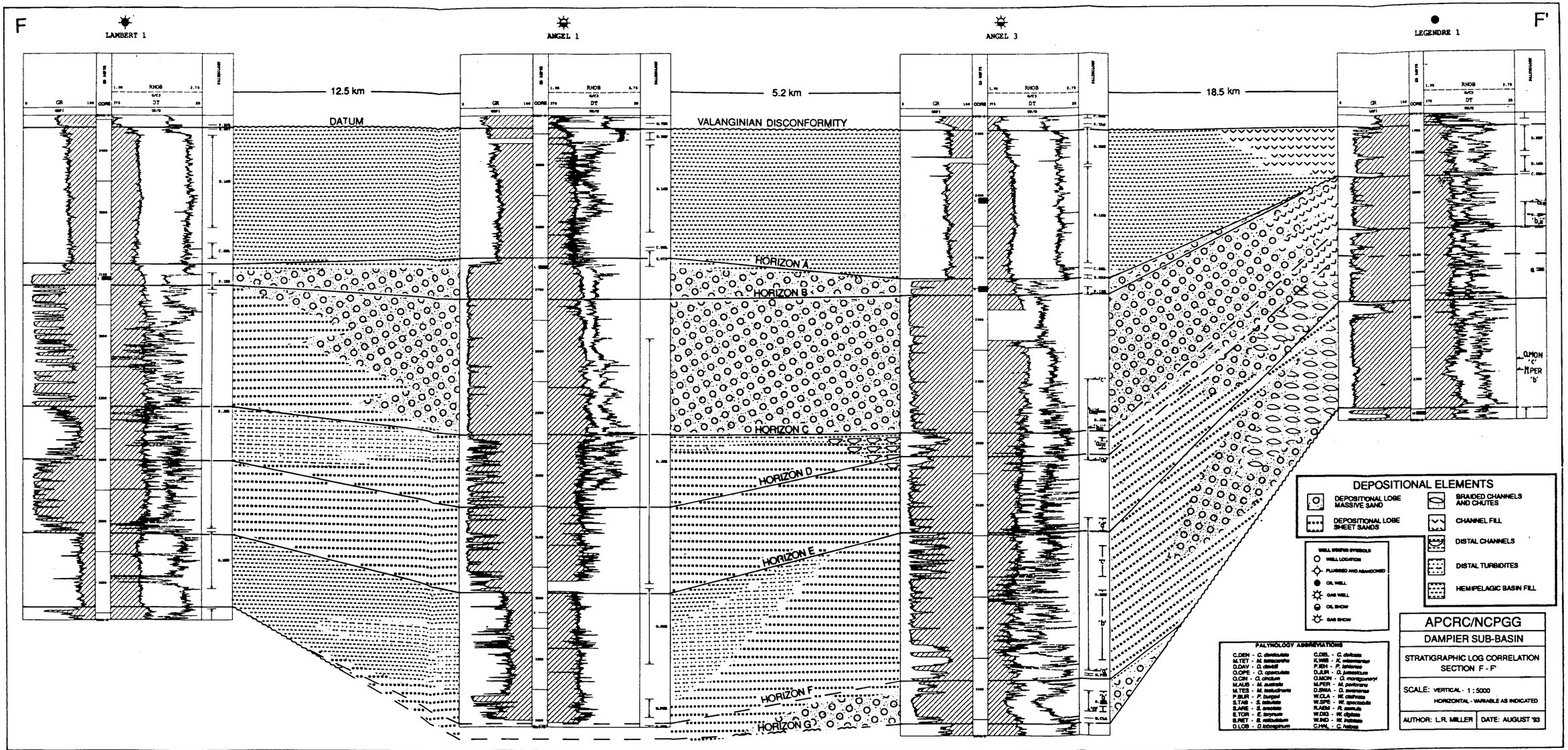

F
F'
LAMBERT 1
ANGEL 1
ANGEL 3
LEGENDRE 1
12.5 km
5.2 km
18.5 km
DATUM
VALANGINIAN DISCONFORMITY
HORIZON A
HORIZON B
HORIZON C
HORIZON D
HORIZON E
HORIZON F
HORIZON G
DEPOSITIONAL ELEMENTS
DEPOSITIONAL LOBE MASSIVE SAND
DEPOSITIONAL LOBE SHEET SANDS
BRAIDED CHANNELS AND CHUTES
CHANNEL FILL
DISTAL CHANNELS
DISTAL TURBIDITES
HEMIPELAGIC BASIN FILL
WELL LOCATION
PLUGGED AND ABANDONED
OIL WELL
GAS WELL
OIL SHOW
GAS SHOW
APCRC/NCPGG
DAMPIER SUB-BASIN
STRATIGRAPHIC LOG CORRELATION SECTION F - F'
SCALE: VERTICAL - 1 : 5000
HORIZONTAL - VARIABLE AS INDICATED
AUTHOR: L.R. MILLER
DATE: AUGUST '93

Figure 4.19.

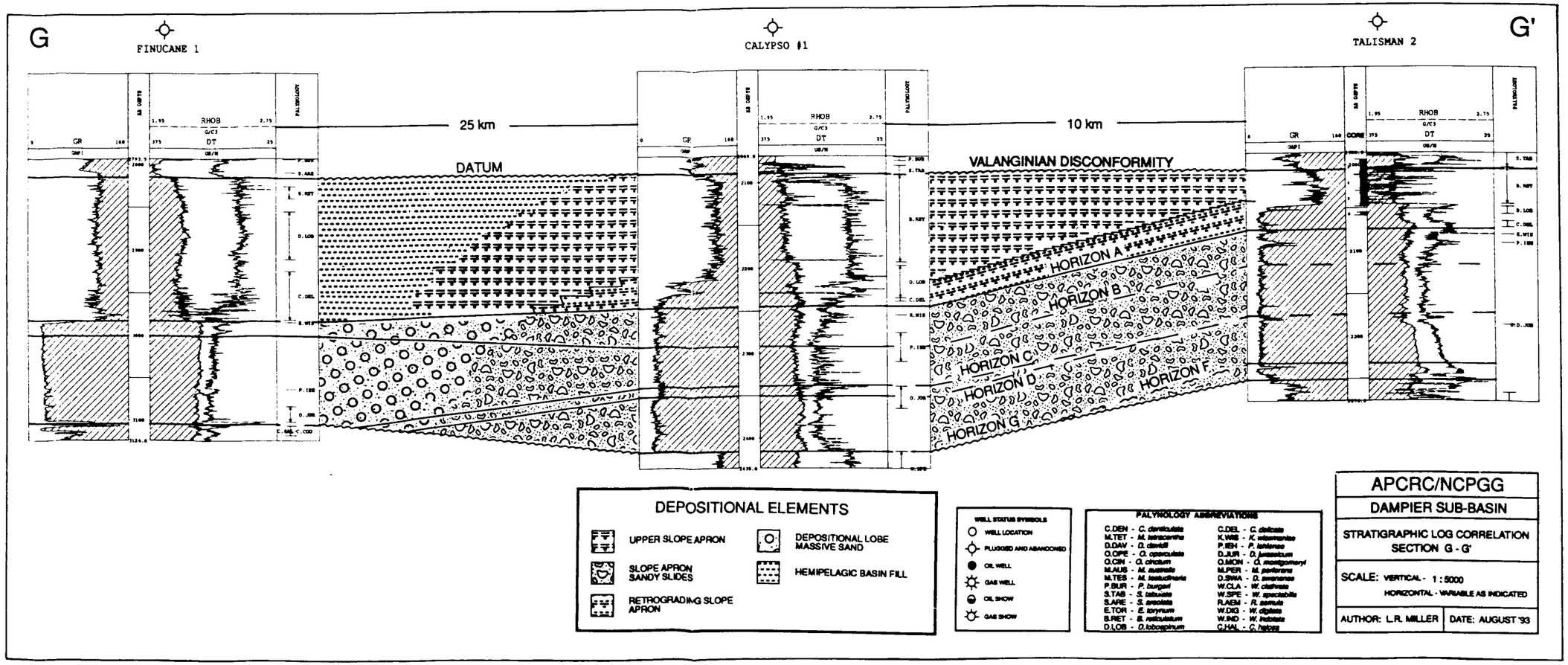

G
G'
FINUCANE 1
CALYPSO #1
TALISMAN 2
25 km
10 km
DATUM
VALANGINIAN DISCONFORMITY
HORIZON A
HORIZON B
HORIZON C
HORIZON D
HORIZON F
HORIZON G
GR
RHOB
DT
CORE
DEPOSITIONAL ELEMENTS
UPPER SLOPE APRON
SLOPE APRON SANDY SLIDES
RETROGRADING SLOPE APRON
DEPOSITIONAL LOBE MASSIVE SAND
HEMIPELAGIC BASIN FILL
WELL STATUS SYMBOLS
WELL LOCATION
PLUGGED AND ABANDONED
OIL WELL
GAS WELL
OIL SHOW
GAS SHOW
PALYNOLOGY ABBREVIATIONS
C.DEN - C. denticulata
C.DEL - C. delicata
M.TET - M. tetracantha
K.WIS - K. wisemaniae
D.DAV - D. davidii
P.BEH - P. behlensis
O.OPE - O. operculata
D.JUR - D. jurassicum
O.CIN - O. cinctum
O.MON - O. montgomeryi
M.AUS - M. australis
M.PER - M. perforans
M.TES - M. testudinaria
D.SWA - D. swanense
P.BUR - P. burgeri
W.CLA - W. clathrata
S.TAB - S. tabulata
W.SPE - W. spectabilis
S.ARE - S. areolata
R.AEM - R. aemula
E.TOR - E. toxynum
W.DIG - W. digitata
B.RET - B. reticulatum
W.IND - W. indotata
D.LOB - D. lobospinum
C.HAL - C. halosa
APCRC/NCPGG
DAMPIER SUB-BASIN
STRATIGRAPHIC LOG CORRELATION
SECTION G - G'
SCALE: VERTICAL - 1 : 5000
HORIZONTAL - VARIABLE AS INDICATED
AUTHOR: L.R. MILLER
DATE: AUGUST '93

Figure 4.20.

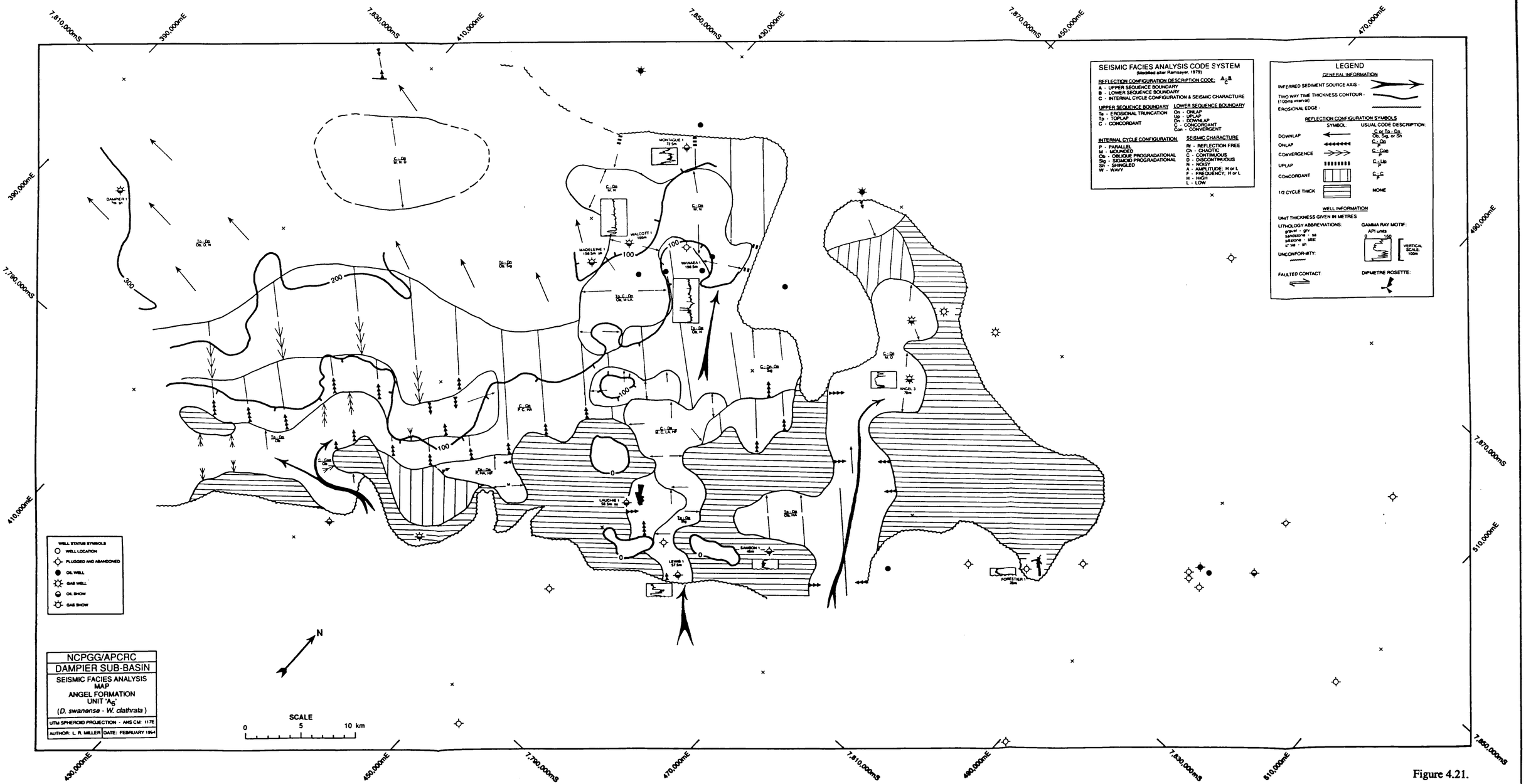

7,810,000mS
390,000mE
7,830,000mS
410,000mE
7,850,000mS
430,000mE
7,870,000mS
450,000mE
470,000mE
490,000mE
510,000mE
7,790,000mS
7,850,000mS
SEISMIC FACIES ANALYSIS CODE SYSTEM
(Modified after Ramsayer, 1979)
REFLECTION CONFIGURATION DESCRIPTION CODE: A=B/C
A - UPPER SEQUENCE BOUNDARY
B - LOWER SEQUENCE BOUNDARY
C - INTERNAL CYCLE CONFIGURATION & SEISMIC CHARACTURE
UPPER SEQUENCE BOUNDARY
Te - EROSIONAL TRUNCATION
Tp - TOPLAP
C - CONCORDANT
LOWER SEQUENCE BOUNDARY
On - ONLAP
Dp - DOWNLAP
Cv - CONVERGENT
Con - CONVERGENT
INTERNAL CYCLE CONFIGURATION
P - PARALLEL
M - MOUNDED
Obp - OBLIQUE PROGRADATIONAL
Sig - SIGMOID PROGRADATIONAL
Sh - SHINGLED
W - WAVY
SEISMIC CHARACTURE
Re - REFLECTION FREE
Ch - CHAOTIC
C - CONTINUOUS
D - DISCONTINUOUS
N - NOISY
A - AMPLITUDE; H or L
F - FREQUENCY; H or L
H - HIGH
L - LOW
LEGEND
GENERAL INFORMATION
INFERRED SEDIMENT SOURCE AXIS -
TWO WAY TIME THICKNESS CONTOUR - (100ms interval)
EROSIONAL EDGE -
REFLECTION CONFIGURATION SYMBOLS
SYMBOL
USUAL CODE DESCRIPTION
DOWNLAP
C or Te - Dp, Obp, Sig, or Sh
ONLAP
C - On P
CONVERGENCE
C - Con P
UPLAP
C - Up P
CONCORDANT
C - C P
1/2 CYCLE THICK
NONE
WELL INFORMATION
UNIT THICKNESS GIVEN IN METRES
LITHOLOGY ABBREVIATIONS:
gravel - grv
sandstone - ss
siltstone - sltst
shale - sh
UNCONFORMITY:
FAULTED CONTACT:
GAMMA RAY MOTIF:
API units
0
150
VERTICAL SCALE 100m
DIPMETRE ROSETTE:
WELL STATUS SYMBOLS
WELL LOCATION
PLUGGED AND ABANDONED
OIL WELL
GAS WELL
OIL SHOW
GAS SHOW
MONTAGUE 1
75 Sm
DAMPIER 1
WALCOTT 1
100m
MADELEINE 1
156 Sm
WANAEA 1
186 Sm
LAUCHIE 1
58 Sm
LEWIS 1
57 Sm
SAMSON 1
45m
ANGEL 3
70m
FORESTIER 1
25m
100
200
300
0
N
SCALE
0
5
10 km
NCPGG/APCRC
DAMPIER SUB-BASIN
SEISMIC FACIES ANALYSIS MAP
ANGEL FORMATION
UNIT 'A6'
(D. swanense - W. clathrata)
UTM SPHEROID PROJECTION - ANS CM: 117E
AUTHOR: L. R. MILLER
DATE: FEBRUARY 1994

Figure 4.21.

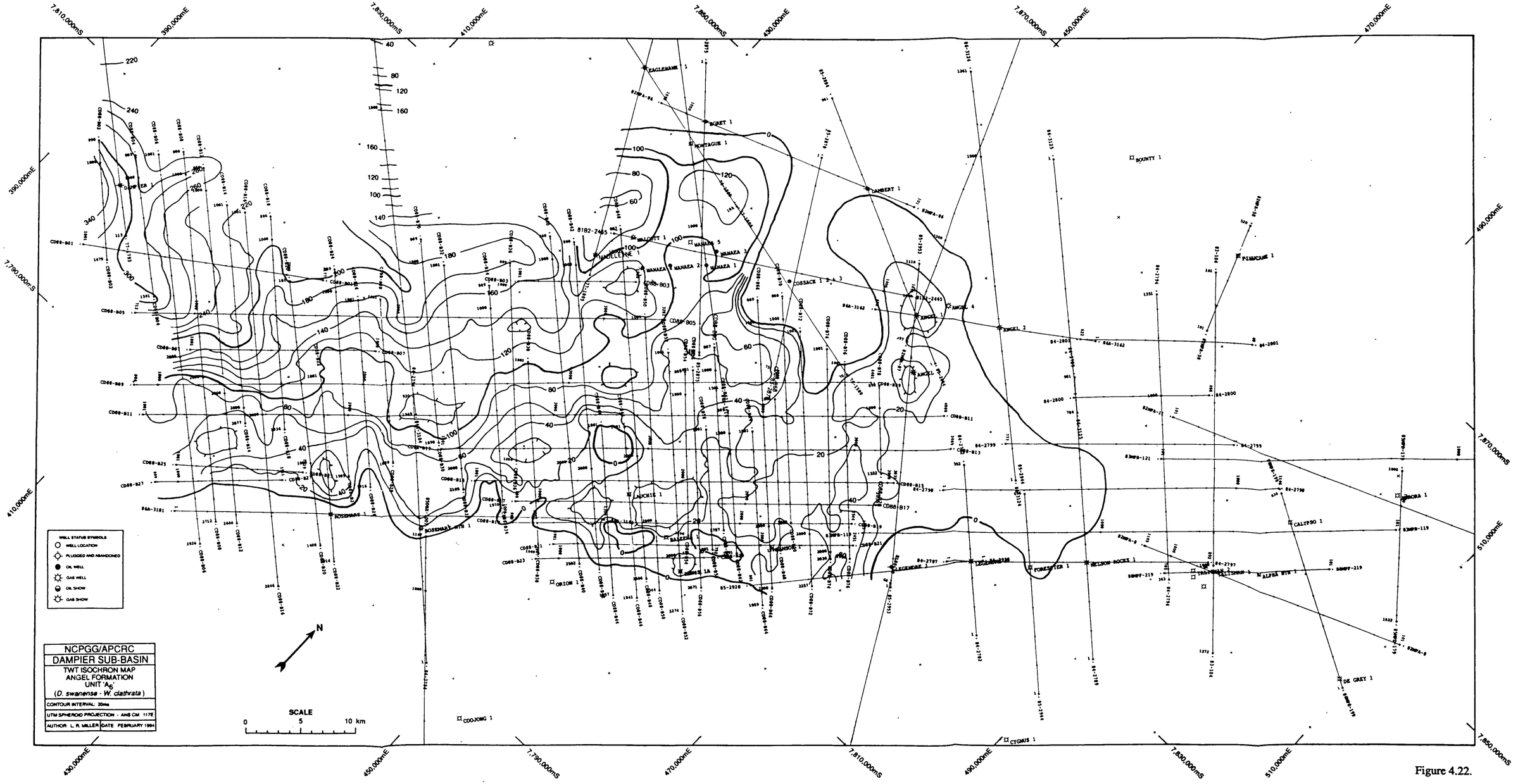

NCPGG/APCRC
DAMPIER SUB-BASIN
TWT ISOCHRON MAP
ANGEL FORMATION
UNIT 'A6'
(D. swanense - W. clathrata)
CONTOUR INTERVAL: 20ms
UTM SPHEROID PROJECTION - ANS CM 117E
AUTHOR L. R. MILLER
DATE FEBRUARY 1994
WELL STATUS SYMBOLS
WELL LOCATION
PLUGGED AND ABANDONED
OIL WELL
GAS WELL
OIL SHOW
GAS SHOW
SCALE
0 5 10 km
N
7,810,000mS
390,000mE
7,830,000mS
410,000mE
7,850,000mS
430,000mE
7,870,000mS
450,000mE
470,000mE
490,000mE
510,000mE
7,790,000mS
7,770,000mS
7,750,000mS
EAGLEHAWK 1
SCRET 1
MONTAGUE 1
DUMPER 1
MALCOTT 1
MAHAZA 1
MAHAZA 2
MAHAZA 3
MAHAZA 4
MAHAZA 5
MADELEINE 1
COSSACK 1
LAMBERT 1
BOUNTY 1
ANGEL 1
ANGEL 2
ANGEL 3
ANGEL 4
PLUMCAKE 1
ROSEMARY 1
ROSEMARY STH 1
LAUCHIE 1
ORION 1
COOJONG 1
LEGENDRE 1
FORESTIER 1
NELSON ROCKS 1
CALYPSO 1
ALPHA STH 1
DE GREY 1
CYGNUS 1
CD88-801
CD88-803
CD88-805
CD88-807
CD88-809
CD88-811
CD88-813
CD88-815
CD88-817
CD88-819
CD88-821
CD88-823
CD88-825
CD88-827
82MPA-96
82MPA-9
83MPA-121
83MPA-119
86MPA-219
84-2799
84-2800
84-2801
84-2797
84-2790
86A-3162
86A-3101
85-2928
8182-2465

Figure 4.22.

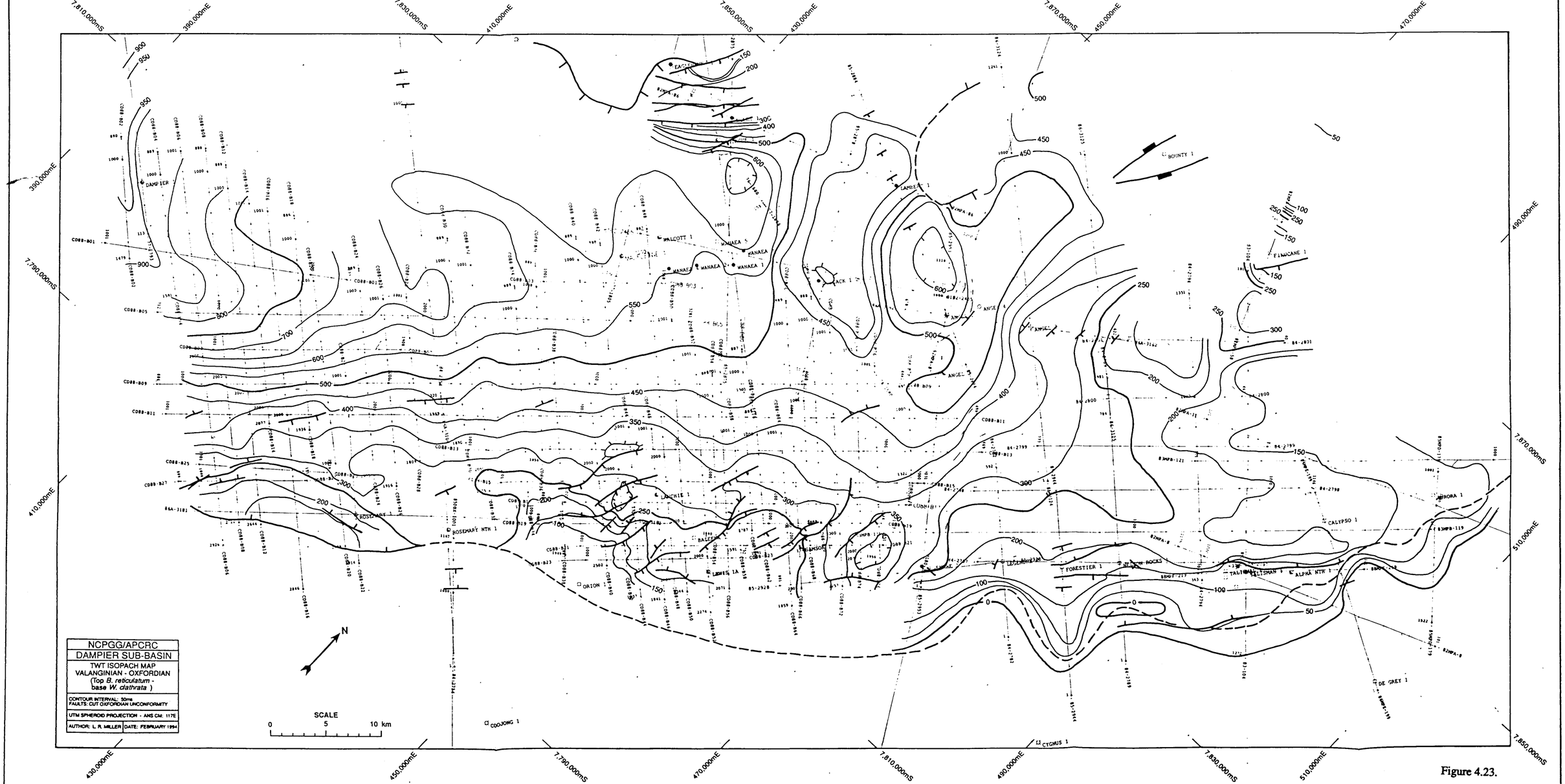

NCPGG/APCRC
DAMPIER SUB-BASIN
TWT ISOPACH MAP
VALANGINIAN - OXFORDIAN
(Top B. reticulatum - base W. clathrata)
CONTOUR INTERVAL: 50ms
FAULTS: CUT OXFORDIAN UNCONFORMITY
UTM SPHEROID PROJECTION - ANS CM: 117E
AUTHOR: L R. MILLER
DATE: FEBRUARY 1994
SCALE
0 5 10 km
N
7,810,000mS
390,000mE
7,830,000mS
410,000mE
7,850,000mS
430,000mE
7,870,000mS
450,000mE
470,000mE
490,000mE
510,000mE
7,790,000mS
DAMPIER
ROSEMARY 1
ROSEMARY NTH 1
WALCOTT 1
WANAEA 1
LAMEE 1
ANGEL 1
LOCHNE 1
BALLEENY 1
THAMSON 1
ORION 1
COOJONG 1
CYGNUS 1
BOUNTY 1
FLAMBANE 1
CALYPSO 1
AURORA 1
FORESTIER 1
TALISMAN 1
ALPHA NTH 1
DE GREY 1

Figure 4.23.

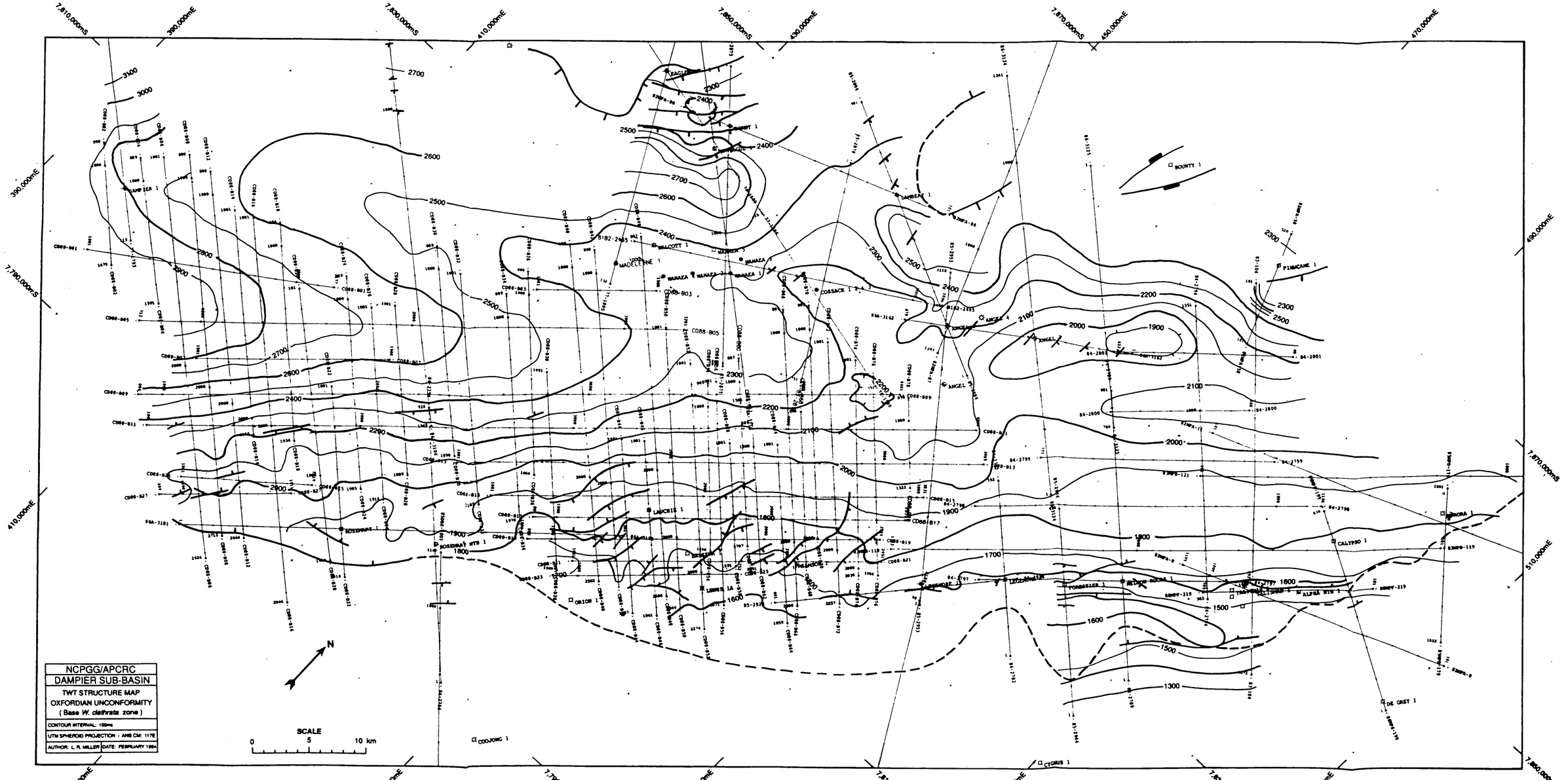

NCPGG/APCRC
DAMPIER SUB-BASIN
TWT STRUCTURE MAP
OXFORDIAN UNCONFORMITY
(Base W. clathrata zone)
CONTOUR INTERVAL: 100ms
UTM SPHEROID PROJECTION - ANS CM: 117E
AUTHOR: L. R. MILLER DATE: FEBRUARY 1994
SCALE
0 5 10 km
N
7,810,000mS
390,000mE
7,830,000mS
410,000mE
7,850,000mS
430,000mE
7,870,000mS
450,000mE
470,000mE
490,000mE
510,000mE
7,790,000mS
7,890,000mS
EAGLE 1
BOUNTY 1
LAMBERT 1
MADELEINE 1
WALCOTT 1
WAMEA 1
WAMEA 2
WAMEA 3
COSSACK 1
PIMLICO 1
ANGEL 1
ANGEL 2
ANGEL 3
ANGEL 4
LAURIE 1
ROSEMARY 1
ROSEMARY NTH 1
ORION 1
LEANYER 1A
FORRESTER 1
HESTIA 1
CALYPSO 1
ARGUS 1
ALPHA NTH 1
DE GREY 1
COOJONG 1
CYGNUS 1

Figure 4.24.

Angel Formation Unit A5

Schematic palaeogeography : Figure 4.25.

Seismic facies map : Figure 4.26.

Seismic examples : Figures 3.25, 3.27, 3.35, 3.38, 3.39, 3.49, 3.50 and 3.51.

Stratigraphic log correlations : location map, Figure 4.15; section C - C', Figure 4.16; section D - D', Figure 4.17; section E - E', Figure 4.18; section F - F', Figure 4.19; section G - G', Figure 4.20.

Isochron map : Figure 4.27.

Structure/isochron map : Valanginian Disconformity to base Angel Formation, Figure 4.23.

Structure map : base Angel Formation, Figure 4.24.

Montages: Enclosures IIIb and IIIc.

Core data : Madeleine 1 core 4 - Facies E1.1; Angel 1 core 3 - Facies F2.2.

Angel Formation unit A5 is considered to have a retrogradational relationship with the underlying unit A6. This contact is considered slightly erosional near the margin (e.g. see Lewis 1 and Forestier 1 on section C - C', Figure 4.16), and aggradational within the depocentre (e.g. see Madeleine 1 and Wanaea 1 on section E - E', Figure 4.18). As with unit A6, this unit has the same three major sediment source axes. The sediment source axis at Lewis 1 (Figure 3.38) bifurcates around a palaeogeographic high area (coincident with Baleena 1 area). This unit contains the second stage of interpreted channel cut and fill which is shown in Figures 3.49, 3.50 and 3.51. Similar sedimentological relationships are expected in this unit, as with unit A6.

Braided Channels and Chutes are noted at Legendre 1 (Figure 3.27). This is interpreted to be associated with distal sheet sands at Angel 1 and Angel 3 (Figure 3.57).

A highlight of this unit is the well developed seismic lens features that are seen on the southeastern flank of the Lewis Trough (Figures 3.39 and 3.42). These features contain massive sand at Rosemary 1 and Lauchie 1, interpreted to be Slope Apron Depositional Sand.

A debris flow (Facies F2.2) occurs at Angel 1, core 3. This facies is expected to occur within the Slope Apron Slides and Slumps depositional element, the likely result of relief and instabilities provided by nearby fault movement. A fault is interpreted in the general vicinity of this depositional element on the structure/isochron map (Figure 4.23; see also tectonic elements map, Figure 4.40).

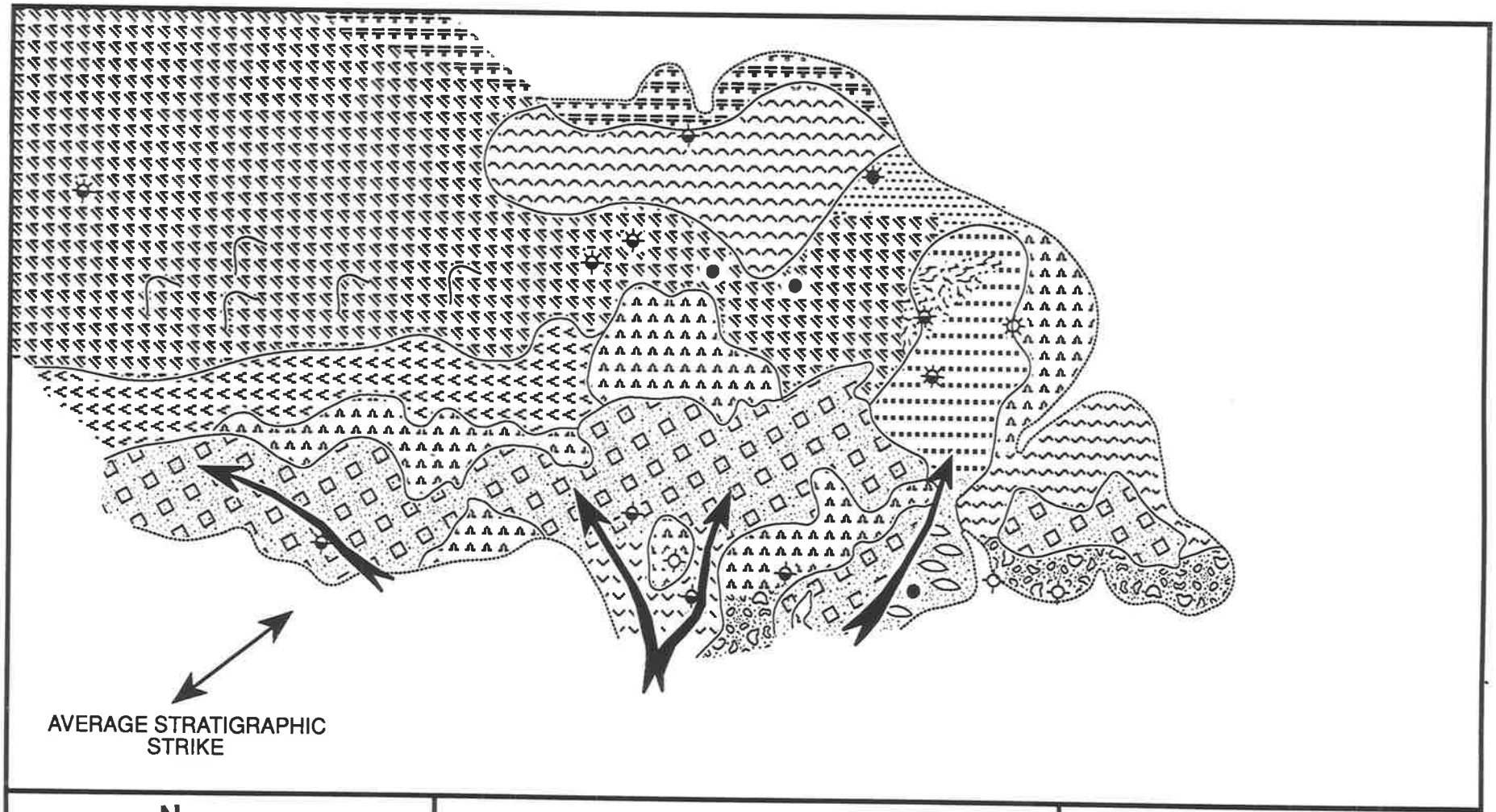

AVERAGE STRATIGRAPHIC STRIKE
N
0
10
20km
SCHEMATIC PALAEOGEOGRAPHY
ANGEL FORMATION UNIT A5

Figure 4.25.

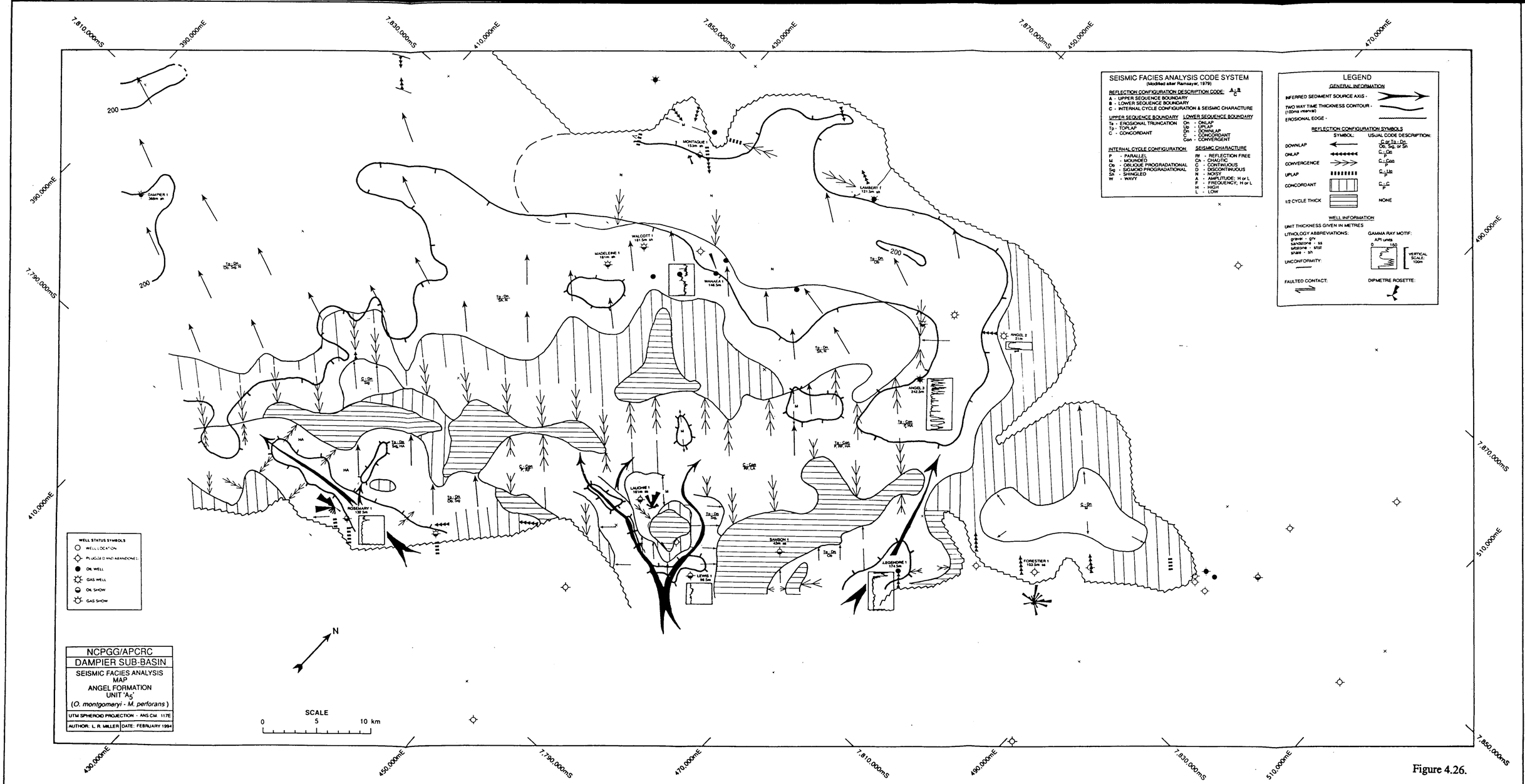

7,810,000mS
390,000mE
7,830,000mS
410,000mE
7,850,000mS
430,000mE
7,870,000mS
450,000mE
470,000mE
490,000mE
510,000mE
7,790,000mS
SEISMIC FACIES ANALYSIS CODE SYSTEM
(Modified after Ramsayer, 1979)
REFLECTION CONFIGURATION DESCRIPTION CODE: A-B-C
A - UPPER SEQUENCE BOUNDARY
B - LOWER SEQUENCE BOUNDARY
C - INTERNAL CYCLE CONFIGURATION & SEISMIC CHARACTURE
UPPER SEQUENCE BOUNDARY
Ta - EROSIONAL TRUNCATION
Tp - TOPLAP
C - CONCORDANT
LOWER SEQUENCE BOUNDARY
On - ONLAP
Up - UPLAP
Dn - DOWNLAP
Co - CONCORDANT
Con - CONVERGENT
INTERNAL CYCLE CONFIGURATION
P - PARALLEL
M - MOUNDED
Ob - OBLIQUE PROGRADATIONAL
Sig - SIGMOID PROGRADATIONAL
Sh - SHINGLED
W - WAVY
SEISMIC CHARACTURE
RF - REFLECTION FREE
Ch - CHAOTIC
C - CONTINUOUS
D - DISCONTINUOUS
N - NOISY
A - AMPLITUDE; H or L
F - FREQUENCY; H or L
H - HIGH
L - LOW
LEGEND
GENERAL INFORMATION
INFERRED SEDIMENT SOURCE AXIS -
TWO WAY TIME THICKNESS CONTOUR - (100ms intervals)
EROSIONAL EDGE -
REFLECTION CONFIGURATION SYMBOLS
SYMBOL:
USUAL CODE DESCRIPTION:
DOWNLAP
C or Ta - Dn, Ob, Sig, or Sh
ONLAP
C - On, P
CONVERGENCE
C - Con, P
UPLAP
C - Up, P
CONCORDANT
C - C, P
1/2 CYCLE THICK
NONE
WELL INFORMATION
UNIT THICKNESS GIVEN IN METRES
LITHOLOGY ABBREVIATIONS:
gravel = GTV
sandstone = SS
siltstone = SLST
shale = SH
UNCONFORMITY:
GAMMA RAY MOTIF:
API units
0
150
VERTICAL SCALE: 100m
FAULTED CONTACT:
DIPMETRE ROSETTE:
WELL STATUS SYMBOLS
WELL LOCATION
PLUGGED AND ABANDONED
OIL WELL
GAS WELL
OIL SHOW
GAS SHOW
DAMPIER 1
366m sh
MONTAGUE 1
153m sh
LAMBERT 1
121.5m sh
WALCOTT 1
181.5m sh
MADELEINE 1
181m sh
WANAEA 1
146.5m
ANGEL 2
21m
ANGEL 3
242.5m
ROSEMARY 1
132.5m
LAICHIE 1
181m sh
SAMSON 1
134 m
LEWIS 1
94.5m
LEGENDRE 1
174.5m
FORESTIER 1
103.5m sh
N
SCALE
0
5
10 km
NCPGG/APCRC
DAMPIER SUB-BASIN
SEISMIC FACIES ANALYSIS MAP
ANGEL FORMATION
UNIT 'A5'
(O. montgomeryi - M. perforans)
UTM SPHEROID PROJECTION - ANS CM 117E
AUTHOR: L.R. MILLER
DATE: FEBRUARY 1994

Figure 4.26.

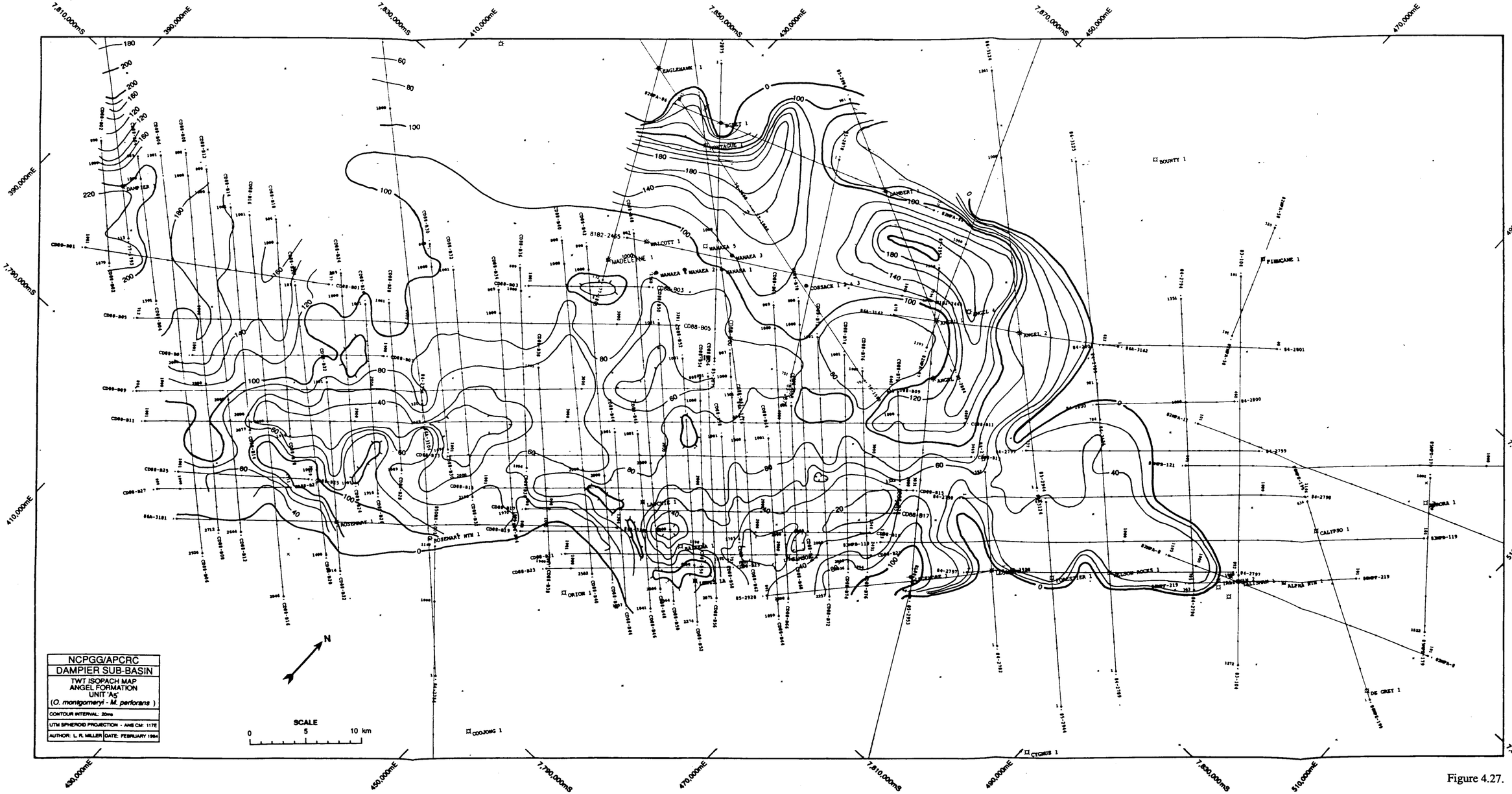

NCPGG/APCRC
DAMPIER SUB-BASIN
TWT ISOPACH MAP
ANGEL FORMATION
UNIT 'As'
(O. montgomeryi - M. perforans)
CONTOUR INTERVAL: 20ms
UTM SPHEROID PROJECTION - AMS CM: 117E
AUTHOR: L. R. MILLER
DATE: FEBRUARY 1994
SCALE
0 5 10 km
N
7,810,000mS
390,000mE
7,830,000mS
410,000mE
7,850,000mS
430,000mE
7,870,000mS
450,000mE
470,000mE
7,790,000mS
490,000mE
510,000mE
DAMPIER
EAGLEHAWK 1
MONTAPUK 1
BOUNTY 1
ANGEL 1
ANGEL 2
ANGEL 3
ANGEL 4
ANGEL 5
PIMMICANE 1
MADELEINE 1
WALCOTT 1
MANAEA 1
MANAEA 2
MANAEA 3
MANAEA 5
COSSACK 1
ROSEMARY 1
ROSEMARY NTH 1
LAVERNE 1
LA LAVERNE 1
ORION 1
CALYPSO 1
ALPHA NTH 1
DE GREY 1
CYGNUS 1
COOJONG 1

Figure 4.27.

Other features noted within unit A5 include seismic mounding in the Kendrew Trough region, seismic convergence and distally associated asymptotic downlap. Seismic trough anomalies are possibly associated with distal turbidite sands. These features are similar in description to those in unit A6.

Angel Formation Units A3 and A4

Schematic palaeogeography : Figure 4.28.

Seismic facies map : Figure 4.29.

Seismic examples : Figures 3.24, 3.30, 3.36, 3.37 and 3.40.

Stratigraphic log correlations : location map, Figure 4.15; section C - C', Figure 4.16; section D - D', Figure 4.17; section E - E', Figure 4.18; section F - F', Figure 4.19; section G - G', Figure 4.20.

Isochron map : Figure 4.30.

Structure/isochron map : Valanginian Disconformity to Angel Formation horizon 'C' (top of unit A3 and A 4), Figure 4.31.

Structure map : Angel Formation horizon 'C' (top of unit A3 and A 4), Figure 4.32.

Montage: Enclosures IIIb and IIIc.

Core data : Legendre 1 core 11 - Facies B1.2; Madeleine 1 core 3 - Facies E1.3; Dampier 1 core 12 - Facies E1.1.

Angel Formation units A3 and A4 are confined by horizons 'C' and 'E' and are divided by horizon 'D'. Unit A3 is a relatively thinner, muddy unit that was deposited during a period of waning sand influx to the basin. Units A3 and A4 are log defined units and were mapped as one seismic interval because of limits in seismic resolution. These units are retrogradational with respect to A5. No active faulting is interpreted to occur within the Angel Formation above horizon 'E', although minor faults are mapped on the structure maps (Figures 4.31 and 4.32). These faults are considered to be palaeogeographic remnants from earlier faulting activity.

The deposition of the Slope Apron Depositional Sand over the Legendre Trend area waned during this period (e.g. see Figure 3.40), while extensive slumps and slides occurred over areas of previous Channel Fill (e.g. Lewis 1, Figure 3.37), and previous palaeo-highs such as at Samson 1 (Figure 3.36). Braided Channels and Channel Fill occur at Legendre 1 (Figure 3.30; core 11, Facies B2.1) which correlates with interpreted Depositional Lobe Sheet Sands at Angel 3.

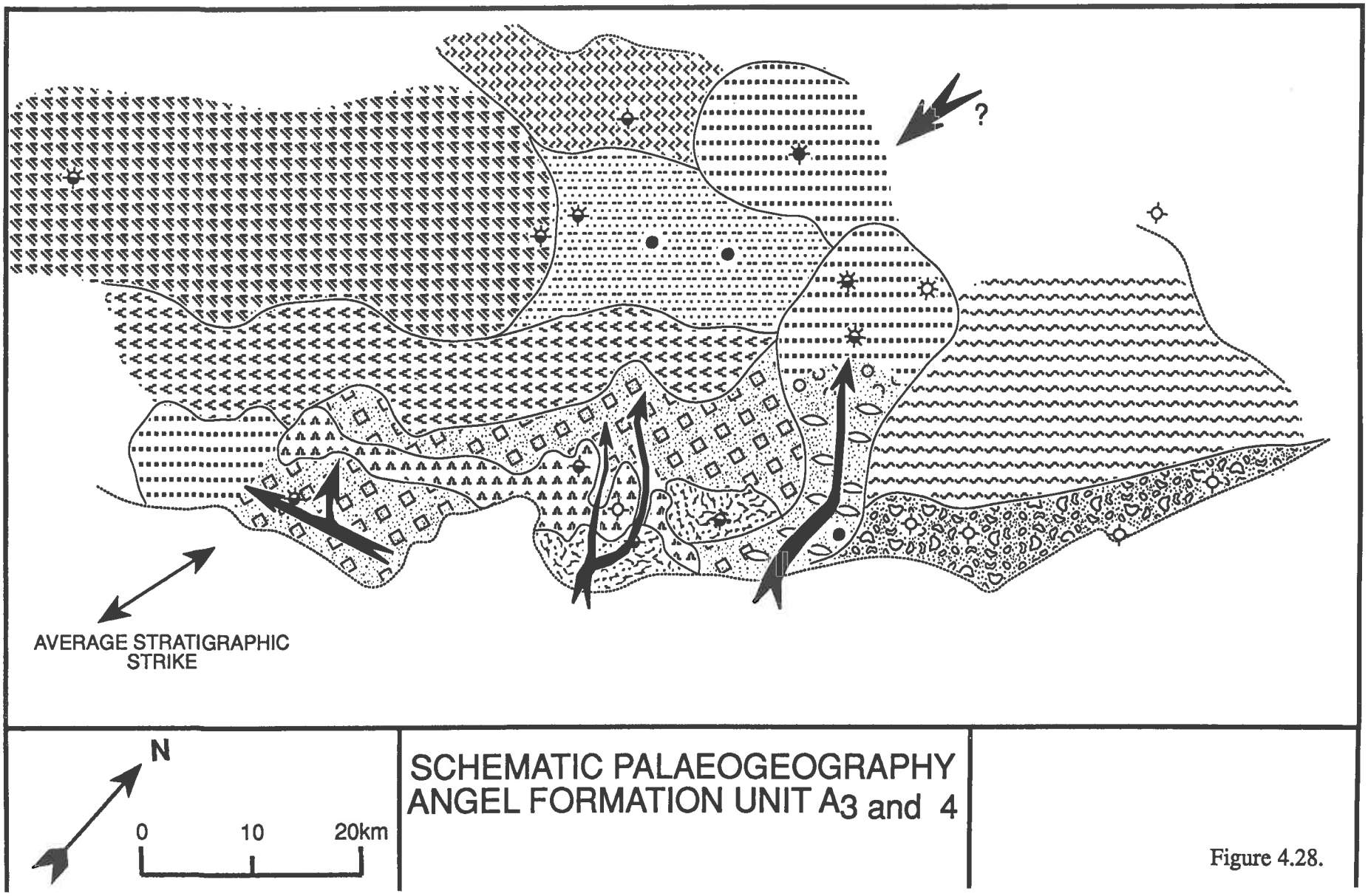

?
AVERAGE STRATIGRAPHIC STRIKE
N
0
10
20km
SCHEMATIC PALAEOGEOGRAPHY
ANGEL FORMATION UNIT A3 and 4

Figure 4.28.

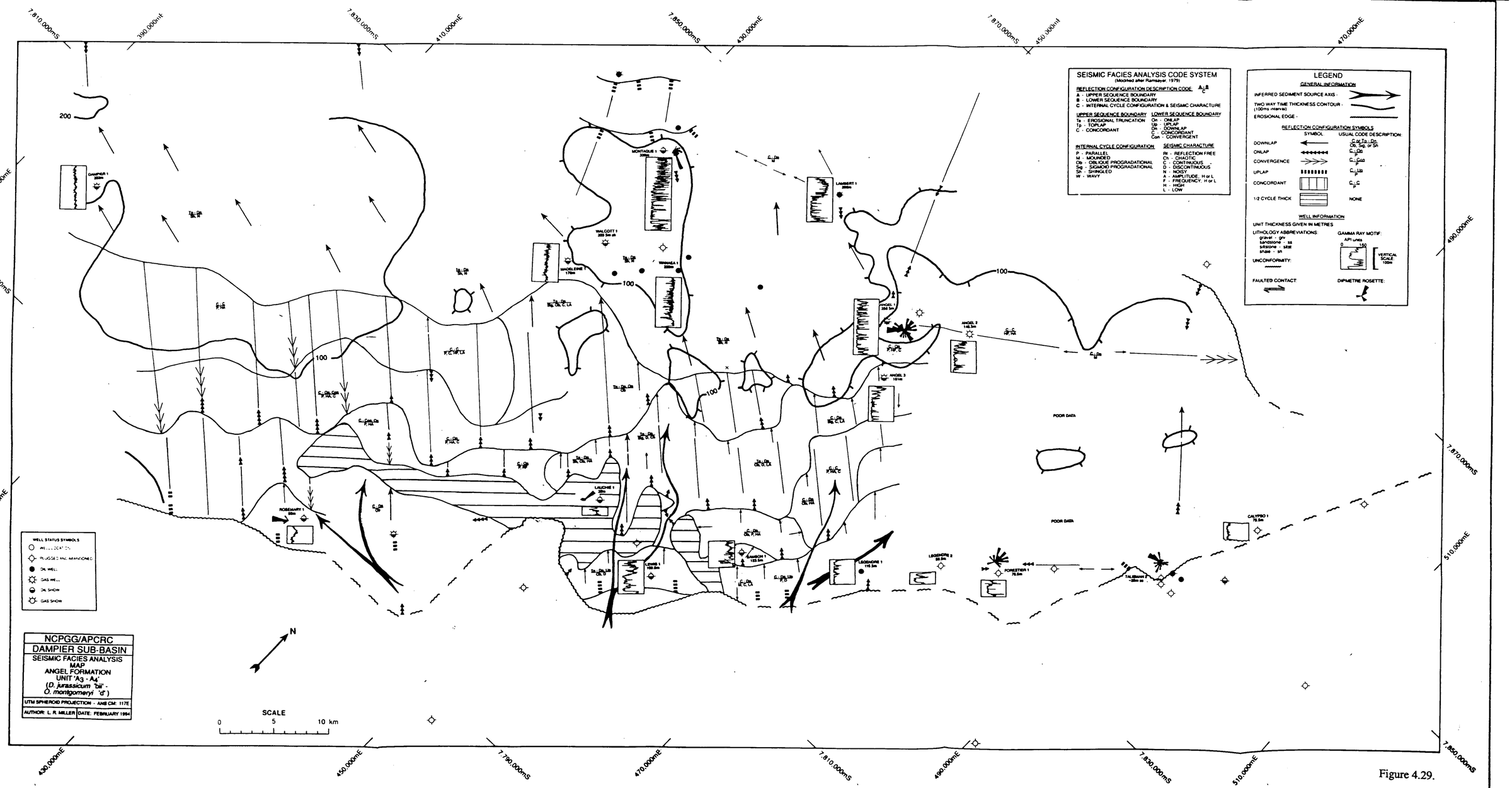

SEISMIC FACIES ANALYSIS CODE SYSTEM
(Modified after Ramsayer, 1979)
REFLECTION CONFIGURATION DESCRIPTION CODE
A - UPPER SEQUENCE BOUNDARY
B - LOWER SEQUENCE BOUNDARY
C - INTERNAL CYCLE CONFIGURATION & SEISMIC CHARACTURE
UPPER SEQUENCE BOUNDARY
Te - EROSIONAL TRUNCATION
Tp - TOPLAP
C - CONCORDANT
LOWER SEQUENCE BOUNDARY
On - ONLAP
Dn - DOWNLAP
Con - CONCORDANT
Con - CONVERGENT
INTERNAL CYCLE CONFIGURATION
P - PARALLEL
M - MOUNDED
Ob - OBLIQUE PROGRADATIONAL
Sig - SIGMOID PROGRADATIONAL
SH - SHINGLED
W - WAVY
SEISMIC CHARACTURE
RF - REFLECTION FREE
Ch - CHAOTIC
C - CONTINUOUS
D - DISCONTINUOUS
N - NOISY
A - AMPLITUDE, H or L
F - FREQUENCY, H or L
H - HIGH
L - LOW
LEGEND
GENERAL INFORMATION
INFERRED SEDIMENT SOURCE AXIS -
TWO WAY TIME THICKNESS CONTOUR - (100ms interval)
EROSIONAL EDGE -
REFLECTION CONFIGURATION SYMBOLS
SYMBOL
USUAL CODE DESCRIPTION:
DOWNLAP
ONLAP
CONVERGENCE
UPLAP
CONCORDANT
1/2 CYCLE THICK
NONE
WELL INFORMATION
UNIT THICKNESS GIVEN IN METRES
LITHOLOGY ABBREVIATIONS:
gravel - gv
sandstone - ss
siltstone - sltst
shale - sh
UNCONFORMITY:
FAULTED CONTACT:
GAMMA RAY MOTIF:
API units
VERTICAL SCALE 100m
DIPMETRE ROSETTE:
WELL STATUS SYMBOLS
OIL WELL
GAS WELL
OIL SHOW
GAS SHOW
DAMPIER 1
MONTAGUE 1
WALCOTT 1
MACKLEINE 1
YAMANEA 1
LAMBERT 1
ANGEL 1
ANGEL 2
ANGEL 3
LAUCHIE 1
ROSEMARY 1
LEGENDRE 1
LEGENDRE 2
FORESTIER 1
CALYPSO 1
POOR DATA
POOR DATA
NCPGG/APCRC
DAMPIER SUB-BASIN
SEISMIC FACIES ANALYSIS MAP
ANGEL FORMATION
UNIT 'A3 - A4'
(D. jurassicum 'bii' - O. montgomeryi 'd')
UTM SPHEROID PROJECTION - AMG CM: 117E
AUTHOR: L. R. MILLER
DATE: FEBRUARY 1994
N
SCALE
0 5 10 km
7,810,000mS
390,000mE
7,830,000mS
410,000mE
7,850,000mS
430,000mE
7,870,000mS
450,000mE
470,000mE
490,000mE
510,000mE
7,790,000mS
200
100

Figure 4.29.

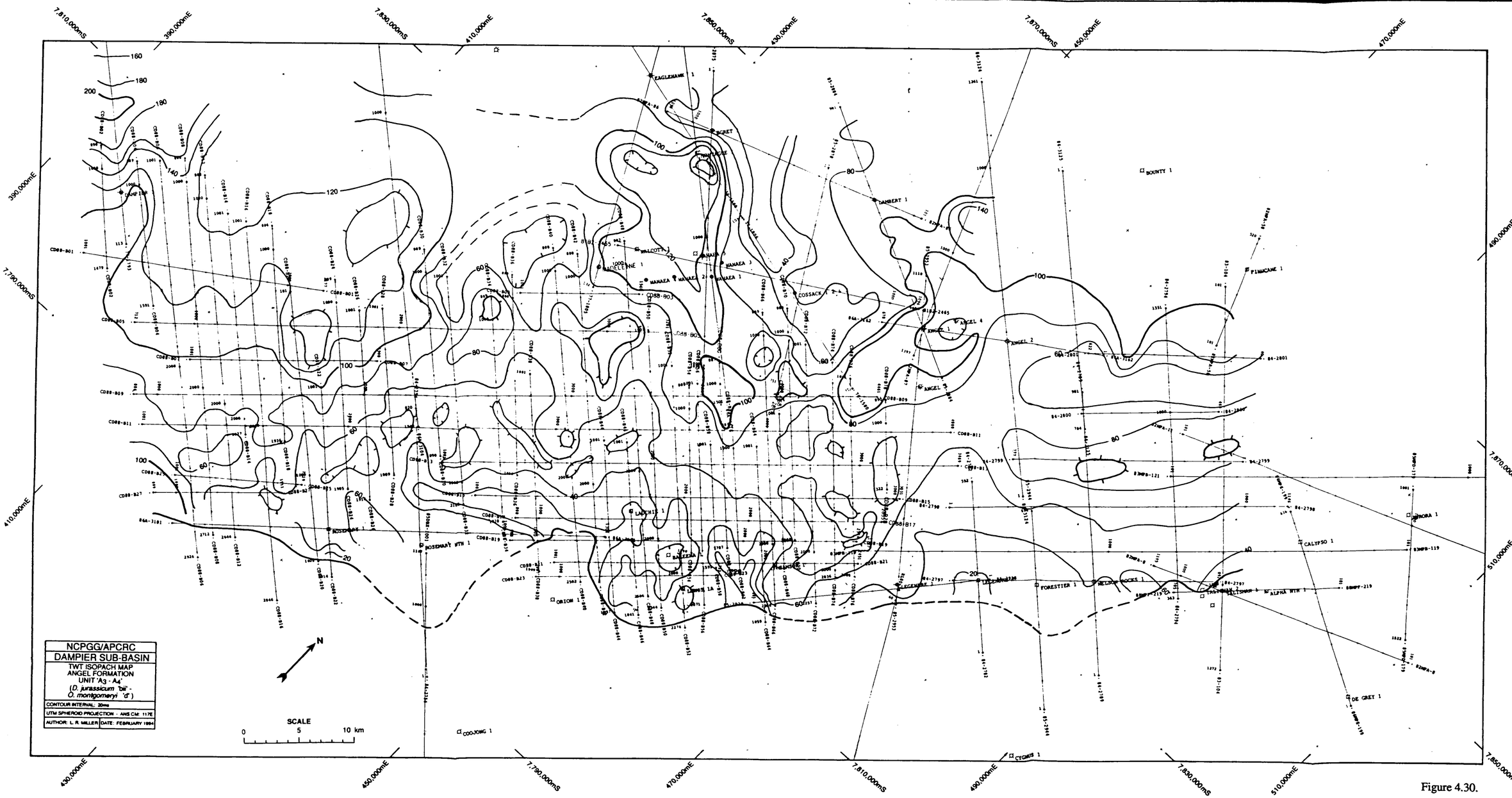

NCPGG/APCRC
DAMPIER SUB-BASIN
TWT ISOPACH MAP
ANGEL FORMATION
UNIT 'A3 - A4'
(D. jurassicum 'bii' -
O. montgomeryi 'd')
CONTOUR INTERVAL: 20ms
UTM SPHEROID PROJECTION - AMS CM: 117E
AUTHOR: L R MILLER
DATE: FEBRUARY 1994
SCALE
0 5 10 km
N
7,810,000mS
390,000mE
7,830,000mS
410,000mE
7,850,000mS
430,000mE
7,870,000mS
450,000mE
470,000mE
7,790,000mS
490,000mE
510,000mE
EAGLEHAWK 1
EGRET
WAHOO
WALCOTT
MADELEINE 1
MANAEA 1
MANAEA 2
MANAEA 3
MANAEA 4
COSSACK 1
LAMBERT 1
BOUNTY 1
ANGEL 1
ANGEL 2
ANGEL 3
ANGEL 4
PLUMCANE 1
ROSEMARY 1
ROSEMARY NTH 1
LADYHILL 1
ORION
CYGNUS 1
LEGENDRE 1
FORESTIER 1
NELSON ROCKS 1
ALPHA NTH 1
CALYPSO 1
ORRA 1
DE GREY 1
COO-JONG 1

Figure 4.30.

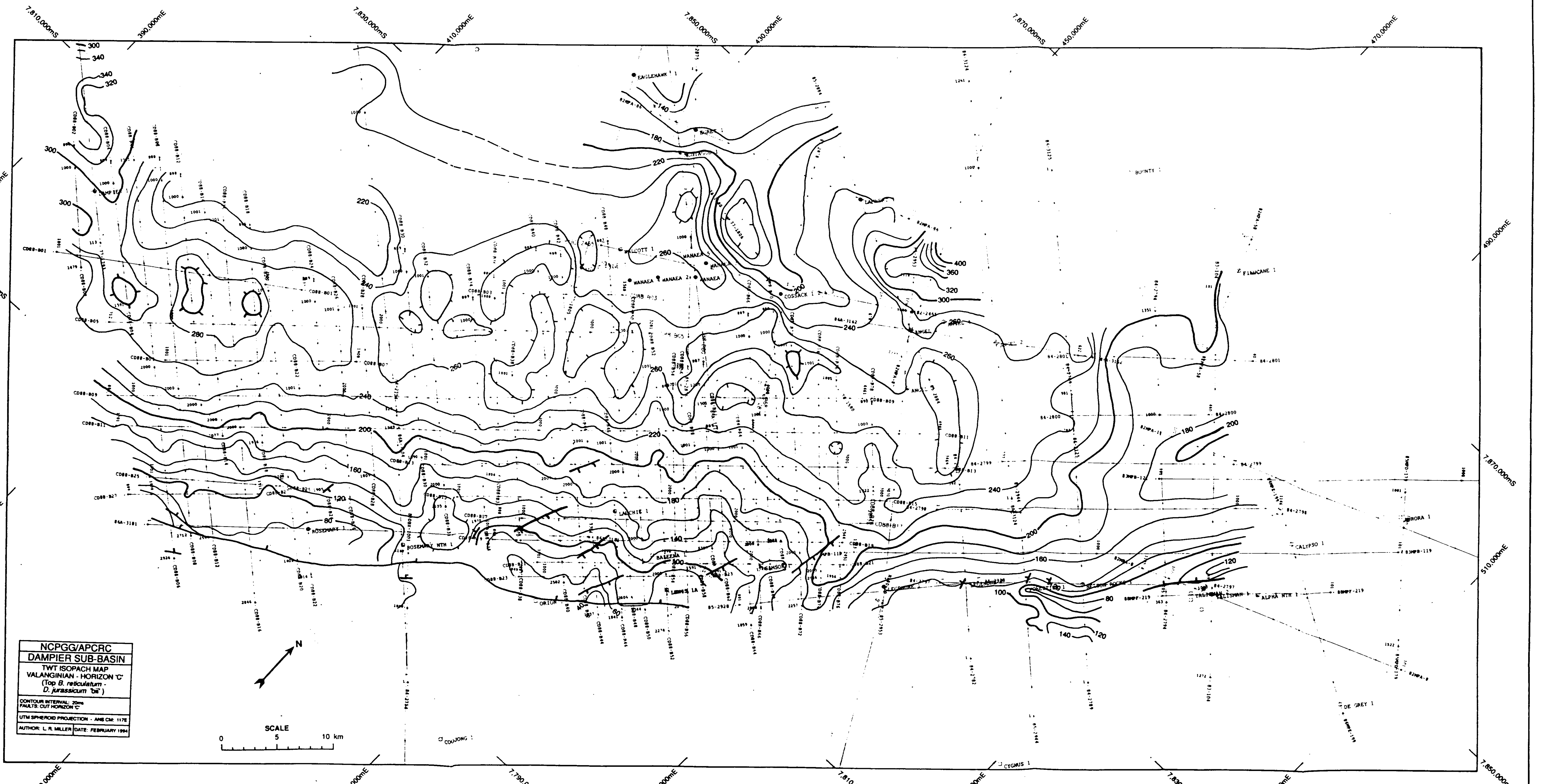

NCPGG/APCRC
DAMPIER SUB-BASIN
TWT ISOPACH MAP
VALANGINIAN - HORIZON 'C'
(Top B. reticulatum - D. jurassicum 'bii')
CONTOUR INTERVAL: 20ms
FAULTS: CUT HORIZON 'C'
UTM SPHEROID PROJECTION - ANS CM: 117E
AUTHOR: L. R. MILLER
DATE: FEBRUARY 1994
SCALE
0
5
10 km
N
EAGLEHAWK 1
WALCOTT 1
WANAEA
COSSACK 1
BOUNTY 1
FINUCANE 1
ROSEMARY 1
ROSEMARY NTH 1
LAMBERT
CALYPSO 1
DE GREY 1
COOJONG 1
CYGNUS 1
ORION
BALEENA
ALPHA NTH 1
7,810,000mS
7,830,000mS
7,850,000mS
7,870,000mS
390,000mE
410,000mE
430,000mE
450,000mE
470,000mE
490,000mE
510,000mE
7,790,000mS

Figure 4.31.

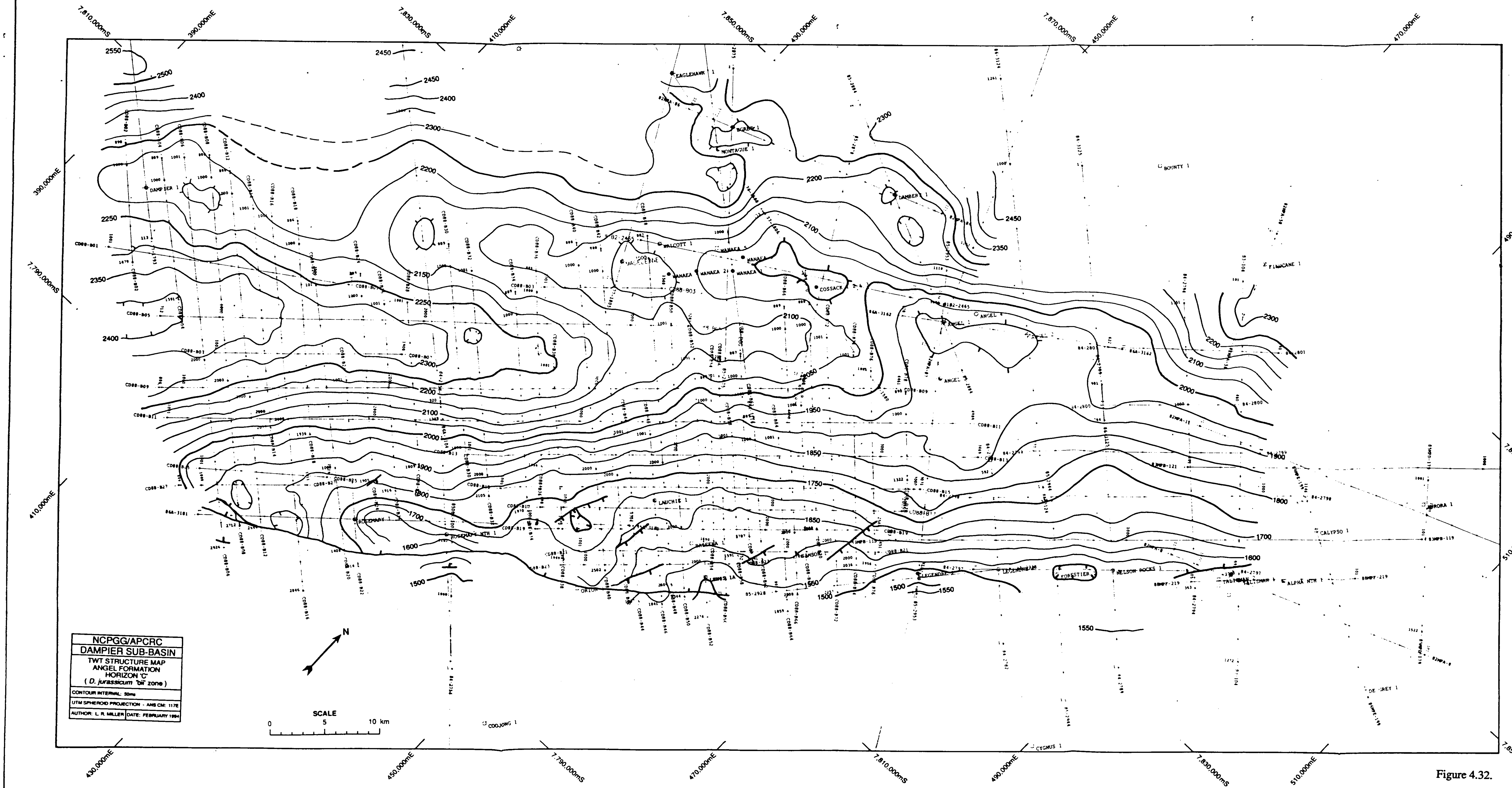

NCPGG/APCRC
DAMPIER SUB-BASIN
TWT STRUCTURE MAP
ANGEL FORMATION
HORIZON 'C'
(*D. jurassicum* "bii" zone)
CONTOUR INTERVAL: 50ms
UTM SPHEROID PROJECTION - ANS CM: 117E
AUTHOR: L. R. MILLER
DATE: FEBRUARY 1994
SCALE
0 5 10 km
N
EAGLEHAWK 1
MONTAGUE 1
DAMPIER 1
LAMBERT 1
BOUNTY 1
WALCOTT 1
WANAEA
COSSACK
ANGEL 1
ANGEL 3
FINUCANE 1
LAUCHIE 1
ROSEMARY
ROSEMARY NTH 1
ORION
FORESTIER
NELSON ROCKS 1
LEGENDRE 2
ALPHA NTH 1
CALYPSO 1
DE GREY 1
COOJONG 1
CYGNUS 1
7,810,000mS
7,830,000mS
7,850,000mS
7,870,000mS
390,000mE
410,000mE
430,000mE
450,000mE
470,000mE
490,000mE
510,000mE
7,790,000mS
7,810,000mS
7,830,000mS
7,850,000mS

Figure 4.32.

Slope Apron Braided Channels are interpreted at Montague 1 which suggests that some sediment was being sourced from the Rankin Platform. It is possible that a sediment source axis exists to the north of Lambert 1. However, due to the lack of seismic data over the area, this is not conclusive.

Slope Apron Sandy Slides are interpreted to the west of Legendre 1, (e.g. Legendre 2, Forestier 1, Talisman 2, Calypso 1), suggesting that relief pre-existed due to the Legendre Fault in this area.

Angel Formation Units A_1 and A_2

Schematic palaeogeography : Figure 4.33.

Seismic facies map : Figure 4.34.

Seismic examples : Figures 3.29, 3.43.

Stratigraphic log correlations : location map, Figure 4.15; section C - C', Figure 4.16; section D - D', Figure 4.17; section E - E', Figure 4.18; section F - F', Figure 4.19; section G - G', Figure 4.20.

Isochron map : Figure 4.35.

Structure/isochron map : Valanginian Disconformity to Angel Formation horizon 'C', Figure 4.31.

Structure map : Angel Formation horizon 'C' (base of unit A_1 and A_2), Figure 4.32.

Montage: Enclosures IIIb and IIIc.

Core data : Angel 1 core 1 - Facies B1.1; Angel 2 core 1 and 3 - Facies B1.1; Angel 3 core 2 - Facies B1.1; Angel 4 core 1, 2, 3 and 4 - Facies B1.1, B2.1, C1.2, and D1.3; Cossack 1 core 1 and 2 - Facies B1.1, C2.1, and D1.3; Dampier 1 core 10 and 11 - Facies C1.2 and D1.3; Lambert 1 core 1 - Facies B1.1; Madeleine 1 core 1 and 2 - Facies B1.1, E1.1, E1.3.

Angel Formation units A_1 and A_2 have extensive sand development and constitute a sand rich depositional system. As with units A_3 and A_4, these units were also mapped together due to limits of seismic resolution. The base of unit A_2, horizon 'C', represents the base Angel Formation over the Wanaea and Cossack Fields according to di Toro (1994).

A renewed sediment pulse of massive sand flow deposition is represented by unit A_2, overlying the thinner, muddier unit A_3. The thinner Unit A_1 is interpreted as a waning pulse of Angel Sand in areas where deposition of the Angel Formation had ceased. The top of the Angel Formation is slightly diachronous. It ranges from middle *P. iehiense* Zone at Wanaea 1 to middle *K. wisemaniae* Zone at Angel 3.

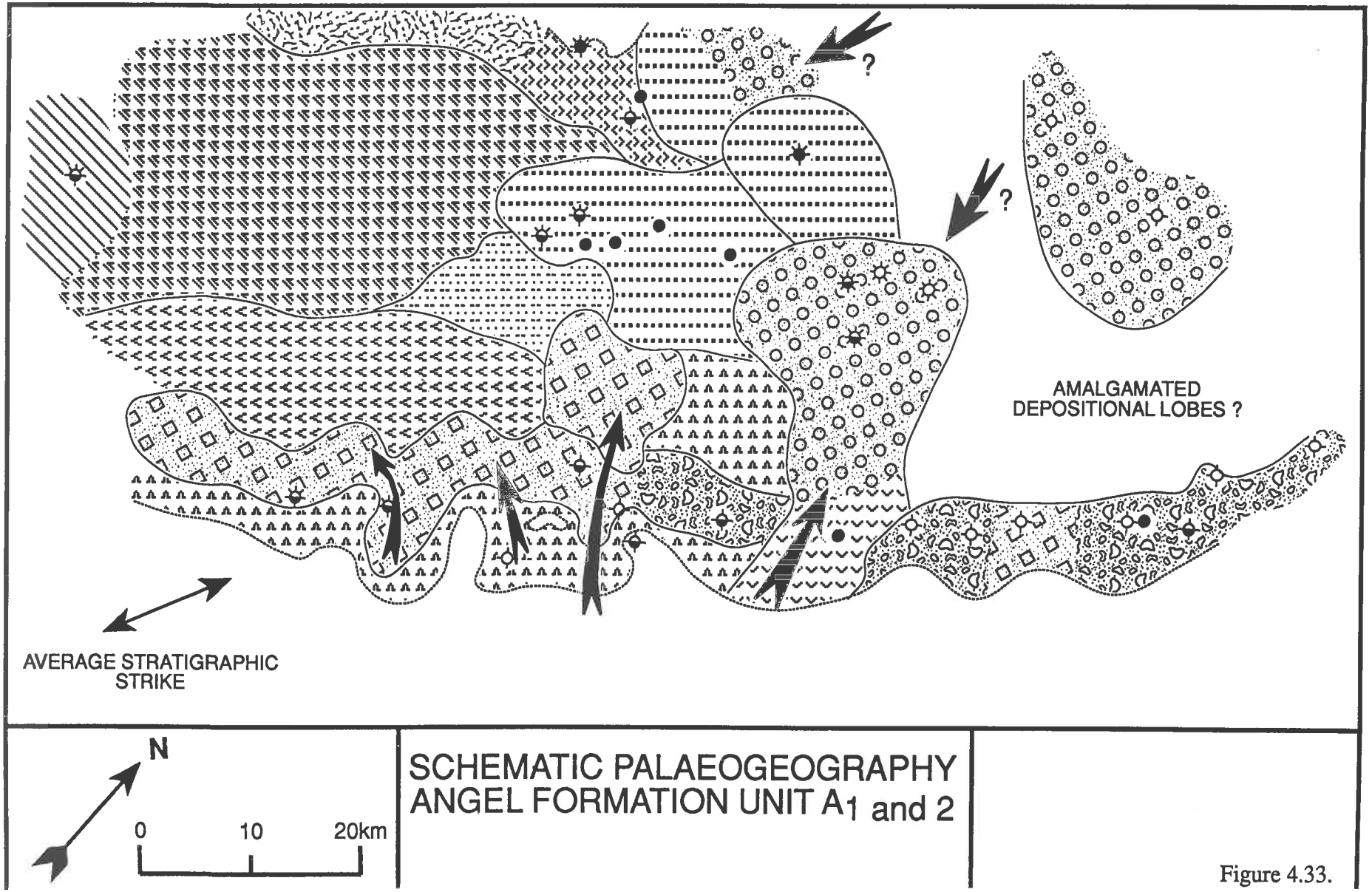

?
?
AMALGAMATED
DEPOSITIONAL LOBES ?
AVERAGE STRATIGRAPHIC
STRIKE
N
0
10
20km
SCHEMATIC PALAEOGEOGRAPHY
ANGEL FORMATION UNIT A1 and 2

Figure 4.33.

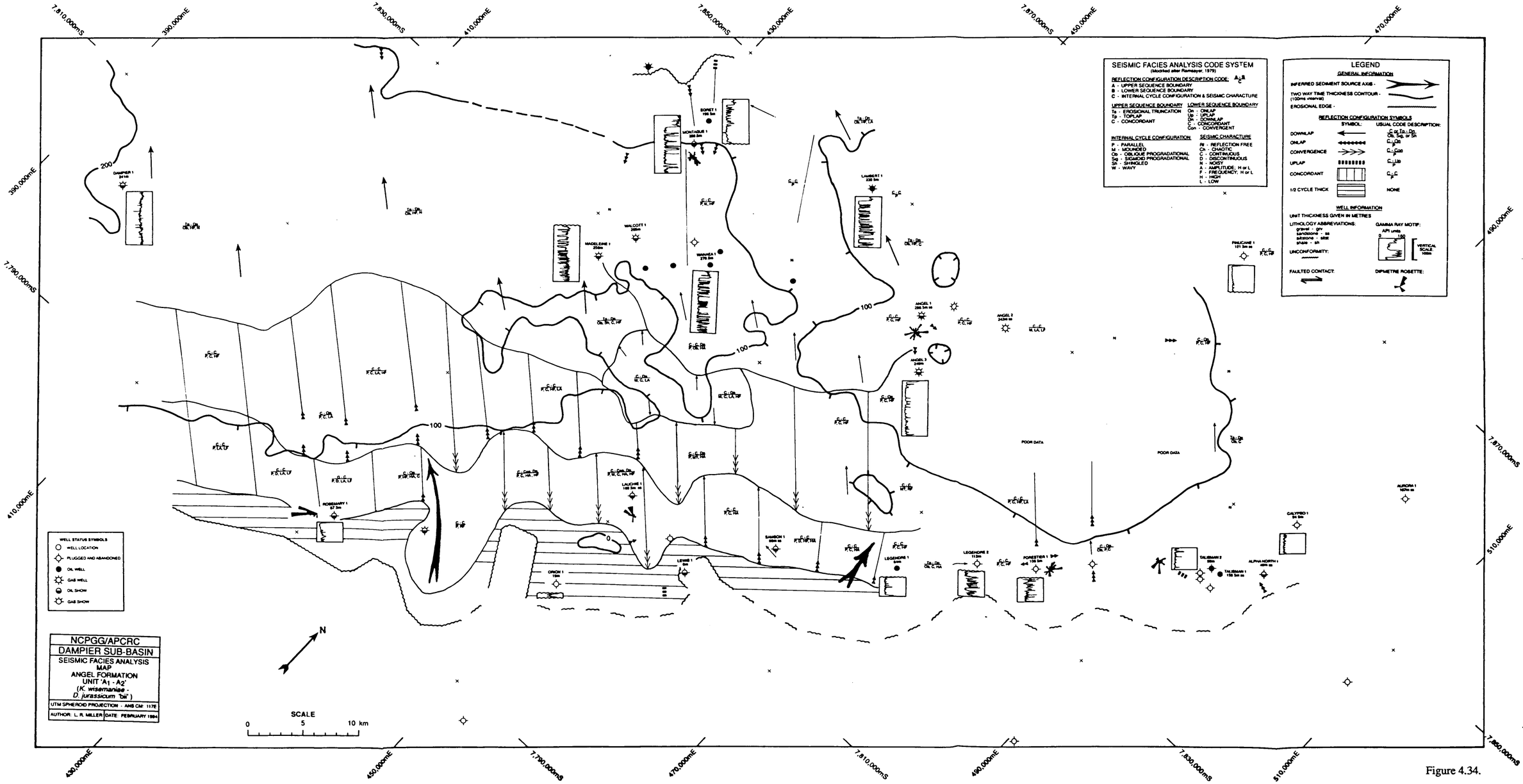

SEISMIC FACIES ANALYSIS CODE SYSTEM
(Modified after Ramsayer, 1979)
REFLECTION CONFIGURATION DESCRIPTION CODE:
A - UPPER SEQUENCE BOUNDARY
B - LOWER SEQUENCE BOUNDARY
C - INTERNAL CYCLE CONFIGURATION & SEISMIC CHARACTURE
UPPER SEQUENCE BOUNDARY
Ta - EROSIONAL TRUNCATION
Tp - TOPLAP
C - CONCORDANT
LOWER SEQUENCE BOUNDARY
On - ONLAP
Up - UPLAP
Dn - DOWNLAP
C - CONCORDANT
Con - CONVERGENT
INTERNAL CYCLE CONFIGURATION
P - PARALLEL
M - MOUNDED
Cb - OBLIQUE PROGRADATIONAL
Sig - SIGMOID PROGRADATIONAL
Sh - SHINGLED
W - WAVY
SEISMIC CHARACTURE
Re - REFLECTION FREE
Ch - CHAOTIC
C - CONTINUOUS
D - DISCONTINUOUS
N - NOISY
A - AMPLITUDE; H or L
F - FREQUENCY; H or L
H - HIGH
L - LOW
LEGEND
GENERAL INFORMATION
INFERRED SEDIMENT SOURCE AXIS -
TWO WAY TIME THICKNESS CONTOUR - (100ms interval)
EROSIONAL EDGE -
REFLECTION CONFIGURATION SYMBOLS
SYMBOL
USUAL CODE DESCRIPTION:
DOWNLAP
ONLAP
CONVERGENCE
UPLAP
CONCORDANT
1/2 CYCLE THICK
C or Ta - Dn On, Sig, or Sh
NONE
WELL INFORMATION
UNIT THICKNESS GIVEN IN METRES
LITHOLOGY ABBREVIATIONS:
gravel - gry
sandstone - ss
siltstone - sltst
shale - sh
UNCONFORMITY:
FAULTED CONTACT:
GAMMA RAY MOTIF:
API Units
VERTICAL SCALE 100m
DIPMETRE ROSETTE:
WELL STATUS SYMBOLS
WELL LOCATION
PLUGGED AND ABANDONED
OIL WELL
GAS WELL
OIL SHOW
GAS SHOW
NCPGG/APCRC
DAMPIER SUB-BASIN
SEISMIC FACIES ANALYSIS MAP
ANGEL FORMATION
UNIT 'A1 - A2'
(K. wisemaniae - D. jurassicum 'bii')
UTM SPHEROID PROJECTION - ANS Clkr 1178
AUTHOR: L. R. MILLER
DATE: FEBRUARY 1984
SCALE
0 5 10 km
N
POOR DATA
POOR DATA
7,810,000mS
390,000mE
7,830,000mS
410,000mE
7,850,000mS
430,000mE
7,870,000mS
450,000mE
470,000mE
490,000mE
510,000mE
7,790,000mS
7,850,000mS

Figure 4.34.

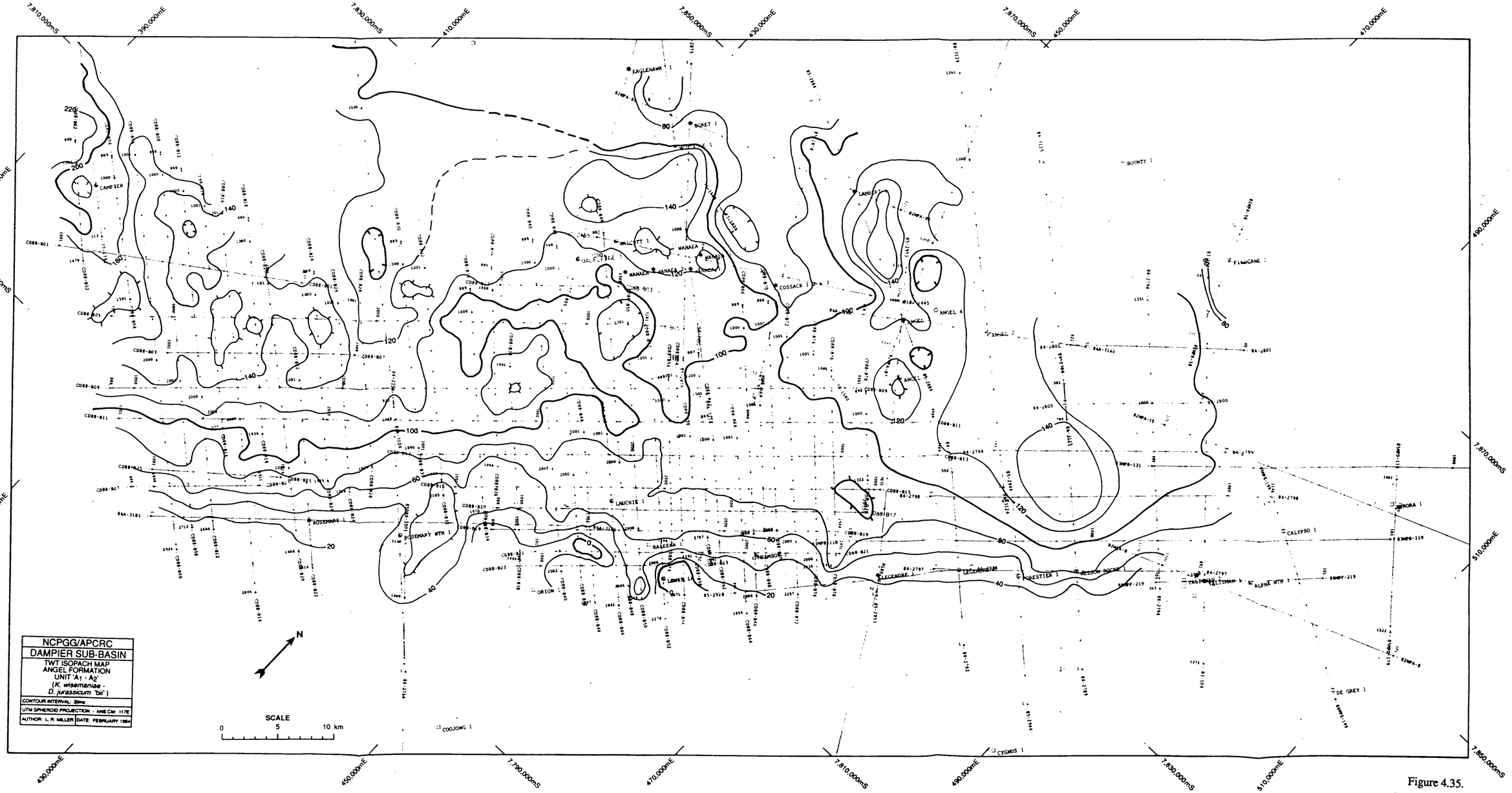

NCPGG/APCRC
DAMPIER SUB-BASIN
TWT ISOPACH MAP
ANGEL FORMATION
UNIT 'A1 - A2'
(K. wisemaniae - D. jurassicum 'bii')
CONTOUR INTERVAL: 20ms
UTM SPHEROID PROJECTION - ANS Cm: 117E
AUTHOR: L. R. MILLER
DATE: FEBRUARY 1994
SCALE
0 5 10 km
N
7,810,000mS
390,000mE
7,830,000mS
410,000mE
7,850,000mS
430,000mE
7,870,000mS
450,000mE
470,000mE
490,000mE
510,000mE
7,790,000mS
CAMPIER
EAGLEHAWK 1
BERET 1
WANAEA
MANAEA
HALLETT 1
COSSACK 1
BOUNTY 1
LANGEY 1
ANGEL
ANGEL 4
FLAMINGO 1
ROSEMARY
ROSEMARY MTH 1
LAURIE 1
BALEENA 1
ORION
LEEMAN 1
THOMSON
LEGENDRE 1
FORESTIER 1
NELSON ROCKS 1
CALYPSO 1
AURORA 1
ALPHA MTH 1
DE GREY 1
COOJONG 1
CYGNUS 1

Figure 4.35.

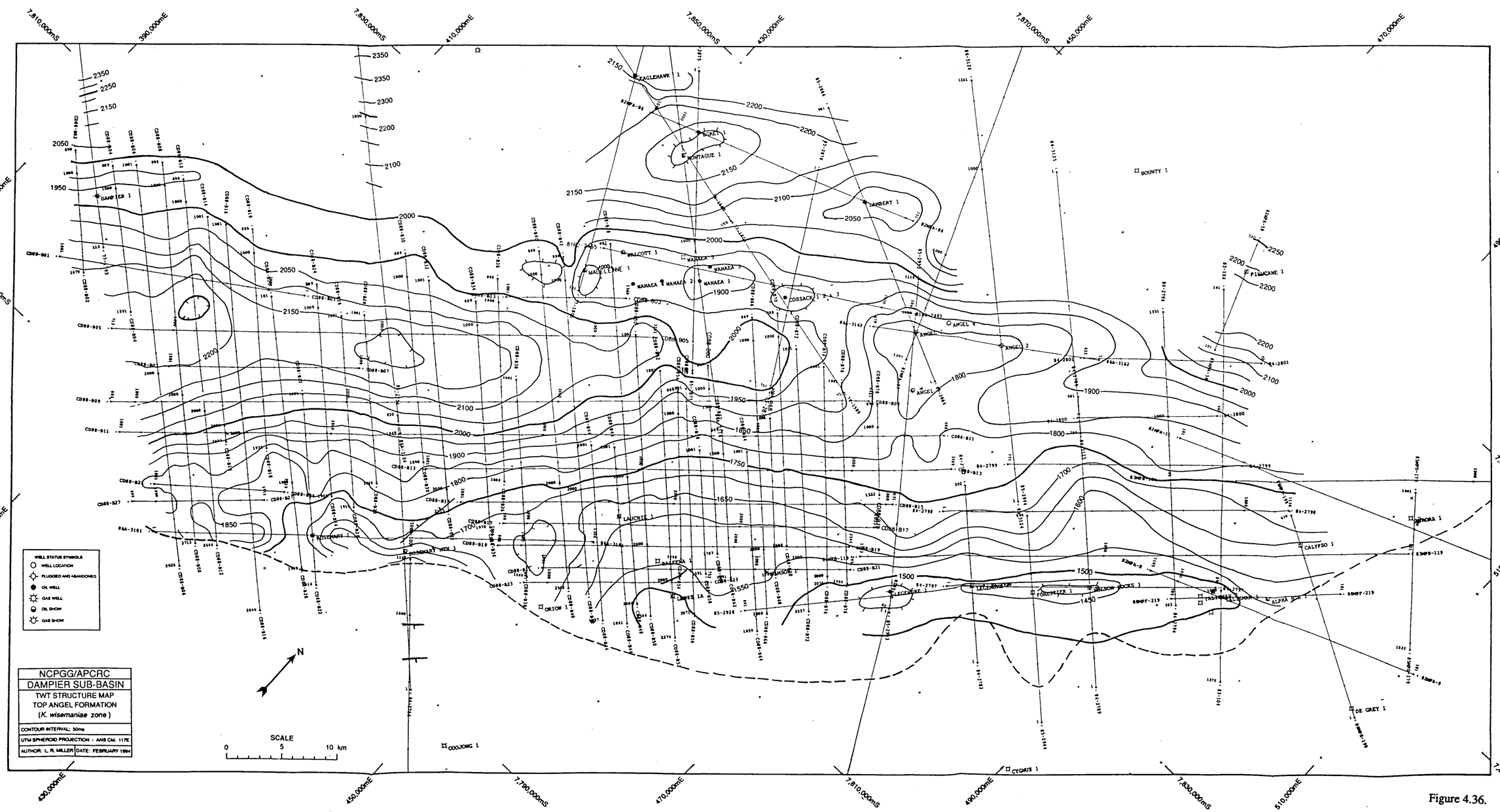

NCPGG/APCRC
DAMPIER SUB-BASIN
TWT STRUCTURE MAP
TOP ANGEL FORMATION
(K. wisemaniae zone)
CONTOUR INTERVAL: 50ms
UTM SPHEROID PROJECTION - ANS CM: 117E
AUTHOR: L. R. MILLER DATE: FEBRUARY 1994
WELL STATUS SYMBOLS
WELL LOCATION
PLUGGED AND ABANDONED
OIL WELL
GAS WELL
OIL SHOW
GAS SHOW
SCALE
0 5 10 km
N
DAMPIER 1
EAGLEHAWK 1
MONTAGUE 1
BOREE 1
LAMBERT 1
BOUNTY 1
WALCOTT 1
MAGELLANE 1
MANAEA 1
MANAEA 2
MANAEA 3
COSSACK 1 2 3
ANGEL 1
ANGEL 2
ANGEL 4
PLEIADE 1
ROSEMARY 1
ROSEMARY WEST 1
LAUCHIE 1
ORION 1
CYGNUS 1
CALYPSO 1
LEGENDRE 1
FORESTIER 1
WILSON ROCKS 1
ALPHA 1
DE GREY 1
CODJONG 1
7,810,000mS
390,000mE
7,830,000mS
410,000mE
7,850,000mS
430,000mE
7,870,000mS
450,000mE
470,000mE
490,000mE
510,000mE
7,790,000mS
7,850,000mS

Figure 4.36.

It is in sand rich systems such as these units that sand piles up and forms some degree of relief, and will not be transported over extensive distances. The extensive sand development here, where some distal sheet sands are observed as far as Madeleine 1, is considered to be a reflection of the amount of sand existing in this system, and not necessarily due to the efficient transport of sand. In addition, the observation that these sheet sands deposited by unconfined turbidity currents rather than distal channel sands associated with confined current flow, coheres with this interpretation.

Most of the existing core database was derived from units A_1 and A_2. Facies B1.1 and B2.1 dominate the sand, and are often interbedded with Facies C1.2, C2.1, and D1.3. Facies B2.1, associated with channelled deposits, appears to be restricted to relatively proximal areas (e.g. Angel 4 core 2, 3, and 4).

In addition to the Angel Field, Depositional Lobe Massive Sand occurs at Finucane 1 and Bounty 1. It is likely that the sand was sourced from the Rankin Platform, as proposed by Hocking (1992). Poor data is available west of the Angel Field . This area is probably dominated by amalgamated Depositional Lobe Massive Sands. A good example of channel incision and subsequent Channel Fill at Legendre 1 is shown in Figure 3.29. This again is considered a major source for the Depositional Lobe Massive Sands that exist over the Angel area, although it may be mixed with possible sediment sourced from the Rankin Platform.

Depositional Lobe Sheet Sands are also relatively extensive and are observed at Lambert 1, Walcott 1, Madeleine 1 and over the Wanaea and Cossack Fields.

Massive sand beds greater than 5m thick and consisting of Facies C1.2 (mottled muddy sands) and interbedded with Facies D1.3 (mottled silt and mud), occur within core 10 and 11 at Dampier 1. These core occur within a section approximately 170m thick that has a serrated, slightly concave egg shaped gamma ray log motif. This section is within unit A_1 and correlates to a relatively thin (<10m) section at Madeleine 1 which is possibly sediment starved (section D - D', Figure 4.17). The sand at Dampier 1 is well sorted, very fine grained, with a silty, argillaceous and calcareous matrix. This section is interpreted to have been deposited by contour currents.

Units A_1 and A_2 are retrogradational with respect to units A_3 and A_4. A_1 and A_2 are more areally extensive, backstepping and onlapping onto the Eliassen - Orion Terrace and Enderby Platform. This is demonstrated by a sand of unit A_2 at Orion 1 (19m thick) which is bounded above and below by unconformities. It is possible that thin isolated erosional remnants of unit A_1 and A_2 exist in down-faulted areas over the Eliassen-Orion Terrace and Enderby Platform. The retrogradational nature of A_1 and A_2 is also observed in the Angel, Wanaea and Madeleine areas by more proximal facies overlying more distal depositional elements of units A_3 and A_4 (e.g. see stratigraphic log correlations D - D', and E - E', Figures 4.17 and 4.18).

Units A_4 to A_1 appear to be related to a similar tectonic event and regime. As previously mentioned, no significant active faults were interpreted over this section. The isopach maps (Figures 4.30 and 4.35) display little relief, indicating that the Lewis Trough depocentre was virtually non-existent during this period. It is

suggested that this section was deposited in a ramp style setting (Hellar and Dickinson, 1985) which resulted from broad regional tilting to the northwest (approximately perpendicular to the stratigraphic strike of the units). Nearshore equivalent sediments underwent repeated gravity flow erosional episodes into more offshore areas. As a result, no nearshore sediments have been interpreted in wells from the area, suggesting they were eroded by this process. Some isolated bodies of nearshore sediments possibly exist in palaeo-low areas such as down-faulted blocks over the Eliassen-Orion Terrace and Enderby Platform.

Forestier Claystone

Seismic examples : Figures 3.22, 3.23 and 3.28.

Stratigraphic log correlations : location map, Figure 4.15; section C - C', Figure 4.16; section D - D', Figure 4.17; section E - E', Figure 4.18; section F - F', Figure 4.19; section G - G', Figure 4.20.

Isochron map : Figure 4.37.

Structure maps : top Angel Formation, Figure 4.36; Valanginian Disconformity, Figure 4.38.

Montage: Enclosure IIId.

Core data : Angel 3 core 1, Facies E1.1; Dampier 1 core 9, Facies E1.1; Legendre 1 core 10, Facies B2.1; Legendre 2 core 1, Facies B1.1; Talisman 2 core 3, 4, 5 and 6, Facies C1.1, C1.2, and F2.2; Talisman 3 core 2, Facies C1.1 and F2.2.

The Forestier Claystone is time equivalent to the Talisman Sand Member which is confined to marginal areas of the study area. Little variation in seismic stratal patterns were noted within this unit and so no seismic facies analysis or schematic palaeogeographic diagram was warranted. The seismic character generally consists of parallel, continuous events of moderate amplitude and frequency. The amplitude and frequency decreases distally. This system is dominated by Hemipelagic Basin Fill (e.g. Facies E1.1 at Angel 3 core 1 and at Dampier 1 core 9). Significant seismic onlap of hemipelagic sediment is noted along the flank of the Legendre Trend (e.g. Figure 3.22).

Upper Slope Apron sections are observed at Samson 1, Lewis 1, Forestier 1, Talisman 2 and Calypso 1 (e.g. see stratigraphic log correlations Figures 4.16, 4.18, and 4.20) suggesting that this type of sedimentation dominated along the margin of the Rosemary-Legendre Fault. Upper Slope Apron deposits containing Facies F2.2 can be observed at Talisman 2 in core 2, 3, 4 and 5 and at Talisman 3 in core 1 and 2. These core contain interpreted slump blocks several metres thick which are bound by synsedimentary fault surfaces. Intraformational breccias are also extensive. A seismic example of Upper Slope Apron at Lewis 1 is shown in figure 3.23.

The Talisman Member Sandstone occurs at Legendre 1 as Channel Fill (core 10, Facies B2.1), at Legendre 2 as Slope Apron Sandy Slides (core 1, Facies B1.1), and at Talisman 2 as Retrograding Slope Apron (core 6, Facies C1.2). It appears that all sand development in this system is restricted to relatively thinner areas (<80ms) and near the basin margin along the Rosemary-Legendre Fault in the northeast. There are no seismic stratal patterns that would indicate sand development elsewhere. This

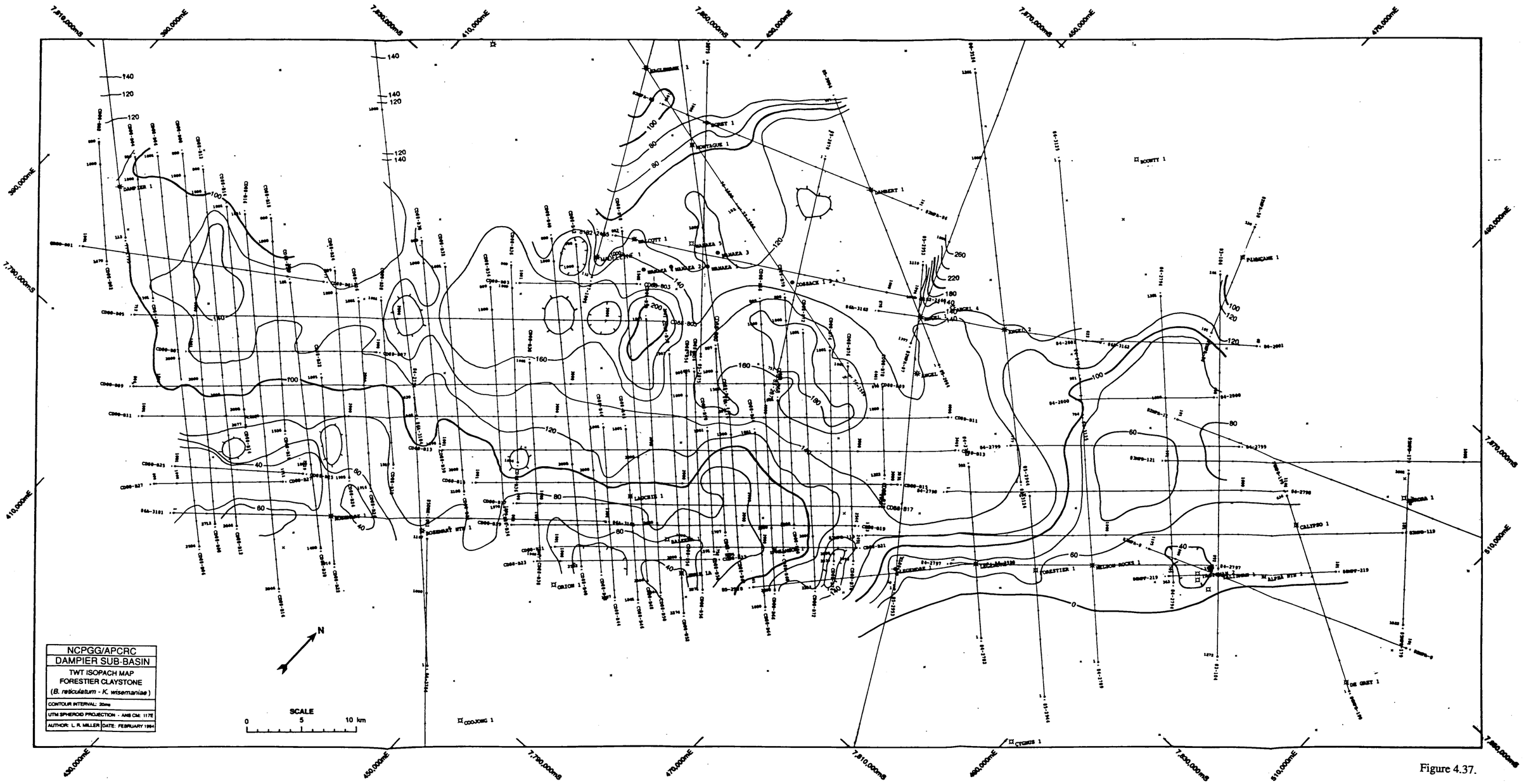

NCPGG/APCRC
DAMPIER SUB-BASIN
TWT ISOPACH MAP
FORESTIER CLAYSTONE
(B. reticulatum - K. wisemaniae)
CONTOUR INTERVAL: 20ms
UTM SPHEROID PROJECTION - ANS Clkt. 1178
AUTHOR: L R. MILLER DATE: FEBRUARY 1994
N
SCALE
0 5 10 km
7,810,000mS
360,000mE
7,850,000mS
410,000mE
7,890,000mS
450,000mE
7,870,000mS
470,000mE
7,790,000mS
430,000mE
7,730,000mS
450,000mE
7,770,000mS
470,000mE
7,810,000mS
490,000mE
7,850,000mS
510,000mE
7,890,000mS
DAMPIER 1
MONTAGUE 1
LAMBERT 1
MURAZA 1
MURAZA 2
MURAZA 3
POSEIDON 1
ANGEL 1
ANGEL 2
ANGEL 3
ANGEL 4
ANGEL 5
ANGEL 6
SCOTT 1
PLUMCAKE 1
LADCHIT 1
ROSEMARY HTT 1
BALLADE 1
ORION 1
COOJONG 1
CYGNUS 1
CALYPSO 1
FORESTIER 1
NELSON ROCKS 1
ALPHA RTE 1
DE GRAT 1

Figure 4.37.

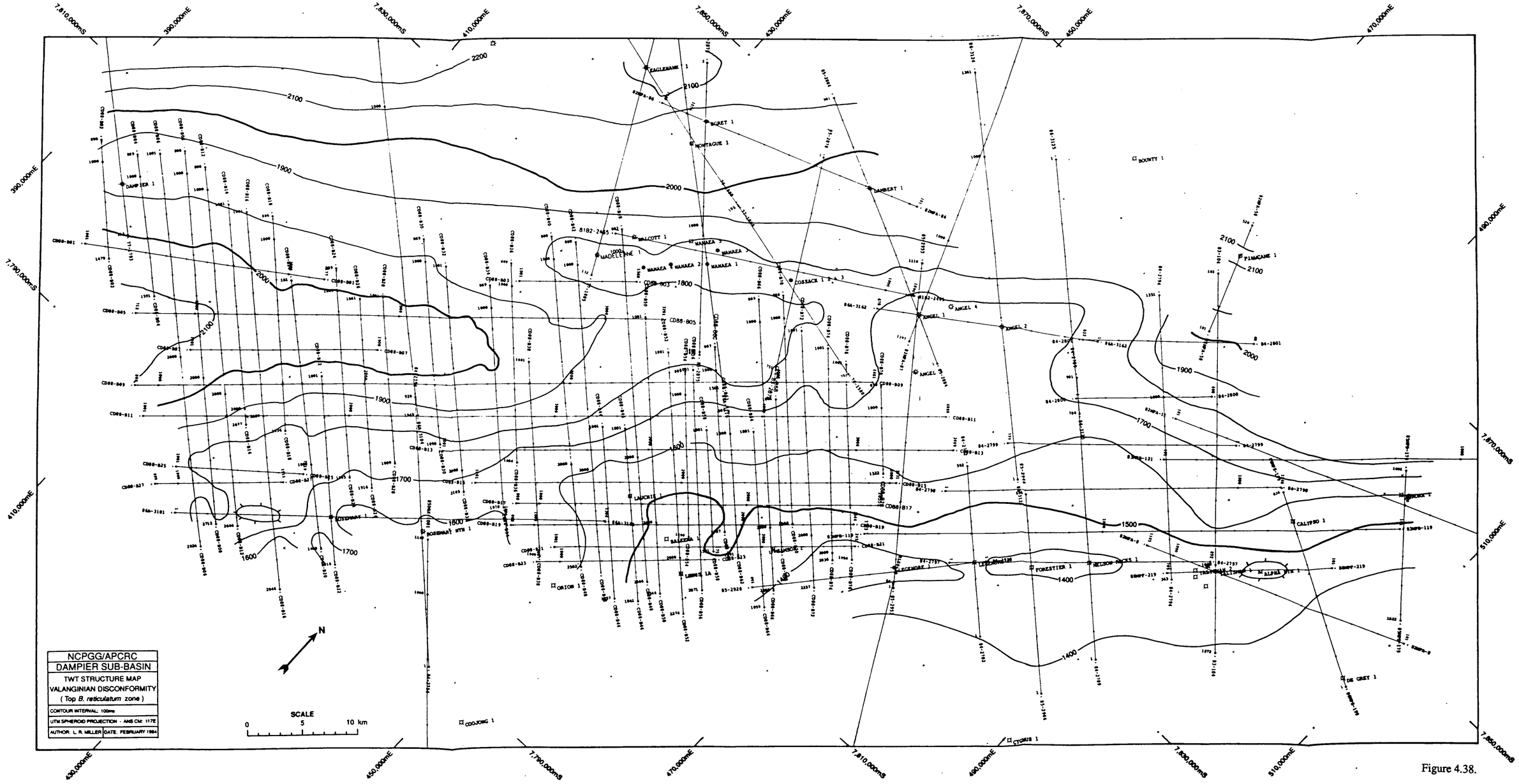

NCPGG/APCRC
DAMPIER SUB-BASIN
TWT STRUCTURE MAP
VALANGINIAN DISCONFORMITY
(Top B. reticulatum zone)
CONTOUR INTERVAL: 100ms
UTM SPHEROID PROJECTION - ANS Cht 117E
AUTHOR: L. R. MILLER
DATE: FEBRUARY 1984
SCALE
0 5 10 km
N
DAMPIER 1
EAGLEHAWK 1
MONTAGUE 1
SCRET 1
LAMBERT 1
BOUNTY 1
MADELEINE 1
WALCOTT 1
MANAEA 1
MANAEA 2
MANAEA 3
COSSACK 1
ANGEL 1
ANGEL 2
ANGEL 4
PINNACLE 1
LAUCHLI 1
ROSEMARY 1
ROSEMARY STR 1
BALCOMA 1
NELSON 1
ORION 1
COOJONG 1
FORESTIER 1
NELSON SOUTH 1
ALPHA STR 1
CALYPSO 1
DE GREY 1
CYGNUS 1
2200
2100
2000
1900
1800
1700
1600
1500
1400

Figure 4.38.

suggests that the sediment source for deposition of the Angel Formation had been cut off before the onset of this relatively mud rich system. Sand remained near the margin, and was not being transported into the basin. It is likely that regionally static tectonic conditions existed over the Dampier Sub-basin during this period. Some definition of the Lewis Trough can be observed on the isochron map (Figure 4.37). This suggests that some accommodation was being provided by differential subsidence within the Lewis Trough.

A local unconformity is interpreted in the region between Orion 1 and Legendre 1 at the time corresponding to near the base of *D. lobospinum* Zone. Missing section can be observed at Legendre 1, Samson 1, Lauchie 1, and Lewis 1 (see Figures 4.16 and 4.18). Erosional truncation can be observed on the seismic examples shown in Figures 3.28 and 3.50. Lewis 1 has the most extensive missing section which is from within *B. reticulatum* Zone to near the top of *D. jurassicum* Zone.

Lithostratigraphic variations outside the area of the unconformity do not reveal the exact timing for when the unconformity occurred. This suggests that sea level fluctuations were probably not responsible. The relative thicknesses of *D. lobospinum* Zone hemipelagic sections varies quite dramatically over the distal portion of the region (e.g. approximately 200m at Walcott 1, <50m at Dampier 1, approximately 150m at Angel 1). This unconformity may have been caused by local uplift and subsequent erosion in the form of slumping. The region of uplift may be defined roughly by the 100ms isochron (Figure 4.37) that encloses wells between Lauchie 1 and Samson 1 and extending to Legendre 1. In addition, an anticlinal trend may be defined by a relatively thin isochron region that trends to the north from Lewis 1. Erosional truncation of horizon 'C' at Lewis 1 and anticlinal dips of horizons 'D', 'E' and 'F' (Figure 4.16) supports this proposed uplift and development of a local low relief anticline. The area is the likely source area for the unusually thick *D. lobospinum* Zone sections in some wells.

Winning Group units M_1 and M_2

Stratigraphic log correlations : location map, Figure 4.39; section A - A', Figure 4.40; section B - B', Figure 4.41.

Isochron map : Aptian disconformity to Valanginian disconformity, Figure 4.42.

Structure maps : Valanginian disconformity, Figure 4.38; Aptian disconformity, Figure 4.43.

Montage: Enclosure IIId.

Core data : Talisman 2 core 3, Facies C1.1, C1.2 and F2.2; Talisman 3 core 1, Facies C1.2.

Units M_1 and M_2 contain the Muderong Shale, Birdrong Sandstone and Mardie Greensand. Limited data was collated for these units, as it is not considered to be the main scope of this study. However, this data enable the basin evolution of a post-rift super-sequence to be interpreted. Limited variations of seismic stratal configuration can be observed within this system. This is characteristic of depositional systems that are transgressive in style. The discussion of these units is somewhat generalised, although it appears that fairly simple processes and associations exist.

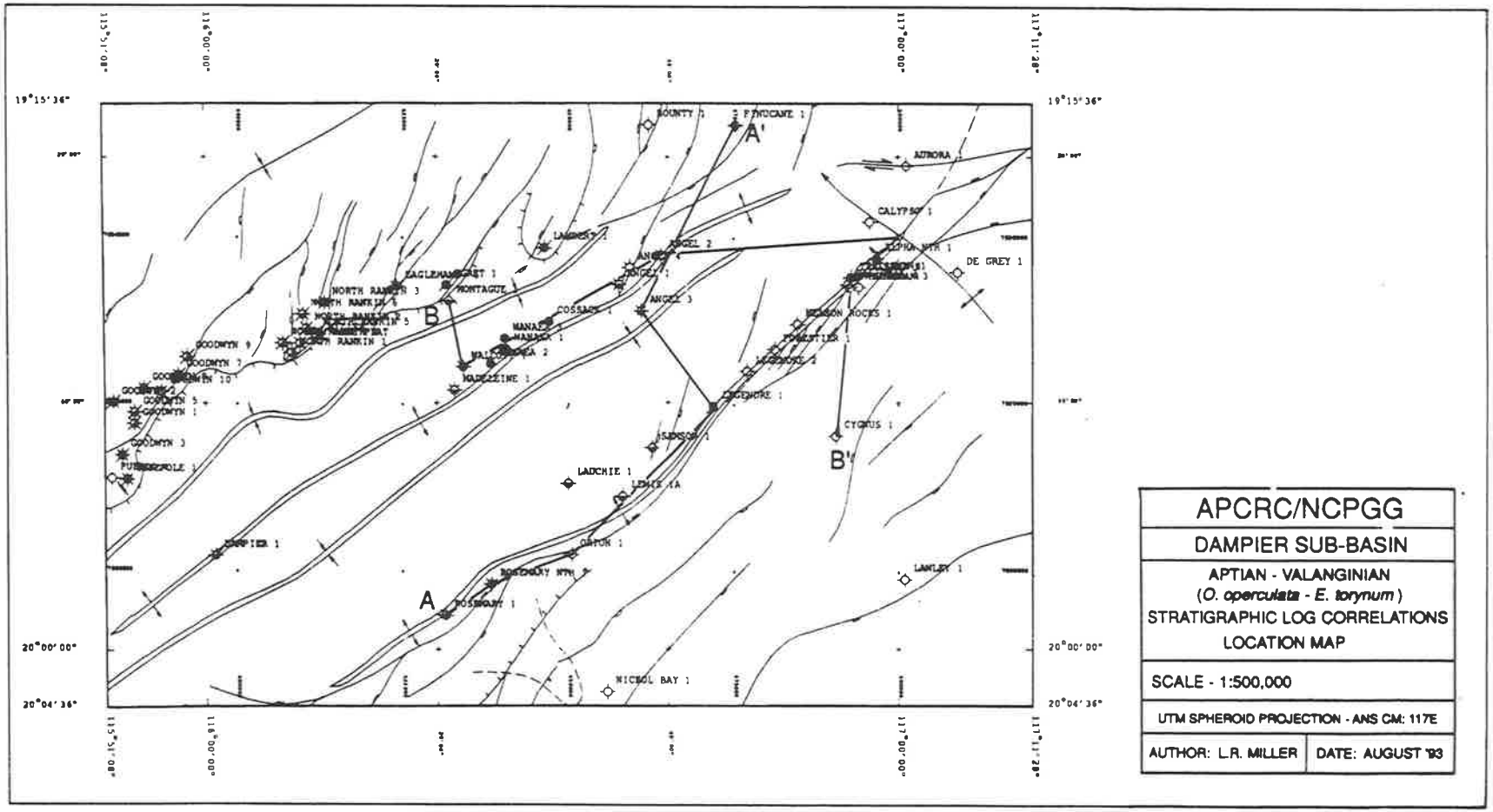

APCRC/NCPGG
DAMPIER SUB-BASIN
APTIAN - VALANGINIAN
(O. operculata - E. torynum)
STRATIGRAPHIC LOG CORRELATIONS
LOCATION MAP
SCALE - 1:500,000
UTM SPHEROID PROJECTION - ANS CM: 117E
AUTHOR: L.R. MILLER
DATE: AUGUST '93
A
A'
B
B'
BOUNTY 1
PINDAN 1
AURORA 1
CALYPSO 1
DE GREY 1
ANGEL 1
ANGEL 2
ANGEL 3
LAGRANGE 1
EAGLEHAWK 1
MONTAGUE
NORTH RANKIN 1
NORTH RANKIN 3
COSSACK 1
MANAS
MANASH 1
MALUS
MADDEEINE 1
GOODWYN 1
GOODWYN 2
GOODWYN 3
GOODWYN 5
GOODWYN 7
GOODWYN 9
GOODWYN 10
PURDOE
DAMPIER 1
LADCHIE 1
LEMAIRIA
DAMPIER 1
ROSEMARY NTH 1
ROSEMARY 1
CYGNUS 1
LAWLEY 1
NICHOL BAY 1

Figure 4.39.

UNIVERSITY OF ADELAIDE
22/3/96
LIBRARY

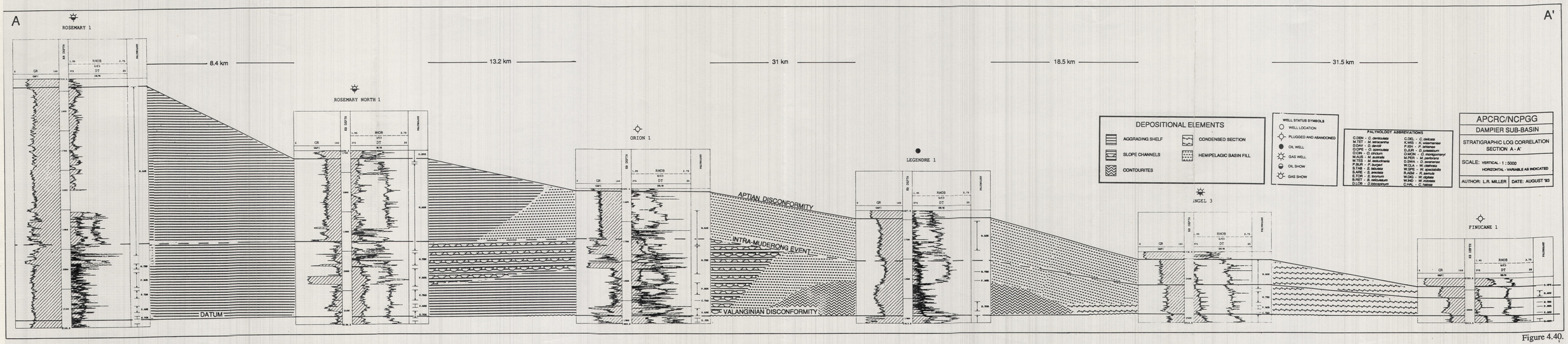


Figure 4.40.

UNIVERSITY OF ADELAIDE LIBRARY 22/3/96

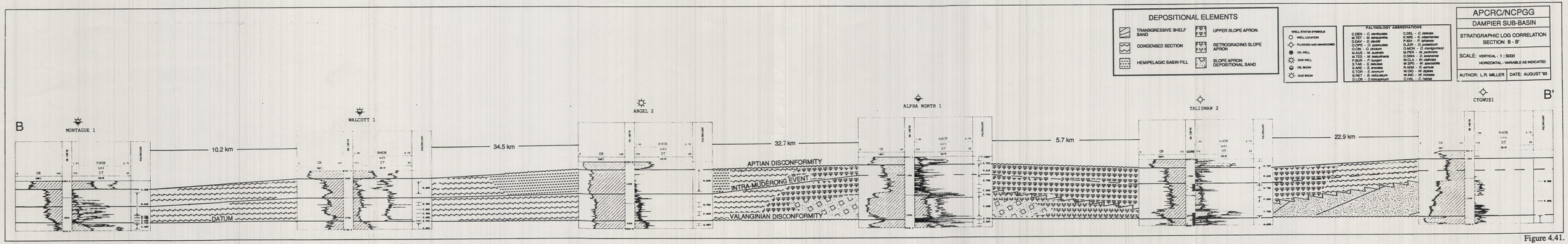


Figure 4.41.

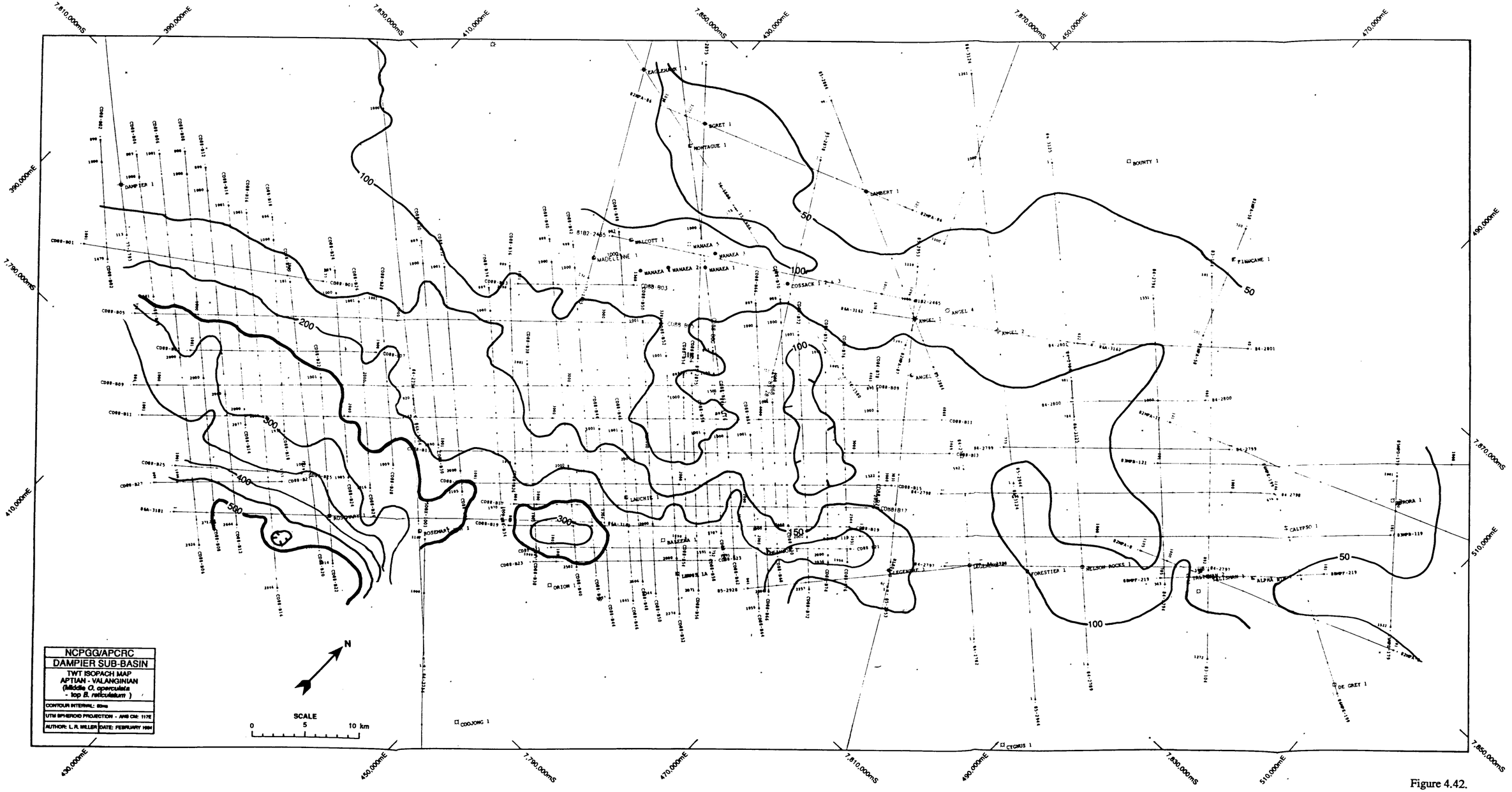

NCPGG/APCRC
DAMPIER SUB-BASIN
TWT ISOPACH MAP
APTIAN - VALANGINIAN
(Middle O. operculata - top B. reticulatum)
CONTOUR INTERVAL: 50ms
UTM SPHEROID PROJECTION - AMG CM: 117E
AUTHOR: L. R. MILLER DATE: FEBRUARY 1998
SCALE
0 5 10 km
N
7,810,000mS
390,000mE
7,830,000mS
410,000mE
7,850,000mS
430,000mE
7,870,000mS
450,000mE
470,000mE
490,000mE
510,000mE
7,790,000mS
7,850,000mS
DAMPIER 1
EAGLEHAWK 1
AGRET 1
MONTAGUE 1
LAMBERT 1
BOUNTY 1
WALCOTT 1
MADELEINE 1
MANAEA 1
MANAEA 2
MANAEA 3
MANAEA 5
COSSACK 1
FINUCANE 1
ANGEL 1
ANGEL 2
ANGEL 4
LAURIE 1
ROSEMARY 1
BALEENA 1
ORION 1
LEGENDRE 1
FORESTER 1
NELSON ROCKS 1
CALYPSO 1
ALPHA 1
DE GREY 1
CYGNUS 1
CDO JONG 1
100
50
200
300
400
500

Figure 4.42.

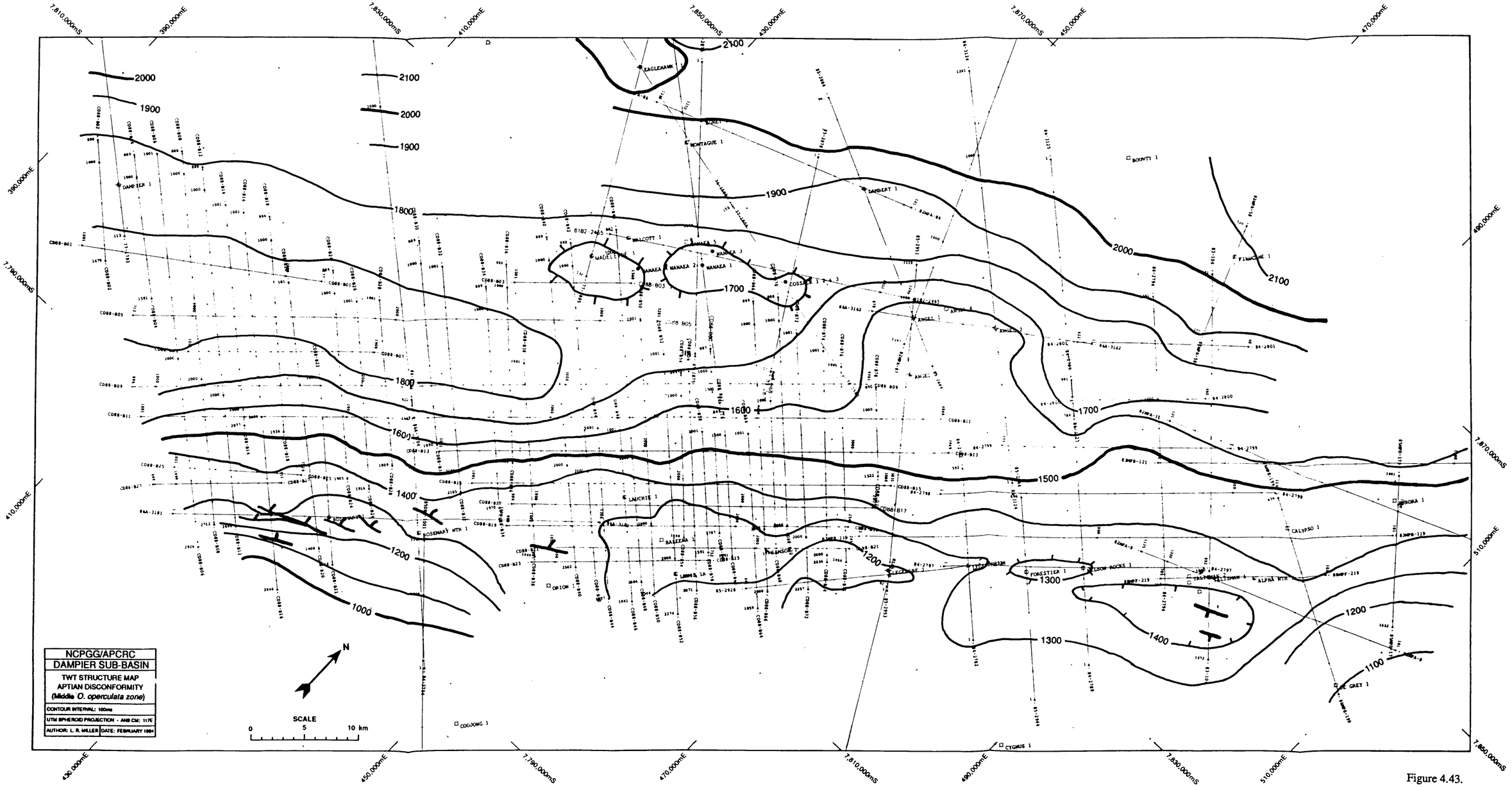

NCPGG/APCRC
DAMPIER SUB-BASIN
TWT STRUCTURE MAP
APTIAN DISCONFORMITY
(Middle O. operculata zone)
CONTOUR INTERVAL: 100ms
UTM SPHEROID PROJECTION - ANS CM: 117E
AUTHOR: L. R. MILLER DATE: FEBRUARY 1994
N
SCALE
0 5 10 km
7,810,000mS
390,000mE
7,830,000mS
410,000mE
7,850,000mS
430,000mE
7,870,000mS
450,000mE
470,000mE
490,000mE
510,000mE
7,790,000mS
7,850,000mS
430,000mE
450,000mE
7,790,000mS
470,000mE
7,810,000mS
490,000mE
7,830,000mS
510,000mE
2100
2000
1900
1800
1700
1600
1500
1400
1300
1200
1100
1000
EAGLEHAWK 1
MONTAGUE 1
DAMPIER 1
WALCOTT 1
MADELEINE 1
MANAEA 1
MANAEA 2
MANAEA 3
MANAEA 5
COSSACK 1
2
3
4
ANGEL 1
ANGEL 2
ANGEL 3
ANGEL 5
BOUNTY 1
FINUCANE 1
ROSEMARY 1
ROSEMARY NTH 1
LAURITE 1
BALEENA 1
LAMBERT 1
LAMBERT A1
LAMBERT A2
LAMBERT A3
ORION 1
COOJONG 1
CYGNUS 1
FORESTIER 1
NELSON ROCKS 1
ALPHA NTH 1
CALYPSO 1
PHORA 1
LE GREY 1

Figure 4.43.

A wedge that progrades north from Rosemary 1 to near Madeleine 1 is revealed on the isochron map (Figure 4.42). This area corresponds to offlapping stratal configurations on seismic. Isochron values vary from between 100ms and 50ms to the north of Madeleine 1, and to less than 50ms in the vicinity of Finucane 1, Bounty 1 and Lambert 1. The region to the north, defined approximately by the 100ms isochron, is considered a condensed section. This wedge to condensed section relationship is clearly observed on the stratigraphic log correlation A - A' (Figure 4.40).

Normal faults with significant displacements are observed on the Aptian horizon in the Rosemary 1 and Rosemary North 1 vicinities (Figure 4.43). There is not adequate seismic coverage over this area to ascertain the lateral extent of these faults. However, related fault movements may have provided relief for erosion and subsequent sedimentation to produce this offlapping wedge. The Winning Group succession is considered transgressive overall. Therefore, it is reasonable to suggest that the progradation observed in this area is tectonically related. The tectonic aspects of this area are discussed in section 4.2.

An interesting observation that can be made from the isochron map is that there is no definition of the Lewis Trough, except possibly by the 100ms isochron to the northeast of Angel 3 and Legendre 1. This suggests that very limited relief of the Lewis Trough depocentre would have existed during Valanginian to Aptian time.

Units M_1 and M_2 are separated by the Intra-Muderong Event (Butcher, 1989; Wiseman, 1979). Although Wiseman considers this a regional surface associated to a relative fall in sea level, it is considered here to represent a flooding surface, at least in this area, if not regionally. This surface occurs within the lower portion of the *M. australis* Zone. Thickness variations shown on the log correlations indicate that it marks the time of onset of fault movements in the Rosemary area.

The stratigraphic log correlations demonstrate the lateral distribution of depositional elements in a succinct manner. Sand beds 5 to 20m thick at Rosemary North 1 and Orion 1 are interpreted as Slope Channels that developed on a depositional slope.

A contourite succession is suggested at Legendre 1 in unit M_2 owing to a serrated egg shaped gamma ray log motif. This interpretation agrees with the stratigraphy that is observed at Legendre 1. Most of the depositional elements observed at Legendre 1 are associated with channels. Schematic palaeogeography diagrams indicate that Legendre 1 is often coincident with a sediment source axis. During unit M_2 time, it is likely that an area of negative relief still existed adjacent to a major sediment source area and was later cut off from sediment supply. This area of negative relief provided a focus through which water bottom currents were directed.

Sections of Mardie Greensand are observed at Alpha North 1 and Talisman 2, and coincide with the S. *tabulata* Zone. These sections are interpreted as Retrograding Slope Apron depositional elements and are interpreted as Facies C1.1 (poorly sorted muddy sands).

The Birdrong Sandstone exists at Cygnus 1 and is interpreted as Transgressive Shelf Sand. This sand unconformably overlies the Legendre Formation of Bathonian Age,

demonstrating the onlapping nature of this transgressive unit onto the Enderby Platform. A transgressing shoreline possibly existed to the southeast of Cygnus 1, approximately parallel with the Lambert Shelf.

Late Cretaceous development

The Campanian to Aptian section contains the Toolonga Calcilutite, Haycock Marl, Gearle Siltstone and Windalia Radiolarite. These formations developed on a broad marine shelf with open marine circulation. The Haycock Marl is the distal equivalent of the Gearle Siltstone and occurs in wells on the Madeleine Trend and to the northwest. The Gearle Siltstone and Haycock Marl were deposited in water depths of about 200m (Kopsen and McGann, 1985). An isopach map (Figure 4.44) and a structure map (Figure 4.45) of the top Toolonga Calcilutite were produced to gain a insight into the influence of post depositional subsidence and tectonics on the underlying post rift Oxfordian to Aptian succession.

The isopach map (Figure 4.44) has a thickening trend within the Lewis Trough. The Lewis Trough, which showed no relief during the Aptian to Valanginian, became active once more due to differential subsidence occurring over the area. This differential subsidence may have been the result of compaction of varying thicknesses of the underlying sedimentary succession occurring over the Legendre Trend, Lewis Trough, Madeleine Trend and Kendrew Trough. Since the Lewis Trough has the thickest underlying sedimentary section, it would have undergone the most amount of compaction, resulting in the Lewis Trough structural morphology to return. However, the possibility that this subsidence is related to mild compressional tectonics is not excluded.

The top Toolonga structure map (Figure 4.45) reveals a relatively planar surface, with the exception of an anticline in the Legendre 2 to Nelson Rocks 1 area. The relatively planar surface has a general dip to the northwest, mainly as a result of post-depositional passive margin subsidence.

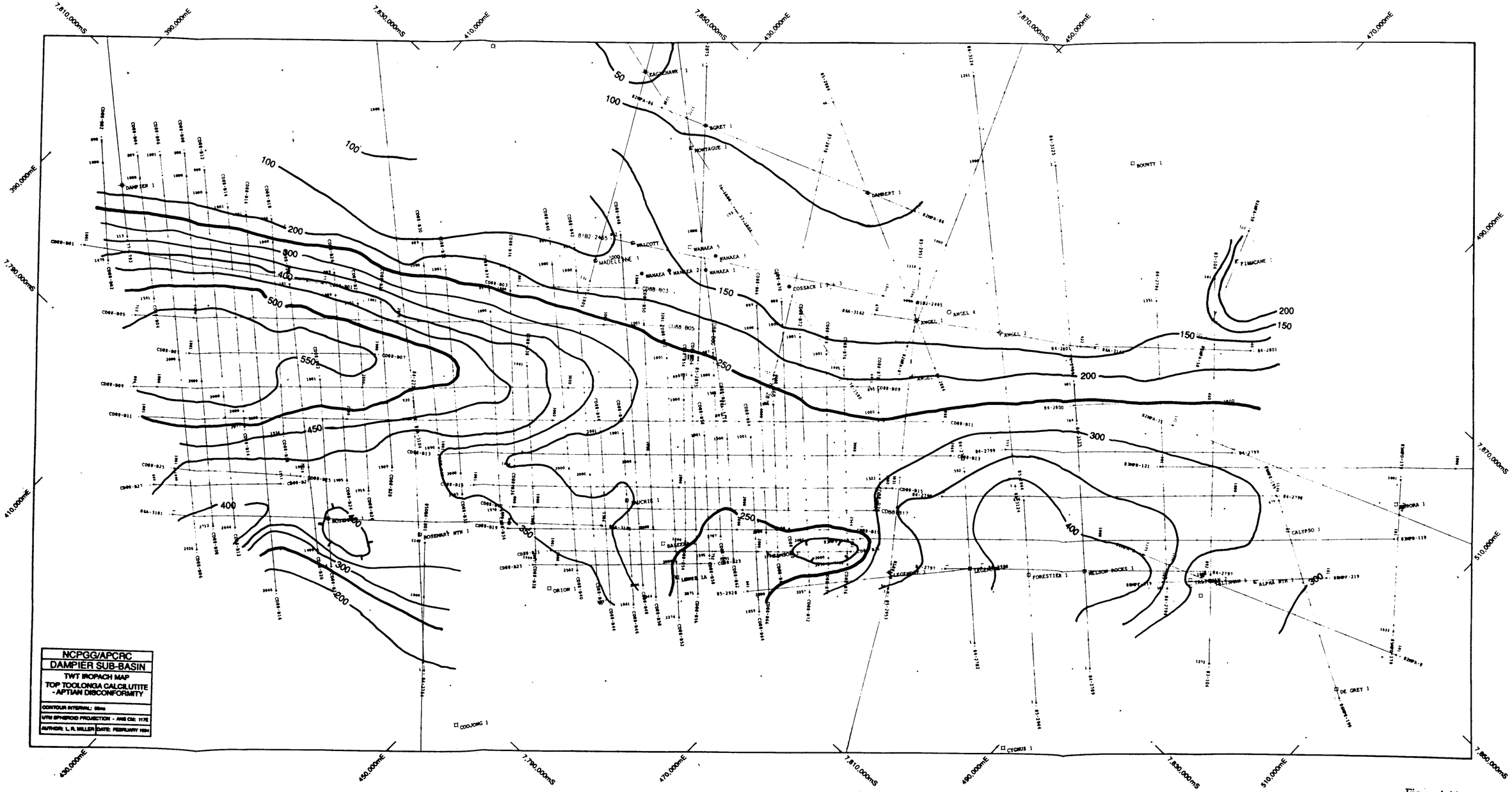

NCPGG/APCRC
DAMPIER SUB-BASIN
TWT ISOPACH MAP
TOP TOOLONGA CALCILUTITE - APTIAN DISCONFORMITY
CONTOUR INTERVAL: 50ms
UTM SPHEROID PROJECTION - ANS CM: 117E
AUTHOR: L.R. MILLER DATE: FEBRUARY 1994
7,810,000mS
390,000mE
7,830,000mS
410,000mE
7,850,000mS
430,000mE
7,870,000mS
450,000mE
470,000mE
490,000mE
510,000mE
7,790,000mS
7,770,000mS
7,750,000mS
430,000mE
450,000mE
470,000mE
7,790,000mS
7,810,000mS
490,000mE
7,830,000mS
510,000mE
7,850,000mS
DAMPIER 1
EAGLEHAWK 1
MONTAGUE 1
BOUNTY 1
LAMBERT 1
WALCOTT
MADELEINE 1
WANAEA 1
WANAEA 2
WANAEA 3
WANAEA 4
COSSACK 1
ANGEL 1
ANGEL 2
ANGEL 4
PIMLICANE 1
ROSEMARY 1
ROSEMARY NTH 1
ORION 1
BALLEZA 1
LEGENDRE 1
FORESTIER 1
NELSON ROCKS 1
CALYPSO 1
ALPHA NTH 1
DE GREY 1
CYGNUS 1
COOJONG 1
50
100
150
200
250
300
350
400
450
500
550
600

Figure 4.44.

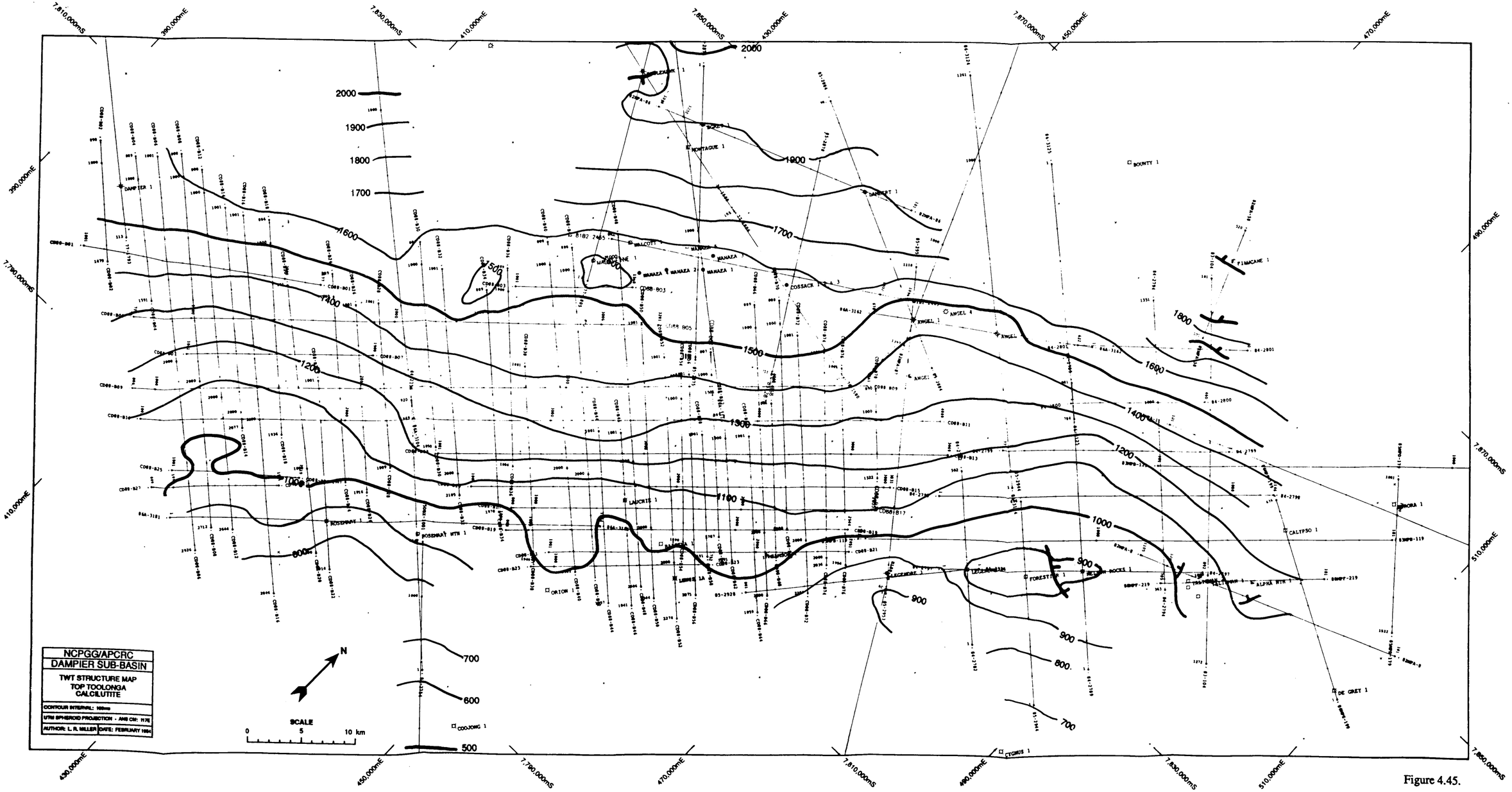

NCPGG/APCRC
DAMPIER SUB-BASIN
TWT STRUCTURE MAP
TOP TOOLONGA CALCILUTITE
CONTOUR INTERVAL: 100ms
UTM SPHEROID PROJECTION - AMG CM: 117E
AUTHOR: L. R. MILLER DATE: FEBRUARY 1984
SCALE
0 5 10 km
N
7,810,000mS
390,000mE
7,830,000mS
410,000mE
7,850,000mS
430,000mE
7,870,000mS
450,000mE
470,000mE
490,000mE
510,000mE
7,790,000mS
DAMPIER 1
ROSEMARY 1
ROSEMARY WTR 1
LAVERIS 1
ORION 1
MAHAEA 1
MAHAEA 2
MAHAEA 3
MARMION 1
WALCOTT 1
MONTAGUE 1
BOREE 1
COSSACK 1
ANGEL 1
ANGEL 2
ANGEL 3
ANGEL 4
BOUNTY 1
DAMPIER 1
FLAMACANE 1
CALYPSO 1
FORESTIER 1
ALPHA WTR 1
DE GREY 1
CYGNUS 1
CODJONG 1
2000
1900
1800
1700
1600
1500
1400
1300
1200
1100
1000
900
800
700
600
500

Figure 4.45.

4.1.3 Conclusions

A west to east structural cross section of the project area is shown in Figure 4.46. This section was constructed with the use of isopach and combination structure/isopach maps. It is located near the stratigraphic dip of the Oxfordian to Valanginian succession. The present day Lewis Trough fold line is indicated over the Eliassen and Angel Formations. There is an eastward progression of this fold line up-section. This fold line has implications for development of stratigraphic traps with respect to sand pinching out up dip on the flank of the Madeleine Trend.

The easterly transport of reservoir quality sand past the Lewis Trough present day fold line, would be required for an up dip pinch out trap to occur along the southwest flank of the Madeleine Trend. It is possible that this occurred over most of the units with the exception of the Eliassen Formation unit E_1, and the Forestier Claystone, both of which are mud dominated systems. These distal sand bodies may be represented by the high amplitude anomalies discussed in this section. The best potential for reservoir development in this area occurs within unit E_2, since palaeo-topographic relief would have resulted in significant onlap onto the Madeleine Trend. This relief is poorly developed or non-existent over the Angel Formation. Another factor needs to be considered with this style of pinch out play for units A_1 to A_4. This is the retrogradational progression of these units which make overlying seals crucial to any sand pinch out.

Structural/stratigraphic pinch out plays remain high risk along the Legendre Trend. Up dip seal is crucial for such plays here. Most structural four way closures and three way closures against the Rosemary Fault have been tested to the top Angel Formation (see top Angel Formation structure map, Figure 4.36). Lauchie 1 and Baleena 1 were structural/stratigraphic plays which appear to have lacked up dip seal towards the Rosemary Fault. With the number of dry wells along the Legendre Trend, it is likely that the Rosemary Fault did not prevent hydrocarbon leakage and petroleum migration to the adjacent Enderby Platform. The existence of the Wandoo Field supports this hypothesis, where oil was thought to have been sourced from the Lewis Trough (Christiansen, 1992). Indeed, Delfos and Boardman (1994) suggested long distance migration for of oil into the Wandoo Field.

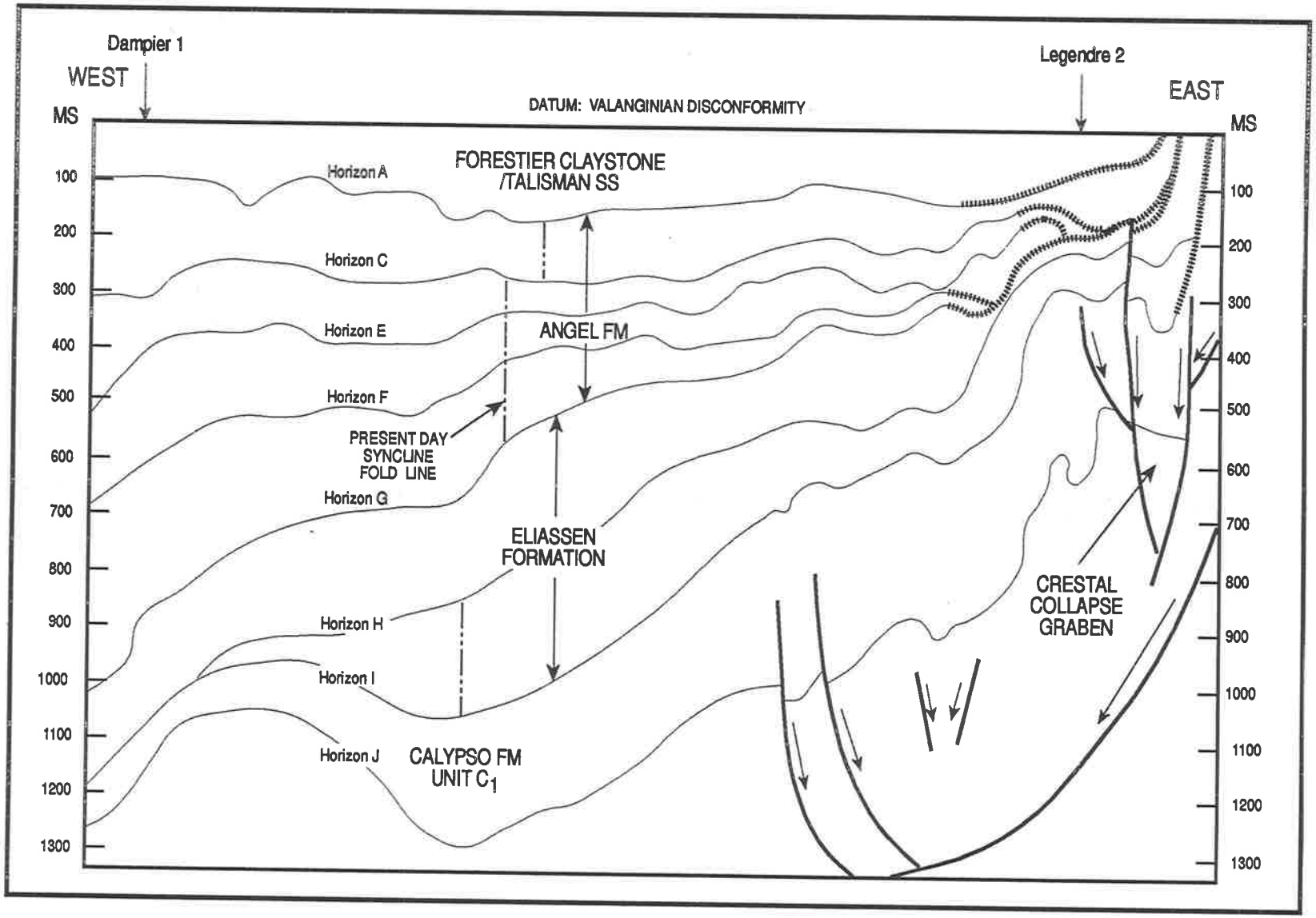


Figure 4.46. Structural cross section of the Valanginian to Callovian section in a diagonal direction across the Lewis Trough. Note the east-ward progression up-section of the present day fold line of the Lewis Trough.

Barber (1994) attributes the failure of the Lauchie 1 and Baleena 1 wells to 'thief zone' downlapping shingled sands of low and high sea level stand offlapping wedges and not to the lack of up dip seal. The palaeo-geography discussed in this section demonstrates that a lack of up dip shales, and the existence of channel style sands up to and against the probable 'non-sealing' Rosemary Fault was responsible for the failure of these wells. The existence of offlapping wedges in this succession is limited to local slope apron gravity deposits. In general, a lack of offlap occurred within any one unit. Processes associated with marine onlap in proximal areas and asymptotic downlap in distal areas (as opposed to discrete downlap where shingled sands may inhibit sealing potential), dominated the whole Oxfordian to Valanginian succession.

The interpretation provided in this section is contrary to the one of Barber (1994) in several other respects. Sand development in wells along the Legendre Trend, such as Legendre 1 are considered by Barber to be associated with low stand (low sea level) systems tract wedges (e.g. Barber 1994, see his Figure 10). His interpretation implies that these sand packages are relatively younger than the genetically related distal 'basin floor sands' in the Angel area. Palynological evidence does not support this interpretation (e.g. see section F - F' Figure 4.19, units A_2, A_4 and A_5 at Legendre 1 to Angel 3 palynological correlations). A more symbiotic relationship may have existed in the development of these relatively distal and proximal sands.

Barber's interpretation implies the development of a broad shelf where eustatic variations may significantly control sequence formation. Low stand wedges were to have prograded from the Enderby Platform into the Lewis Trough. The associated onlapping sections on the Enderby Platform are considered to have been eroded later (at some point in time which is not stated) in response to dramatic uplift. This also implies that the accommodation, provided by continuous movement of the Rosemary Fault, was filled at the time of each successive sequence boundary (sediment accumulation rate equals subsidence rate). The movement of the Rosemary Fault would need to have been relatively continuous from the Valanginian to Callovian with continual filling of relief in order to apply the eustatic systems tract concepts that Barber used on this area. An alternative suggestion is proposed here.

Significant relief was provided by the Rosemary Fault during deposition of the Eliassen Formation. The relief provided by the fault movement was probably both topographic and bathymetric. A significant fault scarp, relatively coincident to a shoreline, would have resulted. While sedimentation nearly kept pace with subsidence during deposition of the Calypso Formation, subsidence related to fault movement outpaced sedimentation during deposition of the Eliassen Formation. This resulted in significant accommodation space becoming available. Sediment filling, accompanied by headward erosion of the fault scarp, would have progressed during deposition of the Angel Formation. Units A_4 to A_1 of the Angel Formation represent retrogradation associated with filling of scarp related relief provided by the Rosemary Fault. A discussion of this relationship follows (Section 4.2), where a headward erosion surface associated with a fault scarp is shown on seismic section in Figures 4.66 and 4.67.

Both the Eliassen Formation and Calypso Formation exist at Orion 1, which is located on the footwall block of the Rosemary Fault. This succession is overall transgressive, with intermediate marine palynological indicators occurring at the base, and offshore marine palynological indicators occurring near the top of the succession. This demonstrates that there was likely concomitant movement on the Eliassen-Orion Fault during movement on the Rosemary Fault. It is suggested that movement ceased at some stage on the Eliassen-Orion Fault while movement continued on the Rosemary Fault. It is likely that the section at Orion 1 either onlaps a fault 'ramp' that is associated with juxtaposition of the Rosemary and Eliassen-Orion Faults; or the section uplaps onto the Eliassen Fault; or both. Seismic data is not available to interpret the correct situation. Sediment subsequently uplapped the Rosemary Fault in the area adjacent to the Orion/Eliassen Terrace during deposition of the Angel Formation. This is supported by the presence of gravity induced slope apron deposits in the Angel Formation which fringe the Rosemary Fault.

In a scarp related margin the nearshore area would be steep and narrow. Prograding wedges most likely did not develop in such a narrow margin because either the gradient would have been too extreme for deposition to occur, or any minor wedge that did develop would have been subsequently eroded due to sediment cannibalisation and continued mass wasting processes. Eustatic rises of sea level would have been accompanied by headward erosion and mass wasting of scarp areas. However, in this style of setting, sediment bypass into the basin would be relatively continuous irrespective of relative sea level (see Figure 4.47). For this reason, an observed eustatic response in the sedimentary succession is not expected. The relationship of eustacy and relative sea level to the stratigraphy is discussed in detail in Section 4.3.

The interpretation of the development of a significant fault scarp is supported by Veenstra (1985). His seismic interpretation indicates that the margin of the Dampier Sub-basin, adjacent to the Rankin Platform, must have had some 2400m of relief in the form of an escarpment. This escarpment formed previous to the break-up and sea floor spreading of the Argo Abyssal Plain. Veenstra (1985) also states that the Dampier Sub-basin must have been more than 2000m deep immediately following this fault movement. It is therefore reasonable to presume from this interpretation that a similar history of fault scarp development on the opposite margin (ie. Rosemary Fault) of the Dampier Sub-basin is quite plausible. This 'fault scarp' hypothesis is considered further in the following section (Section 4.2).

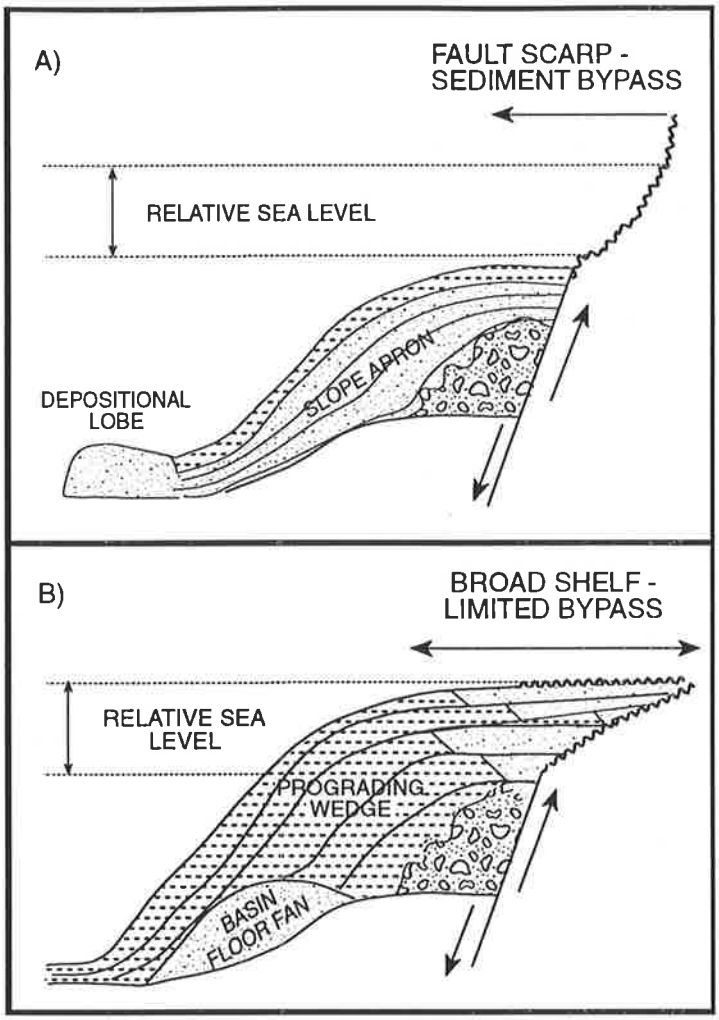


Figure 4.47. Comparison of the effect of relative sea level change on A) a narrow fault scarp where sediment has not filled all topographic relief of a graben; and B) a broad shelf area that has developed after most of the topographic relief due to the graben has been filled in with sediment. In A) initial fault movement was significant and sediment is progressively filling the graben. In B) fault movement can be relatively continuous and the resulting accommodation is continuously being filled by sediment. Eustatic sea level influences the stratigraphy of B) to a greater degree than A). See text for further discussion.

4.2 TECTONIC DEVELOPMENT AND STRUCTURE WITH RESPECT TO SEDIMENTATION

4.2.1 Introduction

This section discusses two aspects that deal with structure and tectonic development. The first aspect is a review of the recent advances made and the new ideas that exist in the literature on structural development, and the degree of support the work in this project owes to them. The second aspect is a direct summary of the structural development of the Dampier Sub-basin as it is observed from the evidence obtained from the database of this project. These two aspects are indeed closely related, and accordingly, are discussed concurrently throughout the section.

A generalised tectonic elements map of the Dampier Sub-basin is shown in Figure 4.48. Although a detailed study of the structure and tectonic development of the Dampier Sub-basin is not within the scope of this thesis, there are some interesting inferences and conclusions that can be made from the results of this work. The database for the study was compiled with the primary focus on stratigraphy and sedimentology. Consequently, there is only limited faulting interpreted, as the majority of the data covers the Lewis Trough depocentre. The Legendre Fault, for example, was difficult to correlate because it only occurs near the ends of long seismic lines. Future research should include the mapping of an extensive seismic database of the Enderby Platform, Rankin Trend and Kendrew Trough. This mapping would provide additional detail for interpreting the structure and tectonic development of the area.

Tectonic History

Earlier conceived ideas of the evolution of the Barrow-Dampier rift (e.g. Kopsen and McGann, 1985; Veenstra, 1985; Boote and Kirk, 1989) were that the present day rift configuration was attributed to rifting associated with the breakup and subsequent sea floor spreading between a micro-continent and northern Gondwana in the Callovian. Woodside (1988) also suggested that the Kendrew Trough formed due to a deep seated wrench zone. The rift was then reactivated due to extension that was related to the breakup of Greater India from east Gondwana in the Valanginian (Fullerton et al., 1989; Veevers et al., 1991; Exon and von Rad, 1994). The initial event, which was considered to have the most influence on the Dampier rift basin, resulted in a regional unconformity at the time of continental breakup. This unconformity has been referred to by Woodside (1988) as the "Main" or "Breakup" unconformity (this label has been confusingly placed at various stratigraphic levels in the literature). Although the two rifting and sea floor spreading events had a significant effect on the structure and stratigraphy of the Barrow-Dampier region, recent ideas consider that the present rift configuration is a result of rifting as early as the Permian (e.g. Hill, 1994). The common theme in the most recent literature is structural inheritance of older basin morphologies and reactivation of older fault patterns (e.g. Ethridge and O'Brien, 1994; Stagg and Colwell, 1994; Hill, 1994). In this section, I will also demonstrate the importance that this factor had on the Dampier Sub-basin.

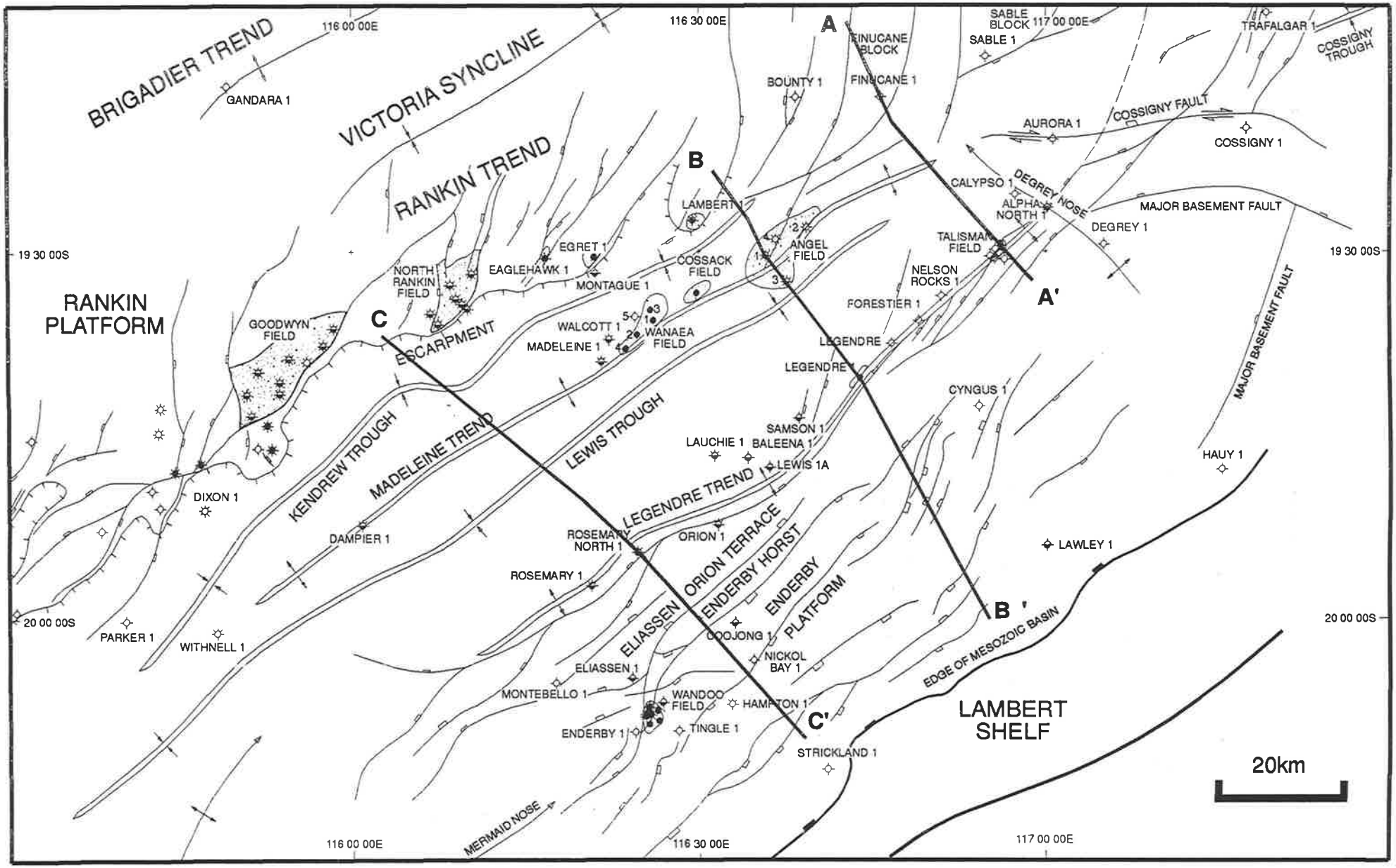


Figure 4.48. Tectonic elements map of the Dampier Sub-basin (modified after Woodside, 1988; Delfos and Boardman, 1994). Note the locations of regional seismic line composites of structural/stratigraphic interpretations that are labelled by cross section letters and which are discussed in this section.

New ideas on structural evolution are presently being formulated by AGSO, subsequent to the acquisition of regional deep-seismic data over the main basin elements of the North West Shelf. The initial results of the project are summarised with respect to the Northern Carnarvon Basin by Stagg and Colwell (1994). Hill (1994) demonstrated the role that pre-existing fault patterns had on successive rift episodes in the Dampier Sub-basin by using the East Africa rift system as an analogue. The tectonic history that he described helps to explain the structure and stratigraphy observed in this study.

The structural and tectonic development of the Dampier Sub-basin is illustrated in Figure 4.49. The North West Shelf is considered by Veevers (1988) to have been initiated in the Cambrian in response to oceanic spreading of the Palaeo-Tethys to the north-northwest. The resulting succession is termed Pre-Westralian Superbasin sediments by Stagg and Colwell (1994). They also defined five subsequent megasequences which are related to the following major tectonic events:

- "Carboniferous - initiation of the Westralian Superbasin, according to Yeates et al. (1987) (pre-Westralian/sag phase-1);
- Late Permian - regional structuring event (sag phase-1 / sag phase-2);
- Late Triassic - major episode of structuring and erosion with both crustal shortening and extension (sag phase-2 / sag phase-3);
- Callovian - initiation of sea-floor spreading in the Argo Abyssal Plain (sag phase-3 / intra-breakup);
- Valanginian - initiation of sea-floor spreading in the Gascoyne and Cuvier Abyssal plains (intra-breakup / post-rift);" (Stagg and Colwell, 1994).

Hill (1994) has described these tectonic events with respect to the structure in the Dampier Sub-basin. This is summarised below (see Figure 4.49):

Permo-Carboniferous

- Northwest-southeast extension and creation of the Westralian Superbasin;
- breakaway of the Sibumasu Block from the north west margin of the Exmouth Plateau;
- subsequent formation of a new ocean, the Neo-Tethys, in the earliest Triassic;
- the Lewis Trough is considered to have been formed by this rifting event;
- a 'Craton margin' rift valley that formed was modified by the principal stress guides of the pre-existing mobile belt fabric;
- the resulting continental break up resulted in a passive margin and regional subsidence and thermal relaxation in the failed Dampier rift valley;
- deposition of the post-rift Locker Shale and Mungaroo Formation.

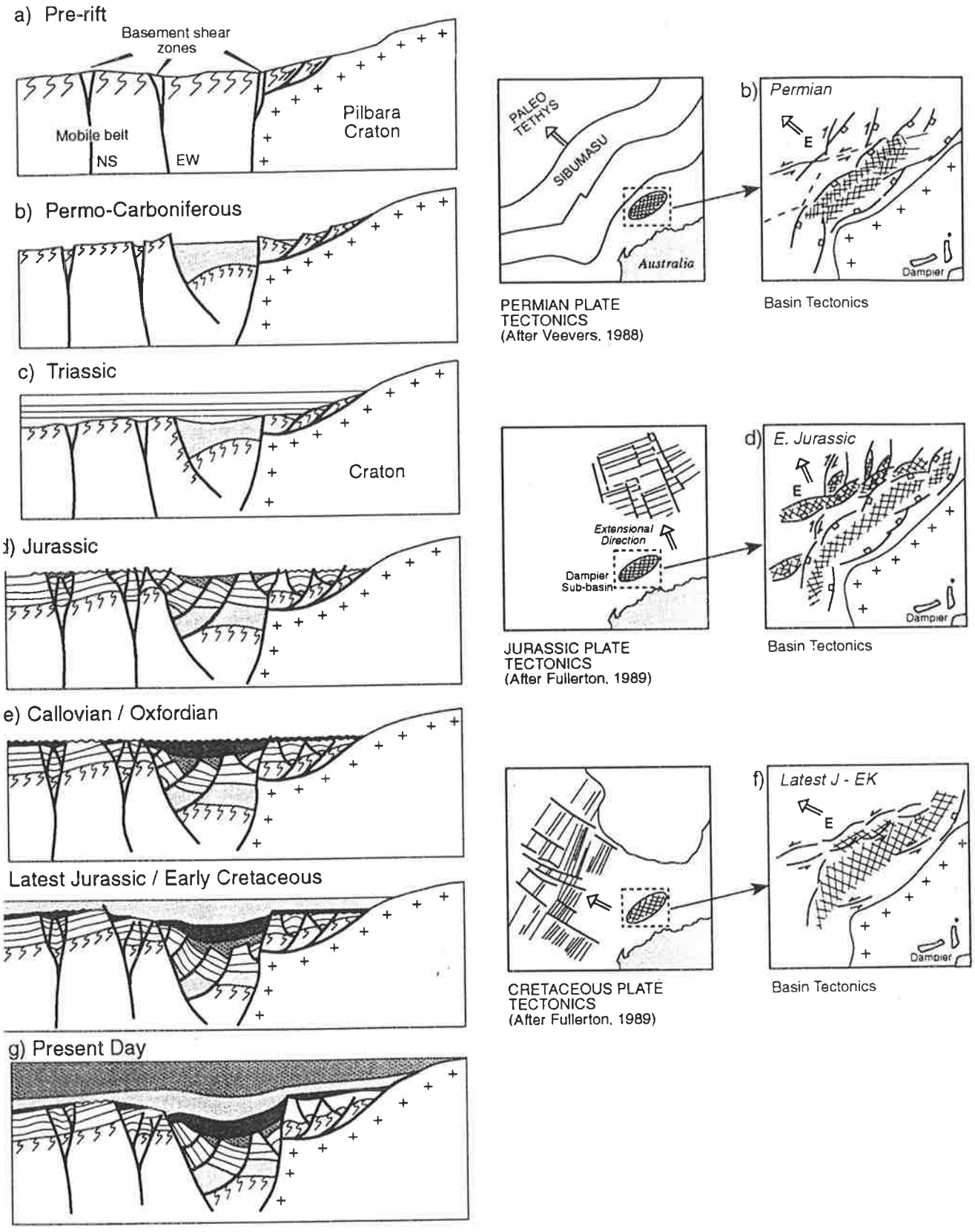


Figure 4.49. Structural development of the Dampier Sub-basin: a) pre-existing mobile belt fabric; b) Permo-Carboniferous extension; c) Triassic post-rift cover; d) Early to Middle Jurassic extension; e) post Callovian break up rebound, erosion and subsidence; f) Late Jurassic to Early Cretaceous minor strike slip and inversion; and, g) post Valanginian passive margin subsidence (after Hill, 1994).

Jurassic

- a new rifting phase in the early Jurassic (Sinemurian - Pleinsbachian ?) lead to continental breakup and sea floor spreading in the Argo Abyssal Plain in the middle Jurassic;
- an extensional vector to the north-northwest induced local oblique shear reactivation of the Pinjarra orogen fabric due to extension sub-parallel to the pre-existing faults;
- the Kendrew Trough formed due to extension and was followed by deposition of the thick Legendre Formation and Athol Formation here and within the rapidly collapsing Lewis Trough;
- a period of isostatic rebound followed and resulted in erosion of the elevated parts of the fault blocks in the sub-basin;
- flexural collapse of the failed Dampier rift and regional extension until the formation of new oceanic crust detached the axis of spreading from the continental crust.

Late Jurassic / Early Cretaceous

- west-northwest to east-southeast extension leads to breakup in the Gascoyne and Cuvier Abyssal plains during the Valanginian (Fullerton et al., 1992);
- strike slip reactivation, induced on the Paterson orogen fabric resulted in minor uplift and erosion of the south-facing flanks of the Rankin Platform blocks and accumulation of Late Jurassic and Early Cretaceous sediment on the down-thrown side of the fault system;
- minor inversion is believed to have occurred near the faults surrounding the Lewis Trough;
- the dominant extensional stress was taken up in basins to the west of the Dampier Sub-basin;
- sea floor spreading in the Cuvier and Gascoyne Abyssal plains resulted in passive margin subsidence of the North West Shelf from the Late Cretaceous to the present day. These sediments consist of thick, open marine carbonates and fine grained clastics; (summarised from Hill, 1994).

Ethridge and O'Brien (1994) suggested that the North West Shelf has undergone a history of a series of minor basin inversion events that are both compressional and extensional in nature. They describe compression for the Latest Triassic to Early Jurassic; extensional deformation in the Middle Jurassic; Late Jurassic to Early Cretaceous compressional inversion; Early Cretaceous extension; and Tertiary to Recent wrench-related deformation that is associated with the convergent margin to the north of Australia. It is possible that these minor inversion events may be localised in nature, and caused by reactivation of the inherited fault systems. Indeed, with the variation of interpretations for the structural history on the North West Shelf, a conclusive history is yet to be presented.

A gravity model across the Dampier Sub-basin (Figure 4.50) demonstrates that the junction between the thick Pilbara Craton and thinner mobile belt crust occurs near the axis of the Dampier Sub-basin where crustal thinning has occurred (Hill, 1994). This thinning is how the Lister (1991) delamination and sub-crustal pure shear model (Figure 4.51) applies to the structural morphology of the Northern Carnarvon Basin. According to Stagg and Colwell (1994), "the Northern Carnarvon Basin formed when most of the lower crust was removed probably by pure shear commencing in the Palaeozoic. Approximately 2/3 of original crust was removed, producing extension of up to 300%."

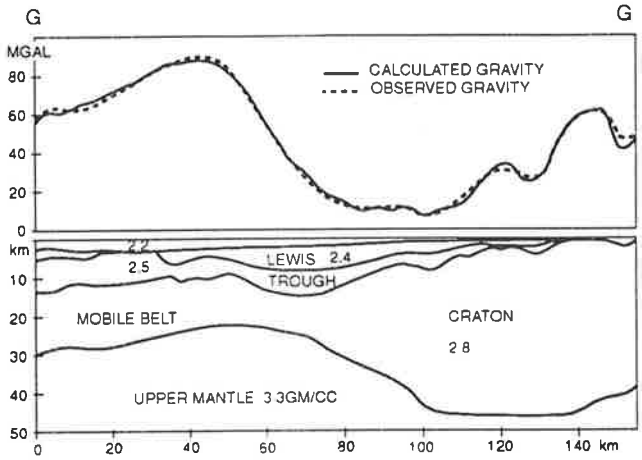


Figure 4.50. Gravity model across the Dampier Sub-basin (after Hill, 1994).

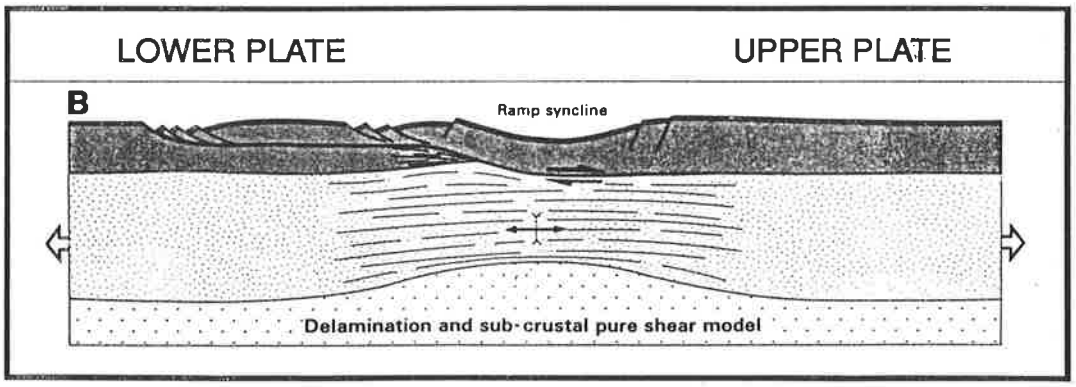


Figure 4.51. Detachment model for extension (after Lister et al., 1991).

Ideas applied by O'Brien (1993) to the Timor Sea region may be relevant to the Northern Carnarvon Basin in the sense of a failed rift rather than a rifted margin. He suggested that the neighbouring Browse Basin, Vulcan Sub-basin and Sahul Platform, and the Calder Graben are compartmentalised into alternating lower-plate and upper plate rifted margins (i.e.. Browse Basin - lower plate rifted margin; Vulcan Sub-basin and Sahul Platform - upper plate rifted margin; Calder Graben - lower plate rifted margin). This idea was suggested by Stagg (pers. comm. 1993) for the Beagle, Dampier and Barrow sub-basins. The Beagle and Dampier sub-basins may be considered to be upper plate portions of a failed rift, while the Barrow Sub-basin may be a lower plate portion of a failed rift. The compartmentalisation of the Barrow and Dampier sub-basins is considered by Ethridge and O'Brien (1994) to

coincide with a north-striking Precambrian fault zone, possibly part of the basement mobile belt that is discussed by Hill (1994). A good example of the lower plate failed rift portion of the Lister shear model is the large roll-over listric detachment fault geometry of the Mermaid Fault as described by Mack (1993). In the Dampier area, the Lewis Trough would be considered the ramp syncline portion of an upper plate (see Figure 4.51).

Sea Floor Spreading

A map of sea floor spreading magnetic lineaments of the Argo, Gascoyne, and Cuvier Abyssal Plains with respect to the Northern Carnarvon Basin is shown in Figure 4.52. The initiation of sea floor spreading in the Argo Abyssal Plain commenced at lineament M26N. This is the polar magnetic lineament that marks the breakup and subsequent formation of the Argo Abyssal Plain. M26N is dated as 155Ma by K/Ar dating of oceanic crust at site 765 of the Deep Ocean Drilling Project (Exon and von Rad, 1994). The most recent geological time scale (Harland, 1989), places 155Ma and M26N near the top of the Oxfordian Stage. This relative age correlation conflicts with previous contentions that breakup of the Argo Abyssal Plain occurred in the Callovian (e.g. Fullerton et al., 1989).

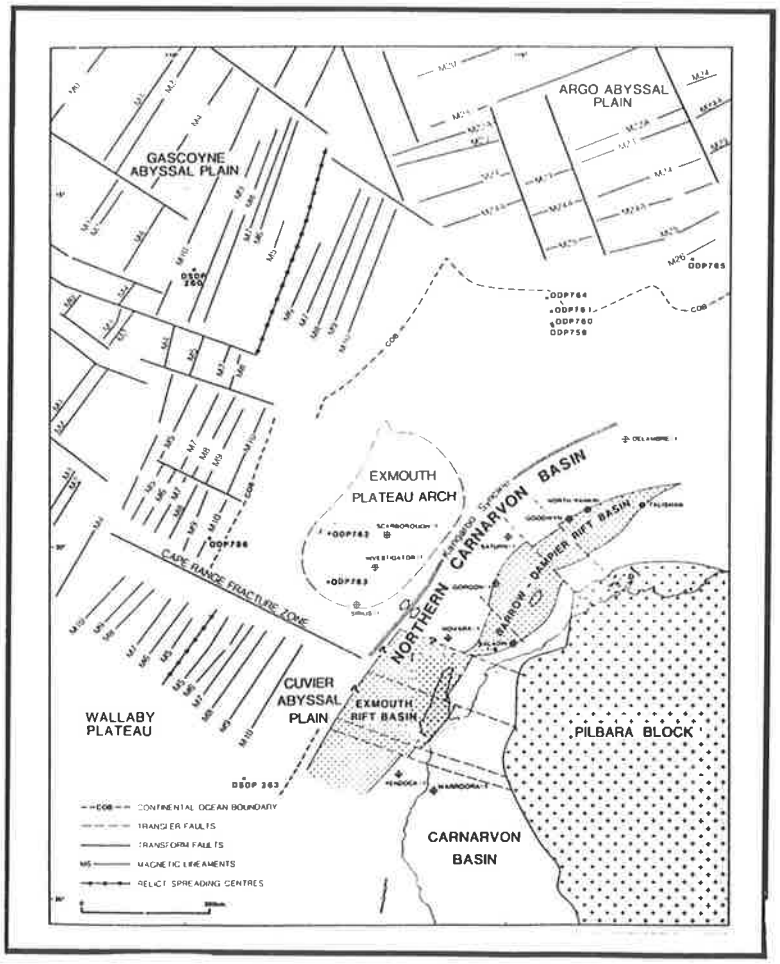


Figure 4.52. Magnetic anomalies and lineaments of the abyssal plains (based on Fullerton, 1989) with respect to the Northern Carnarvon Basin (after Malcolm et al., 1991). Note the location of ODP 765.

The breakup of the Gascoyne, Cuvier and Perth (to the south of Figure 4.52) Abyssal Plains was initiated by lineament M10N. This lineament is dated as 135Ma on the Harland Time Scale (1989) and coincides with the top of the Valanginian Stage (see Figure 4.53). There was a shift in sea floor spreading centres between M5N and M4N. Sea floor spreading on the North West Shelf ceased at M0R (Barremian - Aptian Stage boundary).

4.2.2 Discussion

Tectonic Systems Tracts

In this study it was considered beneficial to describe the Mesozoic stratigraphy and structure of the Dampier Sub-basin using the concept of **tectonic systems tracts** (Prosser, 1993). This concept was adapted from earlier eustatic systems tracts theory in the application of systems tracts to active fault-bounded basins. The term 'systems tract' is defined by Brown and Fisher (1977) as 'a linkage of contemporaneous depositional systems'. Prosser (1993) introduced new terminology in the sense of tectonic systems tracts for areas where depositional systems are considered to be tectonic in origin. According to Prosser (1993), "where sequences are recognised in settings that were obviously active during deposition (or immediately prior to deposition), such as fault-bounded asymmetric grabens, it may be that the reflector dispositions and internal facies characteristics are related to a dominantly tectonic control". Indeed, she noted that studies such as the one by Boote and Kirk (1989) discussing depositional wedge cycles on the North West Shelf could have been 'aided by the use of tectonic systems tracts in interpretation' and would have 'clarified the presentation of basin analysis'.

In this section, the tectonic systems tracts concept is applied with respect to the break up and sea floor spreading of the Argo Abyssal Plain based on the magnetic lineament information provided by Fullerton et al. (1989) and Exon and von Rad (1994). As a result this study suggests that previous rifting events strongly controlled the basin shape and morphology during deposition of the Upper Jurassic and Lower Cretaceous succession. It is important to note that the 'Argo'-related rifting event had inherited a previous basin morphology, and previously existing faults act as zones of incipient weakness vulnerable to reactivation. The 'Cuvier' and 'Gascoyne' related rifting event mildly affected the stratigraphy and structure of the Dampier Sub-basin subsequent to the 'Argo' related rifting.

It can be expected that the higher frequency eustatic signal will overprint the tectonic influence. The tectonic systems tracts defined for this area vary from 5 to 30Ma in duration. Third-order cycles driven by eustacy are expected to range from an apparent .5 to 4Ma in duration (Vail et al., 1988). The effect of eustacy is discussed in the following section (4.3).

The Mesozoic stratigraphy of the Dampier Sub-basin can be placed into pre-rift, rift initiation, rift climax, immediate post-rift and late post-rift tectonic systems tracts, in addition to a later passive margin section (see Figure 4.53, stratigraphic section). Each tectonic systems tract is defined with respect to the style of sedimentation proposed by Prosser (1993). These systems tracts are summarised in Figures 4.54 and 4.55. A short discussion of the stratigraphy and structure for each of the

proposed systems tracts in this study follows. Regional cross sections A - A', B - B' and C - C' (Figures 4.57, 4.58, and 4.59) are referred to throughout the text.

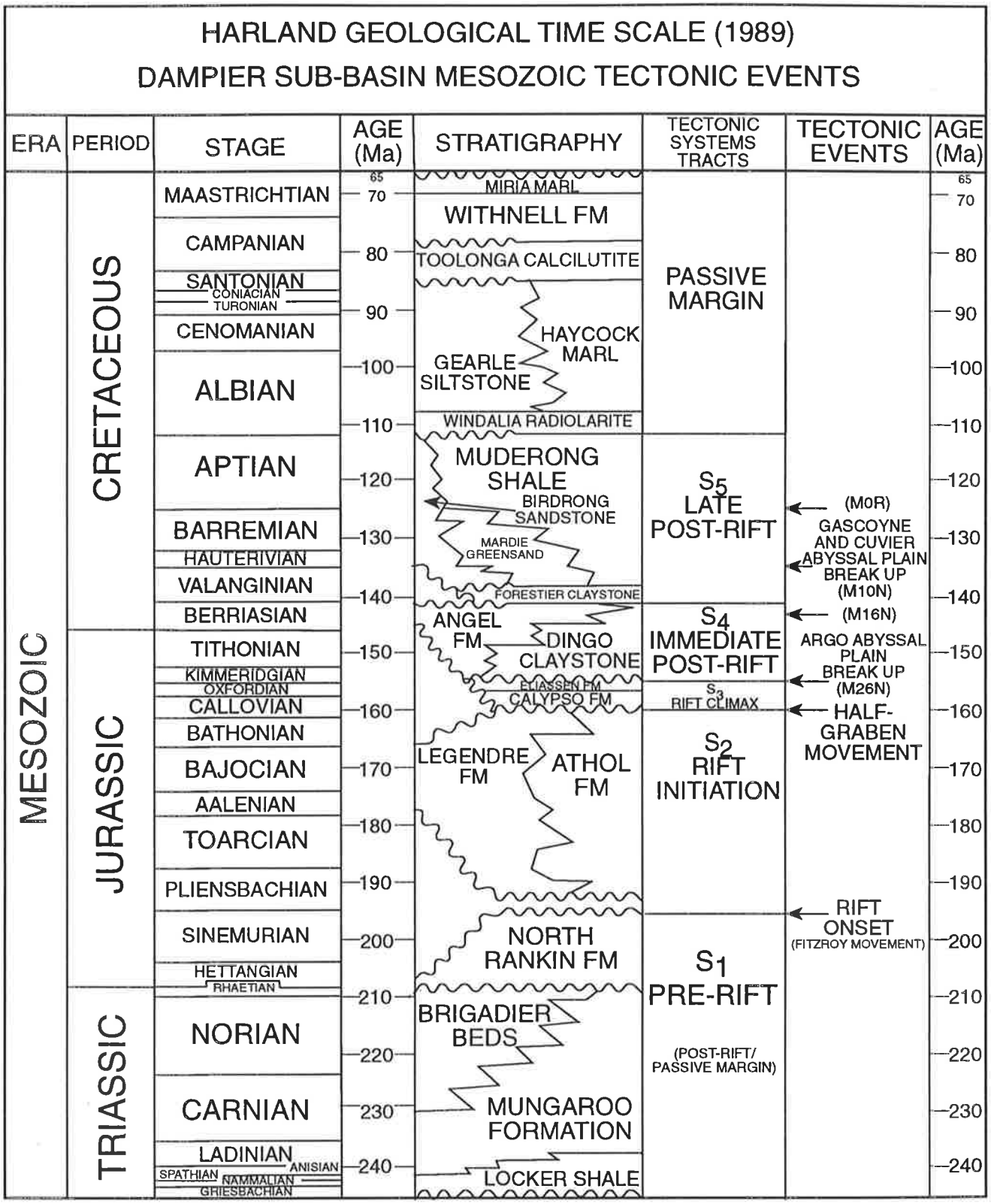


Figure 4.53. Mesozoic stratigraphy of the Dampier Sub-basin with respect to tectonic systems tracts and key tectonic events.

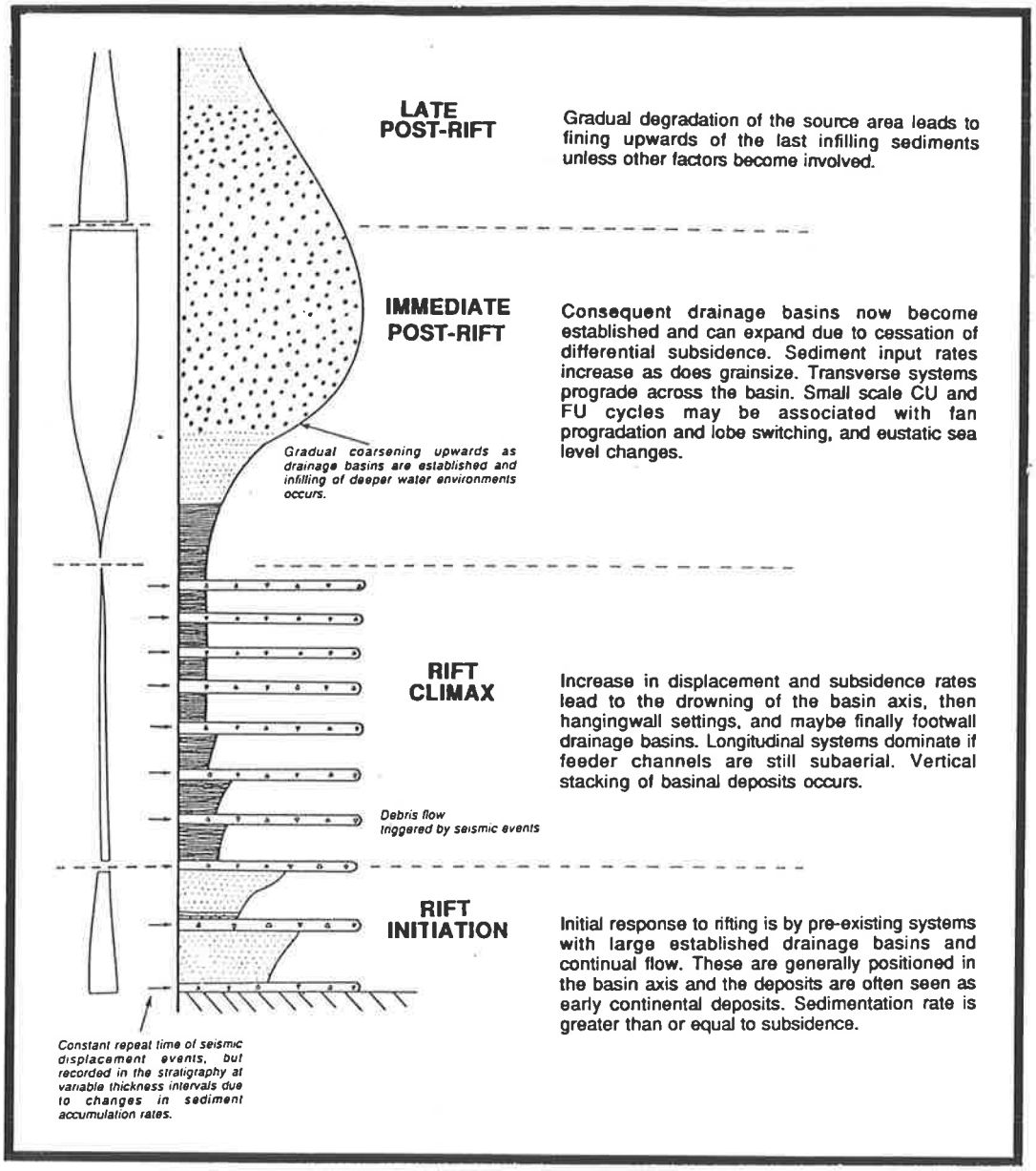


Figure 4.54. An idealised vertical log of the lithostratigraphy reflecting the progression of the rift-related tectonic systems tracts (after Prosser, 1993).

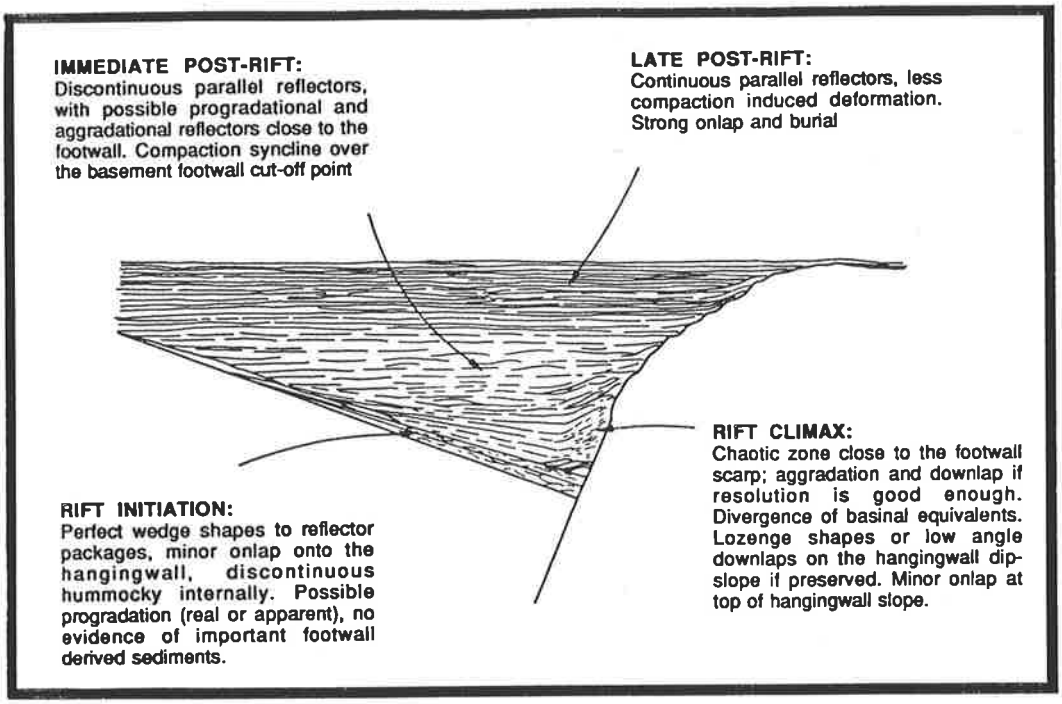


Figure 4.55. An idealised section of seismic stratal patterns across an ideal rifted half graben showing typical tectonic systems tracts and annotated with their characteristic seismic expression (after Prosser, 1993).

Pre-rift

There is no definition of the pre-rift tectonic systems tract, simply because it encompasses the rocks that existed prior to extension.

The pre-rift section of this study is considered to include the Triassic and Early Jurassic succession. It consists of passive margin oceanic sedimentation and prograding fluvio-deltaics. This sedimentation resulted from the establishment of the Lewis Trough, following the Permo-Carboniferous rifting event. The Permo-Carboniferous succession is expected to be relatively thin on the margins of the Lewis Trough and relatively thick within it. Subsurface intersections of Permian rocks exist in only two wells, Enderby 1 and Hampton 1, which are both located on the Enderby Platform. Hampton 1 penetrated 107m below 2477m of silicified siltstone and minor sandstone to 2492m that was underlain by a massive rhyolite, all of indeterminate age (Hampton 1 Well Completion Report). It is presumed that these are Permian rocks. Enderby 1 penetrated 68m at 2081m of rhyolite with minor interbedded sandstone and shale xenoliths. This section is Scythian to Permian in age and a tentative boundary between the Triassic and Permian is placed at 2117.75m (Enderby 1 Well Completion Report). These volcanics produce high amplitude, low frequency events on seismic and provide a good marker for near the top of the Permian succession.

Rift Initiation

The rift initiation is usually associated with the first increment of fault movement that causes a depression in the crust's surface to which gravity-driven sedimentary systems will respond (Prosser, 1993). In the Dampier Sub-basin, however, faults associated with the Lewis Trough were already established from a prior rifting event. Sedimentary systems are to be expected along the basin axis and the sediment accumulation rate is expected to be greater than or equal to the rate of subsidence (Prosser, 1993).

The rift initiation systems tract includes the fluvio-deltaic to nearshore Legendre Formation and the fine grained marine to marginal marine Athol Formation. Synsedimentary faulting is interpreted to occur along the Madeleine and Rosemary Faults. A succession of Legendre and Athol sediments, corresponding to approximately 2 seconds two-way-time, is interpreted to occur within the Lewis Trough depocentre (see Figures 4.58 and 4.59). This is equivalent to approximately 4000m of section. Prosser's ideal Rift Initiation consists of a relatively thin veneer of sediment (approximately 100-200ms two-way-time thickness) that fills most of the accommodation that is produced by fault movement. The relatively thick section here was influenced by the type and style of rifted basin. Prosser applied the concept of tectonic systems tracts to smaller style rifted basins, such as the Magnus Basin in the northern North Sea and the Barents Sea half graben. These two examples are smaller scale rifts, and are more closely associated with basement and crustal faults that have no previous rifting history.

Approximately 800m of lower Jurassic section was penetrated by wells such as Cygnus 1 and Enderby 1 on the Enderby Platform. The Lewis Trough would have been collapsing at this time in response to rifting, while being continually filled with sediment. A line source from the Pilbara Block to the east is expected. Sediment would have been deflected along the axial direction within the Lewis Trough.

The basal contact of this systems tract reveals low relief (approximately 100ms) 'horst and graben' topography on the Enderby Platform. It is interpreted that this faulting occurred early during the onset of rifting and was quickly filled by sediment before the majority of the extension was accommodated by the Rosemary and Madeleine Faults.

Rift Climax

The time of maximum rate of displacement on a fault is termed the rift climax, and sediment accumulation is likely to be outpaced by subsidence and differential relief will be created across the fault scarp (Prosser, 1993). The rift climax systems tract can be subdivided into three stages: early rift climax, mid rift climax and late rift climax systems tracts. The rift climax systems tract is characterised in seismic profiles by an increase in the amount of aggradation, together with the development of divergent forms related to continued tilting of the hanging wall during deposition (Prosser, 1993). The formation of footwall gravity deposits such as slumps is expected. The Calypso Formation is characteristic of the early rift climax, while the Eliassen Formation unit E2 is characteristic mid rift climax. Unit E1 is characteristic of the late rift climax systems tract. These formations are shown on seismic sections

(see regional cross sections) with a wedge-shaped geometry, reflecting the filling of a half graben tilted on the Rosemary Fault. They dominantly occur within the Lewis Trough with the exception of some apron deposits in the Kendrew Trough on sections B - B' and C - C' as well as a slope apron fringing the Eliassen-Orion Terrace on the Enderby Platform (section C - C'). Prosser (1993) noted that in this systems tract, "differential topography is established due to the nature of individual fault growth, the change to a single dominant fault growth, the increase in volume for deposition (accommodation space), the low potential for erosion and high sediment supply, and the relative rates of erosion and deposition relative to subsidence". Basin starvation is a likely characteristic of the rift climax stage. Also, a general feature in the rift climax systems tract, with respect to the depositional system, is the presence of soft sediment deformation structures which indicate seismic triggering, and include rock falls, debris flows, dewatering features and slumping (Prosser, 1993).

early rift climax systems tract - The early rift systems tract is ideally distinguished from the rift initiation systems tract below by a downlap surface. Downlap and onlap can be noted on the basal horizon shown in the seismic examples. The Calypso Formation is a fine grained, nearshore to shallow marine succession of sand, silt and clay. A generally monotonous seismic character is dominated by relatively parallel, continuous events (e.g. see Figure 3.21), suggesting aggradational depositional patterns. The marine influence observed in the Calypso Formation reflects a transgression with respect to the underlying Legendre Formation, probably as a result of the increased subsidence outpacing sediment accumulation. The overall half graben wedge shape of the Calypso Formation can be observed on the Calypso Formation isopach map (Figure 4.7). In addition, lobe shaped contours are also observed, which reflects sedimentary point sources from the scarp produced by the Rosemary Fault.

mid-rift climax systems tract - The onset of the mid-rift climax systems tract is characterised by a change to retrogradational geometries of the reflectors on the hanging-wall dip-slope as a result of transgression (Prosser, 1993). Footwall systems are expected to be small submarine fans. Basinal systems will involve suspension fall-out as hemipelagic muds and silts, and the hanging-wall systems will consist of linear facies belts of regressional shallow marine deposits (Prosser, 1993). Eliassen Formation unit E2 reveals seismic mounded geometries and slope apron wedges (e.g. see section 4.1). The slope apron fringes the Rosemary Fault to the north of where the Eliassen-Orion Terrace disappears (e.g. section B - B), and fringes the Eliassen-Orion Fault to the south (e.g. section C - C'). The seismic database does not cover the area fringing the Eliassen-Orion Terrace satisfactorily, and so this region was not mapped.

The Eliassen Formation spans most of the *W. spectabilis* palynozone. Many wells reveal nearshore palynological indicators near the base (*W. spectabilis 'a'* subzone) while near its top (*W. Spectabilis 'd'* subzone), offshore anoxic conditions are suggested (Morgan Palynological Reports). Indeed, Morgan (1991) suggests an overall transgression at Calypso 1 for the *W. spectabilis* palynozone based on these palynological indicators. It is expected that during this time, the hanging wall was completely submerged and a narrow marine shelf would have existed on the adjacent Enderby Platform.

late rift climax systems tract - Eliassen Formation unit E1 is characteristic of this systems tract. The base of this unit (Horizon 'H') is composed of a relatively continuous reflector that can be easily correlated over the project area (i.e. see section 3.3). Prosser (1993) noted that this stage of the rift climax systems tract is associated with reduced sediment accumulation rates, sediment 'draping', and an extremely continuous reflector, especially over the highest areas where lithology contrasts, and hence, acoustic impedance contrasts will be greatest. Sedimentation of fine-grained siliciclastics from pelagic fall-out and distal turbidite flows is expected. These characteristics can be used to describe unit E1 of the Eliassen Formation.

Immediate Post-rift

The Angel Formation and Dingo Claystone may be described in terms of the immediate post-rift systems tract. It marks the end of active tectonism and displacement on basin-bounding faults which has two implications for the systems tract characteristics: a) tilting of the hanging-wall and differential subsidence across the fault plane ceases; and b) a decreased rate of regional subsidence, although subsidence will continue due to lithospheric thermal cooling effects (Prosser, 1993). In the Dampier Sub-basin, isostatic rebound on the basin margin associated with continental break up and sea floor spreading is likely, as previously discussed. Horizon 'G' (base of the Angel Formation equivalents) is associated with an erosional unconformity, and in some areas appears angular by the existence of underlying erosionally truncated reflectors. Aggradation and progradation are expected in this systems tract.

The features associated with deposition in the immediate post-rift systems tract are those associated with the infilling of a hole (Prosser, 1993). Also characteristic of the Angel Formation, Prosser (1993) states, "if local drainage basins are in subaerial positions at this point of development they will now expand rapidly and the rate of sediment supply to the basin will increase. The coarse-grained material derived from these proximal sources will encroach across the basin and a coarsening-upwards succession will be generated. Together, with a decrease in subsidence rate, there is a greater chance of infilling the basin and gradually shallowing".

It is proposed that some of the Angel Formation was sourced from cannibalisation of the nearshore shelfal development, deposited at the same time as the Eliassen Formation. This section would have been almost, if not completely removed and the underlying section would have also been resedimented as part of the Angel Formation. Evidence of reworked palynomorphs within the Angel Formation is shown in Table 4.1. Interesting to note is that the relatively older reworked palynomorphs tend to some degree to overlie younger ones (e.g. see Rosemary 1 and Legendre 1 evidence). This suggests that progressive erosion into older sediments occurred and lead to resedimentation during the time of Angel Formation deposition.

Well	Zone/unit	reworked palynomorphs
Rosemary 1	lower *P. iehiense*	minor middle Jurassic reworking
	D. jurassicum 'd'	heavy Oxfordian (*W. Spectabilis)* reworking
	D. jurassicum 'biii'	minor Oxfordian reworking
	C. perforans	reworked *W. spectabilis* 'd'
Lewis 1	*D. jurassicum* 'aiii'	minor *W. Spectabilis* reworking
	D. jurassicum 'ai'	reworked *W. digitata*
	unit A5 (2208m)	reworked *W. spectabilis* 'd'
	unit A5 (2250m)	reworked *W. spectabilis* 'a'
	unit A6 (2276m)	reworked *W. spectabilis* 'a'
Samson 1	*D. jurassicum* 'ai'	reworked *W. digitata*
Legendre 1	*D. jurassicum* 'biii'	minor Permian reworking
	D. jurassicum 'a'	reworked Permian
	unit A5 (2174m)	reworked *W. spectabilis* 'd'
	unit A5 (2192m)	reworked *W. digitata*
	unit A5 (2283m)	reworked *W. spectabilis* 'd'

Table 4.1. Detailed information that shows evidence of reworking from palynology interpretations (source: Morgan, 1989).

The Angel Formation is characterised by 'basin infilling' on regional cross sections, taking into account the later, compressional anticline over the Legendre Trend (sections B - B' and C - C'; Figures 4.58 and 4.59). In addition, the stratigraphic log correlations which use the Valanginian Disconformity as a datum (Figures 4.16 to 4.20) supports the idea of basin infilling.

Late Post -rift

The Talisman Sandstone, Forestier Claystone, Birdrong Sandstone, Mardie Greensand and Muderong Shale are considered part of the late post-rift systems tract. This systems tract is characterised by slow peneplanation of the remnant topography of the rift (Prosser, 1993). The seismic character is expected to be typically continuous and parallel reflectors as previously described for the Talisman Sandstone and Forestier Claystone in section 3.4. The reduction of topography leads to a decrease in depositional energy environments and the progression to finer grain sizes up section (Prosser, 1993). The onset of the Forestier Claystone and Talisman Sandstone may be related to the end of sea floor spreading in the Argo Abyssal Plain. In addition, an interpreted transgression during *S. tabulata* at the Valanginian - Hauterivian Stage boundary may be related to the break up of the Gascoyne and Cuvier Abyssal Plains (135Ma) and flooding associated with increased thermal subsidence. The new spreading centre that occurs on the Gascoyne Abyssal Plain at M4N to M5N correlates closely with the 'Intra-Muderong Event', another flooding event which occurs near the base of the *M. australis* Palynozone.

Passive Margin

The succession of Upper Cretaceous sediments, from the base of the Albian Stage, is considered to be associated with passive margin development. There is some amount of sediment thickening of the Albian to Campanian succession over the Lewis Trough (e.g. See Figure 4.46). This is considered to be the result of differential subsidence of the Lewis Trough with respect to its margins, due to compaction of the thicker sedimentary section in the Lewis Trough. It may also have been an effect of mild compression related to wrenching during this time. Evidence for mild wrenching will be discussed later.

Subsidence History

To evaluate the relationship of sedimentation with respect to tectonic history, it is helpful to consider basin subsidence through time. Subsidence curves for the Valanginian to Callovian section and the Valanginian to Sinemurian section, were generated for Lauchie 1. These are shown in Figure 4.56. Lauchie 1 was chosen for this analysis since it is furthest down dip towards the Lewis Trough on the Legendre Trend side of the depocentre. These curves were generated with the aid of *BasinMod 1-D* software. Due to the general layer-cake nature of the stratigraphy within the Lewis Trough, the relative thicknesses of the units and formations are similar in the wells over the Legendre Trend. It was assumed that a subsidence analysis in any of these wells would provide similar results. This assumption was confirmed by viewing additional subsidence curves for the Rosemary 1 and Legendre 1 wells that are contained in Appendix V. The calculation of this curve utilised horizon depth and age in absolute time (Harland 1989 time scale) and generalised lithologies (see Table 4.2).

Lauchie 1 does not penetrate the base of the Calypso Formation. In order to account for the complete depth to the base of the Calypso Formation at 160Ma, 500m of sediment, estimated from seismic interpretation, was added to Horizon 'J' at 3200m in Lauchie 1. In addition, a 3610m thick interval of Legendre Formation was calculated to occur below this level by interpreting approximately 1.3 seconds two-way-time of Legendre Formation near the Rosemary Fault. This calculated thickness is relatively arbitrary, although it is an estimate that is satisfactory for the purposes of this analysis.

Depth (m)	Time (Ma)	Horizon	Estimated net cumulative accommodation	Lithology
2109	125	Valanginian Disc.	150m	
2208	141	A	152m	claystone
2208	143	B	188m	
2368.5	145	C	224m	sandstone
2383	147.5	D	269m	claystone
2403.5	148.5	E	283m	claystone
2564.5	152	F	346m	sandstone
2620	155	G	400m	sandstone
2840	155.75	H	300m	claystone
3003	156.75	I	70m	sandstone/claystone
3200	157.1	J	50m	claystone
3700	160	Callovian Disc.	5m	siltstone
7310	195	Base Legendre Fm.	0m	sandstone/claystone

Table 4.2. Horizon information that was used to generate the subsidence curves for Lauchie 1 that are shown in Figure 4.56.

Compaction was accounted for by using the Falvey and Middleton (1981) compaction correction equation. The effect of compaction is observed by the subtle convergence of the horizon subsidence paths (see Figure 4.56a). It was observed that a large amount of compaction of each unit had occurred prior to complete sedimentation of that unit. The amount of effective compaction occurring on a given unit over a specific period of time can be calculated by taking the difference of the vertical thickness (measured from the subsidence curve) of the unit over that period of time. For example, the vertical thickness of the Calypso Formation unit C2 (Horizons 'J' to 'K') is approximately 600m at 155Ma. This thickness is reduced to approximately 535m at 120Ma. The total compaction from 155Ma to 120Ma of unit C2 is 65m. The average amount of effective subsidence that is attributed to this unit over this period of time calculates to be 0.186cm/thousand years (ma).

The total amounts of 'tectonic subsidence' compared to 'load induced subsidence' are indicated in Figure 4.56a. The amount of subsidence attributed to tectonics is slightly less than one-half of the total subsidence. The most striking feature noted is the dramatic change in the subsidence rate at 155Ma (Horizon 'G' age). The average rate of tectonic subsidence from 155 to 160Ma is approximately 15cm/ma, while from 120 to 155ma it is calculated to be 0.48cm/ma.

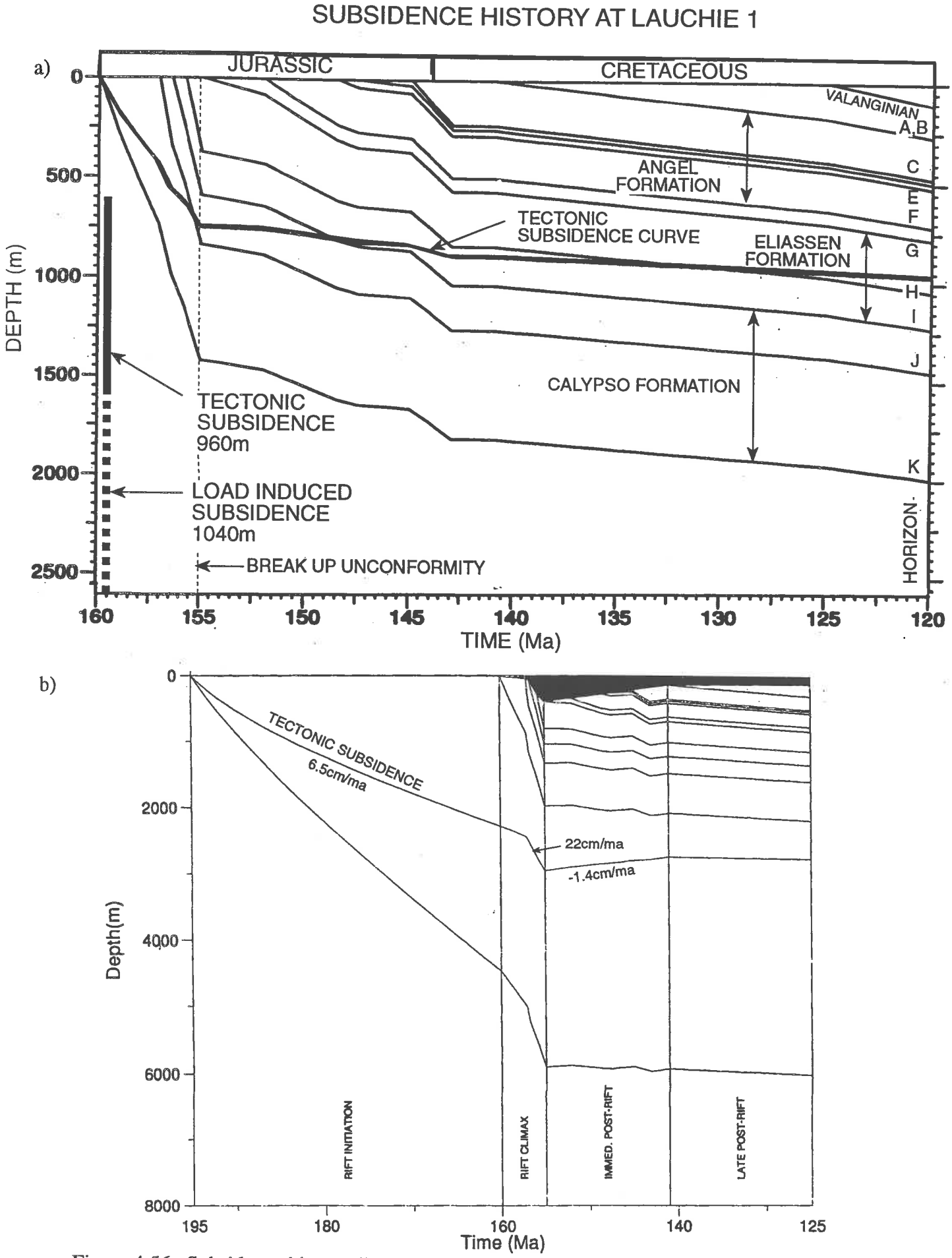


Figure 4.56. Subsidence history diagrams for Lauchie 1: a) - detailed subsidence for Valanginian to Callovian section; b) - subsidence history for the Valanginian to Sinemurian section to show the effect that the rift initiation section has on the relative subsidence of the overlying section. In this example, an estimated increase in net accommodation has been accounted for. See text for discussion.

Figure 4.56a is a detailed account of the subsidence from Valanginian to Callovian Age. In considering this analysis, there are two assumptions which have gross implications. It is assumed that the Callovian disconformity is basement and therefore any subsidence that is attributed to compaction of the underlying section is not taken into account. Secondly, it is assumed that the total amount of subsidence equals the amount of sediment accumulation (not sedimentation), and no relief formed at any time due to either subsidence or uplift. These factors were taken into account to generate the subsidence curve shown in Figure 4.56b.

As mentioned previously, the rift initiation section (Legendre Formation) is only an estimation of thickness from seismic picks. It is interesting to note that a significant amount of compaction occurred on this section during burial (rift climax). There is approximately 350m of compaction of the rift initiation section during the time of rift climax (total thickness is reduced from 4350m to 4000m, approximately). This calculates to 7cm/ma. During rift climax time, the average amount of subsidence attributed to compaction of the rift initiation section is 7cm/ma. The average amount of subsidence attributed to compaction of the rift climax section during rift climax time is 6.5cm/ma. The average amount of subsidence attributed to sediment loading during rift climax time is 12.5cm/ma. By adding these figures together, the net rate of apparent subsidence (subsidence at the sediment-water interface) during rift climax time is 26cm/ma. However, the actual sediment accumulation rate (or total subsidence) for the rift climax section is only 22cm/ma. The result is that -4cm/ma is attributed to tectonic subsidence. Since this is a negative number, it indicates that with these assumptions, tectonic uplift was possible during rift climax time.

Evidence provided from rock and seismic data indicate that there was a significant deepening event during the rift climax. This deepening was too significant to be attributed to a rise in eustatic sea level. In addition, a deepening event would not be expected to occur during a period of tectonic uplift. Therefore, it must be taken into account that subsidence possibly outpaced sediment accumulation during this time. This factor was taken into account to generate the subsidence curve in Figure 4.56b. The expected amount of accommodation generated due to subsidence was estimated and is shown in Table 4.2 as 'cumulative net accommodation'. An estimated 395m of accommodation was estimated to have been produced during the rift climax. During the immediate post-rift section, it is estimated that this accommodation was taken up by 250m of non-compacted sediment accumulation. This sediment filling is noted from the interpreted uplap of seismic reflectors. In addition, a significant shallowing upward trend is noted over the Angel Formation from the rock evidence and seismic facies analysis. A good example of evidence for this accommodation and subsequent sediment filling is shown in Figure 4.67. Although these estimates are relatively arbitrary, they have the correct magnitude and direction for the subsidence/sediment accumulation in this case. It may be that these estimates are, in fact, conservative ones.

The resulting tectonic subsidence curve (Figure 4.56b) reveals an interesting history. During the rift climax, the average tectonic subsidence increased to 14cm/ma from 6.5cm/ma during the rift initiation. The tectonic subsidence peaked at 22cm/ma during the rift climax. The tectonic subsidence curve suggests tectonic uplift of 1.4cm/ma during the immediate post-rift section. Most of this uplift would have easily have been absorbed by compaction induced subsidence (note that the horizons

above the tectonic subsidence curve within the immediate post-rift section in Figure 4.56b are generally subsiding). However, this amount of tectonic uplift acting on the basin margin (i.e. Enderby Platform), where no sediment accumulation is interpreted to occurred at this time, would have been significant enough to have caused mild uplift of the pre-existing rift initiation section. This would have provided a sedimentary provenance for deposition of the Angel Formation.

These calculated rates of tectonic subsidence and sediment accumulation are reasonable when considering recent rifted margin basins. For example, Scott and Govean (1984) discussed sediment accumulation rates for the rifted Gulf of Suez. They calculated successive sediment accumulation rates of 4cm/ma, 106 - 146cm/ma, and 32cm/ma for a vertical section of various formations within the rift. The maximum sediment accumulation rate noted for Lauchie 1 is 25cm/ma for the Eliassen Formation unit E2. This, incidentally, is during a period of relative sediment starvation, when the net amount of accommodation produced during this unit is considered. Scott and Govean did not discuss their rates with respect to tectonic subsidence. However, they referred to the average rate of tectonic subsidence for the Gulf of Suez, which was calculated to be 12.5cm/ma from the Miocene to the present. This figure is a reasonable comparison to the average tectonic subsidence of the rift initiation and rift climax sections at Lauchie 1 which is calculated to be 7.5cm/ma (this includes the estimated net accommodation). This comparison indicates that the estimated net accommodation is a reasonable and, possibly, a conservative estimate.

The tectonic subsidence curve that resulted from estimation of several factors (rift initiation section thickness and amount of net accommodation during rift climax and immediate post-rift) helps to confirm the previous hypothesis on the subsidence and sediment accumulation history for the eastern margin of the Lewis Trough. Even though some estimates were made in producing the tectonic subsidence curve, these estimates are of the correct magnitude. It is likely that estimates provided by more reliable data (i.e. additional core data and seismic across the Rosemary Fault) would not produce dramatic differences in the overall results of this analysis. These overall results suggest mild tectonic subsidence during rift initiation (sediment accumulation generally keeping pace with subsidence); a sudden increase in subsidence during rift climax where subsidence outpaces sediment accumulation; and mild uplift during the immediate post-rift section and sediment accumulation outpacing subsidence. The only interval where contention on the tectonic subsidence may arise is during the immediate post-rift section. More conservative estimates of the subsidence, and/or sediment filling (net accommodation) would produce tectonically static conditions or very mild tectonic subsidence during the immediate post-rift section.

Subtle subsidence inflections noted on the subsidence curves during the immediate post-rift section (Figure 4.56a) may be attributed to varying rates of sediment influx and eustatic sea level. These two factors were not taken into account in this highly generalised analysis. A notable change in tectonic subsidence rate occurs at 145Ma (Horizon 'C' age), possibly suggesting a mild tectonic event at this time. Incidentally, this time closely correlates with magnetic lineament M16N when sea floor spreading ceased in the Argo Abyssal Plain.

The most obvious observation that is made from the subsidence curves is the dramatic decrease in subsidence at 155Ma. Any reasonable estimation in accommodation, sediment influx values or eustatic sea level would not mask the dramatic decrease in tectonic subsidence rate. This time correlates with the base of the Angel Formation as well as the breakup of the Argo Abyssal Plain. The mild tectonic uplift, interpreted from 141 to 155Ma can be associated with the isostatic rebound that is expected to have occurred after breakup. The suggestion by Hill (1994) that isostatic rebound occurred at that time, confirms this likelihood.

Seismic Evidence for Structural Events

The various structural interpretations for the Dampier Sub-basin and/or the North West Shelf as a whole include extension related rifting, lateral movements due to deep seated wrench zones (in which case the Dampier Sub-basin would be a pull-apart basin), and also a history of compressional and extensional inversion events. This indicates that a conclusive structural history and tectonic development remains to be outlined. The evidence outlined in this section shows a history of extension due to rifting events and subsequent sea floor spreading with a minor component of left-lateral wrenching that induced strike slip movement along the Rosemary Fault. This left-lateral strike-slip movement caused a complex history of concurrent extensional and mildly compressional zones along the Legendre Trend which migrated southwestward during the Upper Jurassic and Lower Cretaceous.

A schematic structure map of the study area is shown in Figure 4.60. This map shows the generalised configuration of the northern portion of the Dampier Sub-basin which narrows to the northeast (towards Talisman area). An area of depositional thinning, reflecting periods of sediment starvation, occurred to the north of the Angel area. This reflects basin tilting to the south of this line caused by the overall half graben formation on the Rosemary Fault during the rift climax tectonic systems tract. The opening of the basin to the southwest is a likely reflection of overall rotational extension due to the 'Argo'-related extension direction (as shown). This caused increasing extension and normal fault movement to the southwest (towards the Rosemary area). The Lewis Trough plunges in this direction, indicating increased extension at this time. Indeed, the palaeogeography of unit E2 of the Eliassen Formation (Figure 4.9; mid-rift climax systems tract) reveals an interpreted stratigraphic strike exactly perpendicular to the 'Argo'-related extension direction. This stratigraphic strike was interpreted, incidentally, on the basis of stratigraphy and independent of the 'Argo' extension direction.

Two minor synclinal axes are shown to occur across the Lewis Trough axis. These axes coincide with sediment source directions from the Rosemary Fault during the immediate post rift systems tracts (lower Angel Formation). The distal direction is generally in the direction of the Argo Abyssal Plain which reflects the thermal subsidence that occurred in response to the onset of sea floor spreading at that time. The minor synclines were bathymetric lows along which sediment was transported in the distal direction. These subtle syncline features may be an artifact of an older structural grain which was subsequently draped by sediment and then formed as a result of differential subsidence due to compaction of varying sediment thicknesses.

Minor normal faults appear to splay from the Rosemary Trend and generally strike to the northeast. These faults reflect extension due to left-lateral strike slip movement on the Rosemary Fault. Seismic examples showing the resultant displacement of these faults are shown in Figures 4.61, 4.62, 4.63, and 4.64. These examples can be demonstrated to be the result of oblique or transverse movement on a pre-existing fault plane using sandbox analogue modeling techniques. A summary of this technique as it applies to structure on the North West Shelf is provided by Lemon and Mahmood (1994). In this paper, they show a plan view and transverse sections of a 'side ramp' being subjected to oblique extension in a 3D model sandbox. These sections agreed with interpreted left lateral and minor oblique movement with the Rosemary Fault acting as the effective 'side ramp'. For example, striking similarities can be observed in the fault patterns of my Figure 4.61 with their Figure 9b; and of my Figure 4.64 with their Figure 9a. In addition, the 'kinked' stratal reflectors that abut a fault plane in Figure 4.65 suggest nearly pure left lateral strike slip movement on the fault plane. This was observed by comparing unpublished models (Lemon and Mahmood, pers. comm., 1995) that involve this pure left lateral strike slip movement on a pre-existing fault plane.

If left lateral wrench movement is proposed to occur on the Rosemary Fault, it follows that there must have been minor compressional episodes as well as extensional episodes due to the curvilinear nature of this fault. Areas are outlined on the schematic fault map (Figure 4.60) which reveal minor compressional related anticlines. These areas correspond to zones where the Rosemary Fault curves and strikes in a more westerly direction (i.e. the fault trace outlines a 'confining bend'). Compression-related features and anticlines can be observed in most of the seismic examples. The most striking anticline can be observed to occur on Horizon 'A' in Figure 4.64. Indeed, this example reveals a sequence of compressional and extensional episodes over time. Mild compression is interpreted to occur from Horizon 'I' to Horizon 'A'; a section revealing extensional/left lateral transverse movement overlies Horizon 'A'. This section is followed by a thick 'extensional' section and is followed by compression related features beginning on a reflector just below the Aptian disconformity.

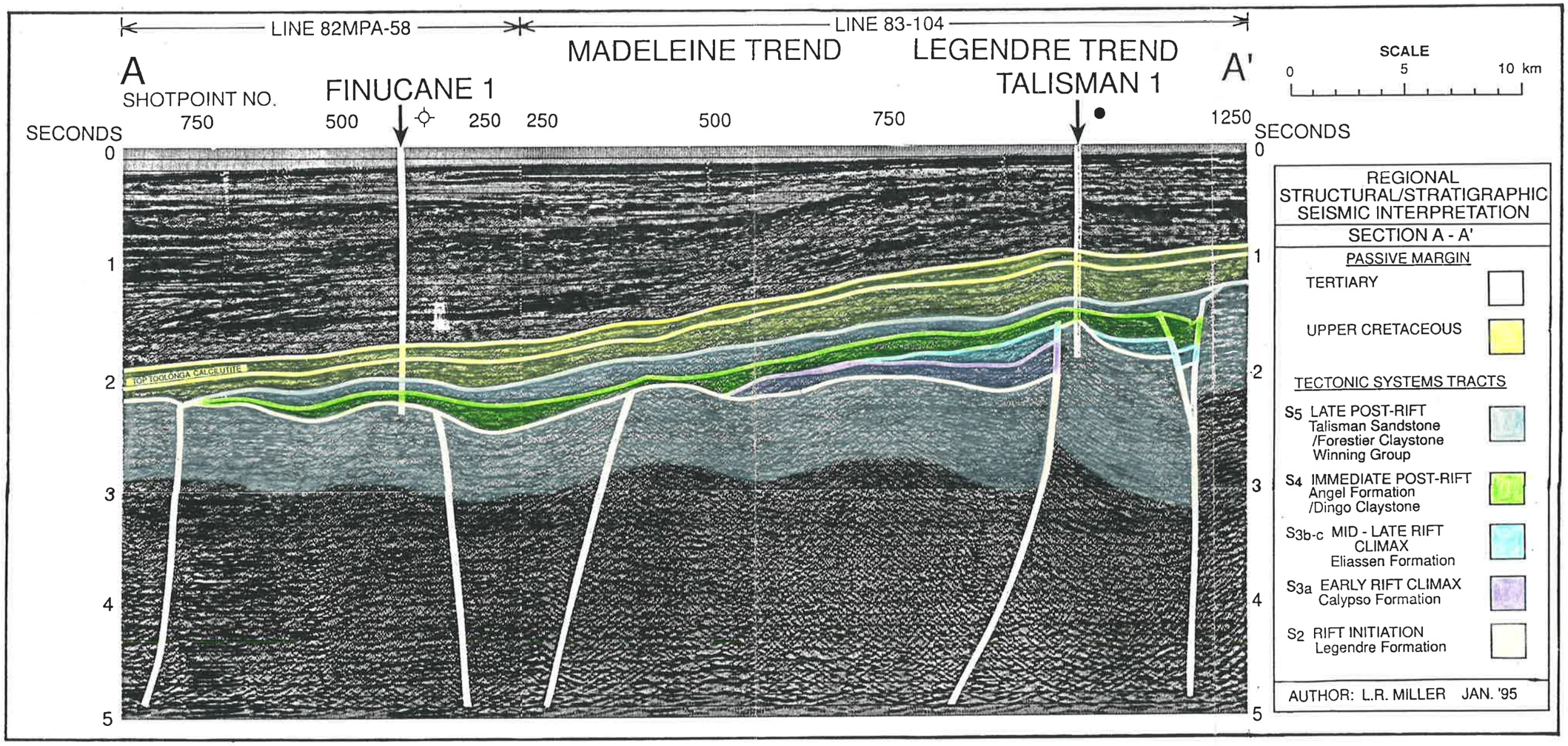


Figure 4.57. Seismic section A - A' showing the regional structure and stratigraphy of the Dampier Sub-basin. See Figure 4.48 for the section location.

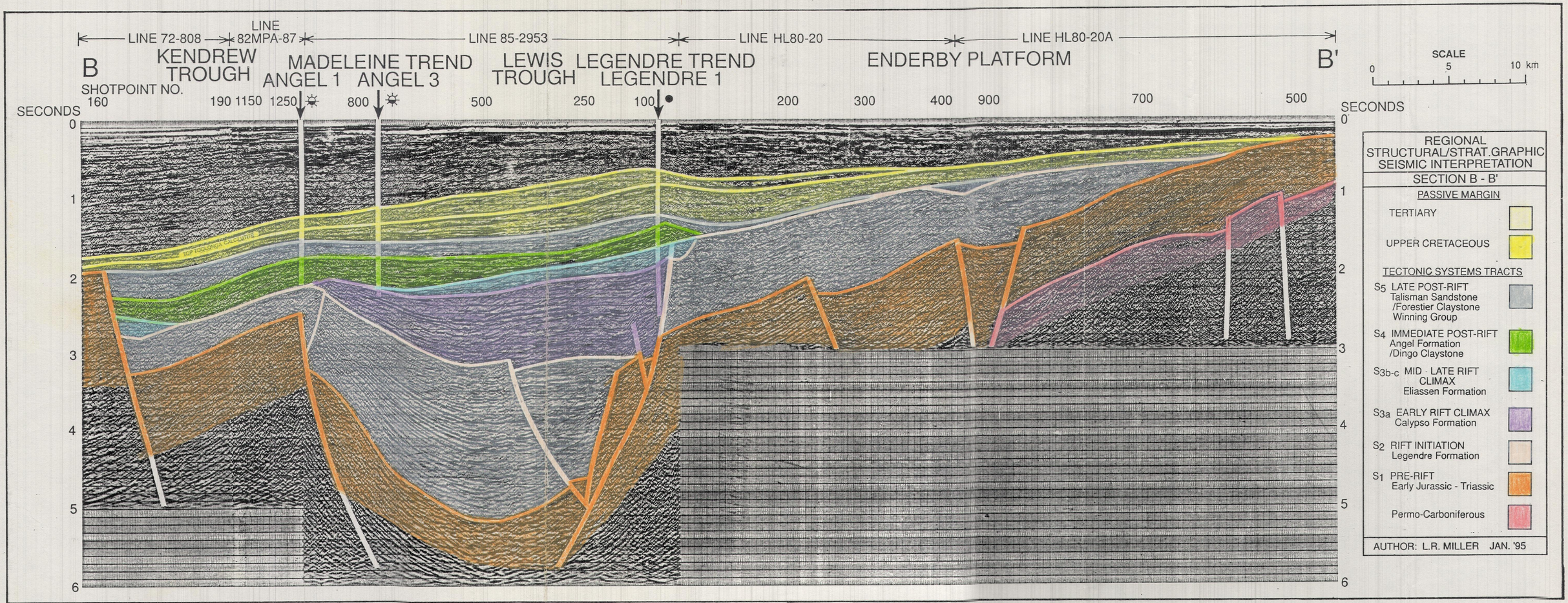


Figure 4.58. Seismic section B - B' showing the regional structure and stratigraphy of the Dampier Sub-basin. See Figure 4.48 for the section location.

UNIVERSITY OF ADELAIDE LIBRARY 22/3/96

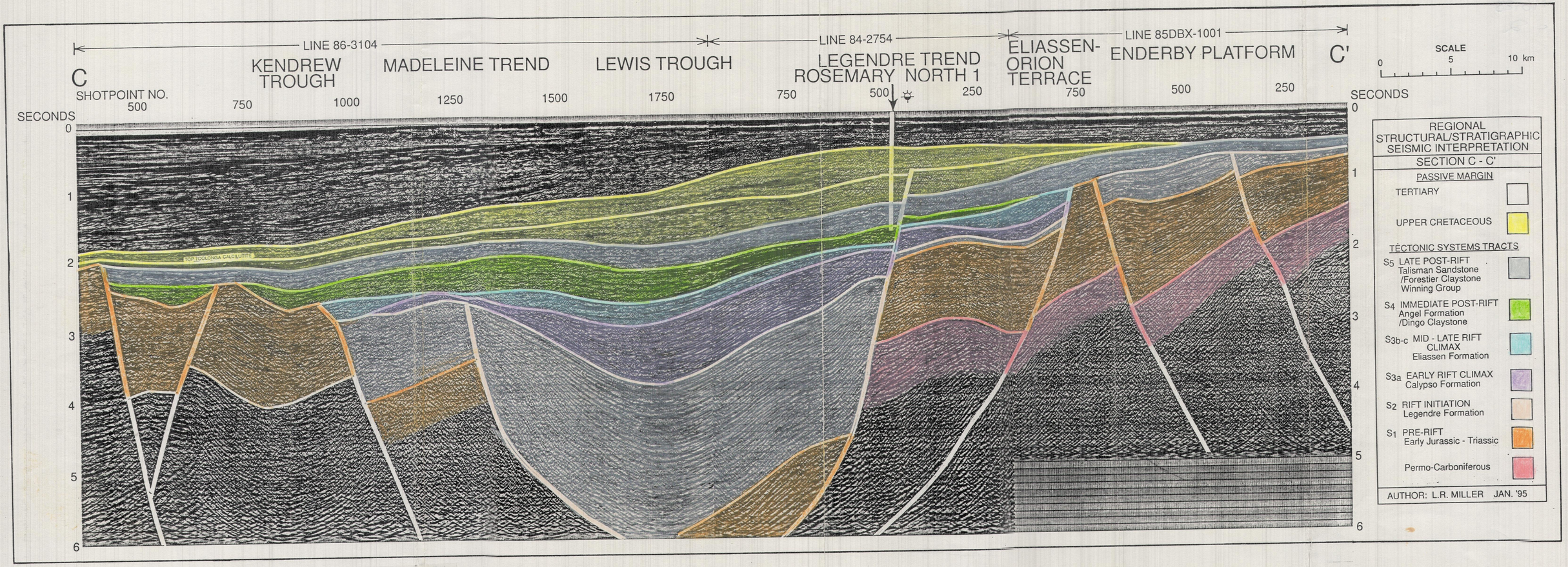


Figure 4.59. Seismic section C - C' showing the regional structure and stratigraphy of the Dampier Sub-basin. See Figure 4.48 for the section location.

This page intentionally left blank.

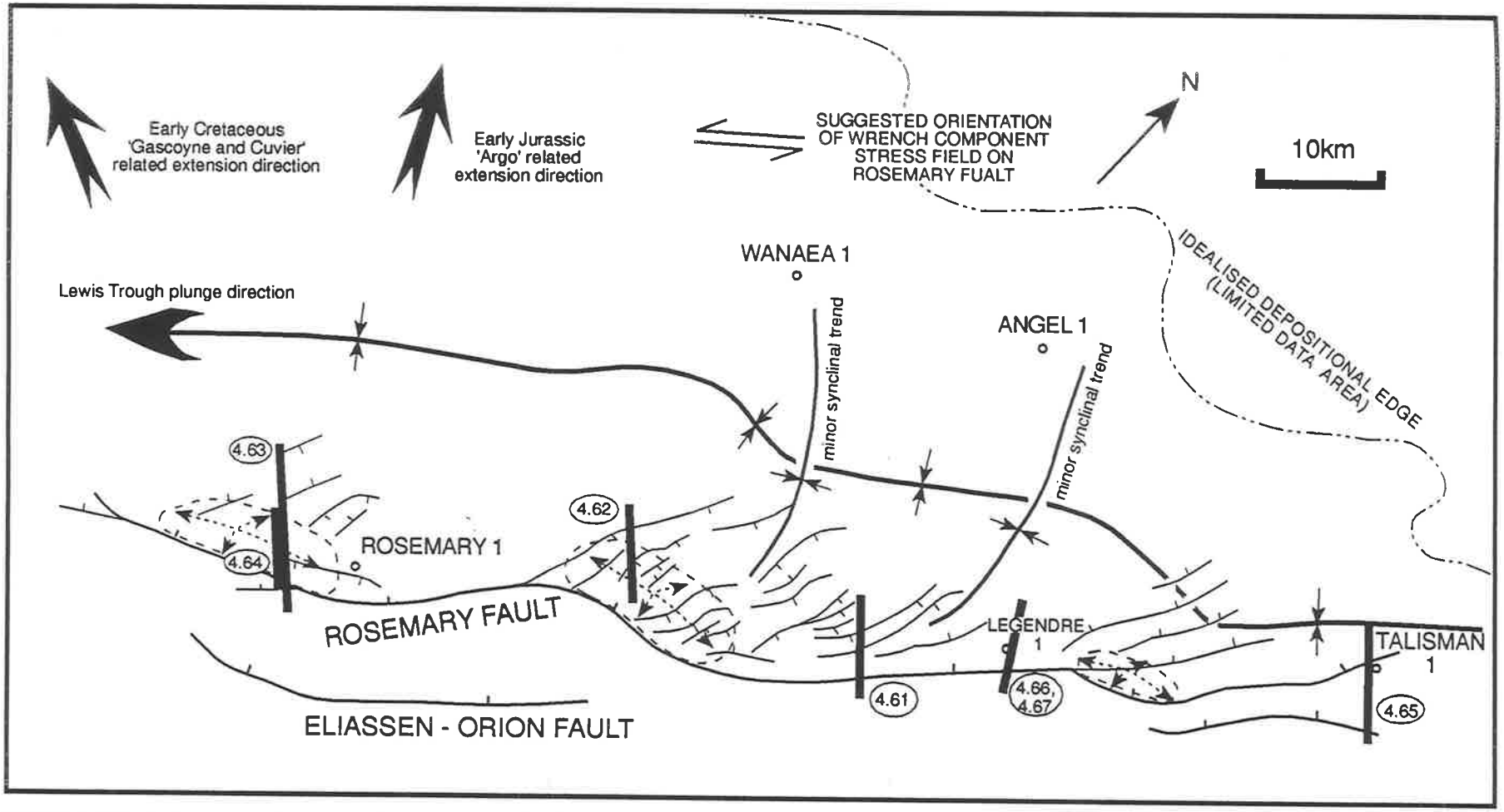


Figure 4.60. Schematic diagram of generalised faults and structure of the study area for the Lower Cretaceous to Upper Jurassic section. The relative intensity of the structures are indicated by increasing line thicknesses. Areas of minor compressional anticline features are outlined by dashed lines and have their trends indicated. Note the suggested orientation of the wrench related stress field that caused lateral displacement on the Rosemary Fault during the Late Jurassic and Early Cretaceous. Seismic examples used in the discussion are indicated by their Figure numbers.

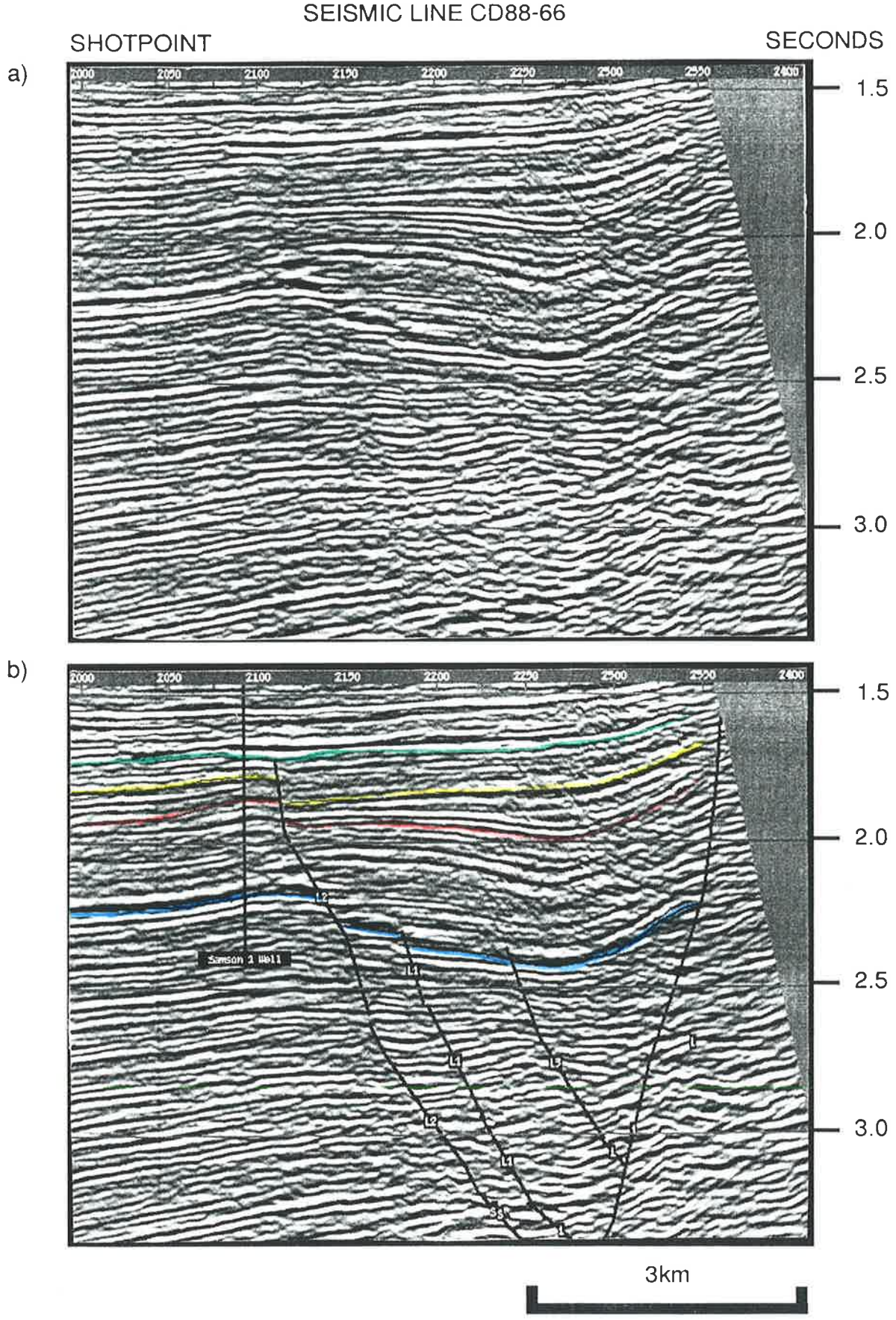


Figure 4.61. a) uninterpreted; and b) interpreted seismic examples revealing a collapse graben structure, considered to be a result of left lateral displacement on the Rosemary Fault. Note the mild compressional features on reflectors to the immediate right of Samson 1 intersection. Refer to Figure 4.60 for example location. See Enclosure IVc) for position on seismic section. Horizon 'G' - green; Horizon 'H' - yellow; Horizon 'I' - red; Horizon 'J' - blue.

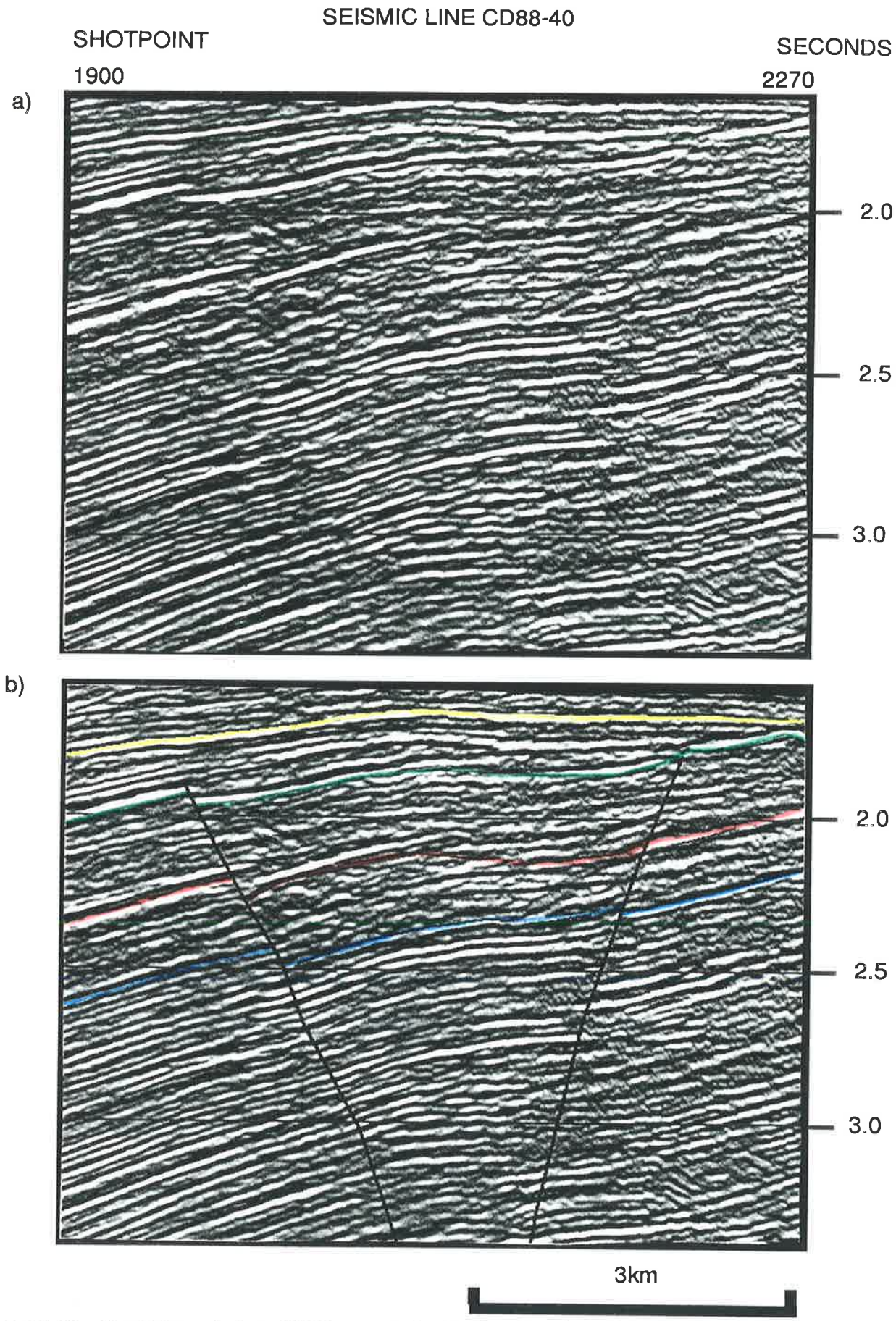


Figure 4.62. a) uninterpreted; and b) interpreted seismic examples revealing low displacement normal faults, considered to be a result of left lateral displacement on the Rosemary Fault. Observe the prominant timing of significant fault movement above Horizon 'G'. Refer to Figure 4.60 for example location. See Enclosure IVk) for position on seismic section. Horizon 'A' - yellow; Horizon 'G' - green; Horizon 'I' - red; Horizon 'J' - blue.

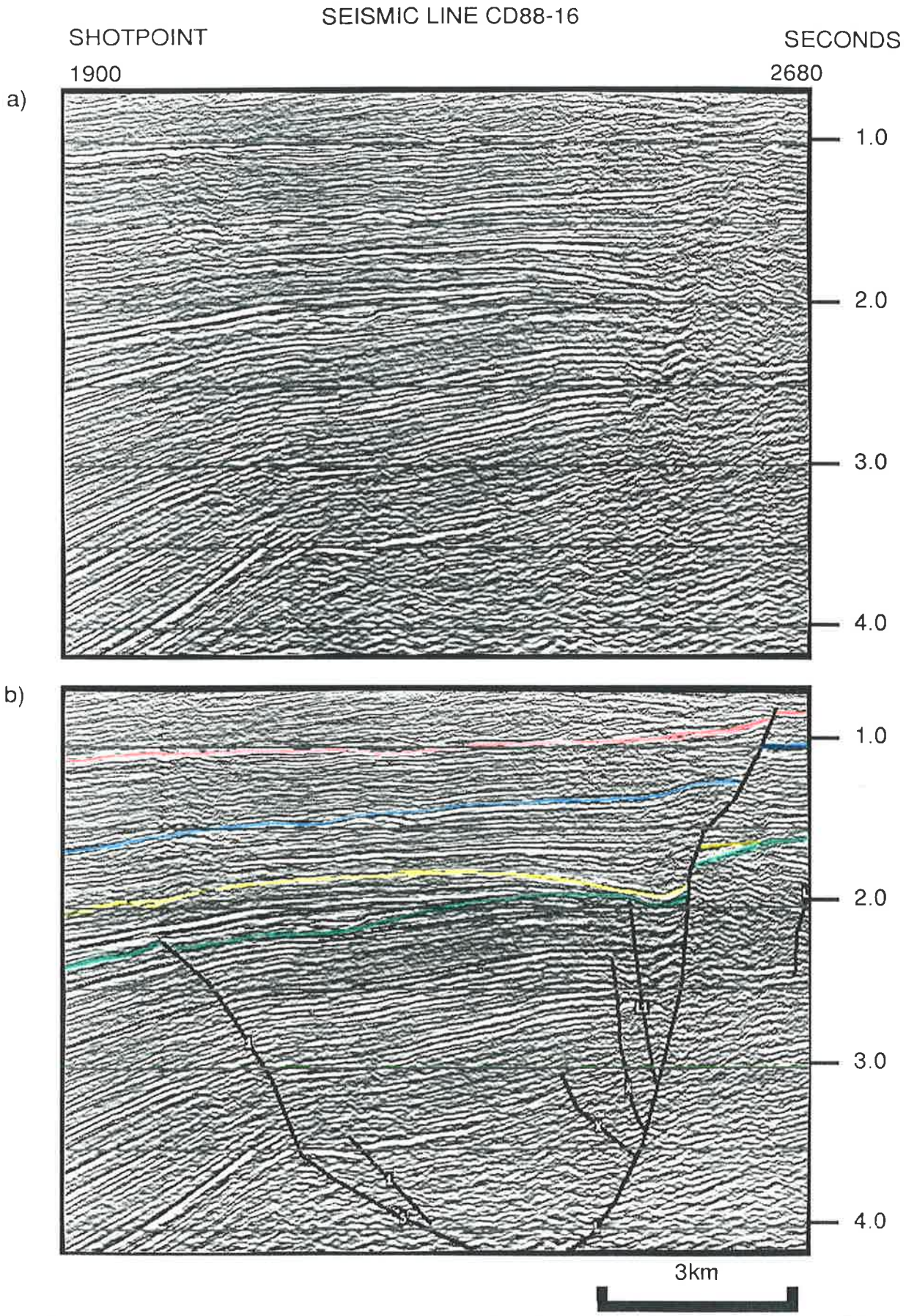


Figure 4.63. a) uninterpreted; and b) interpreted small scale seismic examples showing the stratigraphic result of a structural history of fault reactivation due to alternating extensional and compressional episodes. See Figure 4.64 for a more detailed explanation. Refer to Figure 4.60 for example location. See Enclosure IVa) for position on seismic section. Top Toolonga Calcilutite - red; Aptian Disconformity - blue; Horizon 'A' - yellow; Horizon 'G' - green;.

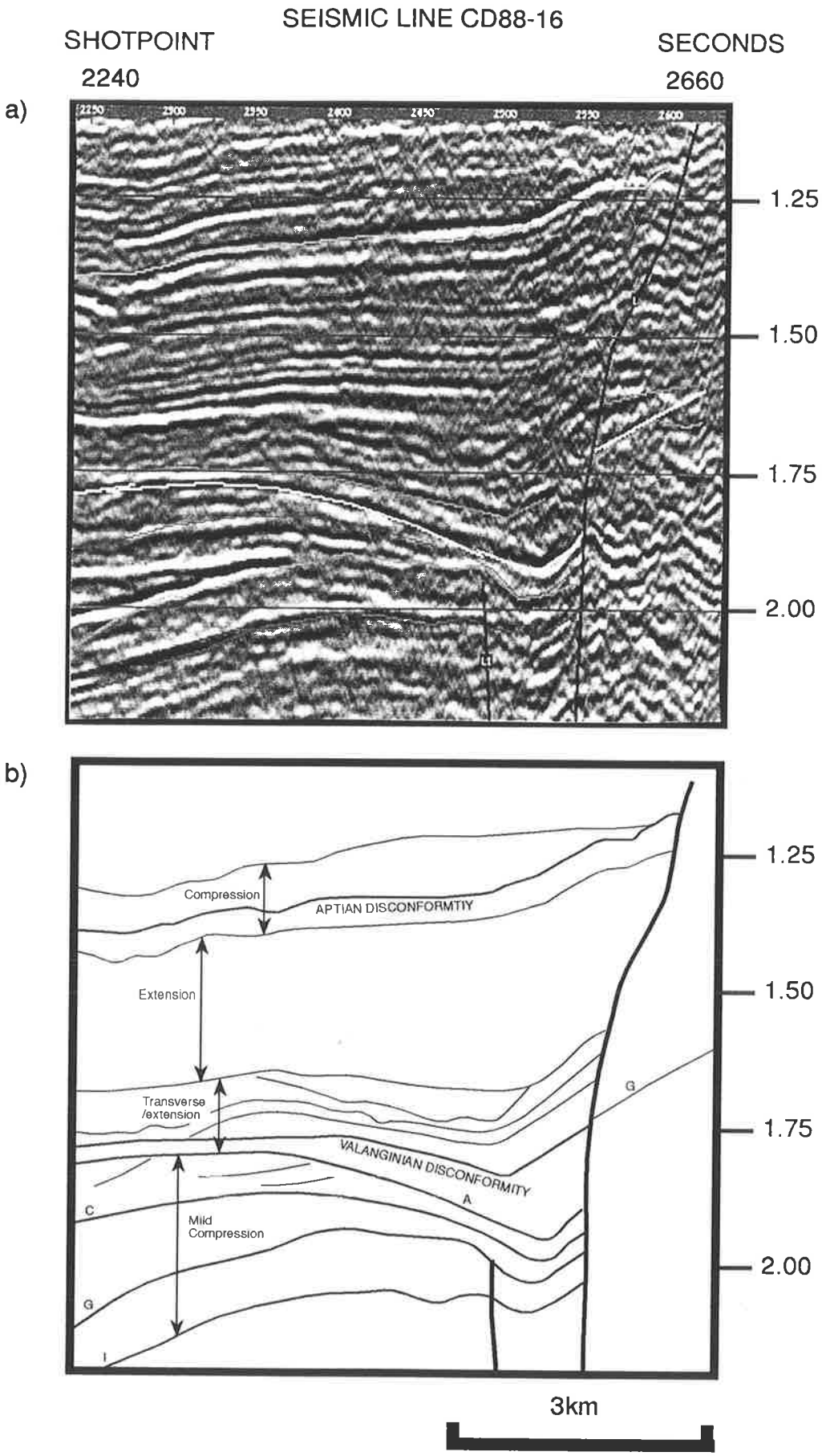


Figure 4.64. a) seismic example; and b) stratal configuration drawing which illustrate a structural history of mildly compressional, to transverse/extensional, to extensional, and finally, to compressional episodes. See Figure 4.63 for a smaller scale example. Refer to Figure 4.60 for example location. See Enclosure IVa) for position on seismic section.

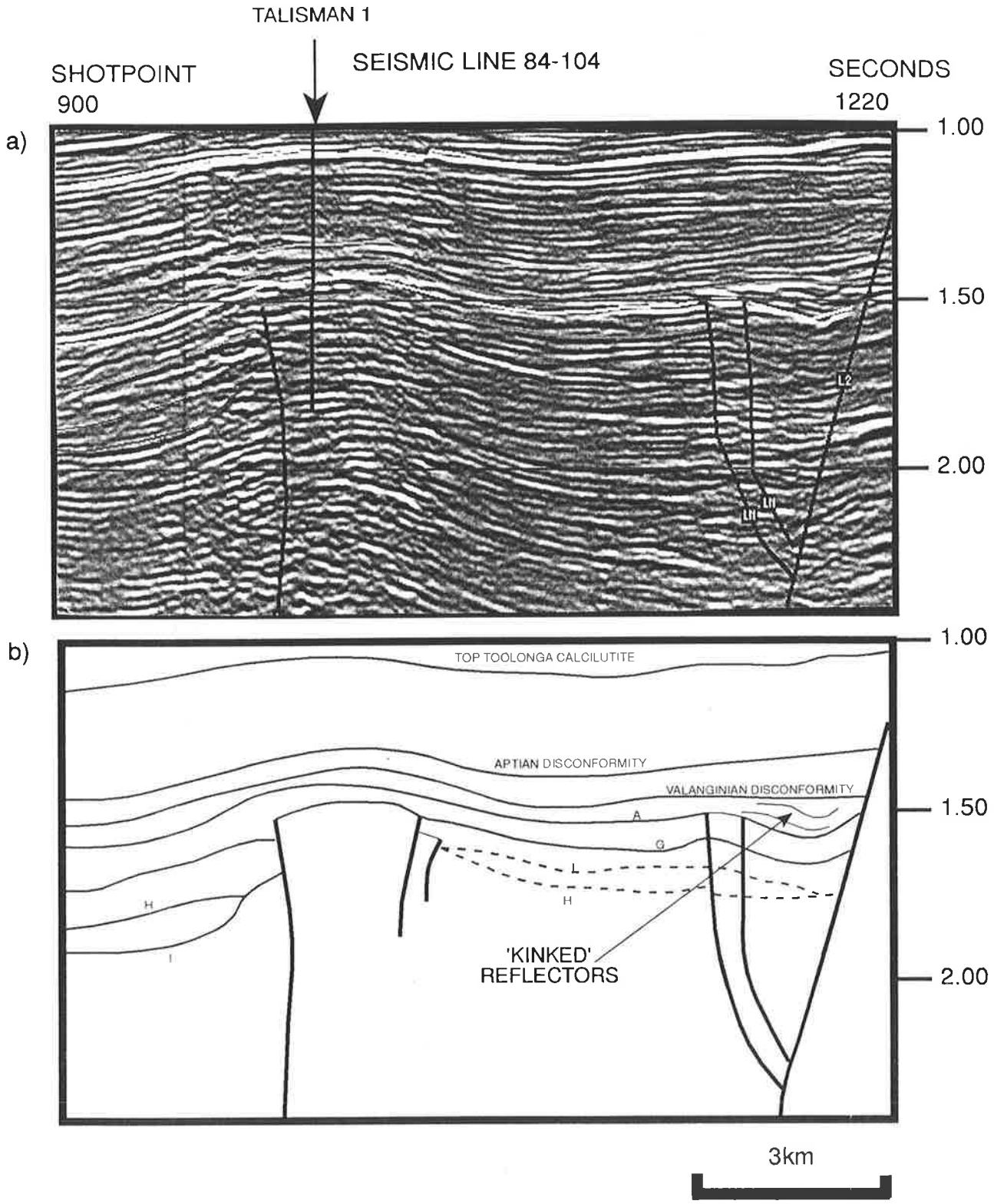


Figure 4.65. a) seismic example; and b) stratal configuration drawing which show the transpressional anticline over the Talisman area which is associated with Tertiary subduction in the Timor Trench. Note the 'kinked' reflectors abutting the fault on the right side of the example. This pattern is considered to be a result of nearly pure left lateral displacement on this fault during the Valanginian. Refer to Figure 4.60 for example location. See Enclosure IVk) for position on seismic section.

The existence of these compressional and extensional events can be explained by the curvature of the Rosemary Fault. When the hangingwall section was moved laterally along areas of the fault plane that curved into the direction of wrench movement, minor compression occurred. As this section progressively moved laterally along the fault plane to where the fault plane curvature deflected away from wrench movement (a 'releasing bend'), it was subjected to extension. It follows then that different dip sections across the Rosemary Fault plane reveal varying histories of compressional and extensional episodes. While one area of the footwall block was subjected to mild compression, another area experienced extension, both as a result of left lateral wrench movement.

The nature of varying extensional episodes is displayed in the data base of this study. The constraints of this study have not allowed details of this complex structural history to be deciphered, and a more complete seismic database across the Rosemary Fault would be required.

The overall character of the structure is a reflection of dominant extension which was overprinted by a minor left lateral wrench component The broad basin morphology was the result of the extension related to rifting. This was subsequently modified, notably along the Legendre Trend, by left lateral wrenching. It is difficult to ascertain the timing and relative intensities of these two tectonic components. It is likely, however, that extensional movements were probably dominant until the break up unconformity (Horizon 'G'). Wrenching was the likely dominant component following break up. This component continued intermittently and varied over different areas up until the middle Cretaceous. Further wrenching occurred in the Tertiary associated with the subduction zone in the Timor Trench. Anticlines associated with this event can be observed on the regional seismic cross sections (Figures 4.57, 4.58, 4.59), and particularly over the Talisman area (Figure 4.65).

It is possible that the timing of the wrenching and extensional components in the Late Jurassic and Early Cretaceous overlap, but it is difficult to say over what period and to what degree. The source of the wrenching component is likely a combination of plate movements in different areas. This wrenching may be somewhat related to the extension caused by the 'Gascoyne' and 'Cuvier' rifting events, and it agrees with this general direction of extension (Figure 4.60, as shown). Hill (1994) suggested that strike slip reactivation of the Paterson Orogen was the 'cause of minor inversion' of fault systems near the Lewis Trough. The Paterson Orogen coincides with the Bedout Sub-basin to the northeast of the study area, and is the northwesterly trending orogen adjacent to the Pilbara Block (see Hill, 1994; his Figure 3). Indeed, the intensity of wrenching is noted to increase to the northeast (i.e. the Talisman area).

The uplift that was associated with the transpressional stress would have had significant effect on palaeogeography and, therefore sand transport directions. Uplifted areas would have been subjected to submarine erosion and/or sediment starvation. Areas adjacent to uplifted areas would have been the locality of sediment transport and possible sand deposition. Indeed, the palaeogeographic maps of the Angel Formation show either condensed sections over uplifted areas or an erosional edge adjacent to them.

The effect of post depositional compression along the Legendre Trend masks the interpretation of a significant fault scarp existing along the Rosemary Fault (i.e. see Figure 4.47) during deposition of the Eliassen Formation and Angel Formation. This is demonstrated by a seismic example over the Legendre Area (Figures 4.66 and 4.67).

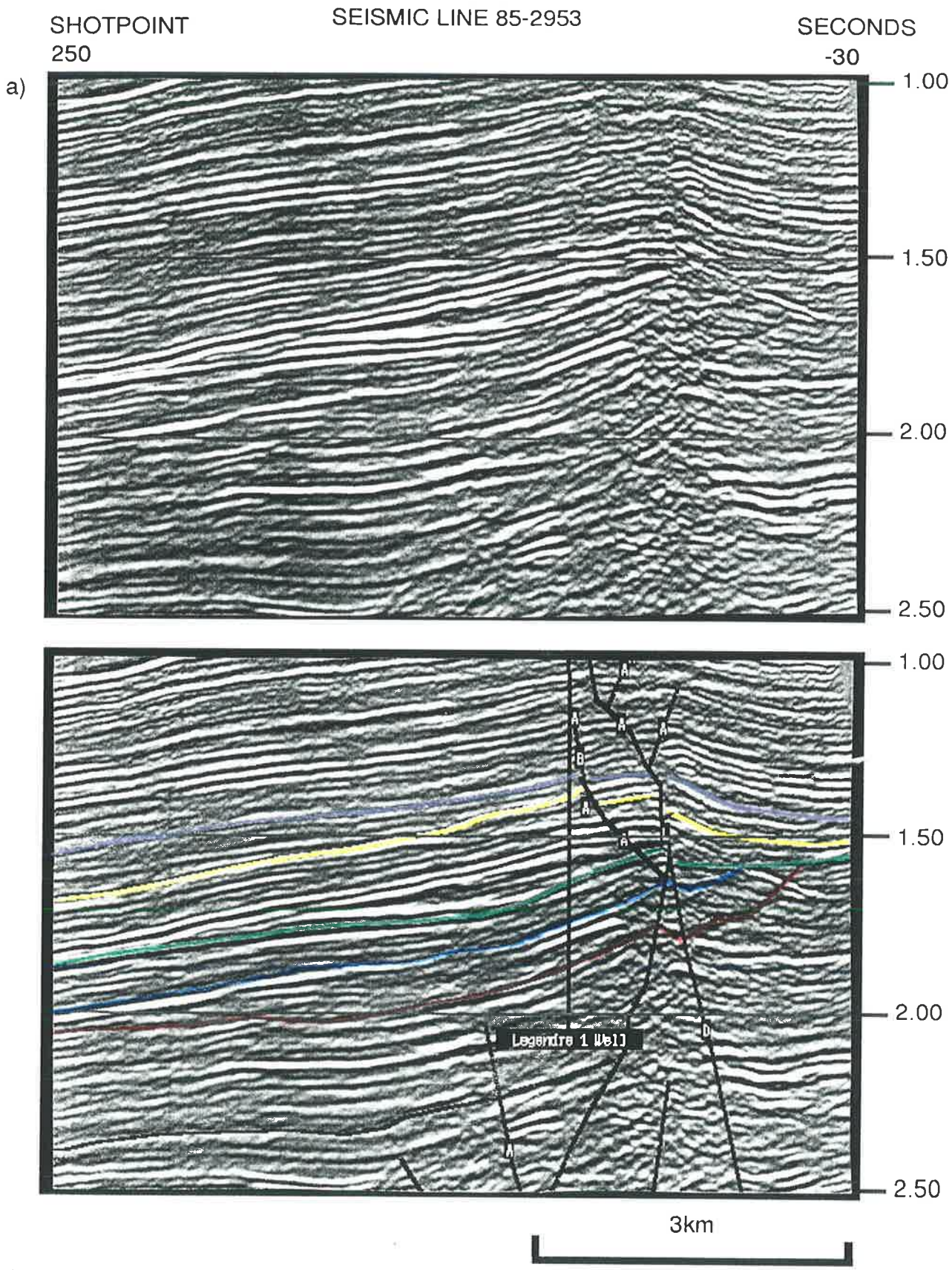


Figure 4.66. a) uninterpreted; and b) interpreted seismic examples near Legendre. Note the interpreted headward erosional surface to the immediate right of fault trace labelled 'L'. It is interpreted that formation of this surface occurred contemporaneously with active normal fault movement during Eliassen Formation time and continued to Angel Formation time when basin filling occurred. See text for further explanation. See Figure 4.67 to view this example flattened on the Valanginian Disconformity. Refer to Figure 4.60 for example location. Valanginian Disconformity - purple; Horizon 'A' - yellow; Horizon 'G' - green; Horizon 'H' - blue; Horizon 'I' - red. See Enclosure IVj) for position on seismic section.

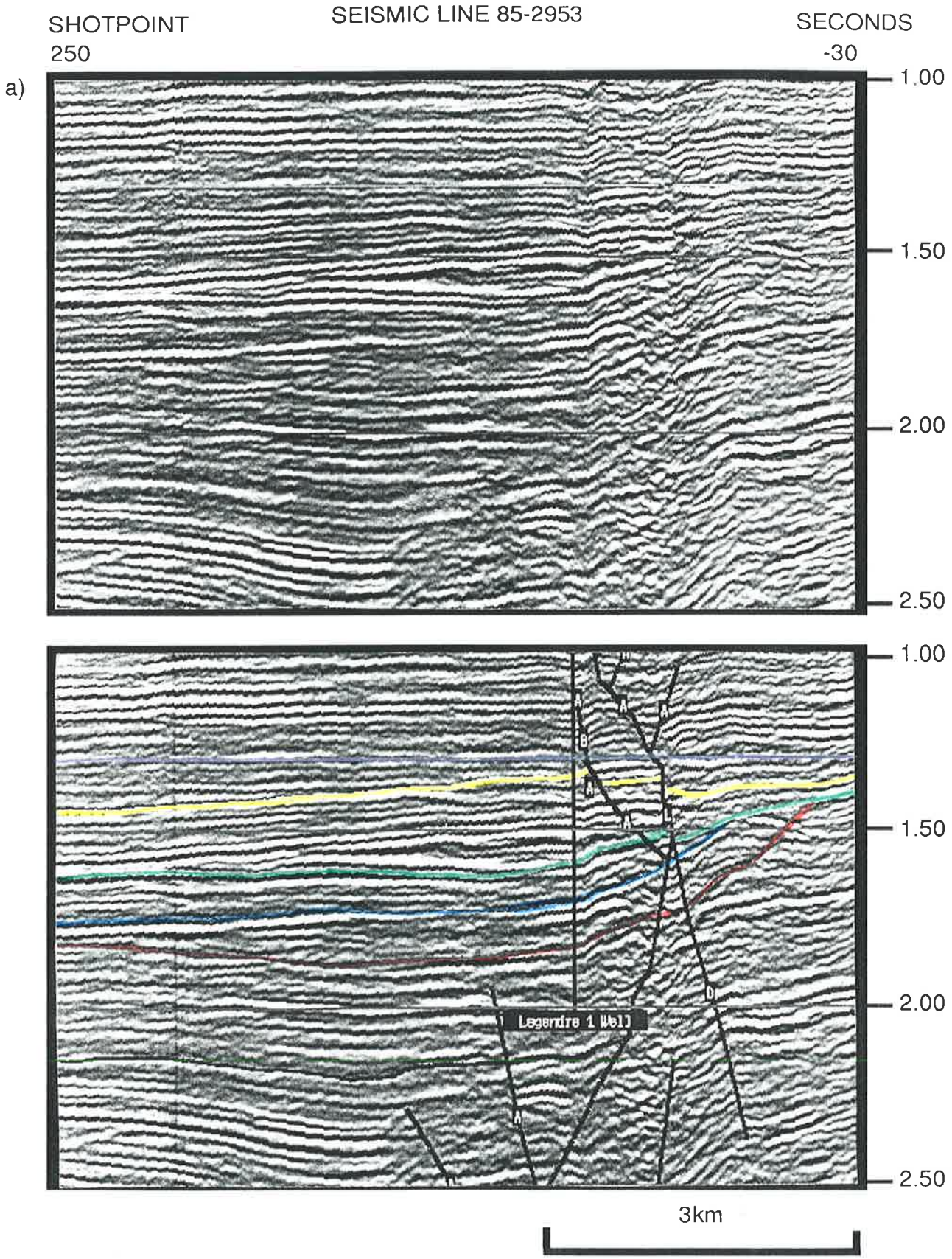


Figure 4.67. a) uninterpreted; and b) interpreted seismic examples flattened on the Valanginian Disconformity. Note the interpreted headward erosional surface to the immediate right of fault trace labelled 'L'. It is interpreted that formation of this surface occurred contemporaneously with active normal fault movement during Eliassen Formation time and continued to Angel Formation time when basin filling occurred. See text for further explanation. See Figure 4.66 to view this example unflattened. Refer to Figure 4.60 for example location. Valanginian Disconformity - purple; Horizon 'A' - yellow; Horizon 'G' - green; Horizon 'H' - blue; Horizon 'I' - red. See Enclosure IVj) for position on seismic section.

A headward erosional surface, or 'degraded footwall crest' (Prosser, 1993) can be observed adjacent to these formations in the hanging-wall block. The effect of most of the transpression-related anticline was removed by flattening on the Valanginian disconformity (Figure 4.67). The flattened seismic example allows an interpretation where synsedimentary headward erosion and normal fault displacement occurred on the Rosemary Fault during deposition of the Eliassen Formation. Subsequently, during deposition of the Angel Formation, lower relief headward erosion can be observed to onlap the erosional surface. The effect of pre-Valanginian compression can be removed by visually flattening the top of the Angel Formation horizon (Horizon 'A'). This onlap would appear to be more like uplap, and possibly represents a more realistic interpretation.

4.2.3 Conclusions

The Mesozoic stratigraphy of the Dampier Sub-basin can be closely related to the rifting and subsequent sea floor spreading events that occurred on the abyssal plains adjacent to the North West Shelf. In stating this, it must be taken into account that there was an established basin fault system and depocentre related to earlier rifting events that was inherited by the middle Jurassic rifting event. The use of tectonic systems tracts helps to demonstrate the relationship between the stratigraphy and the tectonic development of the area. It is suggested that all basins of the North West Shelf should be described in terms of tectonic systems tracts, also keeping in mind the major structural differences that are associated with upper and lower plate rifted margins of the Lister (1991) detachment models as suggested by Stagg (pers. comm., 1993) and O'Brien (1993).

This section demonstrates the close association between the stratigraphy of the Dampier Sub-basin and the stage of rifting and basin development. The Calypso Formation can be described as an early rift climax systems tract. The two defined units of the Eliassen Formation can be placed into the mid rift climax and late rift climax systems tracts, respectively. The Angel Formation can be described in terms of basin filling during the immediate post rift systems tract. This progression of basin filling is reflected by the progressive style of the depositional systems of the Angel Formation as discussed in the previous section. The interpretation of a fault scarp (i.e. the Rosemary Fault) bordering the Angel Formation is masked by the compression-related anticlines that occur along the Legendre Trend (e.g. Figure 4.66).

The implications of the transpression-related anticlines of the Legendre Trend with respect to oil exploration are significant. They have been the target of most drilling sites along the Legendre Trend and the source of only two discoveries (Talisman Field and Legendre 1). The primary reason for the large number of dry wells along the Legendre Trend is likely to be the breach of seal by fault planes. It is suggested in this section that the timing of lateral fault movements also varied along the Legendre Trend. If the complex structural history of compressional and extensional episodes along the Legendre Trend was deciphered in detail, undrilled closures could then be assessed for any existing faults that may have breached the seal. A study of this type by Nelson (1993) considered the effect of successive fault abandonment and reactivation episodes on wrench and inversion structures in the Timor Sea Region.

By applying structural and stratigraphic concepts developed in this study, anticlinal structures may be assessed for reservoir and seal relationships. In doing so, it must be taken into account that syndepositional transpressional episodes would have effected palaeogeography and hence, sand body distribution. For instance, the closure of Horizon 'A' shown in Figure 4.64 warrants investigation with respect to hydrocarbon potential. This closure can be observed in plan view in Figure 4.36 (top Angel Formation Structure Map).

This chapter demonstrates that the 'break up unconformity', previously considered to be near Horizon 'I' or 'J', (near base Calypso Formation or base Eliassen Formation equivalents), actually corresponds to Horizon 'G' (155Ma; base Angel Formation equivalents). This was achieved using the latest known dating on sea floor spreading lineaments with what is considered the most accurate time scale (Harland, 1989). Horizon 'G' is the largest unconformity observed in this study. Previously studies have variably placed the break up unconformity near the base of *W. spectabilis* 'a' and also at the base of *W. digitata* palynozone, depending on which time scale and sea floor spreading dating references were used. It is suspected that these studies referenced the date of the break up unconformity and did not identify the associated unconformity. As demonstrated above, missing section that corresponds to either of these palynozones was not observed. In addition, rocks that lie above the 'break up unconformity' (Horizon 'G') identified in this study, contain palynological evidence that indicate erosion and resedimentation of sediment that is temporally associated with the succession below (Eliassen Formation).

While the effect of eustatic sea level may be overcome by structural movements in the rift initiation and rift climax systems tracts, some effect is expected to be observed within the immediate post-rift and increasingly in the late post-rift sedimentary section, according to Prosser (1993). In the late post-rift section, however, flooding surfaces are related to increased rates of thermal subsidence. The influence of eustacy is discussed in the section to follow.

4.3 GENETIC STRATIGRAPHY AND DEPOSITIONAL SURFACES WITH RESPECT TO SEDIMENT INFLUX, RELATIVE SEA LEVEL AND EUSTACY

4.3.1 Introduction

There is considerable confusion in the literature with respective uses of the terms 'relative sea level' and 'eustacy' (Posamentier and James, 1993; Weimer and Posamentier, 1994). Eustacy is a function of sea-surface movement alone with reference to some fixed point such as the centre of the Earth, while relative sea level is a function of sea surface and sea floor movement (Posamentier and James, 1993; Posamentier et al., 1988). Relative sea level, therefore, incorporates the effect of factors such as local tectonics, sediment influx and subsidence (this includes subsidence due to sediment compaction and loading, as well as thermal and regional tectonic factors). Eustacy is affected either by changes in the absolute volume of global ocean water or by the varying capacities of the oceanic basins of the world. These changes are considered to be caused by world-wide glaciation events, and sea floor spreading rates and times of plate divergence or convergence, respectively (Vail et al., 1984). Posamentier and James (1993) state: "relative sea level changes (regardless of the varying relative contributions of eustacy and tectonics) operating in concert with sediment flux and physiography are the primary control on the stratigraphic succession". With these definitions and concepts in mind, this section deals with the evidence for sediment influx variations and relative sea level changes. The previous section shows that there is a strong tectonic control on the stratigraphy of the Dampier Sub-basin. The effect of physiography was described in the discussion of depositional systems. Here, the relative sea level history of the Dampier Sub-basin (which is dominantly a result of the tectonic history) is described and the effect of eustacy and sediment influx on the stratigraphy is considered.

The Exxon approach divides eustatically driven sequences into systems tracts. The systems tracts are directly attributed to relative sea level (Van Wagoner et al., 1988), and are used within the terminology (e.g. lowstand systems tract, highstand systems tract). The use of these terms tend to implicate the influence of relative sea level into the description of any depositional system. This is misleading and introduces the need for more sequence stratigraphic nomenclature which is complicated and cumbersome. This is an issue that is discussed by Weimer (1992b). For example, a lowstand systems tract is usually perceived as a prograding wedge that occurs on a shelf edge. With this perception, it is differentiated from a highstand systems tract which is also a prograding wedge, but one which occurs on the shelf itself. These perceptions imply that the wedge formed as a result of change in relative sea level. Without considering the influence of tectonics, sediment supply and eustacy, it is wrong to implicate sea level at that point of the interpretation. There are many instances where this has been done with the interpretation of relative sea level carried through to the conclusion (e.g. Ross and Vail, 1994).

The *genetic stratigraphic* approach based on Frazier (1974) and introduced by Galloway (1989a,b) is used in this study. This approach has been combined with the Prosser (1993) approach of *tectonic systems tracts*. I have defined the *genetic stratigraphic sequence* in section 3.31 as defined by Galloway (1994). This contrasts with the *sequence stratigraphic* method of the Exxon group (e.g. Mitchum

et al., 1977; Vail et al., 1977; Van Wagoner et al., 1988) in many respects. While the chronostratigraphic framework of genetically related strata is applied in both methods, the Exxon approach places sequence boundaries at unconformity surfaces which are usually attributed to relative falls in sea level. The initial approach by Galloway subdivides the stratigraphic succession at condensed sections or maximum flooding surfaces (Galloway, 1989a). It accounts for the varying significance of depositional surfaces in different depositional settings. No particular attribute, whether a sequence is tectonically, eustatically or sediment driven, is held accountable without considering the influence of all the variables. These factors are considered to account for the relative changes in accommodation space observed in the sedimentary record.

The effective 'systems tract' used here is the 'depositional system' which consists of various combinations of 'depositional elements'. A particular depositional system is defined within the description of the system itself in a qualitative fashion by using depositional elements. Depositional elements are themselves defined from the available data and are based on the available evidence for depositional processes, relative basinal position, depositional architecture and changes in accommodation space. These depositional elements can be used flexibly and are intended to encompass a spectrum of architectural and process related possibilities that are suitably defined for the style of basin and depositional setting of the Dampier Sub-basin. The focus is on depositional system geometry and no explicit reference to sea level is implied. Only after the complete depositional systems are described and qualified are the effects of tectonics, eustacy, relative sea level and sediment source considered here. In addition, the concept of parasequences (which also introduces another extensive array of complex and rigid terminology) was not adopted in this study. The nomenclature is not practical for marine resedimented depositional systems in rifted margin basins. Indeed, the identification of parasequences was not even achieved on seismic by Weimer (1990) in a study of the Mississippi Fan.

There is enough criticism in the literature to suggest that the eustatic sea level curve published by Vail et al. (1987, 1977) should not be used in many settings, particularly active rift basins. Some of these papers include Miall (1986, 1992), Hubbard et al. (1985a,b) Hubbard (1988), Boyd et al., (1989), Walker (1990), Weimer, (1992a,b) and Sloss (1988). In addition, Cartwright et al. (1993) scrutinise the validity of using onlap and downlap surfaces as discrete surfaces that may be regionally correlated as single chronostratigraphic surfaces. These papers contain many valid, although in some cases contentious, criticisms of the sequence stratigraphic method and in particular, use of the eustatic sea level chart. For example, Sloss (1988) stated: "I persist in the claim that cratons, their margins, and their interior basins do not just lie there passively waiting to be encroached upon by rising sea levels or laid bare to erosion as sea levels fall. Students and practitioners of sequence stratigraphy are, for better or worse, recorders and interpreters of tectonic evolution." I agree with many of the arguments that refute this chart, and so it is included on two stratigraphic sections (Figures 4.68, 4.69) to analyse any correlation or significance the chart has.

In fact, it can be shown that many correlations with the 'Vail' sea level curve are simply 'playing the odds' in the sense that there are sequence boundaries not justified by high resolution biostratigraphy for age dating. The age of any identified surface based on the available data in an area is usually arbitrary enough to be able correlate

it with one of the existing sequence boundaries on the eustatic sea level chart. For example, Labutis (1994) stated: "fewer sequence boundaries, mainly in the middle Cretaceous, could be found in the North West Shelf basins than are presented on the Haq et al. (1988) chart, and it was difficult to identify which of them were actually represented, because of the lack of ties with various zonations." The same result could have been achieved if eustatic sequence boundaries were located by random number generation. With statements similar to the one above recurring in the literature on the use of the eustatic sea level chart, it can be argued that attempts to correlate with it are highly subjective.

The use of geological time scales and age dating

The use of alternative Geological Time Scales on the North West Shelf has caused considerable confusion when attempting to correlate events on a regional and global scale. The standard method of relative age dating of rocks on the North West Shelf is the Dinoflagellate Zonation Scheme of Helby et al., (1987). There is no other retrievable fauna or flora that has successfully been obtained and dated for the Jurassic to middle Cretaceous from wells on the North West Shelf. For this reason, the Dinoflagellate Zonation Scheme has become a relatively informal industry standard on the North West Shelf. Unfortunately, this zonation has been applied to various time scales and has also been allocated to them in various manners. At a time when the Harland (1982) Time Scale was widely accepted in Western Australian studies, the dinoflagellate zonation was correlated by Helby et al. (1987) to this time scale. Almost immediately following this, Haq et al. (1987) published a global cycle chart on a time scale of their own which included biochronostratigraphy. The purpose of this chart was to show the age correlation of the Exxon group's global sea level curve to world biochronostratigraphy and standard chronostratigraphy. Unfortunately, this chart did not include Australian biostratigraphy. To rectify this, an unpublished version of the 'Haq' cycle chart was produced by Partridge and Helby (1988) which included the Australian Biostratigraphy with the Dinoflagellate Zonation Scheme. Due to the popularity of sequence stratigraphy at the time, and the desire to correlate with this cycle chart, many industry geoscientists began to use the Haq scale instead of the older but already accepted Harland (1982) scale.

The significance of the use of the varying time scales on the North West Shelf has immense ramifications when attempting to tie in events which are based on absolute age. For example, there is an approximate 13Ma discrepancy at the Jurassic - Cretaceous boundary between the two scales (e.g. compare Figures 4.68 and 4.69). Attempting to tie in sea floor spreading events such as the break up of the Argo Abyssal plain varies from Kimmeridgian to Callovian in age, depending on which time scale is used. This has dramatic effects on how the geology of an area is interpreted, as discussed in the previous section.

The Harland (1989) Geological Time Scale is adopted here because it is considered to be the most accurate time scale in use on the North West Shelf. For your interest, this scale is annotated with the Haq et al. (1987) eustatic curve. This chart has been modified from the Harland (1982) scale according to more recent absolute age dating and relative age dating from macrofossils. The new stage ages vary by less than one to three million years from the older version, and ages are defined to one decimal place. The most notable variation occurs in the Kimmeridgian to Callovian

succession. Previously a duration of 19Ma, it now represents a duration of 14Ma on the Harland (1989) scale. The shorter time period over this interval better explains the sediment accumulation rate of the mid-rift tectonic systems tract discussed in the previous section. This duration is equivalent to 17Ma on the Haq et al. (1987) scale.

In order to apply the Harland (1989) time scale to North West Shelf biostratigraphy, the dinoflagellate zonations were taken from Partridge and Helby's (1988) correlation to the Haq time scale and annotated to the Harland (1989) scale according to relative age correlations, not absolute age correlations. Furthermore, each dinoflagellate zone was allocated to an age ensuring that they took up the same relative position in the stage, and proportionately, the same length of relative time of the stage. This method was supported by Roger Morgan (pers. comm., 1993) after discussion.

The use of the Harland Chart on the North West Shelf is further supported from recent absolute age dating on the North West Shelf. Bint and Marshall (1994), and di Toro (1994) dated zircon from an ash bed in Wanaea 2 core. The ash bed occurs at the *K. wisemaniae - P. iehiense* boundary. The authors, however, failed to state what the absolute age of these zircons were calculated to be, possibly for reasons of confidentiality. However, Bint and Marshall's Figure 7 (p. 551) shows that the ash bed correlates to 145.6Ma using the Harland (1982) scale. It is presumed that 145.6Ma is approximately the absolute age of this bed. Another instance of absolute dating was performed by AGSO using the Sensitive High Resolution Ion Microprobe (SHRIMP) dating technique. Samples that occurred within a good controlled *K. Wisemaniae* Zone provided a reliable absolute age of 141Ma (Labutis, 1994). This date corresponds to the top of *K. Wisemaniae* Zone on the scale used in this study (see Figure 3.13). These two investigations strongly suggest that the Harland time scale, whether the 1982 or 1989 version, is the more sensible time scale to use on the North West Shelf rather than the Haq et al. (1987) scale.

In addition to the problems association with the use of various time scales on the North West Shelf, there is further complications arising from correlation of the Dinoflagellate Zonation Scheme to any of the geological time scales which are all based on North American and European biostratigraphy. Presently, there are two variations in existence. The first correlation that I believe came into existence allocates the *C. delicata* Zone to the Lower Berriasian. The second correlation, and this is the one that I use for this study, allocates this zone at the Valanginian - Berriasian boundary (Figure 3.13). As a result, the dinoflagellate zones are shifted upwards in relation to the Stages. Frustratingly, both of these correlations are presently in use by various authors, along with the alternate use of the Haq et al.(1988) scale and the Harland 1982 and 1989 scales. The result is that there is four variations of geochronostratigraphy used in the literature (see Table 4.3). This does not include the variations of the alternate Harland 1982 and 1989 scales. The effect of shifting the dinoflagellate zones relative to the Stages (based on biozones), is that it alters the correlation to chronological events based on absolute age such as magnetic lineaments related to sea floor spreading, as well as the eustatic sea level curve. This effect is demonstrated by the example previously described, with the *C. delicata* zone representing an effective shift of an apparent 4Ma in absolute time. The shift of Dinoflaggelate zones with biozones makes the correlation with eustatic sequence boundaries (on average 1Ma duration) meaningless (e.g. See Wulff 1992, his Figure 2; Barber 1994, his Figure 6; Figures 4.68 and 4.69, this study). In

addition, this variation does not include the error margin of tying the eustatic chart with a time scale.

Study	Harland Scale (1982, 1989); 1987 Helby et al. palynology to Stage assignments	Haq Scale (1988); 1987 Helby et al. palynology to Stage assignments	Harland Scale (1982, 1989); New palynology to Stage assignments	Haq Scale (1988); New palynology to Stage assignments
Wulff (1992)	X			
Hocking (1992)			X	
Barber (1994)				X
Labutis (1994)	X			
Robinson et al. (1994)				X
Messent et al. (1994)				X
Ross & Vail (1994)		X		
Bint & Marshall (1994)	X			
Boyd et al., (1993)		X		
This Study			X	

Table 4.3. List of authors for various selected sequence stratigraphic studies on the North West Shelf. The particular geological time scale and the palynological to Stage assignment that was used for each study is indicated. See text for discussion.

The varying allocations of the Dinoflagellate Zonation Scheme to the Stages were discussed with Morgan (pers. comm., 1994) and Partridge (pers. comm., 1995). Although neither could give a satisfactory explanation as to how these two correlations arose, Partridge stated that "it reflects the element of slop involved in the uncertainty of attempting to correlate Australian biostratigraphy to time scales which are based on northern hemisphere macrofossil assemblages", and "although the tenacity of this correlation exists, the Dinoflagellate Zonation Scheme has excellent reliability when the scheme itself is used as the benchmark for correlation purposes on a regional scale" (two statements firmly agreed herein).

It is thought that these two variations in correlation of the dinoflagellate scheme to time scales arose by the following instances. The first correlation was obtained by an attempt to associate the scheme from the original Helby et al. (1987; based on the Harland, 1982 scale) scale to the Haq et al. (1987) scale according to relative position and duration with respect to Stages. The second correlation was obtained when Morgan and Partridge (1988) made a direct correlation to the Haq et al. (1987) scale which was independent of their primary correlation to the Harland (1982) scale. For the purpose of this study, the second correlation was compared to the Harland (1989) scale using the relative stage association method outlined above. This correlation is supported by Hocking (1992), and Morgan (pers. Comm., 1994) agreed that this version is 'likely' the most accurate. Indeed, the absolute age date obtained by AGSO of the *K. wisemaniae* Zone of 141Ma, as discussed previously, agrees exactly to the correlation used on the Harland (1989) scale (see Figure 4.69, position of Horizon 'A').

Ross and Vail (1994) discuss the tenacity involved in correlating Australian biostratigraphy to European biostratigraphy and do not offer a definitive answer. They, however, mention that a new version of the global cycle chart is in progress. On publication of this chart, it is suspected that another attempt will be made to correlate Australian biostratigraphy to geological time scales that are based on biostratigraphy in the northern hemisphere.

Comparison of sequence definitions

Figure 4.68 shows a comparison of units defined in this study with defined sequences of Barber (1994), Hocking (1992) and Wulff (1992) and eustacy. The work by Hocking is a regional study that includes many wells from both the Barrow and Dampier Sub-basins. The Haq et al. (1987) scale was used to so that the variation with the Harland (1989) scale can be observed. Since each of the studies is based on dinoflagellate zones, the use of a different time scale does not change the correlation of the variously defined sequences. It is assumed that each author would identify the same or similar correlatable event markers, regardless of the geological event. The statement by Hocking (1992) likely applies to most sequence stratigraphic interpretations: "In selecting and carrying marker horizons on electric logs, sequence stratigraphic concepts (as outlined by authors such as Haq, Van Wagoner, Galloway, Posamentier, Vail and Loutit) have been born in mind and used where possible, but ultimately a more pragmatic, empirical approach has been used in most areas for reasons of scale and available time." Assuming that most authors would agree with this statement, it is reasonable to presume that many existing markers would have been picked by more than one author, albeit with minor subjectivity.

Horizons 'K', 'I', 'F', and 'E' correlate exactly with some of the sequence boundaries defined by Barber (1994). Remarkably, three of these four horizons correlate exactly with eustatic sequence boundaries (the 160, 150.5, and 136Ma eustatic sequence boundaries). The correlation of Horizons 'G', 'C', and 'A' are also in the vicinity of sequence boundaries defined by Barber. In this case, two of these horizons defined by this study agree exactly with horizons defined by Hocking (1992). Interestingly, in each of these cases, Barber's sequence boundaries all agree exactly with the eustatic sequence boundaries. In addition, there are five remaining sequence boundaries that Barber defined which were not identified as horizons by this study, or by Hocking. However, all of these sequence boundaries agree exactly to eustatic sequence boundaries (the 144, 142, 134, 126, and 123.5Ma).

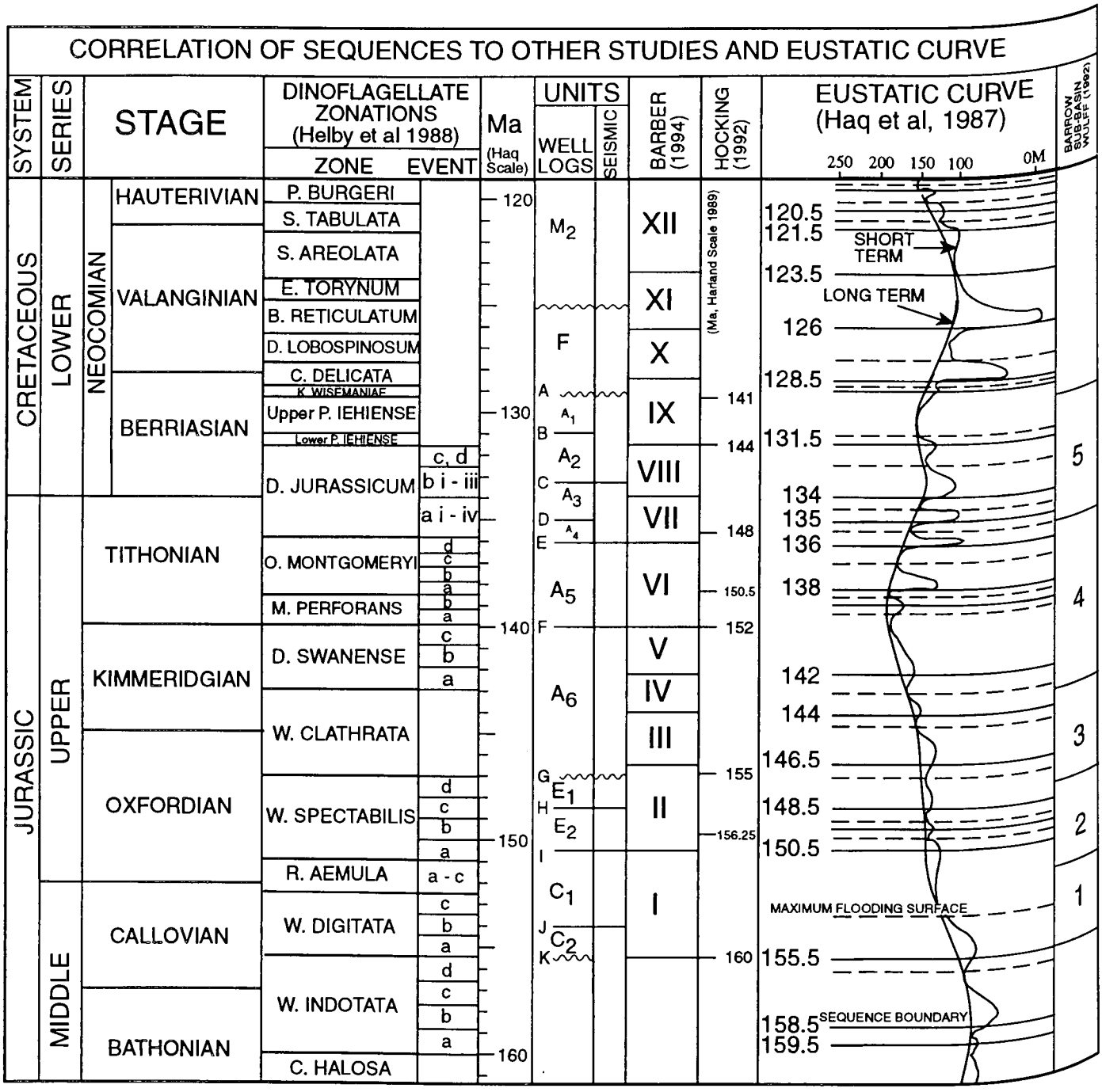


Figure 4.68. Comparison of the defined sequences from this study and those of other projects in the Barrow and Dampier Sub-basins. Note that this time scale is the Haq (1987) scale, and it is not the one used for this study.

There is considerable agreement in the definition of my horizons with those of Hocking. Many correlate exactly (i.e. his 160, 155, 152 and 141Ma horizons), and some show minor discrepancy (i.e. his 156.25, 148, and 144Ma Horizons). On the contrary, he defined a 150.5Ma event not recognised in this study, while Horizons 'C' and 'D' were not recognised by Hocking. That these minor variations may be primarily attributed to different data sets, as Hocking's work includes wells of the Barrow Sub-basin.

The event definitions by Wulff (1992), including the eustatic curve, show poor agreement with those of the other authors. His work was confined to an area within the eastern Barrow Sub-basin. This relative disagreement is probably also constrained by the regional and data set variations of the areas. It is very interesting to note, however, that some of Wulff's boundaries coincide with consecutive tectonic systems tract boundaries (e.g. Wulff's base of sequence 1, top of sequence 2, top of sequence 5; Rift Initiation - Rift Climax, Rift Climax - Immediate Post-rift, Immediate Post-rift - Late Post-rift, respectively). This strongly suggests an excellent regional correlation of these tectonic systems tracts.

Labutis (1994, see his Figure 2, p. 162-3) introduced names for sequences which were intended to be applied to sequence stratigraphic studies on the North West Shelf. The sequence names were adopted from some of the dinoflagellate zones over the relevant section. Labutis defined these sequences from an unlisted database of wells from the Exmouth Plateau and Barrow Sub-basin as well as some other wells over the North West Shelf. Some of the sequences appear to have been derived from previously defined type sections in the literature on specific areas (e.g. Arditto's 1993 description of the Zeepard and Birdrong sequences). The sequences defined by Labutis do not agree with any of the events detailed in Figure 4.68. This disagreement, in addition to the correlation discrepancies between Wulff's Barrow Sub-basin sequences and sequences of the Dampier Sub-basin (Figure 4.68) indicates there is no regional correlation of 'third order sequence boundaries' on the North West Shelf, as interpreted by Labutis. While there may be some correlation on the North West Shelf at the 'supercycle' scale as previously suggested, the disagreement of Labutis's sequences to those events shown in Figure 4.68 is significant. This clearly shows that there is no regional significance of third-order sequences on the North West Shelf. To evaluate any significance of regional third-order sequences would require the definition and association of 'supercycles' or 'tectonic systems tracts' over the North West Shelf. The third-order sequences would then have to be defined independently from data sets with good control (i.e. good quality seismic with good coverage and abundant well control) in each of the North West Shelf basins or sub-basins. Individual comparisons of individual 'third-order sequences' between any two regions and their significance could then be evaluated.

4.3.2 Discussion

The interpreted variations in relative sea level with respect to this study with the 'Vail' eustatic chart are shown in Figure 4.69. The following is a discussion of depositional surfaces and the significance of interpreted relative sea level with respect to the depositional units and related horizons. Refer to Figure 4.70 for the stratal relationships of depositional horizons, and the architectural relationships of depositional elements. The details of the stratigraphy with respect to depositional systems, tectonics, sediment influx and eustacy are summarised in Table 4.4.

Early Rift Climax

Horizon 'K' forms the boundary of the non-marine to brackish Legendre Formation equivalents and the generally nearshore marine Calypso Formation equivalents, as indicated by palynological environmental indicators. This surface occurs at 160Ma within the lower part of the '*W. digitata* 'a' zone. Although this horizon was not mapped due to the lack of well control, the contact was penetrated by Calypso 1, Legendre 2, Samson 1 and Rosemary 1. There is no missing section noted in any of these wells. The nature of the contact is very similar in these wells, each revealing a significant sonic break from wire line logs. In addition, a consistent 15 to 20m thick, interpreted transgressive sand occurs at the base of the Calypso Formation in each case. This surface is considered to be a 'ravinement' surface owing to marine incursion. It is attributed dominantly to tectonics as it marks the boundary between the rift initiation and rift climax systems tracts. It is interpreted that, at this time, half graben movement on the Rosemary Fault commenced relative to the northwestern side of the basin. The resulting increase in subsidence outpaced sediment accumulation and produced enough accommodation space for the marine incursion. While uplap predominated on the developing Rosemary scarp, onlap was occurring on the northwestern margin of the basin (Kendrew Trough region), owing to sediment starvation and the relative lack of accommodation space.

Horizon 'J' marks the onset of a second successive marine deepening event. This horizon was interpreted at the base of condensed sections, (e.g. Rosemary 1), and near the base of intervals of high value gamma ray spikes, very fine-grained sandstones, siltstones and mudstones. The high gamma ray spikes are possibly the result of minerals with volcanic affinities. It is likely that these minerals reflect the sediment provenance, which may be the Permian volcanics observed in some wells on the Enderby Platform. Petrological work would be required to assess this possibility. Attempts at correlating a maximum flooding surface near this horizon, as well as other horizons associated with transgression, (e.g. Horizon 'A', Valanginian disconformity) proved too difficult to produce a satisfactory chronostratigraphic horizon. Flooding surfaces associated with various stages of apparent transgression and subsequent high sea level appear to have varying significance over proximal and distal portions of the region. Better results were achieved by correlating the event with the first indication of marine flooding. This surface is time equivalent to any associated ravinement surface and mass wasting apron (Galloway, 1994). In this style of depositional setting, there is considerable sediment starvation occurring within the basin and uplap, as opposed to onlap, occurs at the basin margin. Here, the onset of any transgression (i.e. first flooding surface) is a more satisfactory surface to

follow rather than any interpreted 'maximum flooding surface'(see Figure 4.70). This is similar to the methods used by Embry (1993) and Johnson et al. (1985), where the transgressive surface forms the boundary of the 'T - R sequence' for regional basin analysis studies.

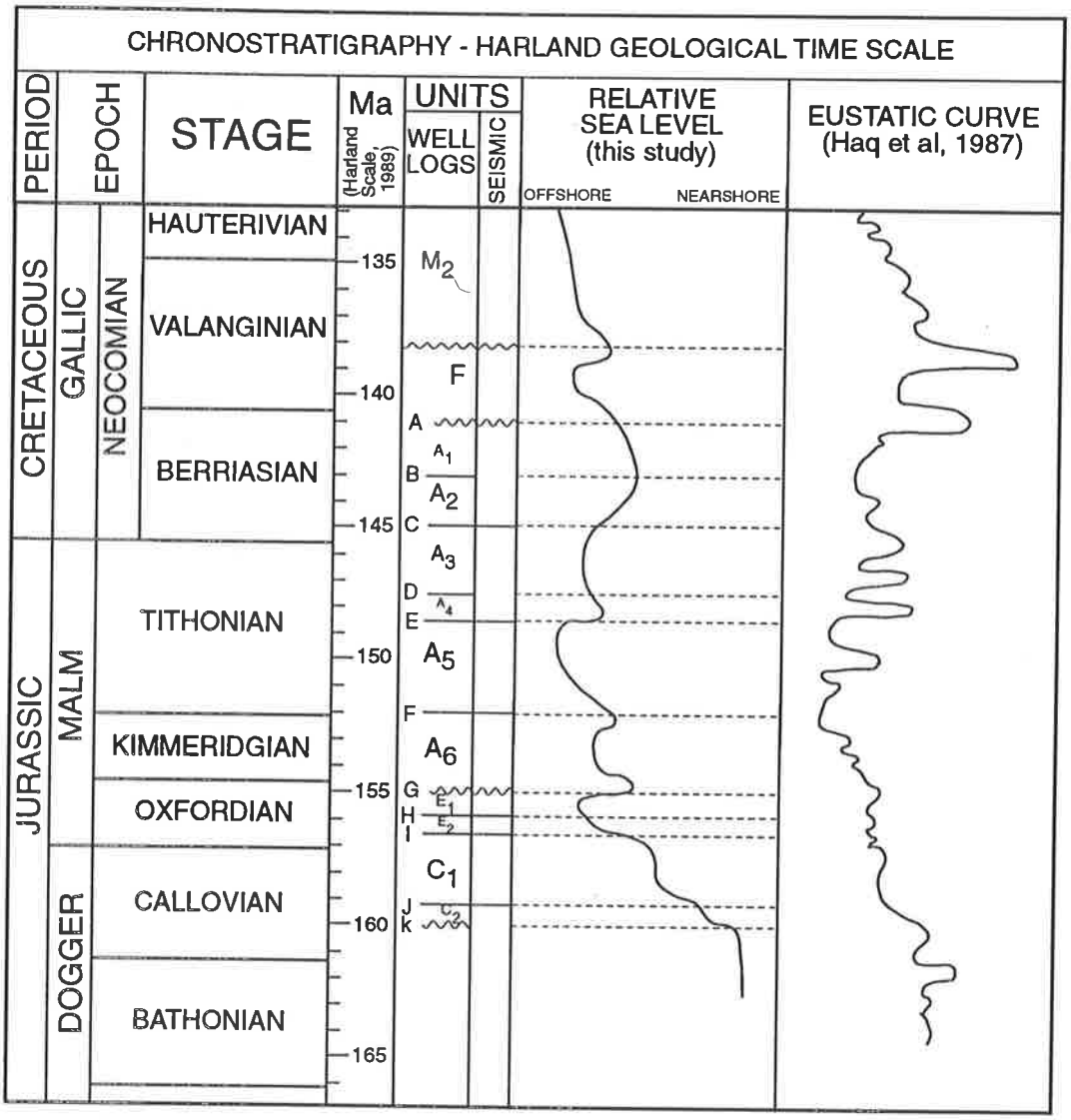


Figure 4.69. The interpreted relative sea level history for the Dampier Sub-basin with respect to the genetic units of this study. The eustatic chart is included for an objective comparison.

Unit	Tectonic Systems Tract	Tectonic Events	Basal Surface	Net Accom.	S : Q	Relative Sea Level	Depositional Systems	Typical Stratal Configurations	Rating
UP. CRET	Passive Margin		TSE						EQT
M1/2	Late Post Rift	thermal subsidence	TSE	+	S>Q	rising/ stillstand	transgressive shelf sands, hemipelagic drape	onlap, parallel, continuous	ETQ
F	ditto	ditto	TSE	+	S>Q	rising/ stillstand	upper slope apron, channel fill, hemipelagic drape	ditto	ETQ
A1	Immediate Post Rift	basin-ward tilting	aggradation	-	S<Q	stillstand	retrogradational ramp: depositional lobe massive sands, sheet sands, contourites	ditto	QET
A2	ditto	ditto	LSE/ aggradation	-	S<Q	falling	ramp: depositional lobe massive sands, sheet sands, distal turbidites	convergence, parallel, asymptotic downlap	QET
A3	ditto	ditto	aggradation	-	S<Q	stillstand	sheet sand lobes, distal channels and turbidites, hemipelagic drape	convergence, parallel, asymptotic downlap	QET
A4	ditto	ditto	aggradation /LSE	-	S<Q	falling	recessive style slope aprons, channel-lobe complexes	convergence, parallel, asymptotic downlap, mounding	QET
A5	ditto	isostatic uplift	TSE	-	S<Q	rising	slope aprons, channel -lobe complexes	convergence, mounding, asymptotic downlap, incised channel fill clinoforms, high amplitude anomalies	QET
A6	ditto	breakup; isostatic uplift,	LSE	--	S<Q	falling	ditto	ditto	TQE
E1	Late Rift Climax	half-graben formation	aggradation	+	S>Q	stillstand	levee complexes, distal turbidites, hemipelagic drape	uplap, parallel, continuous	QTE
E2	Mid-rift Climax	ditto	downlap	++	S>>Q	rising	slope aprons, muddy turbidites, contourites, hemipelagic ponding	uplap, mounding, convergence, high amplitude anomalies	TQE
C1	ditto	ditto	TSE	+	S>Q	rising	undifferentiated aggrading shelf	onlap, uplap, parallel, continuous	TQE
C2	Early Rift Climax	ditto	TSE	+	S> Q	rising	ditto	ditto	TQE

Table 4.4. Summary chart of variables for sequence stratigraphy of the Dampier Sub-basin. TSE - transgressive surface of erosion; LSE - low-stand surface of erosion; '-' - decreasing accommodation; '+' - increasing accommodation ('++' - highly); S - subsidence; Q - sediment influx. The rating is a relatively subjective determination of the order of priority of factors, where T - tectonic influence; Q - sediment influx; E - eustacy. See text for discussion.

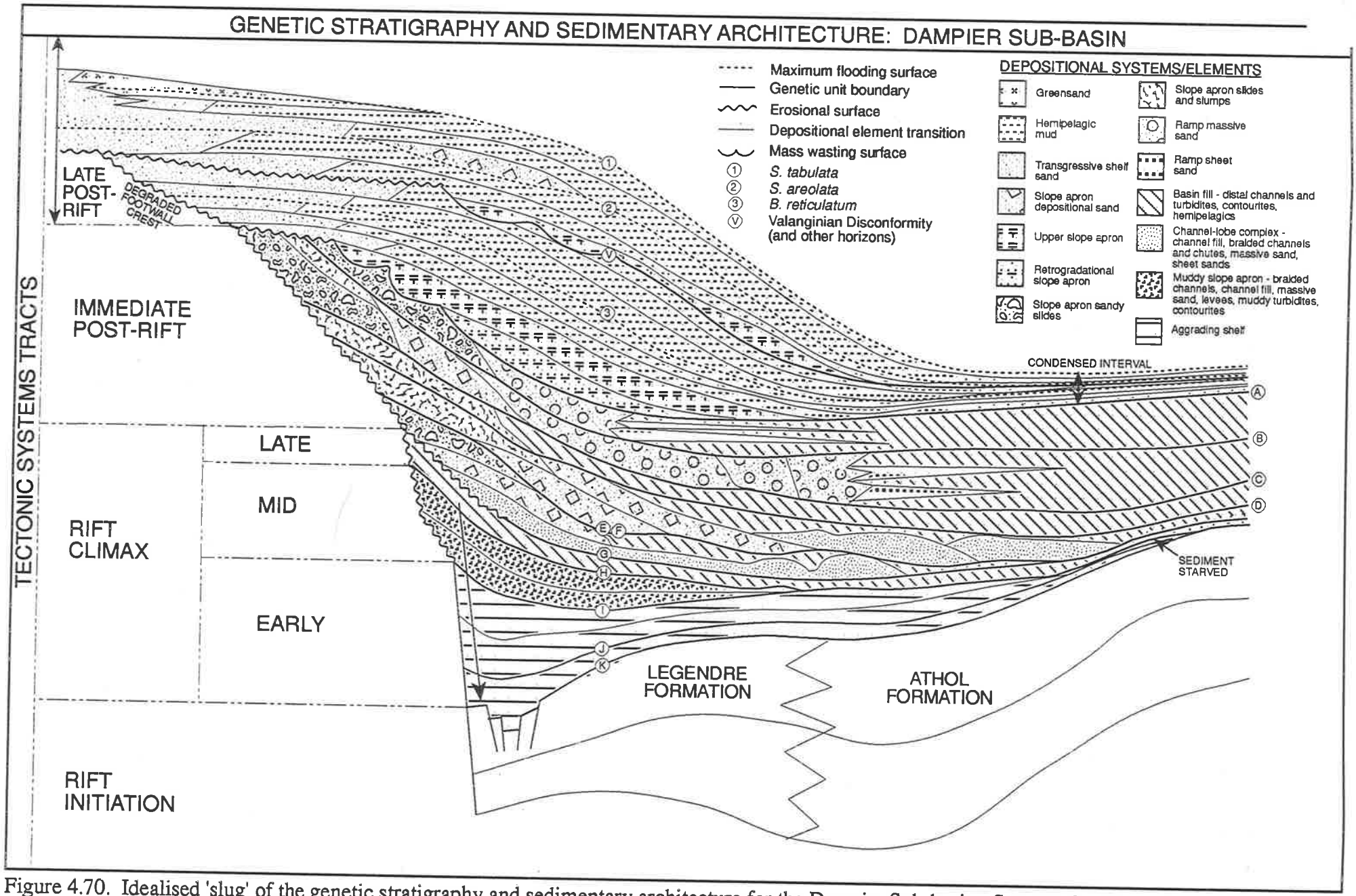


Figure 4.70. Idealised 'slug' of the genetic stratigraphy and sedimentary architecture for the Dampier Sub-basin. See text for discussion.

Horizon 'J' is considered to represent a second 'phase' of marine flooding. With the data available, it is difficult to reflect on which interplay of factors (tectonic subsidence, eustacy, or sediment influx) had the dominating influence on the rise in relative sea level. This surface correlates very closely to the onset of flooding on the eustatic chart (Figures 4.68, 4.69). Indeed, Prosser (1993) attributes any discernible cyclicity or reflection stacking to higher frequency successive faulting increments. Any indication of the effect of eustacy (if preserved) more likely to be recorded near the margin of the rift close to the hinge line. This horizon, unfortunately, has not been intersected by any wells in the region of the hinge line.

Unit C2 of the Calypso Formation interpreted from core, well logs and palynology, displays characteristics of an aggrading shelf. Small scale 'footwall fans' and 'talus cones' (Prosser, 1993) would be subjected to marine currents induced by storms or long shore drift. This marine reworking would result in sediment peneplanation of any topography resultant of gravity style sedimentation. Cores 1, 2 and 3 from Rosemary 1 reveal lithologies and bioturbation that indicate an upward-deepening marine succession. Also, core 1 contains septarian nodules which may provide evidence for fault movement related stresses occurring shortly after sedimentation. It is suggested that the unit was subjected dominantly to sediment aggradation accompanied by minor transgression owing to subsidence slightly outpacing sediment supply.

Mid to Late Rift Climax

The base of the Eliassen Formation equivalents coincide with the change from nearshore to offshore palynological indicators in many wells (e.g. Samson 1, Rosemary 1, Lewis 1). Interestingly, transgression is noted to occur over the *W. Spectabilis* zone, as a transition from nearshore to offshore palynological indicators is noted in Madeleine 1, Angel 3, Calypso 1, Lewis 1 and Legendre 2. Nearshore indicators occur in Legendre 1 (Morgan Palynological Reports, 1987 -1993). No missing section was observed at the base of the formation. Some of the nearshore interpretations may be due to the influence of resedimentation from shallow to deeper water. However, the section in Calypso 1, which is relatively condensed, provides good evidence for a relative rise in sea level. In addition, Angel 3 occurs near the hinge line of the half-graben development, and shows this transition abruptly at horizon 'H', possibly reflecting eustacy.

The base of the Eliassen Formation equivalents are interpreted to mark an event of increased half-graben fault movement, the main cause of sudden sand influx into the basin. Slope Apron of depositional systems contained braided channels, levee complexes, and discrete massive sand bodies. Distally, these systems contained muddy turbidites, contourites and hemipelagic ponding. This sudden increase in fault movement may have been accompanied by a rise in sea level (possibly eustatically induced) on developed scarps or narrow margins on the footwall. The submergence of this area of relatively high gradient may have resulted in submarine erosion and subsequent resedimentation as slope apron deposits. Prosser (1993) suggested that the onset of the mid-rift climax systems tract (corresponding to the base of the Eliassen Formation) is associated with transgression of the hangingwall.

The boundary of the mid-late rift climax systems tracts is associated with the transition to sediment draping, pelagic fall-out, and distal style turbidites (Prosser, 1993). Indeed, unit E1 of the Eliassen Formation is mud dominated, with wide-spread deposition of Contourites and/or Levees, and Hemipelagic Basin Fill depositional elements. Ultimately the exact timing of this transition is likely to be dependent on the interplay of eustacy and sediment influx. Keeping in mind that this horizon was initially identified on seismic, and later found to be a chronostratigraphic surface through well ties, it is a relatively subtle event in well log profiles. This event is attributed mainly to the onset of a static relative sea level with a reduced sediment supply.

Immediate Post-rift

An unconformity that is attributed to submarine erosional processes occurs at the base of the Angel Formation equivalents (Horizon 'G'). It is represented on seismic by erosional truncation of unit E1 in many wells along the Legendre Trend. This unconformity is associated with the breakup and onset of sea floor spreading in the Argo Abyssal Plain. A relative fall in sea level can be directly attributed to isostatic uplift as a result of this event. Offshore palynological indicators of the overlying succession occurs in all wells within the study area. These offshore conditions were fully established during the deposition of units E1 and E2.

Slope aprons and channel-lobe complexes developed during deposition of units A5 and A6. These sediments would have been sourced by headward erosion of the previously developed Rosemary Fault scarp or 'degrading footwall crest' (Prosser, 1993), in addition to terrestrial input from the Enderby Platform. The boundary of these units (Horizon 'F') is considered to be the result of a relative sea level rise which caused more footwall derived section vulnerable to submarine related erosional processes. A considerable amount of topography is considered to have been degraded, effectively lowering the depositional gradient of the margin during this period.

The onset of deposition of unit A4 is attributed to a relative fall in sea level. In contrast to Horizon 'F', Horizon 'E' may be attributed to an increase of sediment influx due to a relative fall in sea level because a lower gradient had been established on the margin. This lower gradient would have been accompanied by the establishment of a relatively wider margin where relative falls in sea level play a bigger role in supplying sediment into the basin. Indeed, Buswell (1989) interpreted a change in provenance or sedimentary source at the base of A4 by noting changes in surface texture, extinction and mincralogy. In particular, he noted frosted sand grains below this horizon, suggesting a resedimented aeolian origin. Sand grains above this surface had a smooth surface texture, suggesting a resedimented shallow marine origin. This evidence supports the above interpretation.

The depositional systems that occur within units A3 and A4 indicate that slope apron systems are thinner and recessive, and channel lobe complexes are more widespread and less confined, relative to units A5 and A6. This is considered to be the result of previous sediment filling of the Lewis Trough which lowered submarine topographic relief. Unit A3 is muddier than unit A4, possibly reflecting a stillstand of relative sea level. While sediment was primarily sourced from the Enderby Platform side of the

basin, sedimentation from north of the Angel area may have commenced during deposition of unit A4.

The subsequent deposition of unit A2 possibly reflects a relative fall in sea level on the margin, which may be related to thermally isostatic-related basin tilting. The depositional systems are more characteristic of a 'ramp' style setting. Slope apron related sediments appear relatively areal confined in which unconfined 'Braided Channels', 'Depositional Lobe Massive Sands and Sheet Sands' dominate and thin distally to 'Distal Turbidites'. This ramp is interpreted to be primarily self-fed from a progressively established margin. Sands were likely resedimented numerous times. Nearshore palynological indicators occur within sheet sands over the Wanaea area which attest to resedimentation from a shallow marine setting.

Unit A1 contains sand bodies which back-step relative to unit A2. It reflects the waning nature of processes related to resedimentation. It was probably accompanied by the onset of a relative rise in sea level during a time when a relatively low depositional gradient was established. The rift basin was basically filled by this time, which may have provided an opportunity for eustacy to control the ensuing stratigraphic succession.

The progression from a point source to a wide margin sediment source up-section within the Angel Formation is confirmed by analysis of the heavy mineral suites by di Bona and Scott (1990). The distribution of identified mineral suites progressively become more widespread up-section, suggesting the transition from point sourced resedimentation to a line source. In particular, their units 'A', 'B' and 'E' are widespread, occurring in wells along the Legendre Trend from Samson 1 to Calypso 1. In this study, the mineral suites occur within units A1 and A2. Although only six wells were used in the area, the progression to more widespread patterns up-section can be observed from their work.

Late Post-rift

An interpreted transgressive ravinement surface of erosion is interpreted to occur at the top of the Angel Formation. Up to 1Ma of missing section is commonly noted in wells along the Legendre Trend at this time. Significant missing section is noted in Lewis 1, attesting to the mild transpression-related uplift which occurred in this area. Minor onlap of the Enderby Platform, which may have been eroded later, commenced at this time. Talisman sands developed on a progressively widening shelf and were also possibly deposited as Channel Fill within channel levee complexes, relatively confined to the margin of the Lewis Trough. In addition, shelfal sands and muds slumped into the margin of the Lewis Trough and filled any remnant relief of the Rosemary Fault scarp that may have existed at this time. This slumping may have also been induced by the sporadic and mild wrenching that occurred over the Legendre Trend. Incidentally, Horizon 'A' corresponds to a eustatic fall and subsequent rapid rise in sea level. This eustatic sea level fall would have likely resulted in a relative sea level stillstand, owing to the interpreted thermal subsidence.

The base of the Winning Group coincides with the Valanginian disconformity (Wiseman, 1979). Indeed, Wiseman documented a relative fall in sea level "of the

order of 200m" to have occurred in the northern Carnarvon Basin from interpretation of the Barrow Island area in the Barrow Sub-basin. He suggested that this fall occurred in the latest Berriasian or earliest Valanginian. The dinoflagellate scheme was not in use at that time, and so it is difficult to ascertain any direct comparison. He also suggested that this eustatic fall may be obscured in other areas due to basin subsidence. As Wiseman (1979) suggested, there is no indication of a relative fall in sea level in this area, and may be owed to basin subsidence.

Minor missing section from 1 to 3Ma in wells northeast of Legendre 1 along the Legendre Trend, is attributed to erosional ravinement during transgression. The Valanginian disconformity has been dated to occur near the base *S. areolata* zone in other studies (e.g. Barber, 1994). The alternate designation to near the top of *B. reticulatum* zone is attributable to the preferred correlation of onset of transgressive related flooding and ravinement. This surface is equivalent to Weimer's (1992a) definition of a transgressive surface of erosion (TSE). Although Weimer suggests that a TSE can be diachronous, in this case it is chronostratigraphic and it proves to be a very good correlation surface. The previous interpretation of the 'Valanginian disconformity' is a likely position for the maximum flooding surface.

Significant onlap of the Enderby Platform commenced at this time. The result was a classic transgressive vertical succession that ranged from the littoral to sub-littoral Birdrong Sandstone and distal equivalent Mardie Greensand (Wiseman, 1979) to the basinal Muderong. An alternative interpretation, (Arditto, 1993), is where this succession is considered to be chronological. These members were related to a final episode of coarse-grained Birdrong sedimentation during early transgression; subsequent terrigenous sediment starvation with later transgression and deposition of the Mardie Greensand; and finally hemipelagic deposition of the Muderong Shale. While this interpretation is slightly contentious, it has some degree of credibility over the Talisman region. The Mardie Greensand is dominantly constrained within the *S. Tabulata* zone. The diachronous nature of this succession is possibly less than previously thought, at least over this area. However, the Birdrong Sandstone is diachronous here, as it is associated with onlap across the Enderby Platform. More work on the temporal and spatial relationship of this succession would provide more detail in this respect.

A subsequent flooding event, known as the 'intra-Muderong' event, occurs within the middle *M. Australis* 'a' subzone (~131Ma). By this time, most of the Enderby Platform had been flooded and Muderong Shale deposition was widespread. It is uncertain whether this event reflects an increase in subsidence rate associated to the breakup of the Cuvier and Gascoyne Abyssal Plains (135Ma) or a eustatic sea level rise. This event corresponds closely to a 'second order' maximum sea level on the eustatic chart.

Passive Margin

The Aptian disconformity corresponds to the top of the Winning Group. This disconformity is regionally correlatable across the North West Shelf is thought to have formed when the Indian Plate extended beyond the Exmouth Plateau (Veevers, 1984). It also correlates to a well documented eustatic fall and subsequent rise in sea level on the eustatic chart. There is no evidence to suggest a relative fall in sea level in the Dampier Sub-basin. This surface may be attributed to a minor relative sea level stillstand followed by sudden flooding. It is possible that the effect of thermal subsidence may have obscured any associated eustatic fall in sea level, as with the Valanginian disconformity. This event represents onset of deposition of the basal transgressive Windalia Sandstone, its distal equivalent Gearle Siltstone and the Haycock Marl. The facies change from Gearle Siltstone to Haycock Marl appears to occur within the central axis of the Lewis Trough. Full oceanic circulation had commenced by this time, and the Dampier Sub-basin continued to subside as part of a broad shelf within a fully developed passive margin.

4.3.3 Conclusions

Previous correlations of the stratigraphy for areas of the North West Shelf to various time scales have caused misleading interpretations with respect to eustacy and tectonic events, in addition to calculations of the rates of subsidence and sediment accumulation. This issue, has been addressed by what is thought to be the most accurate versions of the dinoflagellate zonation scheme and time scale in this study.

Depositional surfaces are a result of fluctuations in sediment influx, tectonic factors and eustacy in varying proportions. In active rifted basins such as this one, it is difficult to quantify the individual effect that each factor had on a depositional event. These considerations remain relatively speculative. While these depositional events have chronological significance on a local scale, the correlation of 'third order events' from region to region can cause biased or erroneous results, particularly with the use of limited databases. In any case, more work on the chronological significance of the timing of tectonically induced 'supercycle' events, or tectonic systems tracts should be conducted across the North West Shelf. When this is done, the relationship of depositional surfaces that are caused by higher frequency events and defined by detailed, independent projects, may be assessed from region to region.

The eustatic chart (Haq et al., 1987) should not be used to interpret rift related depositional systems. It is dubious to attribute relative sea level to eustatic sea level during the Rift Climax and during the early development of the Immediate Post-rift tectonic systems tracts. With respect to depositional surfaces, relative rises in sea level appear to represent the boundaries of depositional episodes that occurred during these systems tracts. Later, during the Immediate Post-rift systems tract when basin filling progressed, and a widening margin developed, relative falls in sea level may have resulted in boundaries (depositional surfaces) associated with depositional episodes. It appears that tectonics had a much greater influence than eustatic sea level on relative sea level during sedimentation of the Rift Climax and Immediate Post-rift tectonic systems tracts.

However, during the Late Post-rift succession, there is a remarkably good correlation of transgressive surfaces of erosion to eustatic rises in sea level that immediately follow significant falls (i.e. Horizon 'A', Valanginian disconformity, Aptian disconformity). Although this may be coincidental, it suggests that there may be some validity with respect to major events on the eustatic curve when applied to settings where it is plausible for eustacy to control the stratigraphy.

CHAPTER 5: CONCLUSIONS

SUMMARY AND IMPLICATIONS FOR PETROLEUM EXPLORATION IN THE DAMPIER SUB-BASIN

5.1 SUMMARY

The Mesozoic succession of the Dampier Sub-basin can be described in terms of tectonic systems tracts with respect to rifting and sea floor spreading of the Argo Abyssal Plain. However, in addition to this event, there are other factors which have major effect on the stratigraphy. These include the inheritance of an already established basin morphology and basin margin faults from older rifting events (e.g. Hill, 1994); the superimposition of various sea floor spreading events that occur over the North West Shelf (i.e. the Argo, Cuvier and Gascoyne Abyssal Plains) during the Jurassic and Cretaceous; and other tectonic factors with respect to cratons adjacent to the basin.

The Legendre Formation and its distal equivalent Athol Formation consist of fluvial-deltaic and shallow marine dominated sequences that are considered to have developed in response to the initiation of rifting. Sedimentation generally kept pace with subsidence and there was virtually no net increase in accommodation space (e.g. see Figures 4.33, 4.58, 4.59). There is much scope for more work on the structure and sedimentology on this Rift Initiation tectonic systems tract.

The Calypso Formation (Mid-Callovian - Oxfordian; Early Rift Climax systems tract) is dominantly a marine shelf sequence where seismic reflection configurations reveal half graben sediment filling under static to slightly transgressive relative sea level conditions (see Figures 4.7 and 4.46). The seismic character of this formation is dominantly parallel and continuous events that onlap or uplap onto the basin margin (Figure 3.21). Core data contain evidence of silty debris flows and turbidity currents, winnowing of fines and repeated bed-load transport of sands by strong bottom currents (e.g. see cores 1, 2, and 3 at Rosemary 1). Nearshore conditions are indicated by palynology interpretations (Morgan, 1987-93). The sub-littoral zone of a marine environment is indicated by *Cruziana* ichnofacies observed in core of Rosemary 1 and Legendre 1 (e.g. see Figure 3.5d). In addition, vertical successions of bedding and structures observed in core 16 and 17 at Legendre 1 are characteristic of storm influenced deposits that occur in water depths below fair weather base but above storm wave base. A transgressive surface of erosion forms the lower boundary of the Calypso Formation. In this study, the formation was sub-divided at a succeeding primary flooding surface which occurred during another transgressive episode. If more core and well data were available, it is likely that additional depositional surfaces could be established, and the Calypso Formation could be further sub-divided.

During lower Oxfordian time, an increased rate of half-graben fault movement gave way to pronounced deeper marine conditions in the Lewis Trough and adjacent Eliassen Terrace, as subsidence dramatically outpaced sediment supply. This marine deepening event is indicated by subsidence analysis in addition to the overlying transgressive transition from nearshore to offshore palynological indicators at

Calypso 1, Samson 1, Orion 1, Lewis 1, Rosemary 1 and Legendre 1 (Morgan, 1987-93). At this time, the Eliassen Formation was deposited as part of the Mid and Late Rift Climax systems tracts (see Figure 4.54). Gravity-induced slope apron depositional systems formed along a contemporaneously developing fault scarp. These slope apron systems contain elements with process affinities of braided channels, levee complexes and channel fill sands (e.g. see Figures 3.32, 3.48, and 4.9). Scismic stratal patterns reveal apron shaped wedges that uplap onto the interpreted scarp of the Rosemary Fault (e.g. see Figures 4.66 and 4.67). This scarp would have been subjected to headward erosion at sediment source inlets and to crestal degradation over the length of the scarp (Figure 4.56). Distal seismic stratal patterns are mounded, and are interpreted to contain muddy distal turbidites, contourites and possibly discrete depositional sand lobes (e.g. see Figures 3.20 and 3.45). As sedimentation progressed into the Late Rift Climax systems tract, increasingly mud rich conditions ensued, owing to depositional elements associated with muddy turbidites, contourites, levee complexes and hemipelagic ponding (e.g. see Figures 3.44 and 3.46). Seismic stratal patterns are continuous and parallel and often highlight the underlying mounded geometries. Low density turbidites were identified by core data at Madeleine 1 (cores 6 and 7). The existence of gravel and very coarse sand-sized material in core 12 at Legendre 1 is a likely function of the proximity to a nearby sediment source.

The formation of an unconformity commenced near the end of Oxfordian time (see Section 4.2.2). This unconformity is directly attributed to break up and subsequent sea floor spreading on the Argo Abyssal Plain. As a result of this break up event, margin-ward isostatic uplift operated contemporaneously with sediment cannibalisation via headward erosion of the previously developed fault scarp. Deposition of the Angel Formation as an immediate post-rift systems tract resulted (Figure 4.54). Palynological evidence indicates cannibalisation of the underlying succession, and possibly from the adjacent Eliassen Terrace and Enderby Platform (Table 4.1). Mud-rich depositional conditions progressed to mud/sand-rich and subsequently to sand-rich conditions as sedimentary gradients subsided and net accommodation space decreased by progressive sediment 'filling' of the basin (see Figure 4.70). Three confined point sources at the base of the Angel Formation became progressively less confined up-section. In fact, the style of source that occurred within units A1 and A2 is more appropriately described in terms of a point source. Concomitantly, there was an evolutionary progression of depositional systems from gravity induced sandy slope aprons and channel-lobe complexes, to a self-fed depositional ramp (see Figures 4.14, 4.25, 4.28, and 4.33). Sedimentation became more widespread and less confined up-section where sand bodies are more correlable laterally . The vertical progression of depositional systems resulted as topographic relief progressively decreased due to basin filling, and later as thermal subsidence induced basin tilting. Six genetically related units were defined using well logs and high resolution palynology (Figure 3.13, and stratigraphic log correlations). These units are interpreted to be distinguished by variations in sediment influx and a tectonically-influenced relative sea level (Table 4.4 and Figure 4.69). The influence of eustacy is considered to be progressively more significant up-section. The mapping of four seismic units together with the well correlations of six genetic units demonstrate the progression that is described above (see Section 4.1).

Seismic stratal patterns within the Angel Formation include seismic convergence (Figure 3.18), asymptotic downlap (Figure 3.19), seismic lens features (Figure 3.52), incised channel features containing clinoforms and mounded geometries (Figures 3.49, 3.50, and 3.51). There is notable erosional truncation of the underlying unit along the southeast flank of the Lewis Trough.

Although there is very limited core data from Angel Formation Units A3 to A6 to interpret depositional environments, evidence from core data within Units A1 and A2 strongly suggest ramp cannibalisation. Occasional broken shell fragments and abundant dispersed detrital glauconite within massive sandstones attest to a shelf depositional environment as a dominant source (e.g. see Angel Field cores). The identification of a distal *Cruziana* and *Zoophycos* Ichnofacies suggests a sublittoral to slope environment of deposition (Figures 3.5f, g, h, and i). The overall lack of vertical grain size variation is characteristic of a ramp style setting (Figure 3.6).

The Angel Formation has previously been considered with respect to the 'Vail' style basin floor fan and the Mutti (1985) type I and II turbidite systems (e.g. Buswell, 1990; Barber, 1994). This study has demonstrated that ramp style models such as those by Heller and Dickinson (1985), Surlyk (1987) and Reading and Richards (1994) which better reflect the sedimentary architecture of the Angel Formation. In particular, these models provide alternatives in predicting sedimentary relationships for hydrocarbon potential (see Section 4.1.3).

Diminishing sediment supply signified the end of widespread Angel Formation sand deposition during the Berriasian. The Dampier rift basin was dominantly filled at this time and deposition of an offshore marine claystone, the Forestier Claystone, commenced as the Late Post Rift systems tract. Onlap onto the adjacent Enderby Terrace had commenced. The seismic character is dominantly continuous and parallel (Figures 3.22 and 3.28). Minor onlap is noted on the Enderby Platform near the Rosemary Fault.

Sands and muds of the Talisman Sandstone and Forestier Claystone slumped into the eastern margin of the Lewis Trough as Upper Slope Apron deposits. This is suggested by core data at Talisman 2 which contains muddy slumps, slides and debris flows and massive sandstone. These processes filled pre-existing remnant relief of the Rosemary Fault scarp.

Mild, sporadic, synsedimentary, left-lateral wrench movements that occurred over the Rosemary Fault system during deposition of the Angel Formation also had some palaeo-topographic control of sedimentation during deposition of the Forestier Claystone and Talisman Sandstone. This wrench component caused contemporaneous mild local uplift and subsidence due to reactivation on the Rosemary Fault in areas that coincide with respective 'constraining bends' and 'releasing bends' (Figure 4.60).

Sediment starvation persisted over most of the basin depocentre during the Late Post Rift systems tract. A retrogressive wedge exists over the Rosemary area and appears to have extended distally to the condensed northerly area. A disconformity within the Valanginian marks the onset of a regional transgression where the Birdrong Sandstone and the Mardie Greensand transgressed over the Enderby Terrace,

primarily due to thermal isostatic subsidence of the basin margin. Eustacy is considered to be the dominant factor that controlled relative sea level and the development of mappable genetic units during the Late Post Rift systems tract.

A disconformity during the Aptian marks the establishment of fully open marine conditions when deposition of the Windalia Sandstone, Gearle Siltstone and Haycock Marl commenced on a passive margin. The Rankin Platform was completely submerged by this time. Differential subsidence occurred over the Lewis Trough area with respect to adjacent areas. Definition of this trough was re-established and was retained until about Campanian time. The differential subsidence was due to either the compaction of a relatively thicker underlying sedimentary section within the Lewis Trough. It may also reflect a mild compressional event.

5.2 IMPLICATIONS OF METHODOLOGY

The Vail et al. 'sea slug' is not suitable for rifted margin basin stratigraphic studies. Discrete prograding wedges that allegedly reflect rises and falls in sea level were not observed in this study. Ramp style models, where thickening distal wedges are common, and slope apron style models have significant relief, are much more appropriate for the Dampier Sub-basin. Furthermore, I suggest that the stratigraphic framework adopted in this study would be equally appropriate for the Jurassic and Lower Cretaceous succession in other areas of the North West Shelf.

'Second-order' super-sequences are clearly controlled by regional tectonics in the Dampier Sub-basin. 'Third-order' scale chronological surfaces are highly useful at a local scale when conducting facies analysis of genetically related units. While these units are often considered to coincide with changes in relative sea level, the real issue is an explanation for relative changes in accommodation space due to the complex interaction between tectonics, sediment influx, and eustacy. The influence of these factors may possibly vary in accordance to the stage of basin development of the rifted basin. For instance, the role of eustacy is considered to become progressively more important as the rifted margin transforms into a passive margin. On a regional scale, the three factors can also be inter-related. Here, regional tectonics and climate may influence the texture and type of sediment being deposited. If the tectonics and/or climate changes have occurred on a global scale, these changes would influence eustacy, and then eustacy is justified for these changes.

In their attempts to correlate and associate cycles on a regional basis as a tool to predict lithofacies in areas of poor data control, stratigraphers are constantly searching for universal types of signatures in the geological record. It appears from this work that there is a poor regional correlation of 'third order' scale sequences on the North West Shelf, particularly during the Rift Climax and Immediate Post Rift systems tracts. Before correlation and the significance of third order sequences on the North West Shelf may be conducted objectively, the regional association of supercycles, or tectonic systems tracts, needs to be evaluated in more detail.

The depositional surfaces defined in this study may be attributed to relative rises and falls in sea level. The nature of these surfaces (e.g. apparent downlap surface, onlapping surface of erosion, onlap surface, unconformity surfaces, etc.) may be attributed to either a relative rise or fall in sea level after the regional extent and

overall significance of the surface on the bounding stratigraphy is evaluated. The preference of the type of surface that was chosen for mapping varied with the relevant stage of basin development. In each case, choice of a surface was made for purposes of accurate correlation. Surfaces defined near the end of the Immediate Post Rift systems tract were attributed to likely falls in relative sea level. During most of the Late Post Rift systems tract, the depositional surfaces defined for best correlation were considered to be primary flooding surfaces (transgressive surfaces).

Primary flooding surfaces were defined by picking the bases of condensed sections, the bases of sections that contain multiple flooding surfaces, and disconformity surfaces where some missing section was noted. It was observed that the interpreted transgressive surface of erosion (disconformity surface) was attributed to primary flooding because it correlated better with these surfaces. In addition, the correlation of the interpreted surfaces of primary flooding (i.e. the bases of condensed sections and 'flooding' intervals) appeared to have more chronological significance than the correlation of maximum flooding surfaces. This approach is an alternative to conventional sequence stratigraphic approaches (either the 'Vail' or 'Galloway' sequence stratigraphic approaches) where interpreted maximum flooding surfaces bear more relative importance than primary flooding surfaces.

Review of literature in sequence stratigraphy on the North West Shelf and globally suggest, that there is a shortcoming, where many interpretations are driven by previously conceived sequence stratigraphic and sedimentological models (e.g. Barber, 1994; Spring and Newell, 1993). This work demonstrates that any particular area must be considered individually on the basis of available data with respect to the age of the rocks, structural regime, stage of basin evolution, and depositional setting. Depositional systems should be independently defined from pre-conceived ideas and 'characterised' by the types of sedimentary processes and respective facies associations that are inferred by interpretation of the data.

The style of sedimentation interpreted to occur within a particular system should be qualified by considering numerous sedimentological models as end-members. These are usually 'type' examples highlighting only a few of the possible parameters. The interpreted character of the depositional system and its respective elements may be allocated accordingly within a spectrum of numerous possibilities (e.g. the spectral variations of submarine channels and lobes due to the texture of the sediment shown in Figures 4.1 and 4.2). In addition, any formulated model for a depositional system should be tested for its validity at every available opportunity to avoid pitfalls, and to gain appreciation for the exploration risks and uncertainties involved with respect to a particular style of play (Reading and Newell, 1994). In the case of marine resedimented clastic rocks, an integrated approach is required which defines the controls on the various systems and their resultant features that may be exhibited in the geological and geophysical record. Ultimately, more understanding is achieved of the facies relationships and architecture in the context of reservoir presence, reservoir geometries and trap integrities. In the search for hydrocarbons, accurate predictions based on a valid understanding of the lithofacies from seismic data can then be conducted.

Dramatic changes in accommodation space have been interpreted to occur during the depositional history of the Upper Jurassic succession of the Dampier Sub-basin. The

development of a significant fault scarp and adjacent basin depocentre during the Oxfordian resulted in a very large increase in net accommodation space. This event preceded progressive basin filling (continual decrease of net accommodation space) and progressive reduction in relief during the Kimmeridgian and Tithonian. The relief of the fault scarp resulted in initial headward erosion and overall degradation of the crest, and inhibited the development of a significant shelf and shoreface. Any shelf development would have been relatively narrow and eustacy would likely have had minimal effect on the stratigraphy. If there was a narrow shelf, significant sediment bypass would have occurred relatively continuously. It is likely that some form of narrow shelf and shoreface developed later, after considerable reduction of relief and basin filling had occurred. The sediment that accumulated on this narrow shelf is considered to have been continually subjected to sediment cannibalisation and resedimented in a ramp style of setting.

There is a considerable lack of coherence as to the use of an accepted time scale for the literature on the North West Shelf. To manifest this problem, two dinoflagellate zonation schemes have been allocated to these time scales. The scale and allocation used in this study was justified by referring to the most up to date material. It is suggested that this time scale and zonation allocation should be used for further studies on the North West Shelf until newer age assignments and more absolute age dating are available (Figure 3.13).

5.3 IMPLICATIONS FOR PETROLEUM EXPLORATION

There is considerable potential for structural/stratigraphic plays to occur on the northwestern flank of the Lewis Trough. It was demonstrated in section 4.1 that turbidite sands likely onlap this flank, or simply pinch-out distally over areas that coincide with this flank, particularly over units A5, A6 and E2.

Indeed, the presence of hydrocarbons within Units A5, A6 and E2 in this region is suggested by multiple shows of sample fluorescence and solvent fluorescence that were observed over these units during the drilling of Madeleine 1. In addition, gas cut formation water was recovered during a formation interval test (FIT) of sheet sands within Unit A2. Sidewall cores retrieved from thin sands of Unit E2 also had good sample fluorescence and sample cut. Cores 7 and 8, within Units E1 and E2, respectively, produced significant traces of oily fluids when they were retorted. Unfortunately, no FIT's were conducted over the prospective intervals of Units E1 and E2 due to mechanical problems during drilling of the well. (Madeleine 1 Well Completion Report, 1969).

It was not in the scope of this study to search the seismic character of units for subtle individual amplitude anomalies that may suggest sand development. However, further investigation is warranted. Additional seismic coverage in this area would therefore be desirable. Higher in the section, there was virtually no topographic relief on this flank of the Lewis Trough to control the deposition of sand. Hence, significant distal turbidites are present in Unit A4 in wells on the Madeleine Trend (e.g. Walcott 1, Wanaea 1). However, there is potential for local stratigraphic closure of sands within Unit A4 due to the overlying claystone of Unit A3. Sands within Units A1 and A2 require virtually total structural closure. Seal potential of any four-

way dip closure of these sandstone-dominated units is almost certain, due to the overlying regionally extensive Forestier Claystone.

There is good potential for sand development with structural or stratigraphic closure within the Kendrew Trough. Unfortunately, seismic coverage over this area was severely limited for this project. However, analysis of the palaeogeography data suggests there was likely transport of sand into the Kendrew Trough from the Angel area. Indeed, there were mounded configurations noted in this area. It is possible that part of the Kendrew Trough was topographically lower than the adjacent Madeleine Trend at some time during deposition of the Eliassen and Angel Formations, which increases the potential for sand development. Further seismic mapping and analysis over the Kendrew Trough is warranted to qualify this possibility. The objectives of such a project could also evaluate the extent of sand being sourced from the Rankin Platform area during deposition of the upper Angel Formation.

The potential for updip seal to occur over Angel Formation sandstone bodies on the southeastern flank of the Lewis Trough is severely downgraded. This is primarily due to the retrogradational nature of the Angel Formation. The definition of a potential sand bearing seismic feature, for example, a seismic lens of a Slope Apron Depositional Sand element, is almost certainly overlain by sand. The potential for the Rosemary Fault to offer the fourth closure of a sandstone body of the Angel Formation is dubious due to the suspected breach of a fault seal. The migration path of the Wandoo Field oil may indeed, have included this fault (e.g., see Christiansen, 1992). The following observation adds credence to the suggestion of a breached of fault seal. Rosemary North 1 was drilled very close to the Rosemary Fault, suggesting that a fault seal would be required as the fourth dip direction of closure. Residual hydrocarbons were observed over a 7m section near the top of the Angel Formation from log analysis (Rosemary North 1 Well Completion Report, 1982). This suggests that more significant hydrocarbon accumulations may have been previously trapped and subsequently escaped, possibly owing to leakage up a fault plane. Another example is from Forestier 1, where 49.2 cubic feet of gas and 400ml of condensate were recovered from the top of the Angel Formation (Forestier 1 Well Completion Report, 1986).

There is remaining potential to generate a hydrocarbon play by defining structural closure of the top Angel Formation sandstone over the Legendre Trend. For instance, there is an area of untested closure southwest of Rosemary 1 (see Figure 4.36). Further detailed seismic analysis would be desirable on a detailed local scale to gain more confidence in reservoir/seal geometry, as well as to evaluate the possibility of a breach of seal via fault planes. The objective of this analysis would be to reduce uncertainty and, if considered feasible, locate a well position.

In spite of the poor updip sealing potential of the Angel Formation along the Legendre Trend, potential of this type is still reasonable for the Eliassen Formation. Good oil shows within the Eliassen Formation have been recovered from several wells along the Legendre Trend. In Samson 1, for instance, 5m and 1.5m hydrocarbon saturated zones were indicated by log analysis within thin sandstones (Samson 1 Well Completion Report, 1984) that were interpreted in this study as levees or contourites. In Lewis 1, good solvent fluorescence was observed in

sidewall cores from this same zone of the Eliassen Formation (Lewis 1 Well Completion Report, 1975). In Rosemary 1, gas cut mud was recovered from an FIT near the base of the Eliassen Formation (Rosemary 1 Well Completion Report, 1972).

The updip sealing potential of the Eliassen Formation along the southeast flank of the Lewis Trough is good for the following reasons. The Eliassen Formation contains mud-rich depositional systems where sands are known to be efficiently transported into the basin. This provides a possibility for channels that contain Channel Fill Sands, such as those at Lauchie 1, to be mud filled updip. However, if these sands do in fact uplap the Rosemary Fault, there is still some chance for a fault seal to occur at the Eliassen Formation level. Because the Eliassen Formation is considered mud-rich, the real problem is defining a reservoir. For example, the Eliassen Formation sandstone was a secondary objective for Baleena 1. The Eliassen Formation at Baleena 1 is a continuous claystone section (see Barber 1994, his Figure 26). Interpretation of this section demonstrates that there is claystone in the Baleena vicinity because it is located on a palaeotopographic high with respect to deposition of the Eliassen Formation. Further seismic analysis to the west of and west-southwest of Baleena 1 over the interpreted Channel Fill fairway shown on the schematic palaeogeography diagram (Figure 4.9) may prove fruitful.

In the event that further seismic acquisition is planned over the study area for the purpose of stratigraphic and structural analysis, it is recommended that a north-south/east-west shotpoint grid be seriously considered. As it was demonstrated in this study, the stratigraphic strike of much of the studied succession is close to north-south. In addition, many relevant faults trend north-south. This is contrary to the conventional approach where seismic was shot perpendicular and parallel to the general strike of the basin morphology. This alternative is suggested because, as demonstrated, the basin morphology was established in the Permo-Carboniferous and inherited by the Valanginian to Callovian stratigraphy. During deposition of the Angel Formation, a north-south relationship to the strike of the stratigraphy and the trend of faults that were active during sedimentation is apparent.

5.4 FURTHER WORK

This study would provide a framework for a diagenesis/petrological project. Detailed petrography and/or mineralogy of the Mesozoic succession could establish more insight into sedimentary provenance and respective source areas. This type of project could be initiated by using the 'pilot' project on heavy mineral suites which was conducted by di Bona and Scott (1990). In addition, the definition of the depositional elements in this study could be tested and refined by observing the textural associations displayed in thin sections. It would also provide additional information with respect to the lithology, and permeability/porosity characteristics of the depositional elements. A diagenetic study combined with petrological work would provide further insight into other questions such as: the source of carbonate cements within Angel Formation sandstones and whether they are related to hydrocarbon migration (e.g., see Ryan-Grigor and Schulz-Rojahn, 1995); the origin of siderite nodules and siderite cemented zones; the emplacement and timing of pyrite cemented zones which may be related to palaeo-oil-water contacts and hydrocarbon migration events.

It is thought that it is the complex structural history of the Legendre Trend is the primary factor affecting the relatively average discovery rate along the Legendre Trend (3 wells out of 18, including Talisman Field wells). In order for success to be achieved in this area, it is crucial to unravel the combined extensional and wrench-related structural history of the Legendre Trend and associated Rosemary Fault. A project of this type would include detailed seismic mapping of the Rosemary Fault and Legendre Trend. Sand-box analogue modelling techniques could be used to confirm and help decipher structural complexities. The aim would be to assess the hydrocarbon trapping potential of faulted areas where suspected fault leakage of hydrocarbons has not been ruled out. In addition, the project should attempt to identify significant hydrocarbon migration events. A diagenetic project would complement this analysis through observation of palaeo-oil-water contacts.

There is much scope for a structural-stratigraphic project on the lower to middle Jurassic Legendre and Athol Formations. This work would entail detailed seismic mapping of the Enderby Platform and Kendrew Terrace. The well database would primarily consist of wells on the Enderby Platform, with a few wells on the Legendre Trend which penetrated the relevant succession. This work could also better assess the extent of this succession within the Lewis Trough. Further knowledge of the structural history of the Rift Initiation sediments of the Dampier Sub-basin would also be obtained. In addition, this type of study would assess the stratigraphic and structural trapping potential of this area including the Lewis Trough. It would also provide further knowledge of the sediment source areas for the Upper Jurassic succession.

Other work that pertains more directly to hydrocarbon play generation have previously been suggested in section 5.3. In addition, the use of seismic attributes for identifying potential sandstone bodies within claystone bearing sections could be evaluated.

In general, there is scope for more seismic stratigraphic projects to be conducted over other areas of the North West Shelf. One aspect of these studies should examine the relationship between super-cycles of various basins (e.g. Boote and Kirk, 1989). When enough of this work is established, the significance of third-order sequences between regions may then be assessed more objectively.

5.5 COMMENT

The informal and non-rigid use of nomenclature has proven to be relatively practical in spite of minor confusion in the literature. The nomenclature should be continued to be used in this way. However, in addition to defining the type and style of lithology in formation definitions, they should be age defined using biostratigraphy (e.g. Hocking, 1992). This should prove to be convenient for future genetic stratigraphy studies. There is much scope for standardising some of the more recent nomenclature on the North West Shelf, in order to avoid future confusion.

REFERENCES

Allaby, A. and Allaby, M. (eds), 1991. *The concise Oxford dictionary of earth sciences.* Oxford: Oxford University Press 410pp.

Apthorpe, M.C., 1979. Depositional history of the Upper Cretaceous of the Northwest Shelf, based upon foraminifera. *APEA Journal*, **19**, 74-89.

Arditto, P.A., 1993. Depositional sequence model for the post-Barrow group Neocomian succession, Barrow and Exmouth Sub-basins, Western Australia. *APEA Journal*, **33**, 151-160.

Barber, P.M., 1988. The Exmouth Plateau deep water frontier: a case history in P.G., Purcell and R.R., Purcell (eds) *The North West Shelf, Australia.* Proceedings of Petroleum Exploration Society Australia Symposium, Perth, 1988, p. 173-88.

Barber, P., 1994. Sequence stratigraphy and Petroleum Potential of Upper Jurassic - Lower Cretaceous Depositional Systems in the Dampier Sub-basin, North West Shelf, Australia. In P.G. and R.R. Purcell (eds), *The sedimentary basins of Western Australia.* Proceedings, West Australian Basins Symposium, Perth, W.A., 1994, p. 525-542.

Berg, O.R., 1982. Seismic detection and evaluation of delta and turbidite sequences: their application to exploration for the subtle trap. *AAPG Bulletin*, **66**, 1271-1288.

Bint, A.N., 1991. Discovery of the Wanaea and Cossack oil fields. *APEA Journal*, **31**, 22-31.

Bint, A.N. and Marshall, N.G., 1994. High resolution palynostratigraphy of the Tithonian Angel Formation in the Wanaea and Cossack oil fields, Dampier Sub-basin. In P.G. and R.R. Purcell (eds), *The sedimentary basins of Western Australia.* Proceedings, West Australian Basins Symposium, Perth, W.A., 1994, p. 543-556.

Boote, D.R. and Kirk, R.B., 1989. Depositional wedge cycles on an evolving plate margin, Western and Northwestern Australia. *AAPG Bulletin*, **73**, 216-243.

Bouma, A.H., 1962. *Sedimentology of some flysch deposits: a graphic approach to facies interpretation.* Amsterdam: Elsevier.

Bouma, A.H., Normark, W.R. and Barnes, N.E., 1985. *Submarine fans and related turbidite systems.* New York, Springer-Verlag, 351 pp.

Boyd, R., Suter, J. and Penland, S., 1989. Relation of sequence stratigraphy to modern sedimentary environments. *Geology*, **17**, 926-929.

Boyd, R., Williamson, P. and Haq, B.U., 1993. Seismic stratigraphy and passive-margin evolution of the southern Exmouth Plateau. In H.W. Posamentier, C.P. Summerhayes, B.U. Haq and G.P. Allen (eds), *Sequence stratigraphy and facies associations*. International Association of Sedimentologists, Special Publication No. 18, Blackwell Publications, p. 581-603.

Bradshaw, M.T., Yeates, A.N., Beynon, R.M., Brakel, A.T., Langford, R.P., Toterdell, J.M. and Yeung, M., 1988. Palaeogeographic evolution of the North West Shelf region. In P.G. and R.R. Purcell (eds), *The North West Shelf, Australia.* Proceedings of Petroleum Exploration Society Australia Symposium, Perth, 1988, p. 29-54.

Brown Jr., L.F. and Fisher, W.L., 1977. Seismic-stratigraphic interpretation of depositional systems: examples from Brazilian rift and pull-apart basins. In *Seismic stratigraphy - applications to hydrocarbon exploration.* AAPG Memoir , 26, p. 213-248.

Busch, D.A., 1959. Prospecting for stratigraphic traps. *AAPG Bulletin,* **43**, 2829-43.

Buswell, A.J.G., 1989. *The Angel formation at Angel 3 Dampier Sub-Basin Western Australia.* Curtin University of Technology unpublished honours thesis.

Butcher, B.P., 1989. *Northwest Shelf of Australia.* In J.D. Edwards and P.A. Santogrossi (eds), *Divergent/Passive Margin Basins.* AAPG Memoir 48, p. 81-115.

Cartwright, J.A., Haddock, R.C. and Pingeiro, L.M., 1993. The lateral extent of sequence boundaries. In G.D. Williams and A. Dobb (eds), *Tectonics and Sequence Stratigraphy.* Geological Society Publication No. 71, p. 15-34.

Chang, K.H., 1975. Unconformity-bounded stratigraphic units. *Geological Society of America Bulletin,* **86**, 1544-52.

Christiansen, D.J., 1992. *The hydrocarbon potential of a western portion of the Lambert Shelf, Dampier Sub-Basin, Western Australia.* University of Adelaide unpublished honours thesis.

Cockbain, A.E. and Hocking, R.M., 1989. *Revised stratigraphic nomenclature in Western Australian Phanerozoic Basins.* Geological Survey of Western Australia, **1989/15**.

Coleman, J.M. and Prior, D.B., 1988. Mass wasting on continental margins. *Annual reviews of Earth and Planetary Science,* **16**, 101-19.

Costella,T. and Barber, P.M., 1980. Triassic-Jurassic depositional history of the Dampier and Beagle Sub-Basins, N.W. Shelf of Australia. *APEA Journal,* **20**, 25-30.

Delfos, E. and Boardman, M., 1994. Wandoo - a new trend. APEA Journal, **34**, 586-601.

di Bona, P. and Scott, J., 1990. Heavy mineral study of the Late Jurassic and Early Cretaceous section from fifteen wells within the Barrow-Dampier Sub-basins, Northwest Shelf, Western Australia. Western Australian Centre for Petroleum Exploration, Curtin University unpublished report.

Dingle, R.V., 1977. The anatomy of a large submarine slump on a sheared continental margin (SE Africa). *Journal of Geological Society of London,* **134**, 293-310.

Di Toro, G.A.E., 1994. The reservoir geology of the Wanaea and Cossack Oil Fields. In P.G. and R.R. Purcell (eds), *The sedimentary basins of Western Australia.* Proceedings, West Australian Basins Symposium, Perth, W.A., 1994, p. 557-72.

Dott, R.H. Jr., 1963. Dynamics of subaqueous gravity depositional processes. *AAPG Bulletin,* **47**, 104-28.

Ehrhard, L.W., O'Reilly, B. J. and Wulff, K.J., 1992. Stratigraphic framework of the Barrow Group and implications for the hydrocarbon potential of the West Barrow area. *APEA Journal*, **32**, 123-37.

Ellis, G.K., 1988. Diagenesis of the Talisman-1 reservoir sequence. In P.G. and R.R. Purcell (eds), *The North West Shelf, Australia.* Proceedings of Petroleum Exploration Society Australia Symposium, Perth, 1988, p. 237-49.

Embry, A.F., 1993. Transgressive-regressive (T-R) sequence analysis of the Jurassic succession of the Sverdrup Basin, Canadian Artic Archipelago. *Canadian Journal of Earth Sciences.,* **30**, 301-20.

Etheridge, M.A. and O'Brien, G.W., 1994. Structural and tectonic evolution of the Western Australian Margin Basin System. Abstract; *APEA Journal*, **34**, 906-8.

Exon, N.F. and von Rad, U., 1994. The Mesozoic and Cainozoic sequences of the Northwest Australian Margin, as revealed by ODP core drilling and related studies. In P.G. and R.R. Purcell (eds), *The sedimentary basins of Western Australia.* Proceedings, West Australian Basins Symposium, Perth, W.A., 1994, p.181-99.

Falvey, D.A. and Middleton, M.F., 1981. Passive continental margins: evidence for a prebreakup deep crustal metamorphic subsidence mechanism. In *Colloquium on Geology of Continental Margins (C3).* Oceanologica Acta, 4 (supplement), p. 103-14.

Forrest, J.T. and Horstman, E.L., 1986. The Northwest Shelf of Australia - geologic review of a potential major petroleum province of the future. In Halbouty, M.T. (ed), *Future Petroleum Provinces of the World.* Proceedings of the Wallace C. Pratt Memorial Conference, Phoenix, 1984, AAPG Memoir 40, 1986, p. 457-86.

Frazier, D.E., 1974. Depositional episodes: their relationship to the Quaternary stratigraphic framework in the north-western portion of the Gulf basin. University of Texas at Austin, Bureau of Economic Geology Circular, 74-101.

Fullerton, L.G., Sager, W.W. and Handschumacher, D.W., 1989. Late Jurassic - Early Cretaceous evolution of the Eastern Indian Ocean adjacent to Northwest Australia. *Journal of Geophysical Research*, **94**, 2937-53.

Galloway, W.E., 1989a. Genetic stratigraphic sequences in basin analysis I: architecture and genesis of flooding-surface bounded depositional units. *AAPG Bulletin*, **73**, 125-42.

Galloway, W.E., 1989b. Genetic stratigraphic sequences in basin analysis II: application to Northwest Gulf of Mexico Cenozoic Basin. *AAPG Bulletin*, **73**, 143-154.

Galloway, W.E., 1993. *Depositional Systems and Sequences in Hydrocarbon Exploration and Production.* National Centre for Petroleum Geology, Adelaide University unpublished in house course notes.

Galloway, W.E., 1994. *Siliciclastic depositional systems and sequences.* National Centre for Petroleum Geology unpublished in house course notes.

Galloway W.E. and Hobday, D.K., (in prep). *Terrigenous clastic depositional systems*. Second edition, New York Springer Verlag.

Guy, M., 1992. Facies analysis of the Kopervik sand interval, Kilda Field, Block 16/26, UK North Sea. In R.F.P. Hardman (ed), *Exploration Britain: geological insights for the next decade.* Geological Society Special Publications **67**, p. 187-220.

Haq, B.U., Hardenbol, J. and Vail P.R. 1987. Chronology of fluctuating sea levels since the Triassic (250 million years ago to present). *Science*, **235**, 1156-1167.

Haq, B.U., Hardenbol, J. and Vail, P.R., 1988. Mesozoic and Cenozoic chrono-stratigraphy and cycles of sea-level change. In C.K. Wilgus, H. Posamentier, C.A. Ross and C.G.St.C. Kendall (eds), *Sea level changes: An integrated approach.* Society of Economic Paleontology and Minerology, Special Publication No. 42, p. 71-108.

Harland, W.B., Armstrong, R.L., Cox, A.V., Craig, L.E., Smith, A.G. and Smith, D.G., 1989. *A geological time scale.* Cambridge University Press, 263pp.

Harland, W.B., Cox, A., Llewellyn, P.G., Picton, C.A.G., Smith, A.G., Walter, R. and Fawcett, R.E., 1982. *Geologic Time Scale.* Cambridge University Press.

Heath, R.S. and Apthorpe, M.C., 1984. New formation names for the Late Cretaceous and Tertiary sequence of the southern North West Shelf. Western Australian Geological Survey **1984/7**.

Helby, R., Morgan, R. and Partridge, A.D., 1987. Mesozoic zonation. In P.A. Jell (ed), *Studies in Australian Mesozoic Palynology.* The Association of Australian Paleontologists, Sydney, p. 71-94.

Heller, P.L. and Dickinson, W.R., 1985. Submarine ramp facies model for Delta-Fed, Sand-Rich turbidite Systems. *AAPG Bulletin*, **69**, 90-976.

Heritier, R.E., Lossel, P. and Wathne, E., 1979. Frigg field large submarine-fan trap in lower Eocene rocks of the North Sea. *AAPG Bulletin*, **63**, 1999-2020.

Hill, G., 1994. The role of the pre-rift structure in the architecture of the Dampier Basin area, North West Shelf, Australia. *APEA Journal*, **34**, 602-13.

Hocking, R.M., 1985. *Revised stratigraphic nomenclature in the Carnarvon Basin.* Western Australia Geological Survey, **1985/1**, p. 985-986.

Hocking, R.M., 1988. Regional geology of the Northern Carnarvon Basin. In P.G. and R.R. Purcell (eds), *The North West Shelf, Australia.* Proceedings of Petroleum Exploration Society Australia Symposium, Perth, 1988, p. 97-114.

Hocking, R.M., 1990. Carnarvon Basin. In *The geology and mineral resources of Western Australia.* Geological Survey of Western Australia Memoir 3, 457-95.

Hocking, R.M., 1992. *Jurassic deposition in the Southern and Central North West Shelf.* Geological Survey of Western Australia, **1992/7**, 101 pp.

Hocking, R.M., 1993. Subdivisions of Western Australian Upper Proterozoic and Phanerozoic sedimentary basins. In preparation.

Hocking, R.M., Moors, H.T. and van de Graaff, W.J.E., 1987. The geology of the Carnarvon Basin, W.A. *Geological Society of Western Australian Bulletin*, **133**.

Hocking, R.M. Voon, J.W.K. and Collins, L.B., 1988. Stratigraphy and sedimentology of the basal Winning group, North Carnarvon Basin. In P.G. and R.R. Purcell (eds) *The North West Shelf, Australia.* Proceedings of the Petroleum Exploration Society Australia Symposium, Perth, 1988 p. 203-24.

Hollenshead, C.T. and Pritchard, R.L., 1961. Geometry of producing Mesa Verde sandstones, San Juan Basin. In J.A. Peterson and J.C. Osmond (eds), *Geometry of sandstone bodies.* AAPG Symposium, 98-118.

Horstman, E.L., 1988. Source maturity, overpressures and production, North West Shelf, Australia. In P.G. and R.R. Purcell (eds), *The North West Shelf, Australia.* Proceedings of Petroleum Exploration Society Australia Symposium, Perth, 1988, p. 529-37.

Hsu, K.J., Kelts, K. and Valentine, J.W., 1980. Resedimented facies in Ventura Basin, California, and model of longitudinal transport of turbidity currents, *AAPG Bulletin*, **64**, 1034-1051.

Hubbard, R.J., 1988. Age and significance of sequence boundaries on Jurassic and early rifted continental margins, *AAPG Bulletin*, **72**, 49-72.

Hubbard, R.J., Pape, J. and Roberts, D.G., 1985a). Depositional sequence mapping as a technique to establish tectonic and stratigraphic framework and evaluate hydrocarbon potential on a passive continental margin. In O.R. Berg and D. Woolverton (eds), *Seismic Stratigraphy - II.* AAPG Memoir 39, p. 79-91.

Hubbard, R.J., Pape, J. and Roberts, D.G., 1985b. Depositional sequence mapping to illustrate the evolution of a passive continental margin. In O.R. Berg and D. Woolverton (eds), *Seismic Stratigraphy - II.* AAPG Memoir 39, p. 93-115.

Ingram, B. and Morgan, R., 1988. The development and status of the Mesozoic palynostratigraphy of the North West Shelf, Australia. In P.G. Purcell and R.R. Purcell (eds), *The North West Shelf, Australia.* Proceedings of Petroleum Exploration Society Australia Symposium, Perth, 1988, p. 581-90.

Johnson, J.G., Klapper, G. and Sandberg, C.A., 1985. Devonian eustatic fluctuations in Euramerica. *Geological Society of America Bulletin,* **99**, 567-87.

Kaye, P., Edmond, G.M. and Challian, A., 1972. The Rankin Trend, Northwest Shelf, Western Australia, *APEA Journal*, **12**, 3-8.

Kirk, R.B., 1985. A seismic stratigraphic case history in the eastern Barrow Sub-basin, North West Shelf, Australia. In O.R. Berg and D. Woolverton (eds), *Seismic Stratigraphy - II.* AAPG Memoir 39, p. 183-207.

Kirk, R.B., 1991. Low stand seismic facies: A Carnarvon-Browse basin comparison. *Exploration Geophysics*, **22**, 207-14.

Kopsen, E., 1994. Northern Carnarvon Basin Hydrocarbon Distribution and Future Petroleum Potential. In P.G. & R.R. Purcell (eds), *The sedimentary basins of Western Australia.* Proceedings, West Australian Basins Symposium, Perth, W.A., 1994, p. 127-40.

Kopsen, E. and Mcgann, G., 1985. A review of the hydrocarbon habitat of the eastern and central Barrow-Dampier sub-basin, Western Australia. *APEA Journal*, **25**(1), 154-76.

Krumbein, W.C. and Sloss, L.L., 1963. *Stratigraphy and sedimentation* (2nd edition). Freeman and Company, San Francisco and London, 660pp.

Labutis, V.R., 1994. Sequence Stratigraphy and the North West Shelf of Australia. In P.G. and R.R. Purcell (eds), *The sedimentary basins of Western Australia.* Proceedings, West Australian Basins Symposium, Perth, W.A., 1994, p.159-180.

Leeder, M.R. and Gawthorpe, R.L., 1987. Sedimentology models for extensional tilt-block/half graben basins. In M.P. Coward, J.F. Dewey and P.L. Hancock (eds), *Continental Extensional Tectonics.* Geological Society Special Publication 28, p. 139-52.

Leithold, E.L. and Bourgeois, J., 1989. Sedimentation, sea-level changes and tectonics on an early Pleistocene continental shelf, northern California. *Geological Society of America Bulletin,* **101**, 1209-24.

Lemon, N.M. and Mahmood, T., 1994. Two and three dimensional analogue modelling of extensional fault systems with application to the North West Shelf, Western Australia. *APEA Journal*, **34**, 555-65.

Link, M.H. and Weimer, P. 1990. Seismic facies and sedimentary processes of submarine fans and turbidite systems: an overview. In P. Weimer and M.H. Link (eds), *Seismic facies and sedimentary processes of submarine fans and turbidite systems, Frontiers in Sedimentary Geology*. New York, Springer-Verlag, p. 3-8.

Lister, G.S., Etheridge, M.A. and Symonds, P.A., 1991. Detachment models for the formation of passive continental margins. *Tectonics*, **10**, 1038-1064.

Lowe, D.R., 1982. Sediment gravity flows II: depositional models with special reference to the deposits of high-density turbidity currents. *Journal of Sedimentary Petrology* **44**, 484-501.

Mack, D.A., 1993. *Seismic stratigraphic interpretation of the Candace Terrace and Preston Shelf, Northern Carnarvon Basin, Western Australia.* University of Adelaide unpublished Masters thesis.

Malcolm, R.J., Pott, M.C. and Delfos, E., 1991. A new tectono-stratigraphic synthesis of the North West Cape Area. *APEA Journal*, **31**, 154-76.

McClure, I.M., Smith, D.N., Williams, A.F., Clegg, L.J. and Ford, C.C., 1988. Oil and gas fields in the Barrow Sub-Basin. In P.G. and R.R. Purcell (eds), *The North West Shelf, Australia.* Proceedings of Petroleum Exploration Society Australia Symposium, Perth, p. 371-90.

McGovney, J.E. and Radovich, B.J., 1985. Seismic stratigraphy and facies of the Frigg Fan Complex. In O.R. Berg, and D. Woolverton (eds), *Seismic stratigraphy - II.* AAPG Memoir 39, 139-54.

Messant, B.E.J., Goody, A.K., Collins, E. and Tobias, S., 1994. Sequence stratigraphy of the Flamingo Group, Southern Bonaparte Basin. In P.G. and R.R. Purcell (eds), *The sedimentary basins of Western Australia.* Proceedings, West Australian Basins Symposium, Perth, W.A., 1994, p.243-258.

Miall, A.D., 1978. Tectonic setting and syndepositional deformation of molasse and other nonmarine-paralic sedimentary basins. *Canadian Journal of Earth Sciences,* **15**, 1613-32.

Miall, A.D., 1986. Eustatic sea level changes interpreted from seismic stratigraphy: a critique of the methodology with particular reference to the North Sea Jurassic record. *AAPG Bulletin*, **70**, 131-137.

Miall, A.D., 1992. Exxon global cycle chart: an event for every occasion? *Geology*, **20**, 131-337.

Miller, L.R. and Stuart, W.J. 1993. Seismic stratigraphic evaluation of a Neocomian submarine fan system, Browse Basin, North West Shelf. *APEA Journal*, **32**, 171-182.

Mitchum, R.M. Jr., 1977. Seismic stratigraphy and global changes of sea level, part 11: Glossary of terms used in seismic stratigraphy. In C.E. Payton (ed), *Seismic Stratigraphy - applications to hydrocarbon exploration.* AAPG Memoir 26, p. 205-12.

Mitchum, R.M. Jr., 1985. Seismic stratigraphic expression of submarine fans. In O.R. Berg and D. Woolverton (eds), *Seismic Stratigraphy - II.* AAPG Memoir 39, p. 117-36.

Mitchum, R.M. Jr. and Vail, P.R., 1977. Seismic stratigraphy and global changes of sea level, part 7: Seismic stratigraphic interpretation procedure. In C.E. Payton (ed), *Seismic stratigraphy - applications to hydrocarbon exploration.* AAPG Memoir 26, p. 135-43.

Mitchum, R.M. Jr., Vail, P.R. and Sangree, J.B., 1977. Seismic stratigraphy and global changes of sea level, part 6: Seismic interpretation of seismic reflection patterns in depositional sequences. In C.E. Payton (ed), *Seismic stratigraphy - applications to hydrocarbon exploration.* AAPG Memoir 26, p. 117-33.

Mitchum, R.M. Jr., Vail, P.R. and Thompson, S., 1977. Seismic stratigraphy and global changes of sea level, part 2: The depositional sequence as a basic unit for stratigraphic analysis. In C.E. Payton (Ed), *Seismic stratigraphy - applications to hydrocarbon exploration.*, AAPG Memoir 26, p. 53-62.

Morgan Palaeo Associates, 1987-93. Palynological Data Sheets (34 wells) (Unpublished).

Morgan Palaeo Associates, 1989. Palynology Review of Angel 3 (Unpublished).

Morgan Palaeo Associates, 1989. Palynology Review of Lauchie 1 (Unpublished).

Morgan Palaeo Associates, 1989. Palynology Review of Legendre 1 (Unpublished).

Morgan Palaeo Associates, 1989. Palynology Review of Legendre 2 (Unpublished).

Morgan Palaeo Associates, 1989. Palynology Review of Madeleine 1 (Unpublished).

Morgan Palaeo Associates, 1989. "Rapid restudy" of the Tithonian of four Dampier wells (Rosemary 1, Lewis 1/1A, Samson 1, Legendre 1) (Unpublished).

Mutti, E., 1985. Turbidite systems and their relations to depositional sequences. In G.,G. Zuffa (ed), *Provenance of arenites*, Holland, Reidel Publishing Company, p. 65-95.

Mutti, E., 1992. *Turbidite sandstones.* Agip, S.p.A., 275pp.

Mutti, E. and Normark, W.R., 1987. Comparing examples of modern and ancient turbidite systems: problems and concepts. In J.R. Legget and G.G. Zuffa (eds), *Marine clastic sedimentology: concepts and case studies.* London, Graham and Trotman, p. 1-37.

Mutti, E. and Normark, W.R. 1990. An integrated approach to the study of turbidite systems. In P. Weimer and M.H. Link (eds), Seismic facies and sedimentary processes of submarine fans and turbidite systems, Frontiers in Sedimentary Geology: New York, Springer-Verlag, p. 75-106.

Mutti, E. and Ricci Lucchi, F., 1972. Turbidites of the northern Apenines: introduction to facies analysis (English translation by T.H. Nilsen, 1978). *International Geology Review*, **20**, 125-166.

Nelson, A., 1993. Wrench and inversion structures in the Timor Sea region. *PESA Journal*, **21**, 3-30.

Nelson, C.H. and Maldonado, A. 1988. Factors controlling depositional patterns of Ebro Turbidite systems, Mediterranean Sea. *AAPG Bulletin*, **72**, 98-716.

Nelson, C.H., Maldonado, A., Barber, J.H. and Alonso, B. 1990. Modern sand-rich and mud-rich siliciclastic aprons: alternative base-of-slope turbidite systems to submarine fans In P. Weimer and M.H. Link (eds) Seismic facies and sedimentary processes of submarine fans and turbidite systems, Frontiers in Sedimentary Geology: New York, Springer-Verlag, p. 171-192.

Normark, W.R., 1970. Growth patterns of deep-sea fans. *AAPG Bulletin*, **54**, 2170-95.

O'Brien G.W., 1993. Some ideas on the rifting history of the Timor Sea from the integration of deep crustal seismic and other data. *PESA Journal*, **21**, 95-113.

Odin, G.S., 1984. Significance of green particles (Glaucony, Betherine, Chlorite) in Arenites. In G.G. Zuffa (ed), *Provenance of Arenites.* Holland, Reidel Publishing Company, p. 297-308.

Oil & Gas Australia, 1992. Production and Development 1991/92, petroleum in Western Australia. In *Oil & Gas Australia,* 28-46.

Partridge, A.D. and Helby, R., 1988. *Australian Biostratigraphy on the Jurassic and Cretaceous Global Cycle Chart* (unpublished version of the Haq et al 1988 Geological Time Scale).

Parry, J.C. and Smith, D.N., 1988. The Barrow and Exmouth Sub-Basins. In P.G. and R.R. Purcell (eds), *The North West Shelf, Australia.* Proceedings of Petroleum Exploration Society Australia Symposium, Perth, 1988, p. 129-46.

Payton, C.E., 1977. *Seismic stratigraphy - applications to hydrocarbon exploration.* AAPG Memoir 26, 516pp.

Pemberton, S.G., Frey, R.W., Ranger, M.J. and MacEachern, J.A., 1992. The conceptual framework of ichnology. In S.G. Pemberton (ed*), Applications of ichnology to petroleum exploration.* A core workshop, SEPM Core Workshop No. 17, Calgary, June 21, 1992, p. 1-32.

Pemberton, S.G., MacEachern, J.A. and Frey, R.W., 1992. Trace fossil models: environmental and allostratigraphic significance. In R.G. Walker and N.P. James (eds), *Facies models: response to sea level change*. Geological Association of Canada, p. 47-71.

Pickering, K.T., Hiscott, R.N. and Hein, F.J., 1989. *Deep marine environments, clastic sedimentation and tectonics*. London, Unwin Hyman Ltd., 416 p.

Pickering, K.T., Stow, D.A.V., Watson, M.P. and Hiscott, R.N., 1986. Deep-water facies, processes and models: a review and classification scheme for modern and ancient sediments. *Earth-science reviews*, **23**(1986), 75 - 174.

Posamentier, H.W. and Erskine, R.D. 1990. Seismic expression and recognition criteria of ancient submarine fans. In P. Weimer and M.H. Link (eds*), Seismic facies and sedimentary processes of submarine fans and turbidite systems, Frontiers in Sedimentary Geology*. New York, Springer-Verlag, p. 197 - 222.

Posamentier, H.W. and James, D.P., 1993. An overview of sequence-stratigraphic concepts: uses and abuses. In H.W. Posamentier, C.P. Summerhayes, B.U. Haq and G.P. Allen (eds), *Sequence stratigraphy and facies associations*. International Association of Sedimentologists, Special Publication No. 18, Blackwell Publications, p. 3-18.

Posamentier, H.W. and Vail, P.R., 1988. Eustatic controls on clastic deposition II: sequences and system tract models. In C.K. Wilgus, H.W. Posamentier, C.R. Ross and C.G.St.C. Kendall (eds), *Sea level changes: an integrated approach.* SEPM Special Publication No. 42, p. 125-54.

Prosser, S., 1993. Rift-related linked depositional systems and their seismic expression. In G.D. Williams and A. Dobb (eds), *Tectonics and seismic sequence stratigraphy.* Geological Society Special Publication No. 71 p. 35-66.

Purcell, P.G. and Purcell, R.R., 1988. The North West Shelf, Australia - an introduction. In P.G. and R.R. Purcell (eds), *The North West Shelf, Australia.* Proceedings of the Petroleum Exploration Society Australia Symposium, Perth, 1988, p. 3-16.

Ramsayer, G.R., 1979. Seismic stratigraphy: a fundamental exploration tool. Offshore Technology Conference Proceedings, 3, p. 1859-67.

Ramsden, C.R.T., Hobson, M.R. and Cooper, R., 1988. The Geophysicists' bane: multiple suppression on the North West Shelf. In P.G. and R.R. Purcell (eds), *The North West Shelf Australia.* Proceedings of the Petroleum Exploration Society Australia Symposium, Perth, 1988, p. 499-508.

Reading, H.G. and Richards, M., 1994. Turbidite systems in deep-water basin margins classified by grain size and feeder system. *AAPG Bulletin*, **78/5** 792-822.

Rider, M.H., 1990. Gamma-ray shape used as a facies indicator: critical analysis of an oversimplified methodology. In A. Hurst, M.A. Lovell and A.C. Morton (eds), *Geological applications of wireline logs.* Geological Society Special Publication No. 48, p. 27-37.

Robinson, P.H., Stead, H.S., O'Reilly, J.B. and Guppy, N.K., 1994. Meanders to fans: a sequence stratigraphic approach to Upper Jurassic - Lower Cretaceous sedimentation in the Sahul Syncline, North Bonaparte Basin. In P.G. and R.R. Purcell (eds), *The sedimentary basins of Western Australia.* Proceedings, West Australian Basins Symposium, Perth, W.A., 1994, p.223-242.

Ross, M.I. and Vail P.R., 1994. Sequence Stratigraphy of the Lower Neocomian Barrow Delta, Exmouth Plateau, Northwestern Australia. In P.G. and R.R. Purcell (eds), *The sedimentary basins of Western Australia.* Proceedings, West Australian Basins Symposium, Perth, W.A., 1994, p.435-448.

Ryan-Grigor, S. and Shulz-Rojahn, J.P., 1995. Seismic delineation of structure-controlled carbonate cement and potential economic implications, Angel Field, North West Shelf. *APEA Journal*, **35**, 280-95.

Sarg, J.F. and Skjold, L.J., 1982. Stratigraphic traps in Paleocene sands in the Balder area, North Sea. In M.T. Halbouty (ed), *The deliberate search for the subtle trap.* AAPG Memoir 32, p. 197-206.

Scott, R.W. and Govean, F.M., 1985. Early depositional history of a rift basin: Miocene in Western Sinai. *Palaeogeography, Palaeoclimatology, Palaeoecology*, **52**, 143-58. Elsevier Science Publishers B.V., Amsterdam.

Selley, R.C. 1979. Dipmeter and log motifs in North Sea submarine-fan sands. *AAPG Bulletin*, **63**, 905-917.

Serra, O., 1984. Fundamentals of well-log interpretation: 1. the acquisition of logging data. *Developments in Petroleum Science*, 15A, Elsevier Science Publishers, 423p.

Shanmugam, G.R., Lehtonen, L.R., Straume, T., Syvertsen, S.E., Hodgkinson, R.J. and Skibeli, M., 1994. Slump and debris-flow dominated upper slope facies in the Cretaceous of the Norwegian and northern North Seas (61-67N): Implications for sand distribution. *AAPG Bulletin*, **78**(6), 910-937.

Shanmugam, G.R. and Moiola, R.J., 1991. Types of submarine fan lobes: models and implications. *AAPG Bulletin*, **75**(1), 156-179.

Shanmugam, G.R., Moiola, R.J. and Damuth, J.E., 1985. Eustatic control of submarine fan development. In A.H. Bouma, W.R. Normark and N.E. Barnes (eds), Frontiers in Sedimentary Geology: Submarine fans and related turbidite systems, Springer-Verlag, New York, p. 23-28.

Shanmugam, G.R., Moiola, R.J., Mcpherson, J.G. and O'Connell, S., 1988. Comparison of turbidite facies associations in modern passive-margin Mississippi fan with ancient active-margin fans. *Sedimentary Geology*, **58**, 63-77.

Sloss, L.L., 1988. Forty years of sequence stratigraphy. *Geological Society of America Bulletin,* **100**, 1661-65.

Spring, D.E. and Newall, N.A., 1993. Depositional systems and sequence stratigraphy of the Cretaceous Warnbro Group, Vlaming Sub-basin, Western Australia. *APEA Journal*, **33**, 190-204.

Stagg, H.M.J. and Colwell, J.B., 1994. The structural foundations of the Northern Carnarvon Basin. In P.G. and R.R. Purcell (eds), *The sedimentary basins of Western Australia.* Proceedings, West Australian Basins Symposium, Perth, W.A., 1994, p.349-364.

Surlyk, F., 1987. Slope and deep gully sandstones, Upper Jurassic, East Greenland. *AAPG Bulletin,* **71**, 464-75.

Thomas, B.M. and Smith, D.N., 1974. A summary of the petroleum geology of the Carnarvon Basin. *APEA Journal*, **14**, 66-76.

Thompson, N.B., Hocking, R.M., Collins, L.B., Voon, J.W.K. and Middleton, M.F., 1990. *Lower Cretaceous deposition in the southern North West Shelf.* Minerals and Energy Research institute of Western Australia unpublished report **55/84**, 112pp.

Thorne, J.A. 1992. An analysis of the implicit assumptions of the methodology of seismic sequence stratigraphy. In Joel Watkins, Feng Zhiqiang and Kenneth McMillen (eds), *Geology and geophysics of continental margins*. AAPG Memoir 53, p. 375-94.

Vail, P.R., Mitchum, R.M. Jr., Todd, R.G., Widmier, J.M., Thompson, S. III, Sangree, J.B., Bubb, J.N., Hatlelid, W.G., 1977. Seismic stratigraphy and global changes of sea level. In C.E. Payton (ed), *Seismic stratigraphy - applications to hydrocarbon exploration.* AAPG Memoir 26, p. 49-212.

Vail, P.R., et al. (22 others), 1987. Cenozoic - Mesozoic Cycle Chart. In A.W. Bally (ed), Atlas of seismic stratigraphy, AAPG studies in geology **27/1**, 224pp.

Vail, P.R., Hardenbol, J. and Todd, R.G., 1984. Jurassic unconformities, chronostratigraphy, and sea-level changes from seismic stratigraphy and biostratigraphy. In J.S. Schlee (ed), Inter-regional unconformities and hydrocarbon accumulations, AAPG Memoir 36, p. 129-144.

Van Wagoner, J.C., Posamentier, H.W., Mitchum, R.M., Vail, P.R., Sarg, J.F., Loutit, T.S. and Hardenbol, J., 1988. An overview of the fundamentals of sequence stratigraphy and key definitions. In C.K. Wilgus, B.S. Hastings, C.G.St.C. Kendall, H.W. Posamentier, C.A. Ross and J.C. Van Wagoner (eds), Sea-level changes - an integrated approach, SEPM Special Publication 42, p. 39-45.

Veenstra, E., 1985. Rift and drift in the Dampier Sub-Basin, a seismic and structural interpretation. *APEA Journal*, **25**, 126-55.

Veevers, J.J. (ed), 1984. Phanerozoic Earth History of Australia, Oxford University Press, Oxford, p. 182-201.

Veevers, J.J., 1988. Morphotectonics of Australia's northwestern margin - a review. In P.G. and R.R. Purcell (eds), *The North West Shelf, Australia.* Proceedings of Petroleum Exploration Society Australia Symposium, Perth, 1988, p. 19-27.

Veevers, J.J., Jones, J.G. and Powell, C.McA., 1982. Tectonic framework of Australia's sedimentary basins. *APEA Journal*, **22**, 283-300.

Veevers, J.J., Powell, C.McA. and Roots, S.R., 1991. Review of seafloor spreading around Australia. I. Synthesis of the patterns of spreading. *Australian Journal of Earth Sciences*, **38**, 373-389.

Vincent, P. and Tilbury, L., 1988. Gas and oil fields of the Rankin Trend and northern Barrow-Dampier Sub-basin. In Purcell, P.G. and R.R. Purcell (Eds), *The North West Shelf, Australia.* Proceedings of Petroleum Exploration Society Australia Symposium, Perth, 1988, 341-69.

von Rad, U. and Exon, N.F., 1982. Mesozoic-Cenozoic sedimentary and volcanic evolution of the starved passive continental margin off northwest Australia. In J.S. Watkins and C.L. Drake (eds), *Studies in Continental Margin Geology.* AAPG Memoir 34, p. 253-81.

Walker, R.G., 1978. Deep-water sandstone facies and ancient submarine fans: models for exploration for stratigraphic trap. *AAPG Bulletin*, **62**, 932-66.

Walker, R.G., 1990. Perspective. Facies modelling and sequence stratigraphy. *Journal of Sedimentary Petrology*, **60**, 777-786.

Walker, R.G., 1992. Turbidites and submarine fans. In R.G. Walker and N.P. James (eds), *Facies models: response to sea level change.* Geological Association of Canada, p. 239-63.

Weimer, P., 1990. Sequence stratigraphy, facies geometries, and depositional history of the Mississippi Fan, Gulf of Mexico. *AAPG Bulletin,* **74**, 47-66.

Weimer, P. and Link, M.H. 1990. Global petroleum occurrences in submarine fans and turbidite systems. In P. Weimer and M.H. Link (eds), *Seismic facies and sedimentary processes of submarine fans and turbidite systems, Frontiers in Sedimentary Geology*. New York, Springer-Verlag, 9-67.

Weimer, P. and Posamentier, H.W., 1994. Recent developments and applications in siliciclastic sequence stratigraphy. In P. Weimer and H.W. Posamentier (eds), *Siliciclastic sequence stratigraphy - recent developments and applications*. AAPG Memoir 58, 3-12.

Weimer, R.J., 1992a. Sequence stratigraphy - a historical perspective. *Applied Sequence stratigraphy, a symposium on applications to oil and gas exploration and production*. Colorado School of Mines, Golden, Colorado, March 25-27, 3 pp.

Weimer, R.J., 1992b. Developments in sequence stratigraphy: Foreland and cratonic Basins. *AAPG Bulletin*, **76**, 965-982.

Well Completion Reports (unpublished):

Alpha North 1, 1989. Marathon Petroleum Australia Ltd.

Angel 1, 1972. Woodside Offshore Petroleum Pty. Ltd.

Angel 2, 1972. Woodside Offshore Petroleum Pty. Ltd.

Angel 3, 1973. Woodside Offshore Petroleum Pty. Ltd.

Angel 4, 1990. Woodside Offshore Petroleum Pty. Ltd.

Aurora 1, 1990. Marathon Petroleum Australia Ltd.

Bounty 1, 1983. Marathon Petroleum Australia Ltd.

Calypso 1, 1985. Marathon Petroleum Australia Ltd.

Cygnus 1, 1989. ARCO Australia Ltd.

Dampier 1, 1969. Woodside Offshore Petroleum Pty. Ltd.

De Grey 1, 1971. Woodside Offshore Petroleum Pty. Ltd.

Eaglehawk 1, 1972. Woodside Offshore Petroleum Pty. Ltd.

Egret 1, 1973. Woodside Offshore Petroleum Pty. Ltd.

Enderby 1, 1970. Woodside Offshore Petroleum Pty. Ltd.

Finucane 1, 1978. Woodside Offshore Petroleum Pty. Ltd.

Forestier 1, 1978. Woodside Offshore Petroleum Pty. Ltd.

Hampton 1, 1974. Woodside Offshore Petroleum Pty. Ltd.

Lambert 1, 1974. Woodside Offshore Petroleum Pty. Ltd.

Lauchie 1, 1990. Philips Australian Oil Company.

Legendre 1, 1968. Woodside Offshore Petroleum Pty. Ltd.

Legendre 2, 1970. Woodside Offshore Petroleum Pty. Ltd.

Lewis 1, 1976. Woodside Offshore Petroleum Pty. Ltd.

Madeleine 1, 1969. Woodside Offshore Petroleum Pty. Ltd.

Montague 1, 1985. Esso Australia Ltd.

Nelson Rocks 1, 1973. Woodside Offshore Petroleum Pty. Ltd.

Orion 1, 1990. Woodside Offshore Petroleum Pty. Ltd.

Rosemary 1, 1973. Woodside Offshore Petroleum Pty. Ltd.

Rosemary North 1, 1982. Woodside Offshore Petroleum Pty. Ltd.

Samson 1, 1984. Woodside Offshore Petroleum Pty. Ltd.

Talisman 1, 1984. Marathon Petroleum Australia Ltd.

Talisman 2, 1985. Marathon Petroleum Australia Ltd.

Talisman 3, 1987. Marathon Petroleum Australia Ltd.

Walcott 1, 1979. Woodside Offshore Petroleum Pty. Ltd.

Wanaea 1, 1990. Woodside Offshore Petroleum Pty. Ltd.

Wilkinson, R., 1988. Australia's oil exploration history. In *Petroleum in Australia: the first century,* Australian Petroleum Exploration Society (APEA) 15-22.

Wiseman, J.F., 1979. Neocomian eustatic changes - biostratigraphic evidence from the Carnarvon Basin, *APEA Journal*, **19**(1), 66-73.

Woodside Offshore Petroleum, 1988. A review of the petroleum geology and hydrocarbon potential of the Barrow / Dampier Sub-Basin and environs. In P.G. and R.R. Purcell (eds), *The North West Shelf, Australia.* Proceedings of Petroleum Exploration Society Australia Symposium, Perth, 1988, 115-28.

Wulff, K., 1992. Depositional history and facies analysis of the upper Jurassic sediments in the eastern Barrow Sub-Basin. *APEA Journal*, **32**, 104-122.

APPENDIX I

CORE LOGS

LIST OF CORE LOGGED IN THE DAMPIER SUB-BASIN

Well	#	Depth (M)	Metres
Angel 1	1	2662.1 - 2667	4.9
	3	3408.3 - 3411.7	3.4
Angel 2	1	2702 - 2707	4.1
	3	2746.9 - 2754	7.1
Angel 3	1	2604.5 - 2613.4	8.9
	2	2746.6 - 2755.7	9.1
Angel 4	1	2698 - 2711	13
	2	2716.5 - 2744	27.5
	3	2744 - 2771	27
	4	2771 - 2798.3	27.3
Cossack 1	1	2891-2909.6	18.6
	2	2909.6-2928.7	19.1
Dampier 1	9	2834.6 - 2838.3	3.7
	10	2898.3 - 2905	6.7
	11	3063.5 - 3070.9	7.4
	12	3282.4 - 3287	4.6
	13	3487.5 - 3492.7	5.2
	14	3710.6 - 3715.2	4.6
	15	3931 - 3935.6	4.6
	16	4134.9 - 4140.4	5.5
Lambert 1	1	3104 - 3109.6	5.6
Legendre 1	10	1933.7 - 1938.2	4.5
	11	2127.2 - 2128.7	1.5
	12	2354.6 - 2359.6	5
	13	2485.6 - 2488.7	3.1
	14	2534.7 - 2538.9	4.2
	16	2974.2 - 2977.8	3.6
	17	3180 - 3184.2	4.2
	18	3383.9 - 3386.6	2.7
Legendre 2	1	2080.3 - 2083.2	2.9

Well	#	Depth (M)	Metres
Madeleine 1	1	2900.1 - 2907.8	7.7
	2	2979.1 - 2984.9	5.8
	3	3185.5 - 3191.9	6.4
	4	3404 - 3408.6	4.6
	5	3632.6 - 3636.3	3.7
	6	3856.9 - 3867.3	10.4
	7	3942.3 - 3947.8	5.5
	8	4160 - 4164.5	4.5
Montague 1	1	3219.5 - 3237.5	18
Rosemary 1	1	2794.4 - 2803.6	9.2
	2	2918.2 - 2927.3	9.1
	3	3185.5 - 3193.7	8.2
Talisman 2	3	1994-2011.3	17.3
	4	2012 - 2030.1	18.1
	5	2030 - 2048.2	18.2
	6	2055 - 2058.7	3.7
Talisman 3	1	1962 - 1965	3
	2	1965 - 1973	8
Wanaea 1	1	2832 - 2845.5	13.5
	2	2889 - 2904.8	15.8
Wanaea 2	1	2075-2077	2
	2	2869-2886	17
	3	2886-2907	21
	4	2907-2930	23

Key

STRUCTURES

 Horizontal bedding

 Fine lamination

 Wavy/wispy bedding

 Inlined bedding

 Convoluted bedding

 Flaser bedding

 Dish structures/dewatering features

 Ripple marks (plan view)

B Highly bioturbated

 Tubes/burrows

 Claystone intraclasts

 Scour surface

 Unconformity surface

 Load casts

 Sand ball

 Sand lens

 Siderite nodule

 Pyrite nodule

 Septarian nodule

 Shell fragments

 Belemnite

 Leaf/plant imprint

 Microfaulting

 Slickensides

 Intraformational breccia

 Dolomite filled fracture

 Carbonaceous material

LITHOLOGY

 Sandstone

 Siltstone

 Claystone

 Shale

 Calcite

 Dolomite

LITHOLOGY DESCRIPTORS

•• Sandy

" Silty

– – Argillaceous

* Glauconitic (5 - 10 %)

* Glauconite (<5%)

▫ Pyrite (disseminated)

L Lithics

O Quartz granule

CEMENT

Ca Calcite

Dol Dolomite

S Siderite

P Pyrite

 Patchy dolomitic cement (or calcite)

OTHER

◀ Sample point

⊂ Photograph point

Lithofacies Codes (modified after Miall, 1978)

GRAVEL:

Gt	- trough cross bedded
Gmm	- massive, matrix supported
Gcm	- massive, clast supported

SAND:

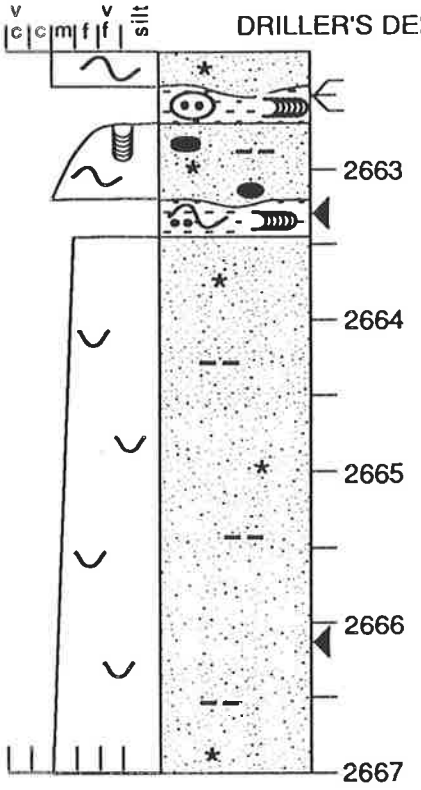
Sb	- bioturbated
Sp	- planar cross bedded
St	- trough cross bedded
Sh	- horizontally bedded
Sq	- graded bedding
Sm	- massive
Se	- erosional scours with intraclasts
Sd	- soft sediment deformation
Sr	- fine rippled sand

SILT & MUD:

Fl	- laminated
Fm	- massive
Fb	- bioturbated
Fr	- ripple laminated
Fd	- soft sediment deformation
Fh	- horizontally bedded

Angel 1 CORE 1 2662.1 - 2667

Angel Formation *K. wisemaniae* Zone RECOVERY: 94% SCALE 1: 50

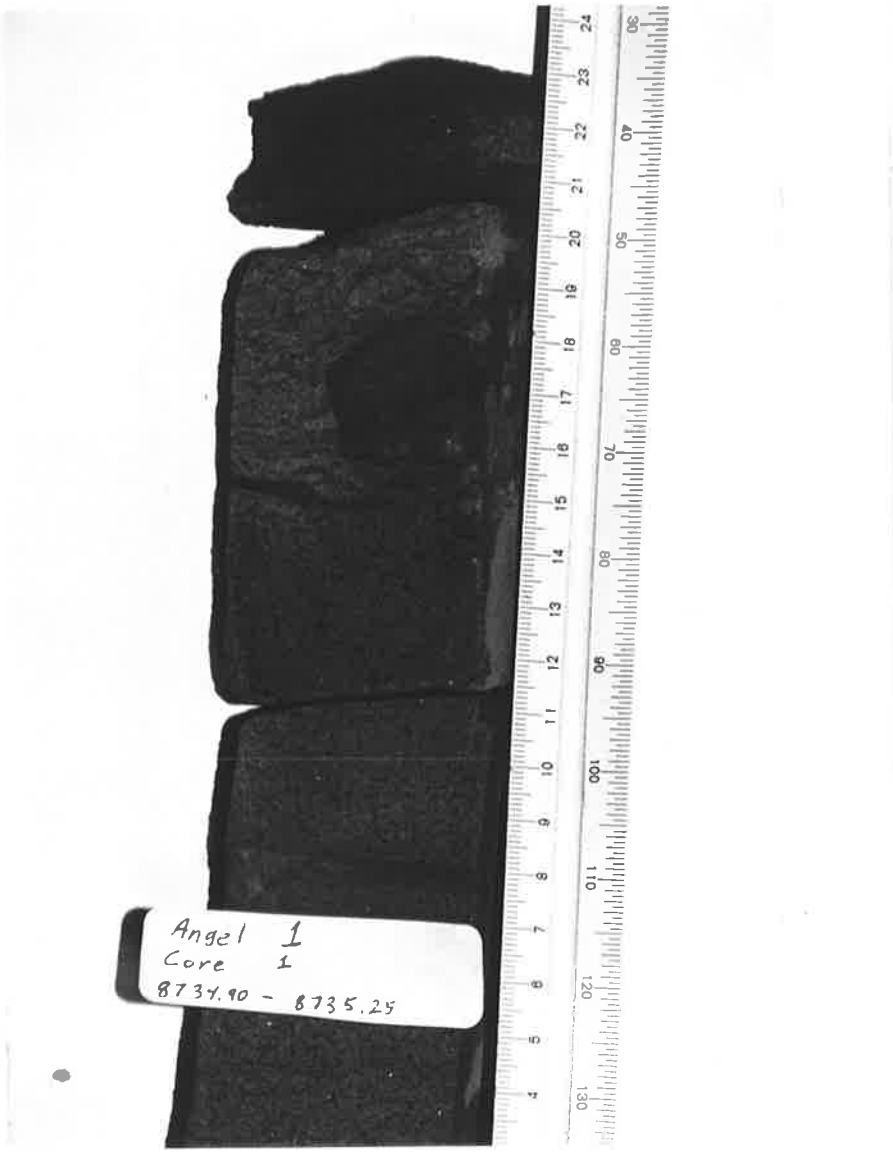


DESCRIPTION & COMMENTS

Claystone: green grey, mica-micaceous, sandy, wispy laminations.

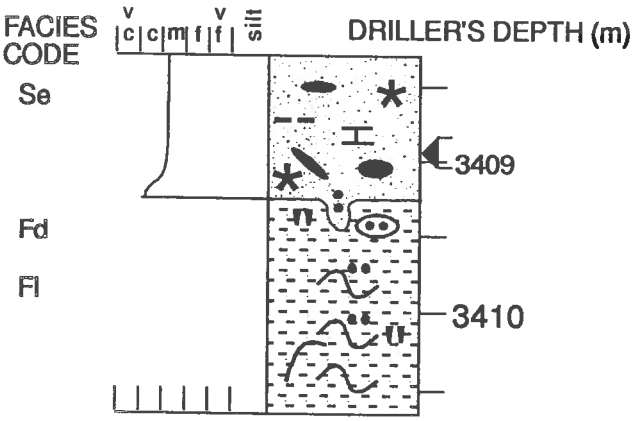
Sandstone: light grey, well sorted, medium to fine grained, 5% glauconite, 5 - 10% argillite; 5 degree dip at sand/clay interface.

Core plug porosity: 16.4 - 22.4% (sandstone).
Core plug permeability: 187 - 723md (sandstone).



Angel 1 CORE 3 3408.3 - 3410.7m

Angel Formation *D. swanense* Zone RECOVERY: 100% SCALE 1: 50



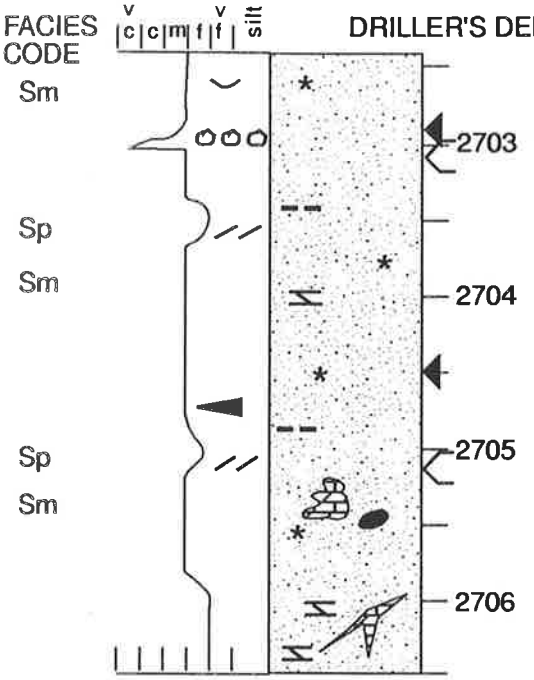
DESCRIPTION & COMMENTS

Sandstone: brown grey, poorly sorted, fine - coarse grained, dominantly medium grained, ~15% glauconite, deformed claystone rip up clasts 1 - 10 cm in diameter; sand filled worm burrows; ~20 degree dip at sand/clay interface. No visual porosity.

Claystone: brown black, wavy sand laminae, sand filled worm burrows, ~25% silt; possible oyster shell at 3410.3 m.

Angel 2 CORE 1 2702.4 - 2706.5m

Angel Formation P. iehiense zone SCALE 1: 50

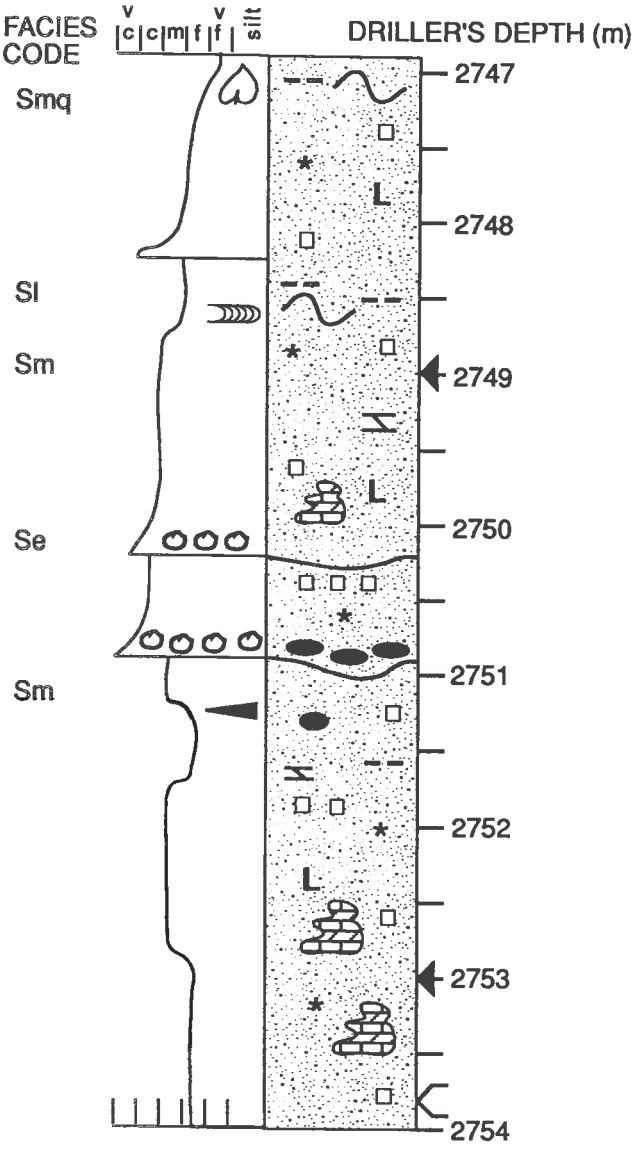


DESCRIPTION & COMMENTS

Sandstone: light brown, brown from 2704 m, well sorted, very fine to medium grained, poor to fair visual porosity; minor inclined bedding in argillaceous bands; dolomite cement increases downwards and fills fractures near the base of core. Belemnite gaurd and leaf fragment noted near 2705 m.

Angel 2 CORE 3 2746.9 - 2754m

Angel Formation *D. jurassicum* Zone SCALE 1: 50

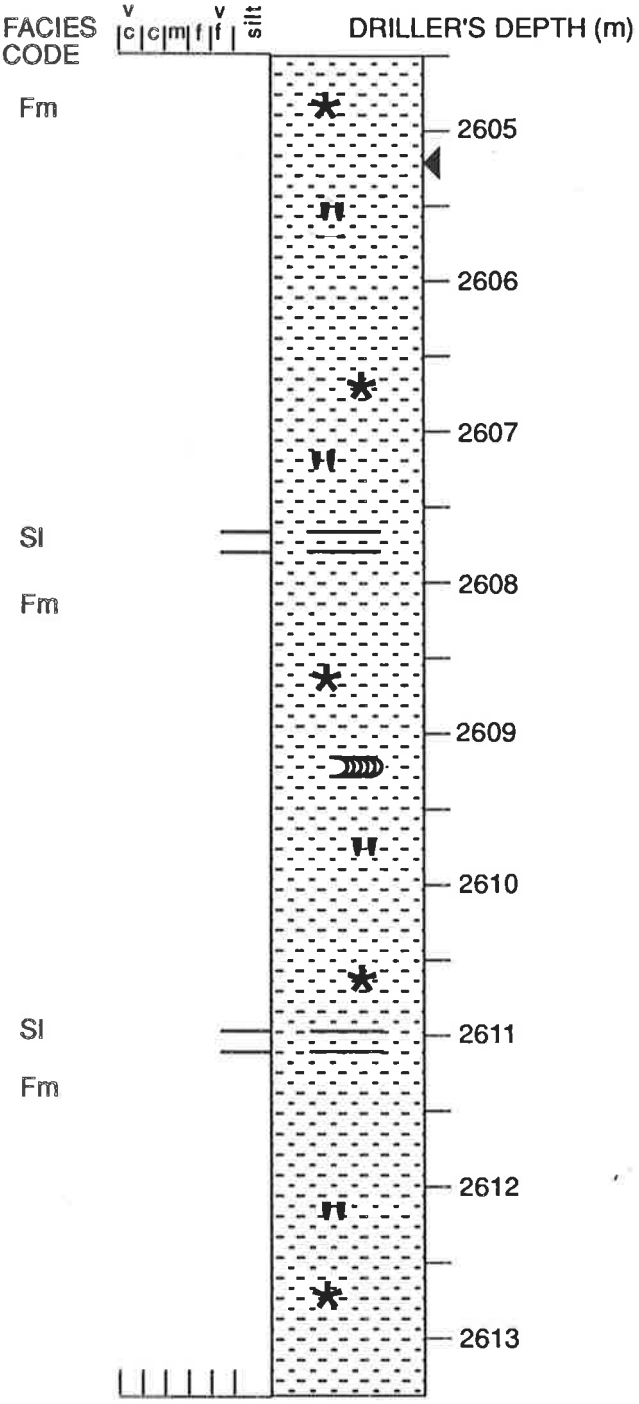


DESCRIPTION & COMMENTS

Sandstone: light grey to clear, very well sorted, fine to coarse grained, dominantly medium grained; good to excellent visual porosity, vuggy and intergranular porosity; dolomite cement increases downwards to spotty; claystone clast at 2751.4 appears coated with coarse quartz grains; possible oil staining at 2748.7; occasional iron staining; pyritized zone at 2750.6 m.

Angel 3 CORE 1 2604.5 - 2613.4m

Forestier Claystone *D. lobospinosum* Zone RECOVERY: 100% SCALE 1: 50



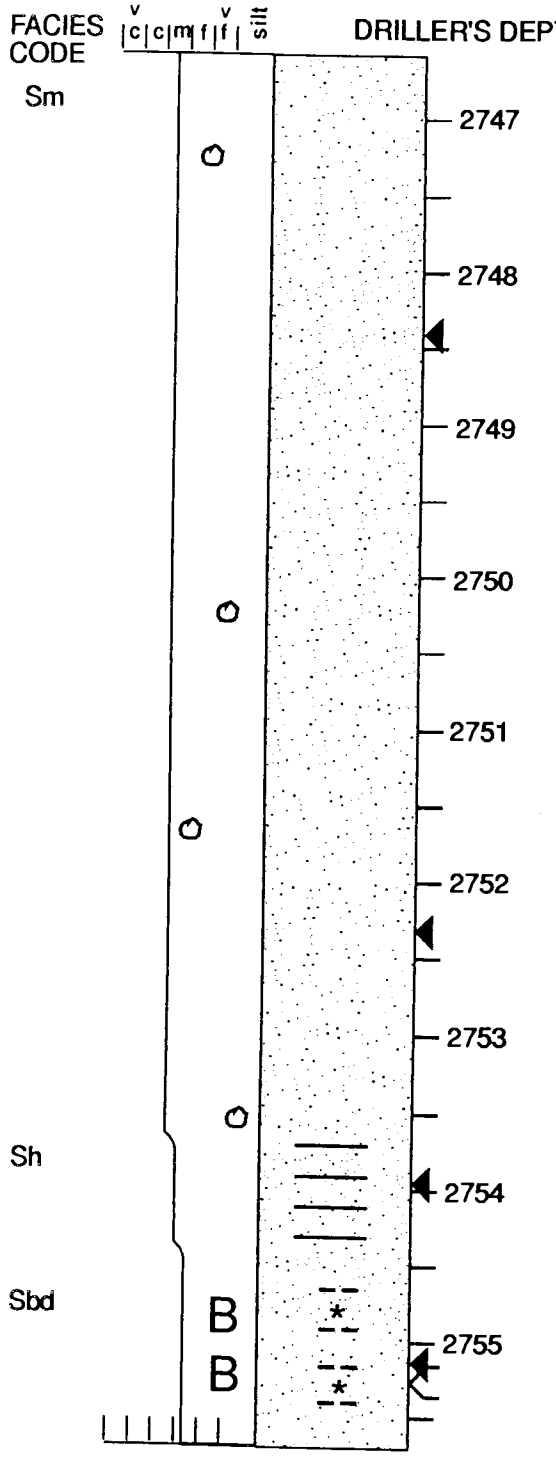
DESCRIPTION & COMMENTS

Claystone: light brown to olive grey, up to 15% glauconite, mica-micaceous.

Sandstone: well sorted, very fine to medium grained, dominantly fine grained; occurs as ~ 5 mm laminae, no visual porosity; dip of 5 - 10 degrees is noted.

Angel 3 CORE 2 2746.6 - 2755.7m

Angel Formation *P. iehiense* Zone RECOVERY: 100% SCALE 1: 50



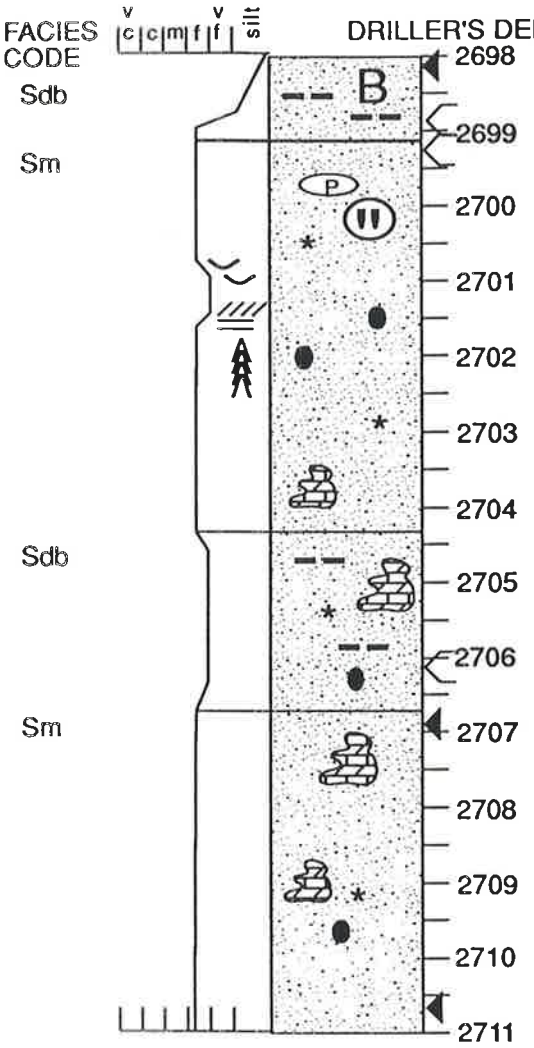
DESCRIPTION & COMMENTS

Sandstone: Light grey, green grey, fine to medium grained, dominantly medium grained; well sorted; smooth and frosted quartz grains; fair to good visual porosity; mm scale quartz granules, lithics and jasper fragments; faint horizontal bedding from 2753.5 m; below 2754.3 m up to 25% argillite and kaolinite, highly bioturbated; no dip seen.

Note: according to the electric log annotation diagram, and the core report in the well completion report, the depths on the core box are labelled top to bottom.

Angel 4 CORE 1 2698 - 2711m

Angel Formation Berriasian Age RECOVERY: 100% SCALE 1: 100



DESCRIPTION & COMMENTS

Sandstone: light grey, well sorted; ~5mm diameter claystone clasts; argillaceous zones are highly bioturbated with occasional *Terebellina, Planolites*, and *Zoophycos* burrows; spotty dolomite cement texture from 2703 to 2710.5 m.

Core unconsolidated from 2710.5 - 2711m.



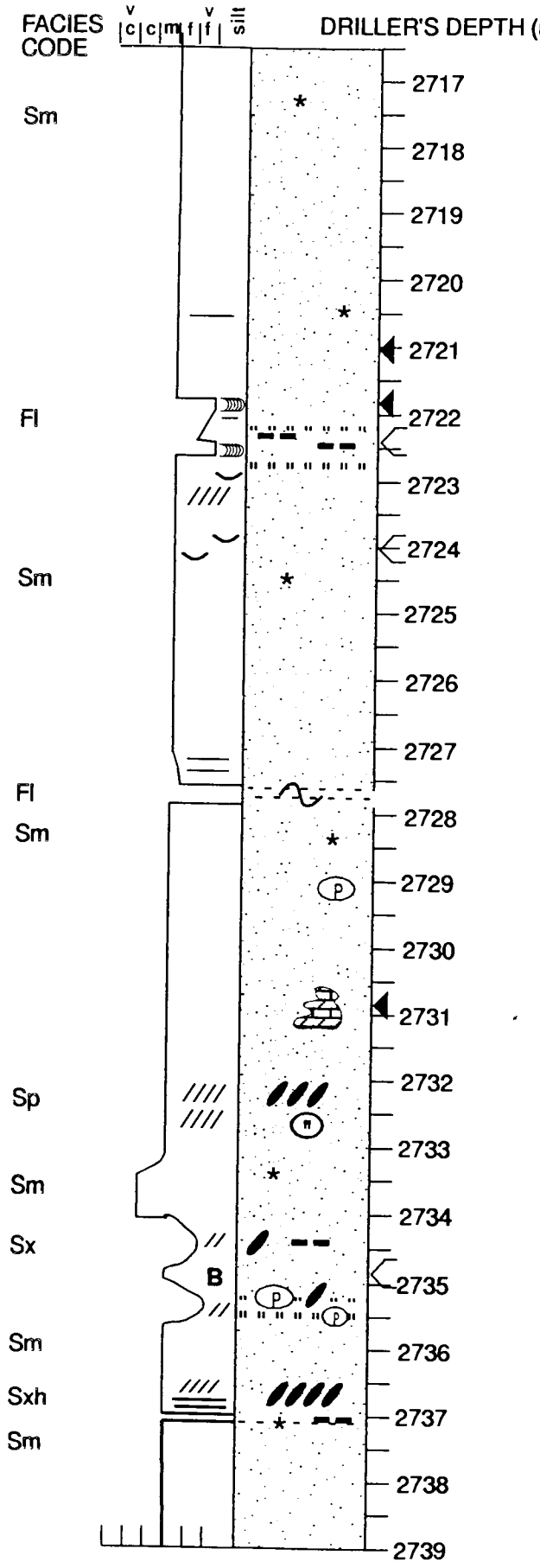
Angel 4 C/ 2698.80 m



cm Scale

Angel 4 CORE 2 2716.5 - 2744m (part 1)

Angel Formation Berriasian - Tithonian Age RECOVERY: 100% SCALE 1: 100



DESCRIPTION & COMMENTS

Sandstone: light grey, well sorted; faint horizontal laminations in argillaceous zones.

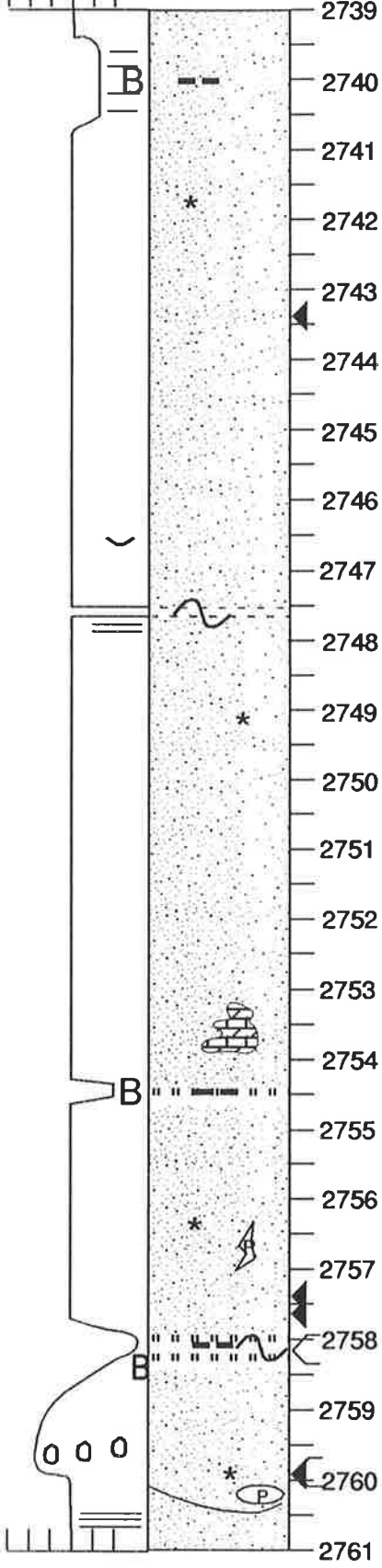
Claystone: Dark grey, wavy laminations, *Rhyzocorallium* and *Plaonolites* burrows.

Claystone rip up clasts, deformed, 3cm long, inclined at 30 degrees.

Anconichnus, *Planolites* burrows.

Angel 4 CORE 2 2716.5 - 2744m (part 2) CORE 3 2744 - 2771m (part 1)

Angel Formation Berriasian/Tithonian Age RECOVERY: 100% SCALE 1: 100

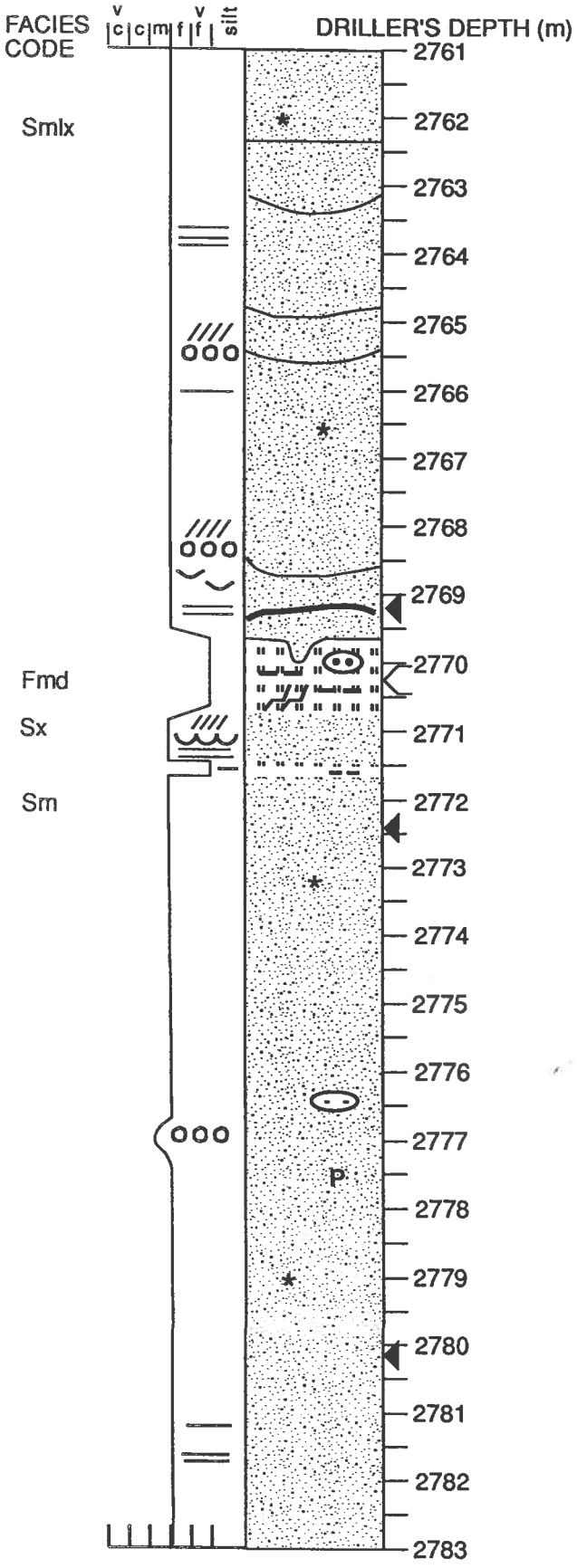


DESCRIPTION & COMMENTS

Sandstone: light grey, well sorted; argillaceous zones are highly bioturbated and soft sediment deformed; occassional mm scale kaolin clasts (ex-feldspar).

Terebellina, Planolites, Rhyzocorallium burrows.

Quartz, chert, jasper, and feldspar in sand matrix.



DESCRIPTION & COMMENTS

Sandstone: light grey, well sorted, 2763 - 2768.5m - poorly to moderately sorted; occasional 3 - 5 mm quartz pebbles above bed contacts; occasional floating pebble size kaolin clasts.

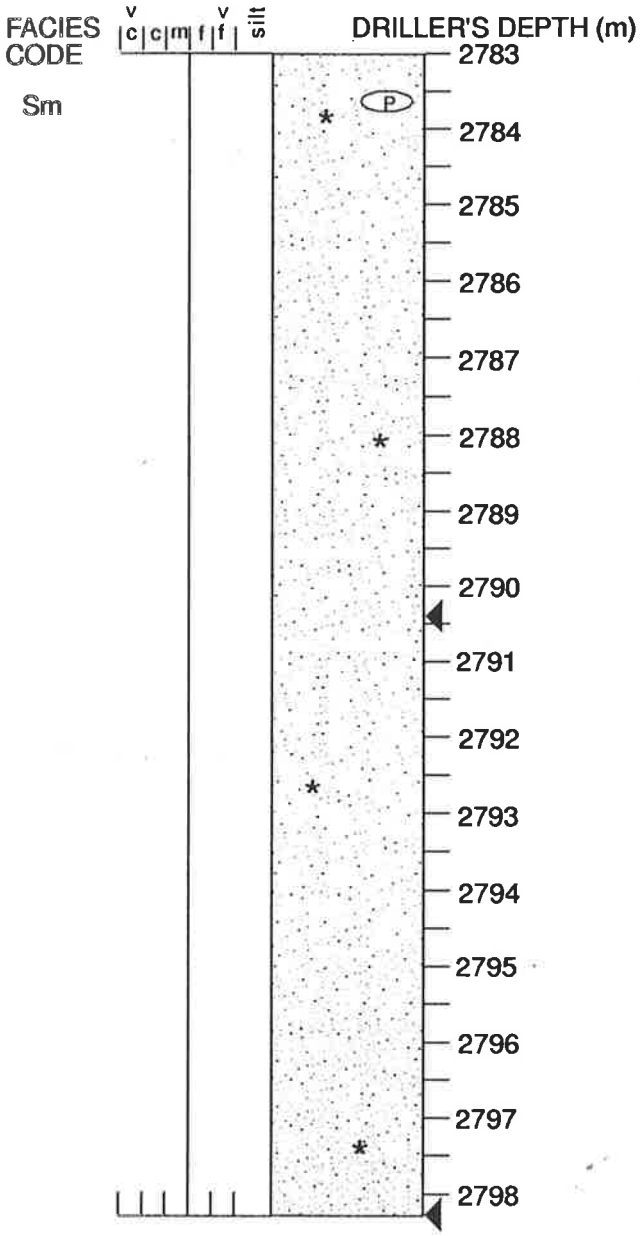
Clast containing fragmented coal squashed to 1mm thick, cuts across core.

2770.5m - synsedimentary normal fault, 1cm throw.

2776.4m - pyritized claystone clast.

Angel 4 CORE 4 (part 2) 2771 - 2798.3m

Angel Formation Tithonian Age RECOVERY: 100% SCALE 1: 100

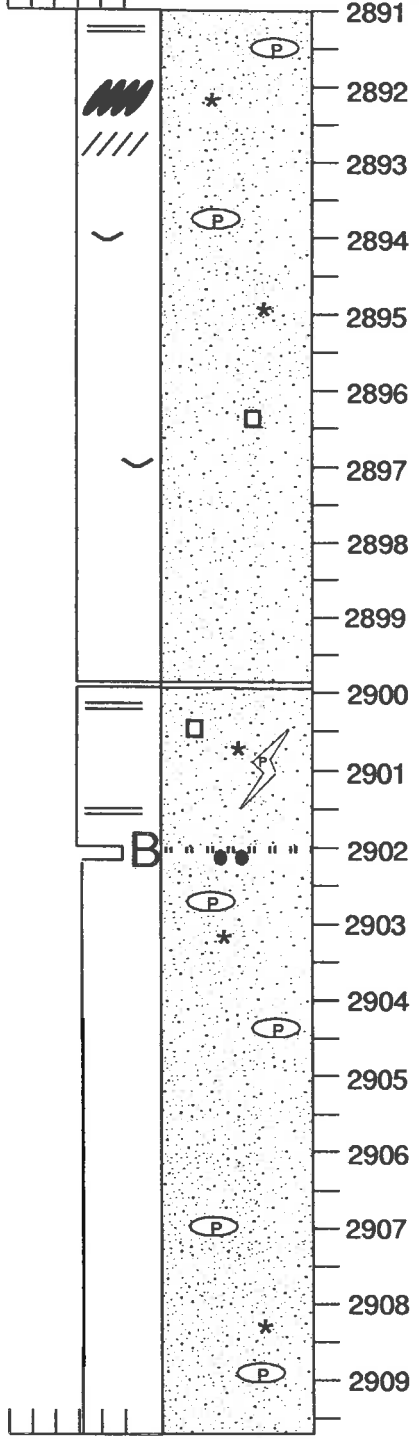


DESCRIPTION & COMMENTS

Sandstone: light grey, well sorted,very fine to medium grained, dominantly fine grained; fair to good visual porosity.

Cossack 1 CORE 1 2891 - 2909.6m

Angel Formation *P. iehiense* Zone RECOVERY: 100% SCALE 1: 100



DESCRIPTION & COMMENTS

Sandstone: light grey, well sorted, 1cm diameter pyrite nodules throughout, disseminated pyrite; 2892.3 - 2892.9m - claystone rip up clasts aligned parallel at 30 degrees.

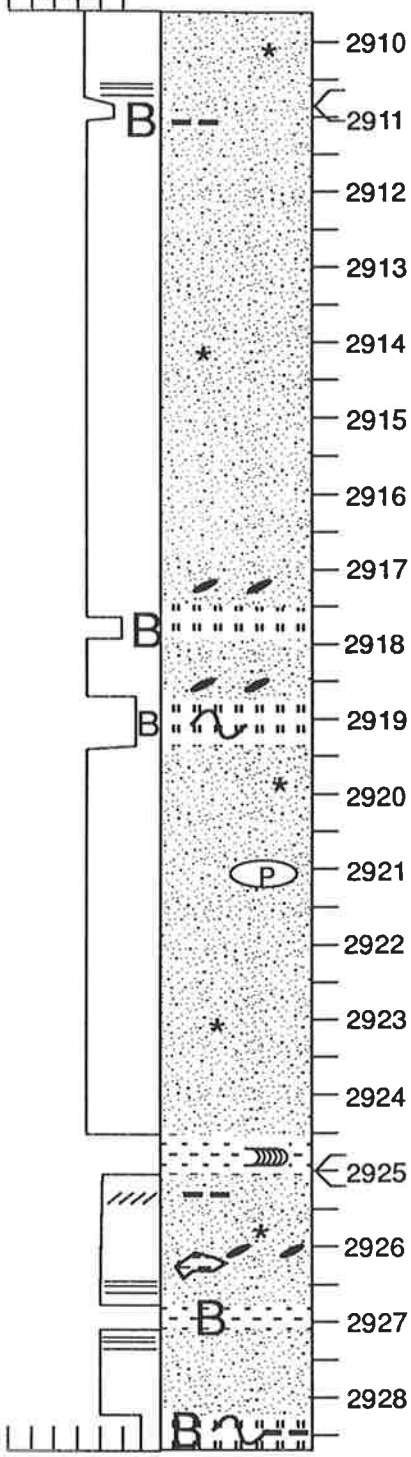
Porosity: sandstone - 11.7 - 18.8% , 16.5% average.
Permeability: sandstone - 63.5 - 1430d, 650 average.

2900.8 - pyrite filled fracture.

Zoophycos burrows common

Cossack 1 CORE 2 2909.6 - 2928.7m

Angel Formation *P. iehiense* Zone RECOVERY: 100% SCALE 1: 100



DESCRIPTION & COMMENTS

Sandstone: light grey, well sorted, fine grained.

Rhyzocorallium and *planolites* burrows.

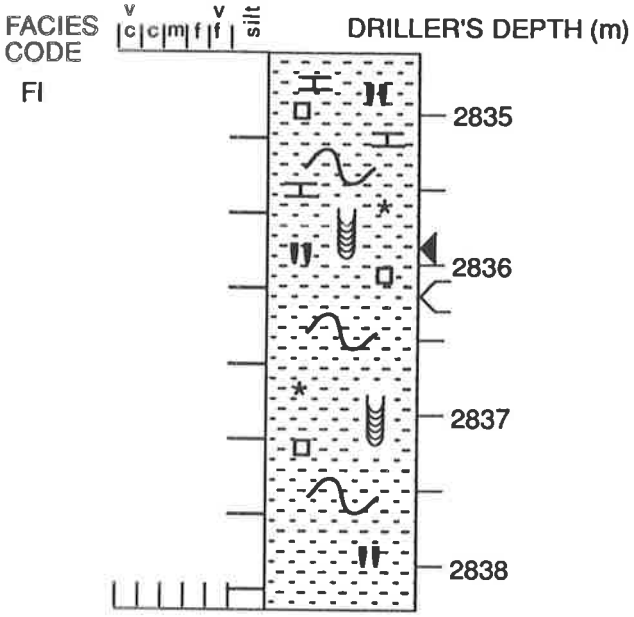
Grey claystone rip up clasts 1 - 2cm by 10cm.

Planolites burrows

Chondrites and *planolites burrows.*

Dampier 1 CORE 9 2834.6 - 2838.3m

Forestier Claystone *D. lobospinosum* Zone RECOVERY: 100% SCALE 1: 50

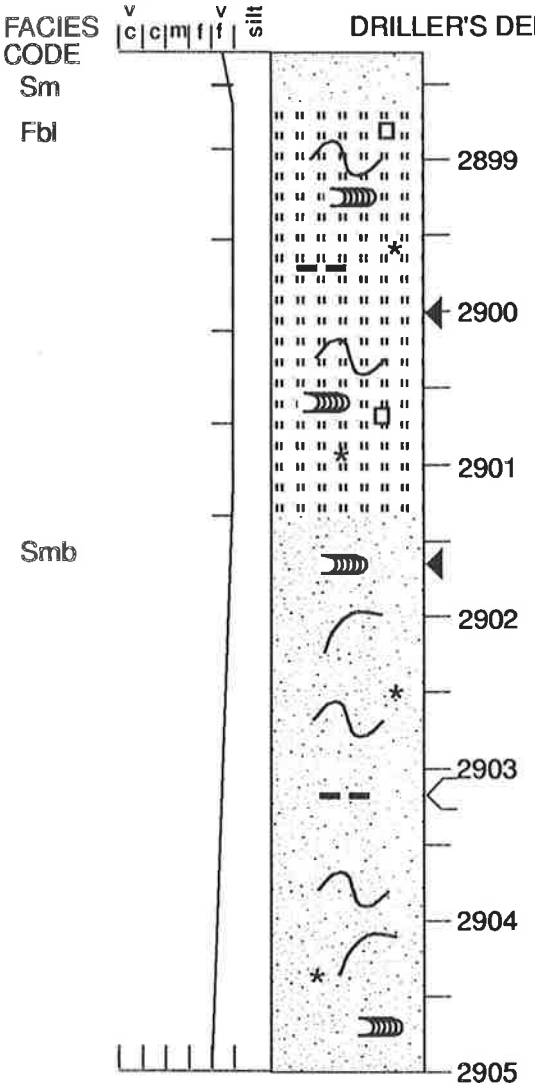


DESCRIPTION & COMMENTS

Claystone: dark brown, laminated silt, slightly bioturbated.

Dampier 1 CORE 10 2898.3 - 2905m

Forestier Claystone *K. wisemaniae* Zone RECOVERY: 100% SCALE 1: 50



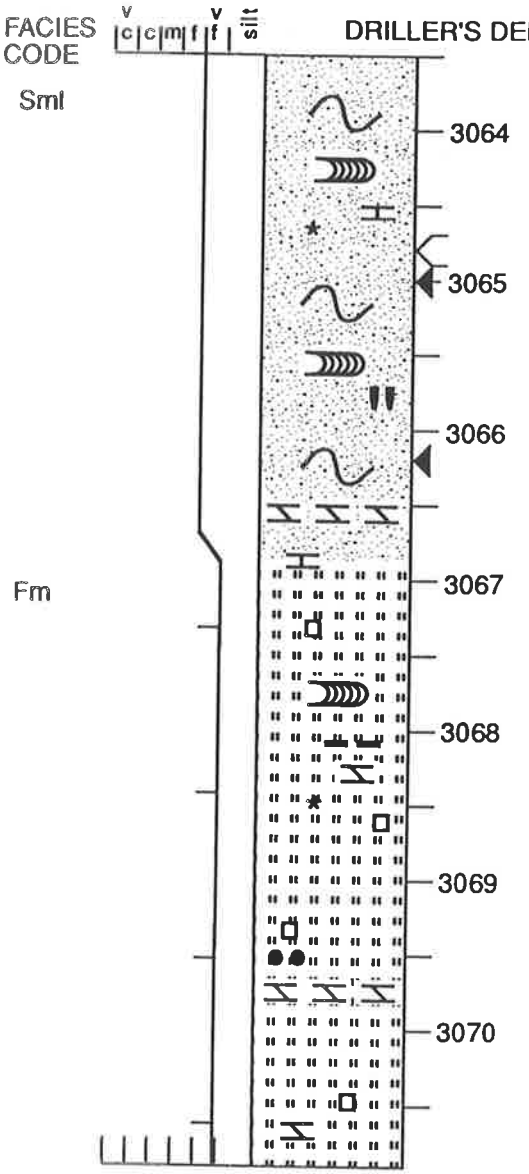
DESCRIPTION & COMMENTS

Siltstone: grey, brown, micaceous, argillaceous; wispy laminae of sand and silt, moderately bioturbated, disseminated pyrite throughout; tight.

Sandstone: dark grey, clear, well sorted, silty and argillaceous; tight; shell fragments.

Dampier 1 CORE 11 3063.5 - 3070.9m

Angel Formation *P. iehiense* Zone RECOVERY: 100% SCALE 1: 50

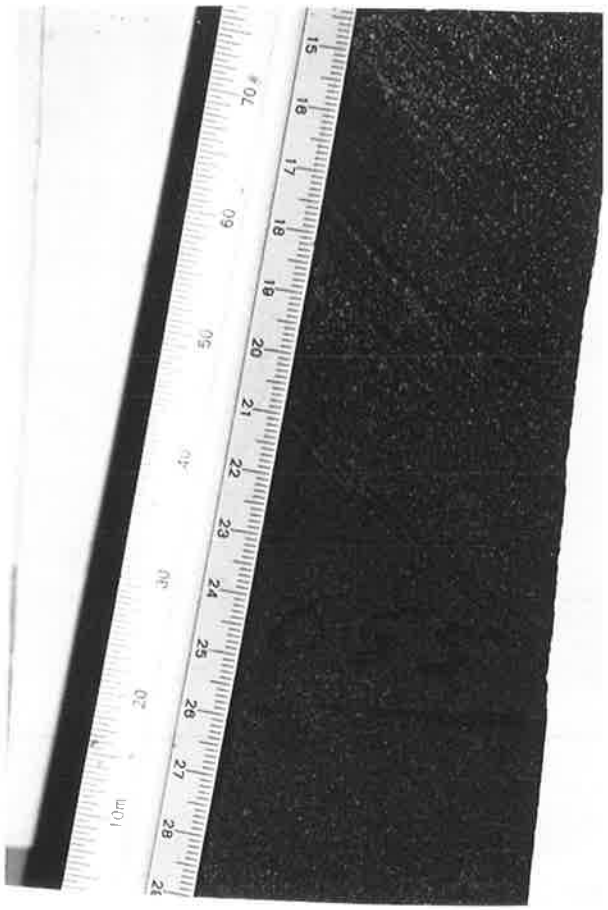


DESCRIPTION & COMMENTS

Sandstone: dark grey, well sorted, slightly calcareous, maroon dolomite or siderite band at 3066.3 m; minor disseminated pyrite.

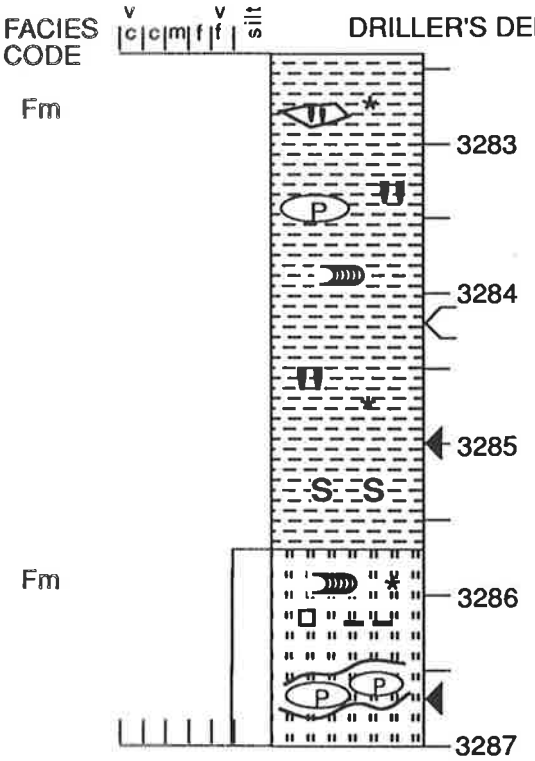
Core plug porosity: (sandstone) 3.6 - 9.1%.
Core plug permeability: (sandstone) 0 md

Siltstone: brown, dark grey, sandy, argillaceous; maroon dolomitized zones; up to 10% disseminated pyrite.



Dampier 1 CORE 12 3282.4 - 3287m

Dingo Claystone *O. montgomeryi* Zone RECOVERY: 100% SCALE 1: 50



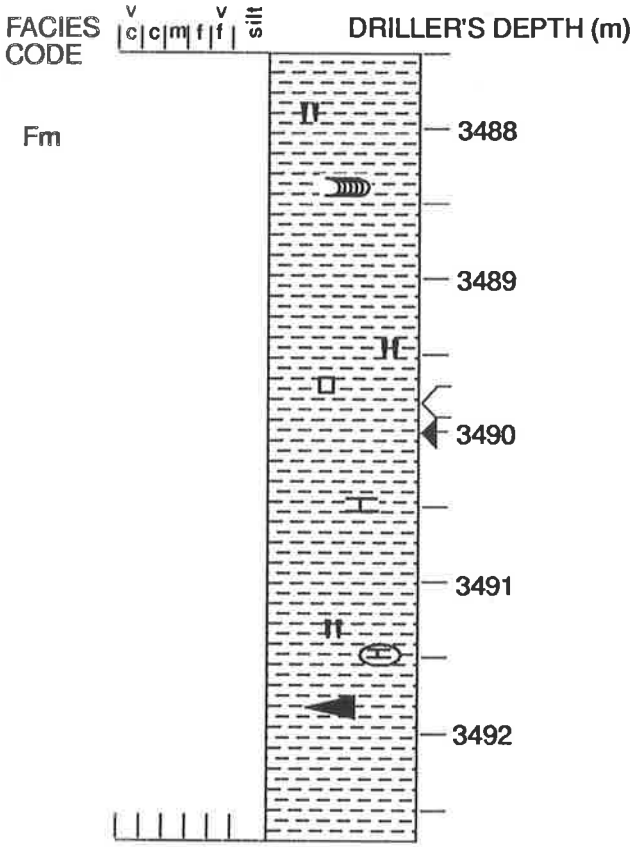
DESCRIPTION & COMMENTS

Shale: dark grey, micaceous, very silty, ~5 mm diametre pyrite nodules, slightly laminated, very fine glauconite throughout.

Siltstone: dark grey, medium grey, argillaceous; 5mm wide worm burrow.

Dampier 1 CORE 13 3487.5 - 3492.7m

Dingo Claystone *O. montgomeryi* Zone RECOVERY: 100% SCALE 1: 50

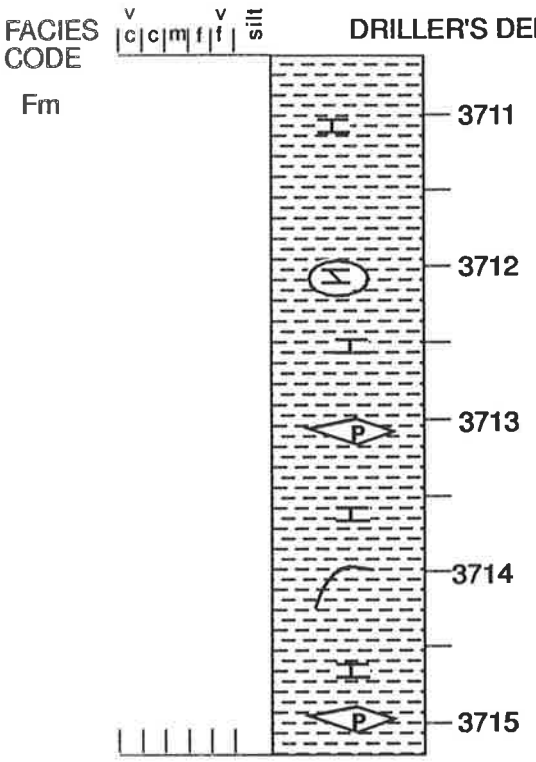


DESCRIPTION & COMMENTS

Shale: dark grey, black, slightly silty, highly micaceous, very minor bioturbation.

Dampier 1 CORE 14 3710.6 - 3715.2m

Dingo Claystone *D. swanenese* Zone RECOVERY: 100% SCALE 1: 50

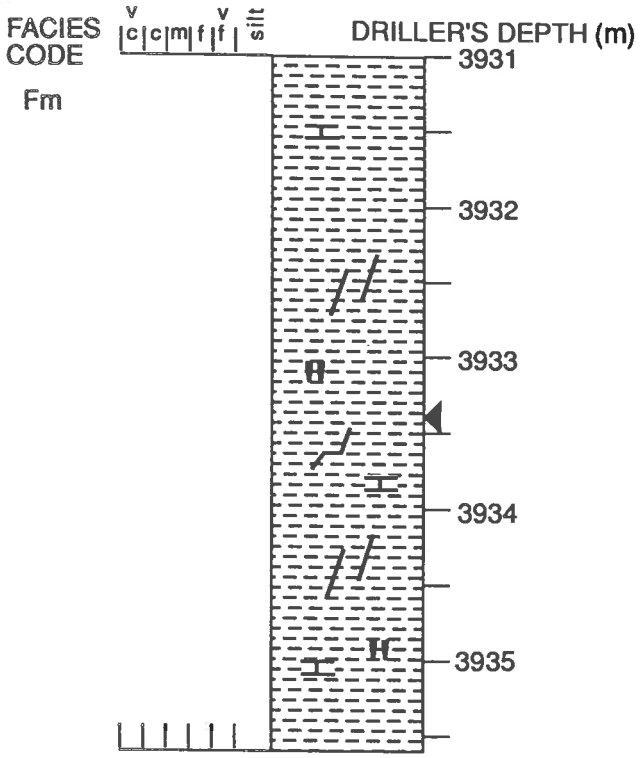


DESCRIPTION & COMMENTS

Shale: dark grey, black, calcareous, micaceous, hard, slightly fissile.

Dampier 1 CORE 15 3931 - 3935.6m

Dingo Claystone *D. swanense* Zone RECOVERY: 100% SCALE 1: 50

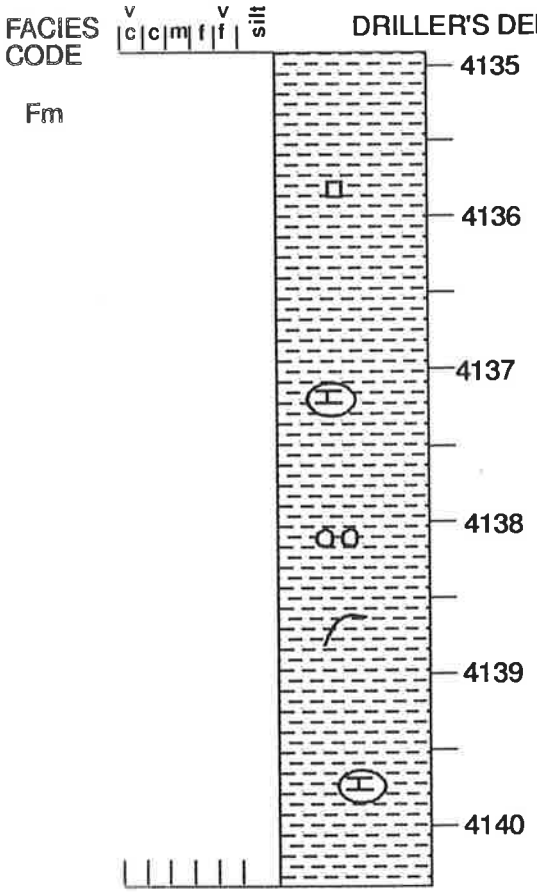


DESCRIPTION & COMMENTS

Shale: dark grey, black, micaceous, slight silt laminations, calcite filled fractures and slickensides; no dip.

Dampier 1 CORE 16 4134.9 - 4140.4m

Dingo Claystone *D. swanense* Zone RECOVERY: 100% SCALE 1: 50

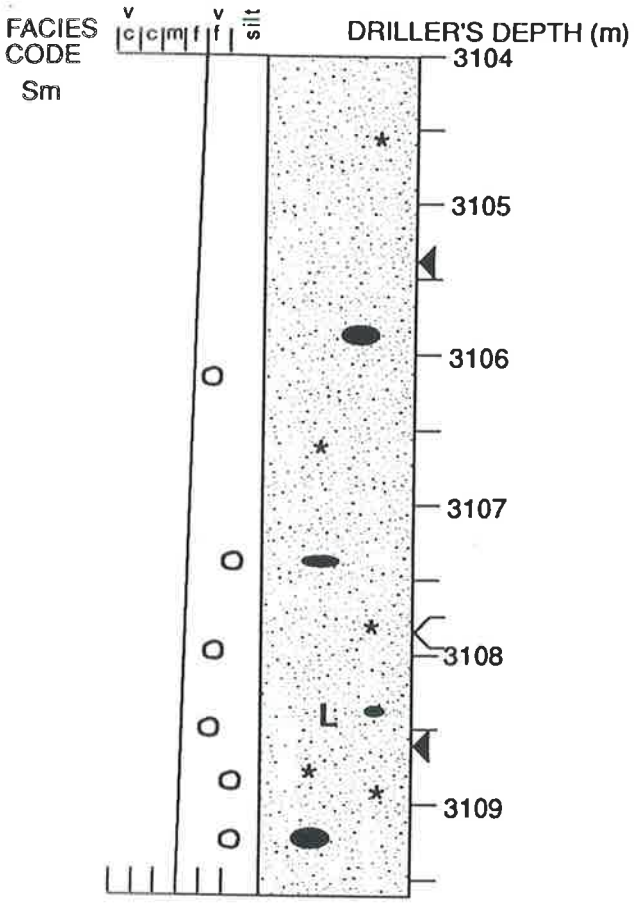


DESCRIPTION & COMMENTS

Shale: dark grey, black, micaceous cleavage, brown crystalline calcite nodules, occasional agregates of a few quartz granules.

Lambert 1 CORE 1 3104 - 3109.6m

Angel Formation *P. iehiense* Zone RECOVERY: 100% SCALE 1: 50



DESCRIPTION & COMMENTS

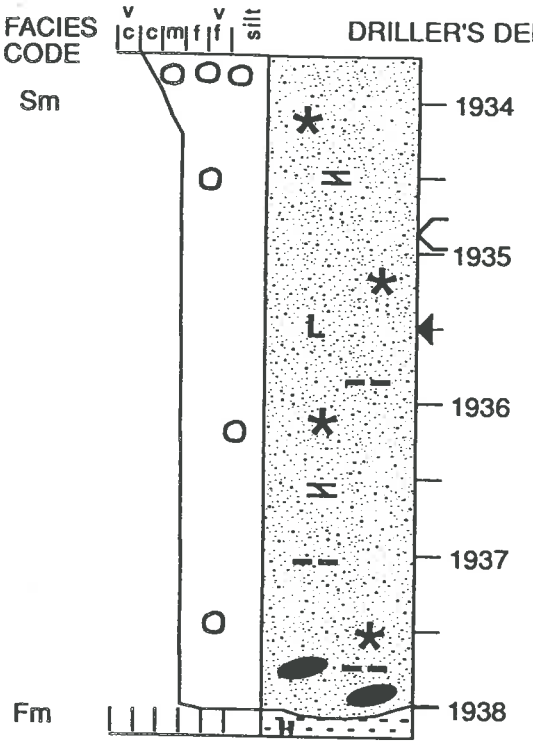
Sandstone: light grey, fine to granule grain size, dominantly medium grained, well sorted near top of core, poorly sorted near base of core; claystone clasts aligned horizontally; occasional jasper clast; ~5% glauconite and increase to 15% near base of core; subtle fining upwards is noted.

Core plug porosity: 18.2 - 20.3%
Core plug permeability: 360 - 735 md



Legendre 1 CORE 10 1933.7 - 1938.2m

Talisman Member (equivalent) *B. reticulatum* Zone RECOVERY: 75% SCALE 1: 50



DESCRIPTION & COMMENTS

Sandstone: cream color , brownish near base of core as argillaceous content increases, clear quartz, fine to coarse grained, dominantly medium, well sorted; up to 20% glauconite; kaolin or dolomite often fills pores, altered feldspar grains, occasional chert fragments, granules are elongate and aligned parallel at 5 - 15 degrees.

Core plug porosity: (sandstone) 10.2 - 23.6%; average - 18.5%.
Core plug permeability: (sandstone) 6 - 45 md; average - 28 md.

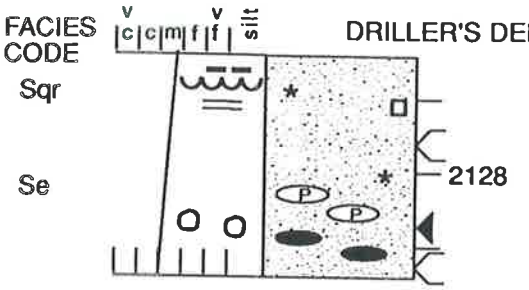
Note: this core appears mixed up in the core box. The positioning of core has been inferred and may not be exactly in the correct position.

Claystone: dark brown, silty.



Legendre 1 CORE 11 2127.2 - 2128.7

Angel Formation *D. jurassicum* Zone RECOVERY: 100% SCALE 1: 50

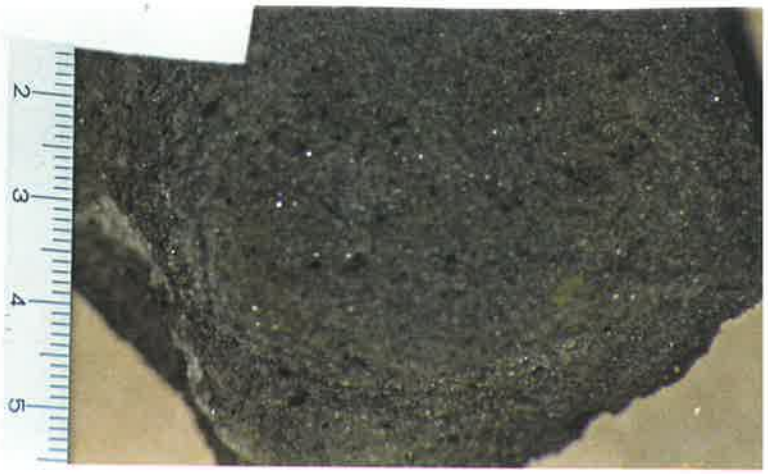


DESCRIPTION & COMMENTS

Sandstone: upper 60 cm - light grey, cream color matrix, well sorted; possible kaolin filling pores; good stratification is noted; ripple marks are seen on one peice of the core and may be ocsillation ripples. Lower 90 cm - light grey, poorly sorted, small scale scour structures, claystone clasts show plastic deformation; alignment of grains dip at ~30 degrees.

Core plug porosity: 3.2 - 9.7% (upper 60cm); 17.2 - 17.9% (lower 90 cm).
Core plug permeability: 0 - 30 md (upper 60 cm); 105 - 151 md (lower 90 cm).

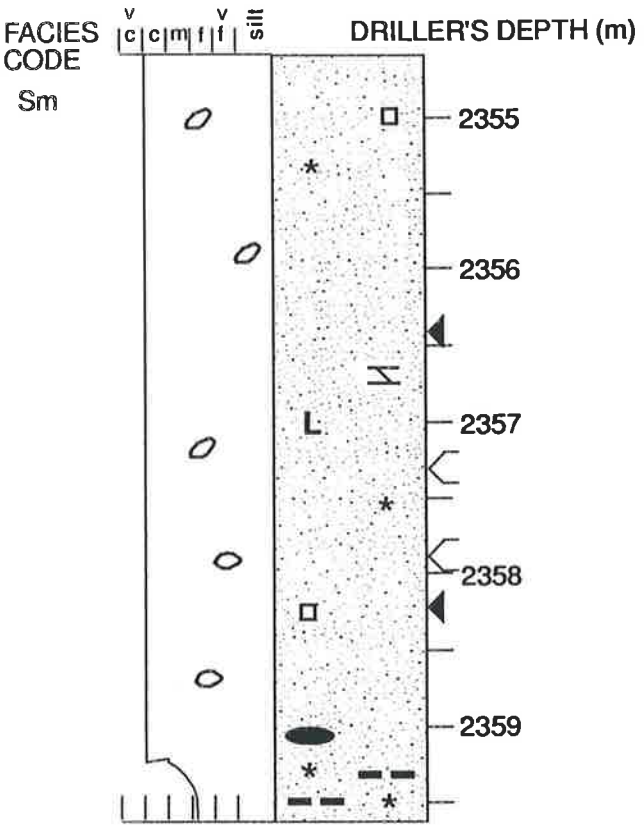
Note: this core appears mixed up in the core box. The positioning of core has been inferred and may not be exactly in the correct position.





Legendre 1 CORE 12 2354.6 - 2359.6m

Eliassen Formation *W. spectabilis* Zone RECOVERY: 81% SCALE 1: 50



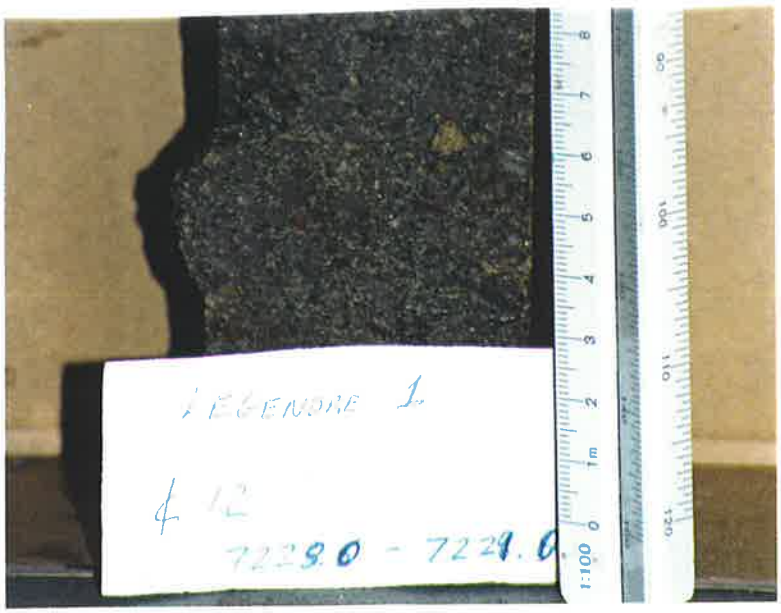
DESCRIPTION & COMMENTS

Sandstone: light grey, pebble to medium grained, dominantly coarse, poorly sorted; possible detrital kaolin grains; up to 5% glauconite; pebbles up to 1 cm and granules are aligned parallel at 30 degrees at the top of the core and decreases to 0 degrees at the base; possible ferroan dolomite cement; silica cement increased downward.

Core plug porosity: clean sandstone- 2.3 - 18% , average 11%;
argillaceous sandstone- 5 - 10%.
Core plug permeability: clean sandstone- 72 - 583 md, two samples at 2356 m > 2,000 md;
argillaceous sandstone- 0 md.

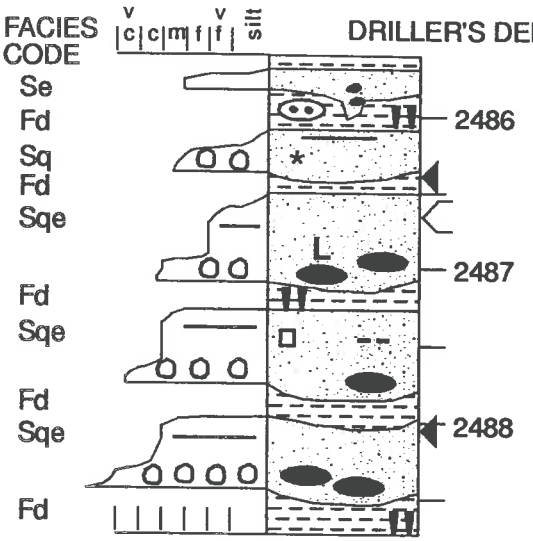
Sandstone: medium grey, brown, poorlly sorted, argillaceous matrix; white kaolin? pebble size clasts; 5 - 10% glauconite occur as rounded sand grains.

Note: this core appears mixed up in the core box. The positioning of core has been inferred and may not be exactly in the correct position.



Legendre 1 CORE 13 2485.6 - 2488.7m

Eliassen Formation *W. spectabilis* Zone RECOVERY: 100% SCALE 1: 50



DESCRIPTION & COMMENTS

Sandstone: cream grey, light grey; sandstone beds up to 30 cm thick interbedded with shale; poorly sorted at base of beds and graded to well sorted at the top of beds; well stratified at bed tops and medium to fine grained; bases of beds are scoured and gravel to medium grained; coarse grains are well rounded, medium to fine grains are subangular; tight, argillaceous and finer grained matrix.

Shale: dark grey, black, plastic deformation, 5 - 10 cm beds interbedded with sandstone beds; micaceous, ball and pillow structures filled with sandstone.

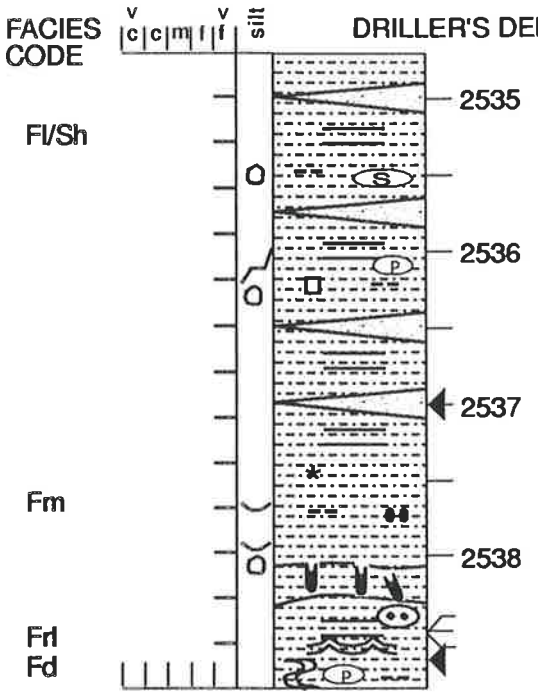
Core plug porosity: sandstone- 0.4 - 11.5%; average 4%
Core plug permeability: sandstone- 0md; one sample at 2487 m with 110.5 md.

Note: this core appears mixed up in the core box. The positioning of core has been inferred and may not be exactly in the correct position.



Legendre 1 CORE 14 2534.7 - 2538.9m

Eliassen Formation *W. spectabilis* Zone RECOVERY: 100% SCALE 1: 50



DESCRIPTION & COMMENTS

Siltstone: dark blue grey, blue black, sandy, argillaceous, mm scale sand laminations and beds, minor microfaulting; up to 30 degree dip in laminations

Sandstone: dark grey, fine to coarse grained, dominantly fine grained, poorly sorted.

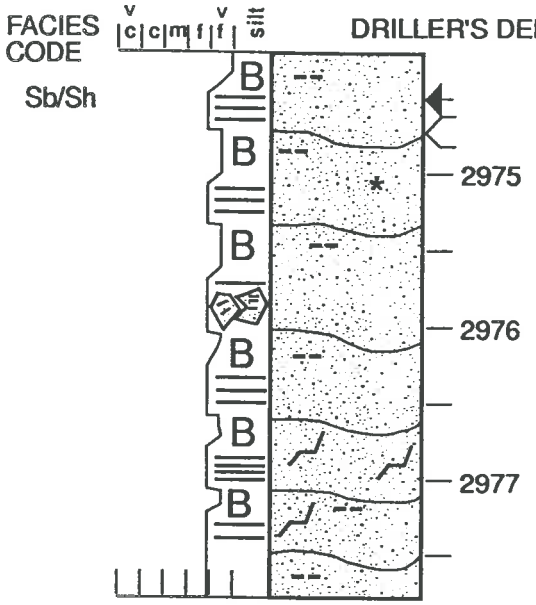
Core plug porosity: 2.0 - 4.5%
Core plug permeability: 0 md

Note: this core appears mixed up in the core box. The positioning of core has been inferred and may not be exactly in the correct position.



Legendre 1 CORE 16 2974.2 - 2977.8m

Calypso Formation *R. aemula* Zone RECOVERY: 80% SCALE 1: 50



DESCRIPTION & COMMENTS

Sandstone: light brown, silt to fine grained, dominantly very fine grained, well sorted, argillaceous matrix, up to pebble size claystone clasts; 30 - 50 cm thick bed sets consist of a scoured base, with a thin massive sand bed, followed by a horizontally laminated unit which is highly bioturbated at the top 20 - 30 cm. This cycle repeats over full core. Microfaulting of laminae and intraformational breccias are also noted. Dip is ~15 degrees.

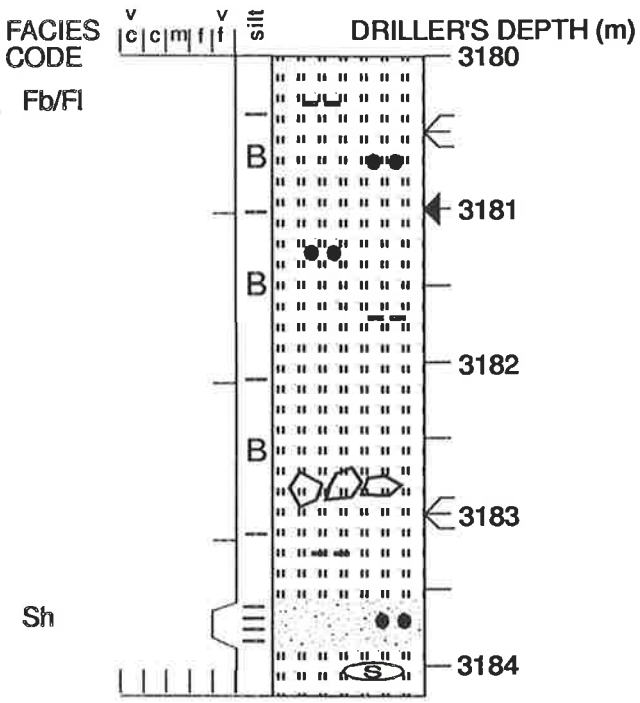
Core plug porosity: 8.5 - 16.8%.
Core plug permeability: 0 md.

Note: this core appears mixed up in the core box. The positioning of core has been inferred and may not be exactly in the correct position.



Legendre 1 CORE 17 3180 - 3184.2m

Calypso Formation *W. digitata* Zone RECOVERY: 100% SCALE 1: 50



DESCRIPTION & COMMENTS

Siltstone: dark brown, medium grey, dark grey; argillaceous and sandy; ~40 degree dip.

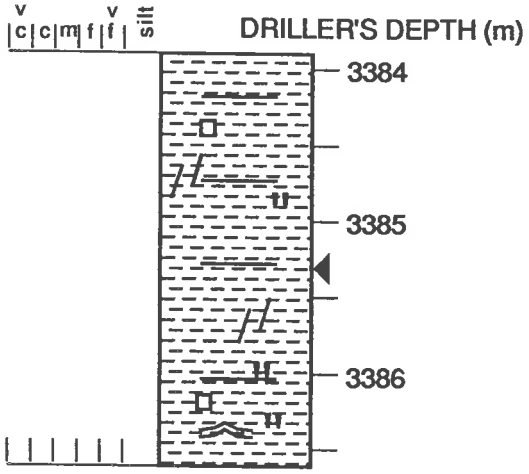
Sandstone: light grey, well sorted, well rounded, very fine grained; poor visible porosity.

Note: this core appears mixed up in the core box. The positioning of core has been inferred and may not be exactly in the correct position.



Legendre 1 CORE 18 3383.9 - 3386.6m

Calypso Formation *W. digitata* Zone RECOVERY: 90% SCALE 1: 50



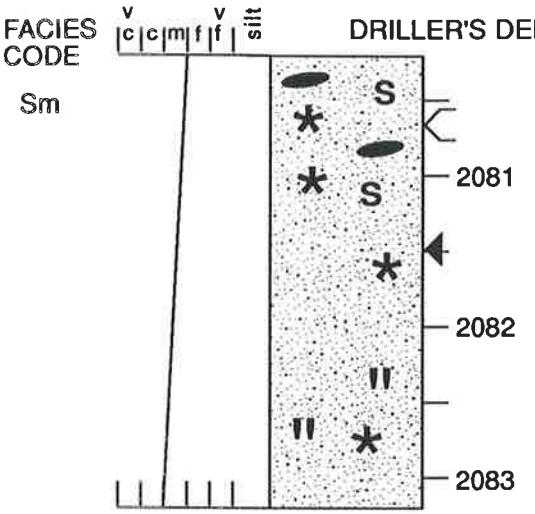
DESCRIPTION & COMMENTS

Shale: black, occasional 1 mm silt laminations; fine carbonaceous material; concoidal fractures often have slickensides at 20 degrees and are quartz filled; ~40 degree dip; thin cm scale siltstone bed near base of core with horizontal laminae and flaser bedding.

Note: this core appears mixed up in the core box. The positioning of core has been inferred and may not be exactly in the correct position. No wire line logs were run over this core interval.

Legendre 2 CORE 1 2080.3 - 2083.2m

Talisman Member *D. lobospinosum* Zone RECOVERY: 28.3% SCALE 1: 50



DESCRIPTION & COMMENTS

Sandstone: orange brown, coarse to fine grained, dominantly medium grained, well sorted, siderite cement, ~10% glauconite.

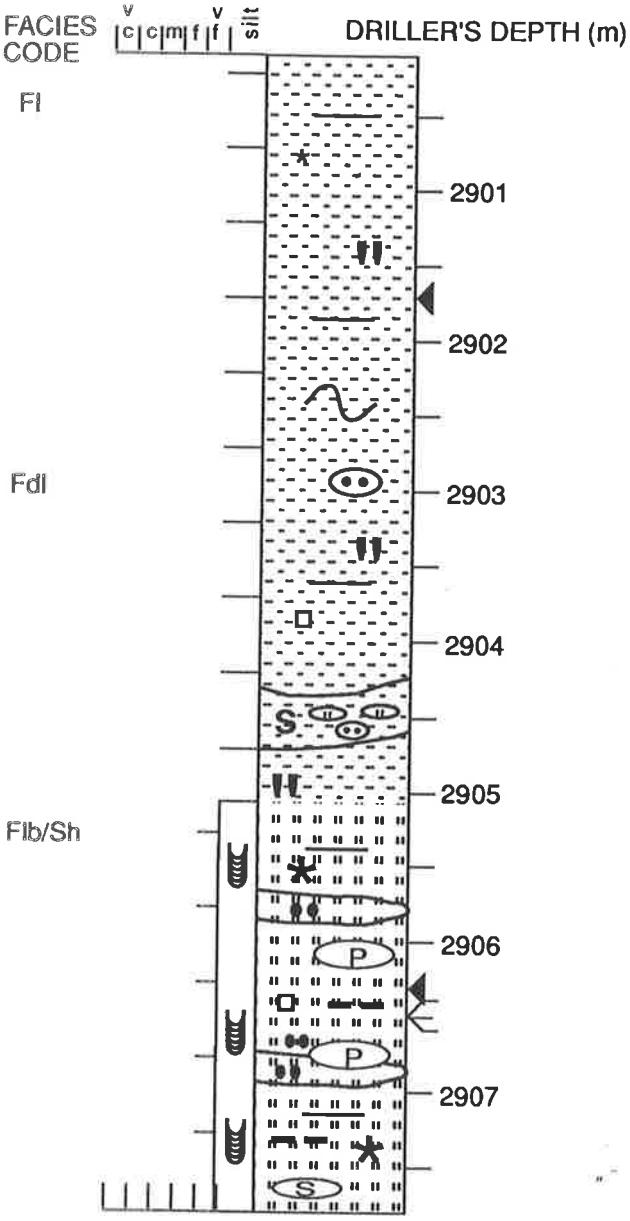
From 2081.5 m - sanstone: light grey, medium to coarse grained dominantly medium grained poorly sorted; core is very friable and broken up.

X-ray analysis at 2081.5 m (well completion report) results: quartz - 50%; microcline feldspar - 10%; calcite - 5%; clay minerals - 5%; siderite - 30%.



Madeleine 1 CORE 1 2900.1 - 2907.8m

Dingo Claystone *P. iehiense* Zone RECOVERY: 100% SCALE 1: 50



DESCRIPTION & COMMENTS

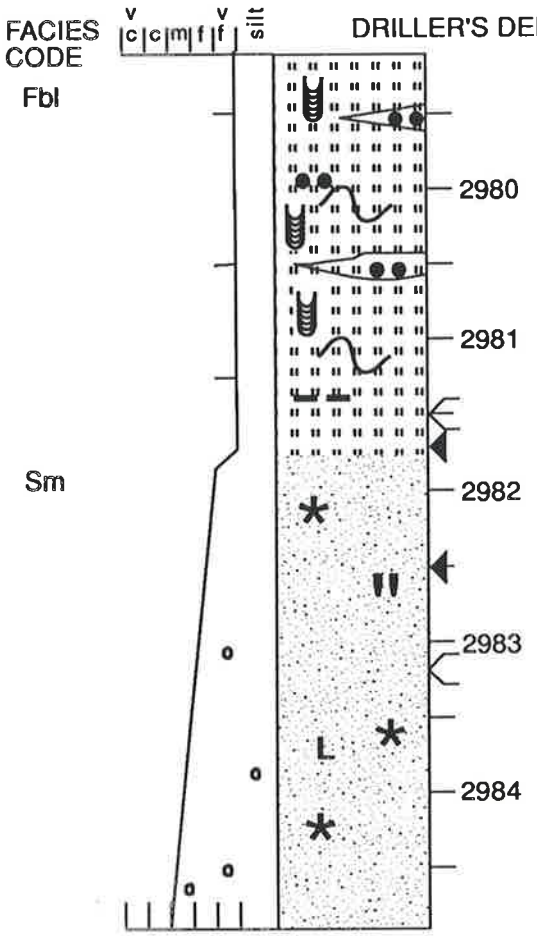
Claystone: dark grey, micaceous, laminated with mm scale beds of sand and silt.

Siltstone: light grey, argillaceous, up to 10% glauconite, sand filled worm burrows.

Sandstone: light grey, well sorted very fine grained; occurs as thin discontinuous laminae in silt and clay, probably indicative of slumping.

Madeleine 1 CORE 2 2979.1 - 2984.9m

Angel Formation *D. jurassicum* Zone RECOVERY: 95% SCALE 1: 50



DESCRIPTION & COMMENTS

Siltstone: dark grey, argillaceous and sandy; horizontal discontinuos laminae of very fine well sorted sand;

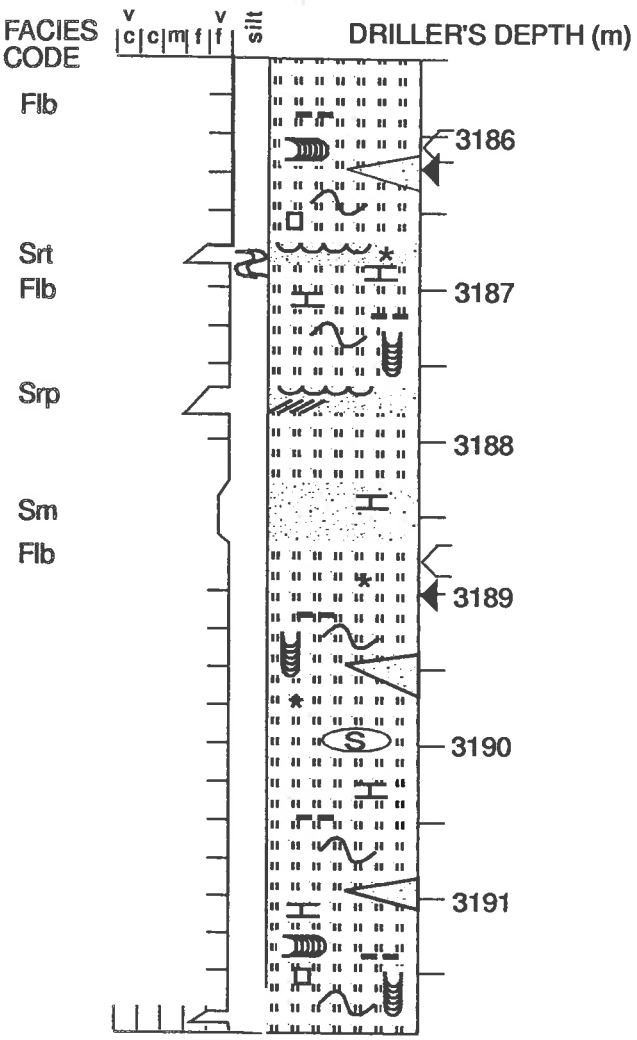
Sandstone: light grey, cream grey, coarse to fine grained, dominantly medium grained near base and fining to fine grained at top of sand unit; good visual porosity; clear and milky quartz grains; no dip.

Core plug porosity: sandstone - 17 - 23%.
Core plug permeability: sandstone- 48 - 880 md; average 300 md; siltstone- 0 md.



Madeleine 1 CORE 3 3185.5 - 3191.9m

Dingo Claystone *D. jurassicum* Zone RECOVERY: 95% SCALE 1: 50



DESCRIPTION & COMMENTS

Siltstone: light grey, dark grey, well sorted, argillaceous and sandy, sand filled worm tubes and burrows, wavy discontinuous beds of up to 5 mm thick very fine grained sand.

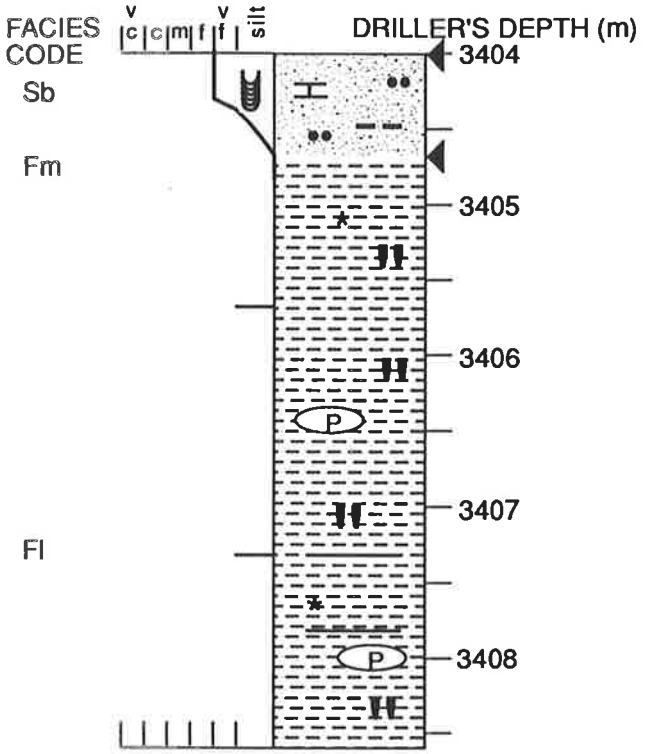
Sandstone: light grey, well sorted, thin convoluted trough? cross bedding is overlain by ripple cross laminations in several beds ~ 10 - 20 cm thick; calcareous cement and kaolinite matrix; no dip.

Core plug porosity: sandstone- 11 - 16.2%.
Core plug permeability: 0 md.

Note: this core appears to be mixed up in the core tray. Exact depths are uncertain and inferred.

Madeleine 1 CORE 4 3404 - 3408.6m

Dingo Claystone *O. montgomeryi* Zone RECOVERY: 67% SCALE 1: 50



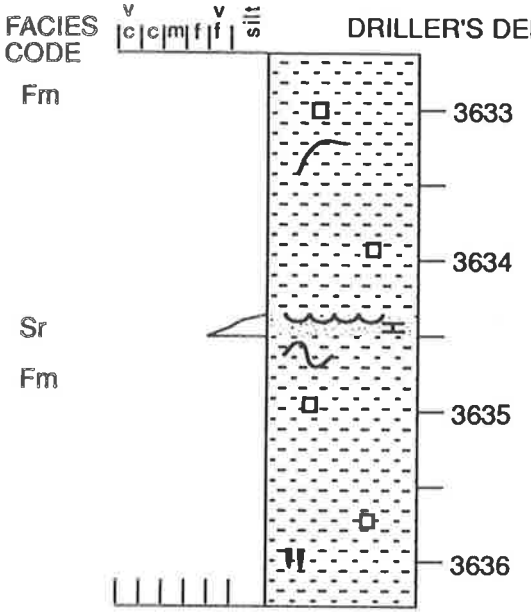
DESCRIPTION & COMMENTS

Sandstone: dark grey, argillaceous and silty, very fine grained, poorly sorted, finely micaceous, highly bioturbated; poor visible porosity.

Shale: dark grey, black, up to ~30% silt, occasional silt laminations, micaceous.

Madeleine 1 CORE 5 3632.6 - 3636.3m

Dingo Claystone *W. clathrata* Zone RECOVERY: 82% SCALE 1: 50



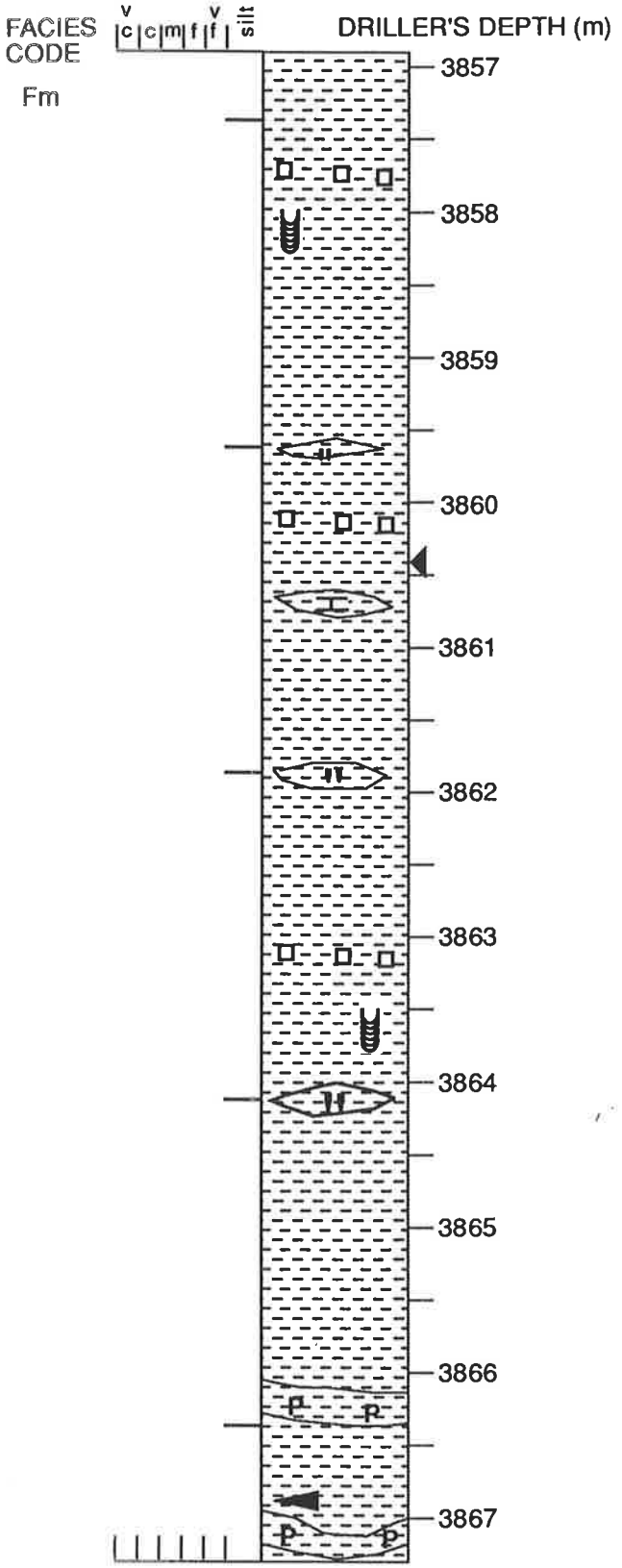
DESCRIPTION & COMMENTS

Claystone: dark grey, micaceous, brachiopod fragment noted, hard, dense; disseminated pyrite; concoidal fractures; occasional discontinuous wavy laminae.

Sandstone: light grey, well sorted, calcareous cement, top surface of bed has ripple cross lamination, poor visibible porosity.

Madeleine 1 CORE 6 3856.9 - 3867.3m

Dingo Claystone *W. spectabilis* Zone RECOVERY: 100% SCALE 1: 50

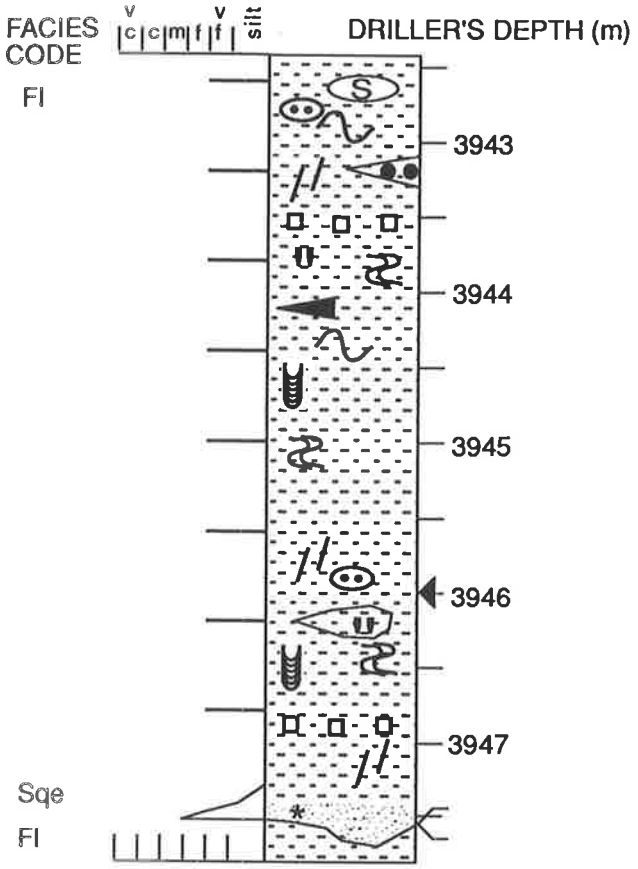


DESCRIPTION & COMMENTS

Shale: dark grey, grey black, micaceous, concoidal fractures, green pyrite bands 1 to several cm's thick; occasional silt lenses and laminations with rare cross bedding and worm burrows; possible fish scales.

Madeleine 1 CORE 7 3942.3 - 3947.8m

Dingo Claystone *W. spectabilis* Zone RECOVERY: 72% SCALE 1: 50



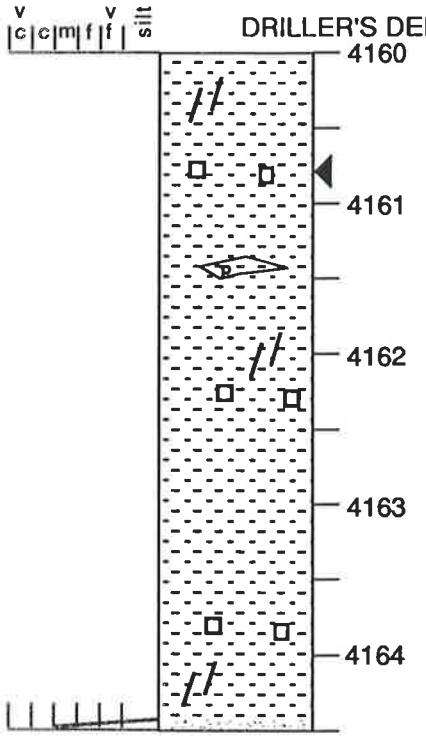
DESCRIPTION & COMMENTS

Claystone: dark grey, hard, dense, siderite nodules and cement, wavy laminations of sand and silt; convoluted bedding and bioturbated throughout.

Sandstone: light grey, poorly sorted, coarse to fine grained; ~10 cm thick bed occurs as a small channel infill at 3147.8 m with scoured base and gradational top; also occurs as discontinuous laminae and 1 cm thick contorted beds.

Madeleine 1 CORE 8 4160 - 4164.5m

Dingo Claystone ? *W. spectabilis* Zone RECOVERY: 68% SCALE 1: 50



DESCRIPTION & COMMENTS

Claystone: dark grey, occasional pyrite lenses, occasional slickensides, massive.

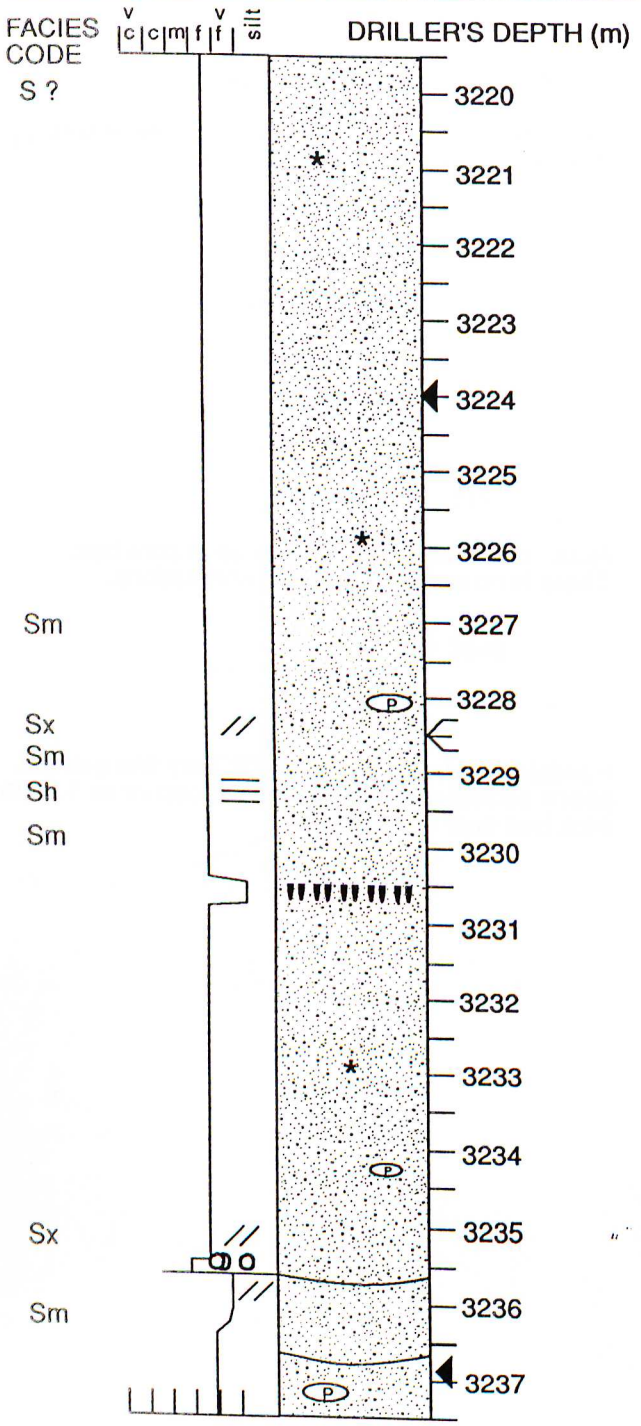
Note: this core is very broken up in core box. There is no certainty of depth annotations.

Sandstone: dark grey, coarse to very fine grained, poorly sorted, argillaceous matrix; occurs as 1.5 cm thick bed near base of core.



Montague 1 CORE 1 3219.5 - 3237.5m

Angel Formation *D. jurassicum* Zone RECOVERY: 100% SCALE 1: 100



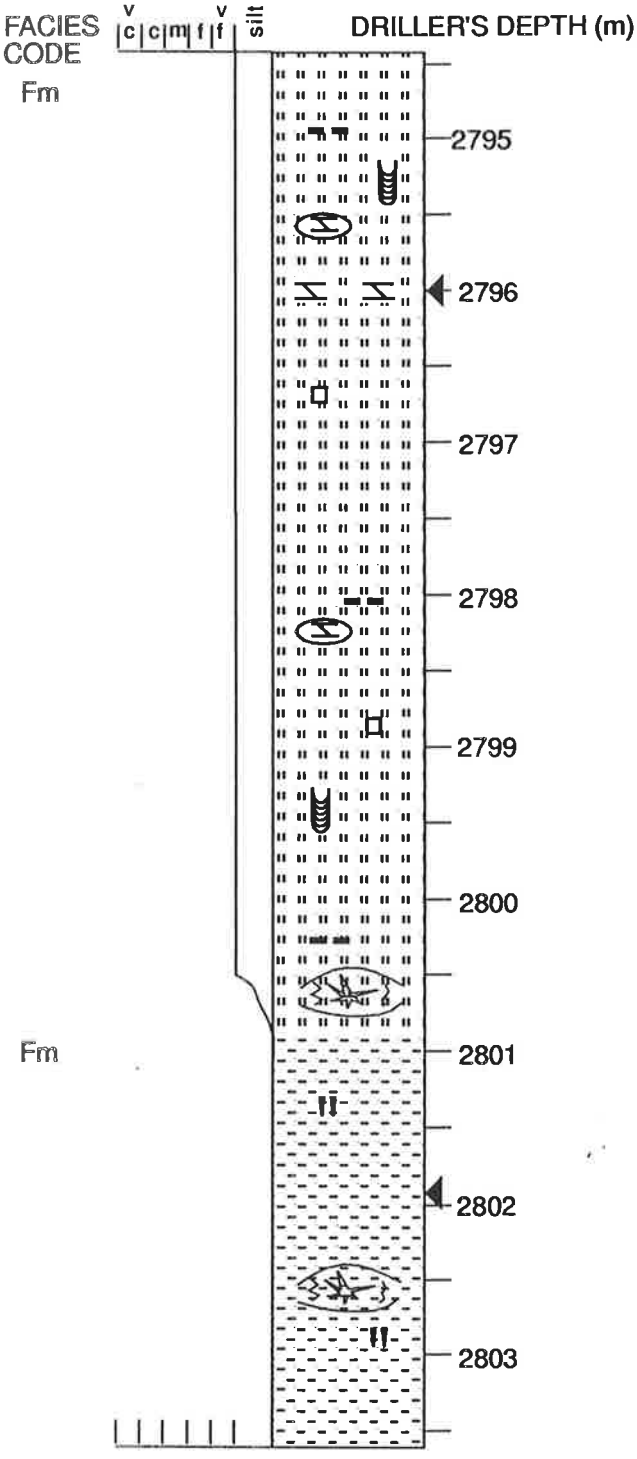
DESCRIPTION & COMMENTS

Sandstone: light grey, moderately to well sorted, fine to very fine grained, silty, dominantly fine grained, core soft and friable, poorly cemented, 3119.5 - 3227m, 3230.9 - 3233.8m core unconsolidated, occasional 1cm diameter pyrite concretions.



Rosemary 1 CORE 1 2794.4 - 2803.6m

Calypso Formation *R. aemula* Zone RECOVERY: 87% SCALE 1: 50



DESCRIPTION & COMMENTS

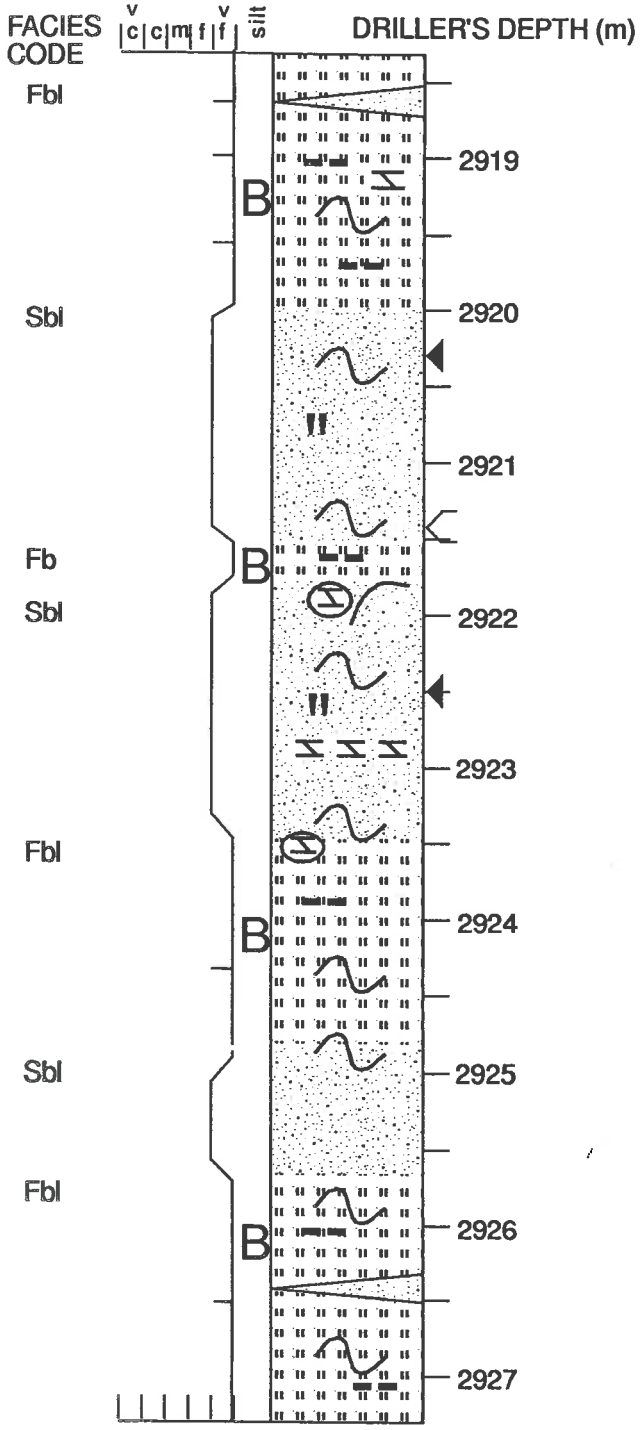
Siltstone: brown grey, grey black, minor bioturbation; silty dolomitic zones; chondrites nodules of dolomite and fracture filled calcite.

Core plug porosity: 0 - 9%; average - 5.3%, excluding sample at 2795 m with 14%.
Core plug permeability: 0 md, sample at 2795 m with 1.6 md.

Claystone: brown black, brown grey, hard, silty, slightly micaceous; dolomite and calcite chondrites nodule.

Rosemary 1 CORE 2 2918.2 - 2927.3m

Calypso Formation *R. aemula* Zone RECOVERY: 88% SCALE 1: 50



DESCRIPTION & COMMENTS

Siltstone: olive black, micaceous, clay laminations, dolomite nodules.

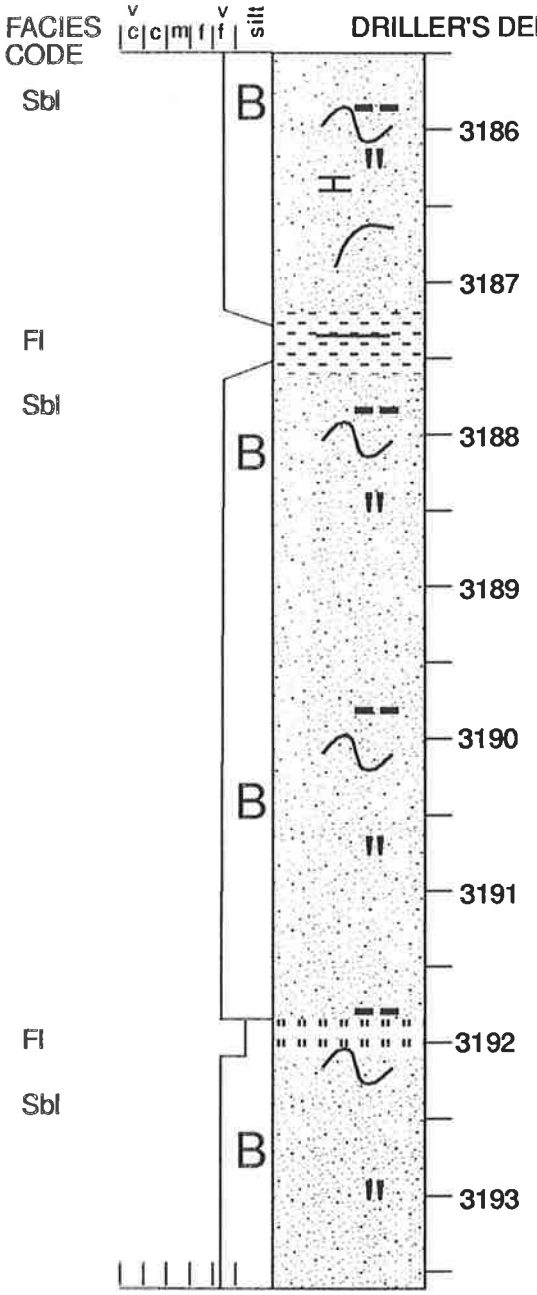
Sandstone: olive grey, well sorted, very fine grained, silty, dolomite cement, clay laminations, highly bioturbated; brachiopod at 2921.7.

Core plug porosity: 1.9 - 10.0%.
Core plug permeability: 0 md.



Rosemary 1 CORE 3 3185.5 - 3193.7m

Calypso Formation *R. aemula* Zone RECOVERY: 90% SCALE 1: 50



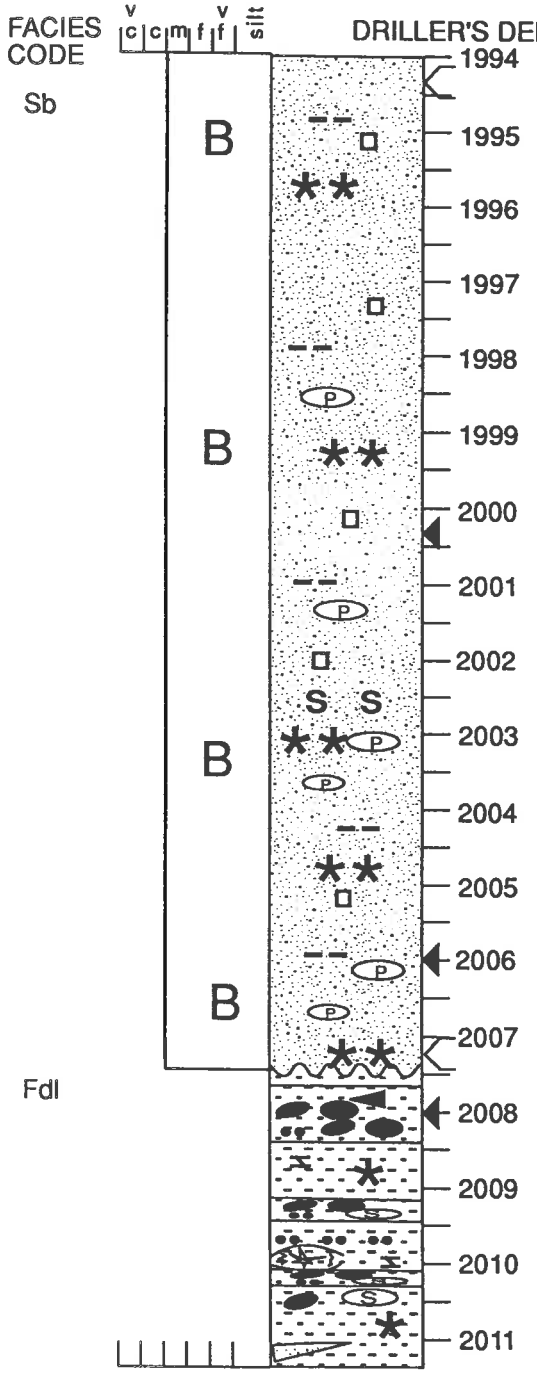
DESCRIPTION & COMMENTS

Sandstone: light grey, very fine grained, well sorted, silty, highly bioturbated, clay laminae, up to 5% calcite cement.

Claystone: dark grey, silty.

Core plug porosity: 7 - 17%.
Core plug permeability: 0 md

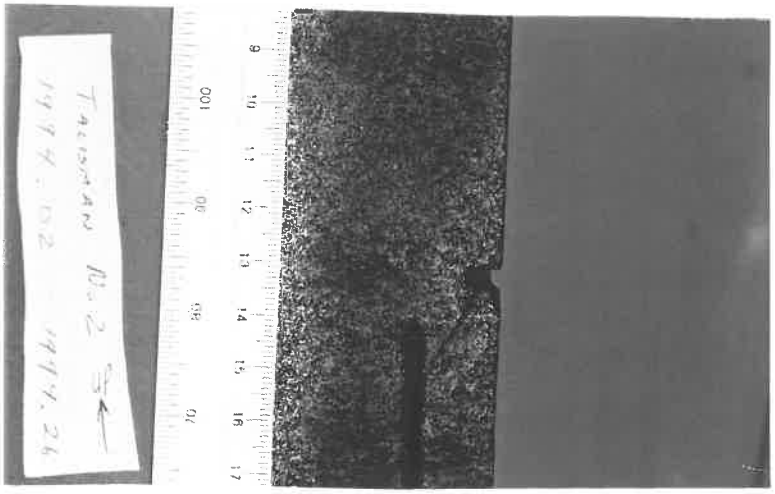
Siltstone: dark grey, up to 30% argillite.



DESCRIPTION & COMMENTS

Greensand: light grey, geen grey, fine to very coarse grained, dominantly medium grained, poorly sorted; occasional fining upwards units ~10 cm thick with sharp or burrowed bases; highly bioturbated throughout; up to 30 % clay; up to 40% glauconite; small pyrite and siderite nodules.

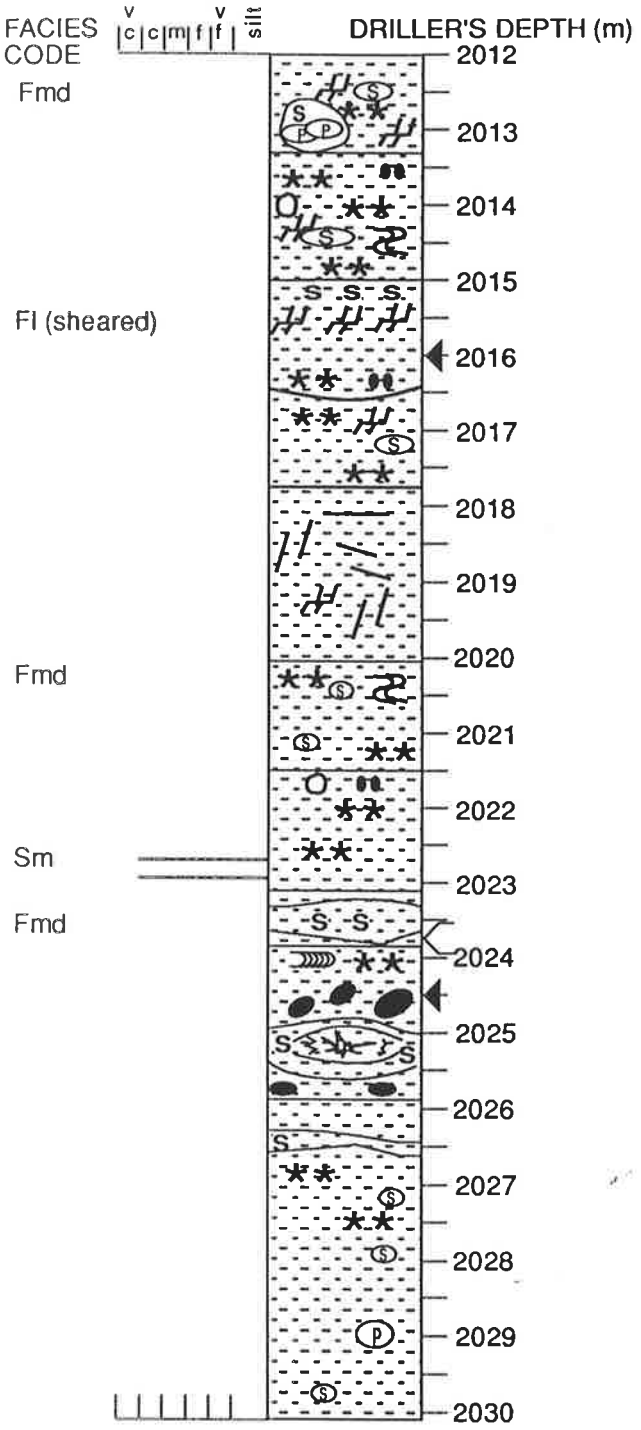
Core plug porosity: sandstone- 4.1 - 19.0%.
Core plug permeability: sandstone- 0.01 - 20.0 md.



Claystone: olive grey, 50 - 90% clay, up to 10% fine to coarse quatrz grains; up to 30% dolomite or siderite cement; intraformational conglomerate beds occur in a sandy glauconitic matrix; up to 5% disseminated or nodular pyrite; possible pyritzed wood fragments at ~2007 m; septarian nodule at 2009.9 m showing several phases of mineral growth of calcite, pyrite, dolomite and quartz; weak horizontal laminations with contorted bedding around intraclasts and nodules

Talisman 2 CORE 4 2012 - 2030.1m

Forestier Claystone *B. reticulatum* Zone RECOVERY: 100% SCALE 1: 100



DESCRIPTION & COMMENTS

Claystone: olive grey, olive black, arenaceous and conglomeritic in part, 40 - 80% argillite, up to 40% quartz grains, up to 30% glauconite; siderite and/or dolomite cement; siderite nodules throughout; siderite nodule around septarian nodule at ~2025.1 m; claystone around nodules often compacted; ~5mm pyrite nodules; 20 cm - 1 m thick mass flow beds of sandy claystone are common.

Slide block: 2015.5m - 2020 m- 20 to 30 degree dip; highly faulted and slickenside surfaces; overlies a contorted bedded claystone, unit top and base is intensely sheared with small faults, may indicate a possible slide block.

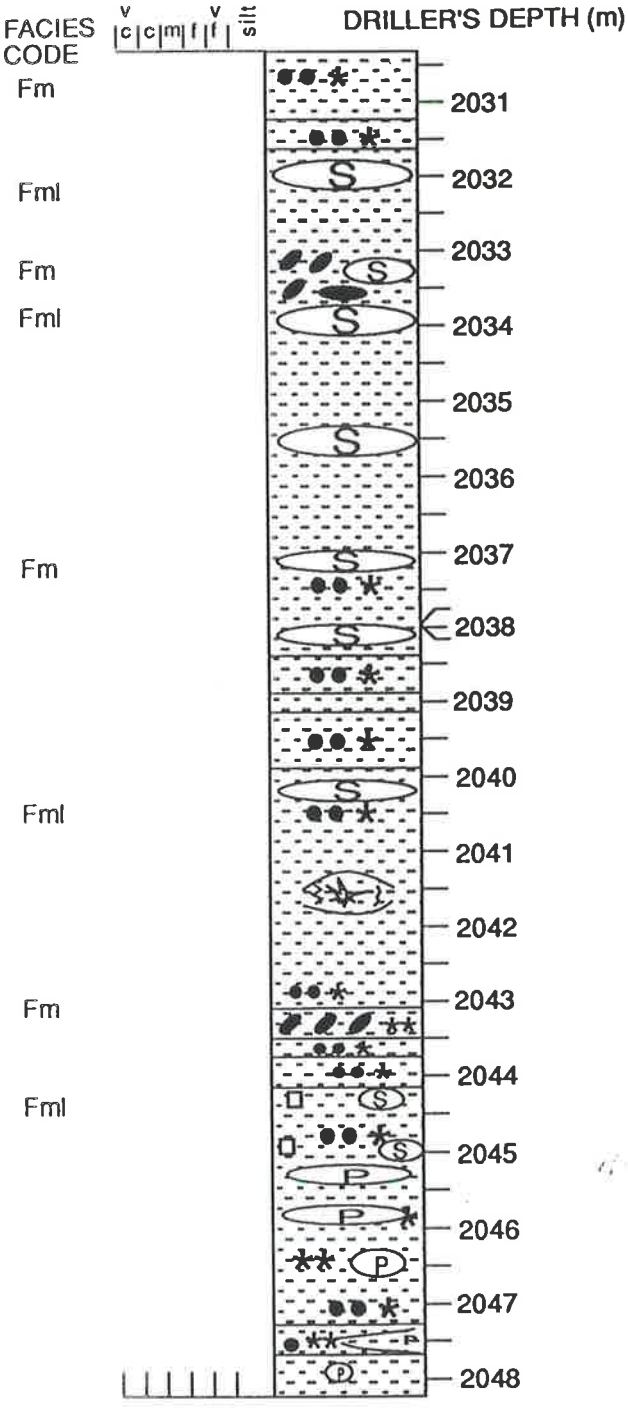
Core plug porosity: sandstone (2021.35 - 2023.25 m)- 9.8 - 15%.
Core plug permeability: sandstone (2021.35 - 2023.25 m)- 0.4 - 2.3 md.

Sandstone: olive grey, dark green grey, fine to pebble grain size, dominantly coarse, up to 30% glauconite; very argillaceous.

Mass flow conglomerate unit: ~2024 m - 2026 m- consists of small conglomerate claystone clasts which are burrowed in a sandy glauconitic matrix.

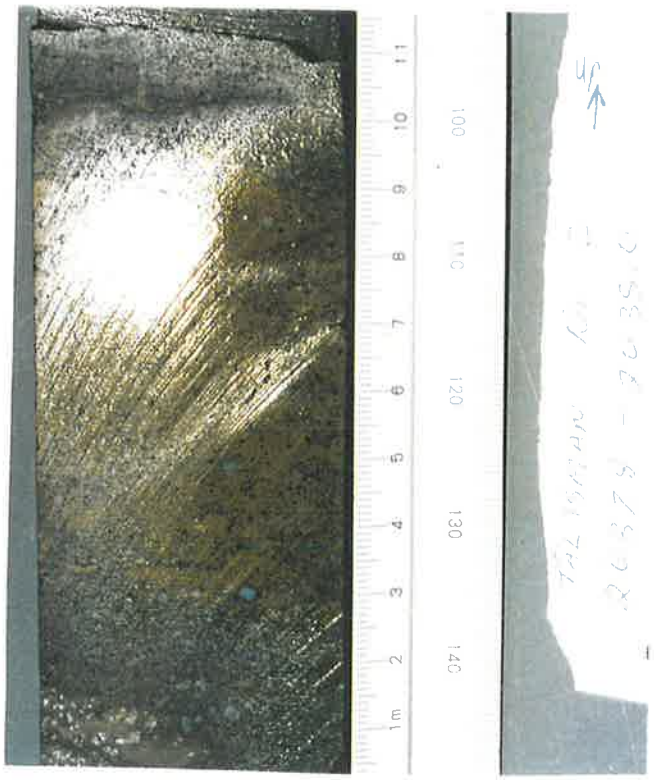
Talisman 2 CORE 5 2030.3 - 2048.2m

Forestier Claystone *B. reticulatum* Zone RECOVERY: 100% SCALE 1: 100



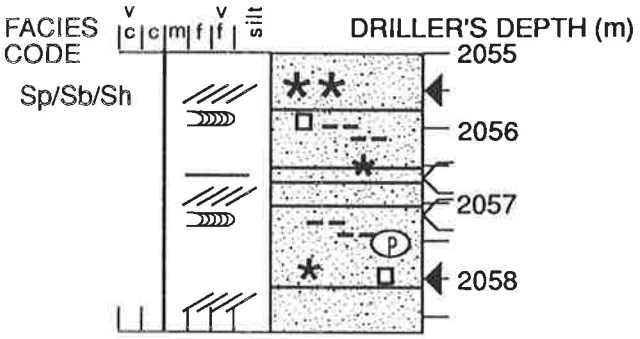
DESCRIPTION & COMMENTS

Claystone: dark grey, grey black, olive black, up to 30% fine to very coarse quartz, up to 15% glauconite; sandy, glauconitic claystone mass flow beds ~10 to 70 cm thick with possible sheared contacts are common ; interbedded with weakly laminated beds ~1 to 1.5 m thick; siderite nodules and pyrite nodules are common throughout; pyrite bands and nodules at ~2045.5 m have cone in cone structures; occasional horizontal burrows throughout mass flow units only; highly pyritized below 2044.5 m.



Talisman 2 CORE 6 2055 - 2058.7 m

Talisman Member *D. lobospinosum* Zone SCALE 1: 100



DESCRIPTION & COMMENTS

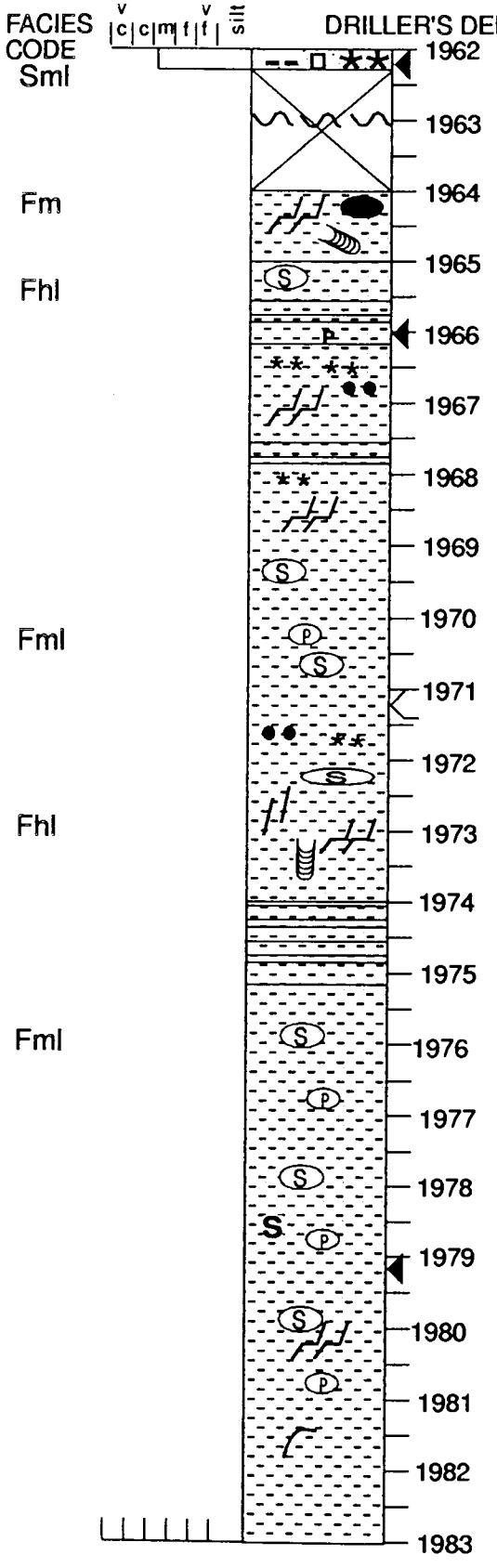
Sandstone: grey, olive grey, dark brown, fine to very coarse grained, predominantly medium to coarse grained, well sorted; up to 30% glauconite; thin beds 20 to 50 cm thick consist of a faint planar cross bedded unit overlain by an argillaceous burrowed sand.

Core plug porosity: 11.7 - 20.0%.
Core plug permeability: 87 - 5300 md.



Talisman 3 CORE 1 1962 - 1965 m CORE 2 1965 - 1983 m RECOVERY: Core 1- 45%
Core 2- 97.5%

Talisman Member/Forestier Claystone *S. areolata - B. reticulatum* Zones SCALE 1: 100



CORE 1

CORE 2

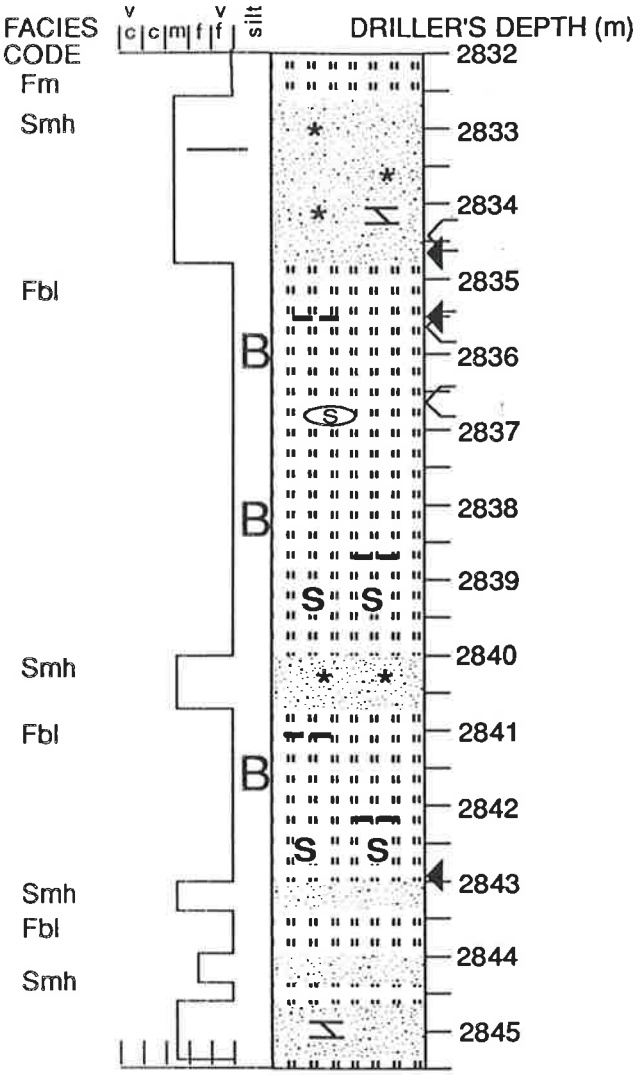
DESCRIPTION & COMMENTS

Sandstone: grey, dark green, medium to granule grain size, dominantly medium grained, well sorted, rounded grains; up to 40% glauconite; up to 20% argillite; dominantly massive with argillaceous streaks.

Claystone: grey, brown grey, cream brown; medium to coarse grained quartz and gluaconite streaks;

Wanaea 1 CORE 1 2832 - 2845.5m

Angel Formation *P. iehiense* Zone RECOVERY: 87% SCALE 1: 100



DESCRIPTION & COMMENTS

Sandstone: light grey, coarse to very fine grained, dominantly medium grained, poorly sorted to well sorted, dominantly well sorted, up to ~5% glauconite, up to ~5% dolomite cement; dominantly massive with weak horizontal and slightly wavy bedding throughout.

Core plug porosity: sandstone- 13..8 - 17.8%; average- 15..8%.

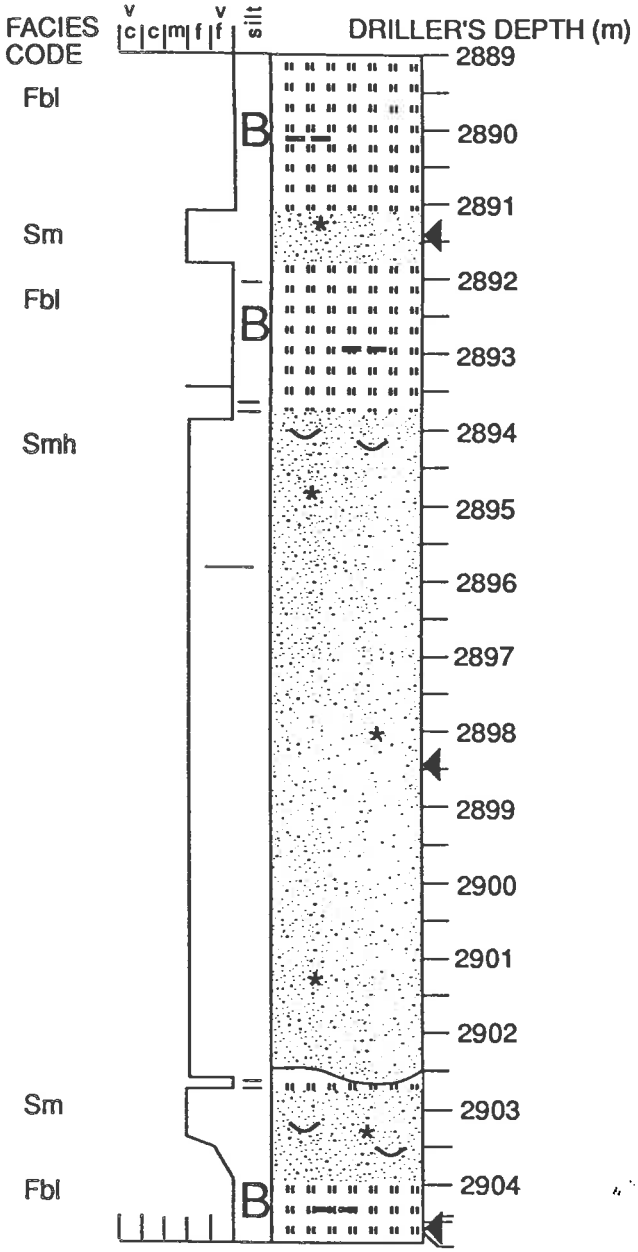
Siltstone: light olive grey, up to 25% quartz sand; up to 15% argillite; primary depositional structures are almost completely destroyed by high bioturbation; bioturbation consists dominantly of horizontal sand filled worm tubes; occasional verticle burrows 1 cm long and 2 cm wide; occasional original lamintions are noted; occasional siderite cemented bands.





Wanaea 1 CORE 2 2889 - 2904.8m

Angel Formation *D. jurassicum* Zone RECOVERY: 88% SCALE 1: 100



DESCRIPTION & COMMENTS

Siltstone: light olive grey, up to 15% sand, up to 15% argillite; original depositional structures neartly completely destroyed by high bioturbation which consists of dominantly horizontal worm tubes; minor pyrite cement, minor glauconite.

Sandstone: light olive grey, granule to very fine grained, dominantly medium grained, well sorted; massive with faint horizontal laminations; up to 15% glauconite; minor dolomite cement; between 2902.7 and 2903.7 heavily contorted with siltstone due to dewatering, also trace coal fragments.

Core plug porosity: sandstone- 12.6 - 21.3%; average- 14.9%.



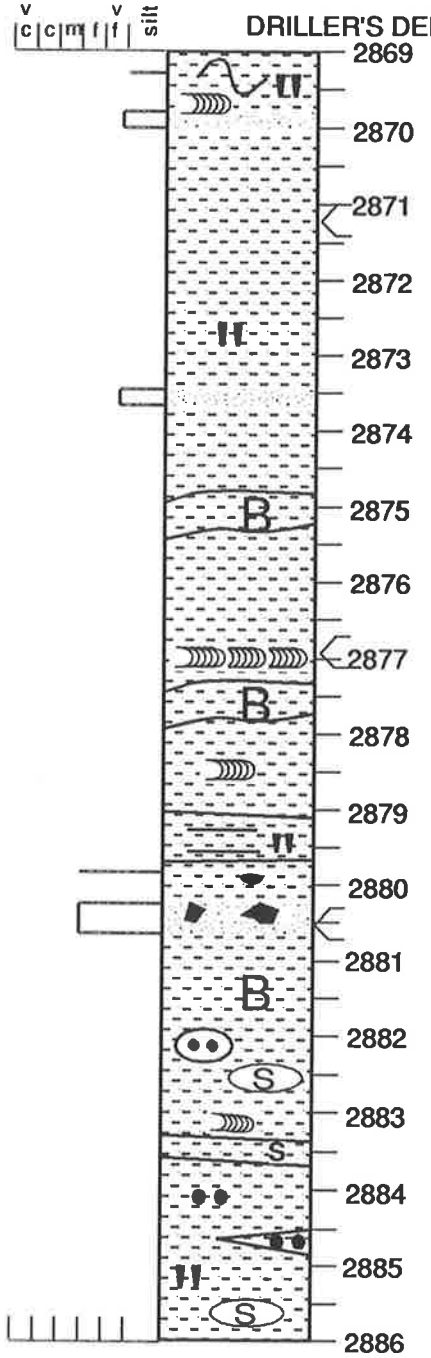
Wanaea 2 CORE 1 2075 - 2077m

Talisman Member (equivalent) *B. reticulatum* Zone RECOVERY: 15% SCALE 1: 50

2075 - 2077 Claystone: grey, all rubble.

Wanaea 2 CORE 2 2869 - 2886m

Angel Formation *P. iehiense* Zone RECOVERY: 100% SCALE 1: 100



DESCRIPTION & COMMENTS

Claystone: grey, silty, low to intense bioturbation

Horizontal worm burrow 1cm thick across complete core - *Rhizocorallium.*

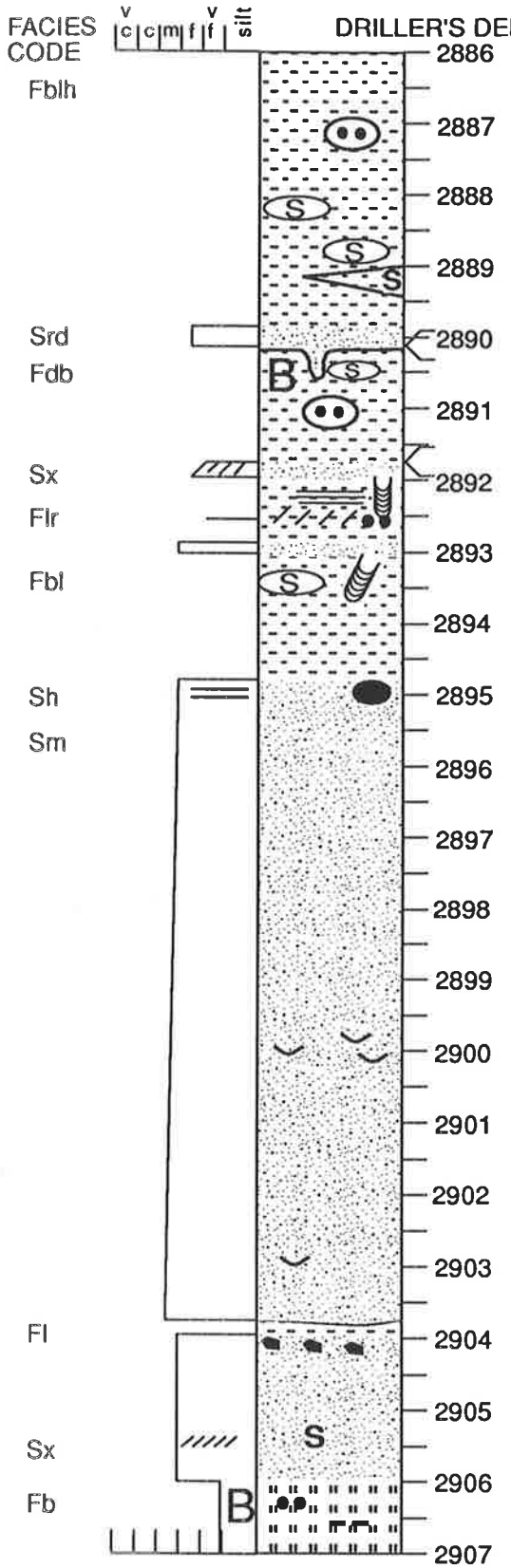
2877.5m - *Zoophycos* burrow

Sandstone: grey, well sorted, clay matrix, cm scale rip up clasts, no porosity; slump bed.

Planolites burrows

Wanaea 2 CORE 3 2886 - 2907m

Angel Formation *P iehiense* Zone RECOVERY: 100% SCALE 1: 100



DESCRIPTION & COMMENTS

Claystone: grey, silty, moderate bioturbation.

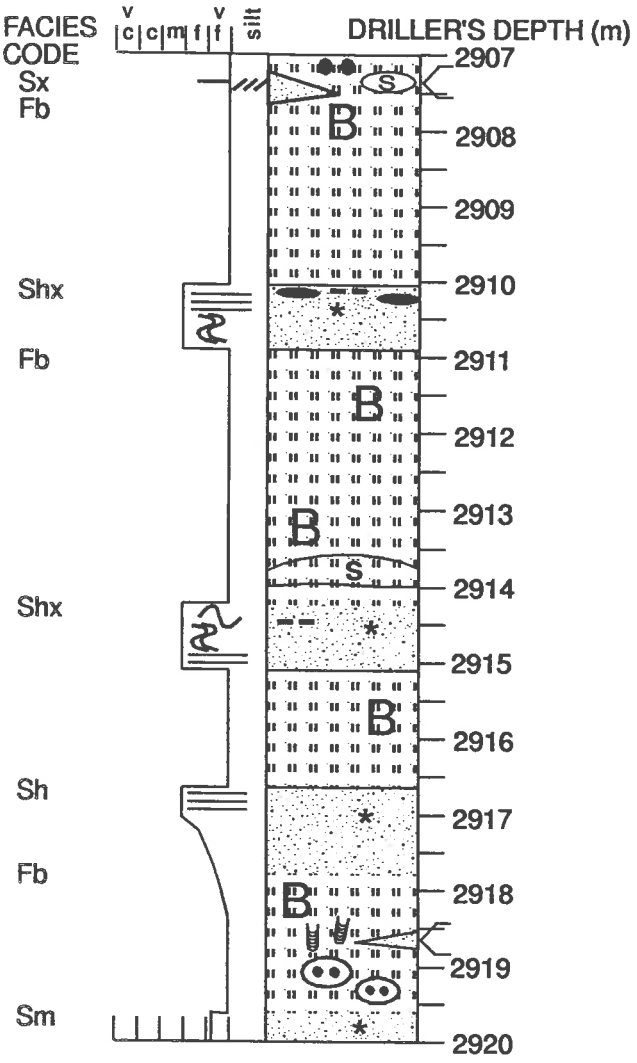
2890.2m - Flame structures

2893m - Inclined escape burrow 6cm deep.

Sandstone: light grey, well sorted fine to medium grained.

Wanaea 2 | CORE 4 (part 1) | 2907 - 2930m

Angel Formation | *P. iehiense* Zone | RECOVERY: 100% | SCALE 1: 100



DESCRIPTION & COMMENTS

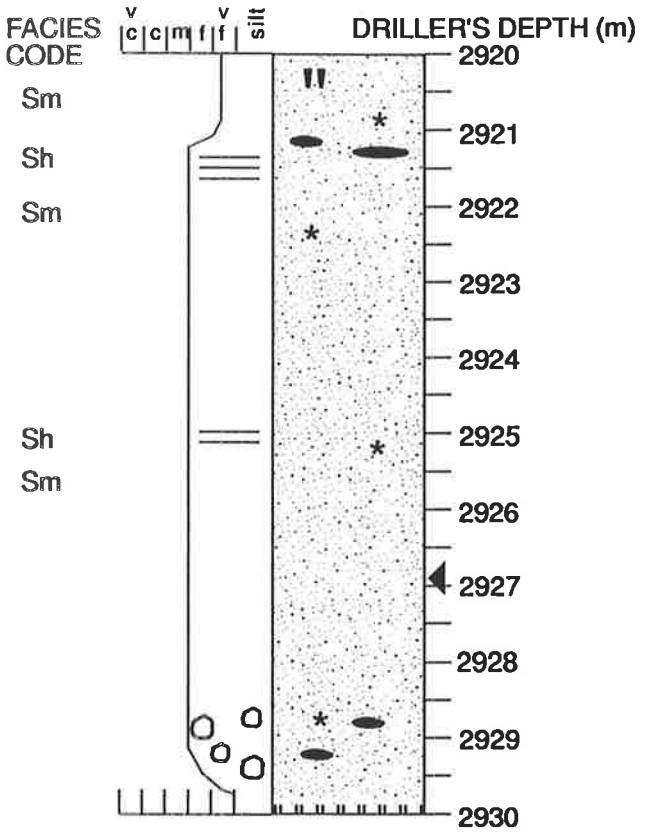
Siltstone: motteled light grey and light brown, argillaceous, sandy, intense bioturbation - *planolites, chondrites,* and *terebellina* burrows common;

Sandstone: light grey, well sorted, planar, wavy and convoluted cross bedding.

2918.7m - *Gastrochaenolites* burrow (firmground); *Tereballina* , *Rhyzocorallium* burrows.

Wanaea 2 CORE 4 (part 2) 2907 - 2930m

Angel Formation *P. iehiense* Zone RECOVERY: 100% SCALE 1: 100



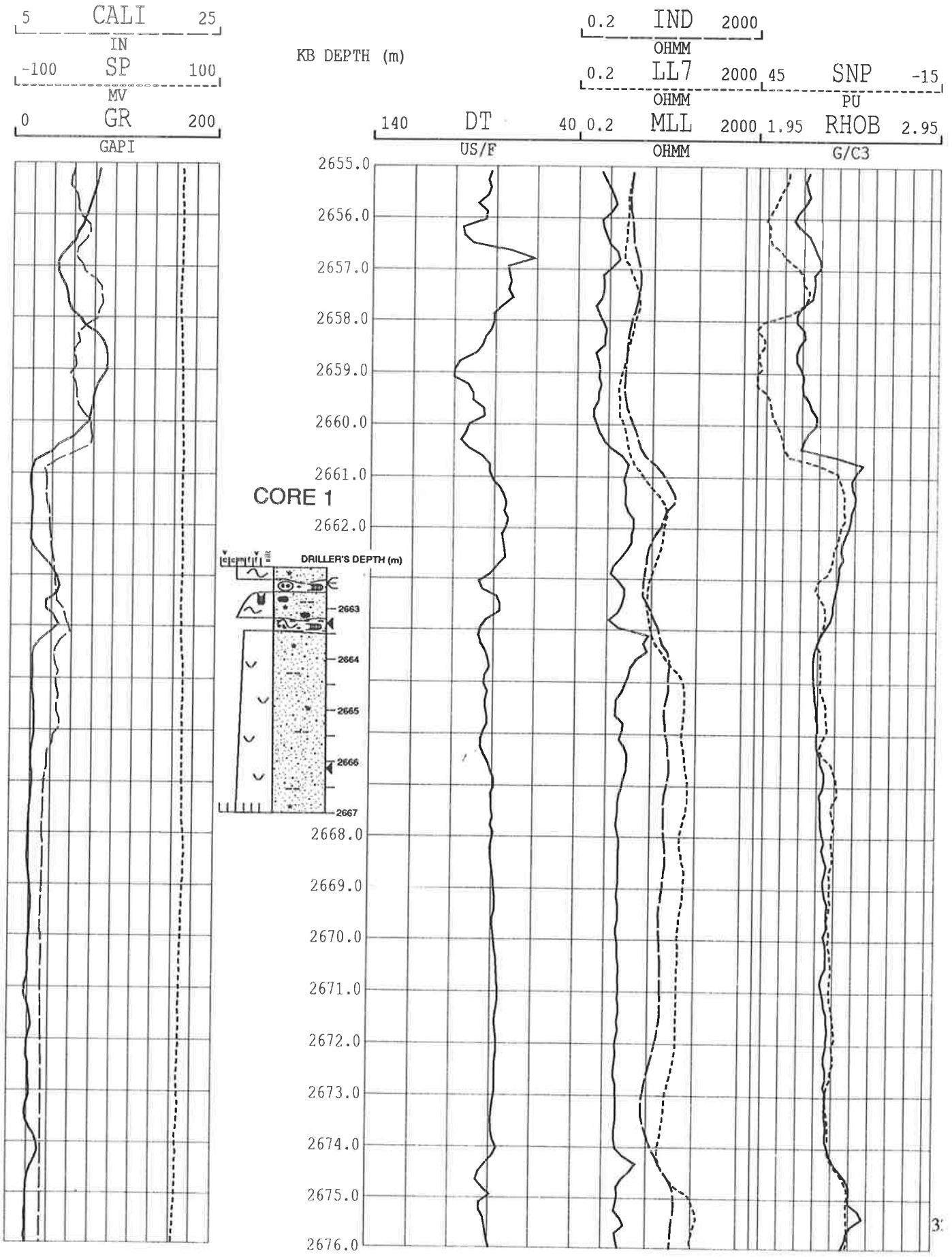
DESCRIPTION & COMMENTS

Sandstone: light grey, well sorted, mm scale rip up clasts at 2921m and 2929m.

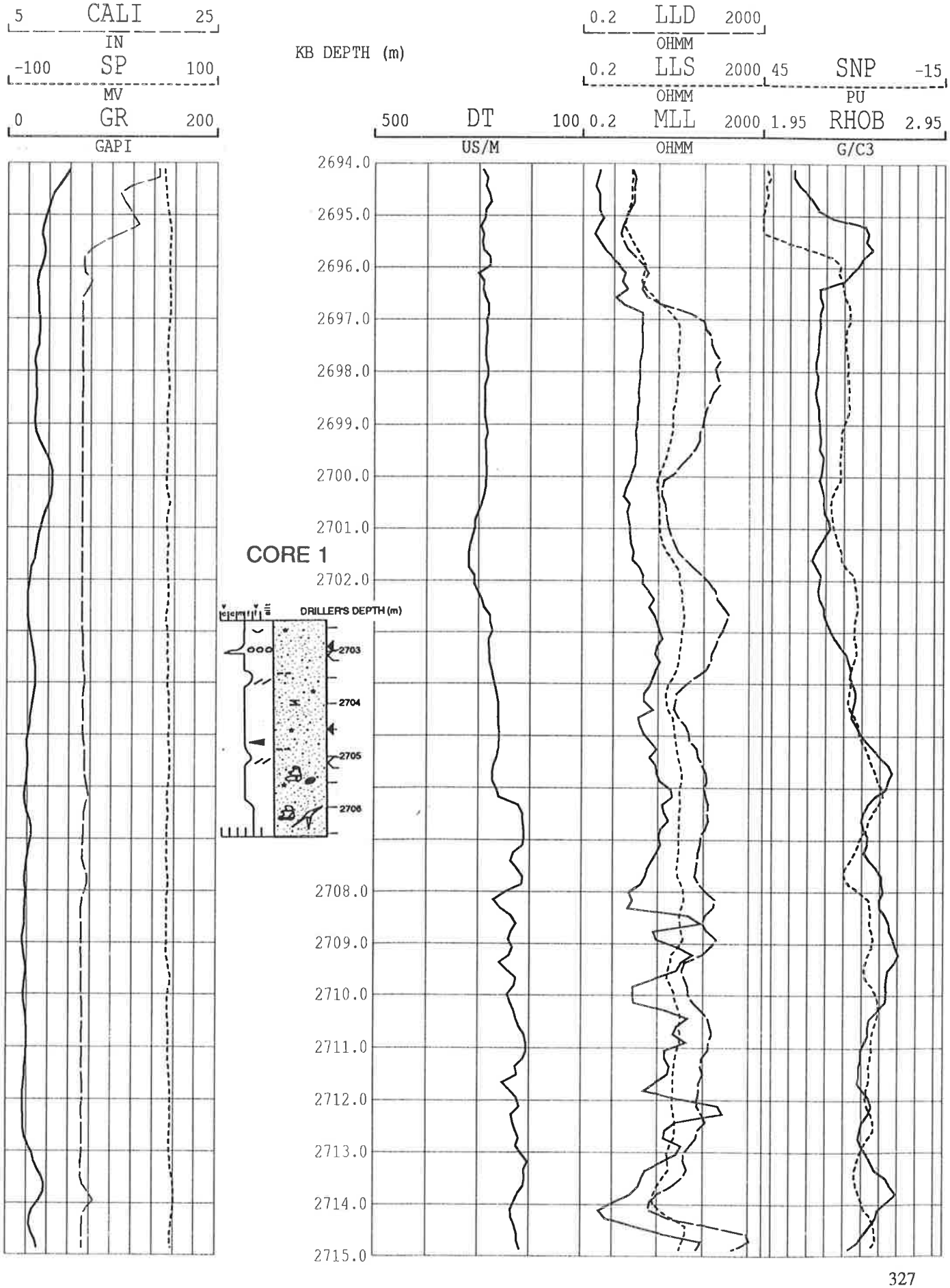
APPENDIX II

CORE LOG TO WIRELINE LOG ANNOTATIONS

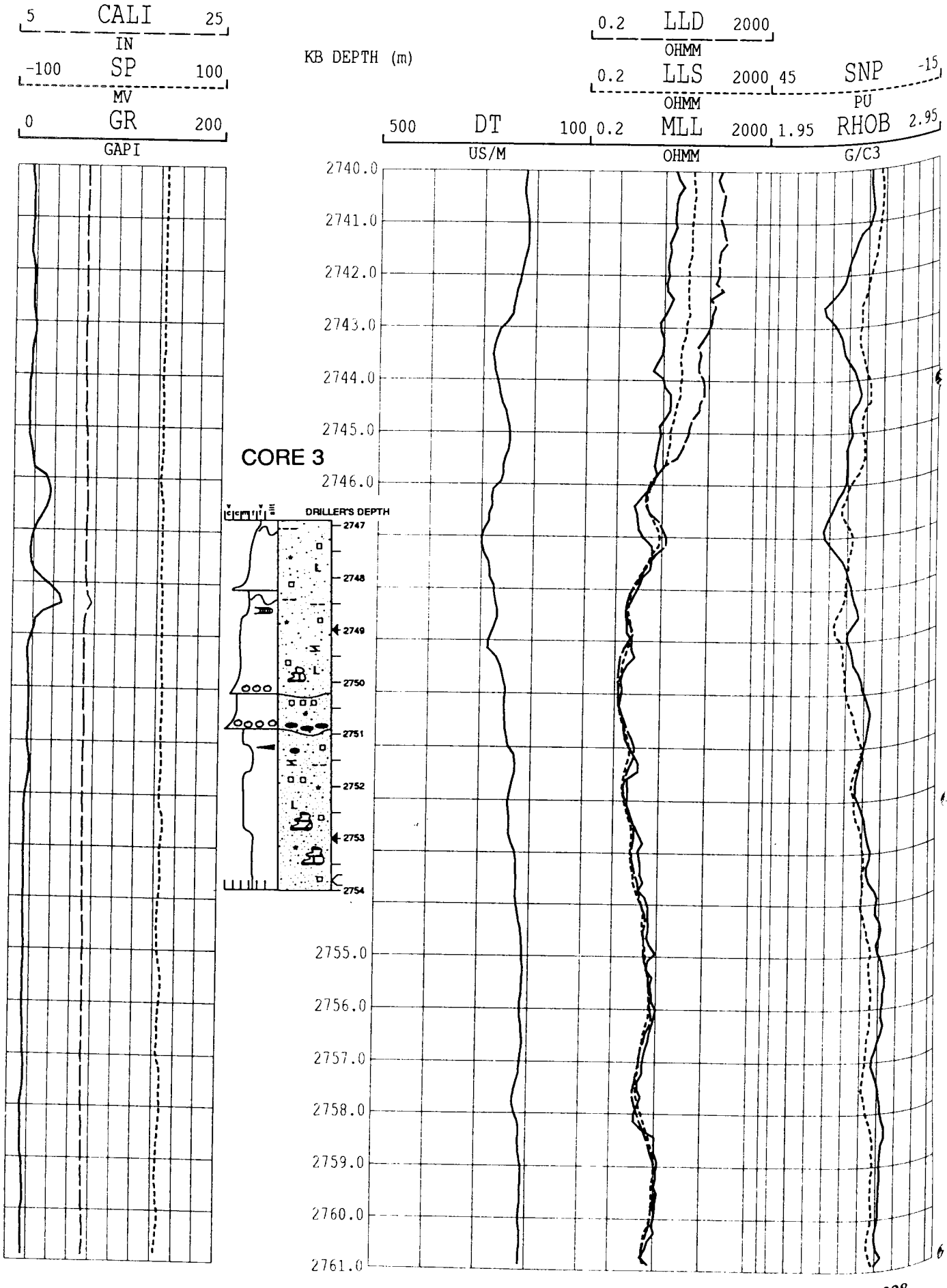
ANGEL_1


5 CALI 25
IN
-100 SP 100
MV
0 GR 200
GAPI
KB DEPTH (m)
0.2 IND 2000
OHMM
0.2 LL7 2000
OHMM
45 SNP -15
PU
140 DT 40
US/F
0.2 MLL 2000
OHMM
1.95 RHOB 2.95
G/C3
2655.0
2656.0
2657.0
2658.0
2659.0
2660.0
2661.0
CORE 1
2662.0
DRILLER'S DEPTH (m)
2663
2664
2665
2666
2667
2668.0
2669.0
2670.0
2671.0
2672.0
2673.0
2674.0
2675.0
2676.0

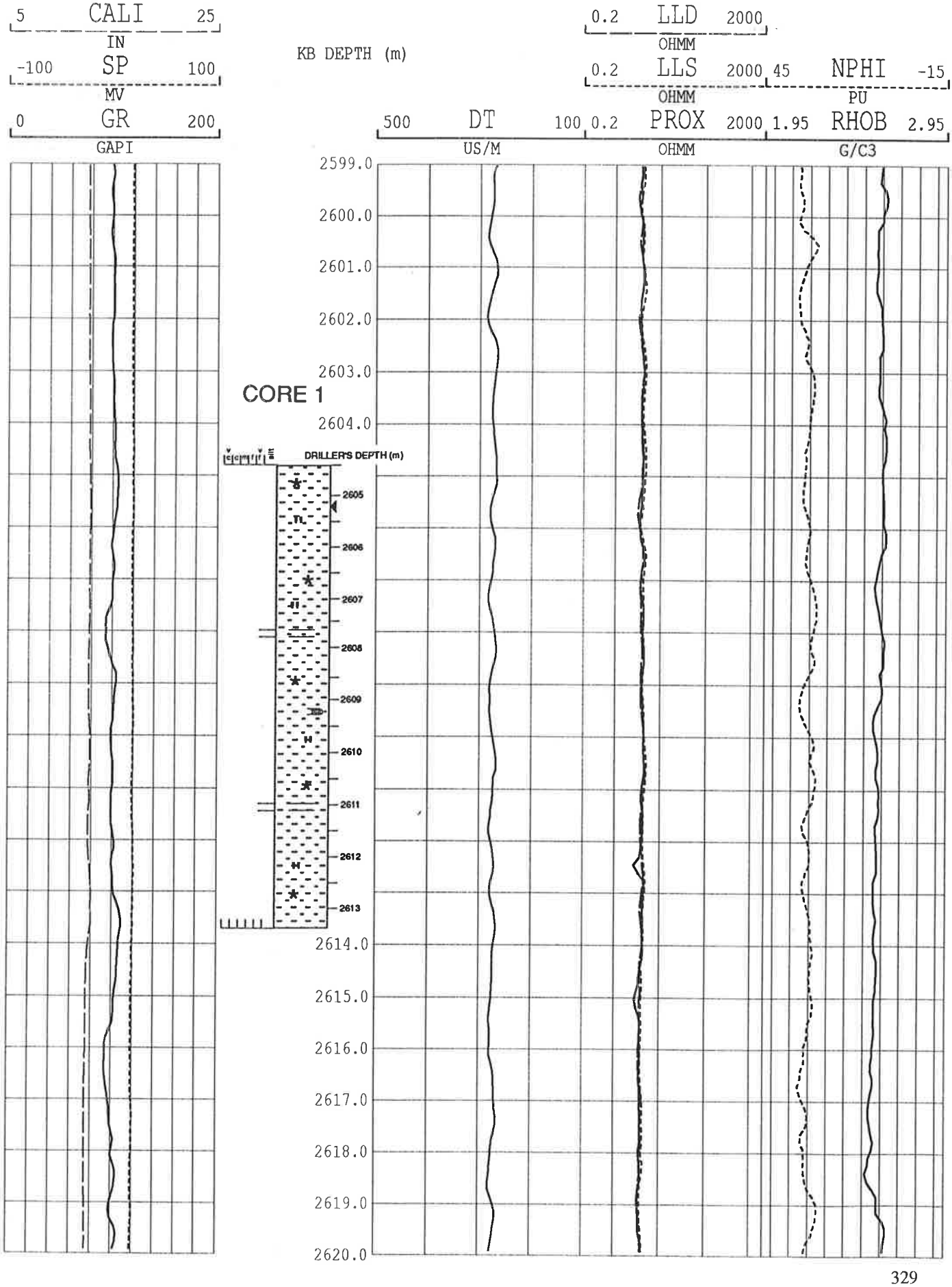
ANGEL_2


5 CALI 25
IN
-100 SP 100
MV
0 GR 200
GAPI
KB DEPTH (m)
0.2 LLD 2000
OHMM
0.2 LLS 2000
OHMM
45 SNP -15
PU
500 DT 100
US/M
0.2 MLL 2000
OHMM
1.95 RHOB 2.95
G/C3
2694.0
2695.0
2696.0
2697.0
2698.0
2699.0
2700.0
2701.0
CORE 1
2702.0
DRILLER'S DEPTH (m)
2703
2704
2705
2706
2708.0
2709.0
2710.0
2711.0
2712.0
2713.0
2714.0
2715.0

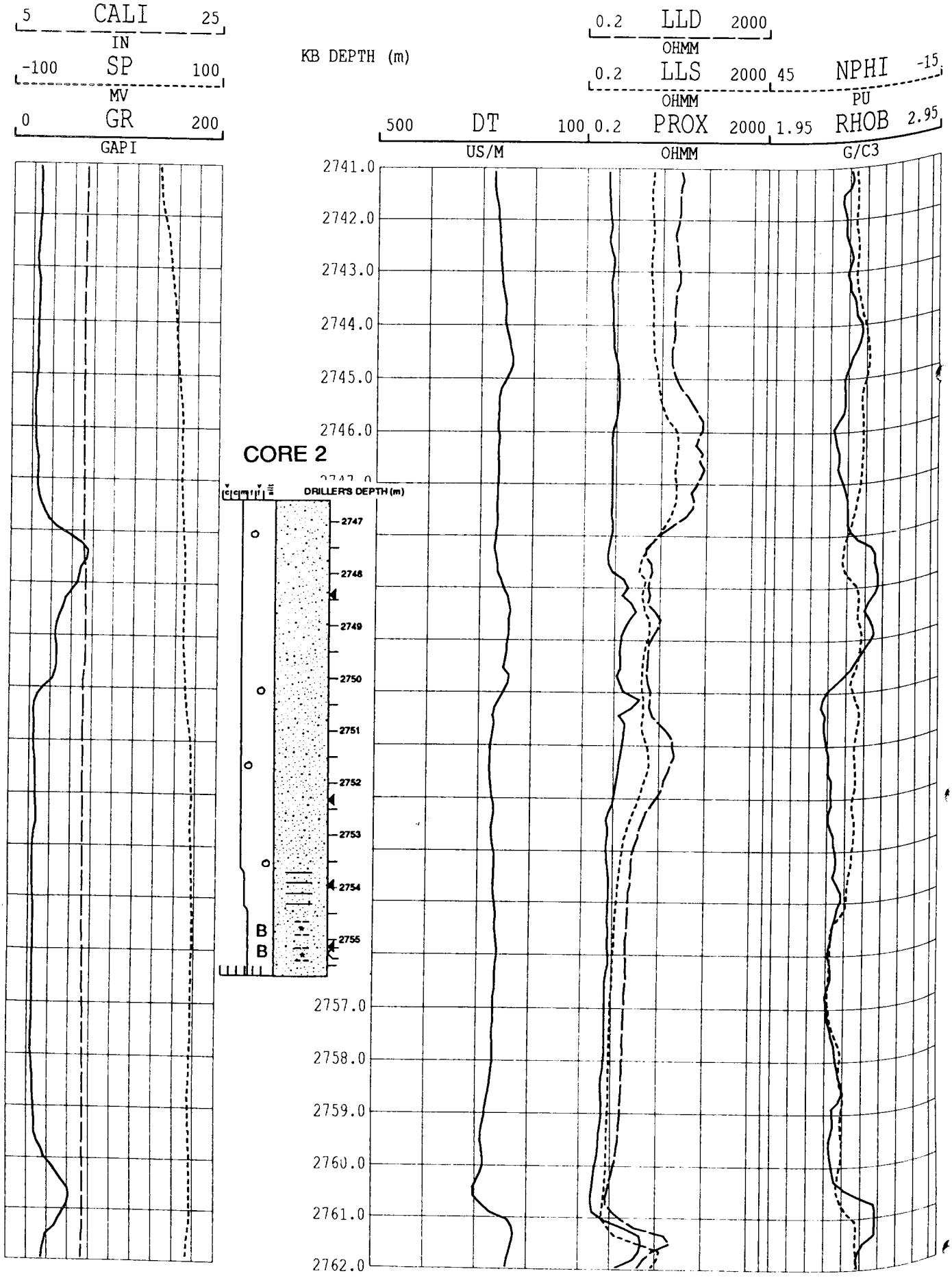
ANGEL_2


5 CALI 25
IN
-100 SP 100
MV
0 GR 200
GAPI
KB DEPTH (m)
0.2 LLD 2000
OHMM
0.2 LLS 2000
OHMM
45 SNP -15
PU
500 DT 100
US/M
0.2 MLL 2000
OHMM
1.95 RHOB 2.95
G/C3
2740.0
2741.0
2742.0
2743.0
2744.0
2745.0
2746.0
CORE 3
DRILLER'S DEPTH
2747
2748
2749
2750
2751
2752
2753
2754
2755.0
2756.0
2757.0
2758.0
2759.0
2760.0
2761.0

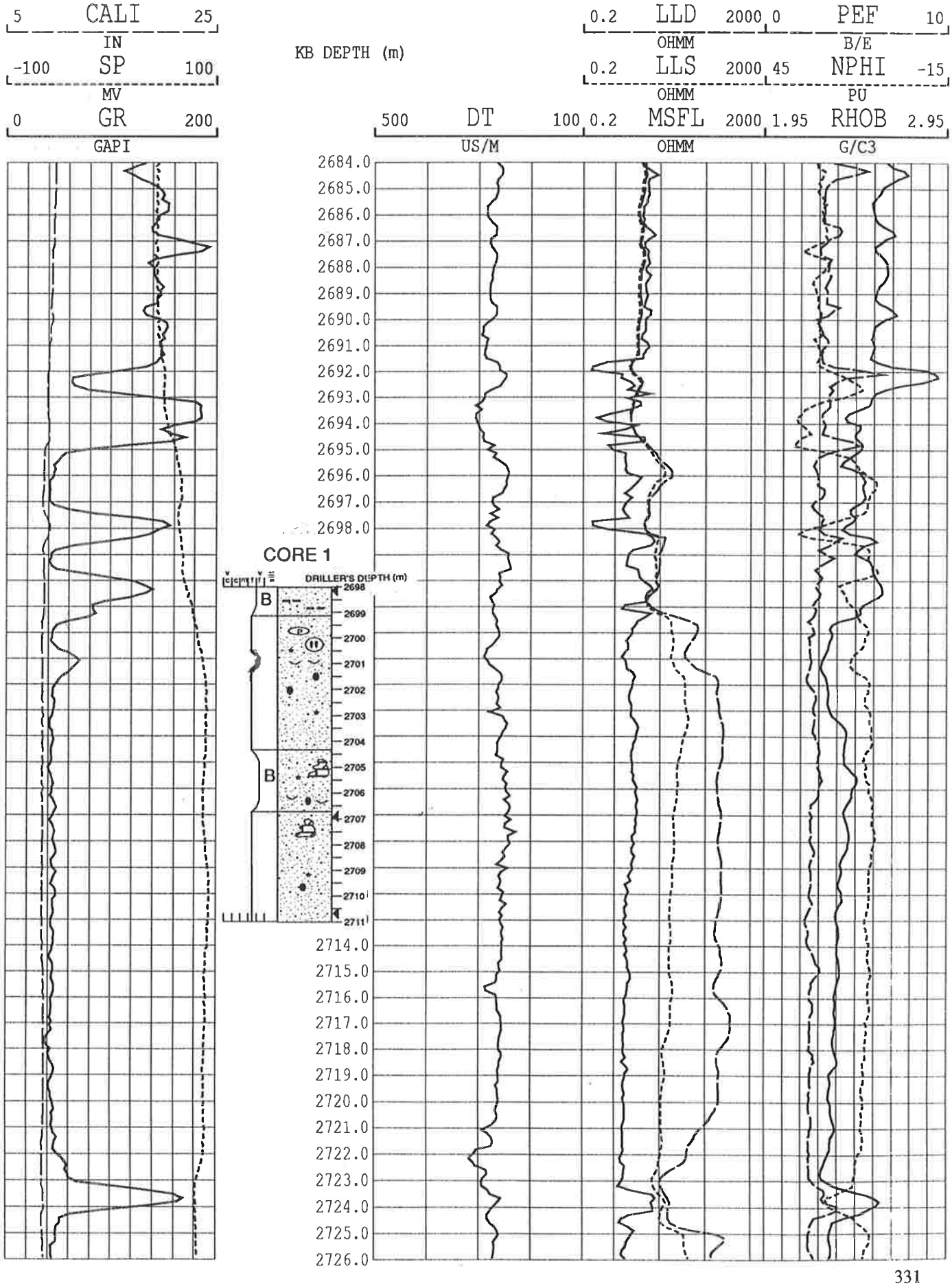
ANGEL_3


5 CALI 25
IN
-100 SP 100
MV
0 GR 200
GAPI
KB DEPTH (m)
0.2 LLD 2000
OHMM
0.2 LLS 2000
OHMM
45 NPHI -15
PU
500 DT 100
US/M
0.2 PROX 2000
OHMM
1.95 RHOB 2.95
G/C3
2599.0
2600.0
2601.0
2602.0
2603.0
2604.0
2614.0
2615.0
2616.0
2617.0
2618.0
2619.0
2620.0
CORE 1
DRILLER'S DEPTH (m)
2605
2606
2607
2608
2609
2610
2611
2612
2613

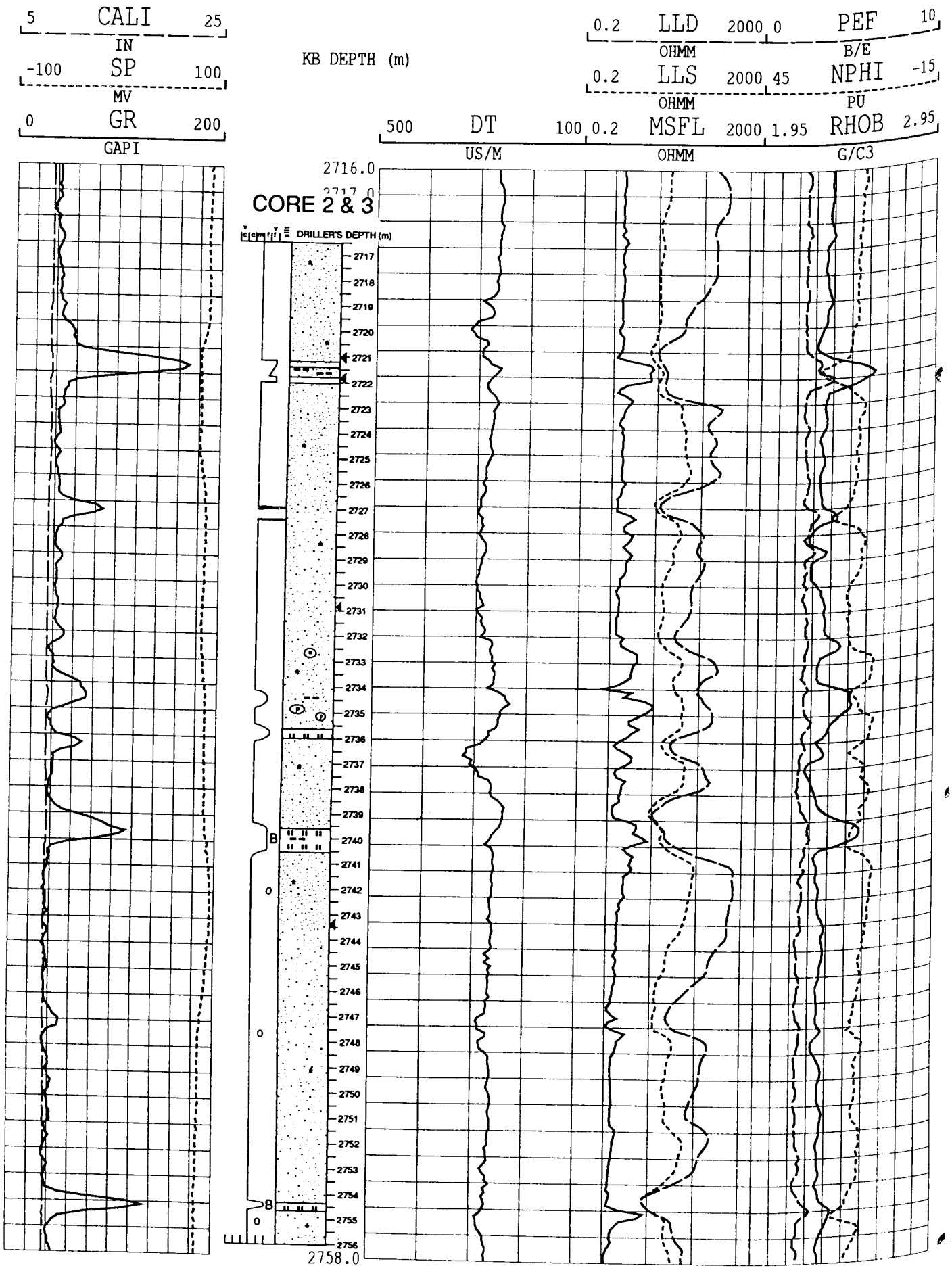
ANGEL 3


5 CALI 25
IN
-100 SP 100
MV
0 GR 200
GAPI
KB DEPTH (m)
0.2 LLD 2000
OHMM
0.2 LLS 2000
OHMM
45 NPHI -15
PU
500 DT 100
US/M
0.2 PROX 2000
OHMM
1.95 RHOB 2.95
G/C3
2741.0
2742.0
2743.0
2744.0
2745.0
2746.0
CORE 2
DRILLER'S DEPTH (m)
2747
2748
2749
2750
2751
2752
2753
2754
2755
B
B
2757.0
2758.0
2759.0
2760.0
2761.0
2762.0

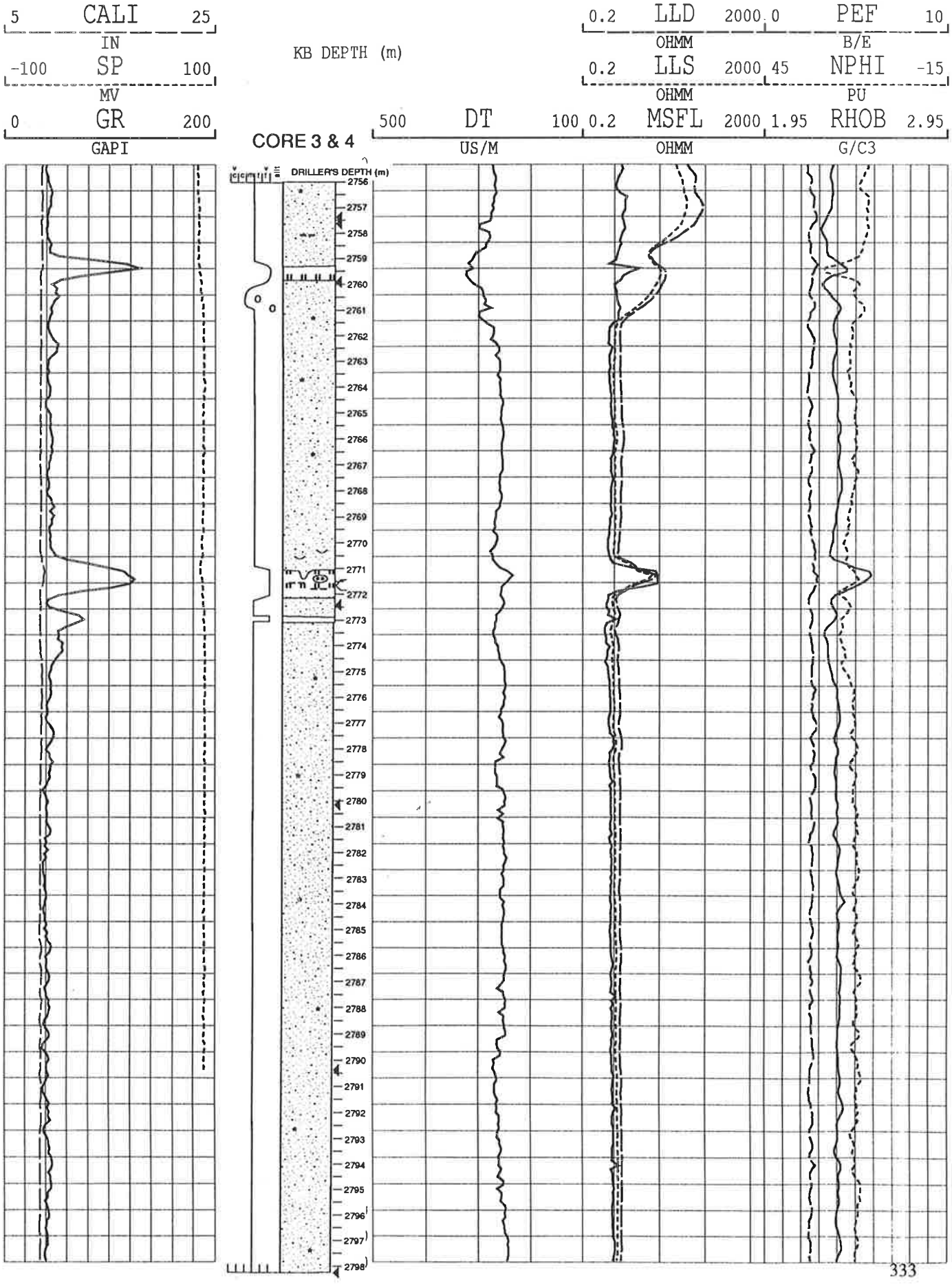
ANGEL_4


5 CALI 25
IN
-100 SP 100
MV
0 GR 200
GAPI
KB DEPTH (m)
0.2 LLD 2000
OHMM
0.2 LLS 2000
OHMM
500 DT 100
US/M
0.2 MSFL 2000
OHMM
0 PEF 10
B/E
45 NPHI -15
PU
1.95 RHOB 2.95
G/C3
2684.0
2685.0
2686.0
2687.0
2688.0
2689.0
2690.0
2691.0
2692.0
2693.0
2694.0
2695.0
2696.0
2697.0
2698.0
CORE 1
DRILLER'S DEPTH (m)
2698
2699
2700
2701
2702
2703
2704
2705
2706
2707
2708
2709
2710
2711
B
B
2714.0
2715.0
2716.0
2717.0
2718.0
2719.0
2720.0
2721.0
2722.0
2723.0
2724.0
2725.0
2726.0

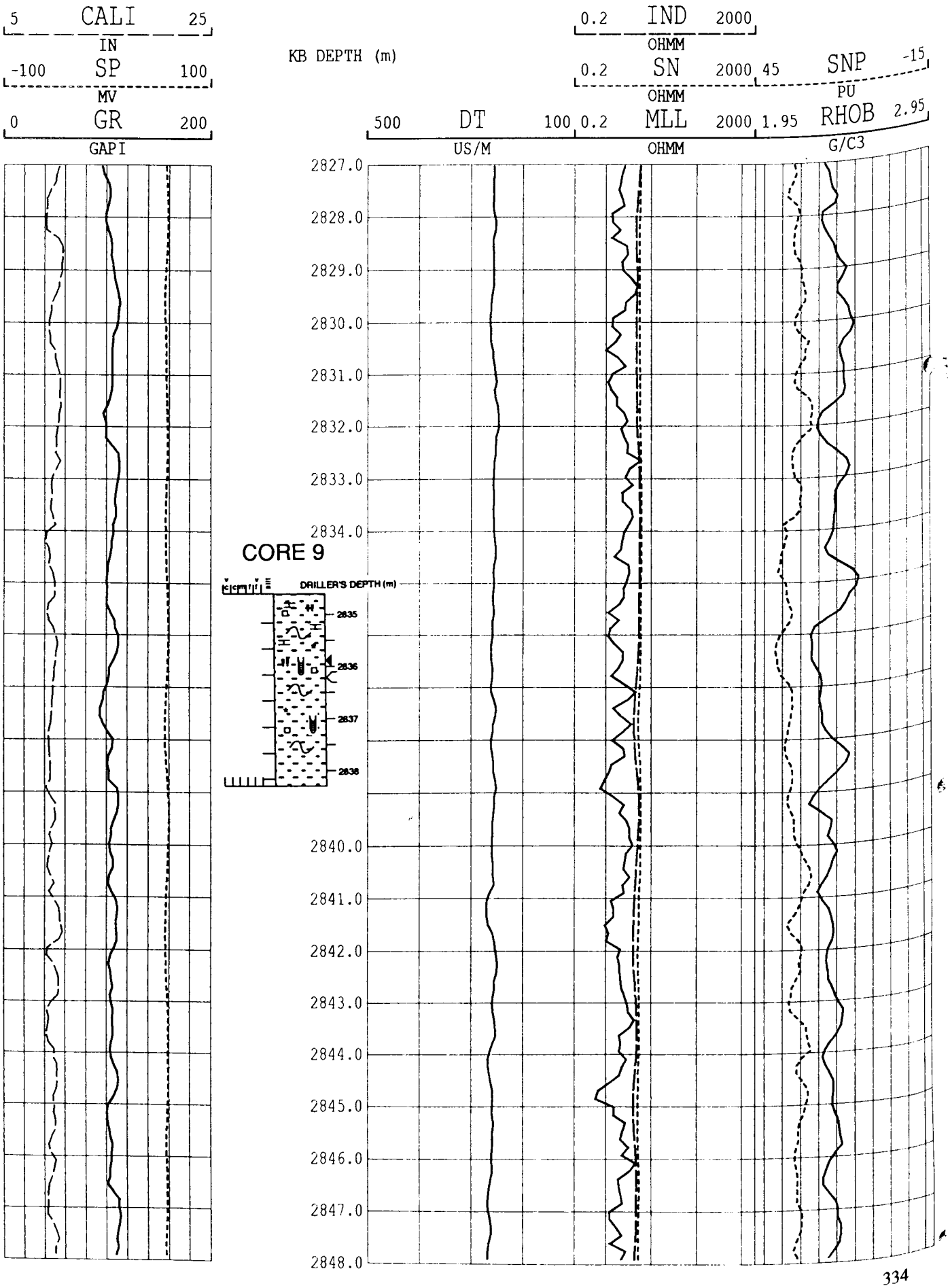
ANGEL_4


5 CALI 25
IN
-100 SP 100
MV
0 GR 200
GAPI
KB DEPTH (m)
0.2 LLD 2000 0 PEF 10
OHMM B/E
0.2 LLS 2000 45 NPHI -15
OHMM PU
500 DT 100 0.2 MSFL 2000 1.95 RHOB 2.95
US/M OHMM G/C3
2716.0
CORE 2 & 3
DRILLER'S DEPTH (m)
2717
2718
2719
2720
2721
2722
2723
2724
2725
2726
2727
2728
2729
2730
2731
2732
2733
2734
2735
2736
2737
2738
2739
2740
2741
2742
2743
2744
2745
2746
2747
2748
2749
2750
2751
2752
2753
2754
2755
2756
2758.0

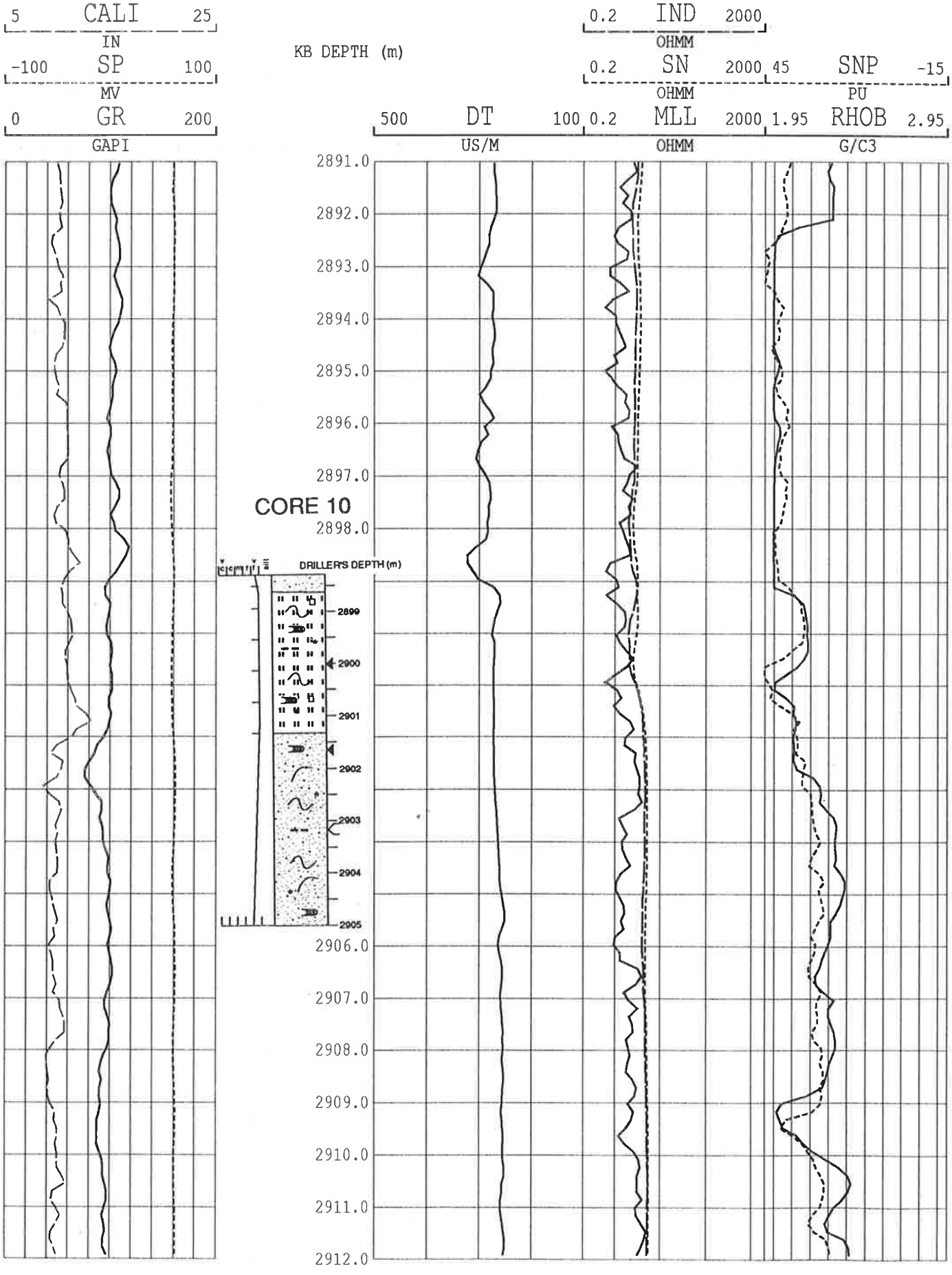
ANGEL_4


5 CALI 25
IN
-100 SP 100
MV
0 GR 200
GAPI
KB DEPTH (m)
CORE 3 & 4
DRILLER'S DEPTH (m)
2756
2757
2758
2759
2760
2761
2762
2763
2764
2765
2766
2767
2768
2769
2770
2771
2772
2773
2774
2775
2776
2777
2778
2779
2780
2781
2782
2783
2784
2785
2786
2787
2788
2789
2790
2791
2792
2793
2794
2795
2796
2797
2798
0.2 LLD 2000
OHMM
0.2 LLS 2000
OHMM
500 DT 100
US/M
0.2 MSFL 2000
OHMM
0 PEF 10
B/E
45 NPHI -15
PU
1.95 RHOB 2.95
G/C3

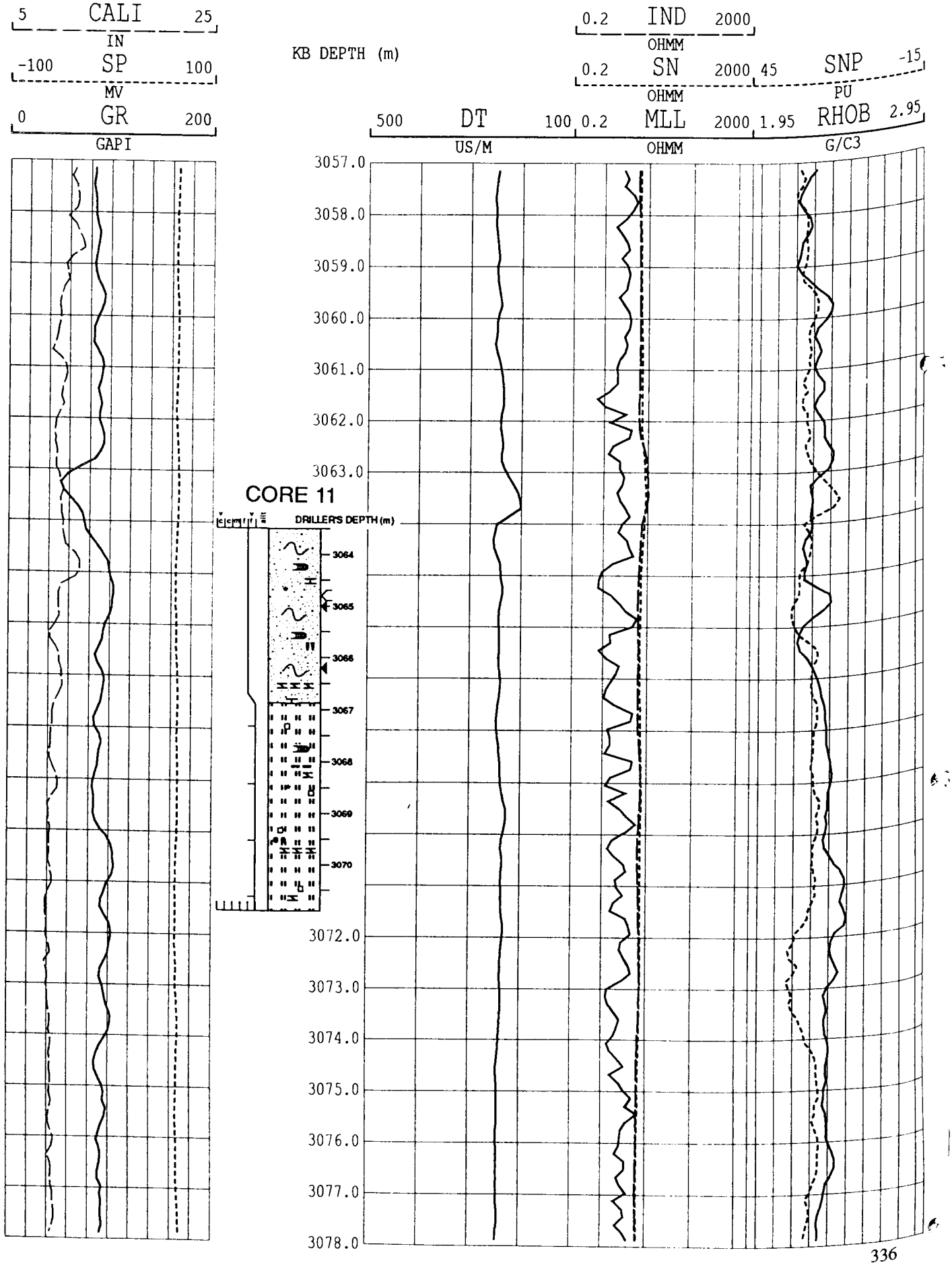
DAMPIER 1


5 CALI 25
IN
-100 SP 100
MV
0 GR 200
GAPI
KB DEPTH (m)
0.2 IND 2000
OHMM
0.2 SN 2000 45 SNP -15
OHMM PU
500 DT 100 0.2 MLL 2000 1.95 RHOB 2.95
US/M OHMM G/C3
2827.0
2828.0
2829.0
2830.0
2831.0
2832.0
2833.0
2834.0
CORE 9
DRILLER'S DEPTH (m)
2835
2836
2837
2838
2840.0
2841.0
2842.0
2843.0
2844.0
2845.0
2846.0
2847.0
2848.0

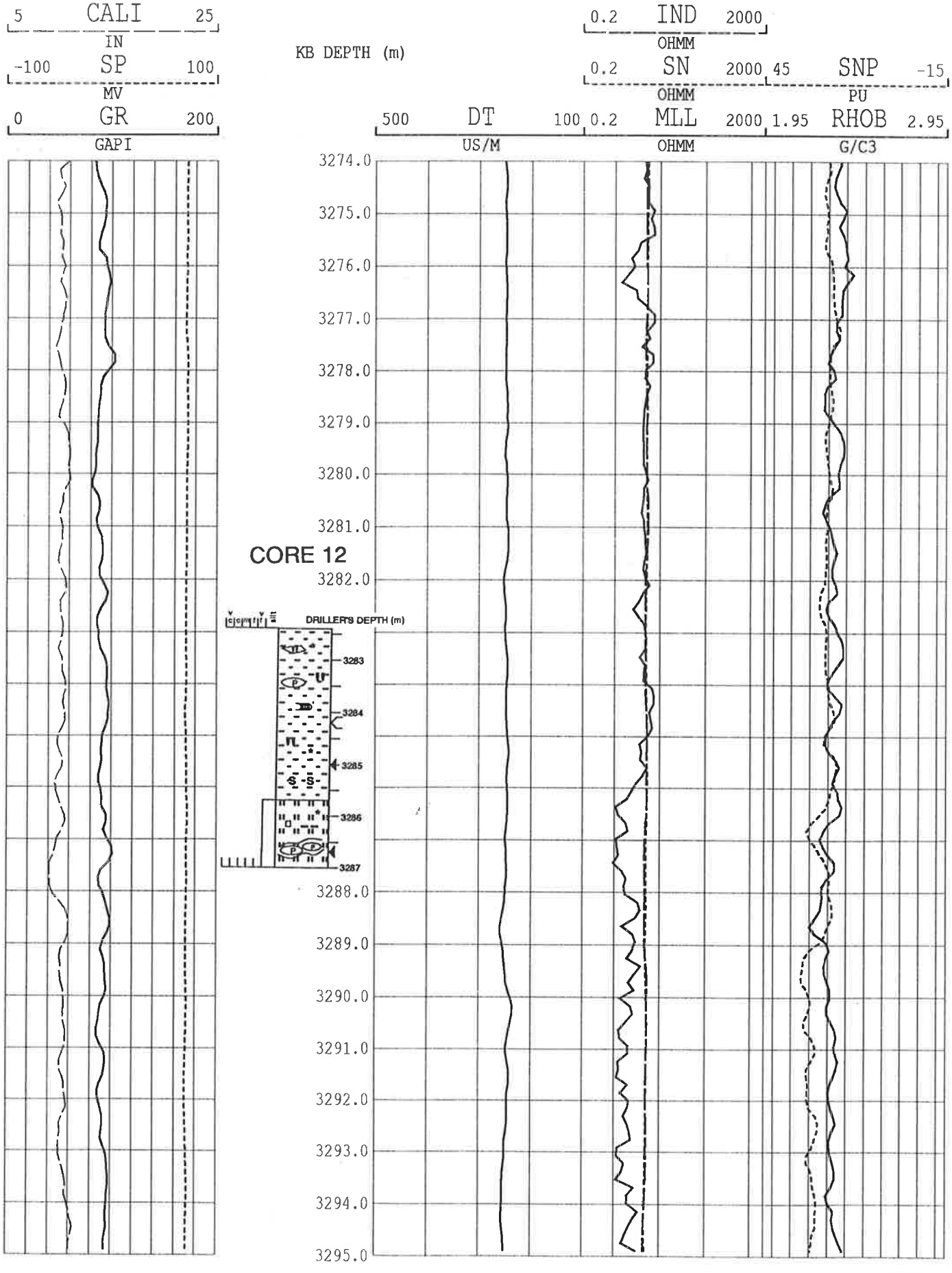
DAMPIER_1


5 CALI 25
IN
-100 SP 100
MV
0 GR 200
GAPI
KB DEPTH (m)
0.2 IND 2000
OHMM
0.2 SN 2000
OHMM
45 SNP -15
PU
500 DT 100
US/M
0.2 MLL 2000
OHMM
1.95 RHOB 2.95
G/C3
2891.0
2892.0
2893.0
2894.0
2895.0
2896.0
2897.0
CORE 10
2898.0
DRILLER'S DEPTH (m)
2899
2900
2901
2902
2903
2904
2905
2906.0
2907.0
2908.0
2909.0
2910.0
2911.0
2912.0

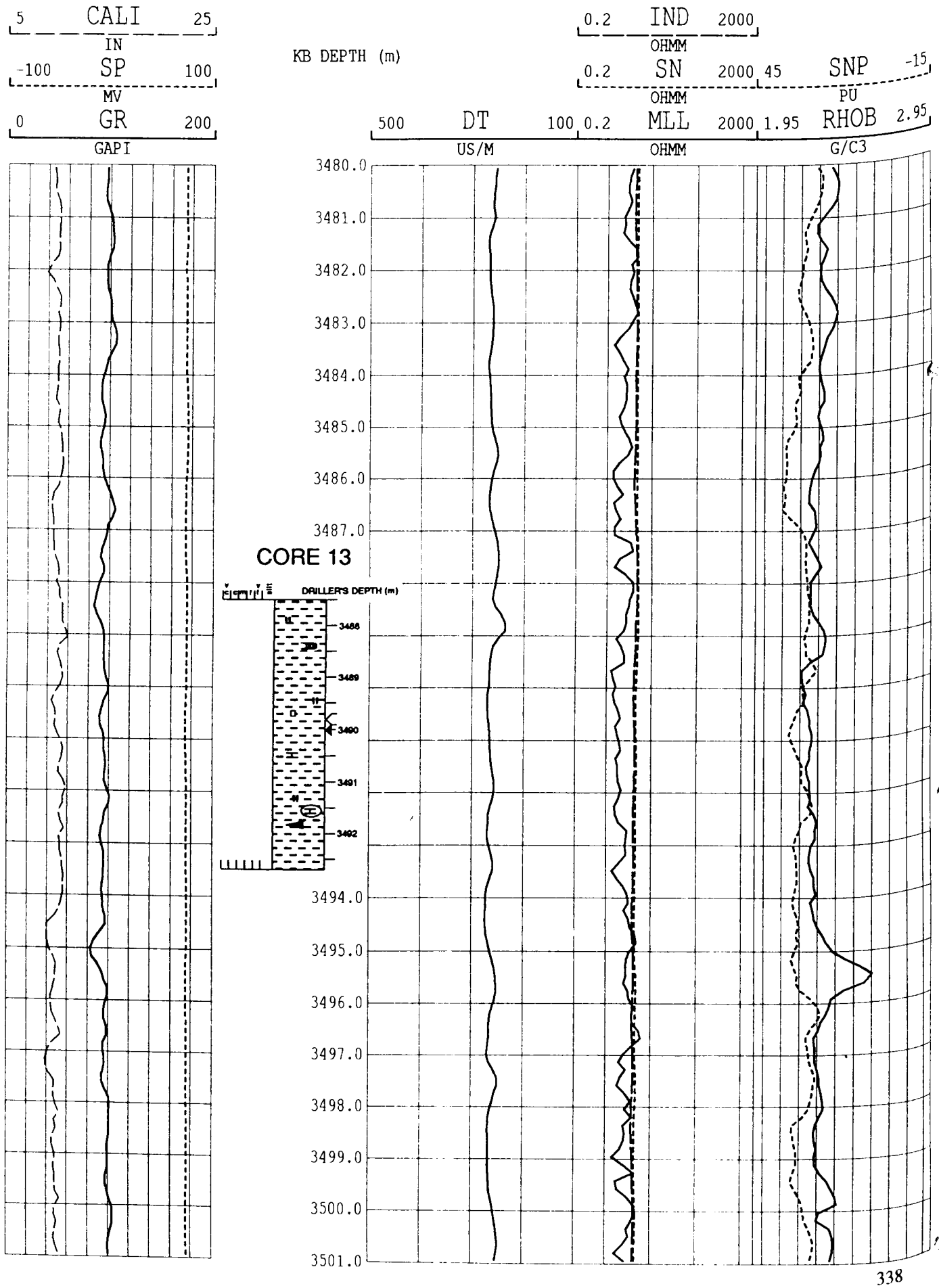
DAMPIER_1


5 CALI 25
IN
-100 SP 100
MV
0 GR 200
GAPI
KB DEPTH (m)
0.2 IND 2000
OHMM
0.2 SN 2000
OHMM
45 SNP -15
PU
500 DT 100
US/M
0.2 MLL 2000
OHMM
1.95 RHOB 2.95
G/C3
3057.0
3058.0
3059.0
3060.0
3061.0
3062.0
3063.0
CORE 11
DRILLER'S DEPTH (m)
3064
3065
3066
3067
3068
3069
3070
3072.0
3073.0
3074.0
3075.0
3076.0
3077.0
3078.0

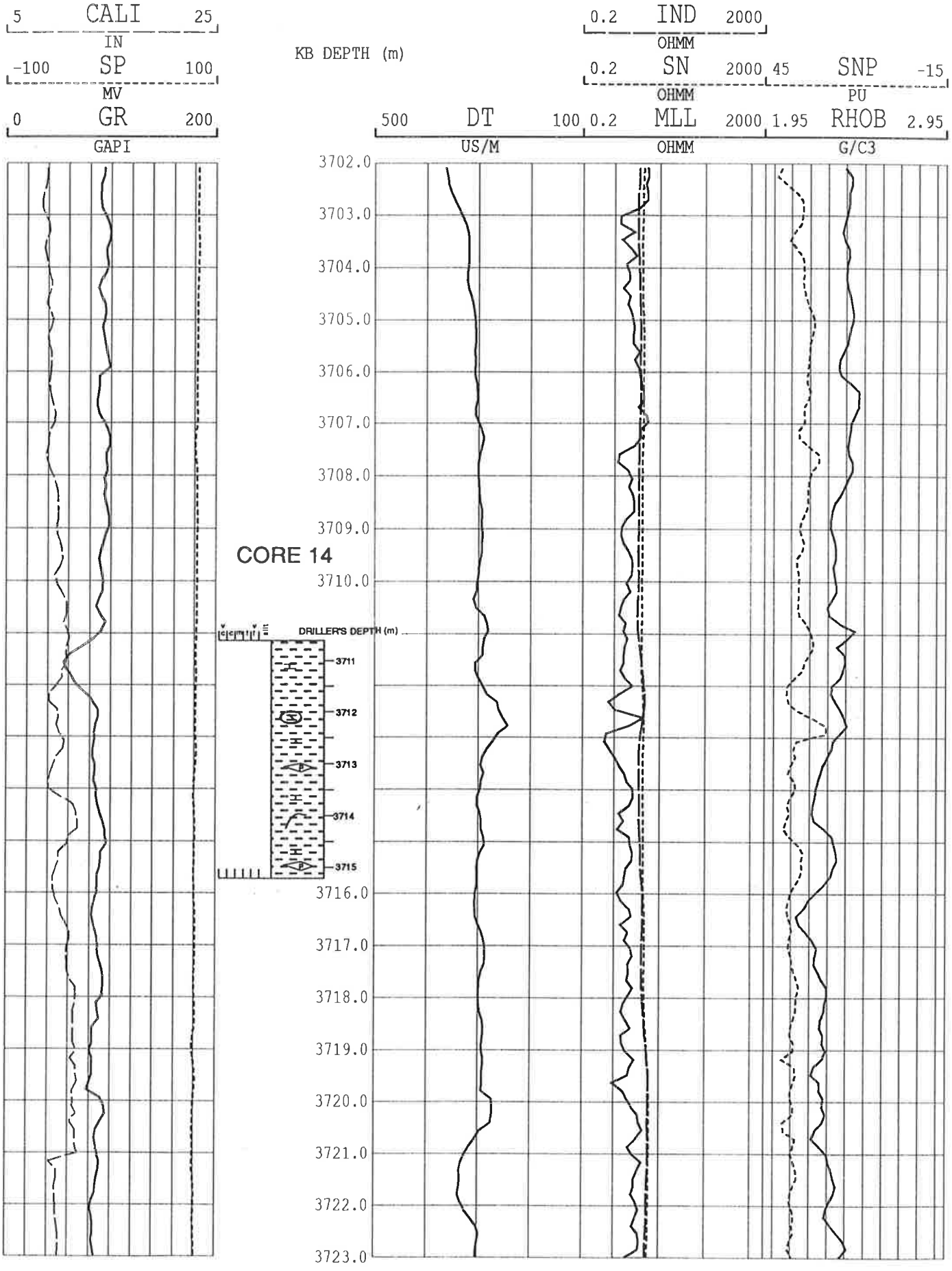
DAMPIER 1


5 CALI 25
IN
-100 SP 100
MV
0 GR 200
GAPI
KB DEPTH (m)
0.2 IND 2000
OHMM
0.2 SN 2000
OHMM
45 SNP -15
PU
500 DT 100
US/M
0.2 MLL 2000
OHMM
1.95 RHOB 2.95
G/C3
3274.0
3275.0
3276.0
3277.0
3278.0
3279.0
3280.0
3281.0
CORE 12
3282.0
DRILLER'S DEPTH (m)
3283
3284
3285
3286
3287
3288.0
3289.0
3290.0
3291.0
3292.0
3293.0
3294.0
3295.0

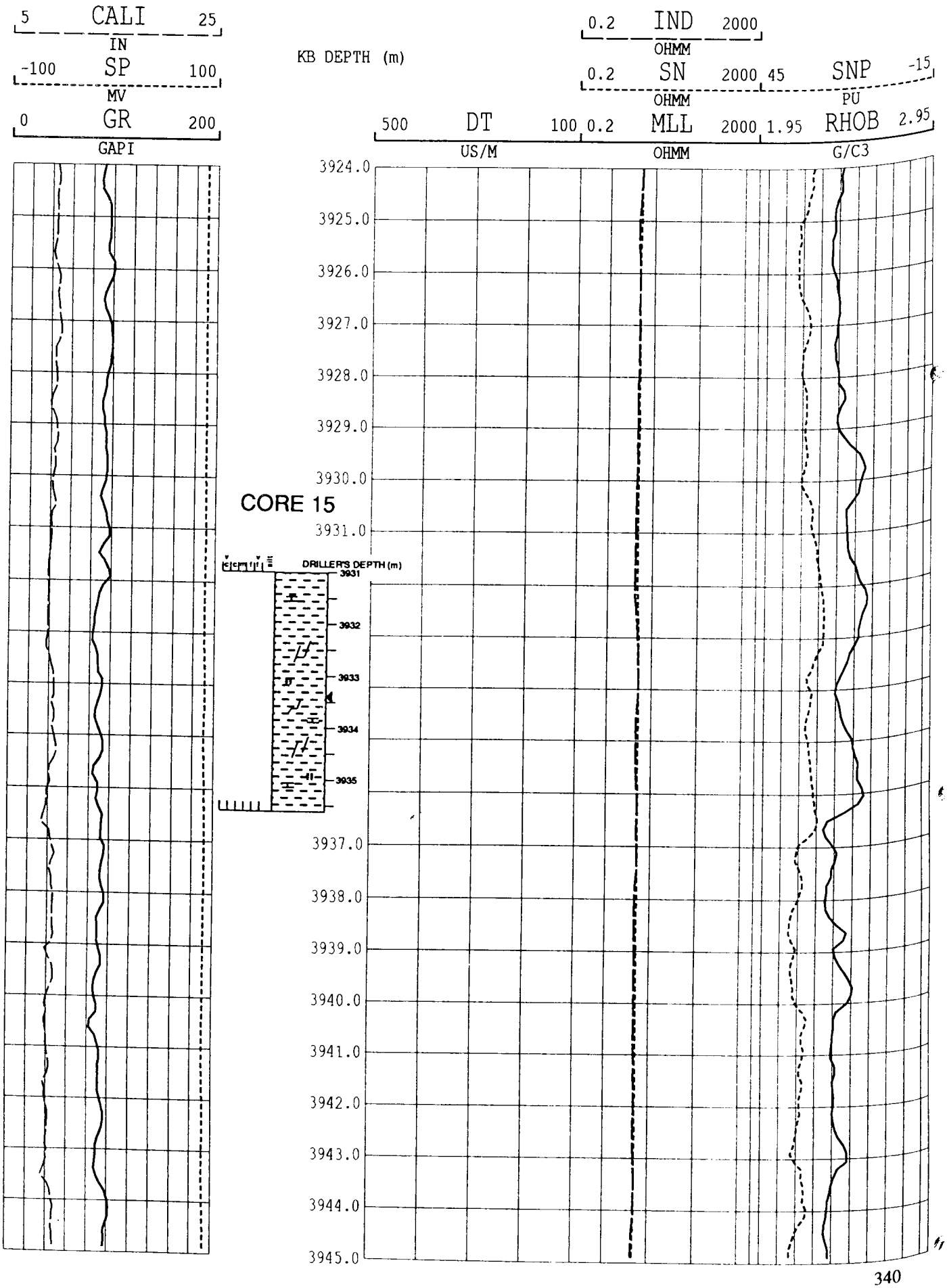
DAMPIER_1


5 CALI 25
IN
-100 SP 100
MV
0 GR 200
GAPI
KB DEPTH (m)
0.2 IND 2000
OHMM
0.2 SN 2000
OHMM
45 SNP -15
PU
500 DT 100
US/M
0.2 MLL 2000
OHMM
1.95 RHOB 2.95
G/C3
3480.0
3481.0
3482.0
3483.0
3484.0
3485.0
3486.0
3487.0
CORE 13
DRILLER'S DEPTH (m)
3488
3489
3490
3491
3492
3494.0
3495.0
3496.0
3497.0
3498.0
3499.0
3500.0
3501.0

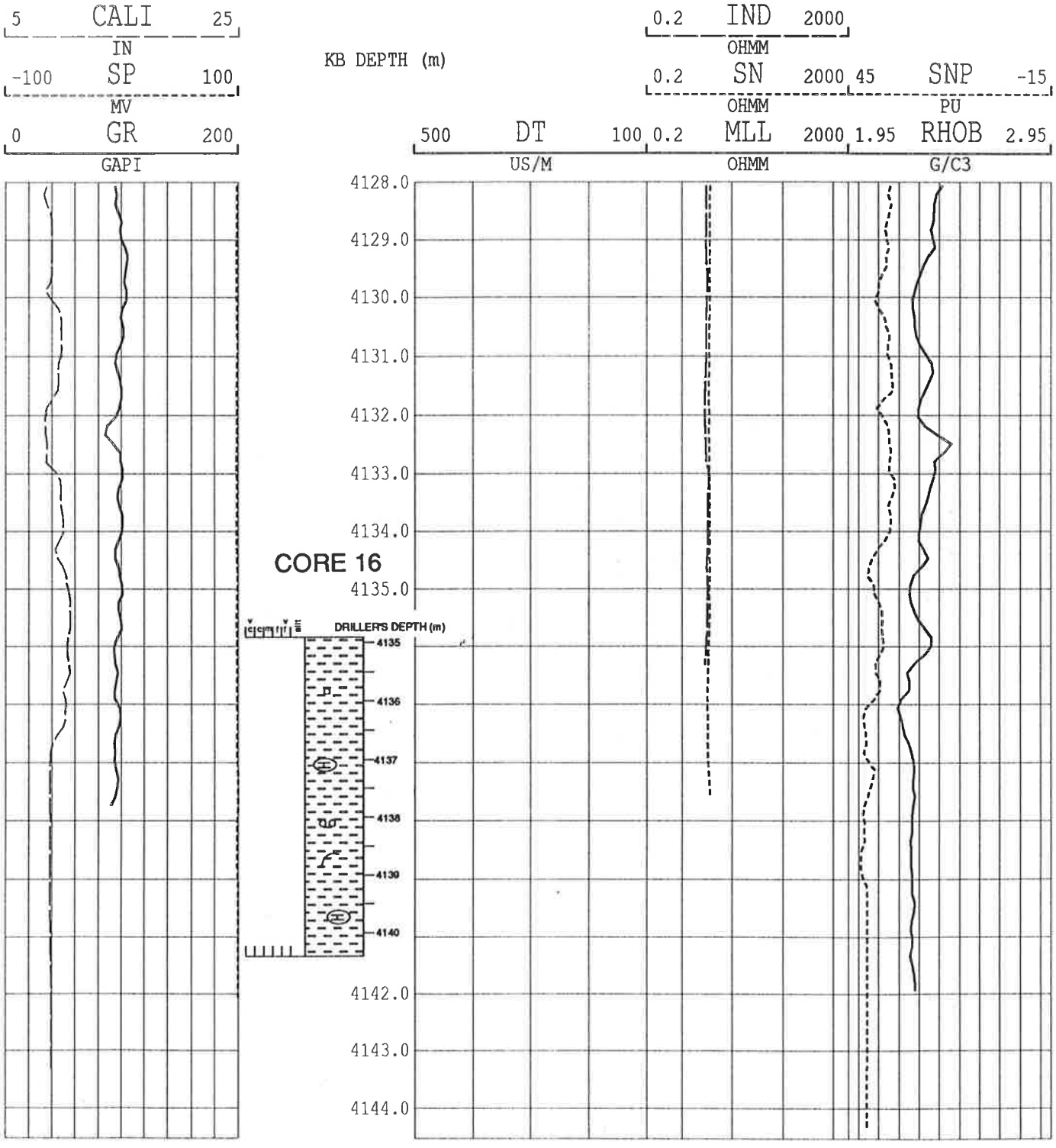
DAMPIER_1


5 CALI 25
IN
-100 SP 100
MV
0 GR 200
GAPI
KB DEPTH (m)
0.2 IND 2000
OHMM
0.2 SN 2000
OHMM
45 SNP -15
PU
500 DT 100
US/M
0.2 MLL 2000
OHMM
1.95 RHOB 2.95
G/C3
3702.0
3703.0
3704.0
3705.0
3706.0
3707.0
3708.0
3709.0
3710.0
3716.0
3717.0
3718.0
3719.0
3720.0
3721.0
3722.0
3723.0
CORE 14
DRILLER'S DEPTH (m)
3711
3712
3713
3714
3715

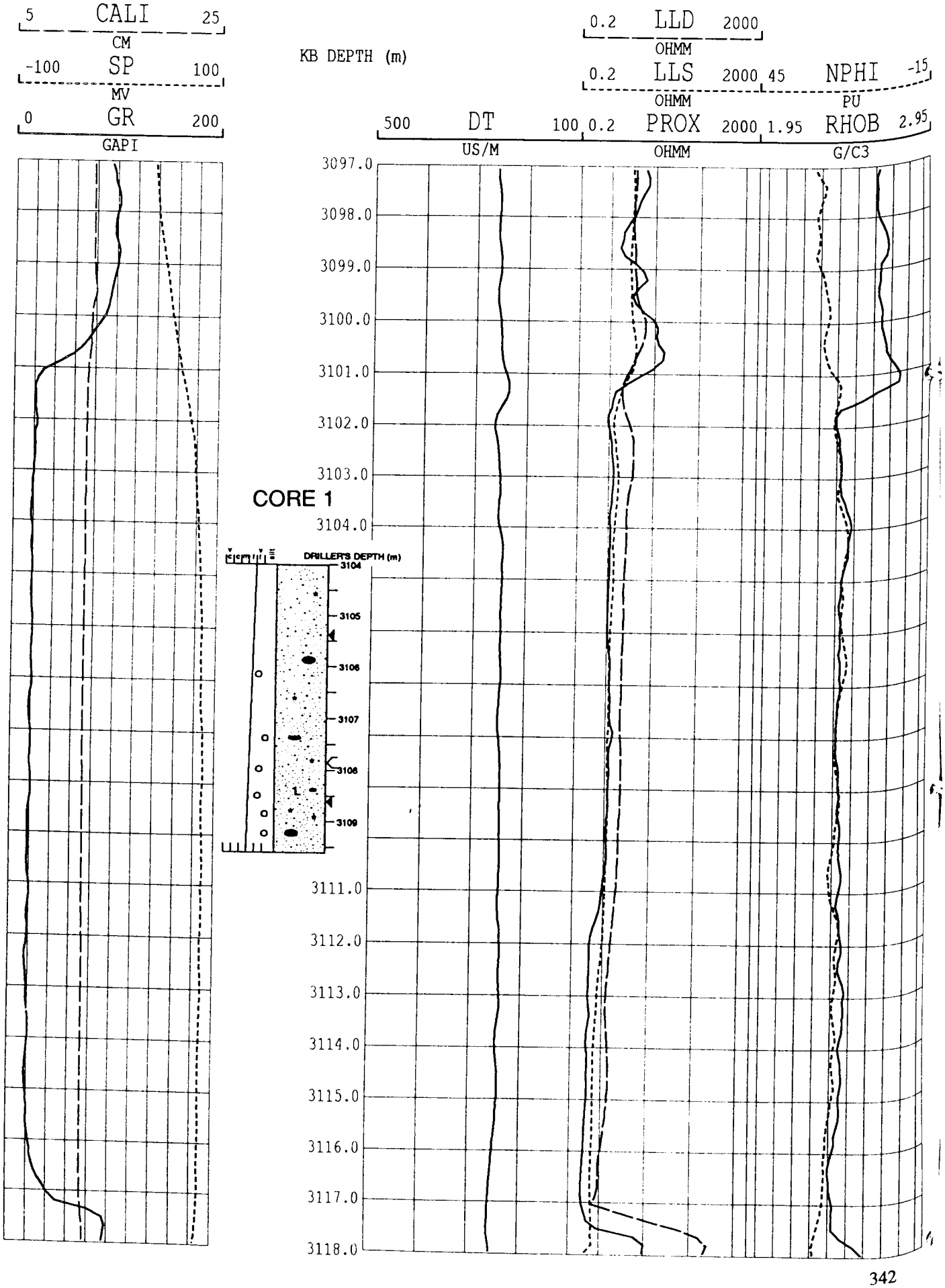
DAMPIER_1


5 CALI 25
IN
-100 SP 100
MV
0 GR 200
GAPI
KB DEPTH (m)
0.2 IND 2000
OHMM
0.2 SN 2000 45 SNP -15
OHMM PU
500 DT 100 0.2 MLL 2000 1.95 RHOB 2.95
US/M OHMM G/C3
3924.0
3925.0
3926.0
3927.0
3928.0
3929.0
3930.0
3931.0
3937.0
3938.0
3939.0
3940.0
3941.0
3942.0
3943.0
3944.0
3945.0
CORE 15
DRILLER'S DEPTH (m)
3931
3932
3933
3934
3935

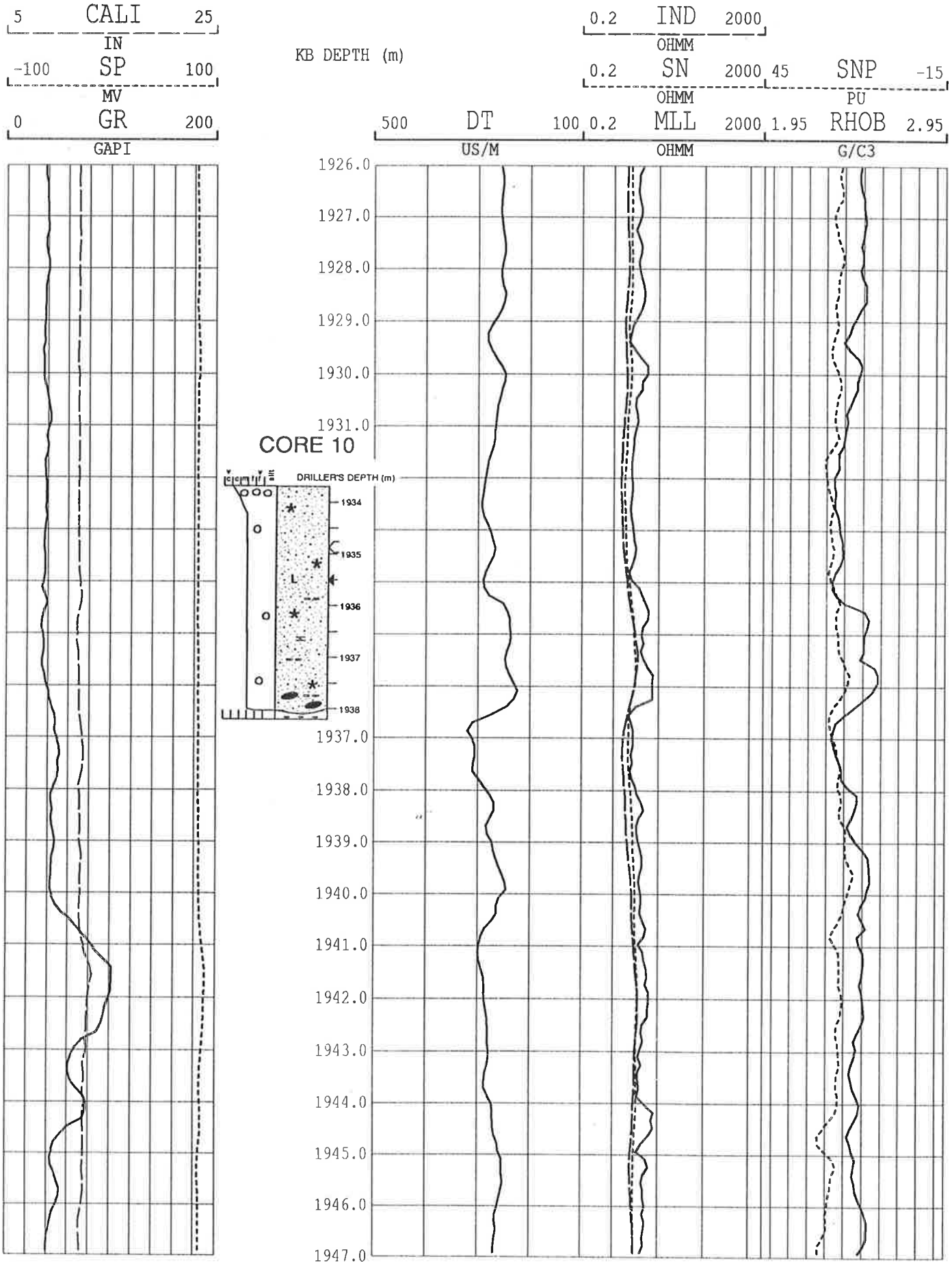
DAMPIER_1


5 CALI 25
IN
-100 SP 100
MV
0 GR 200
GAPI
KB DEPTH (m)
0.2 IND 2000
OHMM
0.2 SN 2000
OHMM
45 SNP -15
PU
500 DT 100
US/M
0.2 MLL 2000
OHMM
1.95 RHOB 2.95
G/C3
4128.0
4129.0
4130.0
4131.0
4132.0
4133.0
4134.0
4135.0
4142.0
4143.0
4144.0
CORE 16
DRILLER'S DEPTH (m)
4135
4136
4137
4138
4139
4140

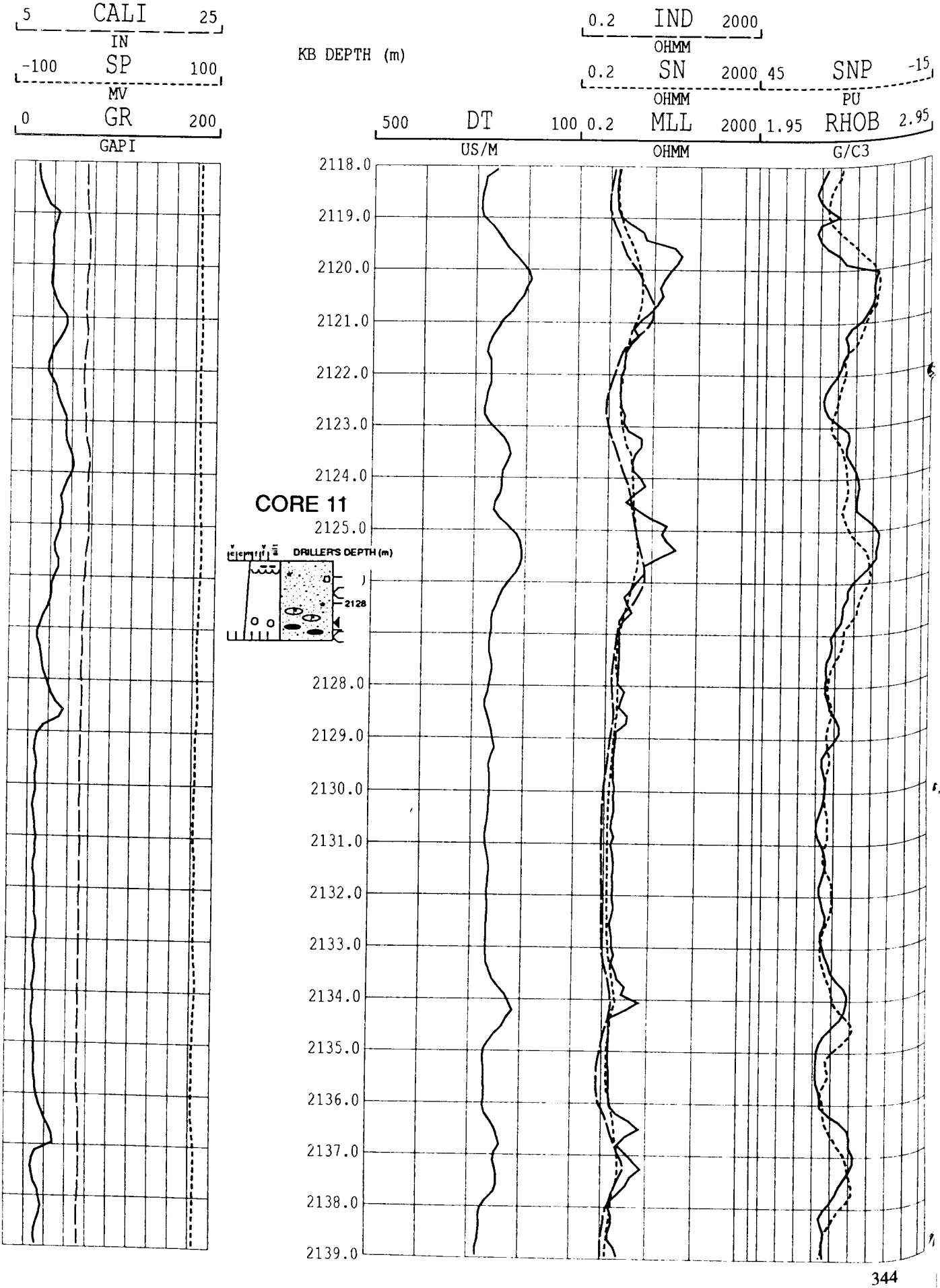
LAMBERT_1


5 CALI 25
CM
-100 SP 100
MV
0 GR 200
GAPI
KB DEPTH (m)
0.2 LLD 2000
OHMM
0.2 LLS 2000
OHMM
45 NPHI -15
PU
500 DT 100
US/M
0.2 PROX 2000
OHMM
1.95 RHOB 2.95
G/C3
3097.0
3098.0
3099.0
3100.0
3101.0
3102.0
3103.0
3104.0
CORE 1
DRILLER'S DEPTH (m)
3104
3105
3106
3107
3108
3109
3111.0
3112.0
3113.0
3114.0
3115.0
3116.0
3117.0
3118.0

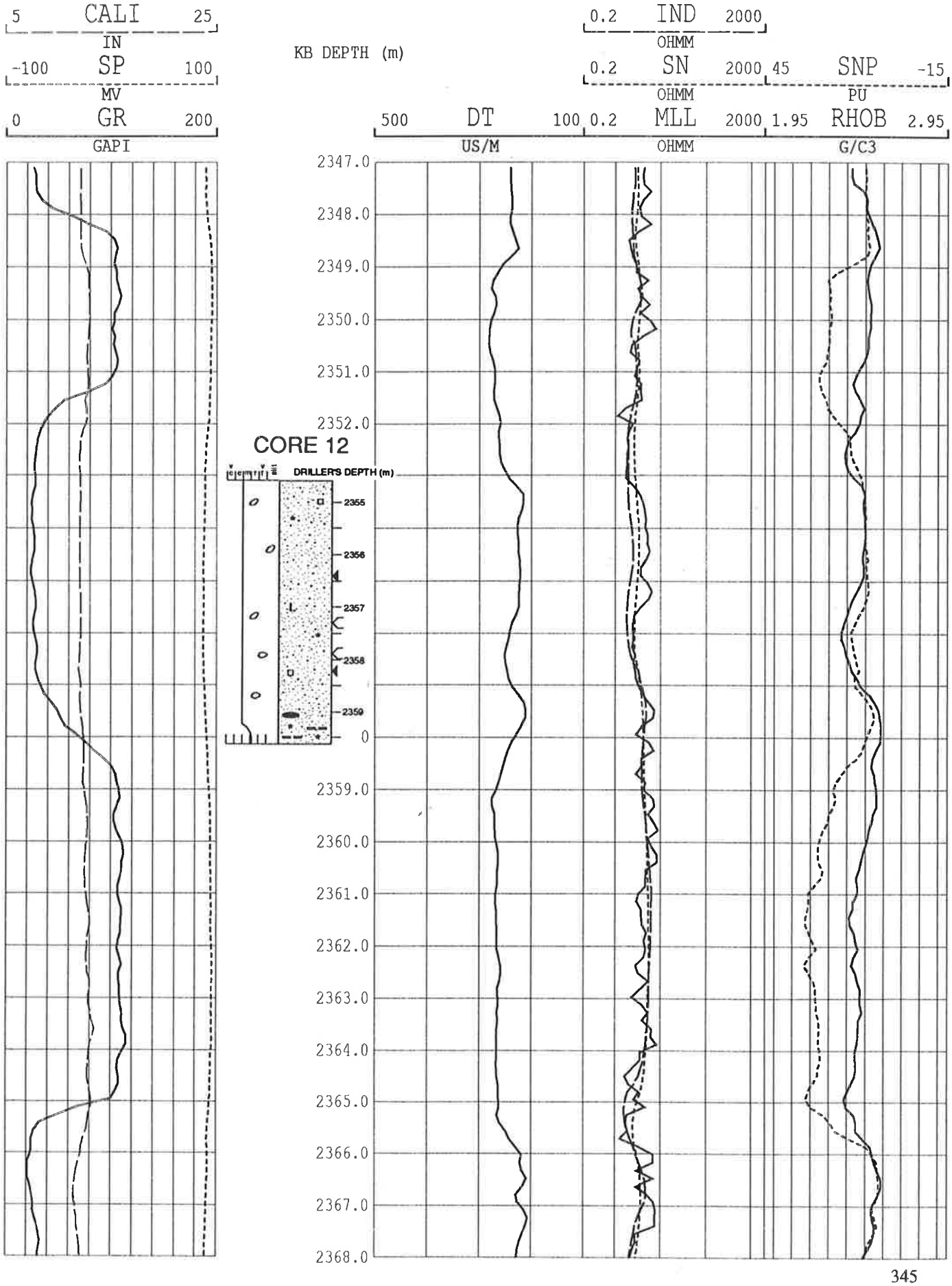
LEGENDRE_1


5 CALI 25
IN
-100 SP 100
MV
0 GR 200
GAPI
KB DEPTH (m)
0.2 IND 2000
OHMM
0.2 SN 2000
OHMM
45 SNP -15
PU
500 DT 100
US/M
0.2 MLL 2000
OHMM
1.95 RHOB 2.95
G/C3
1926.0
1927.0
1928.0
1929.0
1930.0
1931.0
CORE 10
DRILLER'S DEPTH (m)
1934
1935
1936
1937
1938
1937.0
1938.0
1939.0
1940.0
1941.0
1942.0
1943.0
1944.0
1945.0
1946.0
1947.0

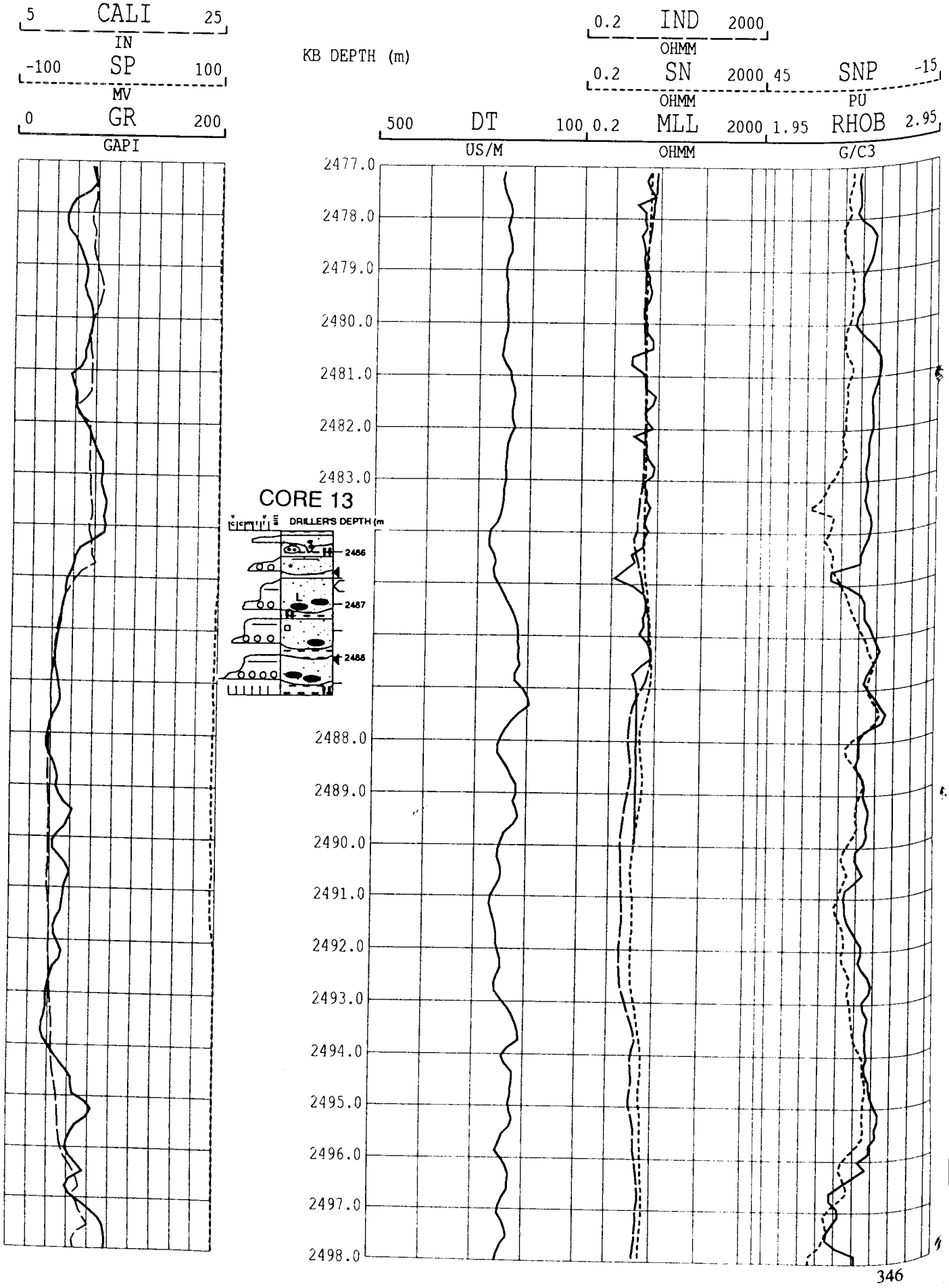
LEGENDRE_1


5 CALI 25
IN
-100 SP 100
MV
0 GR 200
GAPI
KB DEPTH (m)
0.2 IND 2000
OHMM
0.2 SN 2000 45 SNP -15
OHMM PU
500 DT 100 0.2 MLL 2000 1.95 RHOB 2.95
US/M OHMM G/C3
2118.0
2119.0
2120.0
2121.0
2122.0
2123.0
2124.0
2125.0
2128.0
2129.0
2130.0
2131.0
2132.0
2133.0
2134.0
2135.0
2136.0
2137.0
2138.0
2139.0
CORE 11
DRILLER'S DEPTH (m)
2128

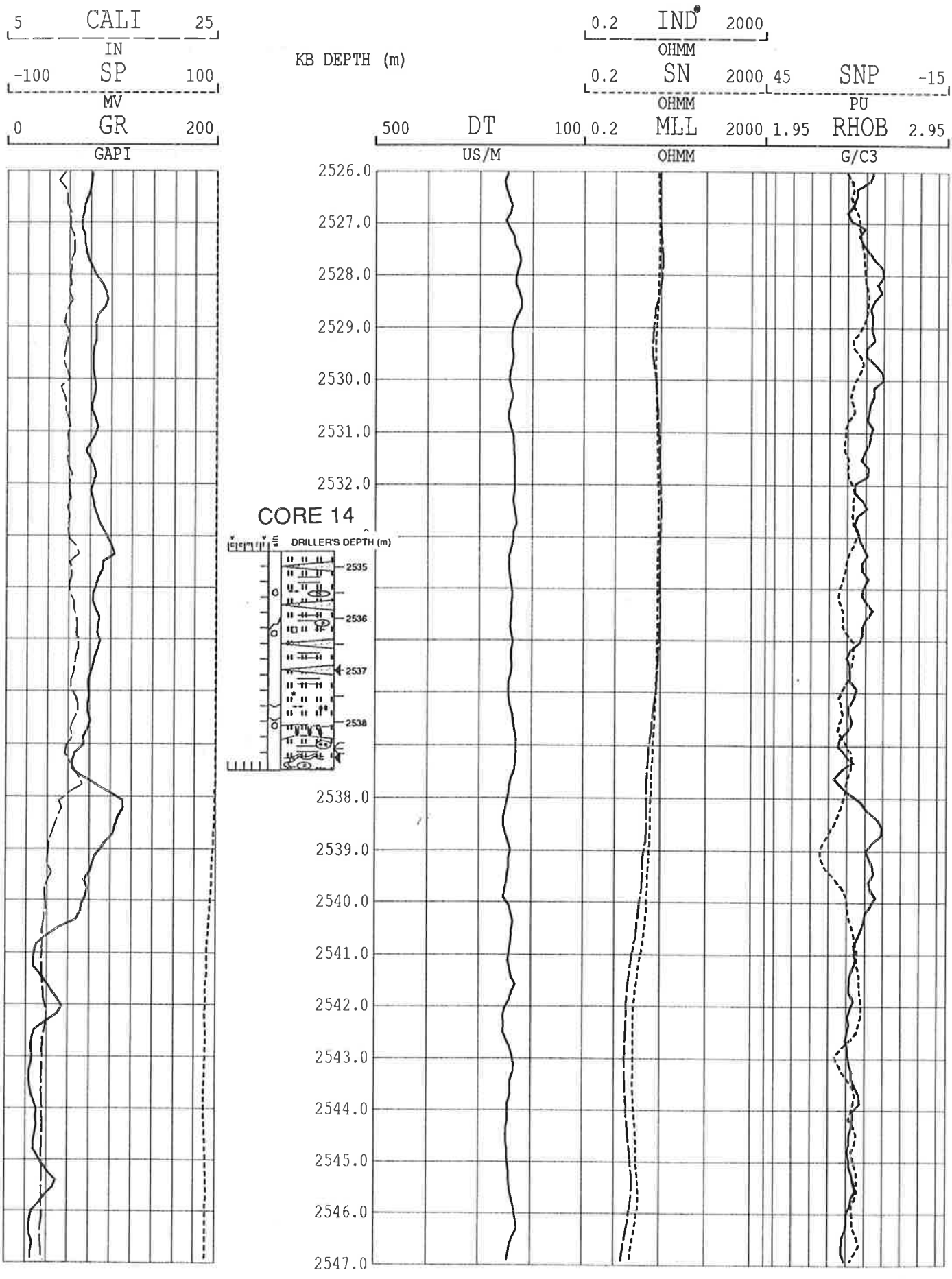
LEGENDRE_1


5 CALI 25
IN
-100 SP 100
MV
0 GR 200
GAPI
KB DEPTH (m)
0.2 IND 2000
OHMM
0.2 SN 2000
OHMM
45 SNP -15
PU
500 DT 100
US/M
0.2 MLL 2000
OHMM
1.95 RHOB 2.95
G/C3
2347.0
2348.0
2349.0
2350.0
2351.0
2352.0
CORE 12
DRILLER'S DEPTH (m)
2355
2356
2357
2358
2359
0
2359.0
2360.0
2361.0
2362.0
2363.0
2364.0
2365.0
2366.0
2367.0
2368.0

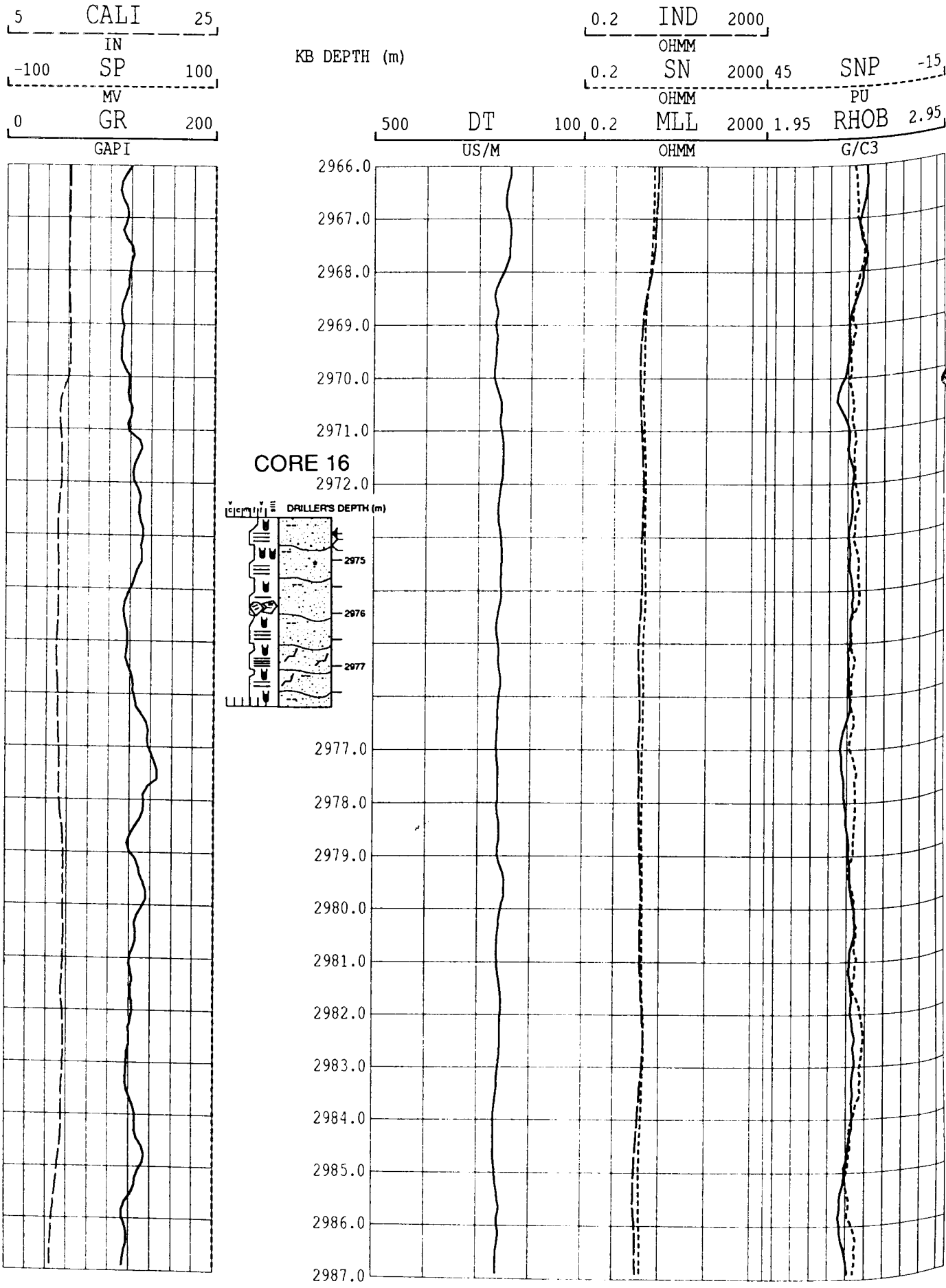
LEGENDRE_1


5 CALI 25
IN
-100 SP 100
MV
0 GR 200
GAPI
KB DEPTH (m)
0.2 IND 2000
OHMM
0.2 SN 2000 45 SNP -15
OHMM PU
500 DT 100 0.2 MLL 2000 1.95 RHOB 2.95
US/M OHMM G/C3
2477.0
2478.0
2479.0
2480.0
2481.0
2482.0
2483.0
CORE 13
DRILLER'S DEPTH (m
2486
2487
2488
2488.0
2489.0
2490.0
2491.0
2492.0
2493.0
2494.0
2495.0
2496.0
2497.0
2498.0

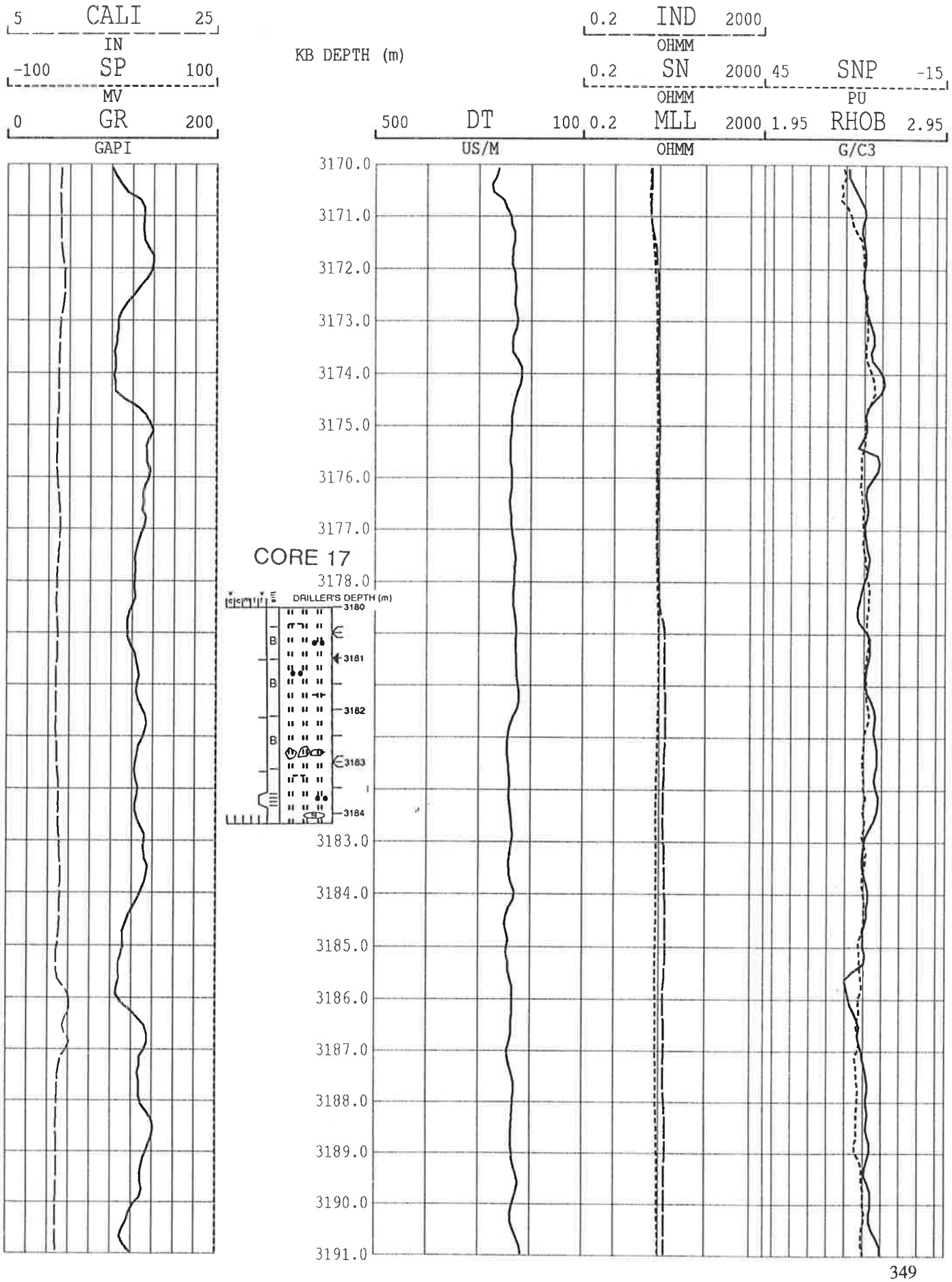
LEGENDRE_1


5 CALI 25
IN
-100 SP 100
MV
0 GR 200
GAPI
KB DEPTH (m)
0.2 IND 2000
OHMM
0.2 SN 2000
OHMM
45 SNP -15
PU
500 DT 100
US/M
0.2 MLL 2000
OHMM
1.95 RHOB 2.95
G/C3
2526.0
2527.0
2528.0
2529.0
2530.0
2531.0
2532.0
CORE 14
DRILLER'S DEPTH (m)
2535
2536
2537
2538
2538.0
2539.0
2540.0
2541.0
2542.0
2543.0
2544.0
2545.0
2546.0
2547.0

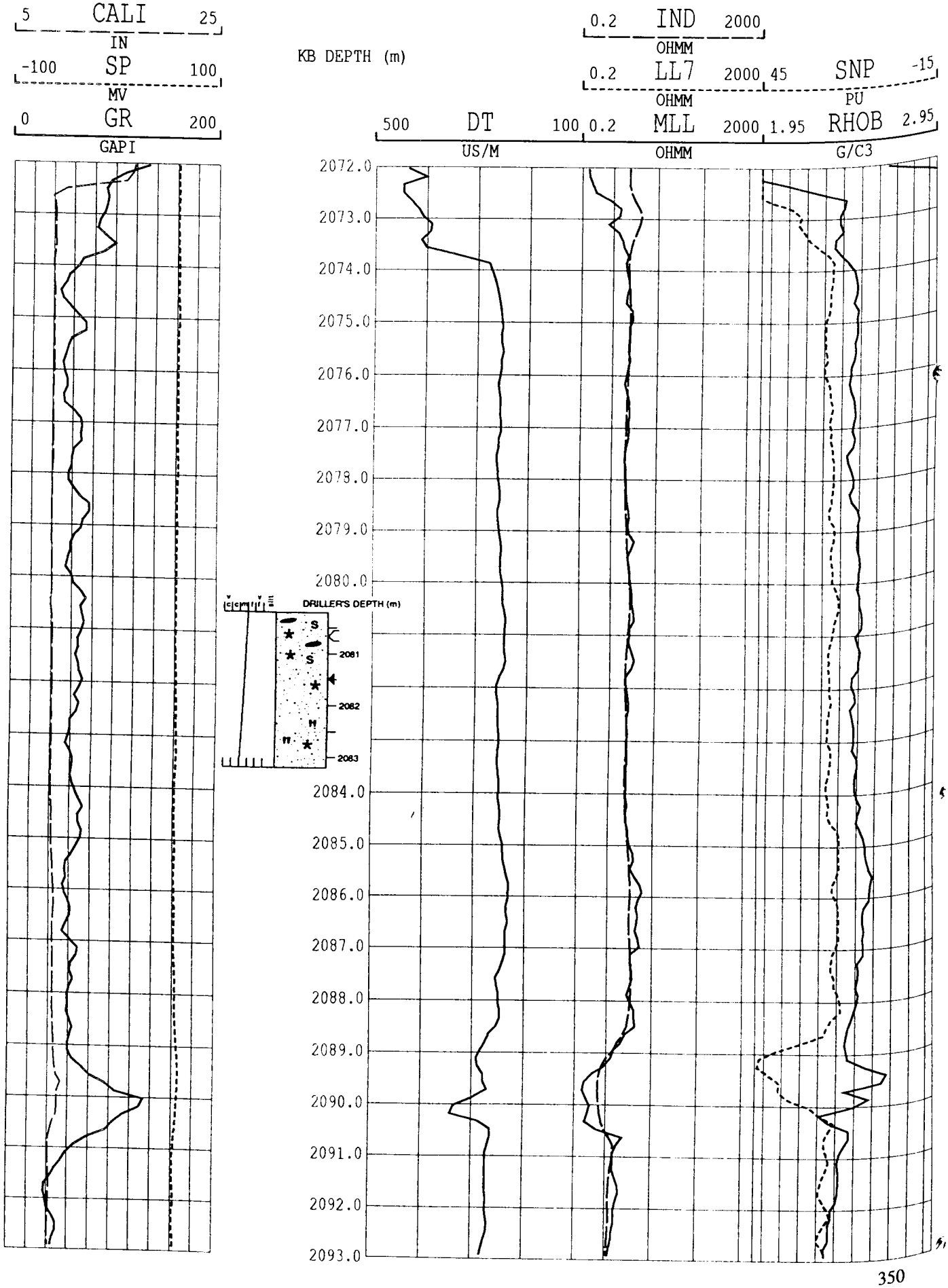
LEGENDRE_1


5 CALI 25
IN
-100 SP 100
MV
0 GR 200
GAPI
KB DEPTH (m)
0.2 IND 2000
OHMM
0.2 SN 2000
OHMM
45 SNP -15
PU
500 DT 100
US/M
0.2 MLL 2000
OHMM
1.95 RHOB 2.95
G/C3
2966.0
2967.0
2968.0
2969.0
2970.0
2971.0
CORE 16
2972.0
DRILLER'S DEPTH (m)
2975
2976
2977
2977.0
2978.0
2979.0
2980.0
2981.0
2982.0
2983.0
2984.0
2985.0
2986.0
2987.0

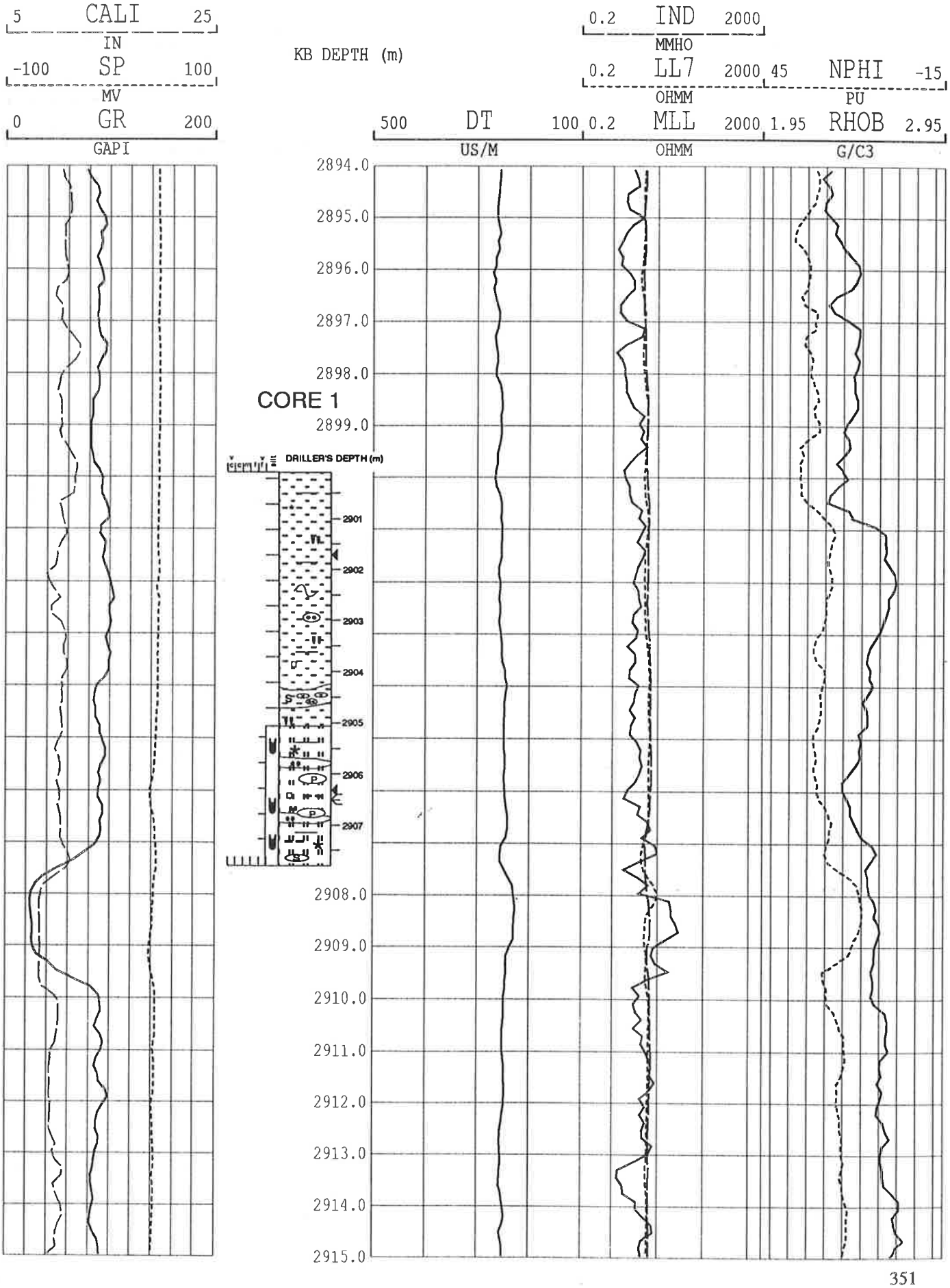
LEGENDRE_1


5 CALI 25
IN
-100 SP 100
MV
0 GR 200
GAPI
KB DEPTH (m)
0.2 IND 2000
OHMM
0.2 SN 2000
OHMM
45 SNP -15
PU
500 DT 100
US/M
0.2 MLL 2000
OHMM
1.95 RHOB 2.95
G/C3
3170.0
3171.0
3172.0
3173.0
3174.0
3175.0
3176.0
3177.0
CORE 17
3178.0
DRILLER'S DEPTH (m)
3180
3181
3182
3183
3184
3183.0
3184.0
3185.0
3186.0
3187.0
3188.0
3189.0
3190.0
3191.0

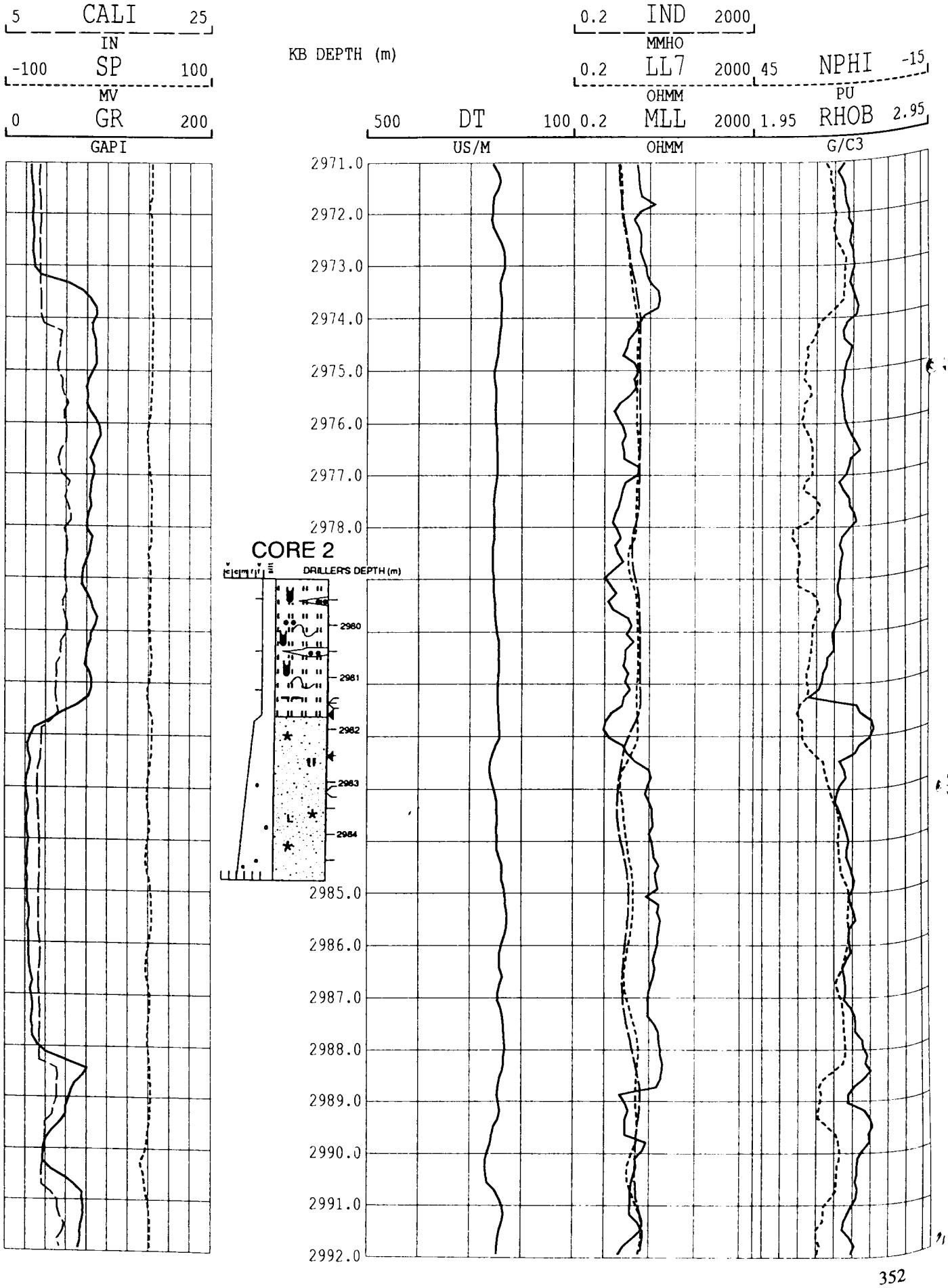
LEGENDRE_2


5 CALI 25
IN
-100 SP 100
MV
0 GR 200
GAPI
KB DEPTH (m)
0.2 IND 2000
OHMM
0.2 LL7 2000
OHMM
45 SNP -15
PU
500 DT 100
US/M
0.2 MLL 2000
OHMM
1.95 RHOB 2.95
G/C3
2072.0
2073.0
2074.0
2075.0
2076.0
2077.0
2078.0
2079.0
2080.0
2084.0
2085.0
2086.0
2087.0
2088.0
2089.0
2090.0
2091.0
2092.0
2093.0
DRILLER'S DEPTH (m)
2081
2082
2083

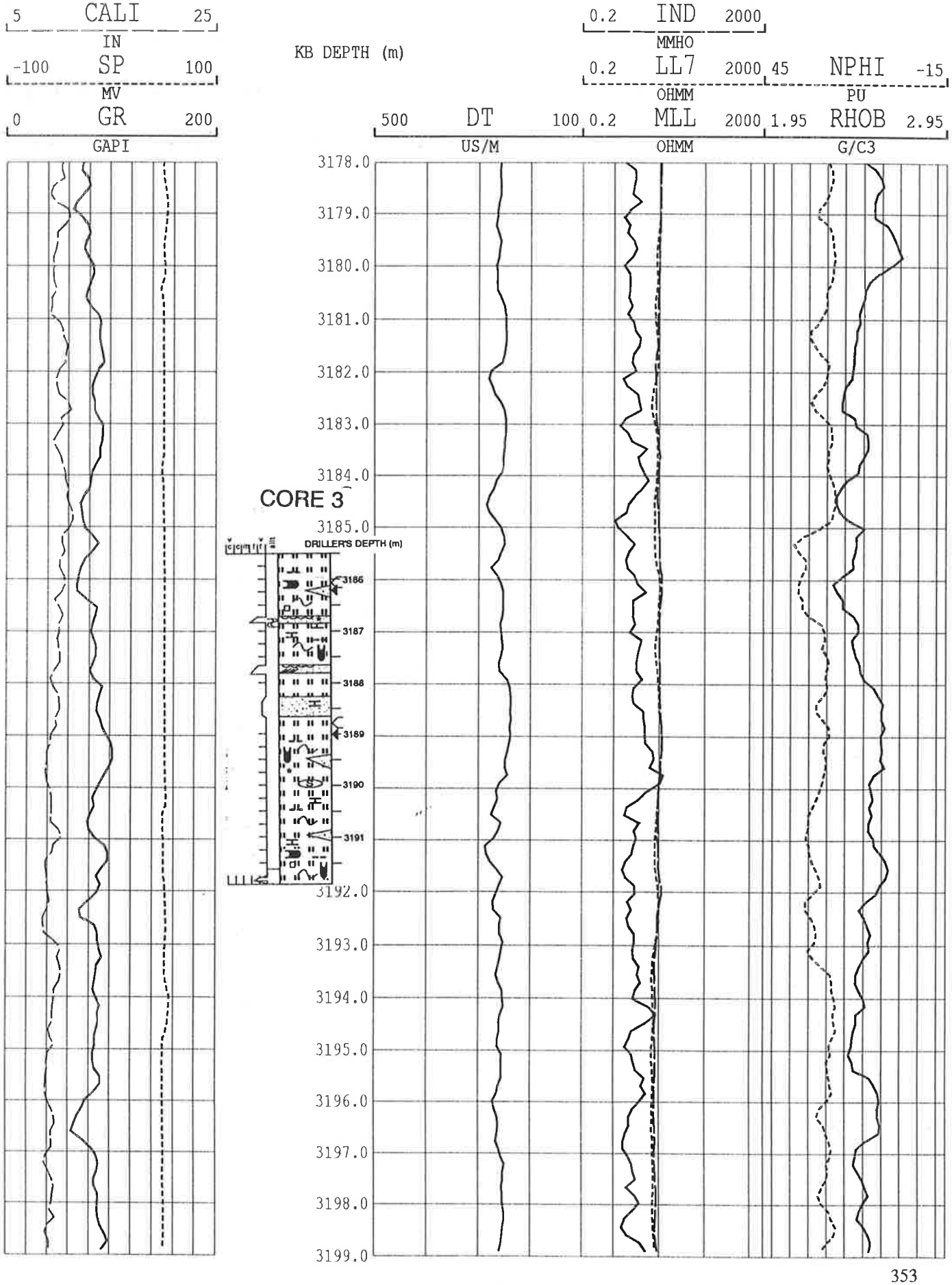
MADELEINE_1


5 CALI 25
IN
-100 SP 100
MV
0 GR 200
GAPI
KB DEPTH (m)
0.2 IND 2000
MMHO
0.2 LL7 2000
OHMM
45 NPHI -15
PU
500 DT 100
US/M
0.2 MLL 2000
OHMM
1.95 RHOB 2.95
G/C3
2894.0
2895.0
2896.0
2897.0
2898.0
CORE 1
2899.0
DRILLER'S DEPTH (m)
2901
2902
2903
2904
2905
2906
2907
2908.0
2909.0
2910.0
2911.0
2912.0
2913.0
2914.0
2915.0

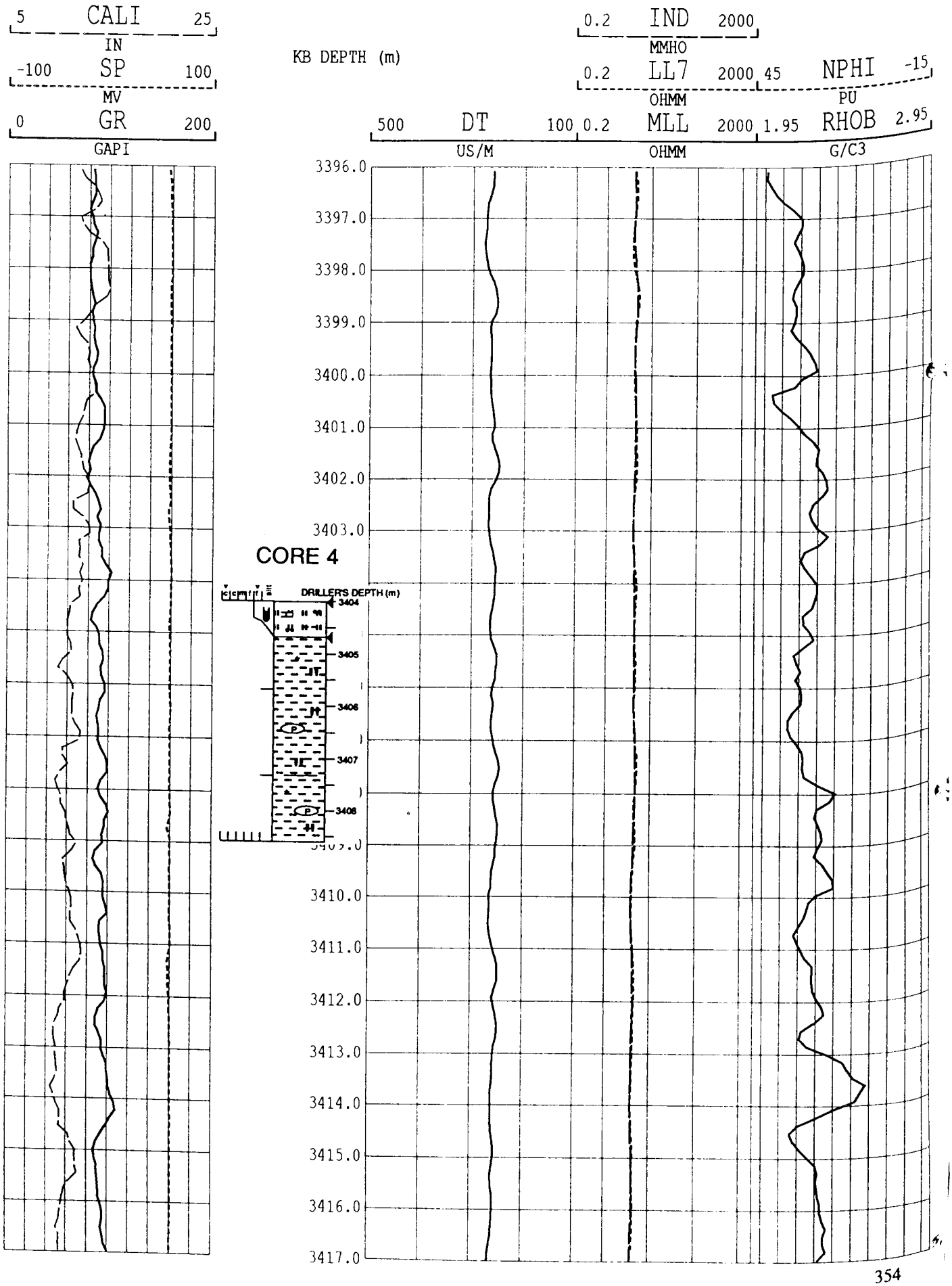
MADELEINE_1


5 CALI 25
IN
-100 SP 100
MV
0 GR 200
GAPI
KB DEPTH (m)
0.2 IND 2000
MMHO
0.2 LL7 2000
OHMM
45 NPHI -15
PU
500 DT 100
US/M
0.2 MLL 2000
OHMM
1.95 RHOB 2.95
G/C3
2971.0
2972.0
2973.0
2974.0
2975.0
2976.0
2977.0
2978.0
2985.0
2986.0
2987.0
2988.0
2989.0
2990.0
2991.0
2992.0
CORE 2
DRILLER'S DEPTH (m)
2980
2981
2982
2983
2984

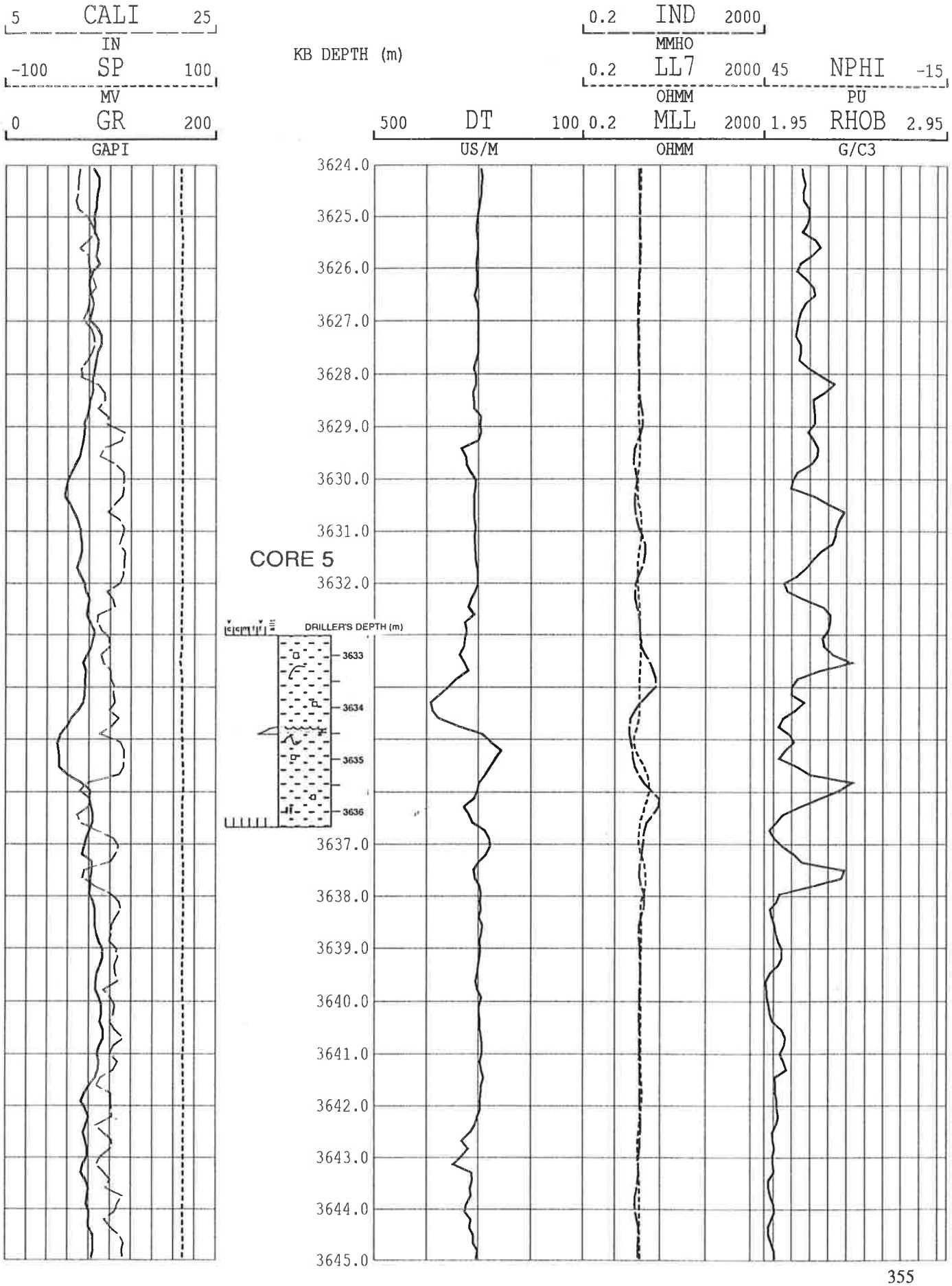
MADELEINE 1


5 CALI 25
IN
-100 SP 100
MV
0 GR 200
GAPI
KB DEPTH (m)
0.2 IND 2000
MMHO
0.2 LL7 2000
OHMM
45 NPHI -15
PU
500 DT 100
US/M
0.2 MLL 2000
OHMM
1.95 RHOB 2.95
G/C3
3178.0
3179.0
3180.0
3181.0
3182.0
3183.0
3184.0
3185.0
3192.0
3193.0
3194.0
3195.0
3196.0
3197.0
3198.0
3199.0
CORE 3
DRILLER'S DEPTH (m)
3186
3187
3188
3189
3190
3191

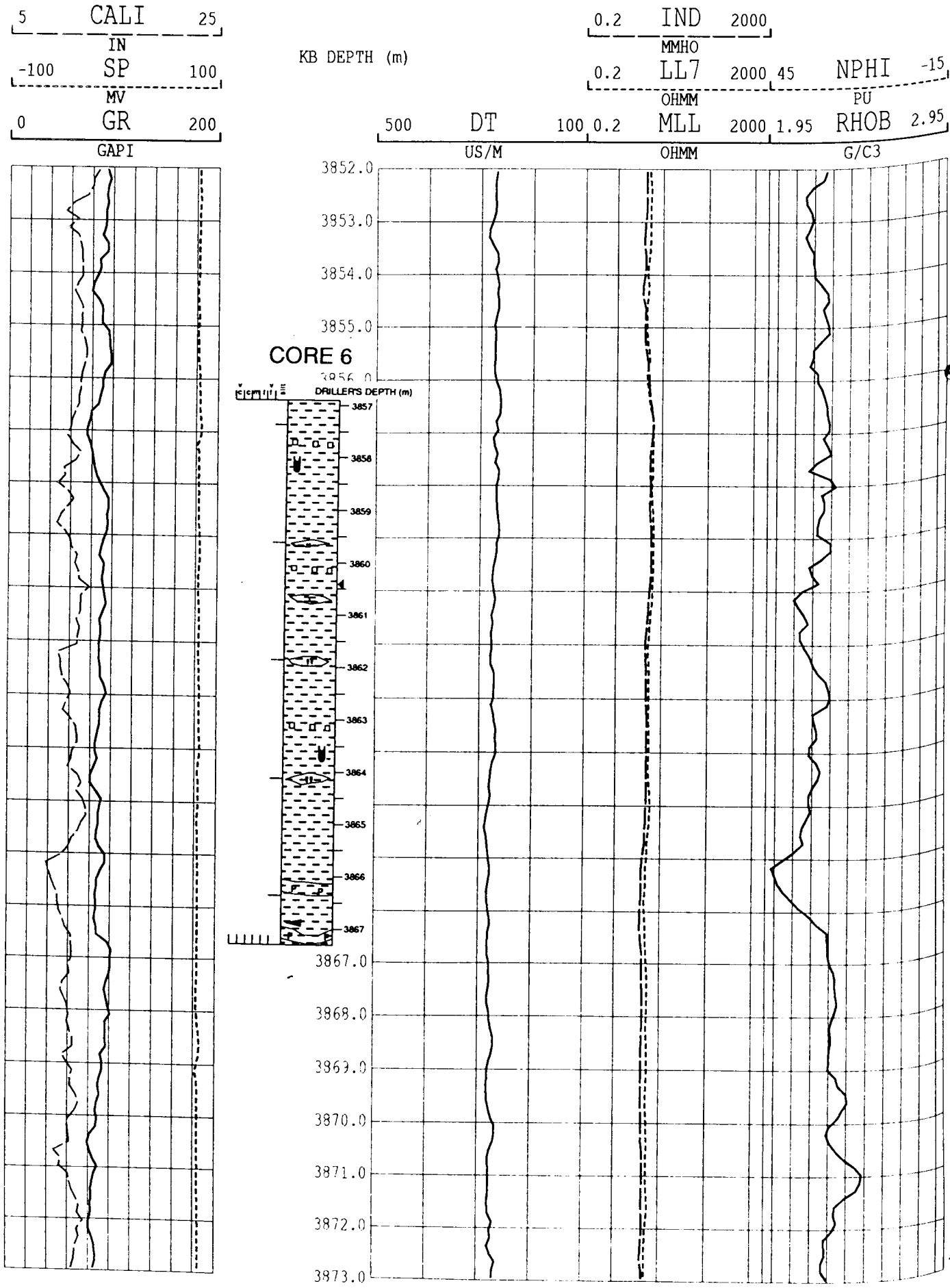
MADELEINE_1


5 CALI 25
IN
-100 SP 100
MV
0 GR 200
GAPI
KB DEPTH (m)
0.2 IND 2000
MMHO
0.2 LL7 2000
OHMM
45 NPHI -15
PU
500 DT 100
US/M
0.2 MLL 2000
OHMM
1.95 RHOB 2.95
G/C3
3396.0
3397.0
3398.0
3399.0
3400.0
3401.0
3402.0
3403.0
CORE 4
DRILLER'S DEPTH (m)
3404
3405
3406
3407
3408
3410.0
3411.0
3412.0
3413.0
3414.0
3415.0
3416.0
3417.0

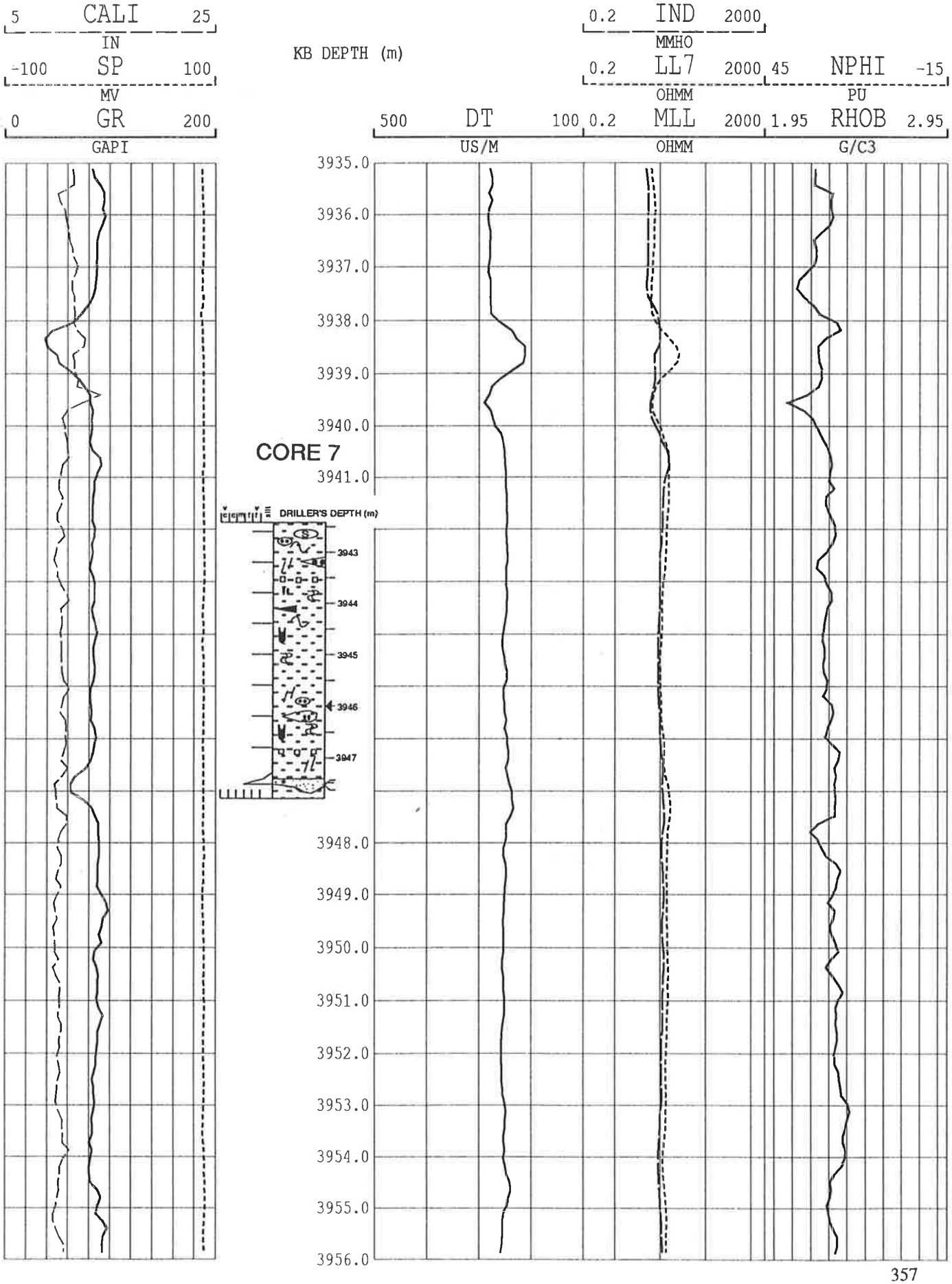
MADELEINE_1


5 CALI 25
IN
-100 SP 100
MV
0 GR 200
GAPI
KB DEPTH (m)
0.2 IND 2000
MMHO
0.2 LL7 2000
OHMM
45 NPHI -15
PU
500 DT 100
US/M
0.2 MLL 2000
OHMM
1.95 RHOB 2.95
G/C3
3624.0
3625.0
3626.0
3627.0
3628.0
3629.0
3630.0
3631.0
CORE 5
3632.0
DRILLER'S DEPTH (m)
3633
3634
3635
3636
3637.0
3638.0
3639.0
3640.0
3641.0
3642.0
3643.0
3644.0
3645.0

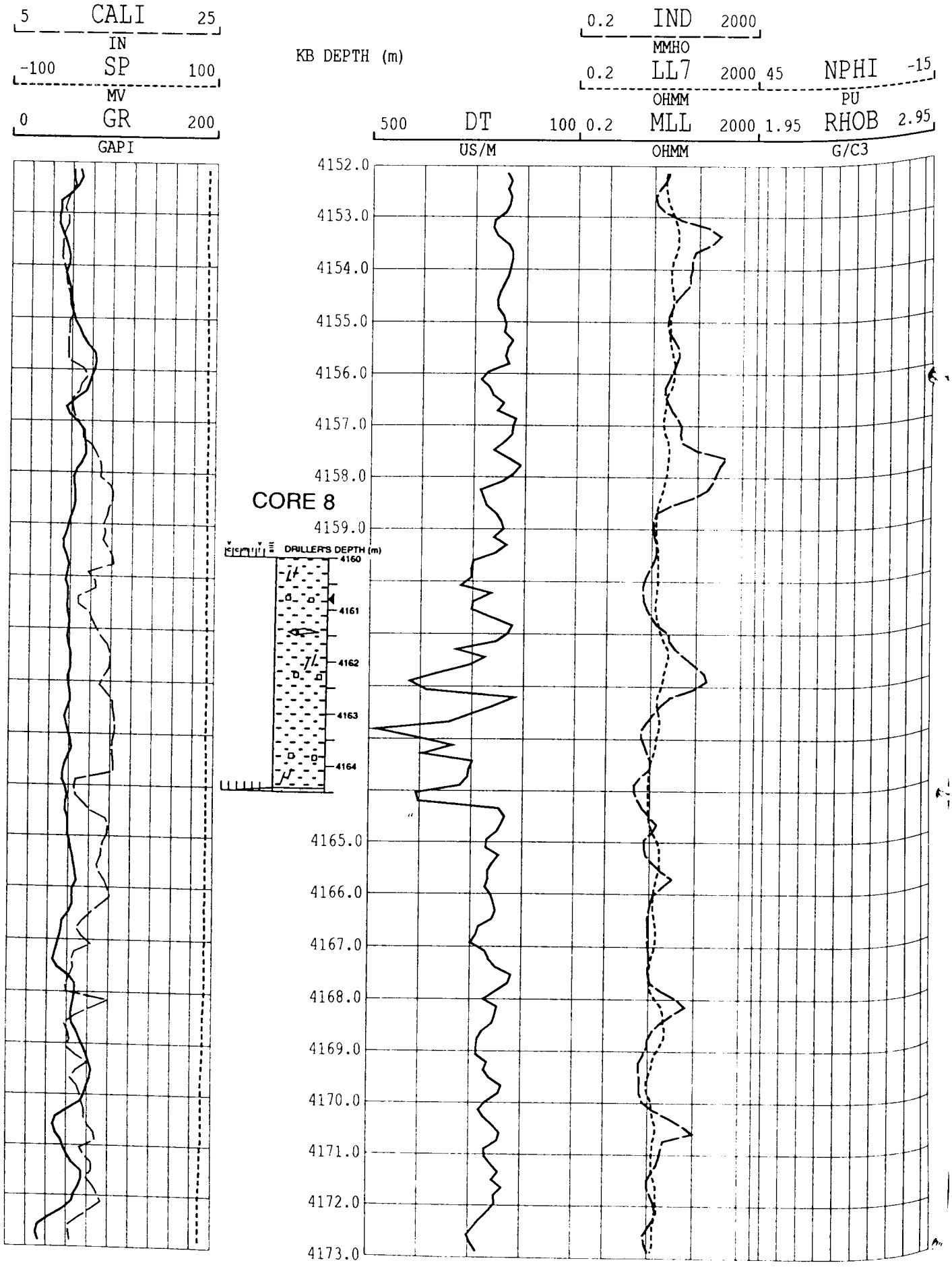
MADELEINE_1


5 CALI 25
IN
-100 SP 100
MV
0 GR 200
GAPI
KB DEPTH (m)
0.2 IND 2000
MMHO
0.2 LL7 2000
OHMM
45 NPHI -15
PU
500 DT 100
US/M
0.2 MLL 2000
OHMM
1.95 RHOB 2.95
G/C3
CORE 6
DRILLER'S DEPTH (m)
3852.0
3853.0
3854.0
3855.0
3856.0
3857
3858
3859
3860
3861
3862
3863
3864
3865
3866
3867
3867.0
3868.0
3869.0
3870.0
3871.0
3872.0
3873.0

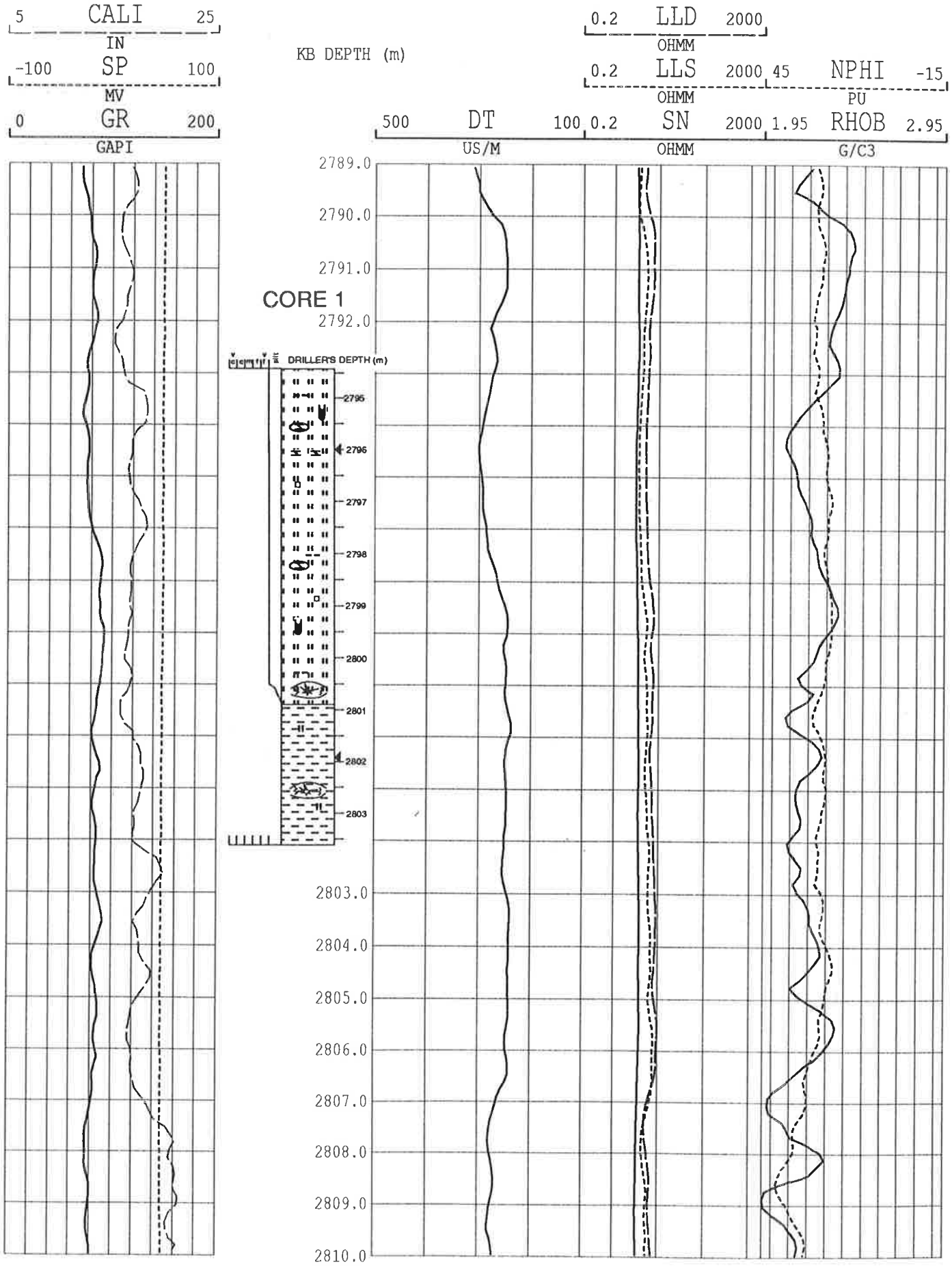
MADELEINE_1


5 CALI 25
IN
-100 SP 100
MV
0 GR 200
GAPI
KB DEPTH (m)
0.2 IND 2000
MMHO
0.2 LL7 2000
OHMM
45 NPHI -15
PU
500 DT 100
US/M
0.2 MLL 2000
OHMM
1.95 RHOB 2.95
G/C3
3935.0
3936.0
3937.0
3938.0
3939.0
3940.0
CORE 7
3941.0
DRILLER'S DEPTH (m)
3943
3944
3945
3946
3947
3948.0
3949.0
3950.0
3951.0
3952.0
3953.0
3954.0
3955.0
3956.0

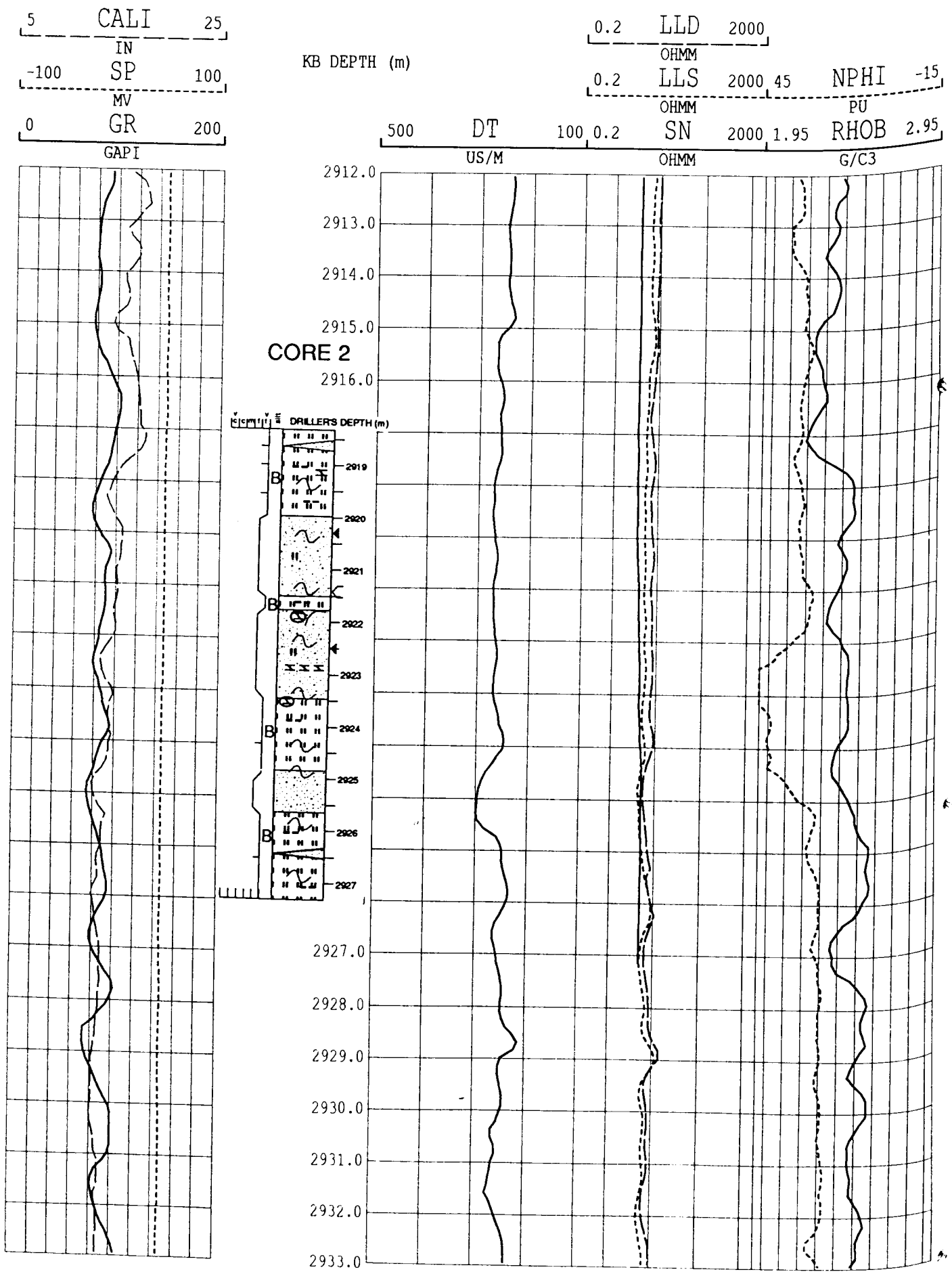
MADELEINE_1


5 CALI 25
IN
-100 SP 100
MV
0 GR 200
GAPI
KB DEPTH (m)
0.2 IND 2000
MMHO
0.2 LL7 2000
45 NPHI -15
OHMM
PU
500 DT 100
0.2 MLL 2000
1.95 RHOB 2.95
US/M
OHMM
G/C3
4152.0
4153.0
4154.0
4155.0
4156.0
4157.0
4158.0
CORE 8
4159.0
DRILLER'S DEPTH (m)
4160
4161
4162
4163
4164
4165.0
4166.0
4167.0
4168.0
4169.0
4170.0
4171.0
4172.0
4173.0

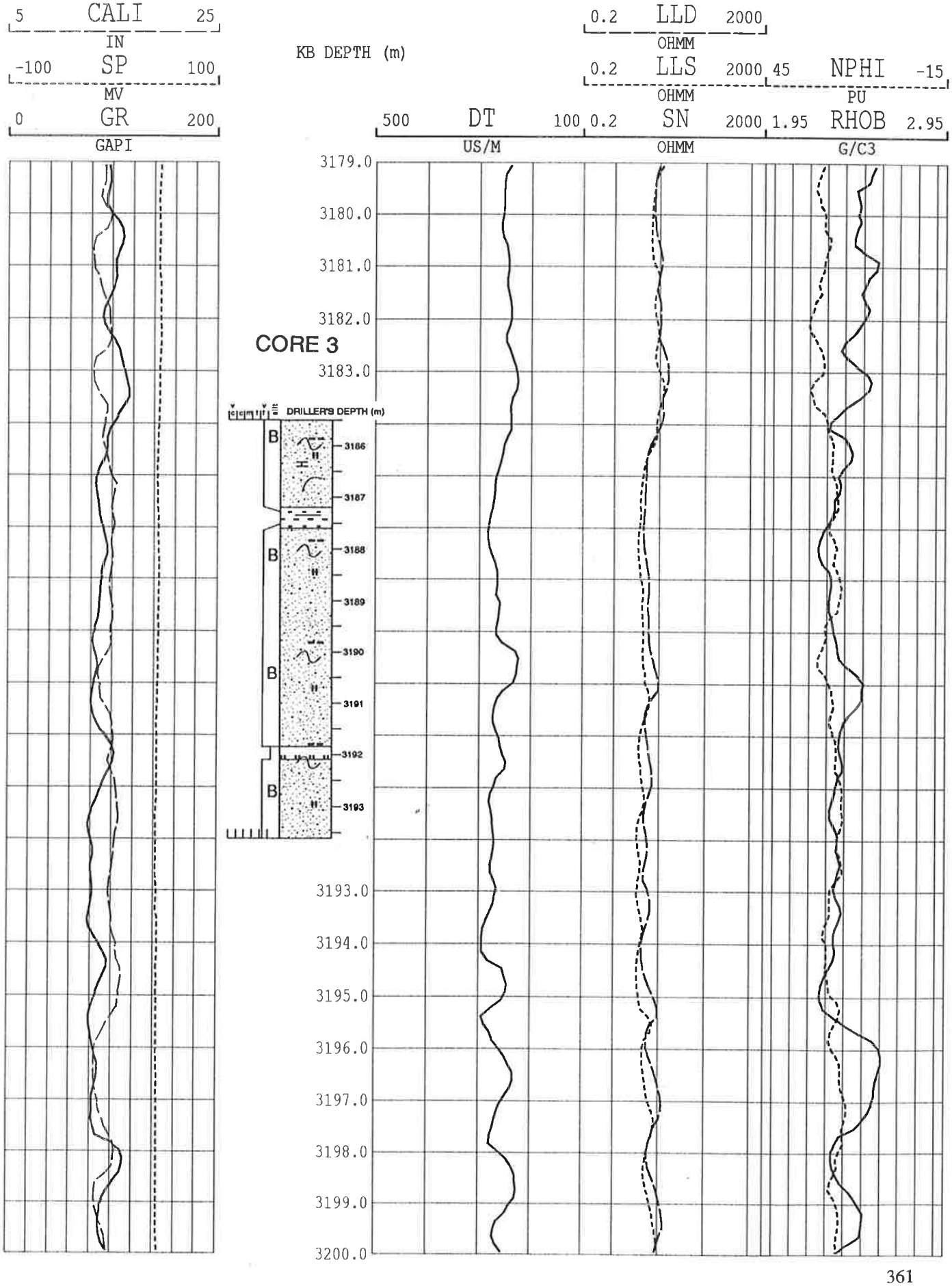
ROSEMARY_1


5 CALI 25
IN
-100 SP 100
MV
0 GR 200
GAPI
KB DEPTH (m)
0.2 LLD 2000
OHMM
0.2 LLS 2000
OHMM
45 NPHI -15
PU
500 DT 100
US/M
0.2 SN 2000
OHMM
1.95 RHOB 2.95
G/C3
2789.0
2790.0
2791.0
CORE 1
2792.0
DRILLER'S DEPTH (m)
2795
2796
2797
2798
2799
2800
2801
2802
2803
2803.0
2804.0
2805.0
2806.0
2807.0
2808.0
2809.0
2810.0

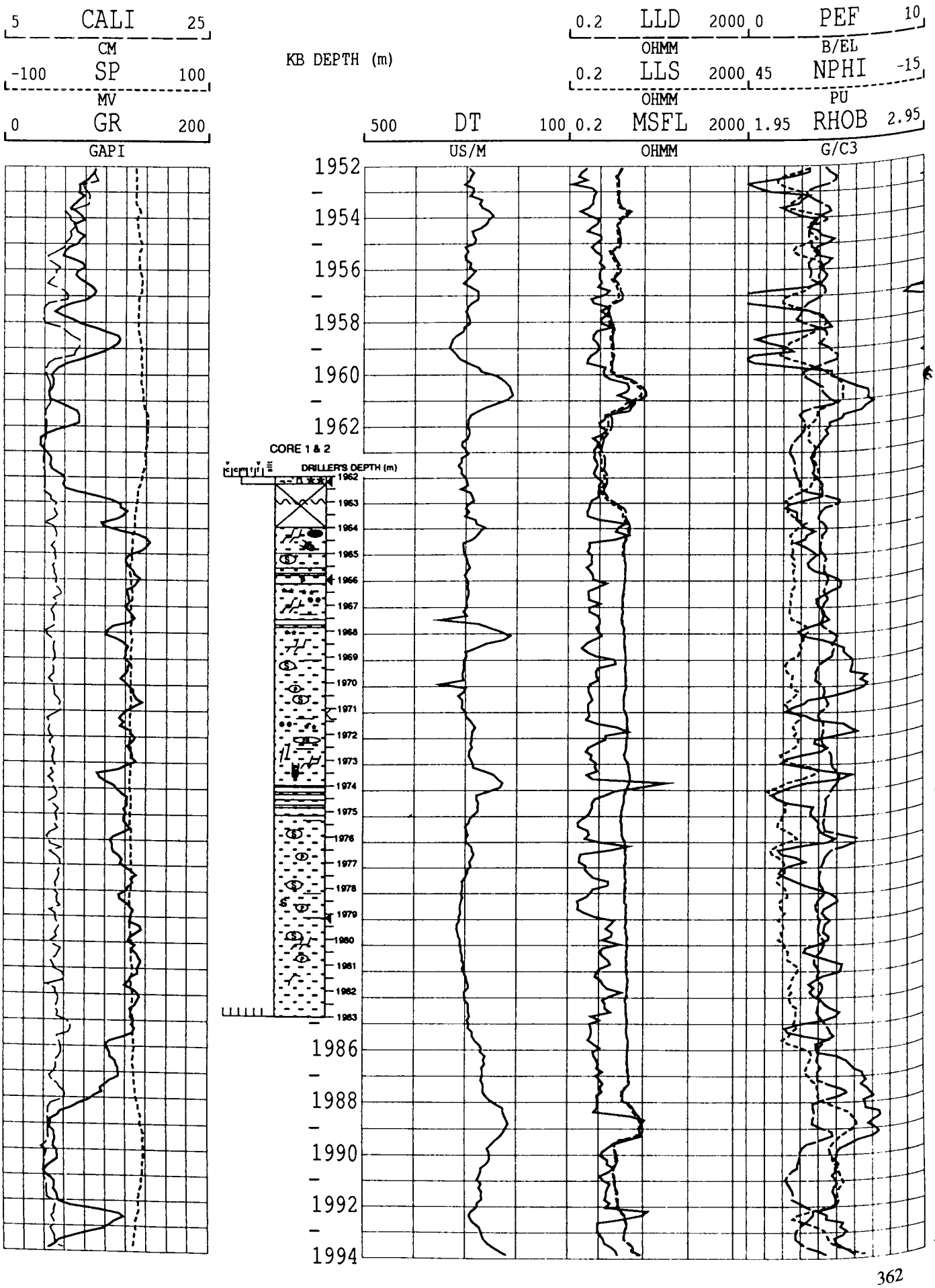
ROSEMARY 1


5 CALI 25
IN
-100 SP 100
MV
0 GR 200
GAPI
KB DEPTH (m)
0.2 LLD 2000
OHMM
0.2 LLS 2000
OHMM
45 NPHI -15
PU
500 DT 100
US/M
0.2 SN 2000
OHMM
1.95 RHOB 2.95
G/C3
2912.0
2913.0
2914.0
2915.0
CORE 2
2916.0
DRILLER'S DEPTH (m)
2919
2920
2921
2922
2923
2924
2925
2926
2927
2927.0
2928.0
2929.0
2930.0
2931.0
2932.0
2933.0

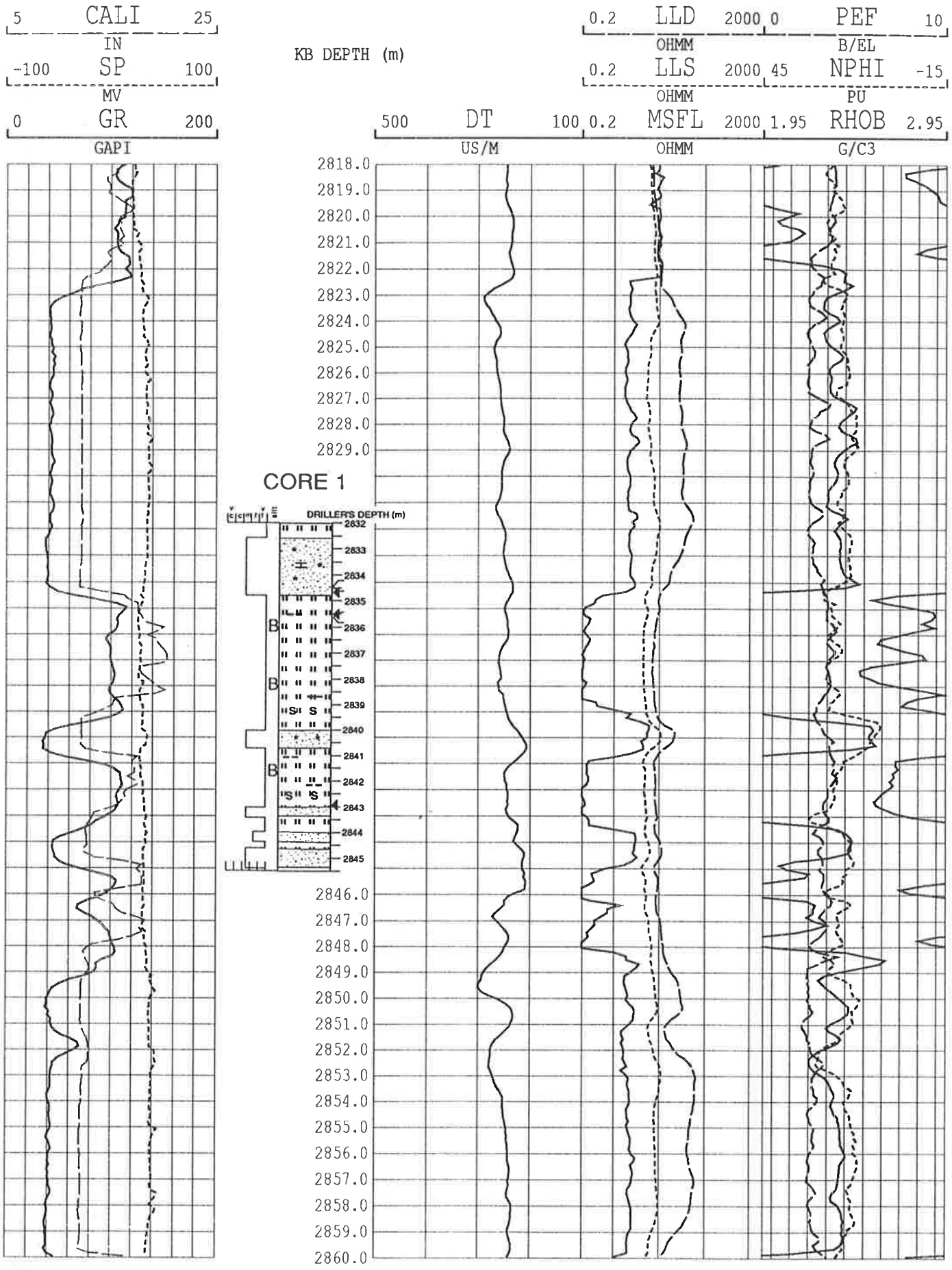
ROSEMARY 1


5 CALI 25
IN
-100 SP 100
MV
0 GR 200
GAPI
KB DEPTH (m)
0.2 LLD 2000
OHMM
0.2 LLS 2000
OHMM
45 NPHI -15
PU
500 DT 100
US/M
0.2 SN 2000
OHMM
1.95 RHOB 2.95
G/C3
3179.0
3180.0
3181.0
3182.0
3183.0
3193.0
3194.0
3195.0
3196.0
3197.0
3198.0
3199.0
3200.0
CORE 3
DRILLER'S DEPTH (m)
B
3186
3187
3188
3189
3190
3191
3192
3193

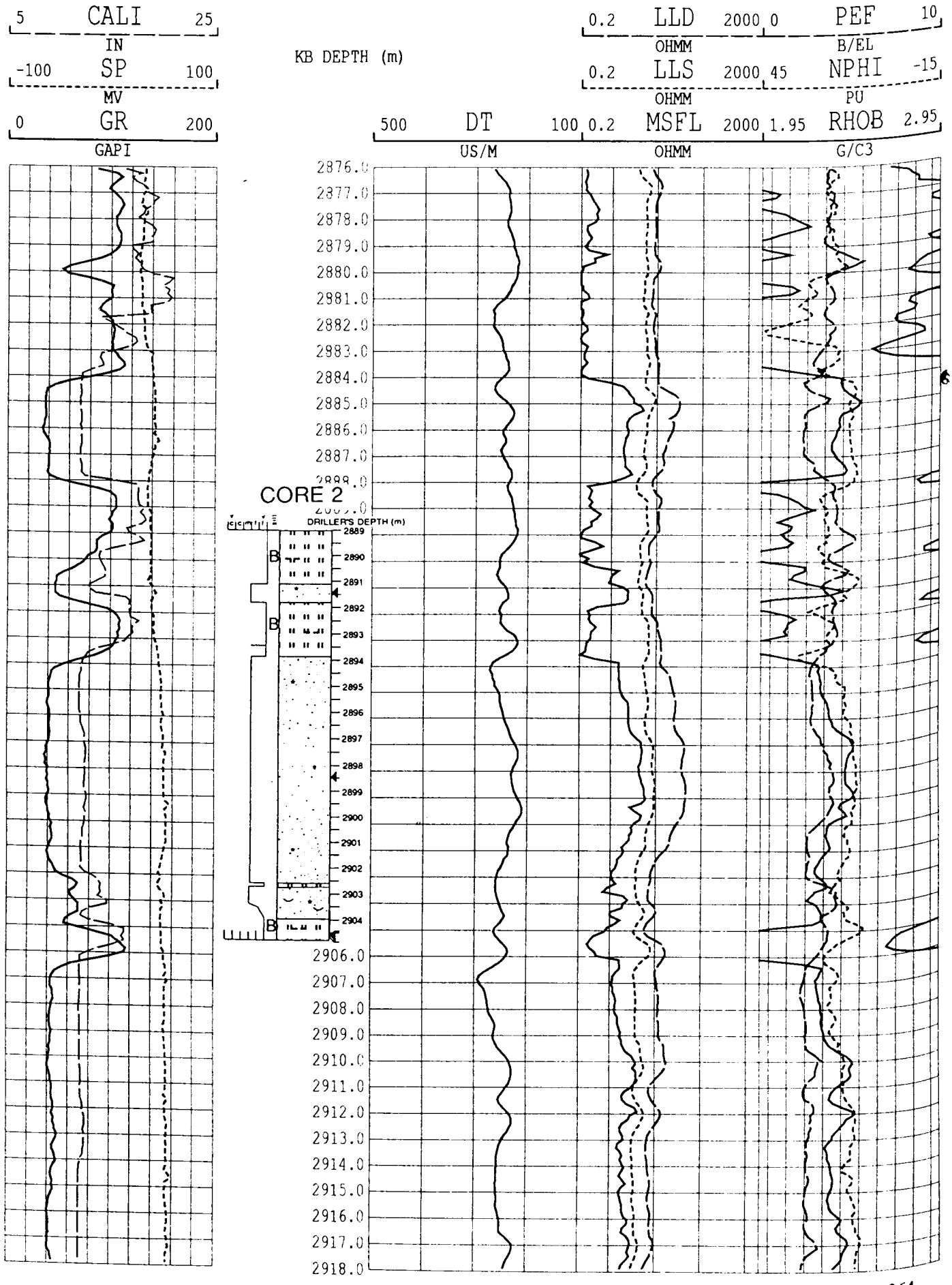
TALISMAN_3


5 CALI 25
CM
-100 SP 100
MV
0 GR 200
GAPI
KB DEPTH (m)
0.2 LLD 2000 0 PEF 10
OHMM B/EL
0.2 LLS 2000 45 NPHI -15
OHMM PU
500 DT 100 0.2 MSFL 2000 1.95 RHOB 2.95
US/M OHMM G/C3
1952
1954
1956
1958
1960
1962
CORE 1 & 2
DRILLER'S DEPTH (m)
1962
1963
1964
1965
1966
1967
1968
1969
1970
1971
1972
1973
1974
1975
1976
1977
1978
1979
1980
1981
1982
1983
1986
1988
1990
1992
1994

WANAEA_1


5 CALI 25
IN
-100 SP 100
MV
0 GR 200
GAPI
KB DEPTH (m)
0.2 LLD 2000
OHMM
0.2 LLS 2000
OHMM
500 DT 100
US/M
0.2 MSFL 2000
OHMM
0 PEF 10
B/EL
45 NPHI -15
PU
1.95 RHOB 2.95
G/C3
2818.0
2819.0
2820.0
2821.0
2822.0
2823.0
2824.0
2825.0
2826.0
2827.0
2828.0
2829.0
CORE 1
DRILLER'S DEPTH (m)
2832
2833
2834
2835
2836
2837
2838
2839
2840
2841
2842
2843
2844
2845
B
B
B
S
S
S
S
2846.0
2847.0
2848.0
2849.0
2850.0
2851.0
2852.0
2853.0
2854.0
2855.0
2856.0
2857.0
2858.0
2859.0
2860.0

WANAEA_1


5 CALI 25
IN
-100 SP 100
MV
0 GR 200
GAPI
KB DEPTH (m)
0.2 LLD 2000 0 PEF 10
OHMM B/EL
0.2 LLS 2000 45 NPHI -15
OHMM PU
500 DT 100 0.2 MSFL 2000 1.95 RHOB 2.95
US/M OHMM G/C3
2876.0
2877.0
2878.0
2879.0
2880.0
2881.0
2882.0
2883.0
2884.0
2885.0
2886.0
2887.0
CORE 2
DRILLER'S DEPTH (m)
2889
2890
2891
2892
2893
2894
2895
2896
2897
2898
2899
2900
2901
2902
2903
2904
2906.0
2907.0
2908.0
2909.0
2910.0
2911.0
2912.0
2913.0
2914.0
2915.0
2916.0
2917.0
2918.0

APPENDIX III

THIN SECTION DESCRIPTIONS

Thin Section Descriptions Sample List

1. Angel 1	Core 1	2666.1m
2. Angel 2	Core 1	2704.5m
3. Finucane 1	Ditch Cuttings	2950m
4. Forestier 1	Ditch Cuttings	2080m
5. Forestier 1	Ditch Cuttings	2325m
6. Hampton 1	Ditch Cuttings	550m
7. Hampton 1	Ditch Cuttings	600m
8. Lambert 1	Core 1	3108.55m
9. Legendre 1	Core 10	1935.5m
10. Legendre 1	Core 11	2128.4m
11. Legendre 2	Core 1	2081.5m
12. Madeleine 1	Core 2	2981.7m
13. Madeleine 1	Core 2	2982.5m
14. Rosemary 1	Ditch Cuttings	2225m
15. Rosemary 1	Core 2	2922.5m
16. Talisman 1	Ditch Cuttings	1920m
17. Talisman 1	Ditch Cuttings	1970m
18. Trafalgar 1	Core 1	2498m

Well: Angel 1 **Depth**: 2666.1 m **Formation**: Angel

Palynological Zone/Age: U. Tithonian **Sample Type**: core

Hand Sample Description: quartz arenite, light grey, medium - fine grained, moderately sorted, slightly glauconitic, fair intergranular porosity.

Thin Section Description:

Grain Size: bimodal - medium grained and fine - very fine grained.

Sorting: moderate.

Roundness: medium sized grains are rounded, fine grains are sub-angular

Spherocity: medium sized grains are high, fine grains are low

Extinction: (quartz) straight - 75%, undulose - 25%, composite - trace.

Mineralogy: quartz - 90%, microcline/perthite - 5%, glauconite - 5%. Accessory chert, dolomite, siderite, opaques, rare zircon.

Cement: early stage quartz overgrowths filling pores provides tangental grain contacts and a relatively open grain framework. This is etched by dolomite. Siderite stains occasionally rim quartz grains. Late stage siderite is seen by rimming dolomite. There is also minor glauconite cement.

Porosity/permeability: (core plug analysis) 19.4% porosity, 535md permeability

Rock Classification: quartz arenite

Comments:

Well: Angel 2 **Depth**: 2704.5m **Formation**: Angel

Palynological Zone: P.iehiense **Sample Type**: core

Hand Sample Description: quartz arenite, fine grained, white spotty texture (dolomite ?), red-brown matrix, well sorted, good visual porosity between white spots.

Thin Section Description:

Grain Size: fine grained

Sorting: well sorted

Roundness: dominantly sub-angular, occasionally sub-rounded

Spherocity: generally moderate and decreases with grain size. Low Spherocity grains appear preferentially oriented.

Extinction: (quartz) straight - 70 %, undulose - 25%, composite - 5%

Mineralogy: quartz - 65%, dolomite - 20%, microcline/perthite - 10%

Cement: dolomite occurs in 50% of the matrix as poikolotopic cement, and reveals corroded quartz grains. Feldspar grains are highly dissolved in areas free of dolomite (post-dates dolomitisation). Late stage glauconitu rims some quartz grains. Non dolomitised areas have silica cement providing tangental contacts and good intergranular porosity.

Porosity/permeability: good (visual). Dolomitised areas are tight.

Rock Classification: quartz arenite

Comments:

Well: Finucane 1 **Depth**: 2950m **Formation**: Forestier Claystone

Palynological Zone/Age: C. delicata **Sample Type**: ditch cuttings

Hand Sample Description: red brown, argillaceous, white sandy wisps

Thin Section Description:

Grain Size: very fine silt, occasional coarse silt

Sorting: well sorted

Roundness: sub-angular

Sphericity:

Extinction: (quartz) undulose - 100%

Mineralogy: clay (dominantly illite, some kaolin) - 80%, quartz - 10%, feldspar - 5%, dolomite - 5%, accessory - siderite, iron oxide, disseminated pyrite, chert

Cement/diagenesis: no cement, rock is clay supported.

Porosity/permeability:

Rock Classification: claystone

Comments:

Well: Forestier 1 **Depth**: 2080m **Formation**: Talisman Member

Palynological Zone/Age: C. delicata **Sample Type**: ditch cuttings

Hand Sample Description: argillaceous quartz arenite, light brown, very coarse to medium grained, limonite (yellow) staining,

Thin Section Description:

Grain Size: fine to coarse, bimodal distribution,

Sorting: coarse grained - well sorted, fine grained - well sorted

Roundness: sub-rounded to sub-angular,

Spherocity: low to high, dominantly high, some broken grains

Extinction: (quartz) undulose - 40%, poly crystalline - 30%, straight - 30%,

Mineralogy: quartz - 60%, clay - 40%, accessory microcline, perthite, dolomite, fine grained glauconite, chert, opaques (carbonaceous matter ?), disseminated pyrite in clay matrix

Cement/diagenesis: very minor quartz cement, etched quartz grains

Porosity/permeability:

Rock Classification: muddy quartz arenite

Comments: One claystone cutting has an oxidation ring on it. This rock appears to have well reworked grains and was deposited in a muddy setting.

Well: Forestier 1 **Depth**: 2325m **Formation**: Angel

Palynological Zone/Age: O. montgomeryi **Sample Type**: ditch cuttings

Hand Sample Description: quartz arenite, white, clear, 95% sand grains, 5% claystone fragments, very coarse to medium grained, dominantly coarse, moderately sorted

Thin Section Description:

Grain Size: medium to very coarse, dominantly coarse

Sorting: well sorted

Roundness: sub-rounded to rounded

Spherocity: moderate

Extinction: (quartz) undulose - 50%, poly crystalline - 30%, straight - 20%; accessory - chert, microcline, clay (illite?)

Mineralogy: quartz - 95%, dolomite (cement) - 5%

Cement/diagenesis: no quartz cement, dolomite cement surrounds some quartz.

Porosity/permeability:

Rock Classification: quartz arenite

Comments: This rock is very clean. There is no glauconite present.

Well: Hampton 1 **Depth**: 550m **Formation**: Mardie Greensand

Palynological Zone/Age: M. australis **Sample Type**: ditch cuttings

Hand Sample Description: argillaceous quartz arenite, grey, granular to medium, dominantly medium, poorly sorted

Thin Section Description:

Grain Size: bimodal - coarse quartz, very fine quartz in argillaceous and carbonate matrix

Sorting: coarse grained - well sorted, very fine grained - well sorted

Roundness: coarse - sub-rounded to rounded (etched), very fine - sub-rounded to angular (etched)

Spherocity: high

Extinction: (quartz) coarse grained: undulose - 90%, poly crystalline - 20%; very fine grained: undulose - 90%, straight - 10%.

Mineralogy: quartz - 20% (very fine and coarse), glauconite - 20% (well rounded very fine grains), dolomite (cement, very fine crystalline) - 20%, clay (dominantly illite) 30%, siderite (cement) 10%, accessory - plagioclase, microcline, biotite, carbonaceous material; trace iron oxide.

Cement/diagenesis: dominantly dolomite cement, some siderite and iron oxide within the dolomite, late stage glauconite cement. Quartz is highly etched.

Porosity/permeability:

Rock Classification: glauconitic sandy mudstone

Comments:

Well: Hampton 1 **Depth**: 600m **Formation**: Birdrong? Member

Palynological Zone/Age: M. australis **Sample Type**: ditch cuttings

Hand Sample Description: argillaceous quartz arenite, grey, granular to medium grained, dominantly medium, poorly sorted

Thin Section Description:

Grain Size: fine to coarse, dominantly medium

Sorting: moderate

Roundness: sub-rounded to rounded, etched quartz grains

Spherocity: high

Extinction: (quartz)

Mineralogy: quartz - 70%, microcline/perthite - 10%, glauconite - 10%, dolomite (cement) - 10%; accessory - calcite, siderite, clay (dominantly illite) opaques (carbonaceous material).

Cement/diagenesis: clay matrix is being replaced by carbonate. There are carbonate cemented aggregates of grains. argillaceous matrix is silty.

Porosity/permeability:

Rock Classification: muddy arenite

Comments: Occasional point contacts of grains occur in the argillaceous matrix.

Well: Lambert 1 **Depth**: 3108.6m **Formation**: Angel

Palynological Zone/Age: P. iehiense **Sample Type**: core

Hand Sample Description: light grey and white matrix with clear quartz grains, Occasional argillaceous siltstone clast 5mm diameter, fine grained, well sorted, rounded grains, fair visual porosity.

Thin Section Description:

Grain Size: fine - coarse, dominantly fine grained

Sorting: moderate

Roundness: dominantly rounded grains,

Spherocity: high spherical quartz, decreases with grain size

Extinction: (quartz) straight - 60%, undulose - 30%, composite - 10%

Mineralogy: quartz - 75%, microcline/perthite - 15%, glauconite - 5%; accessory chert, clay; rare zircon; detrital? siderite

Cement: well cemented by early silica shown by good surface and sutured contacts of quartz grains. Edges of quartz grains are commonly corroded. Minor glauconite rims glauconite grains and nearby quartz grains. Feldspar is highly corroded. Some porosity is filled with illite. Some grains are fractured and filled with an unidentified mineral.

Porosity/permeability: (core analysis) 18.7% porosity, 323md permeability

Rock Classification: subfelds arenite

Comments: the argillaceous clast is a silty claystone with 30% medium grained quartz silt, 20% euhedral pyrite?, dominantly kaolin matrix.

Well: Legendre 1 **Depth**: 1935.5m **Formation**: equivalent Talisman Member

Palynological Zone/Age: B. reticulatum **Sample Type**: core 10

Hand Sample Description: quartz arenite, cream and white, white clay matrix (dolomite?) very coarse to medium grained, moderately sorted, fair porosity, smooth grain surfaces.

Thin Section Description:

Grain Size: very coarse to medium, dominantly medium

Sorting: moderate

Roundness: dominantly rounded

Spherocity: high to low, dominantly high

Extinction: (quartz) undulose - 95%, straight - 5%, occasionally poly crystalline

Mineralogy: quartz - 45% dolomite (matrix) - 40%, glauconite altered faecal pellets? - 10%, microcline/plagioclase - 5%, accessory kaolin

Cement/diagenesis: no cement seen in this sample. Microsparry dolomite comprises the matrix and has interparticle porosity. The rock is matrix supported with occasional tangental grain contacts.

Porosity/permeability: visual - poor, core analysis - 15.8% porosity, 15 md permeability

Rock Classification: dolomitic quartz arenite

Comments: quartz grains appear etched from the dolomitisation. Glauconite is being altered to kaolin?. Feldspars do not appear altered in this sample. Good sample for XRD.

Well: Legendre 1 **Depth**: 2128.4m **Formation**: Angel

Palynological Zone/Age: D. jurassicum **Sample Type**: core 11

Hand Sample Description: quartz arenite, very light grey, fine grained, well sorted, clear, etched quartz grains white matrix, friable, excellent visual porosity.

Thin Section Description:

Grain Size: fine grained

Sorting: well sorted

Roundness: rounded to well rounded

Spherocity: moderate to high

Extinction: (quartz) straight - 70%, undulose - 25%, poly crystalline 5%

Mineralogy: quartz - 95%, microcline - 5%; accessory - glauconite, chert; minor clay rimming quartz grains, rare zircon.

Cement/diagenesis: very minor silica cement, quartz grain contacts are well sutured indicating a good compaction phase. Quartz is highly etched at pore boundaries. Minor late stage glauconite cement.

Porosity/permeability: visual - excellent intergranular porosity, core analysis - 17% porosity, 114md permeability.

Rock Classification: quartz arenite

Comments: This sample has little cement or clay matrix. Quartz grain contacts are highly sutured but there is still a good open framework for excellent porosity.

Well: Legendre 2 **Depth**: 2081.5m **Formation**: equivalent Talisman Member

Palynological Zone/Age: D. lobospinosum **Sample Type**: core 1

Hand Sample Description: light orange grey, buff brown matrix, smooth clear quartz grains, medium to coarse grained, dominantly medium grained, moderately sorted, <10% glauconite, poor to fair porosity.

Thin Section Description:

Grain Size: medium to very coarse, dominantly medium

Sorting: moderate

Roundness: sub-angular to well rounded, dominantly rounded

Spherocity: high to low, dominantly high (80%),

Extinction: (quartz) undulose - 90%, straight - 5%, poly crystalline - 5%

Mineralogy: quartz - 50%, microcline - 10%, siderite (matrix) - 30%, calcite - 5%, accessory kaolin replacing feldspar?.

Cement/diagenesis: matrix is dominantly siderite cement. No quartz cement is seen. Minor late stage glauconite cement. Occasional tangental grain contacts, with relatively open grain framework and siderite matrix.

Porosity/permeability: visual - poor

Rock Classification: sideritic quartz arenite

Comments: see XRD sheet in WCR.

Well: Madeleine 1 **Depth**: 2981.7 **Formation**: Forestier claystone

Palynological Zone/Age: D. jurassicum **Sample Type**: core

Hand Sample Description: sandy siltstone, grey, argillaceous, glauconitic, slightly mica micaceous; horizontal worm tubes are filled with stratified very fine sand.

Thin Section Description:

Grain Size: very fine sand to coarse silt, 50% is matrix

Sorting: moderate

Roundness: sub-angular

Spherocity: low, preferentially oriented

Extinction: (quartz) straight - 80%, undulose - 20%

Mineralogy: quartz - 40%, microcline/perthite 5 - 10%; accessory glauconite, chert and opaques; matrix - dominantly illite, muscovite 5 - 10%.

Cement/diagenesis: early silica cement is etched and replaced by illite, quartz grain contacts are highly sutured, Feldspar grains are slightly altered and highly corroded, late stage glauconite rims.

Porosity/permeability: Visual - tight.

Rock Classification: sandy mudstone

Comments:

Well: Madeleine 1 **Depth**: 2982.5m **Formation**: Angel

Palynological Zone/Age: D. jurassicum **Sample Type**: core

Hand Sample Description: quartz arenite, very light grey, clear etched grains, white matrix, medium grained, glauconitic, well sorted, large (several mm) euhedral dolomite?, gypsum? crystal, excellent porosity.

Thin Section Description:

Grain Size: fine to coarse, dominantly medium

Sorting: moderate

Roundness: sub-angular to sub-rounded, dominantly sub-angular,

Spherocity: coarse grains - low, fine grains - high

Extinction: (quartz) straight - 80%, undulose - 20%

Mineralogy: quartz - 85%, microcline/perthite - 5%, glauconite - <5%, accessory kaolin, chert, dolomite, biotite altering to chlorite, rare zircon.

Cement/diagenesis: minor quartz cement, grain contacts are well sutured and edges are highly etched. Dolomite fills some pore space and replaces microcline, minor kaolin? rims on quartz, minor late glauconite cement.

Porosity/permeability: core analysis - 23.5% porosity, 888md permeability

Rock Classification: quartz arenite

Comments: quartz appears frosted due to etching. This rock is well compacted with little cement and excellent porosity.

Well: Rosemary 1 **Depth**: 2225m **Formation**: Angel

Palynological Zone/Age: P. iehiense **Sample Type**: ditch cuttings

Hand Sample Description: quartz arenite, white, clear, 80% sand grains, 20% claystone, very coarse to coarse grained, dominantly very coarse grained

Thin Section Description:

Grain Size: very coarse to medium, dominantly very coarse

Sorting: moderate

Roundness: originally well rounded or rounded, highly etched

Spherocity: dominantly high

Extinction: (quartz) poly crystalline - 50%, undulose - 45%, straight - 5%

Mineralogy: quartz - 85%, dolomite - 10%, clay (dominantly illite) - 5%, accessory - microcline, chert

Cement/diagenesis: no silica cement, grains are highly etched, many cuttings consist of itched quartz grains within a dolomite cement matrix. Claystone fragments are silty with a dominantly illite matrix. One fragment consists of a very red mineral matrix with quartz and glauconite silt.

Porosity/permeability:

Rock Classification: dolomitic quartz arenite

Comments: Silica cementation did not occur or was subsequently etched away. The absence of glauconitic in the sand portion is conspicuous. There is a high proportion of poly crystalline quartz. These factors makes this sample different from the others, possibly signifying a separate provenance.

Well: Rosemary 1 **Depth**: 2922.5m **Formation**: Dingo Claystone

Palynological Zone/Age: R. aemula **Sample Type**: core

Hand Sample Description: argillaceous siltstone, light brown grey

Thin Section Description:

Grain Size: silt size grains dominantly .05mm

Sorting: well sorted

Roundness: angular - sub-angular

Spherocity: low

Extinction: (quartz)

Mineralogy: quartz - 40%, matrix - 40%, dominantly illite? carbonate?; opaques - 20%

Cement: quartz is highly corroded

Porosity/permeability: (core analysis) 4.7% porosity, 0md permeability

Rock Classification: argillaceous siltstone

Comments:

Well: Talisman 1 **Depth**: 1920m **Formation**: Talisman Member

Palynological Zone/Age: S. tabulata **Sample Type**: ditch cuttings

Hand Sample Description: quartz arenite, light green grey, very coarse to fine dominantly medium, moderately sorted, red fragments

Thin Section Description:

Grain Size: moderate to coarse, dominantly medium

Sorting: moderately sorted

Roundness: sub-angular to rounded, dominantly rounded

Spherocity: high

Extinction: (quartz) undulose - 60%, poly crystalline - 30%, straight - 10%

Mineralogy: quartz - 90%, glauconite - 5%, microsparry ferroan dolomite - 5%; accessory - microcline, siderite, chert, iron oxide altered glauconite

Cement/diagenesis: interstitial iron oxide occurs rimming quartz and replacing some glauconite and dolomite. Dolomite rims quartz grains.

Porosity/permeability:

Rock Classification: iron oxidised quartz arenite

Comments: This sample is just above an unconformity. Exposure is indicated by the presence of iron oxide material and minerals altering to iron oxide. This sand was probably reworked on a marine shelf during a transgression.

Well: Talisman 1 **Depth**: 1970m **Formation**: Talisman Member

Palynological Zone/Age: C. delicata **Sample Type**: ditch cuttings

Hand Sample Description: light grey, clear smooth quartz grains, 20% clay matrix, medium to coarse grained, dominantly medium.

Thin Section Description:

Grain Size: medium to coarse, dominantly medium

Sorting: well sorted

Roundness: rounded although grains are highly etched.

Spherocity: high, occasional broken grain.

Extinction: (quartz) undulose - 80%, straight - 10%, poly crystalline - 10%

Mineralogy: quartz - 75%, microcline/perthite - 10%, siderite (grains) - 5%, glauconite - 10% accessory - chert, kaolin, opaques (carbonaceous material?)

Cement/diagenesis: minor quartz overgrowths on quartz grains

Porosity/permeability:

Rock Classification: feldspathic quartz arenite

Comments:

Well: Trafalgar 1 **Depth**: 2498 **Formation**: Legendre

Palynological Zone/Age: W. digitata **Sample Type**: core 1

Hand Sample Description: quartz arenite, white, clear quartz, very coarse, well sorted, rounded to sub-rounded, quartz cement, excellent porosity, minor disseminated pyrite, minor clay

Thin Section Description:

Grain Size: fine to coarse, dominantly medium

Sorting: moderate

Roundness: rounded, quartz slightly etched

Spherocity: high

Extinction: (quartz) straight - 55%, undulose - 40%, poly crystalline - 5%

Mineralogy: quartz - 95%, microcline/perthite (fine) - 5%, accessory - clay (illite, possibly trace kaolin); rare - tourmaline, zircon, pyrite, chert

Cement/diagenesis: long sutured quartz grain contacts, minor quartz cement follows compaction,

Porosity/permeability: excellent primary intergranular porosity

Rock Classification: quartz arenite

Comments:

APPENDIX IV

UNIT WELL TOPS

Well Horizon	Alpha North 1	Angel 1	Angel 2	Angel 3	Angel 4	Aurora 1	Bounty 1	Calypso 1	Cygnus 1	Dampier 1	Degrey 1	Egret 1	Finucane 1	Forestier 1	Lambert 1
Apt.	1873.5	2330	2365	2352		2260.5	2881	2021	1000	2432.5	1306.5	2906.5	2740	1840	2809.5
Val.	2012.5	2440	2494	2492		2308	2917	2089	1146	2630	1384.5	2981	2813.5	2020	2862.5
A	2078	2649	2689	2735	2684	2459	3132	2245		2899		3091.5	2982.5	2080	3083
B	2104	2716	2716	2760.5	2721.5	2604?	?	2292		3079.5		3128	3000	2086	3116.5
C	2127	2935.5	2932	2984		2626	?	2339.5		3140?		3290	3104	2186.5?	3313.5
D		3007	2984	3022.5			?	2351		3223?		3290		2202.5	3400.5
E		3192	3080.5	3145			3435	2415		3342		3290		2263	3519.5
F		3409.3	3111.5	3386.5						3710		3290?		2366.5	3641
G	2127		3111.5	3456.5		2626		2415				3311?	3104	2394.5	3641
H				3485				2435.5?							
I				3508		2626		2450?							
J						2840.5		2718.5?							
	C. halosa		*W. indotata*						*L. C. halosa*		L. Jurassic	U. Triassic	*D. caddaensis*		*C. turbatus*
Total Depth	2200	3411	4397	3787	2820	3020	3524	2843	2470	4142	2088	3658	3300	2514	3700

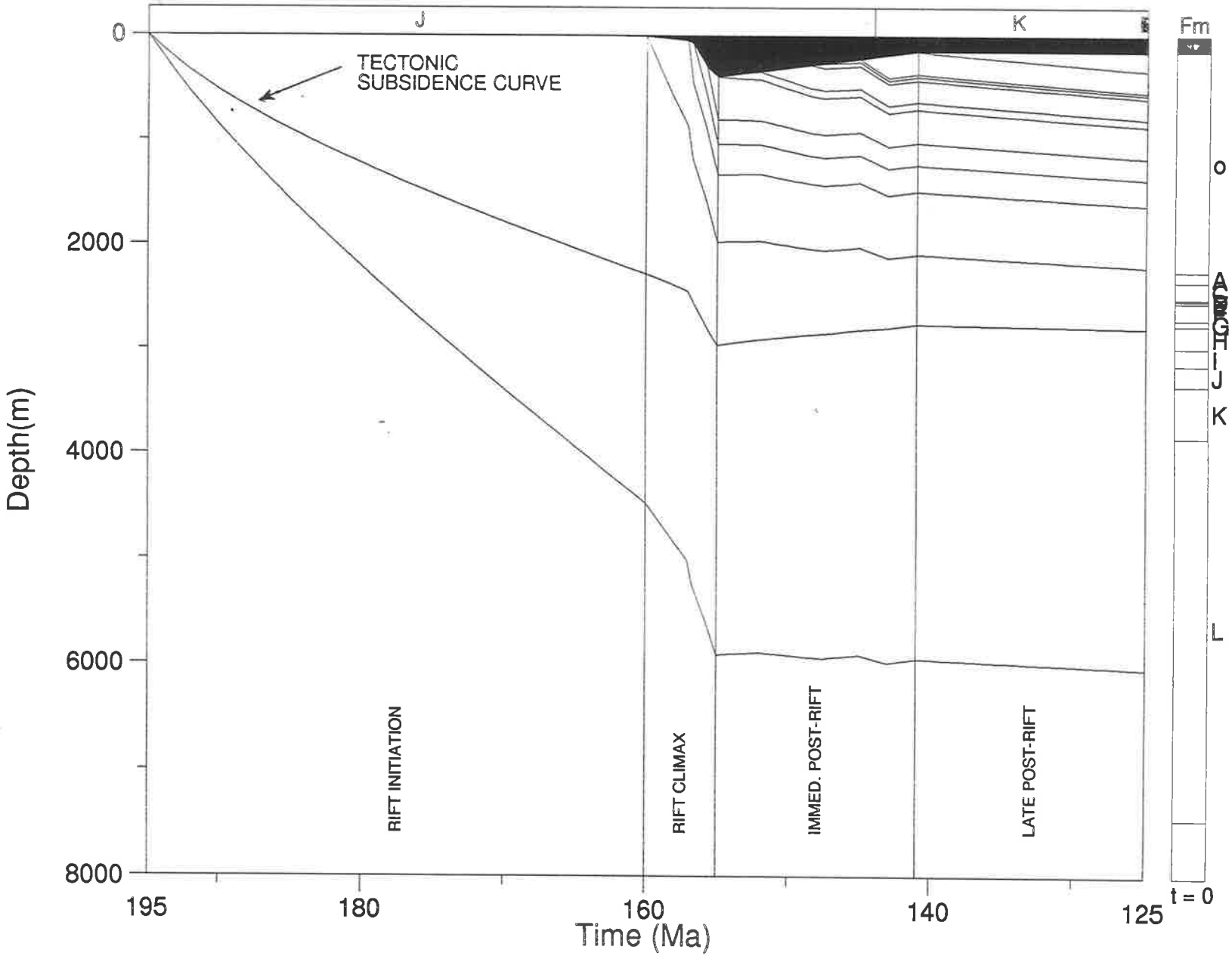
Well Horizon	Lauchie 1	Legendre 1	Legendre 2	Lewis 1	Madelaine 1	Montague 1	Nelson Rocks 1	Nickol Bay 1	Orion 1	Rosemary 1	Rosemary North 1	Samson 1	Talisman 1	Talisman 2	Walcott 1	Wanaea 1
Apt.	1849.5	1647	1843.5	1603.5	2479.5	2928	1833.5	498?	1586.5	1538.5	1714.5	1738	1821	1877.5	2601	2435
Val.	2109	1893	2000.5	1958	2620.5	3014	1962	720	1889	2128	2115.5	1991	1927.5	2005.5	2710	2559.5
A	2208	1974.5	2090	2001?	2890	3169	2057		1889	2203.5	2193.5	2119	1979	2075	2971	2790
B	2208?	2012	2112.5?	2001?	2900.5	3169	2064		1889	2203.5	2193.5	2129	2029.5	2115?	3006.5	2822
C	2368.5	2058.5?	2202?	2001?	3146	3428.5			1908	2291		2205	2137.5?	2165?	3236	3069.5
D	2383	2102?	2202?	2038.5	3223	3485.5				2315		2308.5	?	2165?	3282.5	3129.5
E	2403.5	2174	2252.5	2160.5	3322	3766.5				2371		2328.5			3439.5	3298.5
F	2564.5	2348.5		2257	3503	3919.5				2503.5		2371.5		2232?	3601	3445
G	2620	2348.5	2252.5	2314.5	3659.5	3992			1908	2503.5		2416.5	2163?	2256	3767	3641.5
H	2840	2602.5	2306	2506.5	3937.5	4050			2031	2677		2607			4048	3861
I	3003	2848.5	2578.5	2742	4228	4050			2048	2781.5		2700			4242	4040
J		?	3235	?	4412	4050				3232		3415.5	2163			4155
						M. crenulatus		*L. C. halosa*					*C. cooksonae a*			
Total Depth	3310	3473	3618	3400	4428	4362	2190		2475	3909	2263	3750	2925	2326	4381	4161.3

Appendix IV. Depths below KB of the mapped horizons used in the study. The Palynological zone that total depth was drilled to is indicated for wells that drilled below time horizon 'J'

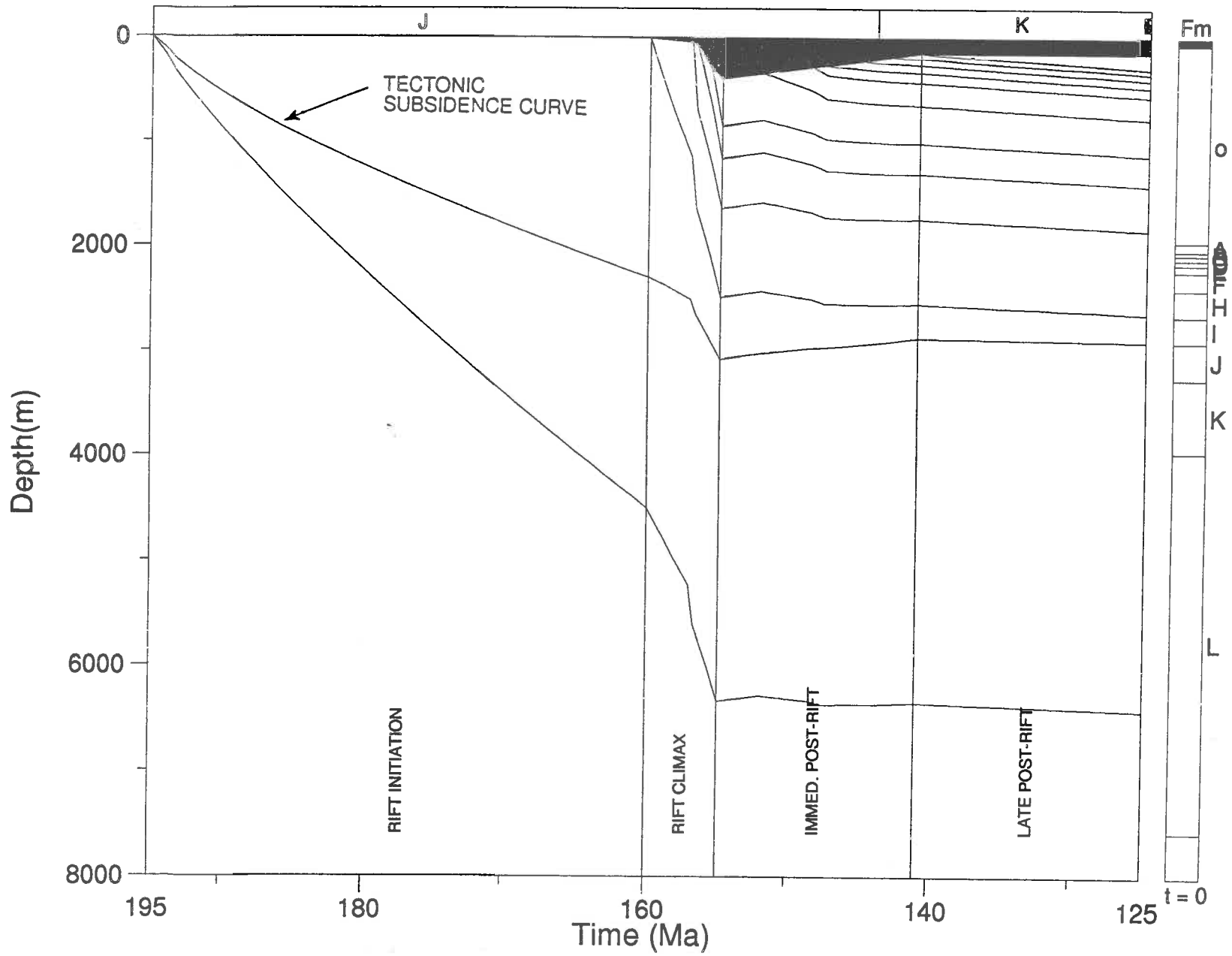
APPENDIX V

SUBSIDENCE CURVES

Lauchie 1 Subsidence



Legendre Subsidence



Rosemary Subsidence

